Springer Theses
Recognizing Outstanding Ph.D. Research

Marie-Hélène Larraufie

Development of New Radical Cascades and Multi-Component Reactions

Application to the Synthesis of Nitrogen-Containing Heterocycles

Springer

Springer Theses

Recognizing Outstanding Ph.D. Research

For further volumes:
http://www.springer.com/series/8790

Aims and Scope

The series "Springer Theses" brings together a selection of the very best Ph.D. theses from around the world and across the physical sciences. Nominated and endorsed by two recognized specialists, each published volume has been selected for its scientific excellence and the high impact of its contents for the pertinent field of research. For greater accessibility to non-specialists, the published versions include an extended introduction, as well as a foreword by the student's supervisor explaining the special relevance of the work for the field. As a whole, the series will provide a valuable resource both for newcomers to the research fields described, and for other scientists seeking detailed background information on special questions. Finally, it provides an accredited documentation of the valuable contributions made by today's younger generation of scientists.

Theses are accepted into the series by invited nomination only and must fulfill all of the following criteria

- They must be written in good English.
- The topic should fall within the confines of Chemistry, Physics, Earth Sciences, Engineering and related interdisciplinary fields such as Materials, Nanoscience, Chemical Engineering, Complex Systems and Biophysics.
- The work reported in the thesis must represent a significant scientific advance.
- If the thesis includes previously published material, permission to reproduce this must be gained from the respective copyright holder.
- They must have been examined and passed during the 12 months prior to nomination.
- Each thesis should include a foreword by the supervisor outlining the significance of its content.
- The theses should have a clearly defined structure including an introduction accessible to scientists not expert in that particular field.

Marie-Hélène Larraufie

Development of New Radical Cascades and Multi-Component Reactions

Application to the Synthesis of Nitrogen-Containing Heterocycles

Doctoral Thesis accepted by
the Université Pierre et Marie Curie, France

Springer

Author
Dr. Marie-Hélène Larraufie
Department of Biological Sciences
Columbia University
New York, NY
USA

Supervisors
Prof. Max Malacria
Prof. Louis Fensterbank
IPCM
Pierre and Marie Curie University
Paris
France

Dr. Emmanuel Lacôte
Laboratoire C2P2 (UMR 5265)
CPE Lyon
Villeurbanne
France

ISSN 2190-5053 ISSN 2190-5061 (electronic)
ISBN 978-3-319-01323-7 ISBN 978-3-319-01324-4 (eBook)
DOI 10.1007/978-3-319-01324-4
Springer Cham Heidelberg New York Dordrecht London

Library of Congress Control Number: 2013945154

Printed on acid-free paper

Springer is part of Springer Science+Business Media (www.springer.com)

Parts of this thesis have been published in the following journal articles:

Reprinted with permission from: Larraufie, M.-H.; Maestri, G.; Malacria, M.; Ollivier, C.; Fensterbank, L.; Lacôte, E. *Synthesis* **2012**, *44*, 1279–1292. Copyright 2012 Georg Thieme Verlag Stuttgart • New York.

Reprinted with permission from: Larraufie, M.-H.; Malacria, M.; Courillon, C.; Ollivier, C.; Fensterbank, L.; Lacôte, E. *Tetrahedron* **2013**, *in press*, doi:10.1016. Copyright 2013 Elsevier.

Reprinted with permission from: Larraufie, M.-H.; Courillon, C.; Ollivier, C.; Lacôte, E.; Malacria, M.; Fensterbank, L. *J. Am. Chem. Soc.* **2010**, *132*, 4381–4387. Copyright 2010 American Chemical Society.

Reprinted with permission from: Larraufie, M.-H.; Ollivier, C.; Fensterbank, L.; Malacria, M.; Lacôte, E. *Angew. Chem. Int. Ed.* **2010**, *49*, 2178–2181. Copyright 2010 Wiley-VCH Verlag GmbH&Co. KGaA, Weinheim.

Reprinted with permission from: Larraufie, M.-H.; Pellet, R.; Fensterbank, L.; Goddard, J.-P.; Lacôte, E.; Malacria, M.; Ollivier, C. *Angew. Chem. Int. Ed.* **2011**, *50*, 4463–4466. Copyright 2011 Wiley-VCH Verlag GmbH&Co. KGaA, Weinheim.

Reprinted with permission from: Maestri, G.; Larraufie, M.-H.; Derat, E.; Ollivier, C.; Fensterbank, L.; Malacria, M.; Lacôte, E. *Org. Lett.* **2010**, *12*, 5692–5695. Copyright 2010 American Chemical Society.

Reprinted with permission from: Larraufie, M.-H.; Maestri, G.; Beaume, A.; Derat, E.; Ollivier, C.; Fensterbank, L.; Courillon, C.; Lacôte, E.; Catellani, M.; Malacria, M. *Angew. Chem. Int. Ed.* **2011**, *50*, *12253–12258*. Copyright 2011 Wiley-VCH Verlag GmbH&Co. KGaA, Weinheim.

To my fabulous parents

Supervisors' Foreword

Welcome to the Larraufie Chemical Show!

In this doctoral thesis, you will first enjoy a bounty of new radical cascades involving cyanamides as 2N, 1C synthetic partners. A very rich crop of valuable derivatives of the vasicinone family and guanidines can be reaped from the versatile inclusion of the cyanamide motif into heterocycles. Generating and taming radicals needs a delicate balance between bond-breaking and bond-forming. Dr. Larraufie has fully mastered that subtle art.

She then went on to coax sunlight into generating radicals from epoxides and aziridines. With this clean and soft source of energy, and the help of crystalline inorganic catalytic salts which store and distribute this energy in a controlled fashion, the game is on for selective construction of C–C bonds. This new development in green radical chemistry has been widely recognized, from the acceptance to a high impact journal to its reception at meetings. Credit for this only belongs to Marie-Hélène Larraufie.

The final part of Dr. Larraufie's exploration of the intricacies of bond formations focused on organometallic catalysis. Swiftly playing with the possibility of chelation in the palladium(II)/palladium(IV) manifold, she evidenced a new twist in palladium catalysis. That led her and Dr. Giovanni Maestri to access a variety of nitrogen heteropolycycles.

The recurrent theme in the thesis is the minute control of the bond-forming events, whether they happen on single-electron species, or in the coordinations sphere of a metal. The research was conducted in collaboration with Max Malacria and Cyril Ollivier at Université Pierre et Marie Curie in Paris and Marta Catellani from Parma University in Milano. It involved dedication, skills, patience, and teamwork, all features that Dr. Larraufie possess. We were fortunate to accompany Marie-Larraufie to her journey through chemistry and watch her develop as a graduate student. Her award is fully deserved!

Paris, June 2013 — Prof. Louis Fensterbank
Villeurbanne, June 2013 — Dr. Emmanuel Lacôte

Marie-Hélène Larraufie is one the most brilliant graduate students I have ever had in my group.

In her first year, I set her to study the scope and limitations of the radical cascades (one of the main topics in my group at this time) involving *N*-acylcyanamides as crucial partners. Marie-Hélène has gone ahead and solved all the problems in order to set up a new approach to natural quinazolinones, to give new insights into the mechanism of homolytic aromatic substitutions, and moreover, to disclose the first radical synthesis of guanidines.

But as you know, the major drawbacks of these methodologies is the necessity to use tin hydride as radical mediator. She has then gone on to get rid of the "tyranny of tin", really stimulated to find sustainable alternatives for the generation of radical species she was able to expand the scope of visible light photoredox catalysis to the ring opening of oxiranes and aziridines and to exploit the thus generated radicals to carbon bond formation.

Not only did she focus on this central problem in her Ph.D., but she found the time to help other students and senior post-docs in the lab on a variety of projects. This notably resulted in an efficient collaboration with Giovanni Maestri, in a completely different area: palladium/norbornene catalyzed multi-components reactions, which led Marie-Hélène to show the first deviation from the ortho effect in the so-called "Catellani reaction". The mechanism of this unexpected behavior was elucidated using theoretical approach. DFT calculations indicated that this is likely originated in a distortion in the reductive elimination pathway from the palladium(IV) intermediate initially formed caused by specific chelation.

Quite frankly, her Ph.D. thesis is a landmark work. Not only has her studies remarkably improved the scope of radical cascades but, more importantly, allowed her to carry out more eco-friendly ways to exploit this methodology, which inspired her younger colleagues in the group. Finally her chelate approach in Pd(IV) chemistry has found new applications that are currently under active investigations in the lab.

On a thematic standpoint one would say her thesis is heterogeneous, overall this is a first class study bringing a lot of opportunities for the future to develop sustainable and efficient new methodologies in radical chemistry as well as in transition metal catalysis.

Paris, June 2013 Prof. Max Malacria

Contents

Part I N-Acylcyanamides as New Partners in Radical Cascades: Synthesis of Polycyclic Quinazolinones and Guanidines

1 Bibliographical Backgrounds 3
1.1 The Cyanamide Moiety, Synthesis and Reactivity 3
1.1.1 Biological Relevance of the Cyanamide Moiety 3
1.1.2 Methods of Synthesis 4
1.2 Homolytic Aromatic Substitutions: State of the Art of the Mechanistic Proposals. 17
1.2.1 Hydrogen as Leaving Group 18
1.2.2 Other Radical Leaving Groups: Ipso Substitutions 26
References 32

2 Results: Developments of New Radical Cascades with *N*-Acylcyanamides 39
2.1 Objectives of the Project 39
2.2 Addition of Alkyl Radicals 39
2.2.1 Synthetic Targets. 39
2.2.2 Synthesis of Cascade Precursors 41
2.2.3 Radical Cyclization of the *N*-Acylcyanamide Precursors. 44
2.3 Addition of Vinyl Radicals to *N*-Acylcyanamides 45
2.3.1 Radical Cyclization of Vinyliodide Precursor Followed by an Unexpected Reduction. 46
2.3.2 Mechanistic Studies 48
2.3.3 Migration of Carbon- or Heteroatom-Substituents 55
2.4 Addition of Nitrogen Centered Radicals 60
2.4.1 Synthetic Targets: Polycyclic Guanidines 61
2.4.2 Generation of Aminyl Radicals 62
2.4.3 Synthesis of the Precursors 67
2.4.4 Optimization of Guanidine Radical Synthesis 71
2.4.5 Scope of the Guanidine Synthesis 73
References 76

3 Supporting Information 79
3.1 General Remarks 79
3.2 Preparation and Cyclization of Alkyl Precursors 79
3.2.1 General Procedures 79
3.2.2 Alkyl Seleno Precursors 82
3.2.3 Cyclized Quinazolinones 88
3.3 Preparation and Cyclization of Vinyl Precursors 90
3.3.1 General Procedures 90
3.3.2 Vinyl Iodide Precursors 91
3.3.3 Cyclized Products 100
3.4 Preparation and Cyclization of Azide Precursors 111
3.4.1 General Procedures 111
3.4.2 Azide Precursors 113
3.4.3 Cyclized Guanidines 127
References 136

Part II Visible-light Photoreductive Catalysis for an Eco-compatible Generation of Radicals

4 Bibliographical Backgrounds: Generation of Radicals by Visible Light Photoredox Catalysis 139
4.1 Photophysical Properties of tris(bipyridyl)ruthenium(II) Complexes 141
4.1.1 Structure and Excited States 141
4.1.2 Absorption Spectrum 142
4.1.3 Deactivation and Quenching of Excited State 143
4.2 State of the Art of the Substrates Amenable to Visible Light Photoredox Catalysis 146
4.2.1 Aromatic Ketones 146
4.2.2 Activated Halides 146
4.2.3 Aryl Enones and Electron-Rich Styrenes 154
4.2.4 α-Keto Sulfonium, Ammonium and Phosphonium Salts 155
4.2.5 *N*-(acyloxy)Phthalimides 156
4.2.6 Diazoniums 157
4.2.7 Azides 158
4.2.8 Iodonium Salts 159
4.2.9 Para-Methoxybenzyl Ethers 160
4.2.10 Naphtols 160
4.2.11 Oxidative Functionalization of Tertiary Amines 161
References 162

5 Results: Visible Light-Induced Photoreductive Generation of Radicals from Epoxides and Aziridines 165
5.1 Epoxides as New Substrates for Visible-Light Triggered Generation of Radicals 165
5.1.1 Objectives of the Project 165
5.1.2 Various Modes of Activation Tested 167
5.1.3 Optimization of the Photoreductive Ring-Opening of Epoxides and Proposed Mechanism 173
5.2 Scope and Limitations of the Reductive Ring-Opening Methodology 176
5.2.1 α,β-Epoxyketones 176
5.2.2 α-Keto-aziridines 181
5.2.3 α-Keto-cyclopropane 183
5.3 Utilization of the Photogenerated Radicals in Carbon–Carbon Bond Formations 185
5.3.1 Optimization of the Allylation Conditions 186
5.3.2 Scope of the Allylation Process 188
5.3.3 Diastereoselectivity of the Allylations 189
References 192

6 Supporting Information 195
6.1 General Remarks 195
6.2 General Procedures 196
6.3 Epoxide, Aziridines and Cyclopropanes Precursors 198
6.4 Reductive Ring-Opening Products 207
6.5 Allylation Products 216
6.5.1 Allylating Agents 216
6.5.2 Allylated Products 218
References 225

Part III New developments in Aryl–Aryl Couplings via Palladium/Norbornene Dual Catalysis: Synthesis of Phenanthridines and Phenanthrenes

7 Bibliographical Background: The Ortho Effect in The Catellani Reaction 229
7.1 The Catellani Reaction 229
7.1.1 Palladacycle Formation 229
7.1.2 Palladacycle Reaction with Alkyl Halides 232
7.1.3 Palladacycle Reaction with Aryl Halides 235

7.2 Synthetic Applications of the *Ortho* Effect 237
7.2.1 Aromatic Arylations Coupled with Heck Reaction 237
7.2.2 Aromatic Arylation Coupled with Suzuki Reaction 239
7.2.3 Aromatic Arylations Coupled with Cyanation 239
7.2.4 Aromatic Arylations Coupled with Addition to C=O or C=N Bonds 240
7.2.5 Aromatic Arylations Coupled with C–H Activations . . . 240
7.2.6 Aromatic Arylations Coupled with *O*-aryl Couplings . . . 242
7.2.7 Aromatic Arylations Coupled with *N*-aryl Couplings . . . 243
7.3 Mechanistic Explanations for the *Ortho* Effect 244
7.3.1 Mechanistic Pathway Followed by Palladacycle 7H Bearing No *Ortho*-substituent 246
7.3.2 Mechanistic Pathway Followed by Palladacycle 7S with an *Ortho*-substituent 250
References 253

8 Results: New Partners for *Ortho*-Substituted Aryl Iodides in Palladium/Norbornene Cocatalysis 257
8.1 Coupling of *Ortho*-Substituted Aryl Iodides and Bromobenzyl Amines: First Reported Catellani Sequence Terminated by *N*-aryl Coupling with Unprotected Amines 257
8.1.1 Objectives of the Project 257
8.1.2 Optimization of the Catalytic Synthesis of Phenanthridines and Proposed Mechanism 258
8.1.3 Scope of the Synthesis of Phenanthridines 264
8.2 Coupling of *Ortho*-Substituted Aryl Iodides and 2-Bromophenyl Acetamides: An Exception to the *Ortho* Effect 271
8.2.1 Previous Work and Objectives of the Project 271
8.2.2 Scope of the Synthesis of Dihydrophenanthrenes 273
8.2.3 The Powerful Effect of Water 275
8.2.4 Mechanistic Investigations by DFT Calculations 280
References 292

9 Supporting Information 295
9.1 General Remarks 295
9.2 Coupling of *Ortho*-Substituted Aryl Iodides and Bromobenzyl Amines 296
9.2.1 General Procedures 296
9.2.2 Preparation of Starting Bromides 297
9.2.3 Phenanthridine-Type Products 299
9.3 Coupling of *Ortho*-Substituted Aryl Iodides and 2-Bromophenyl Acetamides 307

9.3.1 General Procedures 307
9.3.2 Preparation of Bromide Precursors. 308
9.3.3 Dihydrophenanthrene and Spiro Products 309
References 324

General Conclusion 325

Abbreviations

Ac	Acetyl
AcOEt	Ethyl acetate
AIBN	2,2'-Azobis-*iso*-butyronitrile
Ar	Aryl
BDE	Bond dissociation energy
Boc	*tert*-Butoxycarbonyl
Bn	Benzyl
BNAH	1-Benzyl-1,4-dihydronicotinamide
CAN	Ceric ammonium nitrate
cat.	Catalytic
(cpCo(cod))	η5-Cyclopentadienyl-η4-cycloocta-1,5-diene-cobalt(I)
DDQ	2,3-Dichloro-5,6-dicyanobenzoquinone
DFT	Density functional theory
DIB	Diacetoxyiodobenzene
DCP	Dicumyl peroxide
DLP	Dilauroyl peroxide
DMEDA	*N,N'*-Dimethylenediamine
DMF	*N,N'*-Dimethylformamide
DMSO	Dimethylsulfoxide
$DppONH_2$	*O*-(diphenylphosphinyl)Hydroxylamine
dr	Diastereomeric ratio
dtbbpy	Di-*tert*-butylbipyridine
EDPBT	1,1'-(ethane-1,3-diyl)Dipyridinium bistribromide
ee	Enantiomeric excess
equiv	Equivalents
Et	Ethyl
EWG	Electron withdrawing group
EtOH	Ethanol
h	Hour
HE	Hantzsch ester
HFIP	Hexafluoroisopropanol
HOMO	Highest occupied molecular orbital
HPLC	High pressure liquid chromatography
HPDMBI	*p*-Hydroxyl-2-phenyl,*N*,*N*-dimethylbenzimidazoline

HRMS	High resolution mass spectroscopy
IR	Infrared
IPr	1,3-Bis(2,6-di-*iso*-propylphenyl)imidazolylidene
LDBB	Lithium 4,4'-di-*iso*-butylbiphenylide
LUMO	Lowest unoccupied molecular orbital
Me	Methyl
MeCN	Acetonitrile
min	Minute
Mp	Melting point
Ms	Mesyl
NBS	*N*-Bromosuccinimide
n-Bu	Normal butyl
NIS	*N*-Iodosuccinimide
NMM	*N*-methylmorpholine
NMR	Nuclear magnetic resonance
NTBNCC	*tert*-Butyl-*N*-chlorocyanamide
o	*Ortho*
p	*Para*
PDMBI	2-Phenyl,*N*,*N*-dimethylbenzimidazoline
Ph	Phenyl
PMB	*p*-Methoxybenzyl
PMP	*p*-Methoxyphenyl
ppy	Phenylpyridine
PTOC	N-Hydroxypyridine-2(1*H*)thione)
quant.	Quantitative
r.t.	Room temperature
SOMO	Single occupied molecular orbital
TBAF	Tetra-*n*-butyl ammonium fluoride
TBAI	Tetra-*n*-butyl ammonium iodide
TBS	*t*-Butyldimethyl silyl
THF	Tetrahydrofuran
THP	Tetrahydropyranyl
TLC	Thin layer chromatography
TMS	Trimethylsilane
Ts	Tosyl
UV	Ultraviolet

General Introduction

Due to its unique assets, radical chemistry has become over the last 50 years a reliable and efficient tool for synthetic chemists [1, 2]. Radical reactions allow the formation of carbon–carbon and carbon–heteroatom bonds, even at sterically congested quaternary centers. They generally occur under mild conditions, which avoid the requirement of protection/deprotection steps and allow access to high stereocontrol [3–5]. They are thus perfectly suited for the synthesis of complex molecules. However, the broadening of the scope of application of synthetic radical chemistry is hampered by its environmentally unfriendly characteristics. Intense research efforts have been undertaken to bring solutions to this issue, and today, if green radical chemistry is still an ambitious goal, many ways are explored to progress toward that objective (Fig. 1).

During my Ph.D., I have studied two strategies aiming at reducing the ecological impact of radical chemistry.

I focused first on the development of new cascade reactions. Cascade reactions, understood as transformations allowing the formation of two or more bonds in the same flask, represent one of the most challenging and fascinating aspects of

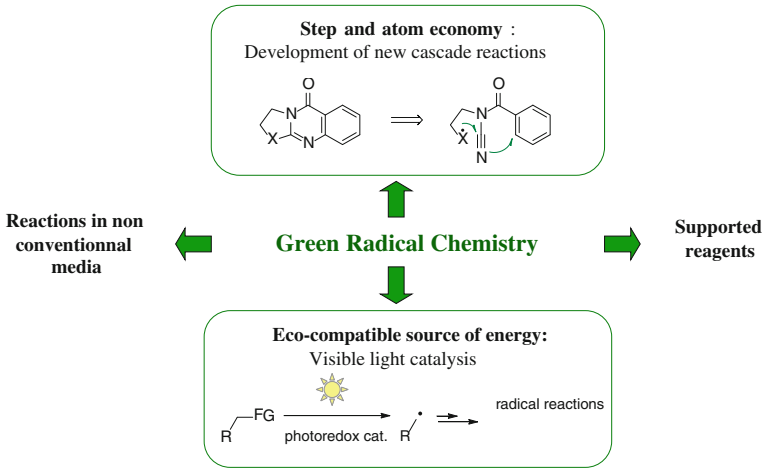

Fig. 1 Different approaches to progress toward green radical chemistry

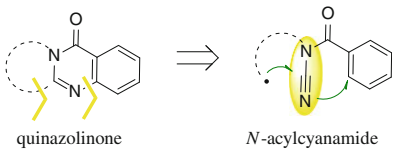

Fig. 2 Radical cyclization of *N*-acylcyanamides

chemistry. They contribute to progress toward green chemistry since they allow a large increase in molecular complexity in a minimum of operational steps, and hence generate much less waste. Since the addition of a radical onto an insaturation generates a new radical species that can further react, organic radicals are inherently prone to engage in cascade reactions. This has been illustrated in many applications in the literature [6–8]. Our group has a strong background in the synthesis of carbon polycyclic compounds via radical cascades [9]. More recently, we turned our attention toward the synthesis of nitrogen heterocycles owing to their high relevancy for biological applications. Our group proposed to build the quinazolinone core by a radical cascade using *N*-acylcyanamides as radical partners (Fig. 2). The first objectives of my Ph.D. were to fully study the polycyclization of C-centered radicals and to extend it to N-centered ones.

If the use of tributyltin hydride—the most commonly employed reagent for the generation of radicals—is very useful in the discovery of new reactivities in an academic setting, it has important drawbacks associated with its toxicity and difficult separation from products [10]. That is why in the second part of my Ph.D., I wished to develop new alternatives for the generation of radicals. The use of visible light has lately appeared to offer promising possibilities for the design of ecologically friendly synthetic radical chemistry [11–13]. Visible light is an abundant and renewable energy source, but most of the molecules do not absorb at these wavelengths, so a photoredox catalyst—such as $Ru(bpy)_3Cl_2$—is required to allow the sensitization of molecules. Photoreduction catalysis has mainly focused on the formation of radicals from halides and enones. We sought to extend it to the ring opening of epoxides, with the objective to access a photocatalytic version of the Nugent–Rajanbabu–Gansäuer reaction (Fig. 3).

Aside from radical chemistry, we have developed a complementary approach to obtain polycyclic compounds via pallado-catalyzed multi-components reactions. In a collaborative effort with the Catellani group in Italy, we got interested in dual palladium/norbornene catalysis. The use of norbornene with palladium to achieve sequential C–halide and C–H activations was pioneered by Catellani in the mid-1980s [14]. Since then, numerous applications have been reported, which allow the construction of up to three carbon–carbon bonds in a single reaction, thanks to a complex catalytic cycle involving multiple oxidation states of palladium (0, II, and potentially IV) [15–18].

We were first interested by the development of a C-amination coupling variant of the Catellani reaction with unprotected amines. Thanks to the use of bromobenzylamine as reaction partners, we studied the possibility to build

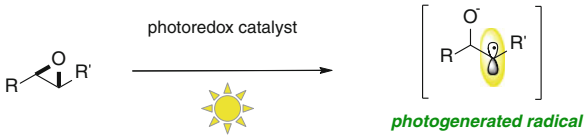

Fig. 3 Visible-light photoreduction of epoxides

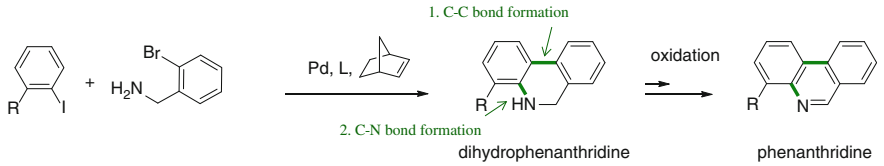

Fig. 4 C-Amination coupling variant of the Catellani reaction

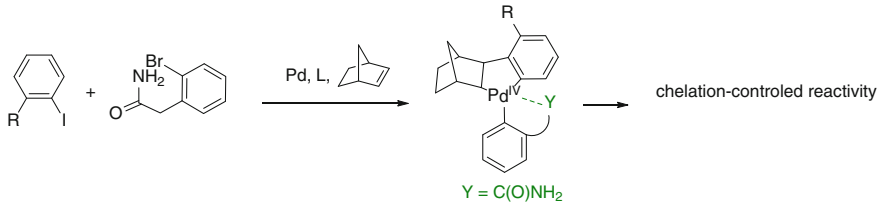

Fig. 5 Bromophenylacetamides as reaction partners

dihydrophenanthridines via sequential carbon–carbon and carbon–nitrogen coupling (Fig. 4).

Our group has been particularly interested in in-depth understanding of the mechanistic pathways involved in the Catellani/Lautens reaction [19]. Using bromophenylacetamides as reaction partners, we disclosed that coordinating substituents might induce different reactivities at the palladium center, and that chelation might thus be a tool to achieve regiocontrol in Pd/norbornene catalysis (Fig. 5). The synthetic results were rationalized on the basis of computational analysis of several reactive pathways.

This manuscript is divided into three chapters dealing, respectively, with cascade reactions using *N*-acylcyanamides, photoredox chemistry, and palladium/norbornene dual catalysis. In each chapter a bibliographical part will first review the literature backgrounds relevant to the topics.

References

1. Renaud, P., & Sibi, M. P. (Eds.) (2001). *Radicals in organic synthesis*. Weinheim: Wiley-VCH.
2. Gansäuer, A. (Ed.) (2006). *Radicals in synthesis I & II* (Vols. 263–264). Springer: Berlin.
3. Curran, D. P., Porter, N. A., & Giese, B. (Eds.) (1996). *Stereochemistry of radicals reactions: Concepts, guidelines and synthetic applications*. Weinheim: Wiley-VCH.
4. Bar, G., & Parsons, A. F. (2003). *Chemical Society Reviews*, *32*, 251–263.
5. Sibi, M. P., Manyem, S., & Zimmerman, J. (2003). *Chemical Reviews*, *103*, 3263–3295.
6. McCarroll, A. J., & Walton, J. C. (2004). *Angewandte Chemie International Edition*, *40*, 2224–2248.
7. Nicolaou, K. C., Edmonds, D. J., & Bulger, P. G. (2006). *Angewandte Chemie International Edition*, *45*, 7134–7186.
8. Godineau, E., & Landais, Y. (2009). *Chemistry–A European Journal*, *15*, 3044–3055.
9. Albert, M., Fensterbank, L., Lacôte, E., & Malacria, M. (2006). *Topics in Current Chemistry*, *264*, 1–62.
10. Baguley, P. A., & Walton, J. C. (1998). *Angewandte Chemie International Edition*, *37*, 3072–3082.
11. Yoon, T. P., Ischay, M. A., & Du, J. (2010). *Nature Chemical*, *2*, 527–532.
12. Narayanam, J. M. R., & Stephenson, C. R. J. (2011). *Chemical Society Reviews*, *40*, 102–113.
13. Teply, F. (2011). *Collection of Czechoslovak Chemical Communications*, *76*, 859–917.
14. Catellani, M., & Chiusoli, G. P. (1985). *Journal of Organometallic Chemistry*, *286*, C13–C16.
15. Catellani, M. (2003). *Synlett*, *3*, 298–313
16. Catellani, M., Motti, E., & Della Ca, N. (2008). *Accounts of Chemical Research*, *41*, 1512–1522.
17. Martins, A., Mariampillai, B., & Lautens, M. (2010). *Topics in Current Chemistry*, *292*, 1–33.
18. Cardenas, D. J., Martin-Matute, B., & Echavarren, A. (2006). *Journal of the American Chemical Society*, *128*, 5033–5040.
19. Maestri, G., Motti, E., Della Ca, N., Malacria, M., Derat, E., & Catellani, M. (2011). *Journal of the American Chemical Society*, *133*, 8574–8585.

Part I
N-acylcyanamides as New Partners in Radical Cascades: Synthesis of Polycyclic Quinazolinones and Guanidines

Chapter 1
Bibliographical Backgrounds

1.1 The Cyanamide Moiety, Synthesis and Reactivity

The cyanamide moiety consists of a nitrogen atom bearing a nitrile group (Fig. 1.1). When the nitrogen atom is substituted with a carbonyl group, one speaks of *N*-acylcyanamide. Thanks to its original structure, it possesses unique properties as a building block in organic synthesis, as a ligand in organometallic applications or as an essential function in bioactive compounds. The synthesis and chemical transformations of mono- and disubstituted cyanamides have been reviewed in depth by Nekrasov in 2004 [1], so only the recent literature will be covered in this section [2].

1.1.1 Biological Relevance of the Cyanamide Moiety

Cyanamides are found in natural products and in several bioactive molecules. Thus, simple cyanamide **1**, produced naturally [3], has been identified as an aldehyde deshydrogenase inhibitor [4]. It consequently blocks ethanol metabolism at the acetaldehyde stage, inducing after alcohol consumption a toxic acetaldehyde syndrome characterized by tachycardia, hypotension, and flushing. For this reason, it is currently assessed in the treatment of alcohol dependence [5]. It is also noteworthy that cyanamide **1**, detected in interstellar clouds, is considered as an important molecule in prebiotic chemistry. Indeed, under UV irradiation or water-iced catalysis, it can isomerize to carbodiimide **2** (Fig. 1.2) [6, 7], which can assemble amino acids into peptides. Furthermore, the condensation of cyanamide **1** with carbohydrate precursors has been proposed as a possible prebiotic route to nucleosides [8].

The cyanamide moiety is also present in more complex molecules exhibiting interesting biological activities. *N*-acylcyanamide **3** thus possesses inhibiting activity against hepatitis C virus NS3 protease [9]. Cyanamide based inhibitors of cathepsin K such as **4** have also been developed [10, 11] and might become valuable alternatives for the treatment of disease involving bone resorption such as osteoporosis (Fig. 1.3).

M.-H. Larraufie, *Development of New Radical Cascades and Multi-Component Reactions*, Springer Theses, DOI: 10.1007/978-3-319-01324-4_1,

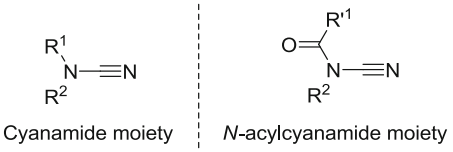

Fig. 1.1 Structure of cyanamide and *N*-acylcyanamide

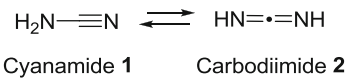

Fig. 1.2 Cyanamide-carbodiimide isomerization

1.1.2 Methods of Synthesis

A limited number of synthetic routes have been reported for the introduction of the cyanamide function. The most straightforward strategy consists in the direct alkylation of cyanamide **1**. However, generally only symmetrically disubstituted cyanamides can be obtained via this methodology since the monoalkylated cyanamide is more nucleophilic and more acid than the starting cyanamide **1**. An example of successful monoalkylation of cyanamide potassium salt **5** has nevertheless been reported by Sharpless, by treatment with tosylate **6** in toluene at 90 °C (Fig. 1.4) [12]. On the other hand, the monoacylation, or monosubstitution with an electron withdrawing group, of cyanamide **1** proceeds smoothly [13–15].

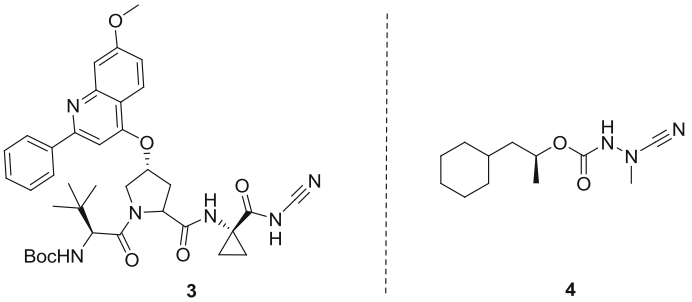

Fig. 1.3 Cyanamide-based bioactive molecules

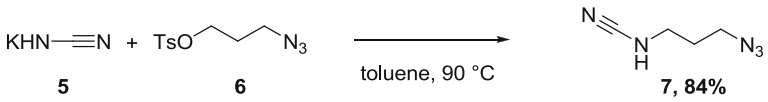

Fig. 1.4 Monoalkylation of cyanamide potassium salt

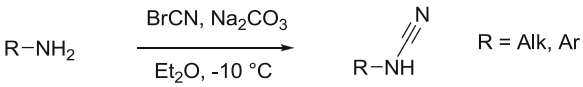

Fig. 1.5 Harrison's methodology for the cyanation of primary amines

In order to achieve the formation of monosubstituted or asymmetrically disubstituted cyanamides, four types of approaches have been developed.

1.1.2.1 Cyanation of Amines by an Electrophilic Cyanating Agent

The most commonly used reagent for electrophilic cyanation is cyanogen bromide. This reagent is very toxic and must consequently be handled with precaution. The efficient synthesis of cyanamides by treatment of a primary amine with BrCN and sodium carbonate in diethyl ether has been reported for the first time in 1976 by Harrison [16] (Fig. 1.5) and has been widely used and adapted since [17–19].

An interesting extension to the electrophilic cyanation by BrCN was the regio- and stereoselective von Braun ring-opening of chiral piperidine (Fig. 1.6). Piperidine **8** containing a phenyl group at C-2 was opened by treatment with BrCN with an inversion of configuration, leading to linear cyanamide **9** [20]. Piperidine **10** containing a trimethylsilylmethyl group at C-2 led, via a similar strategy, to linear cyanamide **11** featuring a terminal double bond, by treatment with TBAF and BrCN [21].

Other electrophilic cyanating agents such as 2-cyanopyridazin-3(2H)-one [22] or 1-cyanoimidazole [23] have been reported as efficient and stable reagents for the synthesis of cyanamides. Nevertheless it should be noted that their preparation involves the use of BrCN, so that their utilization does not circumvent the handling of this toxic reagent.

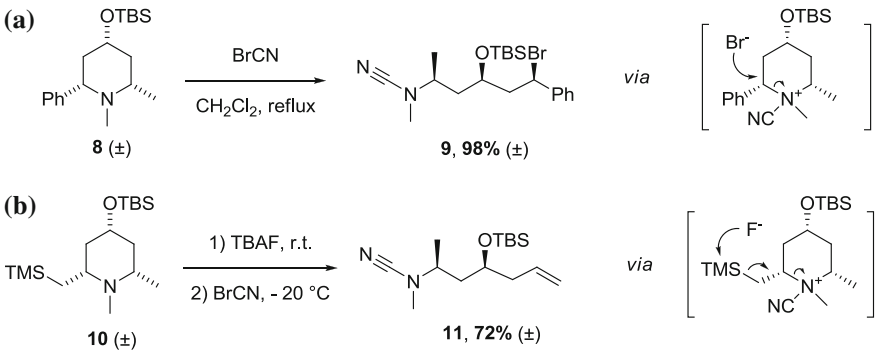

Fig. 1.6 BrCN mediated regioselective ring-opening of piperidines

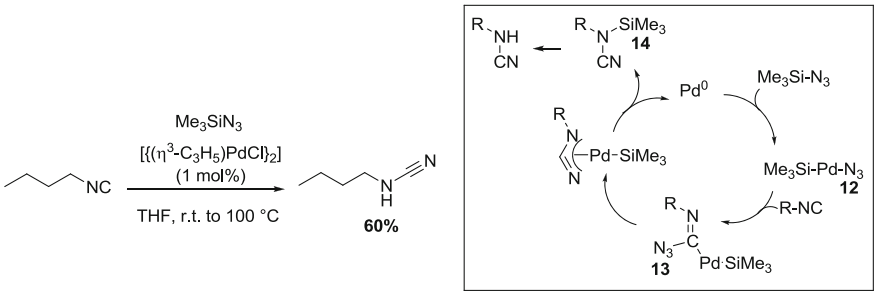

Fig. 1.7 Pallado-catalyzed conversion of alkylisocyanide into the corresponding cyanamide

1.1.2.2 Pallado-Catalyzed Reaction Between Isocyanides and Trimethylsilyl Azide

Alkyl and aryl isocyanides have been converted into the corresponding cyanamides by treatment with Me_3SiN_3 in the presence of $[\{\eta^3\text{-}C_3H_5)PdCl_2]$ as a catalyst (Fig. 1.7) [24]. The reaction proceeds through oxidative addition of Pd^0 into Si–N bond, producing $Me_3Si\text{-}Pd\text{-}N_3$ complex **12**. Insertion of the isocyanide into the $Pd\text{-}N_3$ bond leads to complex **13**. A $Me_3Si\text{-}Pd$ mimic of the Curtius rearrangement followed by reductive elimination affords the TMS protected cyanamide **14** which is then desilylated during silica gel chromatography.

Allyl cyanamides could be synthesized via a related strategy through a pallado-catalyzed three–component coupling reaction between isocyanides, allylcarbonates and $TMSN_3$ [25, 26].

1.1.2.3 Deoxygenation of Isocyanates

An efficient synthesis of cyanamides has been developed by deoxygenation of isocyanates in the presence of the hindered base sodium bis(trimethylsilyl)amide [27]. Alkyl, acyl or aryl isocyanates such as **15** could be converted into the corresponding cyanamides in excellent yields at room temperature. The authors propose the mechanism depicted in Fig. 1.8, which involves a nucleophilic attack by $NaN(SiMe_3)_2$ followed by a 1,2-elimination. Since many isocyanates are commercially available, this methodology is very convenient, however the use of a strong base such as $NaN(SiMe_3)_2$ limits the scope of the substrates.

Interestingly, the same reaction conditions could be applied to the desulfurization of isothiocyanates, leading similarly the corresponding cyanamides in efficient yields [28].

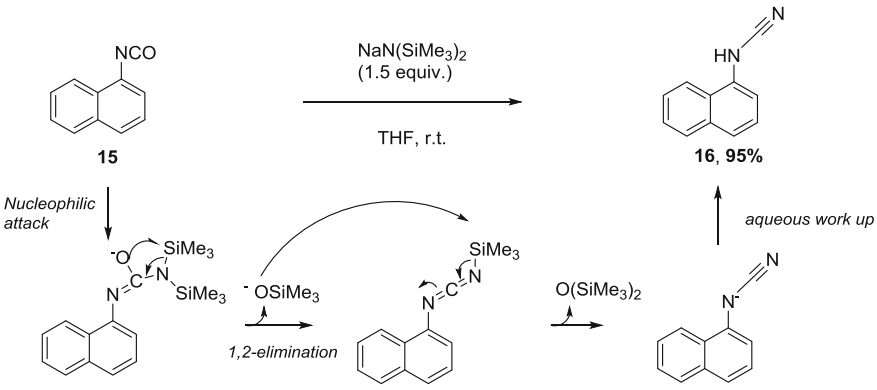

Fig. 1.8 One flask transformation of isocyanates to cyanamide

1.1.2.4 Desulfurization of Isothioureas

Several recent reports in the literature have described the preparation of monosubstituted cyanamides by desulfurization of the corresponding thioureas employing mild reaction conditions. Thus ethylation of phenylthiourea **17** followed by a basic work-up led to phenylcyanamide **18** in four steps (Fig. 1.9) [29].

In a one pot procedure employing diacetoxyiodobezene (DIB) as an oxidative desulfurizating agent, aryl and alkyl dithiocarbamate salts have been converted into the corresponding thioureas and subsequently desulfurizated to provide the cyanamides [30]. Thus, when treated with DIB and ammonia cyclohexyldithiocarbamate salt **19** forms cyclohexylcyanamide **20** in a good yield, by oxidative desulfurization of in situ generated thiourea **21** (Fig. 1.10). Instead of the hypervalent iodine reagent, molecular iodine [31, 32] or bromineless brominating agent EDPBT [33] can also be employed.

Catalytic conditions have recently been developed for the synthesis of cyanamides from thioureas. Thus, using $CuSO_4 \bullet 5H_2O$ as a catalyst, 2-(arylthio)arylcyanamide **22** has been synthesized by domino intra- and intermolecular C–S cross-couplings starting from 2-(iodoaryl)thiourea **21** and aryl iodide (Fig. 1.11) [34].

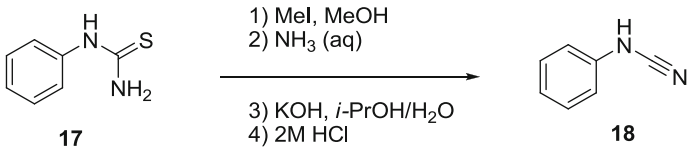

Fig. 1.9 Synthesis of phenylcyanamide via methylation of phenylthiourea

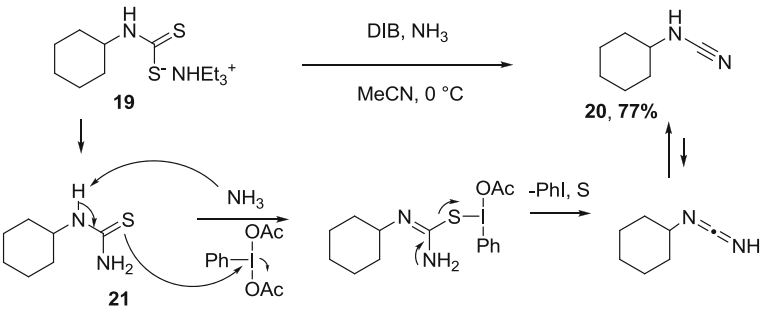

Fig. 1.10 One pot synthesis of cyanamide from thiocarbamate salt

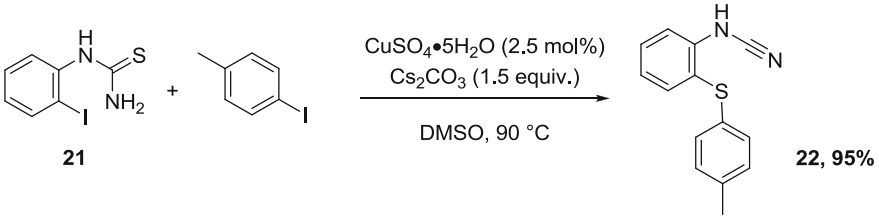

Fig. 1.11 Catalytic synthesis of 2-(arylthio)arylcyanamides

1.1.2.5 Reactivity

Because of their peculiar structure, cyanamides possess original electronic properties. The lone pair of electrons on the amino nitrogen can delocalize into the nitrile group. Thus the N–CN bond length (1.33 Å for Me(*p*-C_6H_4Cl)N–CN) is between the normal N–C bond length (1.47 Å) and the N=C double bond length (1.27 Å). Its cleavage can occur only under harsh conditions or well-designed transition metal catalysis [35]. The basicity of the amino group is strongly decreased compared to the corresponding amine and hence, in the presence of an acid, the nitrile group will be protonated [10]. Finally, the presence of the electron withdrawing amino group enhances considerably the electrophilicity of the nitrile group, as demonstrated by DFT calculations comparing the electrophilicity of diversely substituted nitriles [36]. It is consequently not surprising that a large majority of the reactions using cyanamides imply a nucleophilic attack at the nitrile group. Cyanamides have also been particularly exploited in cyclotrimerizations and cycloadditions as valuable precursors for the synthesis of nitrogen heterocyclic compounds.

1.1.2.6 Nucleophilic Additions at the Nitrile Function

Various types of nucleophiles can add at the carbon atom of the nitrile group under basic or acid conditions, or in the presence of a Lewis acid.

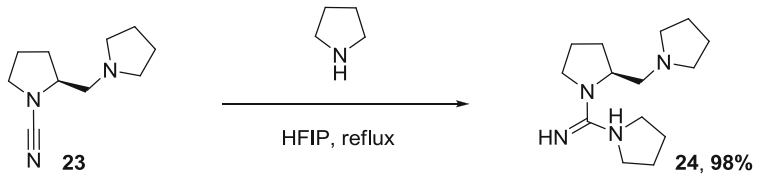

Fig. 1.12 Synthesis of chiral guanidines

– Addition of nitrogen nucleophiles.

The addition of amines on cyanamides allows the straightforward synthesis of guanidine compounds [37–40]. In the aim of preparing chiral superbases, enantiopure cyanamides such as **23** have been synthesized and treated with secondary amines in refluxing hexafluoroisopropanol (HFIP) (Fig. 1.12) [41]. The use of this polar and weakly nucleophilic solvent was essential for the efficiency of the reaction [42].

Alternatively, the guanidines generated can be used as intermediates in the one-pot synthesis of more complex scaffolds [43]. For instance, a rapid access to highly substituted 2-aminoimidazole such as **28** has been developed through a one-pot three-steps sequence starting from diallylamine **26** and propargyl cyanamide **25**. Under $La(OTf)_3$ catalysis, addition of the allyl amine to the cyanamide is followed by the hydroamination of the alkyne and final isomerization to generate the imidazole core (Fig. 1.13) [44].

- Addition of sulfur nucleophiles

Nucleophilic additions of alkyl and aryl thiols to the nitrile group of cyanamides have been reported under acid [45] or basic conditions [46]. As previously,

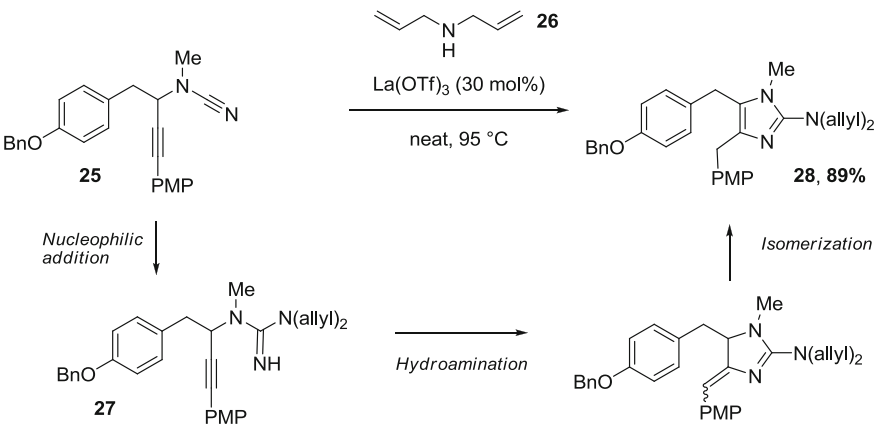

Fig. 1.13 Sequential nucleophilic addition of amine at cyanamide and cycloisomerization

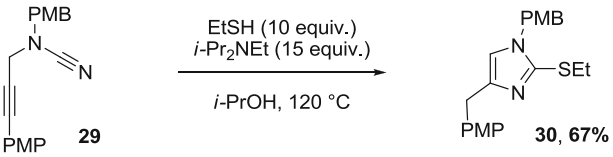

Fig. 1.14 Sequential nucleophilic addition of thiol at cyanamide and cycloisomerization

the intermediate thioureas generated could be engaged in subsequent cycloisomerizations, yielding 2-thioimidazoles in good yields (Fig. 1.14).

- Addition of oxygenated nucleophiles

The successful additions of alkyl and aryl alcoholates to cyanamides have been described, yielding the corresponding imidates. The nucleophiles could either be alcohols in the presence of mild base such as K_2CO_3 [46], or carbonyl functions [47]. Otherwise, an elegant strategy for the in situ generation of alcoholate nucleophile is the ring opening of epoxides by sodium cyanamide. Thus 1,2-anhydroglucopyranose **31** has been treated with NaNHCN in the presence of the strongly oxophile Lewis acid catalyst $TiO(CF_3CO_2)_2$ (Fig. 1.15). After coordination of the titanium catalyst to the oxirane and ring-opening by NaNHCN, the intermediate titanium alcoholate **32** is formed. It then undergoes an intramolecular nucleophilic addition to afford imino-oxazolidine derivative **33** in excellent yield [48].

- Addition of carbon nucleophiles

Finally, carbanions could also perform nucleophilic additions to cyanamides both in intramolecular and intermolecular fashions [49]. A methodology for the regiocontrolled synthesis of highly substituted 1,2 dihydro-2-oxopyridines using an intramolecular carbanion addition to cyanamides as a key step has been

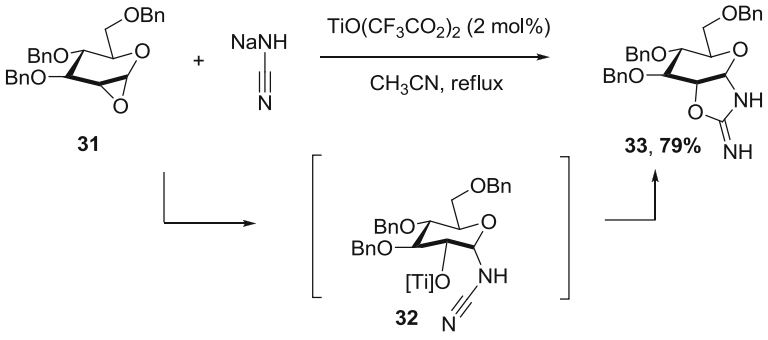

Fig. 1.15 Sequential epoxide ring-opening and nucleophilic addition of titanium alcoholate to cyanamide

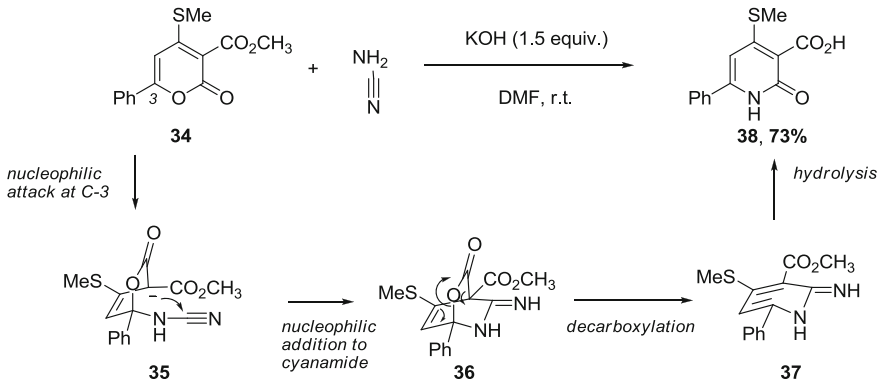

Fig. 1.16 Sequential synthesis of oxopyridine incorporating an intramolecular carbanion addition at cyanamide

reported [50, 51]. Starting from pyran-2-one derivative **34**, the reaction is initiated by nucleophilic attack of the cyanamide at the most electrophilic C-3 center. The stabilized carbanion **35** formed then undergoes a nucleophilic addition to the nitrile function, leading to bicyclic intermediate **36**. Decarboxylation and hydrolysis of the imino and ester groups lead to the functionalized oxopyridine **38** (Fig. 1.16).

The intermolecular addition of 2-fluoro-2′-lithiobiphenyl **42** to the nitrile function of diethylcyanamide followed by an intramolecular S_NAr reaction has been reported [52]. Biphenyllithium adduct **42** was generated from the attack of *o*-fluorophenyllithium **40** on 1,2-aryne **41**, also generated from **40** by elimination of LiF. Hence, in a single procedure, fluorobenzene and diethylcyanamides yielded the 6-amino phenanthridine **43** by simple treatment with *t*-BuLi (Fig. 1.17).

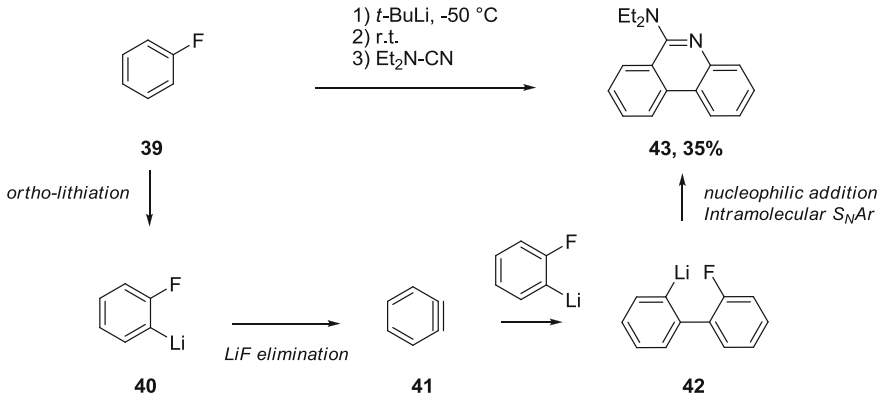

Fig. 1.17 One pot synthesis of 6-amino phenanthridines from fluorophenyl and cyanamide

1.1.2.7 Cycloadditions

- Cyclotrimerizations

Monosubstituted cyanamides tend to undergo spontaneous cyclotrimerizations to give 1,3,5-triazines when stored without particular precautions [53], highlighting their low stability. Disubstituted cyanamides have to be activated to enter such a process, which allows the controlled synthesis of functionalized pyridines. Harsh reagents such as bis(silyl-substituted)methyl lithium [54] or triflic anhydride [55] have proven effective, but recently, an important step forward has been made with the catalytic activation of dialkylcyanamides using organometallic complexes. Thus, hexamethylmelanine **45**, a potent antitumor compound [56], has been synthesized in an atom economical fashion via cyclotrimerization of dimethylcyanamide **44** in the presence of a catalytic amount of $[Al(NMe_2)_3]_2$ (Fig. 1.18) [57]. DFT calculations have suggested that the likely mechanism for this process goes through three insertions of cyanamide functions into Al–N bonds followed by a nucleophilic ring closure.

Cyanamides can also participate to cyclotrimerization processes with other unsaturated partners, extending the scope of the scaffolds reachable. Cobalt catalysis is the most widespread catalyst for such reactions. Thus *N*-cyanopyrrolidine and *N*-cyanopiperidine were cyclotrimerized with 2 equivalents of acetylene in the presence of [CpCo(cod)], delivering 2-aminopyridines under mild conditions (irradiation at room temperature) [58]. Cyanamides could also be cocyclotrimerized with bis-alkynes under $CpCo(CO)_2$ catalysis and thermal conditions [59, 60]. The use of dissymmetrical bis-alkyne **46**, led regioselectively to bicyclic 2-aminopyridine **49**. This regioselectivity can be explained by the minimization of steric interactions between the cyanamide substituent and the cobaltacylopentadiene intermediate [61, 62] **48** during cyanamide incorporation (Fig. 1.19).

Expanding the scope of unsaturations amenable to cycloadditions with cyanamide, our group has recently reported the synthesis of 2,5-diaminopyridine via [2 + 2+2] cycloadditions between yne-ynamides and cyanamides [63]. The reactions were catalyzed by the air-stable catalyst CpCo(CO)(dimethylfumarate) [64] under thermal conditions.

- [3 + 2] Cycloadditions

The [3 + 2] cycloaddition of azide anion and cyanamide has been employed for a long time as a straightforward route for the synthesis of 5-aminotetrazoles.

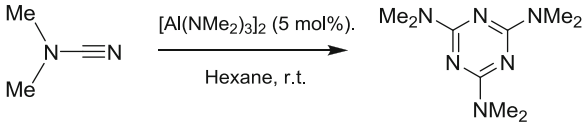

44 **45, 86%**

Fig. 1.18 Cyclotrimerization of dimethylcyanamide catalyzed by aluminium complex

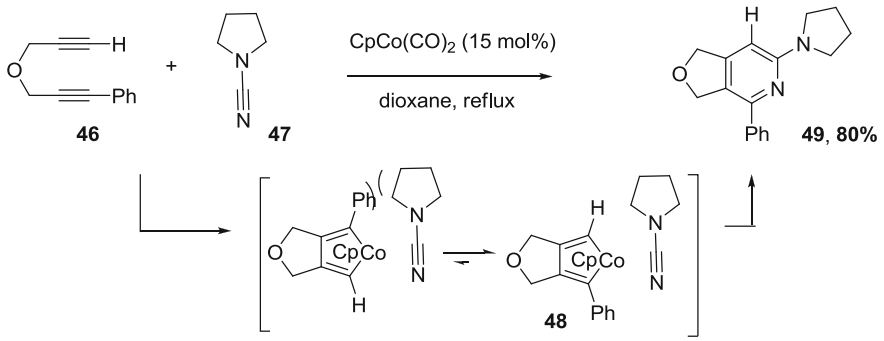

Fig. 1.19 Cobalt-catalyzed cycloaddition of cyanamide and bis-alkyne

Fig. 1.20 Zeolite catalyzed cycloadditions of azide and cyanamide in water

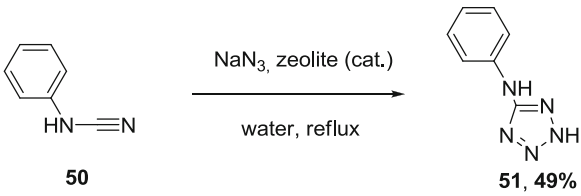

Recent reports have demonstrated that water could be used as solvent despite the low solubility of the starting materials. Zinc salts exhibit efficient catalytic activity for this reaction [65, 66]. Alternatively, natrolite zeolite can be used as a natural and reusable heterogeneous catalyst [67]. For example, cyanamide **50** refluxed in water in the presence of sodium azide and zeolite afforded arylaminotetrazole **51** in 49 % yield (Fig. 1.20).

The first example of intramolecular [3 + 2] cycloadditions between azide and cyanamide has been reported by Sharpless [68], affording the corresponding 1,5-fused tetrazoles under thermal conditions. Cycloaddition of dialkylcyanamides proceeded almost quantitatively at 140 °C (Fig. 1.21a), while monoalkylcyanamides yielded predominantly side products. On the other hand, monosubstituted arylcyanamides were very efficient substrates, since the cycloadditions could occur in good yield at only 60 °C (Fig. 1.21b).

- [2 + 2] Cycloadditions

Cyanamides have been reacted with Woolins' reagent $[PhP(Se)(\mu\text{-}Se)]_2$ **54**, the selenium counterpart of Lawesson's reagent. The reaction led to the formation of selenazadiphosphoaminediselenides such as **57** under thermal conditions (Fig. 1.22). The mechanism is thought to start with a [2 + 2] cycloaddition between the cyanamide and diselanophosphorane **56** which is in equilibrium with Woolins' reagent at high temperature. Here, mono- and disubstituted cyanamides could be employed [69, 70].

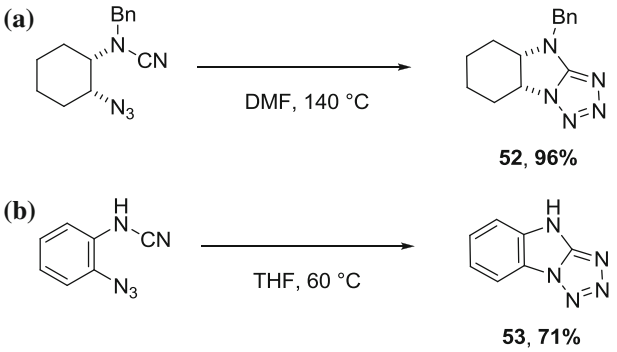

Fig. 1.21 Intramolecular cycloadditions of azidocyanamides

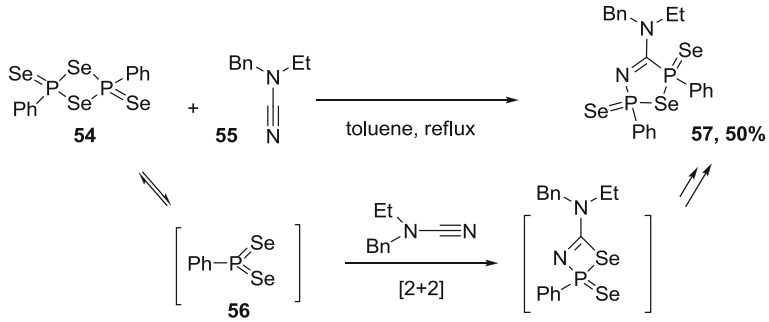

Fig. 1.22 Synthesis of seleno-heterocycles via [2 + 2] cycloadditions

1.1.2.8 Condensation with Aldehydes

The amino nitrogen of cyanamide can condense with aromatic aldehydes, leading to aryl cyanoimino compounds. The imines can then undergo Michael additions or react with other substrates in elaborate multi-component reactions [71–73]. An efficient synthesis of cyanoimidate derivatives such as **62** has hence been developed via the condensation of an aldehyde and cyanamide **1** in the presence of an alcohol, *t*-BuONa and NBS as an oxidant [74]. According to the proposed mechanism, the alcohol performs a Michael addition to cyanoimino intermediate **59**, leading to cyanamide **60**. Bromination by NBS then leads to haloamine **61** which is converted to cyanoimidate **62** after elimination of HBr (Fig. 1.23).

Other miscellaneous reactions have demonstrated the potential of cyanamides for the synthesis of nitrogen polycyclic compounds. For instance, the addition of dialkylcyanamides on vinyl triflates led to benzocycloheptapyridines [75], the hydrolysis of *N*-cyano-*N*-alkylaminoacetates afforded hydantoins [76], and the Holy reaction of cyanamides with arabinose yielded oxazolines [77].

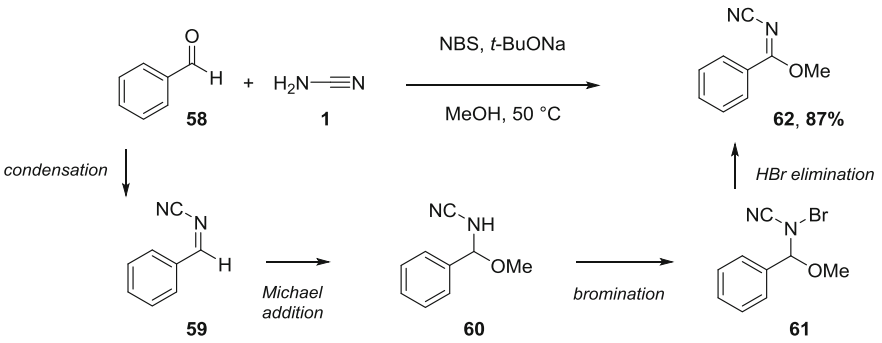

Fig. 1.23 Cyanoimidation of aldehyde

Furthermore, it has recently been demonstrated that cyanamides could undergo carbopalladation with *ortho*-hydroxy or *ortho*-aminoaryl-palladium(II) complexes, opening new perspectives in organometallic applications [78].

1.1.2.9 *Tert*-Butyl-*N*Cchlorocyanamide (NTBNCC), a Versatile Reagent for Chlorination and Oxidation Reactions

NTBNCC **63** is a powerful chlorinating agent because of the electron withdrawing nitrile group attached on the same nitrogen as the chloride atom. It is furthermore stable under ambient conditions, safe and easily recyclable. Its reactivity has been reviewed in depth by Kumar in 2007 [79]. It has for example been employed for the conversion of aldoximes into the corresponding hydroximoyl chlorides [80] (Fig. 1.24), which are important synthons for the synthesis of heterocyclic compounds via 1,3 dipolar additions.

NTBNCC has also been employed successfully for the synthesis of disulfides by coupling of thiols. A wide panel of aliphatic and aromatic thiols could be converted into the corresponding disulfides in less than 5 min at r.t. under treatment with the cyanamide reagent and NaBr (Fig. 1.25) [81].

1.1.2.10 Cyanamides as Radical Partners

Our group introduced the use of cyanamides as radical partners in 2007, for cascade synthesis of polycyclic quinazolinones. Bromo- and iodoaryl precursors

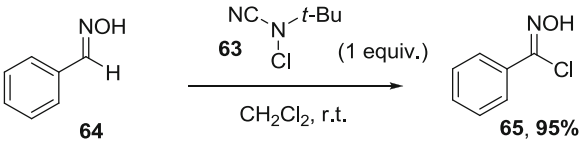

Fig. 1.24 Chlorination of aldoximes by NTBNCC

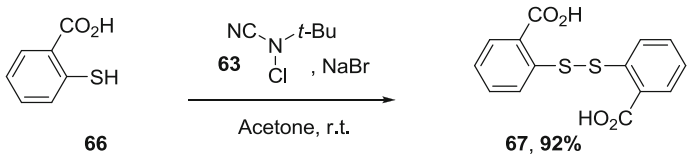

Fig. 1.25 Oxidation of thiols to disulfide by NTBNCC

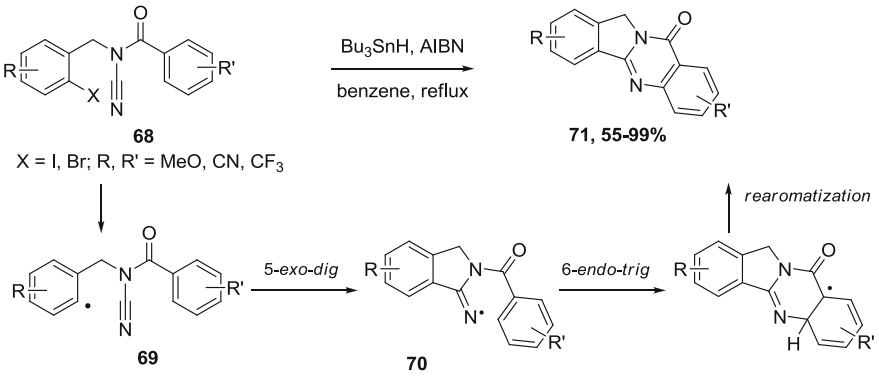

Fig. 1.26 Synthesis of polycyclic quinazolinone via radical cascade employing cyanamide

bearing an *N*-acylcyanamide moiety were treated with Bu_3SnH and AIBN, and underwent the desired radical cyclization sequences with high efficiency (Fig. 1.26) [82]. After halogen abstraction by tin radical, aryl radical **69** is formed and performs a 5-*exo-dig* cyclization on the cyanamide, generating amide-iminyl radical **70**. This N–centered radical is finally trapped by the benzoyl ring. DFT calculations and experimental data tend to prove that this homolytic aromatic substitution occurs directly via a 6-*endo* addition rather than via a 5-*exo* cyclization followed by a neophyl rearrangement [83]. Final rearomatization is presumably induced by AIBN. Alternatively, olefins could be used instead of aryl as the final radical trap, affording the corresponding tricyclic product.

A synthesis of natural alkaloid luotonin A **73** was developed based on this strategy. Previous conditions were unsuccessful for the cyclization of precursor **72**. However its irradiation in the presence of dioxygen and pyridine as an HI scavenger afforded the desired luotonin A under tin-free conditions in 53 % yield (Fig. 1.27).

Samarium diiodide conditions were also employed for the radical cascade cyclization of cyanamides and *N*-acylcyanamides precursors [84]. Aryl iodide **74** was thus treated with SmI_2 in the presence of HMPA and *t*-BuOH and led to polycyclic compound **75** after successive 6-*exo-dig* cyclization and homolytic aromatic substitution (Fig. 1.28).

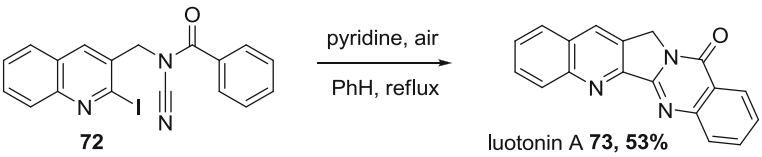

Fig. 1.27 Synthesis of luotonin A via radical cyclization of cyanamide

Fig. 1.28 Radical cyclization of cyanamide promoted by samarium diiodide

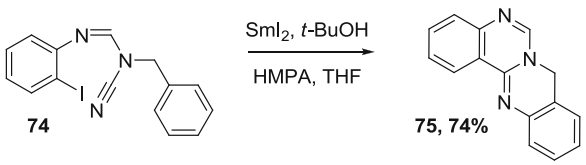

The generation of N-centered radicals at the amino group of monosubstituted cyanamides was recently reported, by treatment with (diacetoxyiodo)benzene and molecular iodine. The radical underwent a 1,6-hydrogen transfer followed by an ionic cyclization leading to spirobycyclic cyanamides [85].

To summarize, cyanamides are precursors of choice for the synthesis of *N*-heterocyclic compounds. Their high synthetic potential is still underexploited, especially in the field of radical chemistry. The study of their reactivity in both intermolecular and intramolecular strategies should lead to new straightforward synthesis of biologically relevant scaffolds.

One of the objectives of my Ph. D. will be to develop new radical cascades using *N*-acylcyanamides as partners. It has been demonstrated in the laboratory that the amide-iminyl radical formed by cyclization on this moiety, could easily perform homolytic aromatic substitutions at benzoyl rings [83]. This radical step offers interesting possibilities for the synthesis of polycyclic products containing fused aromatic ring but its exact mechanism remains unclear. We have wished to review in a second bibliographic part the state of the art of the propositions concerning the mechanism of homolytic aromatic substitutions.

1.2 Homolytic Aromatic Substitutions: State of the Art of the Mechanistic Proposals

Homolytic aromatic substitution refers to the intra- or intermolecular addition of a radical to an aromatic ring with subsequent rearomatization by loss of a leaving group (Fig. 1.29) [86–88]. This reaction is different from aromatic radical nucleophilic substitution ($S_{RN}1$) that features the attack of the radical by a nucleophile delivering an anionic σ-complex. Homolytic aromatic substitution proceeds via the σ-complex **76**, a delocalized cyclohexadienyl radical, whose formation is a reversible process. Radical **76** can rearomatize via two types of pathways. In the

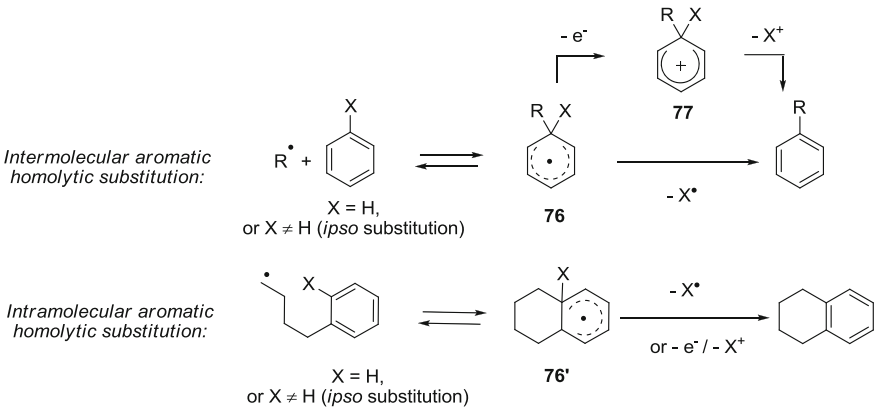

Fig. 1.29 General scheme of homolytic aromatic substitution

first alternative, a radical X• is extruded. Otherwise, an oxidation step can convert the radical σ-complex into cationic σ-complex **77** which subsequently looses a cation X^+. In most cases, the leaving group is hydrogen, and the mechanistic details of the rearomatization step are still under question. Others radical leaving groups have been used occasionally, leading to *ipso*-substitutions.

It should be noted that in the intramolecular cases, σ-complexes such as **76'** can be obtained by direct 6-*endo* cyclization or by 5-*exo* cyclization followed by a neophyl-type rearrangement. However, the focus of this account will be on the rearomatization step.

Homolytic aromatic substitutions have been widely used in radical synthesis. Their involvement in radical cascades offers interesting possibilities for the synthesis of polycyclic products containing fused aromatic rings. Numerous natural alkaloids such as luotonin [89], camphotecin [90], glaucine [91], cavicularin [92], ellipticin [93] have been synthesized using this strategy. A recent example is the synthesis of the tetracyclic core of (±) fortucine **78** by Zard (Fig. 1.30) [94, 95].

1.2.1 Hydrogen as Leaving Group

Despite the widespread utilization of homolytic aromatic substitutions in radical synthesis, their exact mechanisms remain often unclear. Particularly, the rearomatization step after the addition of the attacking radical and the formation of sigma complex **76**, has been an area of debate. The loss of hydrogen, which is not a good leaving group, is indeed required. Several mechanistic studies have been performed, leading to the conclusion that various pathways could be involved according to the reaction conditions [96]. We wish here to review the mechanistic proposals for different sets of conditions, based on a selection of examples including recent ones.

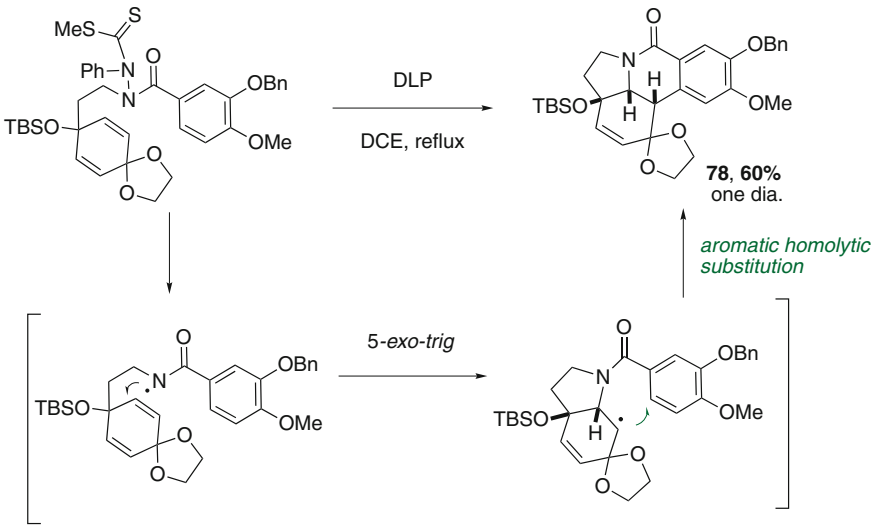

Fig. 1.30 Synthesis of the pentacyclic core of fortucine via tandem cyclization/homolytic aromatic substitution

1.2.1.1 Redox Conditions

In processes where the attacking radical is generated by a redox reaction between the substrate and a metal salt, this latter can play a dual role. It can indeed also oxidize the intermediate sigma radical, leading to rearomatization by further loss of a proton. This strategy has been reported mainly with iron, cerium, copper and manganese salts [97, 98]. Thus in the Miscini reaction, treatment of alkyl iodides with H_2O_2 and $FeSO_4 \bullet 7H_2O$ in the presence of protonated pyridines [99] or electron poor pyrroles [100] in DMSO allows efficient homolytic aromatic substitution. The authors proposed the mechanism depicted in Fig. 1.31 for the transformation. First, H_2O_2 is decomposed by Fe(II) salts, leading to Fe(III) species and hydroxyl radical (eq a). The hydroxyl radical reacts with DMSO, allowing after a fast β-scission, the generation of methyl radical (eq b). This latter can abstract iodide from the alkyliodide, generating an alkyl radical (eq c) that adds to the heteroaryl ring and forms a sigma complex (eq d). This complex is easily oxidized by Fe(III) salts and affords the aromatized product by loss of a proton, along with regeneration of Fe(II) species (eq e).

Recently, aryl boronic acids [101] and potassium alkyltrifluoroborates [102] have been treated with manganese triacetate, generating the corresponding radicals that were engaged in homolytic aromatic substitutions. In both cases, one equivalent of Mn(III) salt is required for the generation of the radical and a second one is needed for the final rearomatization (Fig. 1.32).

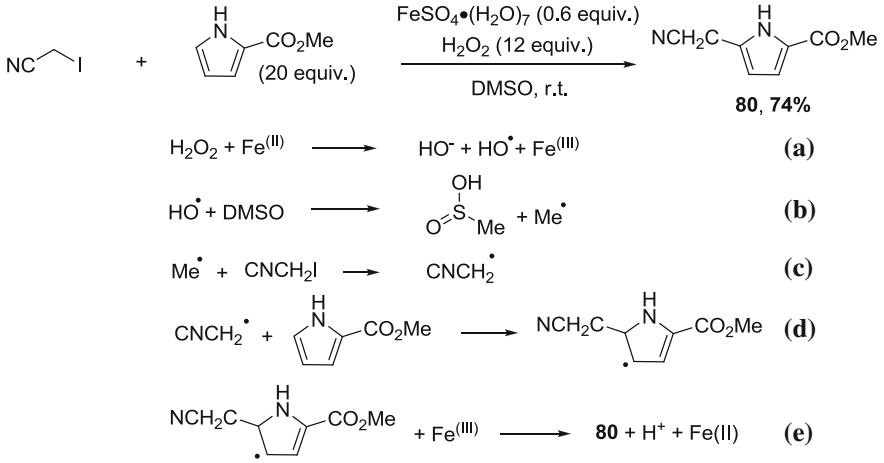

Fig. 1.31 Rearomatization by oxidation with Fe(III) salts

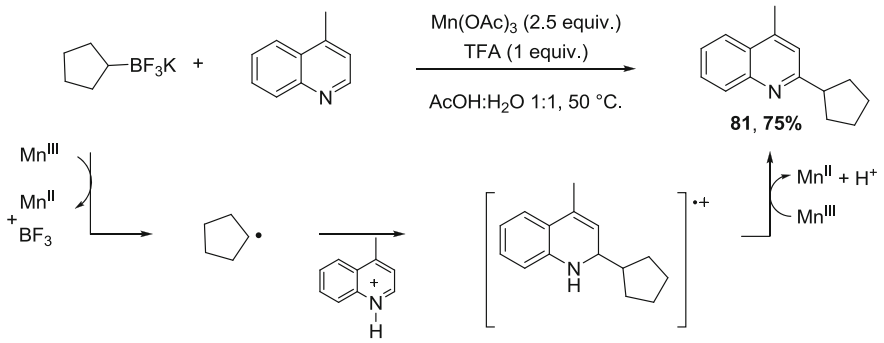

Fig. 1.32 Rearomatization by oxidation with Mn(III) salts

1.2.1.2 Basic Conditions

In the presence of stoichiometric amounts of potassium *tert*-butoxide and additives in catalytic quantities (DMEDA, 1,10-phenanthroline), coupling of aryliodides with unactivated arenes has been reported [103–105]. The reaction is thought to proceed via base-promoted homolytic aromatic substitution (Fig. 1.33) [106]. After initiation by homolysis of the Csp^2-I bond, the aryl radical **82** formed would add to the aryl present in large excess, generating cyclohexadienyl radical **83** (eq a). Deprotonation by the base would lead to radical anion **84** (eq b), which could transfer an electron to the aryliodide, thus completing the chain process (eq c). The role of additives could be to assist the propagation steps, either deprotonation or electron transfer. Intramolecular homolytic aromatic substitution has also been reported in those conditions very recently [107].

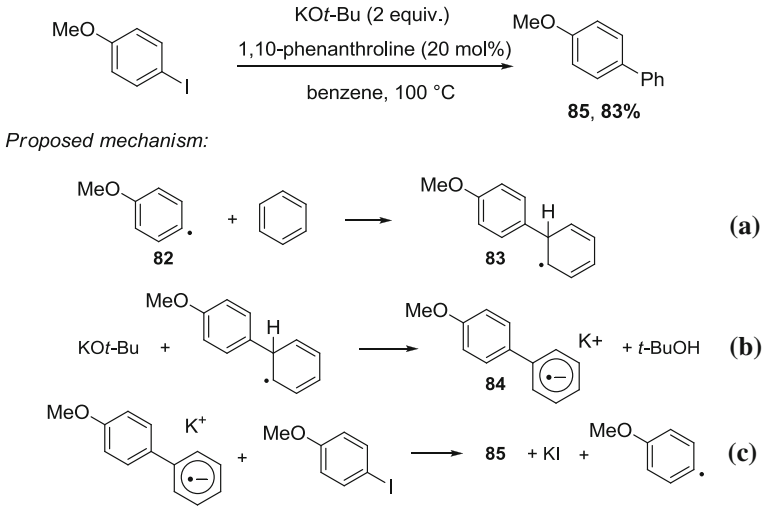

Fig. 1.33 Rearomatization by proton transfer and electron transfer in the presence of KO*t*-Bu

1.2.1.3 Treatment with Peroxides Under Tin-Free Conditions

The precursors commonly used in these conditions are xanthates. Carbon- and nitrogen-centered radicals have been generated through treatment of the corresponding xanthate precursors with dilauroyl peroxide (DLP). They have been engaged in homolytic aromatic substitutions with azoles, quinolones, furans or aryl rings [108–110]. The peroxide has to be introduced in stoichiometric amount since it both initiates the formation of radical **86** and allows the rearomatization of sigma complex **87** (Fig. 1.34). Presumably, **87** and DLP undergo a SET process leading to π-cation **88** that rearomatizes by loss of proton. The reduced peroxide generates a carboxylate anion and a carboxylate radical **89**, which after loss of carbon dioxide affords lauryl radical **91** thus completing the chain mechanism.

Alkyl iodides can also be used as precursors of radicals under tin-free conditions in the presence of peroxides. Thus the the *n*-perfluorobutylation of aromatic compounds by C_4F_9I has been carried out by refluxing the reagents in acetic acid in the presence of benzoyl peroxide [111]. The proposed mechanism is depicted in Fig. 1.35. Since the radical formed was highly electrophilic, it reacted favorably with electron-rich aryl rings, however the regioselectivity of the attack often remained low.

Intramolecular oxidative cyclizations of primary alkyl iodide in the presence of dicumyl peroxide (DCP) have also been reported [112].

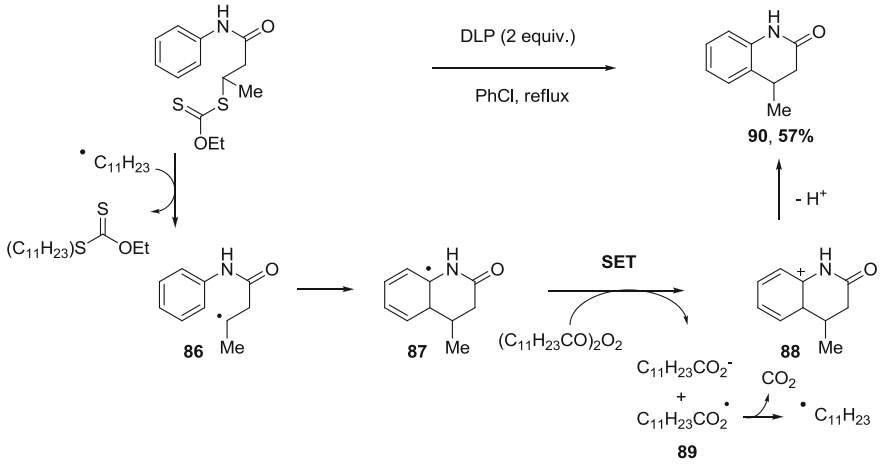

Fig. 1.34 Rearomatization by SET process with peroxide using xanthate precursors

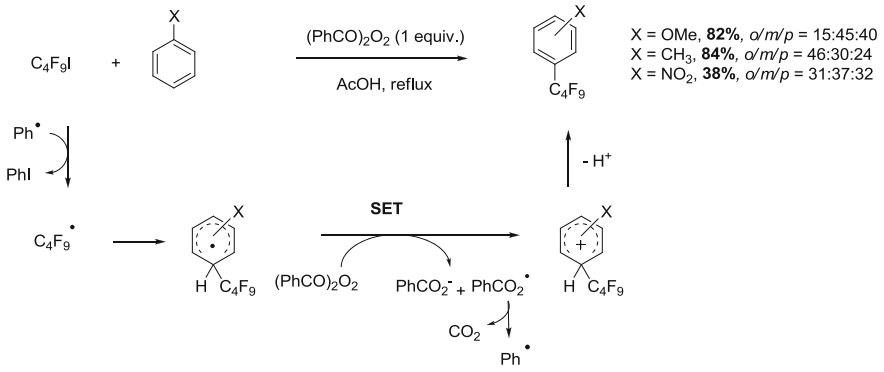

Fig. 1.35 Rearomatization by SET process with peroxide using iodide precursors

1.2.1.4 Use of Arenediazonium Salts as Precursors

When arenediazonium salts are used as precursors of aryl radicals in homolytic aromatic substitutions, they serve as both the radical source and the oxidizing agent [113, 114]. The initiation can be performed by reduction of the diazonium with catalytic amount of $TiCl_3$, leading to phenyl radical **91** [115]. After addition on aryl trap, the sigma complex **92** undergoes a SET process with starting arenediazonium, leading to aromatized product **93** after a loss of proton, and completing the radical chain mechanism (Fig. 1.36).

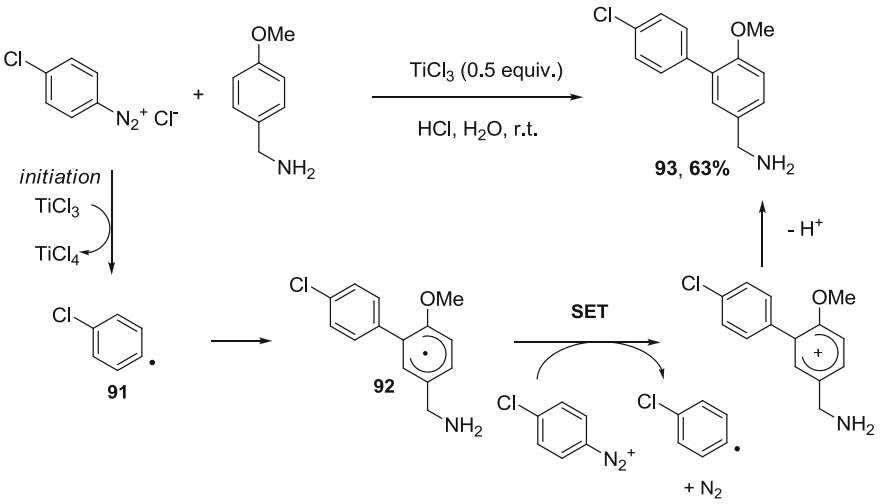

Fig. 1.36 Biaryl coupling with arenediazonium salts as radical sources and oxidizing agents

1.2.1.5 Dioxygen as the Chain Carrier

Oxygen has proven that, in collaboration with a mediator such as $(TMS)_3SiH$, it could trigger inter- and intramolecular homolytic aromatic substitutions at room temperature, without any other initiator and in short reaction times. Thus, aryl iodide **94** has been treated with $(TMS)_3SiH$ in benzene, in an open flask, and yielded after 3 h biaryl **95** in excellent yield (Fig. 1.37) [116]. The key point seems to be that intermediate cyclohexadienyl, formed by addition of aryl radical on benzene, reacts readily ($k \sim 10^9\ M^{-1}\ s^{-1}$) with triplet oxygen to produce biaryl product and hydroperoxyradical $HOO^{\bullet}$ that can propagate the chain.

1.2.1.6 Tin Mediated Homolytic Aromatic Substitutions

A long standing interrogation has been how fully aromatic products can be formed through formal oxidation of intermediate cyclohexadienyl radicals, under the reductive conditions induced by tin mediator. Beckwith, Bowman and Storey have undertaken a careful study of all the possible mechanisms involved in the presence of Bu_3SnH and AIBN to conclude on the most plausible pathway [117].

The first mechanistic proposal assessed was disproportionation of cyclohexadienyl radical **96** leading to aromatized product **97** and dihydro product **98** (Fig. 1.38). Since Crich has demonstrated that dihydro products are not oxidized rapidly in air [118], the maximum yields reachable would be 50 %. This pathway was consequently dismissed. The stability of dihydro products also excludes the direct H transfer from Bu_3SnH to sigma complex **96**.

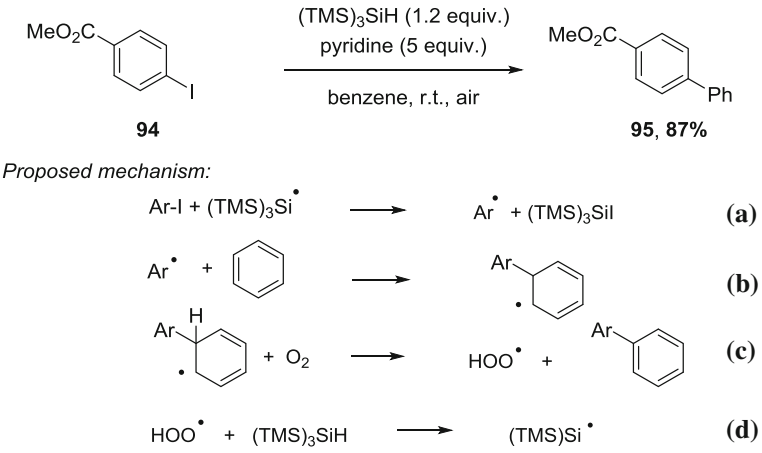

Fig. 1.37 Rearomatization through abstraction of hydrogen from cyclohexadienyl radical by oxygen

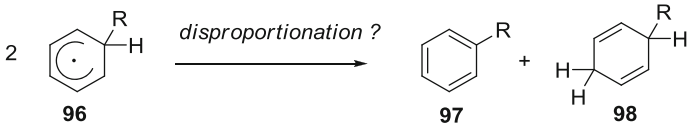

Fig. 1.38 First mechanistic proposal: disproportionation

The second mechanistic proposal suggested that Bu_3SnH could act as a hydride base and deprotonate sigma radical **96** to lead to radical anion **99**, Bu_3Sn^+ and H_2. Starting halide R-X would then undergo a SET reaction with radical anion **99** to generate a new incoming radical **100** and aromatized product **97**. The chain mechanism would be completed and only a catalytic amount of initiator would be needed (Fig. 1.39).

In order to study this hypothesis, Beckwith et al. prepared deuterated precursor **101** and studied its intramolecular homolytic aromatic substitution in the presence of stoichiometric amounts of Bu_3SnH and AIBN (Fig. 1.40). Careful analysis of gaseous products by Raman spectroscopy, NMR and mass spectrometry did not detect any release of HD, thus discarding the mechanistic proposal. Another argument is that most reported homolytic aromatic substitution reactions, except for a few exceptions,[1] [119] require a stoichiometric amount of initiator to reach full conversion.

[1] Only a catalytic amount of AIBN is needed for this homolytic aromatic substitution involving aryl iodides. This result suggests that the mechanism pictured in Fig. 1.39 could be at work in that case.

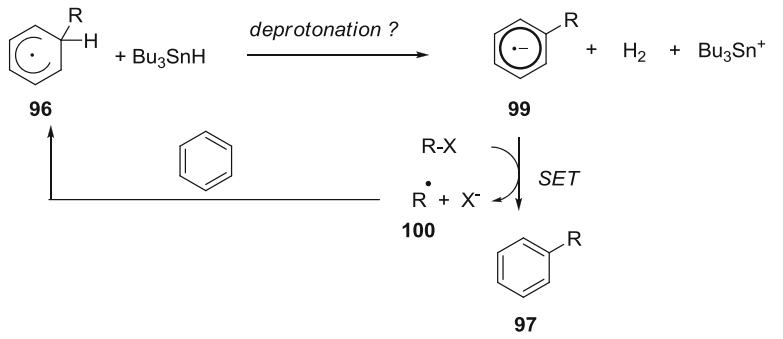

Fig. 1.39 Second mechanistic proposal: deprotonation by Bu_3SnH

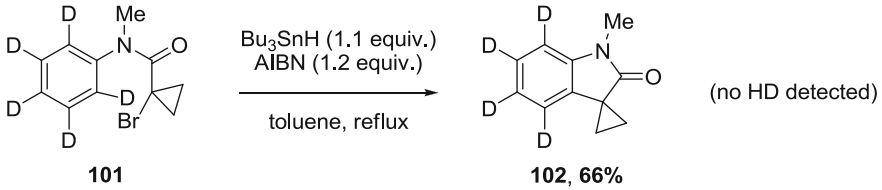

Fig. 1.40 Test reaction for the deprotonation hypothesis

Finally, it was put forward that the initiator could act as the H-abstractor in the rearomatization step. Two pathways could be involved and interplaying (Fig. 1.41). First, cleaved fragments from AIBN could abstract hydrogen from sigma complex **96** leading to aromatized product and isobutyronitrile (path a). Aside, uncleaved molecules of AIBN could accept an hydrogen from sigma complex **96**, leading to radical intermediate **103** that would be reduced by Bu_3SnH (path b). This second route is supported by the fact that azoalkanes have been reported to abstract H from benzydryl radical, affording the corresponding hydrazines [120].

Evidence to support path (a) was brought by careful analysis of the products from radical cyclization of precursor **101** (Fig. 1.40). Indeed, GC–MS and deuterium NMR disclosed the formation of Me_2CDCN in 23 % yield. However, path (a) seems to be a minor pathway since it was established that for every equivalent of AIBN introduced, only 0.25 equivalent of nitrogen gas was evolved, so 0.75 equivalent of AIBN were not cleaved. Efforts to find evidence for path (b) via the isolation of hydrazine **104** were hampered by the instability of this compound. Nonetheless, using analogue AIBMe **105** as the initiator, treatment of precursor **106** with Bu_3SnH afforded 30 % of homolytic aromatic substitution product **107** and 17 % (NMR yield) of hydrazine **108** [121], indicating that path (b) was valid (Fig. 1.42).

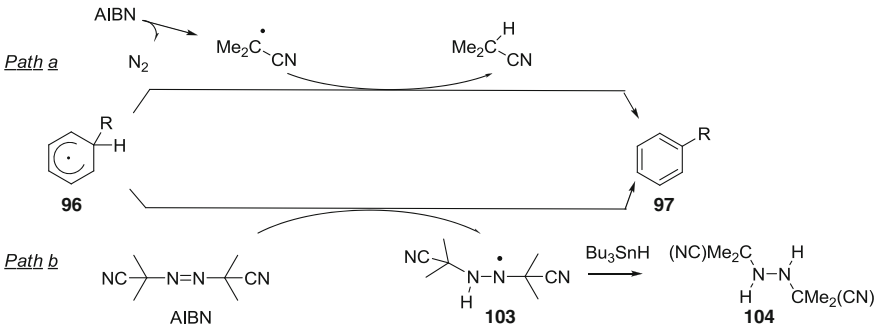

Fig. 1.41 Third mechanistic proposal: H-abstraction by initiator

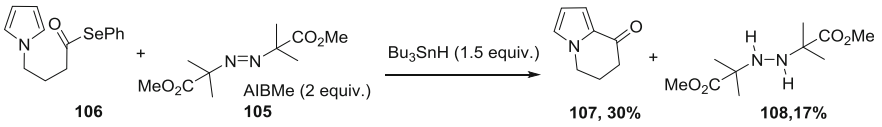

Fig. 1.42 Test reaction for H abstraction by diazo initiator

In the cases where AIBN is replaced with BEt_3 as initiator, it has been suggested that in a similar fashion, rearomatization is obtained by H-abstraction performed by ethyl radicals [122].

To conclude, the mechanism of aromatization in homolytic aromatic substitutions is largely dependent on the reagents used for the reaction. For tin mediated processes, H-abstraction seems to be the main pathway, with a specific involvement of the initiator. One can be sure that several mechanisms of aromatization are still to be discovered.

1.2.2 Other Radical Leaving Groups: Ipso Substitutions

In less widespread cases, the homolytic aromatic substitution occurs on a carbon bearing a substituent, leading to the extrusion of a carbon or heteroatom centered radical by β-scission (Fig. 1.29, X $\neq$ H). Several criteria determine the efficiency of the reaction, especially in intermolecular cases [123]. With electroneutral radicals *ipso* attack can occur selectively only if the σ-complex formed possess a greater stability than the complex derived from addition at an

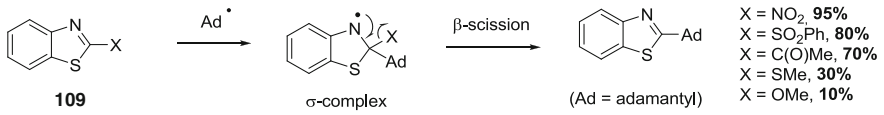

Fig. 1.43 Efficiency of intermolecular *ipso* substitution according to the leaving group

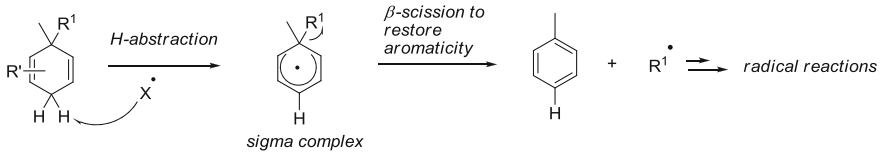

Fig. 1.44 Principle of the use of functionalized cyclohexadiene as radical mediators

unsubstituted position. *Ipso* attacks are much more favored when polar effects can intervene and stabilize the transition state of the addition. For example, the yield of homolytic aromatic substitution of nucleophilic adamantyl radical to benzothiaol derivatives **109** increased strongly with electron withdrawing substituents [124] (Fig. 1.43).

If this area of research remains rather unexplored, on the other hand, the evolution of functionalized cyclohexadienyl radicals obtained by other radical reactions than homolytic aromatic substitution has been studied in depth (Fig. 1.44) [125]. The synthetic potential of the aromatization of these sigma complexes has been beautifully exploited for the tin free generation of silyl-, nitrogen- and carbon–centered radicals. Besides, in depth mechanistic studies undertaken on these systems have been very useful for the understanding of homolytic aromatic substitution mechanistic details and appreciation of the kinetics of β-scissions.

1.2.2.1 Tosyl, Phenylsulfanyl and Phosphinates Leaving Groups

$ArSO_2^{\bullet}$, $ROSO_2^{\bullet}$, $R_2P(O)^{\bullet}$ and $PhS^{\bullet}$ have been used as good radical leaving groups, enabling a precise control of the regioselectivity of homolytic aromatic substitutions. Cyclizations at 2-C of indoles [126], 7-C of indolines, 2-C of imidazoles [127] and 2-C of benzimidazole [128] and arenes [129–132] have been reported by *ipso*-substitution of these groups (Fig. 1.45). For instance, treatment of benzimidazole precursor **110** with Bu_3SnH and AIBN afforded the desired homolytic

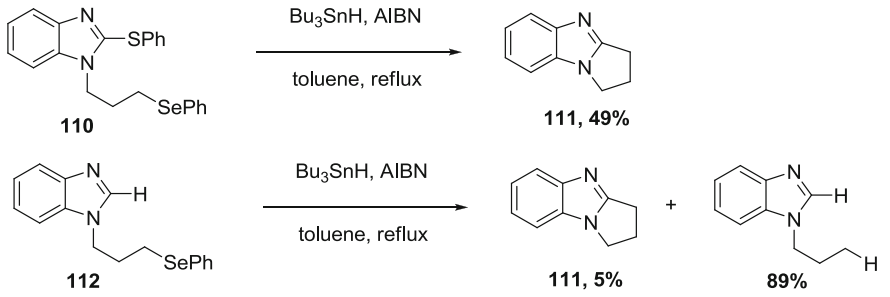

Fig. 1.45 Influence of the radical leaving group for homolytic aromatic substitution at 2-C of benzimidazole

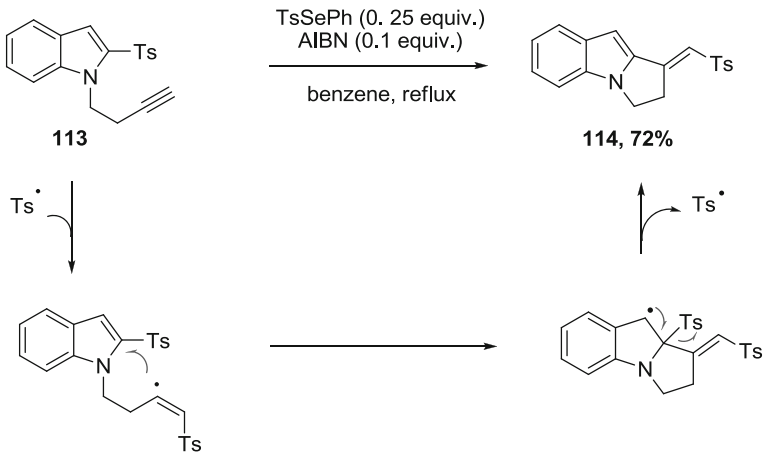

Fig. 1.46 Chain mechanism triggered by tosyl radical extrusion

aromatic substitution with 49 % yield [120]. Strikingly, under the same conditions, the analogue precursor without phenylsulfanyl substituent **112** led to only 5 % of cyclized product, demonstrating that PhS substituent was essential to facilitate homolytic substitution at 2-C of benzimidazole. On a mechanistic point of view, the electrophilic $Ts^{\bullet}$ or $PhS^{\bullet}$ leaving groups may propagate the radical chain by abstracting hydrogen from nucleophilic Bu_3SnH.

Taking advantage of the extrusion of tosyl radical, a catalytic method has been developed, where only a catalytic amount of TsSePh and AIBN allows cyclization

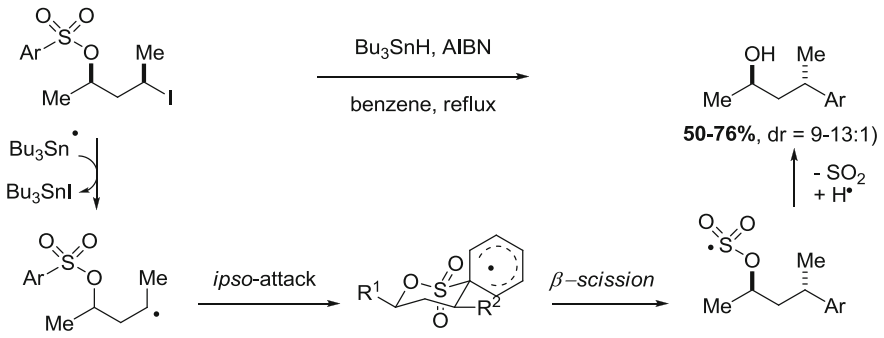

Fig. 1.47 Stereoselective radical aryl migration from sulfur to carbon

onto sulfone-substituted indoles bearing a suitably placed alkyne (Fig. 1.46). Indeed, after initiation and addition of $Ts^{\bullet}$ on the alkyne moiety, the vinyl radical formed performs a homolytic aromatic substitution at 2-C of the indole. Aromatization regenerates a $Ts^{\bullet}$, which allows the propagation of the radical chain.

Studer has shown that the intramolecular *ipso* substitution of sulfur from arenesulfonate was an efficient method for the stereoselective $C(sp^2)$–$C(sp^3)$ bond formation [133]. Starting from alkyl iodides, the corresponding arylated products were obtained with diastereoselectivities of up to 13:1 (Fig. 1.47). The reaction was thought to proceed via intramolecular *ipso* attack at the aryl group. *β*-Fragmentation followed by SO_2 extrusion would lead to the corresponding arylated products with free hydroxyl function.

1.2.2.2 Methoxy and Alkyl Leaving Groups

Radical *ipso* substitutions of alkoxy groups are rare [134–136] and the extruded alkoxy radical have never been trapped. An original synthesis of aza-coumarines has been reported by double *ipso*-substitution. Treatment of bromide precursor **115** with $(TMS)_3SiH$ and AIBN generates aryl radical **116** that undergoes tandem 1,5 *ipso*-substitution forming carbonyloxyradical **117** and 1,6 *ipso*-substitution with concomitant extrusion of methoxy radical (Fig. 1.48). The irreversible extrusion of methoxy radical seems to drives the reaction to completion. In the absence of the 2-methoxy substituent, the analogue precursor does not cyclize efficiently.

Homolytic aromatic substitutions leading to the extrusion of alkyl radicals are scarce in the literature [137, 138]. Along with the preparation of luotonin A via radical cyclization of *N*-acylcyanamide precursors, our group studied cascades

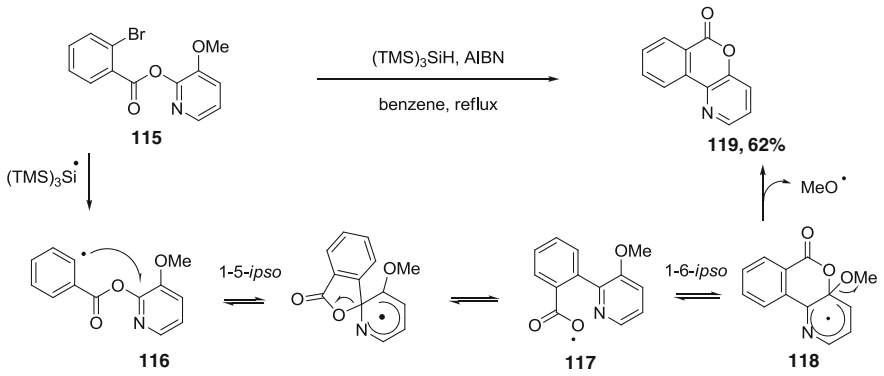

Fig. 1.48 Synthesis of aza-coumarine via tandem homolytic aromatic substitutions

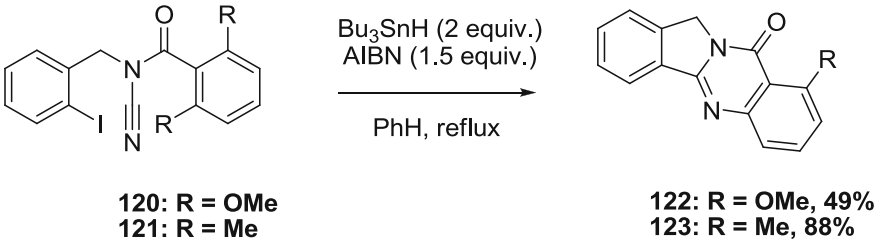

Fig.1. 49 Extrusion of methyl and methoxy radicals in radical cyclizations of *ortho* substituted *N*-acylcyanamides

starting with the addition of an aryl radical to *N*-acylcyanamide and ending with the extrusion of methyl, methoxy radicals [139]. Precursor **120** bearing two *ortho*-methoxy substituents and precursor **121** bearing two *ortho*-methyl substituents were treated with Bu_3SnH and AIBN and led to monosubstituted aromatic compounds with good yields (Fig. 1.49).

In order to prove the extrusion of methoxy and methyl radicals, attempts to trap them with activated olefins were undertaken. The methoxy radical could never be captured. However, the presence of one equivalent of benzylidene malonitrile during the cyclization of **121** allowed the isolation of product **124,** coming from the addition of $Me^{\bullet}$ to the alkene and subsequent reduction (Fig. 1.50).

DFT calculations have been performed to gain insights into the mechanism of these extrusions. A possible transition state for the methyl radical departure was proposed (Fig. 1.51), in which the cost of breaking the C–C bond (14.6 kcal mol^{-1}) is minimal compared to common values.

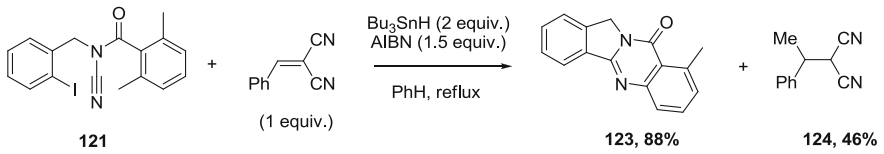

Fig. 1.50 Intermolecular trapping of methyl radical by benzylidene malonitrile

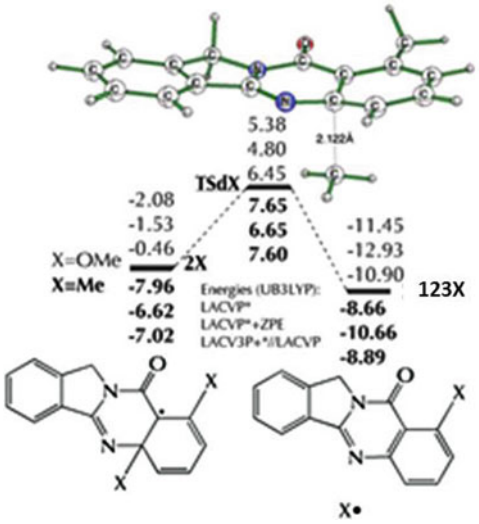

Fig. 1.51 Modelisation of $Me^{\bullet}$ and $MeO^{\bullet}$ extrusion. Geometries are optimized at UB3LYP/BS1 level at 298 K

1.2.2.3 Fluorine as a Leaving Group

Homolytic aromatic substitution leading to the extrusion of a fluorine atom has been reported by our group in 2008 [126]. Indeed treatment of precursor **125** bearing two *ortho*-fluorine substituents afforded monosubstituted product **126a** in 73 % yield along with regioisomer **126b** in 15 % yield (Fig. 1.52). DFT calculations have been performed to confirm the mechanism of the cascade. The result showed that **126a** was probably formed via path a involving a 6-*endo* cyclization, while the formation of **126b** likely occurred via path b involving a 5-*exo* cyclization followed by a rearrangement. The homolytic rupture of very strong C–F bond must be harnessed

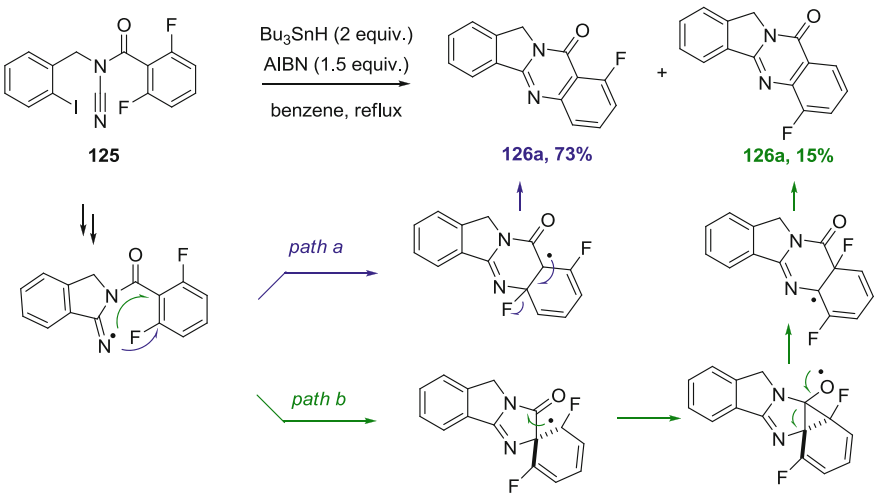

Fig. 1.52 Extrusion of fluorine radical in the radical cyclization of *ortho*-substituted cyanamide

by the restoration of aromaticity, along with hyperconjugation effects due to the presence of an α-radical. One other example of homolytic aromatic substitution at fluorinated aryl ring has been reported since [140].

Thus, homolytic aromatic substitutions possess a high synthetic potential that has been exploited in numerous radical transformations. The use of intramolecular reactions largely eliminates the problems of poor regioselectivity and allows their embedment in complex cascade processes. *Ipso* substitutions of carbon or heteroatom substituents can be very efficient. Interestingly, in a few examples, the extruded radical has been exploited in subsequent radical reactions.

References

1. Nekrasov, D. D. (2004). *Russian Journal of Organic Chemistry, 40*, 1387–1402.
2. Larraufie, M.-H., Maestri, G., Malacria, M., Ollivier, C., Fensterbank, L., & Lacôte, E. (2012). *Synthesis, 44*, 1279–1292. Published as a review in *Synthesis*.
3. Kamo, T., Endo, M., Sato, M., Kasahara, R., Yamaya, H., Hiradate, S., et al. (2008). *Phytochemistry, 69*, 1166–1172.
4. Loomis, C. W., & Brien, J. F. (1983). *Canadian journal of physiology and pharmacology, 61*, 1025–1034.
5. Niederhofer, H., Staffen, W., & Mair, A. (2003). *Alcohol and Alcoholism, 38*, 50–53.
6. Duvernay, F., Chiavassa, T., Borget, F., & Aycard, J. P. (2004). *Journal of the American Chemical Society, 126*, 7772–7773.
7. Duvernay, F., Chiavassa, T., Borget, F., & Aycard, J. P. (2005). *Journal of Physical Chemistry, 109*, 603–608.

8. Anastasi, C., Crowe, M. A., Powner, M. W., & Sutherland, J. D. (2006). *Angewandte Chemie International Edition, 45*, 6176–6179.
9. Ronn, R., Gossas, T., Sabnis, Y. A., Daoud, H., Akerblom, E., Danielson, U. H., et al. (2007). *Bioorganic and Medicinal Chemistry, 15*, 4057–4068.
10. Falgueyret, J. P., Oballa, R. M., Okamoto, O., Wesolowski, G., Aubin, Y., Rydzewski, R. M., et al. (2001). *Journal of Medicinal Chemistry, 44*, 94–104.
11. Barrett, D. G., Deaton, D. N., Hassell, A. M., McFadyen, R. B., Miller, A. B., Miller, L. R., et al. (2005). *Bioorganic and Medicinal Chemistry Letters, 15*, 3039–3043.
12. Demko, Z. P., & Sharpless, K. B. (2001). *Organic Letters, 3*, 4091–4094.
13. Rogister, F., Laeckmann, D., Plasman, P. O., Van Eylen, F., Ghyoot, M., Maggetto, C., et al. (2001). *European Journal of Medicinal Chemistry, 36*, 597–614.
14. Domling, A., Herdtweck, E., & Heck, S. (2006). *Tetrahedron Letters, 47*, 1745–1747.
15. Xiao, Z. L., Yang, M. G., Tebben, A. J., Galella, M. A., & Weinstein, D. S. (2010). *Tetrahedron Letters, 51*, 5843–5844.
16. Cockerill, A. F., Deacon, v., Harrison, R. G., Osborne, D. J., Prime, D. M., Ross, W. J., Todd, A., Verge, J. P. (1976). *Synthesis-Stuttgart* **1976**, 591–593.
17. Lindsey, C. C., O'Boyle, B. M., Mercede, S. J., & Pettus, T. R. R. (2004). *Tetrahedron Letters, 45*, 867–868.
18. Servais, A., Azzouz, M., Lopes, D., Courillon, C., & Malacria, M. (2007). *Angewandte Chemie International Edition, 46*, 576–579.
19. Kumar, V., Kaushik, M. P., Mazumdar, A. (2008). *European Journal of Organic Chemistry*, 1910–1916.
20. McCall, W. S., Grillo, T. A., & Comins, D. L. (2008). *Journal of Organic Chemistry, 73*, 9744–9751.
21. McCall, W. S., & Comins, D. L. (2009). *Organic Letters, 11*, 2940–2942.
22. Kim, J. J., Kweon, D. H., Cho, S. D., Kim, H. K., Jung, E. Y., Lee, S. G., et al. (2005). *Tetrahedron, 61*, 5889–5894.
23. Wu, Y. Q., Limburg, D. C., Wilkinson, D. E., & Hamilton, G. S. (2000). *Organic Letters, 2*, 795–797.
24. Kamijo, S., Jin, T., & Yamamoto, Y. (2002). *Angewandte Chemie International Edition, 41*, 1780–1782.
25. Kamijo, S., Jin, T. N., & Yamamoto, Y. (2001). *Journal of the American Chemical Society, 123*, 9453–9454.
26. Kamijo, S., & Yamamoto, Y. (2002). *Journal of the American Chemical Society, 124*, 11940–11945.
27. Wong F. F., Chen, C. Y., Yeh, M. Y. (2006). *Synlett*, 559–562.
28. Chen, C. Y., Wong, F. F., Huang, J. J., Lin, S. K., & Yeh, M. Y. (2008). *Tetrahedron Letters, 49*, 6505–6507.
29. Brand, H., Mayer, P., Schulz, A., Soller, T., & Villinger, A. (2008). *Chemistry - An Asian Journal, 3*, 1050–1058.
30. Ghosh, H., Yella, R., Ali, A. R., Sahoo, S. K., & Patel, B. K. (2009). *Tetrahedron Letters, 50*, 2407–2410.
31. Nath, J., Patel, B. K., Jamir, L., Sinha, U. B., & Satyanarayana, K. (2009). *Green Chemistry, 11*, 1503–1506.
32. Yella, R., Khatun, N., Rout, S. K., & Patel, B. K. (2011). *Organic and Biomolecular Chemistry, 9*, 3235–3245.
33. Yella, R., Kavala, V., & Patel, B. K. (2011). *Synthetic Communications, 41*, 792–805.
34. Ramana, T., Saha, P., Das, M., & Punniyamurthy, T. (2010). *Organic Letters, 12*, 84–87.
35. Fukurnoto, K., Oya, T., Itazaki, M., & Nakazawa, H. (2009). *Journal of the American Chemical Society, 131*, 38–39.
36. Oballa, R. M., Truchon, J. F., Bayly, C. I., Chauret, N., Day, S., Crane, S., et al. (2007). *Bioorganic and Medicinal Chemistry Letters, 17*, 998–1002.

37. Chen, C. Y., Lin, H. C., Huang, Y. Y., Chen, K. L., Huang, J. J., Yeh, M. Y., et al. (2010). *Tetrahedron, 66*, 1892–1897.
38. Shestakov, A. S., Gusakova, N. V., Shikhaliev, K. S., & Zagoruiko, A. V. (2006). *Russian Journal of General Chemistry, 76*, 1647–1652.
39. Snider, B. B., Ahn, Y., & O'Hare, S. M. (2001). *Organic Letters, 3*, 4217–4220.
40. Prashad, M., Har, D., Chen, L. J., Kim, H. Y., Repic, O., & Blacklock, T. J. (2002). *Journal of Organic Chemistry, 67*, 6612–6617.
41. Kohn, U., Klopfleisch, M., Gorls, H., & Anders, E. (2006). *Tetrahedron-Asymmetry, 17*, 811–818.
42. Snider, B. B., & O'Hare, S. M. (2001). *Tetrahedron Letters, 42*, 2455–2458.
43. Shikhaliev, K. S., Shestakov, A. S., Medvedeva, S. M., & Gusakova, N. V. (2008). *Russian Chemical Bulletin, 57*, 170–176.
44. Giles, R. L., Sullivan, J. D., Steiner, A. M., & Looper, R. E. (2009). *Angewandte Chemie International Edition, 48*, 3116–3120.
45. Shestakov, A. S., Gusakova, N. V., Shikhaliev, K. S., & Timoshkina, A. G. (2007). *Russian Journal of Organic Chemistry, 43*, 1825–1829.
46. Giles, R. L., Nkansah, R. A., & Looper, R. E. (2010). *Journal of Organic Chemistry, 75*, 261–264.
47. Dutta, S., Higginson, C. J., Ho, B. T., Rynearson, K. D., Dibrov, S. M., & Hermann, T. (2010). *Organic Letters, 12*, 360–363.
48. Castilla, J., Marin, I., Matheu, M. I., Diaz, Y., & Castillon, S. (2010). *Journal of Organic Chemistry, 75*, 514–517.
49. Snider, B. B., & Duvall, J. R. (2005). *Organic Letters, 7*, 4519–4522.
50. Pratap, R., Farahanullah, N., Raghunandan, R., Maulik, P. R., & Ram, V. J. (2007). *Tetrahedron Lett, 48*, 4939–4942.
51. Farhanullah, N., Agarwal, A., Goel, V. J., & Ram, J. (2003). *The Journal of organic chemistry, 68*, 2983–2985.
52. Pawlas, J., & Begtrup, M. (2002). *Organic Letters, 4*, 2687–2690.
53. Kurzer, F. (1949). *Journal of the Chemical Society*, 3033–3038.
54. Chen, X., Bai, S. D., Wang, L., & Liu, D. S. (2005). *Heterocycles, 65*, 1425–1430.
55. Herrera, A., Martinez-Alvarez, R., Ramiro, P., Chioua, M., Chioua, R. (2004). *Synthesis-Stuttgart,* 503–505.
56. Foster, B. J., Harding, B. J., Leylandjones, B., & Hoth, D. (1986). *Cancer Treatment Reviews, 13*, 197–217.
57. Dornan, P., Rowley, C. N., Priem, J., Barry, S. T., Burchell, T. J., Woo, T. K., Richeson, D. S. (2008). *Chemical Communication,* 3645–3647.
58. Heller, B., Sundermann, B., Buschmann, H., Drexler, H. J., You, J. S., Holzgrabe, U., et al. (2002). *Journal of Organic Chemistry, 67*, 4414–4422.
59. Bonaga, L. V. R., Zhang, H. C., Maryanoff, B. E. (2004). *Chemical Communication*, 2394–2395.
60. Maryanoff, B. E., Zhang, H. C. (2007). *Arkivoc*, 7–35.
61. Varela, J. A., & Saa, C. (2003). *Chemical Reviews, 103*, 3787–3801.
62. Dazinger, G., Torres-Rodrigues, M., Kirchner, K., Calhorda, M. J., & Costa, P. J. (2006). *Journal of Organometallic Chemistry, 691*, 4434–4445.
63. Garcia, P., Evanno, Y., George, P., Sevrin, M., Ricci, G., Malacria, M., et al. (2011). *Organic Letters, 13*, 2030–2033.
64. Geny, A., Agenet, N., Iannazzo, L., Malacria, M., Aubert, C., & Gandon, V. (2009). *Angewandte Chemie International Edition, 48*, 1810–1813.
65. Demko, Z. P., & Sharpless, K. B. (2001). *Journal of Organic Chemistry, 66*, 7945–7950.
66. Habibi, D., Nasrollahzadeh, M., Faraji, A. R., & Bayat, Y. (2010). *Tetrahedron, 66*, 3866–3870.

67. Nasrollahzadeh, M., Habibi, D., Shahkarami, Z., & Bayat, Y. (2009). *Tetrahedron, 65*, 10715–10719.
68. Demko, Z. P., & Sharpless, K. B. (2001). *Organic Letters, 3*, 4091–4094.
69. Bhattacharyya, P., Slawin, A. M. Z., & Woollin, J. D. (2002). *Chemistry—A European Journal, 8*, 2705–2711.
70. Hua, G. X., Zhang, Q. Z., Li, Y., Slawin, A. M. Z., & Woollins, J. D. (2009). *Tetrahedron, 65*, 6074–6082.
71. Hulme, R., Zamora, O. D. P., Mota, E. J., Pasten, M. A., Contreras-Rojas, R., Miranda, R., et al. (2008). *Tetrahedron, 64*, 3372–3380.
72. Khatab, T. K., El-Bayouki, K. A. M., & Basyouni, W. M. (2011). *Tetrahedron Letters, 52*, 1448–1451.
73. Aberle, N. S., Lessene, G., & Watson, K. G. (2006). *Organic Letters, 8*, 419–421.
74. Yin, P., Ma, W. B., Chen, Y., Huang, W. C., Deng, Y., & He, L. (2009). *Organic Letters, 11*, 5482–5485.
75. Herrera, A., Martinez-Alvarez, R., Chioua, R., Benabdelouahab, F., & Chioua, M. (2004). *Tetrahedron, 60*, 5475–5479.
76. Kumar, V., Kaushik, M. P., Mazumdar, A. (2008). *European Journal of Organic Chemistry,* 1910–1916.
77. Jenkinson, S. F., Jones, N. A., Moussa, A., Stewart, A. J., Heinz, T., & Fleet, G. W. J. (2007). *Tetrahedron Letters, 48*, 4441–4444.
78. Vicente, J., Abad, J. A., Lopez-Saez, M. J., Jones, P. G., & Bautista, D. (2010). *Chemistry—A European Journal, 16*, 661–676.
79. Kumar, V., & Kaushik, M. P. (2007). *Synlett, 19*, 2937–2951.
80. Kumar, V., & Kaushik, M. P. (2006). *Tetrahedron Letters, 47*, 1457–1460.
81. Kumar, V., & Kaushik, M. P. (2008). *Bulletin of the Chemical Society of Japan, 81*, 160–162.
82. Servais, A., Azzouz, M., Lopes, D., Courillon, C., & Malacria, M. (2007). *Angewandte Chemie International Edition, 46*, 576–579.
83. Beaume, A., Courillon, C., Derat, E., & Malacria, M. (2008). *Chemistry—A European Journal, 14*, 1238–1252.
84. Hu, Z., Li, S. D., Hong, P. Z. (2010). *Arkivoc*, 171–177.
85. Martin, A., Perez-Martin, I., & Suarez, E. (2009). *Tetrahedron, 65*, 6147–6155.
86. Studer, A., Brossart M. (2001). In Renaud, P., Sibi, M. P. (Ed.), *Radicals in organic synthesis* (1 st Edn.), (pp. 62–80, Vol. 2) Wiley-VCH, Weinheim, **2001**, .
87. Bowman, W. R., & Storey, J. M. D. (2007). *Chemical Society Reviews, 36*, 1803–1822.
88. Fossey, J., Lefort, D., & Sorba, J. (1995). *Free radicals in organic chemistry* (pp. 167–180). Chichester: Wiley.
89. Bowman, W. R., Cloonan, O. M., Fletcher, A. J., & Stein, T. (2005). *Organic and Biomolecular Chemistry, 3*, 1460–1467.
90. Curran, D. P., Ko, S.-B., & Josien, H. (1995). *Angewandte Chemie International Edition, 34*, 2683–2684.
91. Comins, D. L., Hong, H., & Jianhua, G. (1994). *Tetrahedron Letters, 35*, 5331–5334.
92. Harrowven, D. C., Woodcock, T., & Howes, P. D. (2005). *Angewandte Chemie International Edition, 44*, 3899–3901.
93. Pederson, J. M., Bowman, W. R., Elsegood, M. R. J., Flechter, A. J., & Lovell, P. J. (2005). *Journal of Organic Chemistry, 70*, 10615–10618.
94. Biechy, A., Hachisu, S., Quiclet-Sire, B., Ricard, L., & Zard, S. Z. (2008). *Angewandte Chemie International Edition, 47*, 1436–1438.
95. Biechy, A., Hachisu, S., Quiclet-Sire, B., Ricard, L., & Zard, S. Z. (2009). *Tetrahedron, 65*, 6730–6738.
96. Beckwith, A. L. J., Bowry, V. W., Bowman, W. R., Mann, E., Parr, J., & Storey, J. M. D. (2004). *Angewandte Chemie International Edition, 43*, 95–98.

97. Snider, B., & Kwon, T. (1990). *Journal of Organic Chemistry, 55*, 4786–4788.
98. Citterio, A., Sebastiano, R., & Marion, A. (1991). *Journal of Organic Chemistry, 56*, 5328–5335.
99. Minisci, F., Vismara, E., & Fontana, F. (1989). *Heterocycles, 28*, 489–519.
100. Baciocchi, E., Muraglia, E., & Sleiter, G. (1992). *Journal of Organic Chemistry, 57*, 6817–6822.
101. Dickschat, A., & Studer, A. (2010). *Organic Letters, 12*, 3972–3974.
102. Molander, G., Colombel, V., & Braz, V. A. (2011). *Organic Letters, 13*, 1852–1855.
103. Sun, C.-L., Li, H., Yu, D.-G., Yu, M., Zhou, X., Lu, X.-Y., et al. (2010). *Nature Chemical, 2*, 1044–1049.
104. Shirakawa, E., Itoh, K.-I., Higashino, T., & Hayashi, T. (2010). *Journal of the American Chemical Society, 132*, 15537–15539.
105. Liu, W., Cao, H., Zhang, H., Zhang, H., Chung, K. H., He, C., et al. (2010). *Journal of the American Chemical Society, 132*, 16737–16740.
106. Studer, A., & Curran, D. P. (2011). *Angewandte Chemie International Edition, 50*, 5018–5022.
107. Sustac Roman, D., Takahashi, Y., & Charrette, A. (2011). *Organic Letters, 13*, 3242–3245.
108. Gagosz, F., Moutrille, C., & Zard, S. Z. (2002). *Organic Letters, 4*, 2707–2709.
109. Binot, G., & Zard, S. Z. (2005). *Tetrahedron Letters, 46*, 7503–7506.
110. Florez-Lopez, E., Gomez-Perez, L. B., & Miranda, L. D. (2010). *Tetrahedron Letters, 51*, 6000–6002.
111. Bravo, A., Bjorsvik, H.-R., Fontana, F., Liguori, L., Mele, A., & Minisci, F. (1997). *Journal of Organic Chemistry, 62*, 7128–7136.
112. Menes-Arzate, M., Martinez, R., Cruz-Almanza, R., Muchowski, J. M., Osornio, Y. M., & Miranda, L. D. (2004). *Journal of Organic Chemistry, 69*, 4001–4004.
113. Wetzel, A., Ehrhardt, V., & Heinrinch, M. R. (2008). *Angewandte Chemie International Edition, 47*, 9130–9133.
114. Pratsch, G., Unfried, J. F., Einsiedel, J., Plomer, M., Hübner, H., Gmeiner, P., et al. (2011). *Organic and Biomolecular Chemistry, 9*, 3746–3752.
115. Wetzel, A., Pratsch, G., Kolb, R., & Heinrich, M. (2010). *Chemistry—A European Journal, 16*, 2547–2556.
116. Curran, D. P., & Keller, A. I. (2006). *Journal of the American Chemical Society, 128*, 13706–13707.
117. Beckwith, A. L. J., Bowry, V. W., Bowman, W. R., Mann, E., Parr, J., & Storey, J. M. D. (2004). *Angewandte Chemie International Edition, 43*, 95–98.
118. Crich, D., & Patel, M. (2006). *Tetrahedron, 62*, 7824–7837.
119. Harrowen, D. C., Sutton, B. J., & Coulton, S. (2002). *Tetrahedron, 58*, 3387–3400.
120. Engel, P. S., & Wu, W.-X. (1989). *Journal of the American Chemical Society, 111*, 1830–1835.
121. Allin, S. M., Barton, W. R. S., Bowman, W. R., & McInally, T. (2001). *Tetrahedron Letters, 42*, 7887–7890.
122. Bowman, W. R., Elsegood, M. R. J., Stein, T., & Weaver, G. W. (2007). *Organic and Biomolecular Chemistry, 5*, 103–113.
123. Traynham, J. (1979). *Chemical Reviews, 79*, 323–330.
124. Tiecco, M. (1980). *Accounts of Chemical Research, 13*, 51–57.
125. Walton, J. C., & Studer, A. (2005). *Accounts of Chemical Research, 38*, 794–802.
126. Caddick, S., Aboutayab, K., Jenkins, K., & West, R. I. (1996). Soc. *Journal of the Chemical Society, Perkin Transactions 1, 1*, 675–682.
127. Aldabbagh, F., & Bowman, W. R. (1999). *Tetrahedron, 55*, 4109–4122.
128. Allin, S. M., Bowman, W. R., Karim, R., & Rahman, S. S. (2006). *Tetrahedron, 62*, 4306–4316.
129. Clive, D. L. J., & Kang, S. (2001). *Journal of Organic Chemistry, 66*, 6083–6091.
130. Schulte, B., Fröhlich, R., & Studer, A. (2008). *Tetrahedron, 64*, 11852–11859.
131. Clark, A. J., Fullaway, D. R., Murphy, N. P., & Parekh, H. (2010). *Synlett, 4*, 610–614.

132. da Mata, M. L., Motherwell, W. B., & Ujjainwalla, F. (1997). *Tetrahedron Letters, 38*, 137–140.
133. Studer, A., Brossart, M. (1998). *Chemical Communication*, 2127–2128.
134. Zhang, W., & Pugh, G. (2001). *Tetrahedron Letters, 42*, 5613–5615.
135. Rosa, A. M., Lobo, A. M., Branco, P. S., & Prabhakar, S. (1997). *Tetrahedron, 53*, 285–298.
136. Glover, S. A., Golding, S. L., Goosen, A., & McCleland, C. W. (1981). *Journal of the Chemical Society, Perkin Transactions 1, 1*, 842–844.
137. Du, W., & Curran, D. P. (2003). *Synlett, 9*, 1299–1302.
138. Harrowven, D. C., Nunn, M. I. T., Newman, N. A., & Fenwick, D. R. (2001). *Tetrahedron Letters, 42*, 961–964.
139. Beaume, A., Courillon, C., Derat, E., & Malacria, M. (2008). *Chemistry—A European Journal, 14*, 1238–1252.
140. Laot, Y., Petit, L., & Zard, S. Z. (2010). *Organic Letters, 12*, 3426–3429.

Chapter 2
Results: Developments of New Radical Cascades with *N*-Acylcyanamides

2.1 Objectives of the Project

Since radical cascades using cyanamides have been reported only starting from aryl radicals, we have wished to broaden the scope of these cascades. Our objectives were to test the reactivity of alkyl, vinyl and aminyl radicals in this process. Indeed, the use of alkyl and vinyl radical should provide us with a straightforward access to natural and biologically active quinazolinones; while the use of aminyl radicals should afford the first radical synthesis of guanidines (Fig. 2.1).

2.2 Addition of Alkyl Radicals

We first examined the possibility to engage alkyl radicals in cascades with *N*-acylcyanamides. We wished to explore the scope of the reactivity, by varying the substitution of the alkyl radical and the length of the arm that will determine the size of the first ring formed.

2.2.1 Synthetic Targets

Four synthetic targets were defined (Fig. 2.2), with two of them being natural quinazolinones.

Deoxyvasicinone is a natural alkaloid which was isolated in 1957 from the leaves of *Adhatoda vasica* [1]. This compound possesses anti-depressive, anti-bacterial and anti-inflammatory properties [2]. A wide variety of methodologies have been reported for its synthesis via pallado-catalyzed tandem carbonylation/cyclization [3], transition metal complex-catalyzed reductive *N*-heterocyclization [4] or tandem intramolecular Staudinger/aza-Wittig reactions [5]. In 2007,

M.-H. Larraufie, *Development of New Radical Cascades and Multi-Component Reactions*, Springer Theses, DOI: 10.1007/978-3-319-01324-4_2,

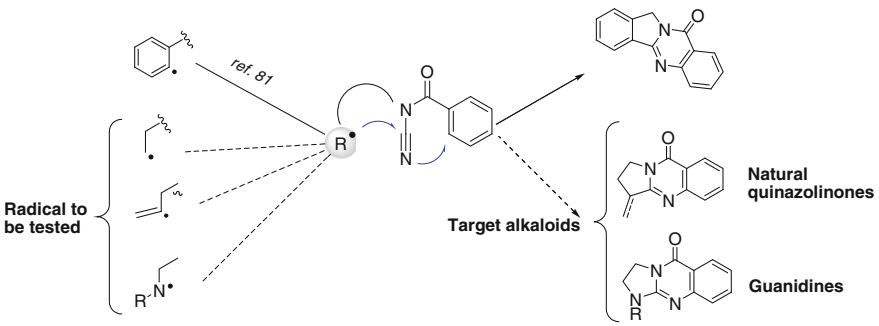

Fig. 2.1 Objectives of the new radical cascades with cyanamides

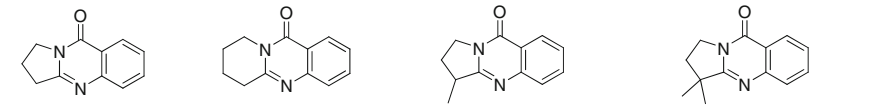

Fig. 2.2 Synthetic targets

Fig. 2.3 Bowman's radical synthesis of deoxyvasicinone

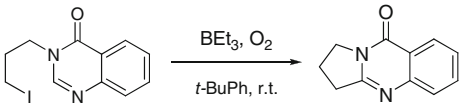

Bowman has reported the first radical synthesis of deoxyvasicinone [6]. Treatment of alkyl iodide **131** with BEt_3 and O_2 allowed the generation of the corresponding alkyl radical and its oxidative cyclization on 3*H*-quinazolin-4-one core (Fig. 2.3).

Mackinazolinone **128** is a natural quinazolinone fused with a piperidine ring. This compound was isolated in 1965 in New Guinea from the leaves of *Mackinlaya subulata* [7] and has demonstrated a large spectra of pharmaceutical activities [8, 9]. Numerous synthetic methodologies similar to those developed for deoxyvasicinone have been applied to the building of mackinazolinone, including Bowman's radical cyclization [5, 6].

α-Methyldeoxyvasicinone **129** is an unnatural analogue of deoxyvasicinone presenting bronchodilator activities [10]. Six syntheses of this compound have been reported, none of them presenting a radical step [11]. α,α'-Dimethyldeoxyvasicinone **130** has never been described.

2.2.2 Synthesis of Cascade Precursors

2.2.2.1 *N*-Acylcyanamide Precursors for Deoxyvasicinone and Mackinazolinone

The synthesis of the desired cyclization precursors was devised according to the retrosynthetic scheme in Fig. 2.4. *N*-Acylcyanamides **132** could be obtained by cyanation of corresponding amides **133** which would derive from acylation of corresponding amines **134**.

Our first idea was to synthesize bromo precursors for the cyclization (Fig. 2.4, X = Br). However, when commercial 3-bromopropylamine hydrobromide **135** was treated with triethylamine and benzoyl chloride, only 28 % of the desired amide **136** was obtained (Fig. 2.5). The major product **137** resulted from an intramolecular O-alkylation side-reaction.

We have consequently substituted the bromine with a phenylselenium group which is known as a good radical leaving group but a poor nucleofuge (Fig. 2.4, X = SePh). 3-Bromopropylamine hydrobromide **135** and 4-bromobutylamine hydrobromide **138** (obtained by treatment of commercial 4-aminobutan-1-ol with HBr as a 48 % aqueous solution) [12] were converted to their seleno derivatives by reaction with diphenyldiselenide and sodium borohydride [13]. Benzoylation of the amino groups were then efficiently performed, affording seleno amides **133a** and **133b** in good yields. Cyanation of the amides under the reaction conditions described for the aryl substrates [14] (3 equivalents of cyanogen bromide and 1 equivalent of sodium hydride) led to disappointing yields of the corresponding *N*-acylcyanamides (20 %). However, switching from sodium hydride to potassium hydride proved very beneficial for the reaction, probably thanks to the formation of a more nucleophilic potassium salt intermediate. With optimum cyanation

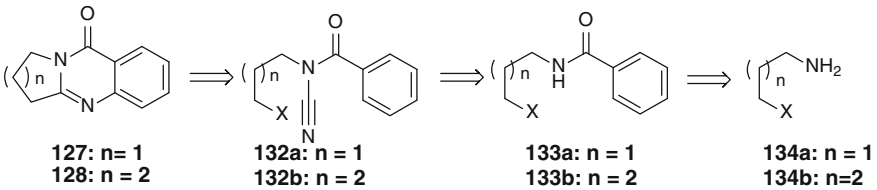

Fig. 2.4 Retrosynthetic scheme

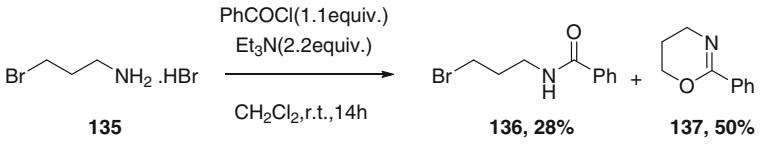

Fig. 2.5 Attempt to perform direct benzoylation of bromoamine

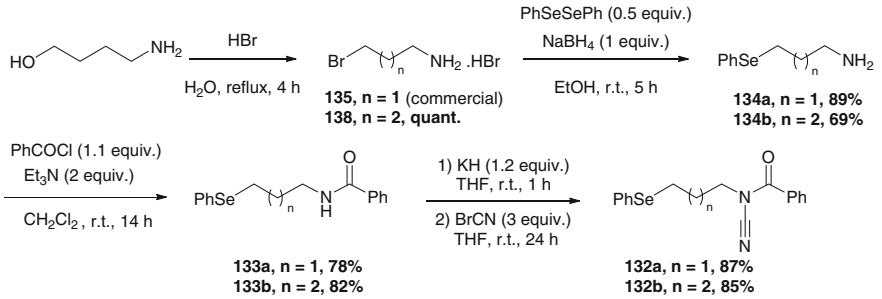

Fig. 2.6 Synthesis of unsubstituted cyclization precursors

conditions in hands (3 equivalents of cyanogen bromide and 1.2 equivalents of potassium hydride), we could obtain the desired *N*-acylcyanamides **132a** and **132b** in more than 85 % yields (Fig. 2.6).

2.2.2.2 *N*-Acylcyanamide Precursor for α-methyldeoxyvasicinone

N-Acylcyanamide precursor **145** for α-methyldeoxyvasicinone was synthesized in six steps from commercially available 1,3-dichlorobutane **139** (Fig. 2.7). Selective monoiodination by Finkelstein reaction afforded 3-chloro-1-iodobutane **140**, which was reacted with potassium phthalimide to provide compound **141**. Conversion of the secondary chloride to phenyl selenium group was achieved by treatment with in situ generated sodium phenylselenoate. Deprotection of the phthalimide group with hydrazine afforded selenoamine **143**. The amine was first

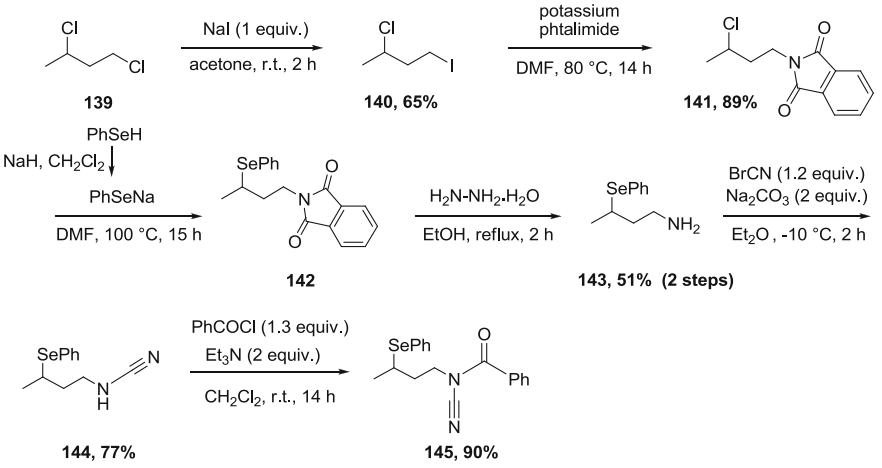

Fig. 2.7 Synthesis of α-methyldeoxyvasicinone precursor

converted into the corresponding cyanamide **144** according to Harrison's methodology, [15] then acylated to obtain the desired *N*-acylcyanamide **145** in satisfying yield.

2.2.2.3 *N*-Acylcyanamide Precursor for α,α'-methyldeoxyvasicinone

The *N*-acylcyanamide precursor for α,α'-methyldeoxyvasicinone was the most challenging to prepare. Its synthesis was carried out in six steps starting from commercially available 3,3-dimethylallyl bromide **146**. Heating **146** with potassium phthalimide at 80 °C led to the desired phthalimide derivative **147**. Hydrobromination of the double bond was then performed by treatment with HBr solution in acetic acid (Fig. 2.8).

Several conditions were tested to displace the tertiary bromide of **148** with phenylselenium. The only successful strategy was the indium mediated procedure developed by Jang et al. [16]. The key feature of this methodology is the reduction of the alkylbromide by indium metal to generate the corresponding alkyl radical **150**. This latter can then perform a homolytic substitution at the selenium atom of diphenyldiselenide to afford selenoester **152** (Fig. 2.9).

Finally, treatment of phthalimide **152** with hydrazine afforded the free amine **153**. For purification issues, the amine was first acylated then cyanated leading in two steps to the desired *N*-acylcyanamide **155** (Fig. 2.10).

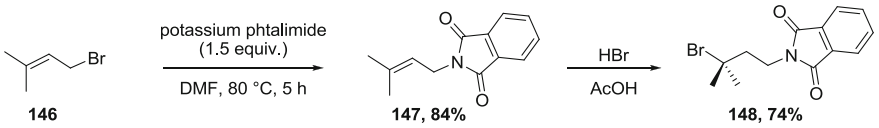

Fig. 2.8 Synthesis of intermediate bromophthalimide 148

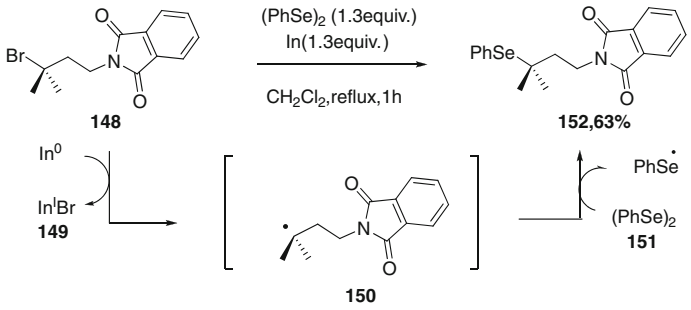

Fig. 2.9 Conversion of tertiary bromide to alkyl phenyl selenide

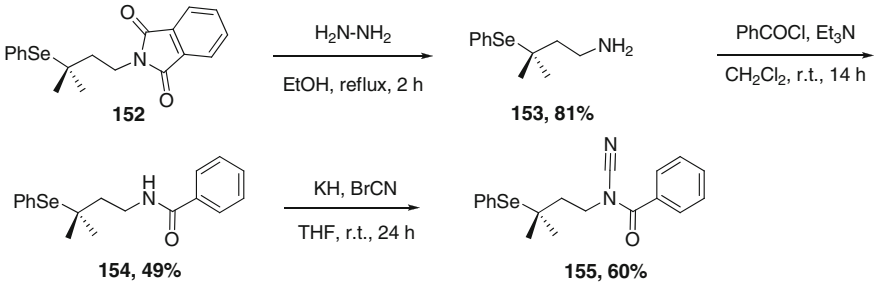

Fig. 2.10 Synthesis of *N*-acylcyanamide precursor for α,α'-methyldeoxyvasicinone

2.2.3 Radical Cyclization of the N-acylcyanamide Precursors

The four *N*-acylcyanamide precursors were then reacted under the reaction conditions that were previously developed in the laboratory for the cyclization of alkyl phenylselenoates [17]. Cyclization proceeded smoothly in all cases, under slow addition of Bu_3SnH (1.2 equivalents) and AIBN (1.5 equivalents) in refluxing benzene (0.017 M). The major tin derivative formed during the reaction is $Bu_3SnSePh$, which is stable on silica gel and non-polar. The purification of quinazolinones was facilitated by their high polarity. A first washing of the column chromatography with pentane eliminated the tin residues, and subsequent elution with polar solvents allowed the isolation of pure products (Fig. 2.11).

Under those conditions, deoxyvasicinone **127** was isolated in 65 % yield. We attempted to replace the tin mediator with $(TMS)_3SiH$, however the yield dropped to only 20 %. Chatgilialoglu's reagent is yet known to react with alkyl phenylselenates readily [18], but proved not adapted to our cascade. Cyclization of precursor **132b** allowed the isolation of mackinazolinone **128** in 51 % yield along with the product of direct reduction. This result could be explained by the lower kinetic constant of 6-*exo-dig* cyclization compared to 5-*exo-dig*. However, the successful isolation of mackinazolinone was the first evidence that the cascade could begin not only with 5-*exo-dig* cyclization but also 6-*exo-dig* processes.

α-Methyldeoxyvasicinone **129** and α,α'-dimethyldeoxyvasicinone **130** were obtained in good 76 and 87 % yields respectively. The trend observed with these few examples seems to show that the more nucleophile is the first radical formed, the more efficient is the cyclization. Thus, it appears that cyclization on the cyanamide moiety could be favored with nucleophilic radicals, which evidences that *N*-acylcyanamides are electrophilic acceptors.

To conclude, this project allowed us to demonstrate that alkyl radicals could take part easily in radical cascades with *N*-acylcyanamides [19]. The size of the first ring formed and the substitution of the radical could be varied, and three biologically active products have been synthesized along with non-reported analogue α,α'-dimethyldeoxyvasicinone, whose activity should be tested. A new range of quinazolinone type products should be now available by using our

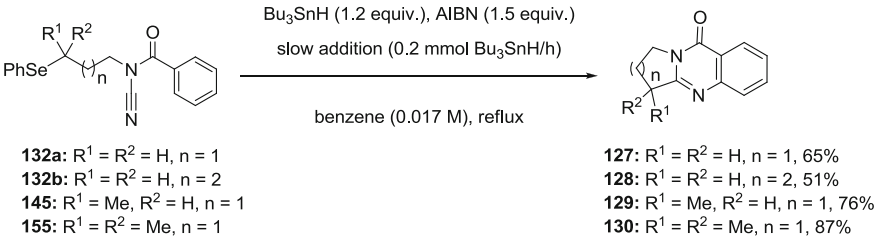

132a: $R^1 = R^2 = H$, n = 1
132b: $R^1 = R^2 = H$, n = 2
145: $R^1 = Me$, $R^2 = H$, n = 1
155: $R^1 = R^2 = Me$, n = 1

127: $R^1 = R^2 = H$, n = 1, 65%
128: $R^1 = R^2 = H$, n = 2, 51%
129: $R^1 = Me$, $R^2 = H$, n = 1, 76%
130: $R^1 = R^2 = Me$, n = 1, 87%

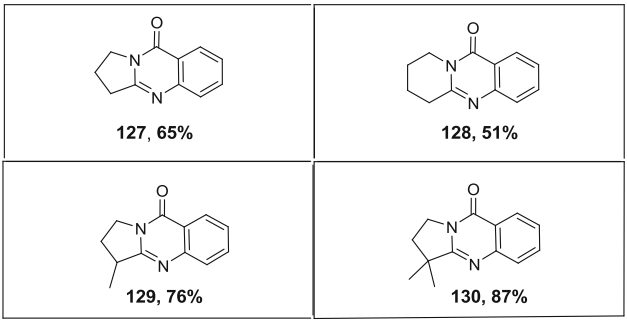

Fig. 2.11 Radical cyclization of *N*-acylcyanamides

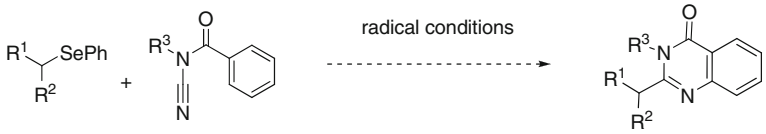

Fig. 2.12 Envisaged intermolecular version of the cascade

methodology. A perspective to broaden again the scope of products would be to develop an intermolecular version as depicted in Fig. 2.12. This strategy should furthermore simplify the synthesis of the precursors, which can be fastidious for intramolecular reactions.

2.3 Addition of Vinyl Radicals to *N*-acylcyanamides

Stimulated by the good reactivity of alkyl radicals with cyanamides, we next turned our attention towards the behavior of vinyl radicals. Our first idea was to synthesize the core of natural alkaloid isaindigotone **156** [20, 21], which possesses interesting antioxidant properties. We proposed that isaindigotone could be constructed via a Heck reaction on key intermediate **157**, obtained by cascade cyclization of *N*-acylcyanamide precursor **158** (Fig. 2.13).

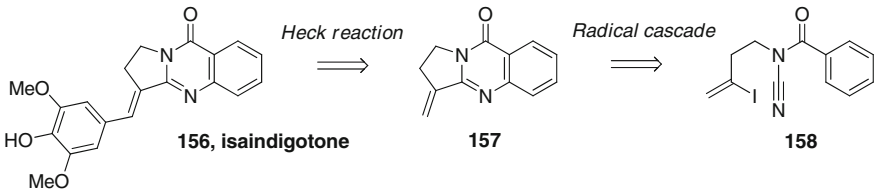

Fig. 2.13 Retrosynthetic plan for the synthesis of isaindigotone

2.3.1 Radical Cyclization of Vinyliodide Precursor Followed by an Unexpected Reduction

2.3.1.1 Synthesis of the Precursor

3-Iodo-but-3-enylamine **161** was first synthesized from 3-butyn-1-ol **159** according to the methodology described by Sugiyama et al. [22]. Regioselective hydroiodination was achieved using sodium iodide, trimethylsilylchloride and water. Subsequent tosylation of the hydroxyl group afforded tosylate **160** which was substituted with sodium azide. Staudinger reduction of the azide function finally yielded the desired amine **161** (Fig. 2.14).

Owing to the volatility of amine **161**, we first planned to install the *N*-acyl cyanamide function by benzoylation followed by cyanation (Fig. 2.15). However, when amide **162** was treated with potassium hydride and cyanogen bromide, we observed the addition of BrCN to the double bond, delivering amide **163**. Indeed, examples of addition of BrCN on furans [23], alkenes [24] and alkynes have been previously reported in the literature [25].

We wondered whether inverting the order of the sequence, hence performing first the cyanation on the primary amine then the acylation, could be beneficial for the outcome of the reaction. Indeed, we hoped that the higher nucleophilicity of the amine compared to the amide would allow it to react faster with BrCN than the

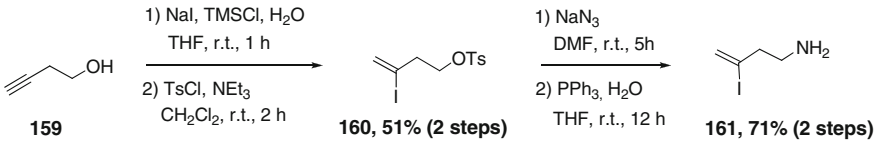

Fig. 2.14 Synthesis of 3-iodo-but-3-enylamine

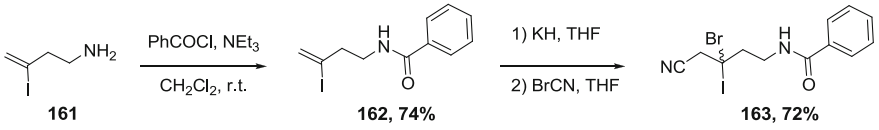

Fig. 2.15 First attempt to install the *N*-acylcyanamide function

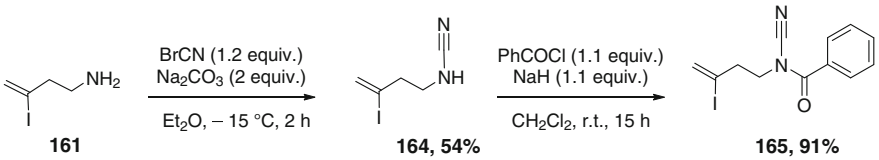

Fig. 2.16 Inversion of the sequence to obtain the *N*-acylcyanamide

alkene. This idea proved valuable, since the inversion of the sequence allowed us to obtain the desired *N*-acylcyanamide **165**. Intermediate cyanamide **164** could be isolated; however it proved quite unstable under air and had to be engaged in the next step immediately (Fig. 2.16).

2.3.1.2 Radical Cyclization

With the desired precursor **165** in hand, we submitted it to the radical cyclization conditions developed for aryl iodides [14]. Under treatment with Bu_3SnH (2 equivalents) and AIBN (1.5 equivalents) slowly added in refluxing benzene, we obtained the desired cyclization, but to our great surprise, in the major product **129** the exocyclic double bond had been fully reduced during the cascade. In the minor product **167**, the double bond had not been reduced but had migrated to an endocyclic position (Fig. 2.17).

After this surprising result, the influence of different parameters on the outcome of the reaction was tested (Fig. 2.18). Running the reaction in boiling toluene led to **129** (59 %) and **167** (15 %), with the apparition of side-product of direct reduction **166** (18 %) (entry 2). The use of *tert*-butanol gave exclusively product **129** in the highest isolated yield (77 %) (entry 3). Following this solvent screening, the amount of initiator was gradually lowered (entries 4-6). The NMR yield of **129** slightly decreased from 79 to 72 %, 64 and 57 % when the loading of AIBN was 1.5 equiv., 1 equiv., 0.5 equiv. and 0.25 equiv. respectively. This shows that the formation of **129** does not require a stoichiometric amount of AIBN and likely steams from a radical chain mechanism. However, the propagation of the chain may be of weak efficiency since below 1 equiv. of AIBN some byproducts as well as starting material were recovered.

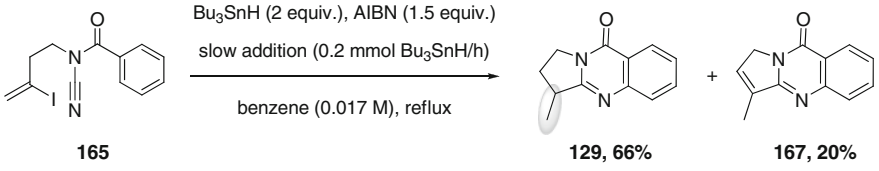

Fig. 2.17 Radical cyclization of vinyliodide precursor

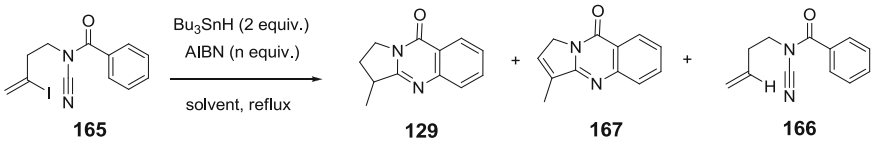

Entry	Solvent	n	Yield **129** [%]	Yield **167** [%]	Yield **166** [%]	SM [%]
1	benzene	1.5	**66**	20	<5%	<5%
2	toluene	1.5	**59**[a]	15	18	<5%
3	*t*-BuOH	1.5	**77 (79)**[a]	12	<5%	<5%
4	*t*-BuOH	1	**72**[a]	13	<5%	<5%
5	*t*-BuOH	0.5	**64**[a]	11	13%	<5%
6	*t*-BuOH	0.25	**57**[a]	10	8%	6%

[a] NMR yields (butadiene sulfone used as internal standard)

Fig. 2.18 Influence of solvent and AIBN loading

2.3.2 Mechanistic Studies

2.3.2.1 Origin of Both Novel Hydrogens

In order to understand the formation of product **129**, we wished first to investigate the origin of both hydrogens causing the reduction of the *exo* double bond. For that purpose, we primary treated vinyl iodide precursor **165** with tributyltin deuteride (Fig. 2.19). Quinazolinone **169** with a deuterium atom on the five-membered ring was isolated, demonstrating that the hydrogen at this position came from the tin mediator.

In a second time, we prepared vinyliodide precursor **170** bearing a *penta*-deuterated benzoyl ring, in a similar fashion to precursor **165** using d_5-benzoyl chloride in the last step (see SI). We then made react deuterated precursor **170** under the usual radical cyclization conditions. We obtained quinazolinone **171** bearing a deuterium on the methyl group. That result taught us that the hydrogen at that position had migrated from the benzoyl ring (Fig. 2.20).

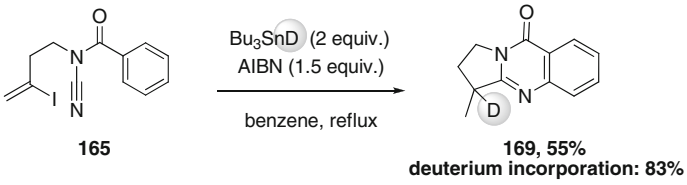

Fig. 2.19 Origin of the internal hydrogen

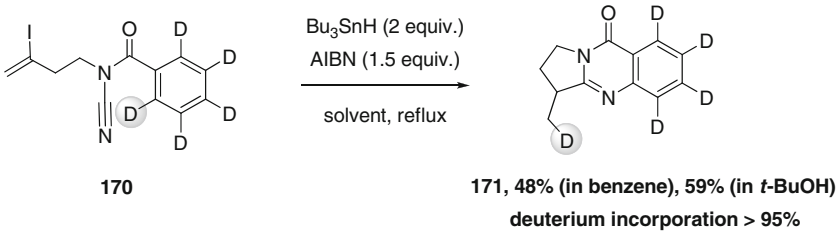

Fig. 2.20 Origin of the external hydrogen

2.3.2.2 Discrimination Between an Intra- and an Intermolecular Mechanism

In order to discriminate between an intra- and an intermolecular migration of hydrogen, we imagined to perform a double tagging experiment, with 0.5 equivalent of a precursor bearing a *penta*-deuterated benzoyl ring and 0.5 equivalent of a precursor bearing hydrogens on its benzoyl ring. To facilitate the separation on silica gel chromatography of the cyclized products, we chose to use precursor **172** bearing a polar *para*-methoxy substituent as a test precursor. Vinyliodide **172** was synthesized as reported in Fig. 2.21, and cyclized under the usual conditions, leading to reduced quinazolinone **173** in 72 % yield.

We then mixed 0.5 equivalent of precursor **170** and 0.5 equivalent of precursor **172** and analyzed the outcome of the cyclization. Four products were isolated (**174** was isolated in mixture with **173** and **175** in mixture with **171**), demonstrating that the hydrogen migration was intermolecular. Indeed, if the mechanism had been intramolecular, **172** would have led to all-hydrogen product **173** only and **170** to all-deuterium product **171** only. The formation of the four products attests that the two precursors have exchanged hydrogen (or deuterium) between one another (Fig. 2.22).

Since hydrogen seemed to migrate in an intermolecular fashion, we attempted to trap it before its addition on the external position of quinazolinone. For that purpose, we introduced in the reaction mixture 5 equivalents of a very good radical acceptor, benzylidene malonitrile **176**. We expected that it would play the role of a sacrificial acceptor (Fig. 2.23). Indeed, the presence of benzylidene malonitrile successfully inhibited the formation of reduced quinazolinone **129**, providing instead adduct **177**. Compound **177** could arise from the addition of hydrogen to

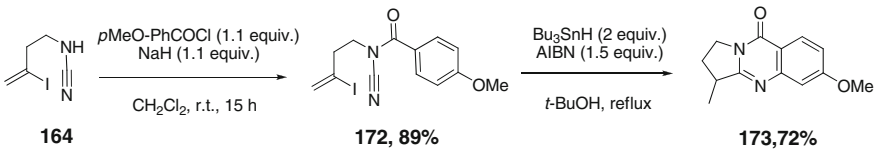

Fig. 2.21 Synthesis and cyclization of *p*-methoxy substituted precursor

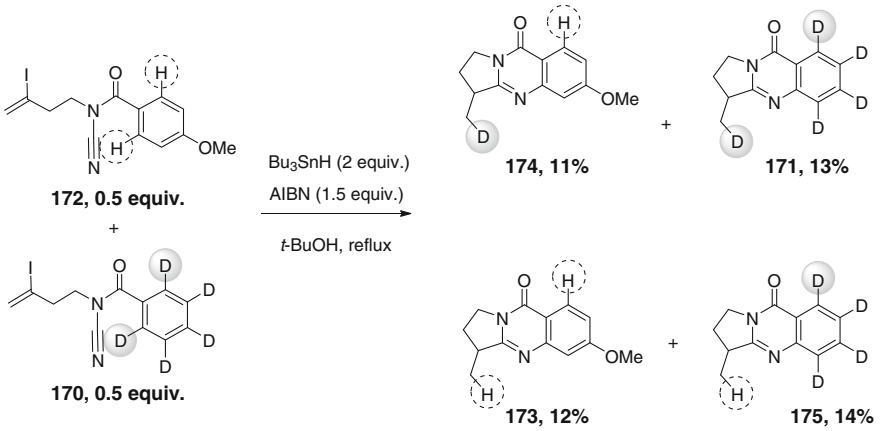

Fig. 2.22 Double tagging experiment

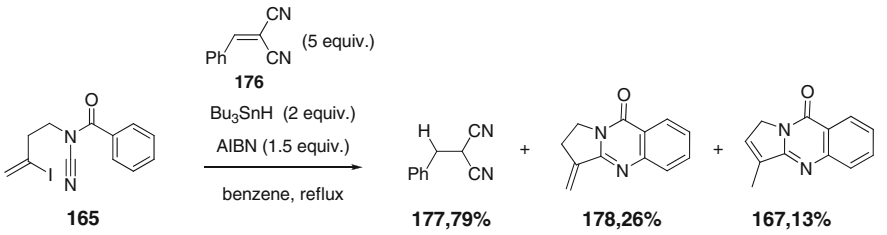

Fig. 2.23 Trapping of the $H^{\bullet}$ with a sacrificial acceptor

benzylidene malonitrile followed by radical termination by transfer of second hydrogen from Bu_3SnH. However, the exomethylene product **178** proved very unstable under the reaction conditions, and was consequently isolated in a disappointing 26 % yield, along with endomethylene product **167**.

In order to ascertain that the sacrificial acceptor had intercepted hydrogen coming from the benzoyl ring of *N*-acylcyanamide precursor, deuterated precursor **170** was reacted under the same reaction conditions. The outcome was very similar and in accordance with our assumption, delivering adduct **179** with a deuterium incorporation of 74 % (Fig. 2.24).

2.3.2.3 Influence of Steric Hindrance

We first wished to assess the influence of steric hindrance at the *exo* methylene on the output of the reaction. Indeed, in the case of a bimolecular approach, the migration of hydrogen should be sensitive to hindrance at the double bond. We envisaged synthesizing precursor **182**, bearing a trisubstituted double bond starting

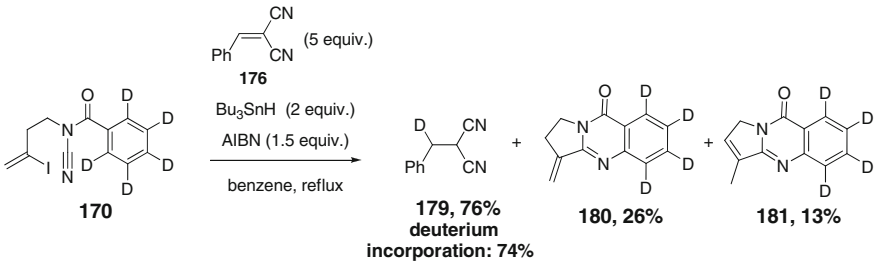

Fig. 2.24 Trapping of $D^{\bullet}$ with a sacrificial acceptor

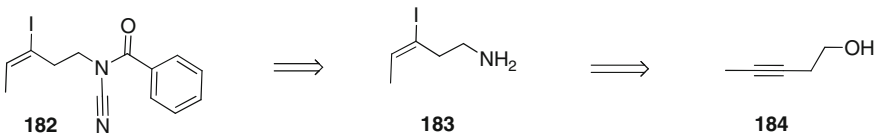

Fig. 2.25 Retrosynthetic plan for the synthesis of methyl substituted vinyliodide

from corresponding alkynol **184**, with a similar strategy to that employed for simple precursor **165** (Fig. 2.25).

The synthesis started under unfavorable auspices, since treatment of alkynol **184** with NaI, TMSCl and H_2O led to an unseparable mixture of two regioisomers **185** and **186** in a 1.5/1 ratio (Fig. 2.26). The methyl substituent on the alkyne had strikingly lowered the regioselectivity of the hydroiodination. Since the amount of product engaged was not negligible, we decided to carry on the reactions with the regioisomer mixture, in the hope of being able to separate them later in the synthesis. We thus tosylated the hydroxyl functions, and obtained an unseparable

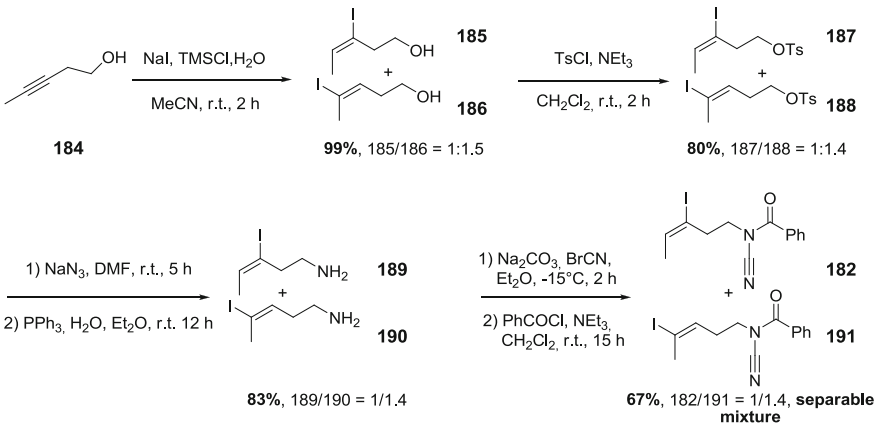

Fig. 2.26 Synthesis of the methyl substituted precursor and its regioisomer

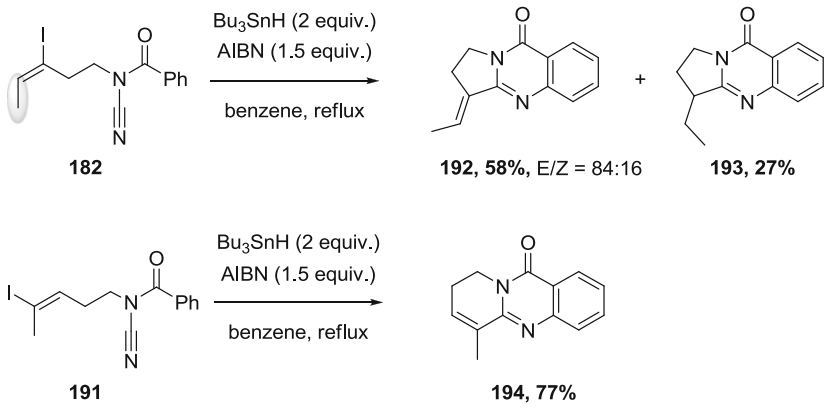

Fig. 2.27 Radical cyclization of precursors bearing a trisubstituted double bond

mixture of tosyls **187** and **188**. Nucleophilic substitution with sodium azide followed by Staudinger reduction afforded unseparable amines **189** and **190** that were submitted to cyanation and subsequent acylation in the previously employed conditions. To our great delight the *N*-acylcyanamides formed could, at last, be separated by flash column chromatography, delivering two cyclization precursors (instead of one!) **182** and **191**.

Both new *N*-acylcyanamides **182** and **191** possessing a trisubstituted double bond were cyclized under the usual radical conditions. Cyclization of **182** led to quinazolinone **192** still bearing the double bond as a major product (58 %) (Fig. 2.27). Reduced quinazolinone **193** was only isolated in 27 % yield. The presence of a methyl substituent at the double bond thus seemed to block the H migration process.

The cyclization of precursor **191** confirmed that when the double bond was *endo*, it could not be affected by H migration. Indeed, the reduction of the double bond was completely inhibited and quinazolinone **194** was isolated as the sole product.

Additionally, the cyclized product **192** bearing a trisubstituted double bond showed a higher stability under our radical conditions. Thus, cyclization of precursor **182** in the presence of 5 equivalents of benzylidene malonitrile led in a high 92 % yield to quinazolinone **192** (Fig. 2.28).

In a second time, we wished to assess the influence of steric hindrance at the *meta* position of the benzoyl ring on the outcome of the cascade reaction. We synthesized precursor **195** bearing *meta* methyl substituents and precursor **196** *meta tert*-butyl substituents. The presence of methyl substituents appeared to have little influence on the cascade process, since reduced quinazolinone **197** was isolated as the sole product in 63 % yield (Fig. 2.29). The presence of the *tert*-butyl substituents impacted more the reaction. Reduced quinazolinone **198** was isolated in 33 % yield. However the major product seemed to be a dearomatized

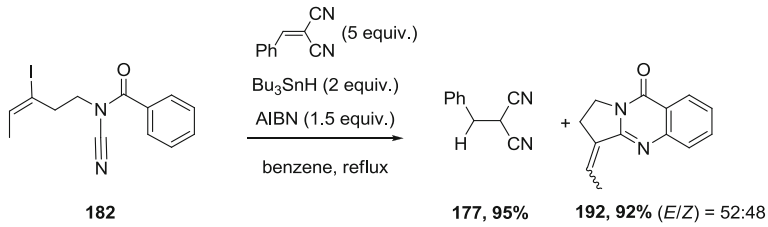

Fig. 2.28 Radical cyclization in the presence of a sacrificial acceptor

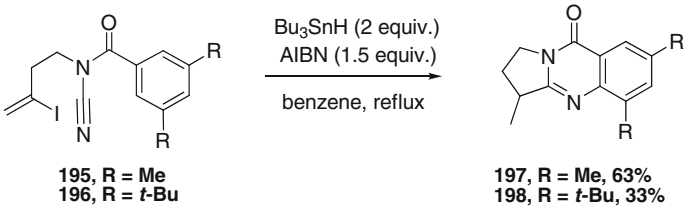

Fig. 2.29 Influence of *meta* substituents on the cascade process

compound according to the crude NMR. Unfortunately, the several attempts we made to isolate the major product were not successful. Hence we were not able to conclude on the influence of *meta*-substituents on the H migration.

2.3.2.4 Influence of Ring Size

Finally, we wanted to investigate the influence of the size of the first ring formed. We thus decided to prepare *N*-acylcyanamide **199**, as a precursor for the synthesis of 6-6-6 tricyclic system. Compound **199** was synthesized similarly to the other precursors, in 5 steps from 5-chloropent-1-yne **200** (Fig. 2.30).

The cyclization of precursor **199** proved surprisingly inefficient, since the dehalogenated product **201** was isolated as the major product in 45 % yield (Fig. 2.31). Among the cyclized products, the two third was still bearing an *endo* double bond (**202**, 16 %) and one third had undergone the H migration (**203**, 8 %). We demonstrated previously that once in the *endo* position, the double bond can no more be reduced by the H migration. Consequently, the lower amount of

Fig. 2.30 Synthesis of the precursor of 6-6-6 tricyclic system

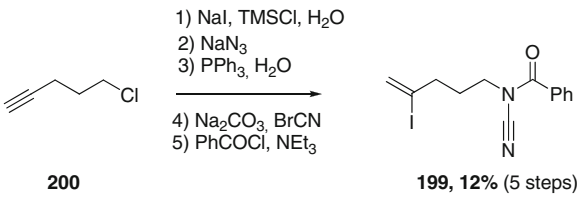

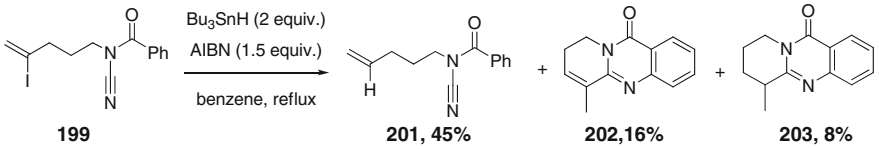

Fig. 2.31 Influence of the ring size on the cascade

reduced product might be explained by a more rapid migration of the *exo* double bond to the *endo* position in the 6-6-6 tricyclic synstem.

2.3.2.5 Mechanistic Proposal

According to all the experiments described previously, we propose the mechanism depicted in Fig. 2.32 for the H migration. After iodide abstraction by the tin radical, vinyl radical **204** would be formed and add to the cyanamide moiety via a 5-*exo-dig* cyclization. The amide-iminyl radical **205** generated would then be trapped by the benzoyl ring, leading to cyclohexadienyl radical **206**. Subsequently, the rearomatization would occur via bimolecular addition of "$H^{\bullet}$" on the *exo* double bond of a previously formed quinazolinone **178**. This step would generate a new molecule of quinazolinone **178** and a tertiary radical **207** that would be reduced by Bu_3SnH. This mechanistic proposal is in accordance with all the investigative experiments performed, however it has not been proven formally.

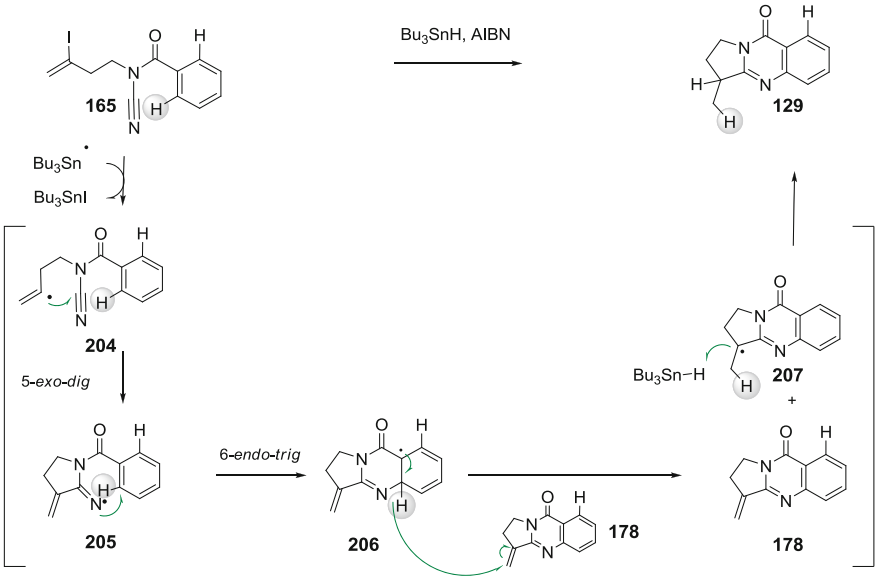

Fig. 2.32 Mechanistic proposal for the H migration

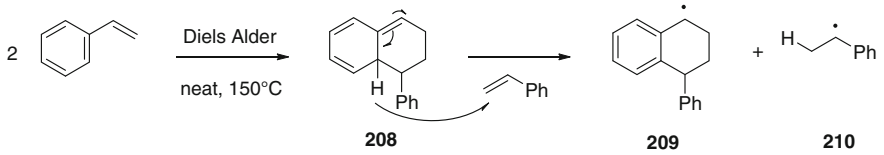

Fig. 2.33 Mayo mechanism for the autoinitiation of styrene

Deeper mechanistic studies on the kinetic of the reaction as well as DFT calculations should be performed to bring new insights into this unprecedented cascade. Alternatively, AIBN could play the role of a temporary radical trap, and the hydrogen could be first transferred to the initiator, generating AIBN(H)$^{\bullet}$ (**103**, Fig. 2.46.) which would then deliver H$^{\bullet}$ to the quinazolinone **178**.

The key hydrogen transfer step that we propose is reminiscent of the Mayo mechanism for the thermal autoinitiation of styrene, which has been confirmed by Rizzardo [26, 27]. In this mechanism (Fig. 2.33) two molecules of styrene undergo a Diels–Alder reaction to provide adduct **208**. This adduct then undergoes hydrogen atom transfer with a third molecule of styrene in a rearomatization step leading to benzyl radical **210** that can initiate the polymerization.

2.3.3 Migration of Carbon- or Heteroatom-Substituents

Having explored the migration of hydrogen, we envisioned to test the outcome of the cascade with precursors bearing *ortho*-substituents at the benzoyl group. As described in the bibliographical part, aromatizations with concomitant extrusion of carbon- or heteroatom- substituents have been reported. These types of processes were described either in the context of homolytic aromatic substitution or via aromatization of cyclohexadienyl radicals obtained by hydrogen abstraction. In some cases, these extruded radical could be trapped by activated olefin. We hoped that in our case, the *N*-acylcyanamide precursor could play the role of both the source of extruded radical and the trap. We would hence obtain a formal migration of substituent from the benzoyl ring to the *exo*-double bond during the cascade cyclization (Fig. 2.34).

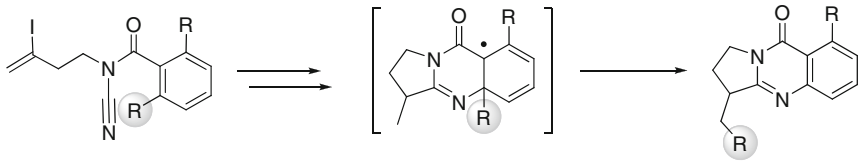

Fig. 2.34 Strategy envisioned for the migration of *ortho* substituents

2.3.3.1 Synthesis of *Ortho,Ortho'*-disubstitued Benzoyl Cyanamides

Conveniently, a set of five *ortho,ortho'*-disubstitued benzoyl cyanamides and one *ortho*-monosubstituted benzoyl cyanamide could be synthesized by reaction of common intermediate **164** with corresponding acyl chlorides. All acylations proceeded smoothly except from the reaction between cyanamide **164** and 2,4,6-triisopropylbenzoyl chloride. Probably because of the steric hindrance involved by *ortho*-substituents, this reaction was very sluggish. After stirring at room temperature during one week, 15 % of desired *N*-acylcyanamide could be isolated in one test reaction; but unfortunately, this reaction could not be reproduced at higher scale (Fig. 2.35).

2.3.3.2 Cyclization of Carbon-Substituted Benzoyl Cyanamides

When treated in the usual radical conditions, precursors **211** and **212** pleasingly afforded, in average yields, the desired quinazolinones **217** and **218** where methyl and isopropyl group respectively underwent the planned migration. Both benzene and *tert*-butanol could be used as solvent with similar efficiency. Methyl radical is not reported to be extruded with a high dissociation rate [28], and its addition to simple alkene is slow ($k = 3.3 \times 10^4\ M^{-1}\ s^{-1}$ for the addition of $Me^{\bullet}$ to ethene at 338 K) [29]. The successful outcome of the cascade in our case could be explained by a bimolecular mechanism, and by the highly conjugated nature of the trapping olefin (Fig. 2.36).

To our great delight, the treatment of precursor **213** with Bu_3SnH and AIBN added at a rate of 0.06 mmol of Bu_3SnH/h in refluxing *tert*-butanol allowed the isolation of quinazolinone **219** in 55 % yield. Running the reaction in benzene proved strongly detrimental. This could be explained by the fact that trifluoromethyl radical is known to add readily to aromatic solvents [30, 31]. The trifluoromethyl group appears in a large number of structures of interest to the pharmaceutical and agrochemical industry [32–35], and the methodologies available to generate trifluoromethyl radicals are not so numerous [36, 37].

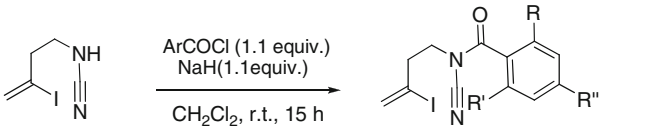

164

211: R = R' = R" = Me, **87%**
212: R = R' = R" = *i*-Pr, **15%**
213: R = R' = CF_3, R" = H, **48%**
214: R = R' = Cl, R" = H, **85%**
215: R = R' = F, R" = H, **96%**
216: R = Me, R' = R" = H, **92%**

Fig. 2.35 Synthesis of *ortho*-substituted *N*-acylcyanamides

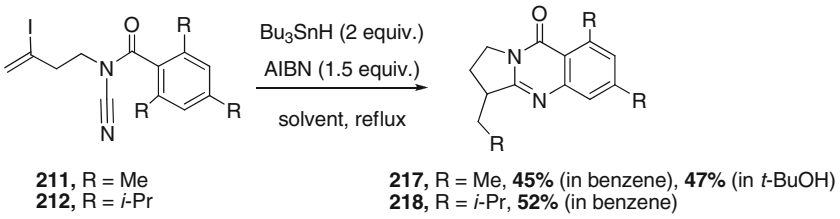

Fig. 2.36 Migration of alkyl radicals

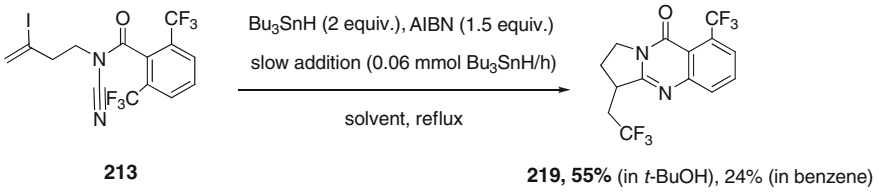

Fig. 2.37 Migration of trifluoromethyl radical

Consequently any new methodology for the generation and trapping of $CF_3^{\bullet}$ is of high interest (Fig. 2.37).

Trifluoromethyl radical is very electrophilic and can consequently abstract hydrogen from cyclohexane or THF. The newly formed radical can then add to activated unsaturations as demonstrated by Fuchs. He reported that treatment of vinyl triflone **220** with AIBN in THF, afforded trisubstituted olefin **221** by the chain transfer mechanism depicted in Fig. 2.38.

We decided to perform our cyclization in THF, to observe if in our conditions, trifluoromethyl radical-mediated H abstraction at THF could prevail to CF_3 migration. When only 2 equivalents of THF were introduced in the reaction mixture, the migration at quinazolinone remained the major pathway. Quinazolinone **219** was isolated in 41 % yield along with 17 % of unsaturated compound **222**. When the reaction was run in THF, the migration was completely inhibited, and olefin **222** was isolated as the sole product. These experiments seem to confirm that the migration occur via the extrusion of a trifluoromethyl radical. When THF is present as a solvent, it reduces $CF_3^{\bullet}$ to CF_3H, generating THF radical. This latter appears to be unable to add to the quinazolinone under our reductive condition (Fig. 2.39).

Finally, we wished to run a competition experiment between hydrogen and methyl group migration. Dissymmetric precursor **216** was cyclized under the usual conditions, leading to quinazolinone **223** as the sole isolated product (Fig. 2.40). This result could be explained by the faster radical addition at the less substituted carbon of the benzoyl ring.

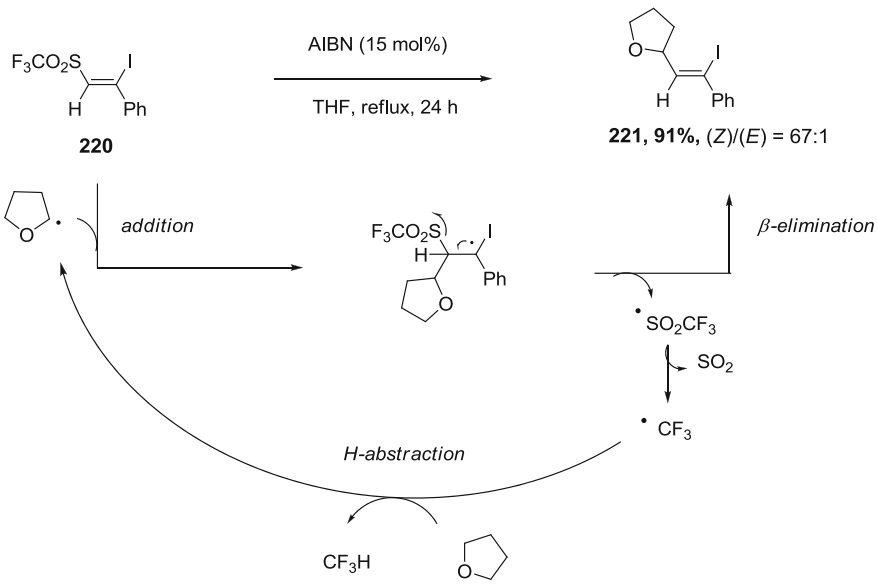

Fig. 2.38 Reaction of vinyl triflone with THF under radical initiation

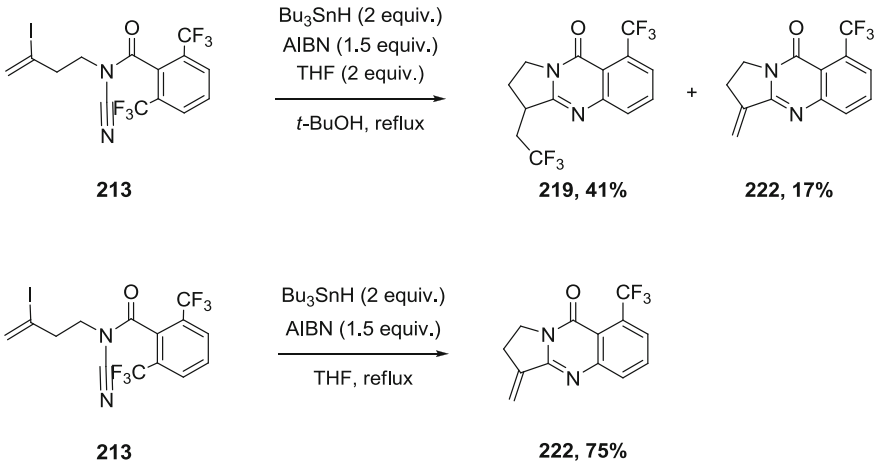

Fig. 2.39 Test of the influence of the presence of THF in our cascade

2.3.3.3 Cyclization of Heteroatom-Substituted Benzoyl Cyanamides

Heteroatom-substituted benzoyl cyanamides led to less clear results than their carbon counterparts. The cyclization of *o,o'*-dichloro precursor **214** resulted in degradation. Further studies would be necessary to understand at which step in the mechanism this degradation occurs. The cyclization of *o,o'*-difluoro precursor **215**

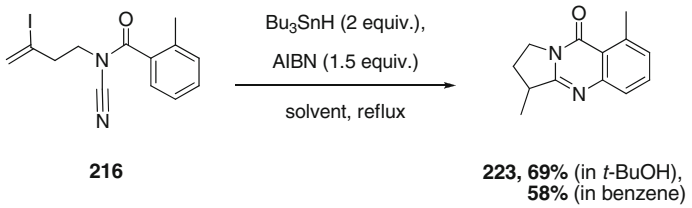

Fig. 2.40 Cyclization of dissymmetric precursor

led to a complex mixture from which quinazolinone **224** could be isolated in 30 % yield. This product was very surprising, and we could imagine the mechanism depicted in Fig. 2.41 to explain its formation. Fluorine radical could be extruded during aromatization and, thanks to its high affinity for tin, add to the mediator. This addition would result in the release of butyl radical that would add to the *exo*-double bond of quinazolinone **225**. Running the reaction with Bu_3SnD indeed provided deuterated quinazolinone **226**, albeit only in 9 % yield. ^{19}F and ^{119}Sn NMR studies are currently performed to gain new insights into this unprecedented outcome. Disappointingly, running the reaction with Ph_3SnH or $(TMS)_3SiH$ instead of Bu_3SnH led to inseparable complex mixtures.

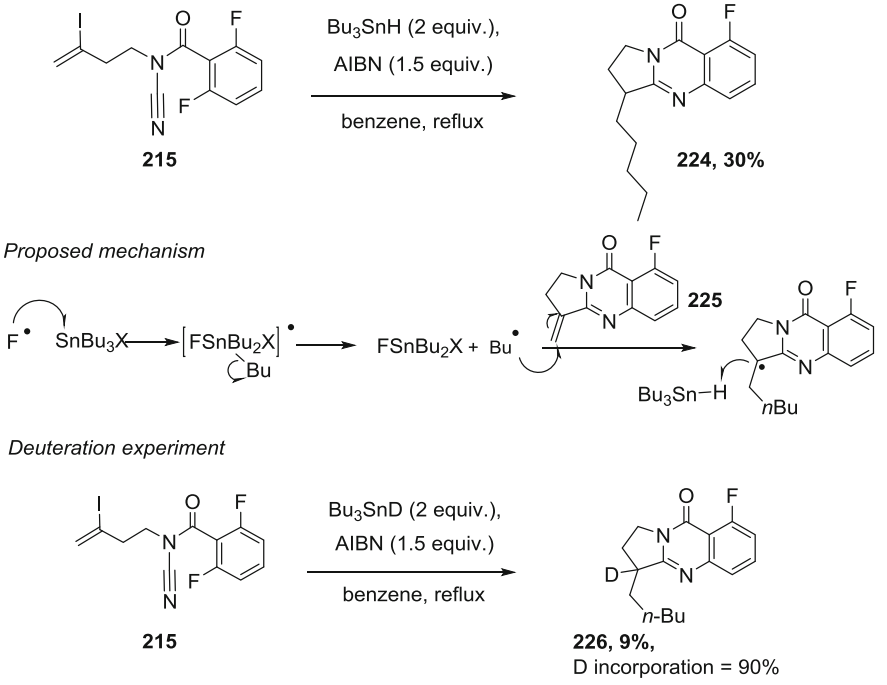

Fig. 2.41 Cyclization of difluoro precursor

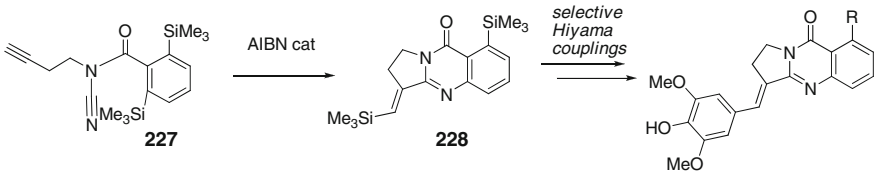

Fig. 2.42 Possible perspective involving TMS migration

To conclude, the study on the behavior of vinyl radicals in cascades with *N*-acylcyanamides allowed us to develop an original domino process, involving unexpected migrations of hydrogen or carbon substituents triggered by homolytic aromatic substitutions [38]. Careful mechanistic studies helped us to get better insights into the cascade. In a broader manner, this study brings precious elements for the better understanding of homolytic aromatic substitutions. As a perspective, many new applications to this migration could be proposed. For instance, in the aim of synthesizing isaindigotone, silylated precursor **227** could be cyclized in the presence of a catalytic amount of AIBN. Quinazolinone **228** may be obtained under those tin free conditions and transformed isaindigotone via selective Hiyama couplings (Fig. 2.42).

2.4 Addition of Nitrogen Centered Radicals

Our next challenge was to test the reactivity of nitrogen centered radicals in cascades with cyanamides. The use of aminyl radicals in cascades is challenging due to kinetic reasons. As illustrated on Fig. 2.43, the lazy amino radical has a lower cyclization rate than the corresponding alkyl radical. Even more importantly, the competition between direct reduction and cyclization is less in favor of cyclization for aminyl radicals compared to alkyl radicals [39].

Nevertheless, we were particularly interested in using aminyl radicals since we realized that their addition on cyanamide followed by homolytic aromatic substitution would provide us with a straightforward synthesis of tricyclic guanidines (Fig. 2.44).

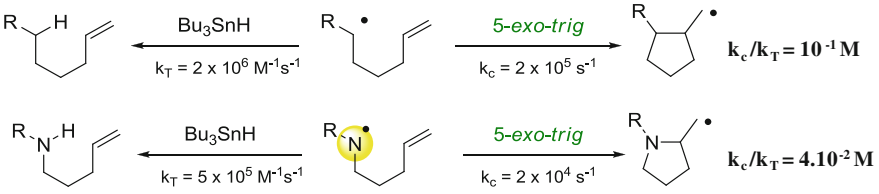

Fig. 2.43 Comparison of the kinetics of cyclization and reduction for aminyl and alkyl radicals

Fig. 2.44 Objective of the project

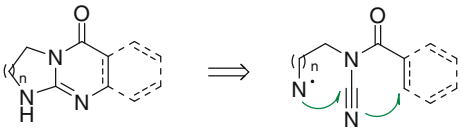

2.4.1 Synthetic Targets: Polycyclic Guanidines

2.4.1.1 Bioactivity

Polycyclic guanidines frameworks are found in a range of natural or bioactive products (Fig. 2.45). Hence, alchornine alkaloid **229** was isolated in 1969 from small rain-forest tree *Alchornea javanensis*; [40] anagrelide **230** is a drug used for the treatment of thrombocytosis; [41] cyclic guanidines saxitoxin, ptilocaulin and tetrodotoxin are potent ion-channel blockers and ptilomycalin A **231** is a marine alkaloid exhibiting remarkable antitumor activities [42].

2.4.1.2 Applications in Bio-inspired Molecular Recognition

In biological systems, the strong ion-pairs formed by arginine side chain with oxoanions, such as carboxylates or phosphates, are critical to stabilize protein tertiary structures. They also play a preponderant role in the interactions between proteins and carbohydrates or nucleic acids. The high affinity of the guanidinium group for oxoanions, due to its geometry and to its high pKa value (pKa $\sim$ 12–13) allowing protonation over a wide pH range, has been extensively used in artificial receptors for molecular recognition [43]. Thus, Mendoza has reported the use of chiral guanidinium based receptor **232** for the enantioselective recognition of zwitterionic amino acids (Fig. 2.46). L-Tryptophane could be for example extracted from a racemic mixture in 40 % efficiency and 99 % *ee* thanks to the hypothetical formation of complex **233** [44].

2.4.1.3 Organocatalysis

Chiral polycyclic guanidines are promising organocatalysts for reactions that proceed through ionic transition states. Guanidines thus act as effective catalysts in

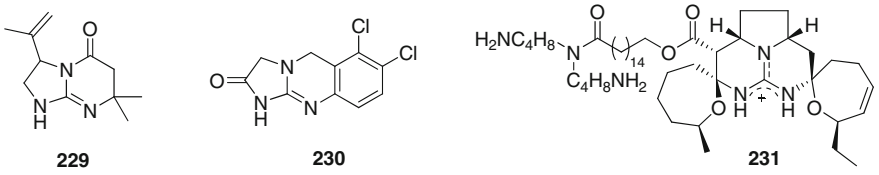

229 **230** **231**

Fig. 2.45 Natural and bioactive polycyclic guanidines

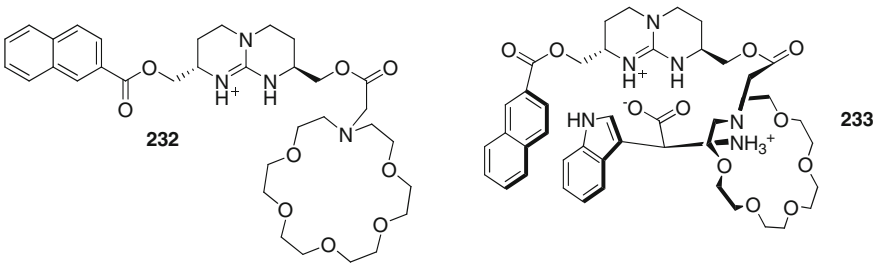

Fig. 2.46 Guanidinium based receptor for the enantioselective recognition of L-tryptophan

several highly enantioselective reactions such as base-catalyzed Diels-Alder, Strecker reaction, conjugate additions or enantioselective protonations [45]. Thus, chiral C_2-symmetric guanidine **234** was used as a bifunctional catalyst for the enantioselective addition of HCN to *N*-benzhydrylimine **235** (Fig. 2.47) [46]. The reaction is thought to proceed via the protonation of catalyst with HCN forming a guanidinium cyanide complex that can serve as hydrogen bond donor to the imine. Pre-transition state assembly **237** then directs the attack of the cyanide at the re face of the imine.

2.4.2 Generation of Aminyl Radicals

Finding the appropriate way to generate the aminyl radical was the most challenging point of the project. N-Centered radicals can be easily obtained by homolytic cleavage of relatively weak bonds, *e.g.* N–N, N–S, N–O and N-Halogen

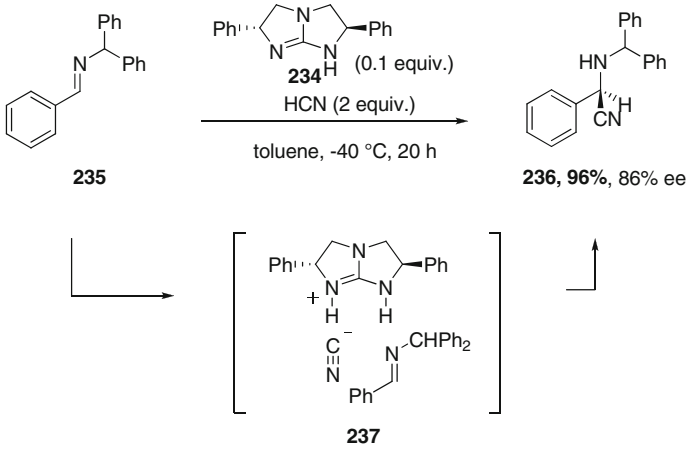

Fig. 2.47 Enantioselective Strecker reaction catalyzed by bicyclic guanidine

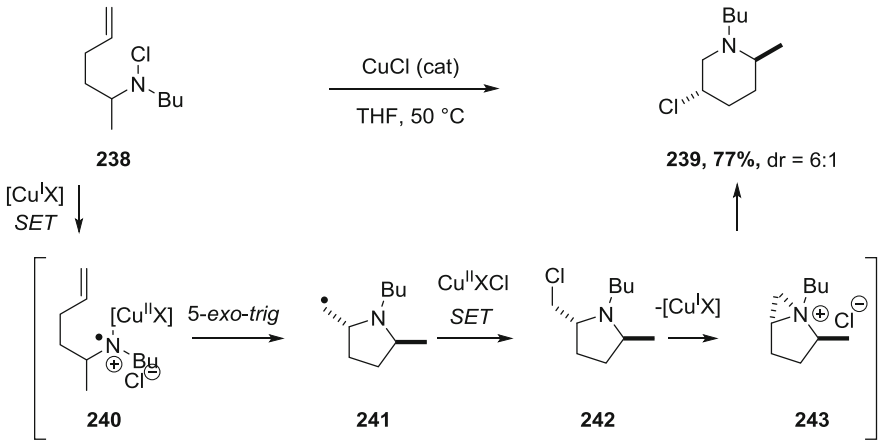

Fig. 2.48 Copper(I) mediated generation of aminyl radical from chloroamine

bonds, but also strong N–H and N–C bonds in specific conditions. This subject has been reviewed in depth by Zard in 2008 [47] and just recently by our group [48]. Only a few significant methodologies will be presented here.

2.4.2.1 Aminyl Radicals by Homolytic N-Halogen Bond Cleavage

Haloamines have been widely used as precursors since they can be conveniently prepared by electrophilic halogenation of the corresponding amines using *N*-halosuccinimides. Their major drawback is their low stability. Homolysis of the N-X bond under photochemical activation is the most widespread way to trigger the radical reaction. Nevertheless, the development of alternative catalytic reduction of haloamines with low valent metal salts allowed the generation of aminyl radicals in a more controlled fashion. Thus, *N*-chloramine **238** has been converted to piperidinyl derivatives **239** in the presence of copper(I) salts (Fig. 2.48) [49]. Single electron transfer from copper (I) catalyst allows the reduction of the N–Cl bond to generate radical cation **240**. The aminyl radical undergoes a fast 5-*exo-trig* cyclization to afford pyrrolidinyl intermediate **241** and release copper(II) complex. The primary alkyl radical formed reacts through a second SET process leading to the formation of the corresponding chlorinated pyrrolidine **242** and the regeneration of the catalyst. Alkyl chloride **242** finally undergoes an anionic stereoselective ring expansion to yield compound **239**.

2.4.2.2 Aminyl Radicals by N–O Bond Cleavage

N-Benzoyloxyamines such as **244** can also be reduced by copper(I) salts and undergo transfer group reactions (Fig. 2.49) [50]. Similarly to the reaction with

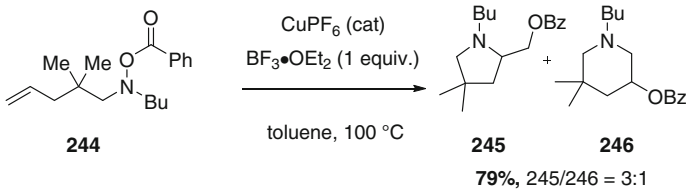

Fig. 2.49 Copper(I)-mediated generation of aminyl radical from *N*-benzoyloxyamine

haloamines, the copper(II)-benzoyl complex formed during the reduction step transfers the acyl group to the primary C-radical obtained after cyclization. This step thus allows the regeneration of the catalyst. It should be noted that no reaction was observed without Lewis acid, which indicates that the acyloxy group must be activated to weaken the N–O bond.

2.4.2.3 Aminyl Radicals by N–C Bond Cleavage

N–C Bonds are generally too strong to lead to efficient homolytic cleavage. In specific cases i.e. the release of ring strain, decarboxylation or aromatization [51], such process can nonetheless occurs. For example, irradiation of carbamate derivative of *N*-hydroxy-3-thiopyridone (*N*-PTOC) **247** in the presence of trifluoroacetic acid leads to carbonyloxylradical **248** that undergoes rapid fragmentation to release a molecule of carbon dioxide and protonated aminyl radical **249** (Fig. 2.50) [52]. This latter performs a fast 5-*exo-trig* cyclization. Finally, chain propagation is achieved by the attack of the resulting alkyl radical on thiocarbonyl

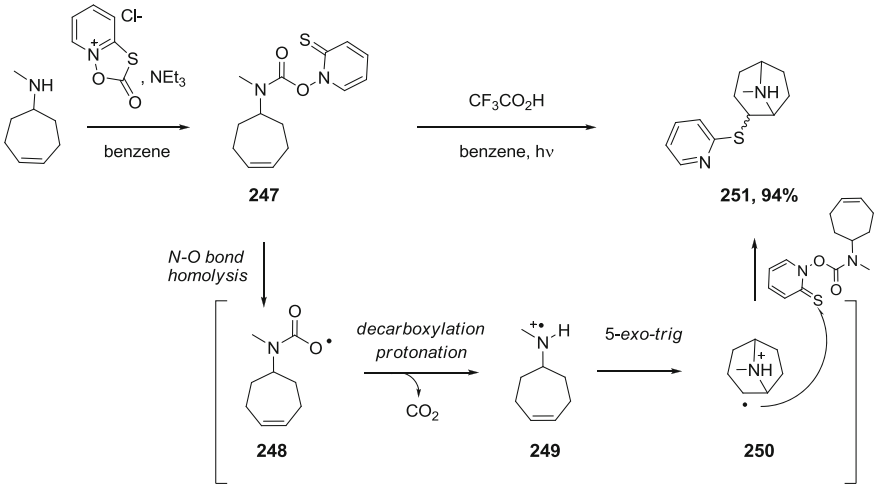

Fig. 2.50 Generation of aminyl radical from *N*-PTOC carbamate

function. The drawback of the methodology is that precursor **247** is poorly stable and must be prepared in situ.

2.4.2.4 Aminyl Radical by N–S Bond Cleavage

Sulfenamine derivatives have been successfully employed for the generation of *N*-centered radicals via homolytic substitution of tin radical at the sulfur atom. As reported by Li, treatment of *N*-(benzenesulfenyl)pent-4-enylamines **252** with the Bu_3SnH/AIBN system affords the corresponding aminyl radicals. These latters can cyclize onto the alkene moiety to provide a mixture of pyrrolidines and piperidines. The nature of the substituents of the alkene is critical for controlling the product distribution [53]. The only limitation to this methodology can be the access to the sulfenyl precursor (Fig. 2.51).

2.4.2.5 Generation of Aminyl Radicals Via N–H Bond Cleavage

Generation of aminyl radicals from tosylamines can be achieved by proton and electron transfer with oxydants such as $Cu(OAc)_2$. The oxidation of tosyl-*o*-allylanilines **255** has thus been reported using $Cu(OAc)_2$ and Cs_2CO_3 at 120 °C. As a result, anilinyl radical **256** is formed and cyclizes in a 5-*exo*-*trig* mode [54]. The alkyl radical generated can subsequently perform a homolytic aromatic substitution. Hence, this intramolecular carboamination of alkenes could lead to straightforward synthesis of hetero-multicyclic compounds (Fig. 2.52) [55].

2.4.2.6 Generation of Aminyl Radical via N–N Bond Cleavage

Carbon- or heteroatom radicals can add at the α or γ position of the azido moiety to give 1,3- or 3,3-triazenyl radicals **259** and **260** [56]. With both aliphatic and aromatic azides, the latter fragment by loss of N_2 to form aminyl radical (Fig. 2.53).

Thus, intermolecular addition of stannyl radicals to alkyl azides provides transient nucleophilic stannylaminyl radicals. Kim was the first to prove that those radicals could cyclize onto unsaturations to form heterocyclic rings (Fig. 2.54). He

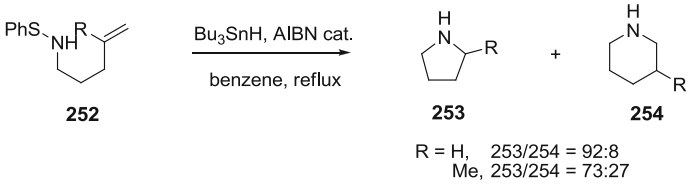

Fig. 2.51 Generation of aminyl radical via homolytic cleavage of N–S bond

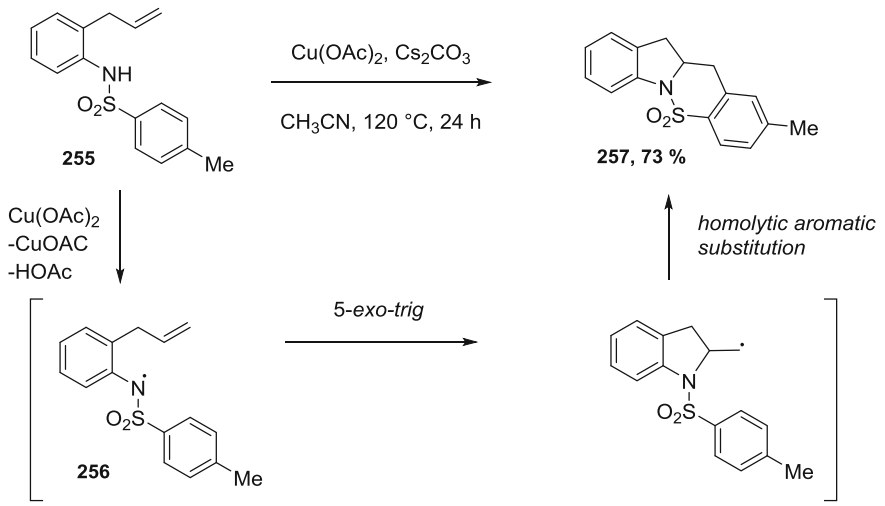

Fig. 2.52 Generation of aminyl radical via proton and electron transfer with Cu(II) salts

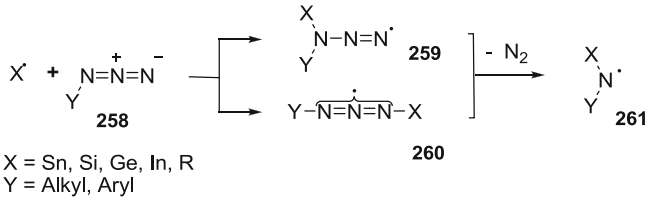

Fig. 2.53 Generation of aminyl radical by homolytic addition to azides

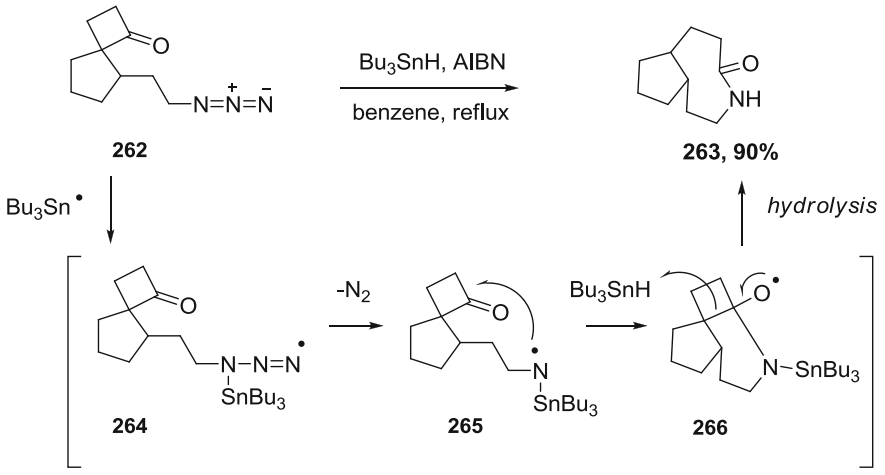

Fig. 2.54 Addition of stannylaminyl radical to carbonyl function

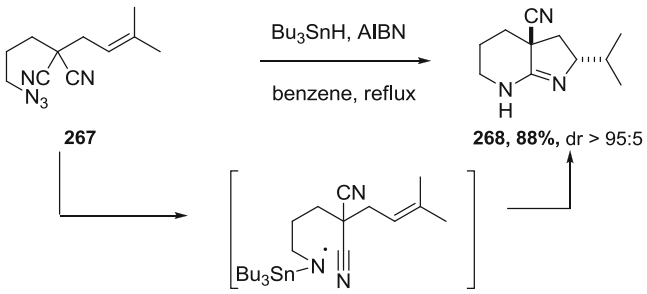

Fig. 2.55 Addition of stannylaminyl radical to nitrile group

treated azido precursor **262** with Bu_3SnH and AIBN, and generated stannylaminyl radical **265** which added to the carbonyl group. Fragmentation and subsequent hydrolysis afforded lactam **263** in 90 % yield.

Spagnolo reported subsequently that stannylaminyl radicals could add intramolecularly to electrophilic cyano groups. The generated aminoimidyl radicals could undergo further cyclizations onto suitably positioned alkenes and aromatic rings (Fig. 2.55) [57].

To decide what strategy we would use for our cascade with *N*-acylcyanamides, we took into account the synthesis of the precursor. Cyanamide functions are prone to hydrolysis under acid or basic aqueous treatment, so we wished to maintain the construction of *N*-acylcyanamide moiety as the last step of the precursor synthesis. Besides, the precursor should not bear more than one free amino group at the cyanation step to prevent polycyanation issues. These requirements oriented us towards the use of azido precursor, since azide functions are stable under a wide range of conditions, easily introduced at any step of the synthesis and cannot undergo undesired cyanation. Furthermore their use for the generation of aminyl radicals is atom economical relatively to the other methodologies, and we could be optimistic about their reactivity with cyanamides after their good behavior with nitriles.

2.4.3 Synthesis of the Precursors

2.4.3.1 Variation of the Link Length Between the Azide and the Cyanamide Functions

Our first objective was to synthesize azido-*N*-acylcyanamide precursors **269**–**271** with increasing length of the alkyl link between the azide and the cyanamide functions (Fig. 2.56).

Precursors **269** and **270** were prepared similarly starting from bromoalkylamines hydrobromide **135** and **138** (Fig. 2.57). Nucleophilic substitution with sodium azide in H_2O afforded, after basic treatment, azidoamines **272** and **273** that

Fig. 2.56 Precursors with variable chain lengths

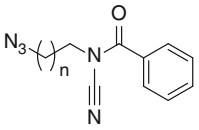

269, n = 1
270, n = 2
271, n = 3

underwent subsequently cyanation and acylation. The synthesis of the *N*-acyl cyanamides was thus very rapid, the only difficulty being related to the volatility of the intermediates.

Precursor **271** was prepared starting from 1,4-dibromobutane **274** (Fig. 2.58). Double nucleophilic substitution with sodium azide in DMF afforded 1,4-diazidobutane **275**. An efficient mono-Staudinger reduction to azido amine **276** was then achieved in biphasic conditions using triphenyl phosphine in Et_2O/EtOAc/5 % HCl aqueous solution [58]. In these conditions, as soon as the azidoamine is formed, it is protonated by HCl and migrates to the aqueous layer, thus preventing over-reduction to diamine. Subsequent cyanation and acylation afforded the desired *N*-acylcyanamide precursor **271**.

2.4.3.2 Variation of the Substituents on the Alkyl Chain Linking Azide and Cyanamide Functions

Next, we endeavored to prepare precursors diversely substituted on the alkyl chain. We decided to prepare precursor **277**–**279** starting from the corresponding amino alcohols (Fig. 2.59).

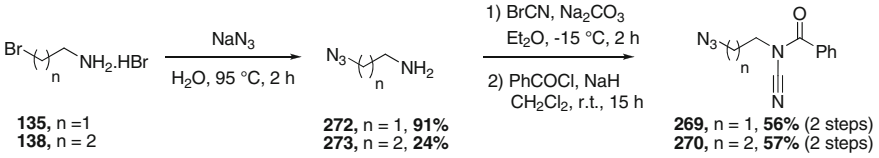

135, n =1
138, n = 2

272, n = 1, **91%**
273, n = 2, **24%**

269, n = 1, **56%** (2 steps)
270, n = 2, **57%** (2 steps)

Fig. 2.57 Synthesis of *N*-acylcyanamides 269 and 270

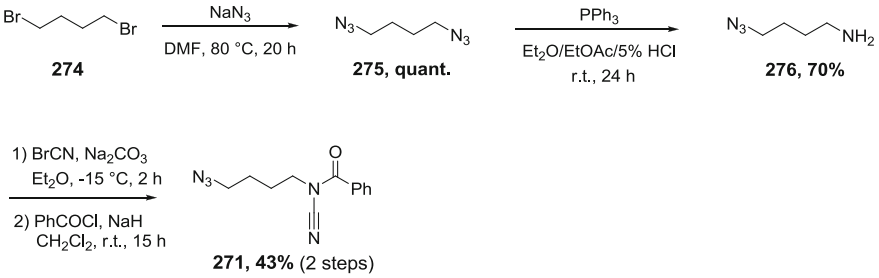

274

275, quant.

276, 70%

271, 43% (2 steps)

Fig. 2.58 Synthesis of *N*-acylcyanamide precursor 271

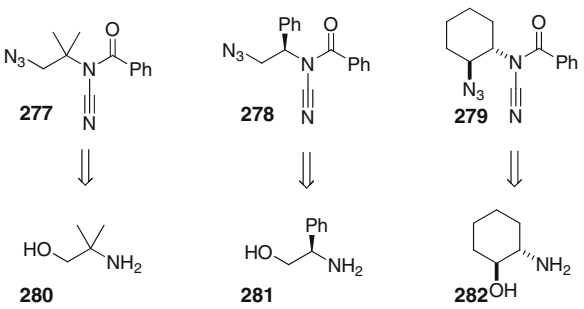

Fig. 2.59 Precursors with various substituents on the alkyl chain

N-protection of **280**–**282** with Boc group gave protected amino alcohols which were subsequently mesylated to **283**–**285** [59]. Deprotection with HBr as a 2 M solution in acetic acid allowed the isolation of amino mesylates **286**–**288** as their hydrobromide salts. The protonation of the amine conveniently prevents intramolecular nucleophilic substitution. Conversion of mesylates into azides **289**–**291** was achieved by treatment with sodium azide in water. Final cyanations and acylations afforded the desired precursors (Fig. 2.60).

2.4.3.3 Variation of the Benzoyl ring

In order to check the scope and limitations of the cascade, we sought to prepare precursors **295**–**299** bearing different types of substituents on their benzoyl ring, as well as heteroaryl rings. We treated cyanamide **293**, with various acyl chlorides in the presence of sodium hydride and obtained the corresponding *N*-acylcyanamides with medium to good yields (Fig. 2.61).

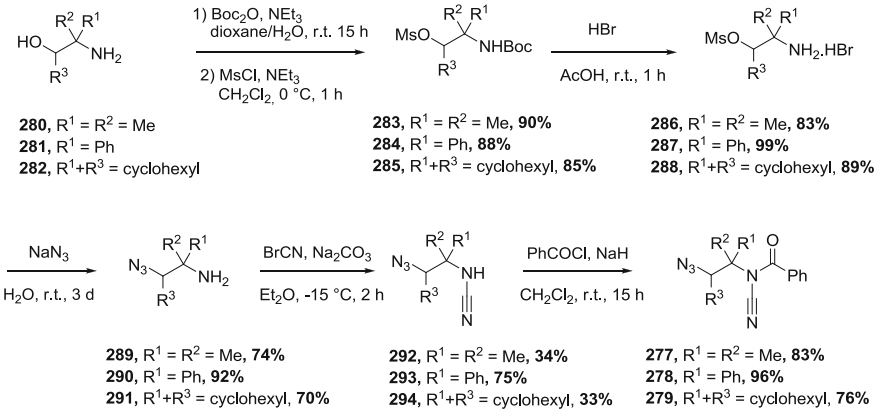

Fig. 2.60 Synthesis of *N*-acylcyanamides 277–279

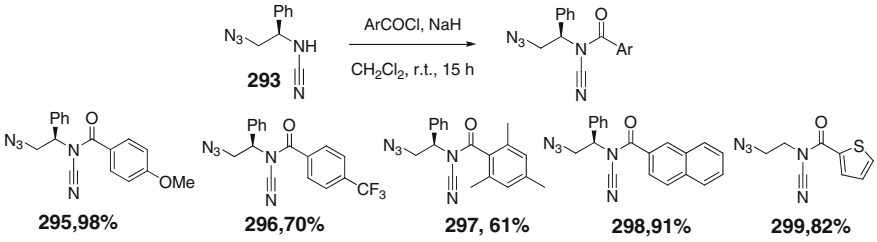

Fig. 2.61 Synthesis of precursors with various aryl traps

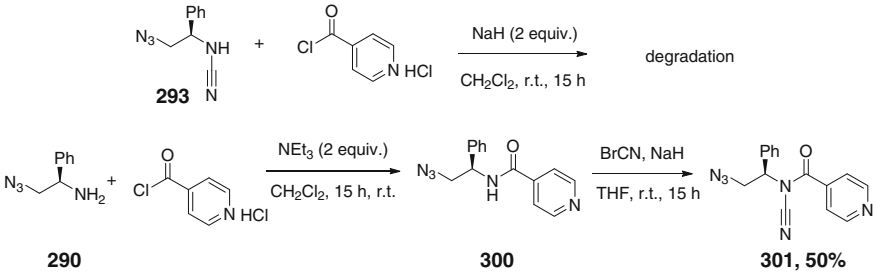

Fig. 2.62 Synthesis of isonicotinoyl precursor

Treatment of cyanamide **293** with isonicotinoyl chloride hydrochloride led only to degradation (Fig. 2.62). Fortunately, inverting the acylation and the cyanation steps allowed us to isolate the desired isonicotinoyl precursor **300** successfully.

Finally, the final aryl acceptor was replaced with olefins. Precursors **302**, **303** and **304** bearing substituted double bonds could be synthesized starting from the corresponding cyanamides and acyl chlorides (Fig. 2.63).

2.4.3.4 Synthesis of Aryl Azide Precursor

Finally we decided to test a precursor with an aryl azide function. Starting from 2-nitro aniline **305**, 2-azido aniline **307** was conveniently obtained by a 5 steps procedure reported by Hall [60]. This procedure involved first the protection of the amino group by conversion to phthalimide, followed by the reduction of the nitro group with iron and acetic acid. Diazotization of the amino group followed by treatment of the diazonium with sodium azide then afforded the 2-phthalimidophenyl azide. This latter was finally deprotected by treatment with hydrazine in methanol to give 2-azidoaniline **307** (Fig. 2.64).

Two strategies for the preparation of the *N*-acylcyanamide **39**8 were then tested. Direct cyanation of the aryl amine by treatment with BrCN and Na_2CO_3 was not successful. However, an acylation/cyanation sequence allowed us to obtain the desired precursor **308** incorporating aryl azide and *N*-acylcyanamide functions (Fig. 2.65).

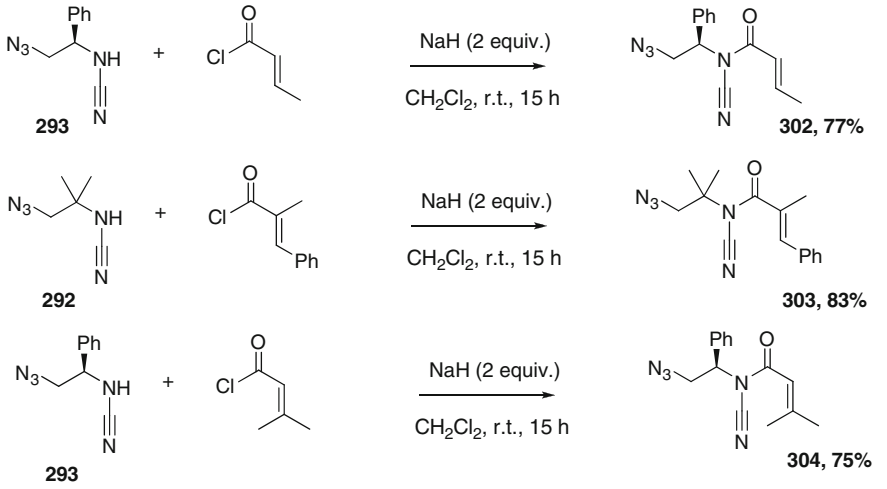

Fig. 2.63 Synthesis of precursors with olefins as acceptors

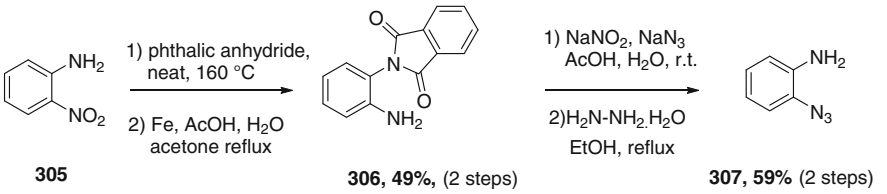

Fig. 2.64 Synthesis of 2-azido amine

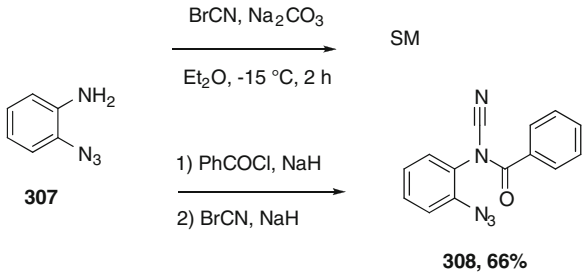

Fig. 2.65 Synthesis of aryl azide precursor

2.4.4 Optimization of Guanidine Radical Synthesis

The simplest substrate **269** was selected to test the feasibility of the cascade and optimize the radical conditions (Fig. 2.66). The first set of conditions we used were the one developed for the cyclization of vinylcyanamides, i.e. treatment with

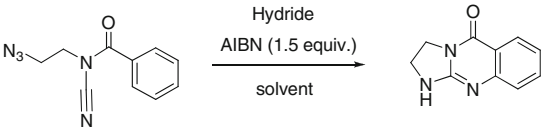

269 **309**

Entry	Solvent, Temp.	Addition rate (mmol/h)	Hydride (equiv.)	Additives	Yield **399** [%]
1	benzene, reflux	**0.2**	Bu_3SnH (2)	-	**41**
2	toluene, reflux	**0.2**	Bu_3SnH (2)	-	**30**
3	*t*-BuOH, reflux	**0.2**	Bu_3SnH (2)	-	**31**
4	benzene, reflux	**one batch**	Bu_3SnH (2)	-	**20**
5	benzene, reflux	**0.06**	Bu_3SnH (2)	-	**76**
6	benzene, reflux	**0.06**	Bu_3SnH (1.2)	-	**43**
7	benzene, reflux	**0.06**	$(TMS)_3SiH$ (2)	-	**<10**
8	benzene, reflux	**0.06**	Bu_3SnH (2)	$BF_3.Et_2O$ (1 equiv.)	**38**
9	benzene, 50°C	**0.06**	Bu_3SnH (2)	-	**25**
10	benzene, r.t.	**0.06**	Bu_3SnH (2)	Irradiation	**<10**
11	benzene, r.t.	**0.06**	Bu_3SnH (2)	BEt_3, air, no AIBN	**<10**

Fig. 2.66 Optimization of the radical cyclization of azidocyanamide 269

Bu_3SnH (2 equivalents) and AIBN (1.5 equivalents) slowly added (0.2 mmol Bu_3SnH/h) in refluxing benzene. To our great delight, guanidine **309** could be isolated after silica gel column chromatography in 41 % yield (entry 1). A rapid solvent screening showed that replacing benzene with *t*-BuOH or toluene led to reduced yields (entries 2,3). We then investigated the influence of the rate of addition of Bu_3SnH (entries 4,5). Addition in one batch resulted in poor isolated yield of 20 %, while slower addition (0.06 mmol Bu_3SnH/h) allowed us to obtain the desired guanidine in 76 % yield. We then sought to reduce the amount of Bu_3SnH to 1.2 equivalents (entry 6) or to replace it with $(TMS)_3SiH$ as a mediator (entry 7) but both attempts proved detrimental for the conversion and consequently for the yield. Several Lewis acids were tested in the idea of improving the cyclization of the aminyl radical. Indeed, kinetic studies have demonstrated that Lewis acids activate aminyl radicals towards cyclizations by increasing their rate constants more by 3 orders of magnitude. One of the most efficient Lewis acid was reported to be BF_3 [61]. In our case, the addition of Lewis acids resulted in a decrease in the yield of final product (entry 8), possibly because of the presence of multiple sites of complexation in the *N*-acylcyanamide precursor. We finally tried to reduce the temperature of the reaction which resulted in a progressive drop of the yield (entries 9–11). Two types of initiations at room temperature were tested: AIBN under irradiation and BEt_3 with O_2, but they both led to less than 50 % conversion and less than 10 % yield of desired guanidine. The major side product was uncyclized aminocyanamide. We consequently conserved the conditions of entry 5 as our best conditions.

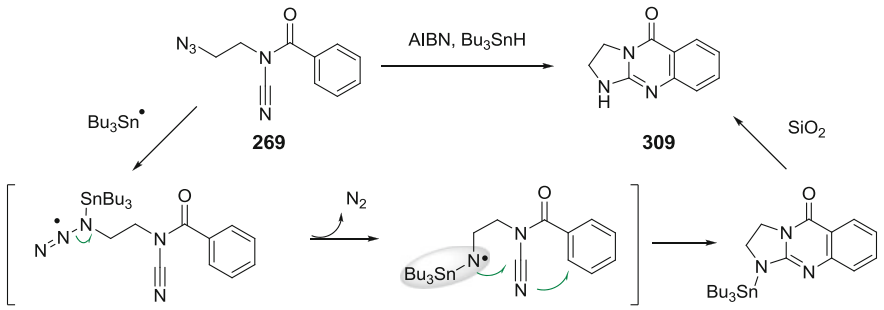

Fig. 2.67 Proposed mechanism for the radical synthesis of guanidines

We think that the cascade proceeds as depicted in Fig. 2.67. Addition of tin radical to the azide function leads after loss of nitrogen to a nucleophilic stannylaminyl radical that can cyclize on the cyanamide moiety. The resulting amide iminyl radical performs a homolytic aromatic substitution at the benzoyl ring, leading to stannylated guanidine. Silica gel chromatography finally allows the isolation of the free guanidine **309**.

2.4.5 Scope of the Guanidine Synthesis

With our optimized conditions in hands, we examined the scope of our methodology. We first investigated the influence of the length and substitution of the alkyl chain on the outcome of the reaction (Fig. 2.68). Cyclization of precursors **270** and **271** showed that increasing the number of carbons between the azide and the cyanamide function led to a progressive decrease of the efficiency of the reaction. This trend seems logical owing to the slower kinetics of 6-*exo-dig* and 7-*exo-dig* cyclizations compared to 5-*exo-dig*. This explanation was confirmed by the observation of uncyclized amino cyanamides as side products. Furthermore, the cyclization of precursor **271** can be prevented by competitive 1,5-hydrogen transfer. On the other hand, the substitution on the alkyl chain did not seem to have a strong impact on the cascade, and all the 5,6,6-tricyclic guanidines derived from precursors **280**–**282** were obtained in good yields.

Next, we investigated the influence of variations on the benzoyl ring thanks to the cyclization of precursors **295**–**301** (Fig. 2.69). Overall, our radical cascade proved rather general. The introduction of *para* substituents on the aryl ring, either electron donor or electron withdrawing groups, did not affect the efficiency of the radical cascade. Thus, precursors **295** and **296** delivered the desired guanidines **315** and **316** with the same 82 % yield. Naphtyl derivative **298** and pyridyl **301** cyclized successfully, yielding the corresponding polyheterocyclic guanidines **318** and **320** in 81 and 71 % yield respectively. The thiophene ring could also serve as final radical trap but proved more fragile under our reaction conditions. The

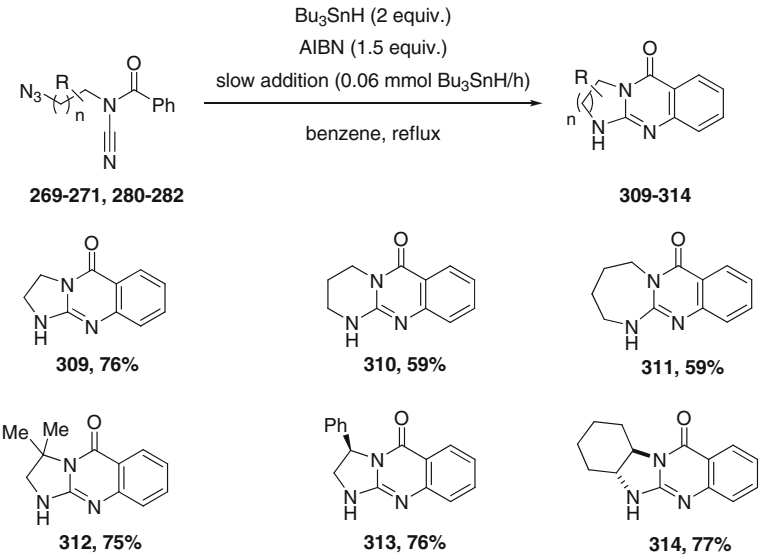

Fig. 2.68 Scope 1 of the guanidine synthesis

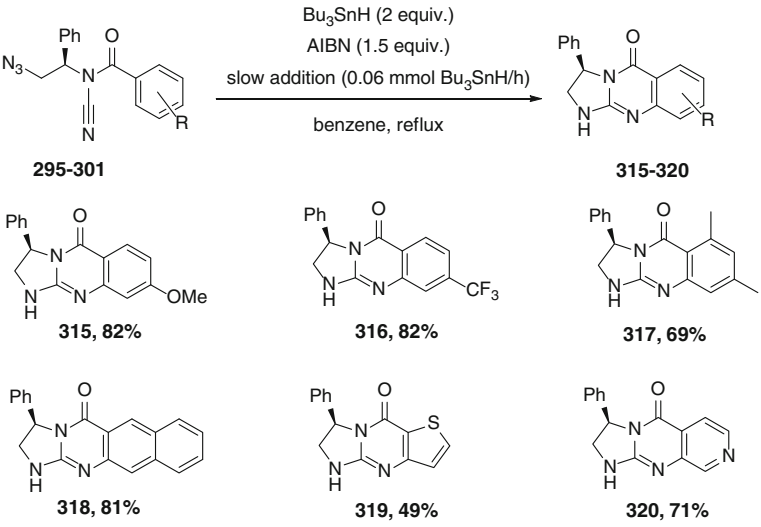

Fig. 2.69 Scope 2 of the guanidine synthesis

corresponding guanidine **319** was only isolated in 49 % yield, and the crude NMR showed that some degradation had occurred during the cyclization. Finally, the cascade could also end with the extrusion of a methyl radical, as demonstrated by the formation of desmethyl adduct **317** from precursor **299**.

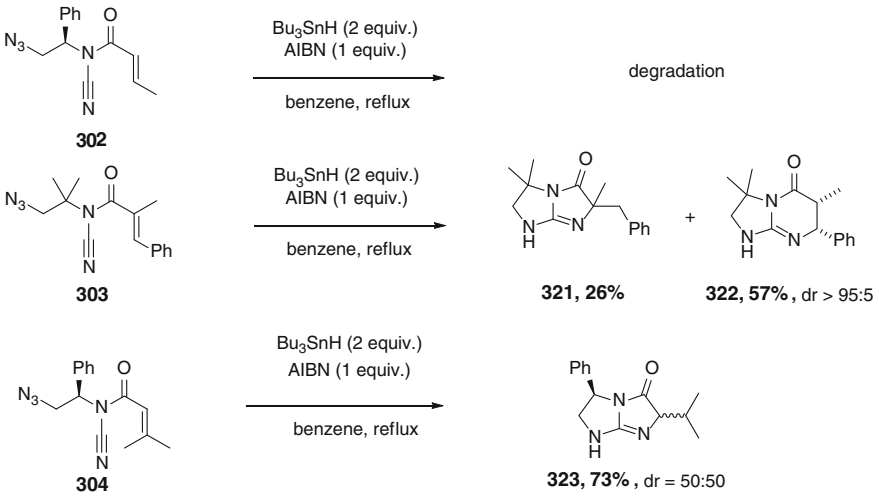

Fig. 2.70 Cyclization of *N*-enoyl cyanamides

Subsequently, we examined the possibility of replacing the final aryl acceptor with an olefin (Fig. 2.70). Cyclization of precursor **302** bearing a disubstituted activated double bond afforded mainly degradation. The stability of the precursors in our reaction conditions seemed to be highly influenced by the substitution patterns of the olefins, since when we used precursor **303** bearing a trisubstituted double bond, the cascade occur cleanly. Two bicyclic guanidines were isolated **321** (26 %) showing a 5,5 framework arising from final 5-*exo-trig* cyclization and **322** (57 %) possessing a 5,6 framework arising from final 6-*endo-trig* cyclization followed by a diastereoselective hydrogen transfer. Precursor **304** behaved equally well and allowed us to obtain selectively the 5-*exo-trig* final cyclization, delivering guanidine **323** in 73 % yield.

Finally, we tested the cyclization of arylazide precursor **308**. Unfortunately only degradation was observed in our previous conditions (Fig. 2.71). One explication could be that aryl azides have been reported to undergo [3+2] cycloadditions with cyanamides at only 60 °C (the temperature required for the same reactions with alkyl cyanamides are >130 °C) [62]. The corresponding tetrazoles are besides known to be unstable when they are substituted with electron withdrawing group, which would be the case with our precursor. Heating **308** in refluxing benzene could thus possibly lead to tetrazole **324** that would further decompose. In order to extend our methodology to aryl azide, we consequently have to develop conditions which allow an efficient cascade at room temperature. Liu has recently developed a methodology for the generation of aminyl radical by visible light triggered reduction of arylazide under $Ru(bpy)_3$ catalysis, at room temperature [63]. We plan to test these mild conditions for the cyclization of **308**.

To conclude, we reported the first radical synthesis of cyanamides, which was achieved via addition of aminyl radicals on cyanamides as starting point of a

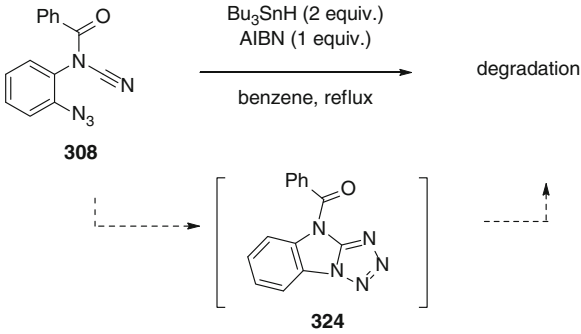

Fig. 2.71 Attempt to cyclize aryl azide precursor

radical cascade [64]. Most of the bicyclic and tricyclic guanidines we have synthesized have not been described previously and might possess interesting biological properties as DNA intercalating agents for example. We are currently trying to find collaborations to have them tested.

As perspectives, owing to the wide scope of products accessible via our methodology, we could try to design new chiral organocatalysts; even if the reduction of the carbonyl function present in our guanidines would probably be a prerequisite to employ them as chiral bases. The development of an intermolecular version of this reaction, starting from an azide and a *N*-acylcyanamide would allow a huge extension of the scope and should also be studied. Finally, we can envisage testing the reactivity of heteroatom-centered radicals with cyanamides, such as sulfur, silicium or phosphorous radicals.

References

1. Amin, A. H., & Mehta, D. R. (1959). *Nature, 183*, 1317–1318.
2. Al-Shamma, A., Drake, S., Flynn, D. L., Mitscher, L. A., Park, Y. H., Rao, G. S. R., et al. (1981). *Journal of Natural Products, 44*, 745–747.
3. Mori, M., Kobayashi, H., Kimura, M., & Ban, Y. (1997). *Heterocycles, 46*, 541–543.
4. Akazome, M., Kondo, T., & Watanabe, Y. (1993). *Journal of Organic Chemistry, 58*, 310–312.
5. Takeuchi, H., Hagiwara, S., & Eguchi, S. (1989). *Tetrahedron, 45*, 6375–6378.
6. Bowman, W. R., Elsegood, M. R. J., Stein, T., & Weaver, G. W. (2007). *Organic & Biomolecular Chemistry, 5*, 103–113.
7. Johns, S. R., & Lamberton, J. A. (1965). *Chemical Commun*ications, 267–269.
8. Hart, N. K., Johns, S. R., & Lamberton, J. A. (1971). *Australian Journal of Chemistry, 24*, 223–224.
9. Liu, J. F., Wilson, C. J., Ye, P., Sprague, K., Sargent, K., Si, Y., et al. (2006). *Bioorganic & Medicinal Chemistry Letters, 16*, 686–690.
10. Hermecz, I., Vasvari-Debreczy, L., Horvath, A., Balogh, M., Kökösi, J., DeVos, C., et al. (1987). *Journal of Medicinal Chemistry, 30*, 1543–1549.
11. Elmuradov, B. Z., & Shakhidoyatov, K. M. (2004). *Chem. Nat. Comp., 40*, 496–498.
12. Minin, P. L., & Walton, J. C. (2003). *Journal of Organic Chemistry, 68*, 2960–2963.

13. Bowman, W. R., Stephenson, P. T., Terrett, N. K., & Young, A. R. (1995). *Tetrahedron, 51*, 7959–7980.
14. Servais, A., Azzouz, M., Lopes, D., Courillon, C., & Malacria, M. (2007). *Angewandte Chemie International Edition, 46*, 576–579.
15. Cockerill, A. F., Deacon, A., Harrison, R. G., Osborne, D. J., Prime, D. M., & Ross, W. J., et al. (1976). *Synthesis-Stuttgart*, 591–593.
16. Munbunjong, W., Lee, E. H., Chavasiri, W., & Jang, D. O. (2005). *Tetrahedron Letters, 46*, 8769–8771.
17. Coulomb, J., Certal, V., Larraufie, M.-H., Ollivier, C., Corbet, J.-P., Mignani, G., et al. (2009). *Chemistry–A European Journal, 15*, 10225–10232.
18. Shanks, D., Berlin, S., Besev, M., Ottosson, H., & Engman, L. (2004). *Journal of Organic Chemistry, 69*, 1487–1491.
19. Larraufie, M.-H., Malacria, M., Courillon, C., Ollivier, C., Fensterbank, L., & Lacôte, E. (2013). *Tetrahedron.* doi:10.1016. Copyright 2013 Elsevier (in press).
20. Wu, X., Qin, G., Cheung, K. K., & Cheng, K. F. (1997). *Tetrahedron, 53*, 13323–13328.
21. Molina, P., Tarraga, A., Gonzales-Tejero, A., Rioja, I., Ubeda, A., Terencio, M. C., et al. (2001). *Natural Products, 64*, 1297–1300.
22. Sugiyama, H., Yokokawa, F., & Shiori, T. (2000). *Organic Letters, 14*, 2149–2152.
23. Klopp, A. H., & Wright, G. F. (1939). *Journal of Organic Chemistry, 4*, 142–149.
24. Mc Elvain, S. M., & Mc Leish, W. L. (1955). *Journal of the American Chemical Society, 77*, 3786–3789.
25. Iwai, I., Iwashige, T., Yura, R., Nakamura, N., & Shinozaki, K. (1964). *Chemical & Pharmaceutical Bulletin, 12*, 1446–1451.
26. Mayo, F. R. (1968). *Journal of the American Chemical Society, 90*, 1289–1295.
27. Chong, Y. K., Rizzardo, E., & Solomon, D. H. (1983). *Journal of the American Chemical Society, 105*, 7761–7762.
28. Walton, J. C., & Studer, A. (2005). *Accounts of Chemical Research, 38*, 794–802.
29. Zytowski, T., & Fischer, H. (1997). *Journal of the American Chemical Society, 119*, 12669–12878.
30. Stefani, A. P., & Szwarc, M. (1962). *Journal of the American Chemical Society, 84*, 3661–3666.
31. Whittemore, I. M., Stefani, A. P., & Szwarc, M. (1962). *Journal of the American Chemical Society, 84*, 3799–3803.
32. Dolbier, W. R, Jr. (2005). *J. Fluor. Chem., 126*, 157–163.
33. Bégué, J. P., & Bonnet-Delpon, D. (2006). *J. Fluor. Chem., 127*, 992–1012.
34. Kirk, K. L. (2006). *J. Fluor. Chem., 127*, 1013–1029.
35. Billard T, & Langlois B. R. (2007). *European Journal of Organic Chemistry,* 891–897.
36. Ma, J.-A., & Cahard, D. (2004). *Chemical Reviews, 104*, 6119–6146.
37. Bertrand, F., Pevere, V., Quiclet-Sire, B., & Zard, S. Z. (2001). *Organic Letters, 3*, 1069–1071. References therein.
38. Larraufie, M.-H., Pellet, R., Fensterbank, L., Goddard, J.-P., Lacôte, E., Malacria, M., et al. (2011). *Angewandte Chemie International Edition, 50*, 4463–4466.
39. Musa, O. M., Horner, J. H., Shahin, H., & Newcomb, M. (1996). *Journal of the American Chemical Society, 118*, 3862–3868.
40. Hart, N. K., Johns, S. R., & Lamberton, J. A. (1969). *Chemical Communications*, 1484–1485.
41. Palmblad, J., et al. (2008). *International Journal of Medicine and Science, 5*, 87–91.
42. Kashman, Y., Hirsh, S., McConnell, O. J., Ohtani, I., Kusumi, T., & Kakisawa, H. (1989). *Journal of the American Chemical Society, 111*, 8925–8926.
43. Blondeau, P., Segura, M., Perez-Fernandez, R., & de Mendoza, J. (2007). *Chemical Society Reviews, 36*, 198–210.
44. Galan, A., Andreu, D., Echavarren, A. M., Prados, P., & de Mendoza, J. (1992). *Journal of the American Chemical Society, 114*, 1511–1512.
45. Ishikawa, T., & Isobe, T. (2002). *Chemistry–A European Journal, 8*, 553–557.
46. Corey, E. J., & Grogan, M. J. (1999). *Organic Letters, 1*, 157–160.

47. Zard, S. Z. (2008). *Chemical Society Reviews, 37*, 1603–1618.
48. Baralle, A., Baroudi, A., Daniel, M., Fensterbank, L., Goddard, J.-P., & Lacôte, E., et al. (2012). In C. Chatgilialoglu & A. Studer (Eds.), *Encyclopedia of radicals in chemistry, biology and materials.* New York: Wiley.
49. Heuger, G., Kalsow, S., & Göttlich, R. (2002). *European Journal of Organic Chemistry, 11*, 1848–1854.
50. Noack, M., & Göttlich, R. (2002). *Chemical Communications*, 536–537.
51. Kemper, J., & Studer, A. (2005). *Angewandte Chemie International Edition, 44*, 4914–4917.
52. Newcomb, M., Marquardt, D. J., & Deeb, T. M. (1990). *Tetrahedron, 46*, 2329–2344.
53. Liu, F., Liu, K., Yuan, X., & Li, C. (2007). *Journal of Organic Chemistry, 72*, 10231–10234.
54. Sherman, E. S., Chemler, S. R., Boon Tan, T., & Gerlits, O. (2004). *Organic Letters, 6*, 1573–1575.
55. Chemler, S. R., & Fuller, P. H. (2007). *Chemical Society Reviews, 36*, 1153–1160.
56. Minozzi, M., Nanni, D., & Spagnolo, P. (2009). *Chemistry–A European Journal, 15*, 7830–7840.
57. Benati, L., Bencivenni, G., Leardini, R., Minozzi, M., Nanni, D., Scialpi, R., et al. (2004). *Organic Letters, 6*, 417–420.
58. Lee, J. W., Jun, S. I., & Kim, K. (2001). *Tetrahedron Letters, 42*, 2709–2711.
59. Wannaporn, D., & Ishikawa, T. (2005). *Molecular Diversity, 9*, 321–331.
60. Hall, J. H., & Patterson, E. (1967). *Journal of the American Chemical Society, 89*, 5856–5961.
61. Ha, C., Musa, O. M., Martinez, F. N., & Newcomb, M. (1997). *Journal of Organic Chemistry, 62*, 2704–2710.
62. Demko, Z., & Sharpless, K. B. (2001). *Organic Letters, 3*, 4091–4094.
63. Chen, Y., Kamlet, A. S., Steinman, J. B., & Liu, D. R. (2011). *Nature Chem*, *3*, 146–153.
64. Larraufie, M.-H., Ollivier, C., Fensterbank, L., Malacria, M., & Lacôte, E. (2010). *Angewandte Chemie International Edition, 49*, 2178–2181.

Chapter 3
Supporting Information

3.1 General Remarks

Reactions were carried out under argon, with magnetic stirring and redistilled solvents. THF and Et_2O were distilled from sodium/benzophenone. CH_2Cl_2, acetonitrile, NEt_3 and *t*-BuOH were distilled from CaH_2. Benzene and toluene were distilled from sodium/potassium amalgam. 2,2-Azobis(2-methylpropionitrile) (AIBN) was precipitated in acetone at 0 °C. Thin layer chromatography (TLC) was performed on Merck 60 F254 silica gel. Merck Geduran SI 60 Å silica gel (35–70 mm) was used for column chromatography. The melting points reported were measured with a Reichert hot stage apparatus and are uncorrected. IR spectra were recorded with a Bruker Tensor 27 ATR diamant PIKE spectrometer. Optical rotations were measured using a Perkin-Elmer 341 polarimeter. ^1H, ^{13}C and ^{19}F NMR spectra were recorded at 400, 100 and 377 MHz respectively, using a Bruker 400 AVANCE spectrometer fitted with a BBFO probehead. Chemical shifts are given in ppm using the $CDCl_3$ or the d_4-MeOD signal as reference ($^1H = 7.26$ ppm, $^{13}C = 77.16$ ppm and $^1H = 3.31$ ppm, $^{13}C = 49.00$ ppm respectively). Unless noted, NMR spectra were recorded in $CDCl_3$ at 300 K. The terms m, s, d, t, q, quint., and sext. represent multiplet, singlet, doublet, triplet, quadruplet, quintuplet, and sextuplet, respectively, and the term br means a broad signal. Exact masses were recorded at UPMC by the laboratory of Prof. J.-C. Tabet (UMR 7201) (electrospray source).

3.2 Preparation and Cyclization of Alkyl Precursors

3.2.1 General Procedures

General procedure 1 (GP1): Conversion of alkyl bromides into phenylseleno derivatives [1]

M.-H. Larraufie, *Development of New Radical Cascades and Multi-Component Reactions*, Springer Theses, DOI: 10.1007/978-3-319-01324-4_3,

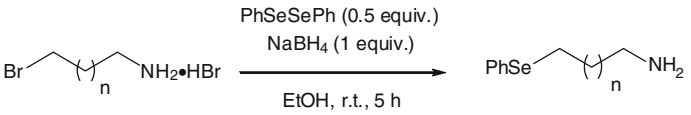

To a solution of diphenyldiselenide (0. 5 equiv) in EtOH (0,02 M) at r.t. was added $NaBH_4$ (1 equiv.). The reaction mixture was stirred at r.t. during 30 min, then a solution of the amine bromide hydrobromide (1 equiv.) in EtOH (0.2 M) was added. The reaction mixture was stirred under reflux during 4 h. Aqueous NaOH 1 M was added and the amine was extracted two times with CH_2Cl_2. The combined organic layers were washed with water, dried over $MgSO_4$ and concentrated *in vacuo* to afford the desired phenyl seleno derivative as an orange oil.

General Procedure 2 (GP2): Preparation of phthalimides

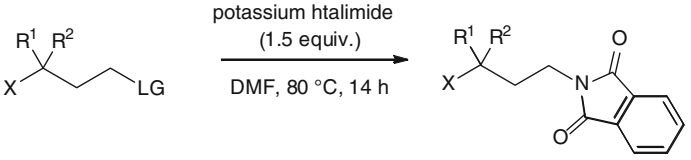

To a solution of halide (1 equiv.) in DMF (0.6 M) was added potassium phthalimide (1.5 equiv.). After 3 h at 90 °C, the mixture was quenched with water. The aqueous layer was then extracted with Et_2O. The organic extracts were combined, dried over $MgSO_4$, and concentrated under reduced pressure. The residue was purified by flash column chromatography to afford the desired phthalimide.

General Procedure 3 (GP3): Preparation of amines from phthalimides

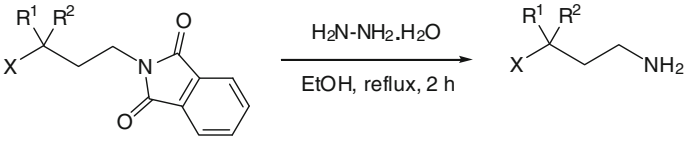

To a solution of phthalimide (1 equiv.) in EtOH (0.1 M) was added hydrazine monohydrate (2 equiv.). After refluxing for 2 h, a solution of HCl 6 M was added. The mixture was filtered and the filtrate was neutralized by a solution of NaOH 2 M. The aqueous layer was then extracted with Et_2O. The organic extracts were combined, dried over $MgSO_4$, and concentrated under reduced pressure to afford the desired amine.

General procedure 4 (GP4): Benzoylation of seleno amines

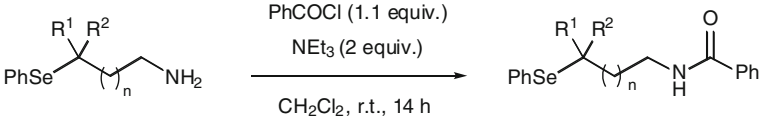

To a solution of seleno amine (1 equiv.) in CH_2Cl_2 (0.1 M) at 0 °C was added NEt_3 (2 equiv.), and 15 min later, benzoyl chloride (1.1 equiv.). The reaction mixture was stirred at r.t. during 14 h, then hydrolyzed by a saturated solution of NH_4Cl. The aqueous layer was extracted two times with CH_2Cl_2. The combined organic layers were washed with water, dried over $MgSO_4$ and concentrated *in vacuo*. Purification by flash column chromatography afforded the seleno amide as a white solid.

General procedure 5 (GP5): Preparation of *N*-acylcyanamides

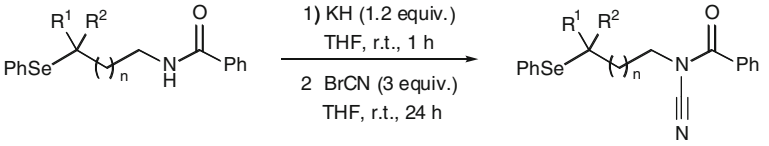

To freshly degreased KH (1.2 equiv.) was added a solution of seleno amide (1 equiv.) in THF (0.14 M) at r.t.. The reaction mixture was stirred during 45 min, then a solution of BrCN (3 equiv.) in CH_2Cl_2 (3.0 M) was added. The resulting reaction mixture was stirred at r.t. during 24 h and filtered through a short pad of silica. The filtrate was concentrated under reduced pressure and purified by flash column chromatography to afford the cyanamide as a pale yellow oil.

Caution: Cyanogen bromide is volatile, and readily absorbed through the skin or gastrointestinal tract. Therefore, toxic exposure may occur by inhalation, physical contact, or ingestion. It is acutely toxic, causing a variety of nonspecific symptoms. Exposure to even small amounts may cause convulsions or death. LD_{50} orally in rats is reported as 25–50 mg/kg. It must be carefully manipulated under a ventilated hood. All the glassware must be washed with a NaOH solution (0.5 M) and bleach (10 %).

General procedure 6 (GP6): Cyclization of *N*-acylcyanamides

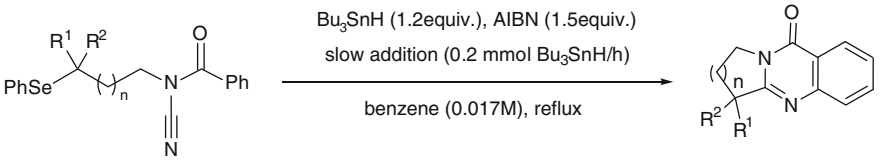

To a degassed solution of *N*-acylcyanamide (1 equiv.) and AIBN (0.3 equiv.) in benzene (final concentration = 0.017 M, 75 % final volume) under reflux was added Bu_3SnH (2 equiv.) and AIBN (1.2 equiv.) in benzene (25 % final volume) over 2 h (0.2 mmol Bu_3SnH/h). The reaction mixture was refluxed for an additional hour, cooled to r.t. and concentrated under reduced pressure. Purification of the residue by flash column chromatography afforded the cyclization product.

3.2.2 Alkyl Seleno Precursors

3-Phenylselanyl-1-propylamine (134a)

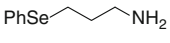

$C_9H_{13}NSe$ M = 214.17 g/mol

Following **GP1** with 3-bromopropylamine hydrobromide (7 mmol; 1.53 g), **134a** was isolated as an orange oil (1.33 g; 89 %). Spectral data are in accordance with those reported in the literature [1].

^{1}H NMR (400 MHz, $CDCl_3$): δ = 1.46 (br s, 2 H, NH_2), 1.79–1.86 (m, 2 H, PhSe–CH_2–CH_2), 2.78 (t, J = 7.2 Hz, 2 H, PhSe–CH_2), 2.94 (t, J = 7.1 Hz, 2 H, NH_2–CH_2), 7.21–7.26 (m, 3 H, arom.), 7.47–7.49 (m, 2 H, arom.); ^{13}C NMR (100 MHz, $CDCl_3$): δ = 25.0 (PhSe–CH_2–CH_2), 29.7 (PhSe–CH_2), 41.6 (NH_2–CH_2), 126.8 (CH arom.), 129.2 (2 CH arom.), 130.2 (C arom.), 132.4 (2 CH arom.).

4-Phenylselanyl-butylamine (134b)

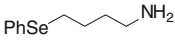

$C_{10}H_{15}NSe$ M = 228.19 g/mol

4-Aminobutan-1-ol (3.9 mmol; 350 mg) was refluxed for 3 h in an aqueous solution of HBr 48 % wt (30 mL). After concentration *in vacuo*, 4-bromobutylamine hydrobromide was obtained as a white solid. Following **GP1** with crude 4-bromobutylamine hydrobromide, **134b** was isolated as an orange oil (606 mg; 69 %). Spectral data are in accordance with those reported in the literature [1].

^{1}H NMR (400 MHz, $CDCl_3$): δ = 1.22 (br s, 2 H, NH_2), 1.45–1.49 (m, 2 H, PhSe–CH_2–CH_2), 1.62–1.70 (m, 2 H, NH_2–CH_2–CH_2), 2.60 (t, J = 7.0 Hz, 2 H, PhSe–CH_2), 2.84 (t, J = 7.3 Hz, 2 H, NH_2–CH_2), 7.12–7.18 (m, 3 H, arom.), 7.40–7.42 (m, 2 H, arom.); ^{13}C NMR (100 MHz, $CDCl_3$): δ = 27.3, 27.5 (PhSe–CH_2–CH_2 + NH_2–CH_2–CH_2), 33.6 (PhSe–CH_2), 41.4 (NH_2–CH_2), 126.5 (CH arom.), 128.8 (2 CH arom.), 130.3 (C arom.), 132.2 (2 CH arom.).

2-(3-Chloro-butyl)-isoindole-1,3-dione (141)

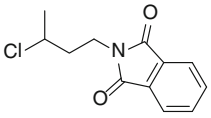

$C_{12}H_{12}NO_2Cl$ M = 237.68 g/mol

To a solution of sodium iodide (60 mmol; 1 equiv.; 8.99 g) in acetone (20 mL) was added 1,3-dichlorobutane (60 mmol; 1 equiv; 6.83 mL). The reaction mixture was stirred for 2 h at r.t. and filtered. The filtrate was concentrated under reduced pressure and Et_2O (30 mL) was added to precipitate inorganic salts. After a second filtration the filtrate was concentrated under pressure to afford 3-chloro-1-iodobutane **140** (8.50 g; 65 %) as a yellow oil [2]. Following **GP2** with **140** (8.72 mmol, 1.90 g),

2-(3-chloro-butyl)-isoindole-1,3-dione **141** (petroleum ether: Et_2O = 10: 1; 1.84 g; 89 %) was isolated as a white solid.

IR (ATR): ν = 2,922, 1,764, 1,698, 1,494, 1,443, 1,401, 1,380, 1,290, 1,085, 959, 712 cm^{-1}; ^1H NMR (400 MHz, $CDCl_3$): δ = 1.55 (d, J = 6.6 Hz, 3 H, Me), 2.02–2.12 (m, 2 H, N–CH_2–CH_2), 3.77–3.91 (m, 2 H, N–CH_2), 3.99–4.08 (m, 1 H, MeC*H*), 7.69–7.71 (m, 2 H, arom.), 7.81–7.84 (m, 2 H, arom.); ^{13}C NMR (100 MHz, $CDCl_3$): δ = 25.4 (Me), 35.8 (N–CH_2–*C*H_2), 38.8 (N–CH_2), 55.7 (Me*C*H), 123.4 (2 CH arom.), 132.2 (2 C arom.), 134.1 (2 CH arom.), 168.3 (2 CO); HRMS calcd. for $C_{12}H_{12}NO_2ClNa$ ($[M + Na]^+$) 260.0449, found 260.0449.

3-phenylselanyl-butylamine (143)

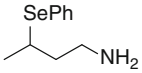

$C_{10}H_{15}NSe$ M = 228.20 g/mol

To a solution of sodium phenylselenolate (8.4 mmol; 1 equiv.; 1.50 g) in DMF (8 mL) was added **141** (8.4 mmol; 1 equiv.; 2.00 g). After 14 h at 110 °C, the mixture was quenched with water. The aqueous layer was then extracted with CH_2Cl_2 (15 mL). The organic extracts were combined, dried over $MgSO_4$, and concentrated under reduced pressure to afford 2-(3-phenylselanyl-butyl)-isoindole-1,3-dione **142** (2.02 g; 67 %) as a pale yellow oil. Following **GP3** with **142** (4.5 mmol; 1.63 g), 3-phenylselanyl-butylamine **143** (780 mg; 76 %) was isolated as a pale yellow oil.

IR (ATR): ν = 3,295, 3,024, 2,950, 2,917, 2,860, 1,649, 1,578, 1,476, 1,436, 1,375, 1,253, 1,066, 1,021, 739, 691 cm^{-1}; ^1H NMR (400 MHz, $CDCl_3$): δ = 1.31 (s, 2 H, NH_2), 1.45 (d, J = 6.8 Hz, 3 H, Me), 1.72–1.84 (m, 2 H, N–CH_2–CH_2), 2.84–2.91 (m, 2 H, N–CH_2), 3.39 (sextet, J = 6.9 Hz, 1 H, Se–CH), 7.25–7.30 (m, 3 H, arom.), 7.55–7.57 (m, 2 H, arom.). ^{13}C NMR (100 MHz, $CDCl_3$): δ = 22.6 (CH–*Me*), 37.2 (Se–CH), 40.6 (N–CH_2–*C*H_2), 41.6 (N–CH_2), 127.6 (2 CH arom.), 129.1 (CH arom.), 129.2 (C arom.), 135.2 (2 CH arom.); HRMS calcd. for $C_{10}H_{16}NSe$ ($[M + H]^+$) 230.0442, found 230.0440.

2-(3-Methyl-3-phenylselanyl-butyl)-isoindole-1,3-dione (152)

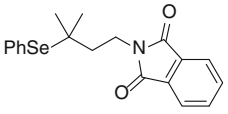

$C_{19}H_{19}NO_2Se$ M = 372.32 g/mol

Following **GP2** with 3,3-dimethylallylbromide **146** (20.0 mmol; 2.66 mL), **147** (petroleum ether: Et_2O = 6: 2; 3.20 g; 74 %) was isolated as a white solid [3]. A solution of **147** (12.5 mmol; 1 equiv.; 2.70 g) and HBr (33 % in AcOH, 20 mL) was stirred at r.t. for 2 h. Water was then added and the aqueous layer was extracted with Et_2O. The organic extracts were combined, dried over $MgSO_4$ and concentrated under reduced pressure to afford **148** (3.45 g; 93 %) as a white solid. To a solution of indium (2.7 mmol; 1.3 equiv.; 313 mg) and diphenyl diselenide

(2.7 mmol; 1.3 equiv.; 844 mg) in CH_2Cl_2 (30 mL), was added **148** (2.1 mmol; 616 mg). The reaction mixture was refluxed for 1 h, then hydrolyzed with a 1 M HCl solution. The aqueous layer was extracted with CH_2Cl_2. The combined organic layers were washed with water, dried over $MgSO_4$ and concentrated *in vacuo*. Purification by flash column chromatography (petroleum ether: EtOAc = 10: 3) afforded **152** (490 mg; 63 %) as a white solid [4].

IR (ATR): ν = 1,767, 1,705, 1,396, 1,365, 1,331, 1,143, 722 cm^{-1}; ^1H NMR (400 MHz, $CDCl_3$): δ = 1.43 (s, 6 H, CMe_2), 1.78–1.82 (m, 2 H, N–CH_2–CH_2), 3.93–3.97 (m, 2 H, N–CH_2), 7.30–7.36 (m, 3 H, arom.), 7.68–7.76 (m, 4 H, arom.), 7.83–7.85 (m, 2 H, arom.); ^{13}C NMR (100 MHz, $CDCl_3$): δ = 29.9 (CMe_2), 35.6 (N–CH_2–CH_2), 40.9 (CMe$_2$), 44.9 (N–CH_2), 123.3 (2 CH arom.), 127.4 (C arom.), 128.8 (3 CH arom.), 132.3 (2 C arom.), 134.0 (2 CH arom.), 138.5 (2 CH arom.), 168.3 (2 CO); HRMS calcd. for $C_{19}H_{19}NO_2SeNa$ ($[M + Na]^+$) 396.0473, found 396.0470.

3-Phenylselanyl-butylamine (153)

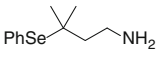

$C_{11}H_{17}NSe$ M = 242.22 g/mol

Following **GP3** with **152** (1.05 mmol; 390 mg), 3-methyl-3-phenylselanyl-butylamine **153** (205 mg; 81 %) was isolated as a yellow oil.

IR (ATR): ν = 2,922, 1,577, 1,465, 1,435, 1,364, 1,121, 1,022, 1,000, 739, 693 cm^{-1}; ^1H NMR (400 MHz, $CDCl_3$): δ = 1.37 (s, 6 H, CMe_2), 1.42 (s, 2 H, NH_2), 1.68–1.72 (m, 2 H, N–CH_2–CH_2), 2.89 (t, J = 8.0 Hz, 2 H, N–CH_2), 7.28–7.32 (m, 2 H, arom.), 7.34–7.37 (m, 1 H, arom.), 7.61–7.63 (m, 2 H, arom.). ^{13}C NMR (100 MHz, $CDCl_3$): δ = 30.23 (CMe_2), 39.2 (N–CH_2–CH_2), 46.0 (CMe$_2$), 47.4 (N–CH_2), 127.8 (C arom.), 128.7 (2 CH arom.), 128.8 (CH arom.), 138.3 (2 CH arom.); HRMS calcd. for $C_{11}H_{18}NSe$ ($[M + H]^+$) 244.0599, found 244.0595.

***N*-(3-Phenylselanyl-propyl)-benzamide (133a)**

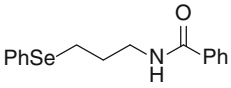

$C_{16}H_{17}NOSe$ M = 318.27 g/mol

Following **GP4** with **134a** (7.47 mmol; 1.60 g), **133a** was purified by flash column chromatography (petroleum ether: EtOAc = 8: 2) and isolated as a white solid (1.85 g; 78 %). Spectral data are in accordance with those reported in the literature [5].

^1H NMR (400 MHz, MeOD): δ = 1.95–2.00 (m, 2 H, PhSe–CH_2–CH_2), 2.97 (t, J = 7.2 Hz, 2 H, PhSe–CH_2), 3.47 (t, J = 7.0 Hz, 2 H, NH–CH_2), 7.22–7.26 (m, 3 H, arom.), 7.42–7.47 (m, 2 H, arom.), 7.49–7.57 (m, 3 H, arom.), 7.78–7.80 (m, 2 H, arom.); ^{13}C NMR (100 MHz, MeOD): δ = 25.6 (PhSe–CH_2–CH_2), 31.2 (PhSe–CH_2), 40.9 (NH–CH_2), 127.9 (CH arom.), 128.3 (2 CH arom.), 129.6 (2 CH arom.), 130.2 (2 CH arom.), 131.5 (C arom.), 132.6 (CH arom.), 133.7 (2 CH arom.), 135.7 (C arom.), 170.3 (CO).

***N*-(4-Phenylselanyl-butyl)-benzamide (133b)**

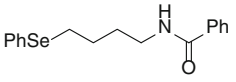

$C_{17}H_{19}NOSe$ M = 332.30 g/mol

Following **GP4** with **134b** (1.07 mmol; 244 mg), **133a** was purified by flash column chromatography (petroleum ether:EtOAc = 5:1) and isolated as a white solid (290 mg; 82 %). Spectral data are in accordance with those reported in the literature [5].

^{1}H NMR (400 MHz, $CDCl_3$): δ = 1.73–1.82 (m, 4 H, PhSe–CH_2–CH_2–CH_2), 2.96 (t, J = 6.9 Hz, 2 H, PhSe–CH_2), 3.46 (q, J = 6.8 Hz, 2 H, NH–CH_2), 7.23–7.26 (m, 3 H, arom.), 7.41–7.50 (m, 5 H, arom.), 7.71–7.72 (m, 2 H, arom.); ^{13}C NMR (100 MHz, $CDCl_3$): δ = 27.5 (2 CH_2, PhSe–CH_2–*C*H_2–*C*H_2), 29.8 (PhSe–*C*H_2), 39.5 (NH–*C*H_2), 127.0 (3 CH arom.), 128.7 (2 CH arom.), 129.2 (2 CH arom.), 130.2 (C arom.), 131.5 (CH arom.), 133.8 (2 CH arom.), 134.8 (C arom.), 167.7 (CO).

***N*-cyano-(3-Phenylselanyl-propyl)-benzamide (132a)**

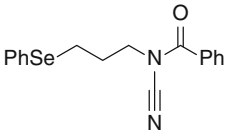

$C_{17}H_{16}N_2OSe$ M = 343.29 g/mol

Following **GP5** with **133a** (1.64 mmol; 524 mg), **132a** was purified by flash column chromatography (petroleum ether:EtOAc = 3:1) and isolated as a pale yellow oil (491 mg; 87 %).

IR (neat): ν = 2,230, 1,700, 1,578, 1,477, 1,447, 1,437, 1,269, 1,113, 1,021, 691, 670 cm^{-1}; ^{1}H NMR (400 MHz, $CDCl_3$): δ = 2.17–2.24 (m, 2 H, PhSe–CH_2–CH_2), 2.98 (t, J = 7.1 Hz, 2 H, PhSe–CH_2), 3.89 (t, J = 7.0 Hz, 2 H, N–CH_2), 7.26–7.30 (m, 3 H, arom.), 7.47–7.50 (m, 2 H, arom.), 7.54–7.60 (m, 3 H, arom.), 7.78–7.80 (m, 2 H, arom.); ^{13}C NMR (100 MHz, $CDCl_3$): δ = 24.2 (PhSe–CH_2–*C*H_2), 28.2 (PhSe–*C*H_2), 47.7 (N–*C*H_2), 111.1 (CN), 127.6 (CH arom.), 128.7 (4 CH arom.), 129.3 (2 CH arom.), 129.4 (C arom.), 131.0 (C arom.), 133.3 (CH arom.), 133.4 (2 CH arom.), 168.5 (CO); HRMS calcd. for $C_{17}H_{16}N_2OSeNa$ ([M + Na]$^+$) 367.0321, found 367.0321.

***N*-cyano-(3-Phenylselanyl-propyl)-benzamide (132b)**

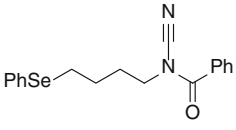

$C_{18}H_{18}N_2OSe$ M = 357.32 g/mol

Following **GP5** with **133b** (0.85 mmol; 283 mg), **132b** was purified by flash column chromatography (petroleum ether:EtOAc = 7:3) and isolated as a pale yellow oil (258 mg; 85 %).

IR (neat): ν = 2,928, 2,232, 1,705, 1,438, 1,329, 1,279, 730, 711, 686, 652 cm^{-1}; ^1H NMR (400 MHz, $CDCl_3$): δ = 1.78–1.97 (m, 4 H, PhSe–CH_2–CH_2–CH_2), 2.96 (t, J = 7.1 Hz, 2 H, PhSe–CH_2), 3.77 (t, J = 7.1 Hz, 2 H, N–CH_2), 7.25–7.28 (m, 3 H, arom.), 7.44–7.61 (m, 5 H, arom.), 7.74–7.77 (m, 2 H, arom.); ^{13}C NMR (100 MHz, $CDCl_3$): δ = 26.9, 27.1 (PhSe–CH_2–CH_2–CH_2), 27.8 (PhSe–CH_2), 47.3 (N–CH_2), 111.1 (CN), 127.2 (CH arom.), 128.7 (4 CH arom.), 129.3 (2 CH arom.), 129.8 (C arom.), 131.1 (C arom.), 133.2 (2 CH arom.), 133.3 (2 CH arom.), 168.5 (CO); HRMS calcd. for $C_{18}H_{18}N_2OSeNa$ ($[M + Na]^+$) 381.0477, found 381.0481.

3-Phenylselanyl-butyl-cyanamide (144)

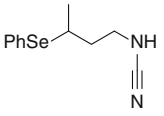

$C_{11}H_{14}N_2Se$ M = 253.20 g/mol

To a solution of cyanogen bromide (1.9 mmol; 1.2 equiv.; 219 mg) in Et_2O (3 mL) at −15 °C was added Na_2CO_3 (3.18 mmol; 2 equiv.; 337 mg) and amine **143** (1.59 mmol; 363 mg). The reaction mixture was stirred for 2 h at −15 °C, allowed to reach r.t., and filtered through a short pad of silica. The filtrate was concentrated under reduced pressure and purified by flash column chromatography (petroleum ether:Et_2O = 1:2) to afford cyanamide **144** as a pale yellow oil (310 mg; 77 %). This product proved unstable and was immediately used for the next step.

IR (neat): ν = 3,198, 2,918, 2,217, 1,578, 1,476, 1,436, 1,375, 1,246, 1,158, 1,066, 1,021, 999, 738, 691 cm^{-1}; ^1H NMR (400 MHz, $CDCl_3$): δ = 1.42 (d, J = 7.0 Hz, 3 H, Me), 1.81–1.87 (m, 2 H, N–CH_2–CH_2), 3.17–3.21 (m, 2 H, N–CH_2), 3.24–3.32 (m, 1 H, Se–CH), 4.35 (br s, 1 H, NH), 7.23–7.29 (m, 3 H, arom.), 7.52–7.54 (m, 2 H, arom.); ^{13}C NMR (100 MHz, $CDCl_3$): δ = 22.5 (Me), 36.1 (Se–CH), 37.1 (N–CH_2–CH_2), 44.5 (N–CH_2), 116.4 (CN), 127.9 (CH arom.), 128.1 (C arom.), 129.1 (2 CH arom.), 135.3 (2 CH arom.); HRMS calcd. for $C_{11}H_{14}N_2SeNa$ ($[M + Na]^+$) 277.0214, found 277.0215.

***N*-Cyano-(3-phenylselanyl-butyl)-benzamide (145)**

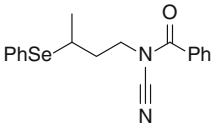

$C_{18}H_{18}N_2OSe$ M = 357.31 g/mol

To a solution of cyanamide **144** (0.75 mmol; 190 mg) in CH_2Cl_2 (20 mL) at 0 °C was added NEt_3 (1.5 mmol; 2 equiv.; 211 μL) and benzoyl chloride (0.97 mmol; 1.3 equiv.; 113 μL). The reaction mixture was stirred 15 min at 0 °C

and 14 h at r.t., concentrated under reduced pressure and purified by flash column chromatography (petroleum ether:Et_2O = 10:2), to afford *N*-acylcyanamide **145** as a white solid (240 mg; 90 %).

Mp: 62–63 °C; IR (neat): ν = 2,954, 2,230, 1,701, 1,579, 1,476, 1,448, 1,345, 1,272, 1,074, 1,022, 909, 788, 732 cm^{-1}; ^1H NMR (400 MHz, $CDCl_3$): δ = 1.51 (d, J = 7.0 Hz, 3 H, Me), 1.99–2.17 (m, 2 H, N–CH_2–CH_2), 3.30 (sext., J = 6.9 Hz, 1H, Se–C*H*), 3.86–4.04 (m, 2 H, N–CH_2), 7.27–7.36 (m, 3 H, arom.), 7.44–7.52 (m, 2 H, arom.), 7.56–7.64 (m, 3 H, arom.), 7.80–7.76 (m, 2 H, arom.); ^{13}C NMR (100 MHz, $CDCl_3$): δ = 22.5 (Me), 35.2 (N–CH_2–*C*H_2), 36.1 (Se–*C*H), 46.7 (N–*C*H_2), 111.1 (CN), 127.9 (C arom.), 128.2 (CH arom.), 128.7 (4 CH arom.), 129.2 (2 CH arom.), 131.0 (C arom.), 133.3 (CH arom.), 135.8 (2 CH arom.), 168.4 (CO); HRMS calcd. for $C_{18}H_{18}ON_2SeNa$ ([M + Na]$^+$) 381.0477, found 381.0479.

***N*-cyano-N-(3-methyl-3-(phenylselanyl)butyl)benzamide (155)**

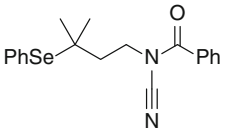

$C_{19}H_{20}N_2OSe$ M = 371.33 g/mol

Following **GP4** with **153** (0.71 mmol; 172 mg), **154** was purified by flash column chromatography (petroleum ether:Et_2O = 1:1) and isolated as a white solid (120 mg; 49 %). Following **GP5** with **154** (0.29 mmol; 100 mg), **155** was purified by flash column chromatography (pentane:Et_2O = 5:1) and isolated as a pale yellow oil (65 mg; 60 %).

Mp: 62–63 °C; IR (neat): ν = 2,956, 2,230, 1,702, 1,599, 1,579, 1,448, 1,345, 1,270, 1,075, 694 cm^{-1}; ^1H NMR (400 MHz, $CDCl_3$): δ = 1.45 (s, 6 H, 2 Me), 1.93–1.97 (m, 2 H, N–CH_2–CH_2), 4.02–4.06 (m, 2 H, N–CH_2), 7.33–7.42 (m, 3 H, arom.), 7.48–7.50 (m, 2 H, arom.), 7.57–7.61 (m, 1 H, arom.), 7.67–7.69 (m, 2 H, arom.), 7.78–7.80 (m, 2 H, arom.); ^{13}C NMR (100 MHz, $CDCl_3$): δ = 30.1 (2 Me), 40.3 (N–CH_2–*C*H_2), 44.2 (Me_2*C*), 46.0 (N–*C*H_2), 111.2 (CN), 127.2 (C arom.), 128.7 (2 CH arom.), 128.7 (2 CH arom.), 129.1 (3 CH arom.), 131.1 (C arom.), 133.3 (CH arom.), 138.4 (2 CH arom.), 168.4 (CO); HRMS calcd. for $C_{19}H_{20}N_2OSeNa$ ([M + Na]$^+$) 395.0633, found 395.0633.

3.2.3 Cyclized Quinazolinones

Deoxyvasicinone (127)

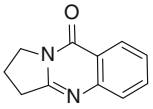

$C_{11}H_{10}N_2O$ M = 186.21 g/mol

Following **GP6** with *N*-acylcyanamide **132a** (1.41 mmol; 484 mg), **127** was purified by flash column chromatography (pentane then CH_2Cl_2:EtOAc = 1:1) and isolated as a white solid (171 mg; 65 %). Spectral data are in accordance with those described in the literature [6].

Mp: 105–106 °C; IR (neat): ν = 2,962, 2,924, 1,670, 1,609, 1,483, 1,424, 1,334, 770, 693 cm^{-1}; ^1H NMR (400 MHz, $CDCl_3$): δ = 2.25 (quin, J = 7.8 Hz, 2 H, N–CH_2–CH_2), 3.14 (t, J = 7.9 Hz, 2 H, C–CH_2), 4.17 (t, J = 7.3 Hz, 2 H, N–CH_2), 7.40 (ddd, J = 7.4, 6.8, 1.3 Hz, 1 H, arom.), 7.59–7.60 (m, 1 H, arom.), 7.66–7.70 (m, 1 H, arom.), 8.23 (dd, J = 8.0, 1.4 Hz, 1 H, arom.). ^{13}C NMR (100 MHz, $CDCl_3$): δ = 19.5 (N–CH_2–CH_2), 32.6 (C–CH_2), 46.5 (N–CH_2), 120.5 (C arom.), 126.2 (CH arom.), 126.4 (CH arom.), 126.8 (CH arom.), 134.1 (CH arom.), 149.2 (C arom.), 159.5 (N–C–N), 161.0 (CO); HRMS calcd. for $C_{11}H_{11}O_1N_2$ ($[M + H]^+$) 187.0866, found 187.0866.

Mackinazolinone (128)

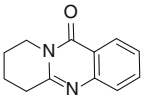

$C_{12}H_{12}N_2O$ M = 200.24 g/mol

Following **GP6** with *N*-acylcyanamide **132b** (0.46 mmol; 164 mg), **128** was purified by flash column chromatography (pentane, then CH_2Cl_2:EtOAc = 1:1) and isolated as a white solid (47 mg; 51 %). Spectral data are in accordance with those described in the literature [6].

Mp: 95–96 °C; IR (neat): ν = 2,955, 1,658, 1,610, 1,583, 1,564, 1,467, 772 cm^{-1}; ^1H NMR (400 MHz, $CDCl_3$): δ = 1.90–2.02 (m, 4 H, N–CH_2–CH_2–CH_2), 2.97 (t, J = 6.7 Hz, 2 H, C–CH_2), 4.06 (t, J = 6.3 Hz, 2 H, N–CH_2), 7.39 (ddd, J = 7.6, 7.0, 1.1 Hz, 1 H, arom.), 7.55–7.58 (m, 1 H, arom.), 7.66–7.69 (m, 1 H, arom.), 8.23 (d, J = 7.3, 1.4 Hz, 1 H, arom.). ^{13}C NMR (100 MHz, $CDCl_3$): δ = 19.4 (N–CH_2–CH_2), 22.2 (C–CH_2–CH_2), 32.1 (C–CH_2), 42.4 (N–CH_2), 120.5 (C arom.), 126.2 (CH arom.), 126.5 (CH arom.), 126.7 (CH arom.), 134.3 (CH arom.), 147.5 (C arom.), 155.0 (N–C–N), 162.3 (CO); HRMS calcd. for $C_{12}H_{13}N_2O$ ($[M + H]^+$) 201.1022, found 201.1023.

α-Methyldeoxyvasicinone (129)

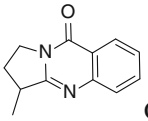

$C_{12}H_{12}N_2O$ M = 200.24 g/mol

Following **GP6** with *N*-acylcyanamide **145** (0.45 mmol; 162 mg), **129** was purified by flash column chromatography (CH_2Cl_2:EtOAc = 10:1 to 1:1) and isolated as a white solid (68 mg; 76 %). Spectral data are in accordance with those described in the literature [7].

Mp: 120–121 °C; IR (neat): ν = 2,965, 2,928, 1,663, 1,609, 1,560, 1,468, 782, 734 cm^{-1}; ^1H NMR (400 MHz, $CDCl_3$): δ = 1.45 (d, J = 7.0 Hz, 3 H, Me), 1.83 (dq, J = 12.9, 8.5 Hz, 1 H, N–CH_2–C*H*H), 2.39–2.51 (m, 1 H, N–CH_2–CH*H*), 3.23–3.33 (m, 1 H, Me–C*H*), 3.91–4.01 (m, 1 H, N–C*H*H), 4.23 (ddd, J = 12.4, 8.7, 3.9 Hz, 1 H, N–CH*H*), 7.40 (ddd, J = 8.2, 6.7, 1.6 Hz, 1 H, arom.), 7.62–7.70 (m, 2 H, arom.), 8.22–8.25 (m, 1 H, arom.). ^{13}C NMR (100 MHz, $CDCl_3$): δ = 17.2 (Me), 28.6 (N–CH_2–*C*H_2), 38.8 (Me–*C*H), 44.6 (N–CH_2), 120.7 (C arom.), 126.2 (CH arom.), 126.4 (CH arom.), 127.0 (CH arom.), 134.1 (CH arom.), 149.4 (C arom.), 161.0 (N–C–N), 162.4 (CO); HRMS calcd. for $C_{12}H_{12}N_2ONa$ ($[M + Na]^+$) 223.0842, found 223.0843.

α,α'-Dimethyldeoxyvasicinone (130)

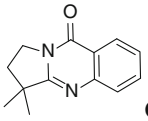

$C_{13}H_{14}N_2O$ M = 214.26 g/mol

Following **GP6** with *N*-acylcyanamide **155** (0.08 mmol; 30 mg), **130** was purified by flash column chromatography (CH_2Cl_2:EtOAc = 10:1 to 1:1) and isolated as a white solid (15 mg; 87 %). Spectral data are in accordance with those described in the literature.

Mp: 128–129 °C; IR (neat): ν = 2,961, 1,671, 1,613, 1,470, 772 cm^{-1}; ^1H NMR (400 MHz, $CDCl_3$): δ = 1.43 (s, 6 H, 2 Me), 2.10 (t, J = 7.2 Hz, 2 H, C–C*H*$_2$), 4.12 (t, J = 7.2 Hz, 2 H, N–C*H*$_2$), 7.41–7.43 (m, 1 H, arom.), 7.70–7.72 (m, 2 H, arom.), 8.28 (d, J = 8.1 Hz, 1 H, arom.). ^{13}C NMR (100 MHz, $CDCl_3$): δ = 26.1 (2 Me), 35.6 (N–CH_2–*C*H_2), 43.2 (N–CH_2), 43.6 (Me_2*C*), 120.9 (C arom.), 126.2 (CH arom.), 126.5 (CH arom.), 127.3 (CH arom.), 134.1 (CH arom.), 149.8 (C arom.), 161.3 (N–C–N), 165.1 (CO). HRMS calcd. for $C_{13}H_{14}N_2ONa$ ($[M + Na]^+$) 237.0998, found 237.0995.

3.3 Preparation and Cyclization of Vinyl Precursors

3.3.1 General Procedures

General procedure 1 (GP1): Preparation of cyanamides

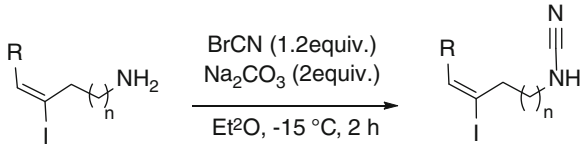

To a solution of cyanogen bromide (1.2 equiv.) in Et_2O (0.5 M) at −15 °C was added Na_2CO_3 (2 equiv.) and the corresponding vinyl iodo amine (1 equiv.). The reaction mixture was stirred for 2 h at −15 °C, allowed to reach r.t., and filtered through a short pad of silica. The filtrate was concentrated under reduced pressure and purified by silica gel flash chromatography to afford the cyanamide.

Caution: Cyanogen bromide is a very toxic reagent and must be carefully manipulated under a ventilated hood. All the glassware must be washed with a NaOH solution (0.5 M) and bleach (10 %).

General procedure 2 (GP2): Preparation of *N*-acylcyanamides

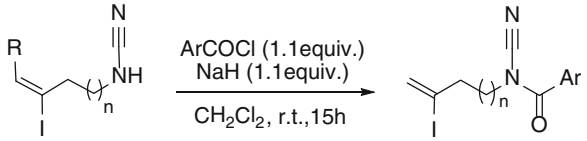

To a solution of cyanamide (1 equiv.) in CH_2Cl_2 (0.05 M) at 0 °C was added the acyl chloride (1.1 equiv.) immediately followed by NaH (1.1 equiv.; [60 % in mineral oil]). The reaction mixture was stirred 15 min at 0 °C and an additional hour at r.t., concentrated under reduced pressure and purified by flash column chromatography to give the *N*-acylcyanamide.

General procedure 3 (GP3): Cyclization of *N*-acylcyanamides (classical conditions)

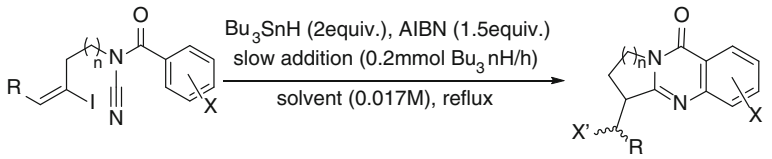

To a degassed solution of *N*-acylcyanamide (1 equiv.) and AIBN (0.3 equiv.) in benzene (*tert*-butanol) (final concentration = 0.017 M, 75 % final volume) under

reflux was added Bu_3SnH (or Bu_3SnD) (2 equiv.) and AIBN (1.2 equiv.) in benzene (*tert*-butanol) (25 % final volume) over 2 h (0.2 mmol Bu_3SnH/h). The reaction mixture was refluxed for an additional hour, cooled to r.t. and concentrated under reduced pressure. Purification of the residue by flash column chromatography afforded the cyclization product(s).

General procedure 4 (GP4): Double tagging experiments

To a degassed solution of *N*-acylcyanamide A (0.5 equiv.) and *N*-acylcyanamide B (0.5 equiv.) and AIBN (0.3 equiv.) in *tert*-butanol (final concentration = 0.017 M, 75 % final volume) under reflux was added Bu_3SnH (2 equiv.) and AIBN (1.2 equiv.) in *tert*-butanol (25 % final volume) over 2 h (0.2 mmol Bu_3SnH/h). The reaction mixture was refluxed for an additional hour, cooled to r.t. and concentrated under reduced pressure. Purification of the residue by flash column chromatography afforded the cyclization product(s).

General procedure 5 (GP5): Cyclization of *N*-acylcyanamides in the presence of benzylidene malonitrile

To a degassed solution of *N*-acylcyanamide (1 equiv.), benzylidene malonitrile (5 equiv.) and AIBN (0.3 equiv.) in benzene (final concentration = 0.017 M, 75 % final volume) under reflux was added Bu_3SnH (2 equiv.) and AIBN (1.2 equiv.) in benzene (25 % final volume) over 2 h (0.2 mmol Bu_3SnH/h). The reaction mixture was refluxed for an additional hour, cooled to r.t. and concentrated under reduced pressure. Purification of the residue by flash column chromatography afforded the cyclization product(s).

3.3.2 Vinyl Iodide Precursors

Toluene-4-sulfonic acid 3-iodo-but-enyl ester (160)

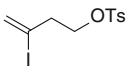

$C_{11}H_{13}IO_3S$ M = 352.19 g/mol

To a solution of NaI (40 mmol; 2 equiv.; 6.00 g) in acetonitrile (30 mL) was added at r.t. TMSCl (40 mmol; 2 equiv.; 5.08 mL) followed by H_2O (20 mmol; 1 equiv.; 360 μL). The reaction mixture was stirred for 10 mon, then a solution of 3-butyn-1-ol **159** (20 mmol; 1 equiv.; 1.40 g) in acetonitrile (5 mL) was added. The resulting mixture was stirred at r.t. for 1 h, then quenched with H_2O (60 mL) and extracted with Et_2O (3 × 50 mL). The combined organic layers were dried over $MgSO_4$ and concentrated under reduced pressure to afford the crude 3-iodo-but-3-en-1-ol (3.90 g) as an orange oil.

To the crude iodo alcohol dissolved in CH_2Cl_2 (25 mL), were added TsCl (35 mmol; 1.75 equiv.; 5.72 g) and NEt_3 (40 mmol; 2 equiv.; 5.58 mL) at 0 °C. The reaction mixture was stirred at 0 °C for 30 min then at r.t. for 30 min, quenched with H_2O (50 mL) and extracted with Et_2O (3 × 50 mL). The combined

organic layers were dried over $MgSO_4$ and concentrated under reduced pressure. Purification by flash column chromatography (petroleum ether:Et_2O = 10:2) afforded **160** (10.7 g; 51 %) as an orange oil. Spectral data are in accordance with those reported in the literature [8].

^{1}H NMR (400 MHz, $CDCl_3$): δ = 2.46 (s, 3 H, Me), 2.72 (dt, J = 6.3, 0.7 Hz, 2 H, O–CH_2–CH_2), 4.13 (t, J = 6.2 Hz, 2 H, O–CH_2), 5.79 (d, J = 1.8 Hz, 1 H, = C*H*H), 6.11 (dd, J = 1.3 Hz, 2.7 Hz, 1 H, = CH*H*), 7.36 (d, J = 8.0 Hz, 2 H, arom.), 7.80 (d, J = 8.2 Hz, 2 H, arom.); ^{13}C NMR (100 MHz, $CDCl_3$): δ = 21.8 (Me), 44.5 (O–CH_2–*C*H_2), 68.2 (O–CH_2), 103.7 (= C), 128.1 (2 CH arom.), 129.3 (= CH_2), 130.0 (2 CH arom.), 132.9 (C arom.), 145.0 (C arom.).

3-Iodo-but-3-enylamine (161)

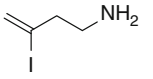

C_4H_8NI M = 197.02 g/mol

To a solution of tosylate **160** (11.1 mmol; 1 equiv.; 3.90 g), in DMF (28 mL) at 0 °C was added NaN_3 (33.3 mmol; 3 equiv.; 2.16 g). The reaction was stirred at r.t. for 2 h then at 50 °C for 3 h, and finally quenched with H_2O (70 mL) and extracted with Et_2O (3 × 10 mL). The combined organic layers were dried over $MgSO_4$ and concentrated under reduced pressure to afford the crude 4-azido-2-iodobut-1-ene (1.90 g) as a volatile yellow oil, which was used for the next step without further purification.

To the crude azide dissolved in Et_2O (30 mL), were added triphenyl phosphine (12.7 mmol; 1.5 equiv.; 3.33 g) and H_2O (12.7 mmol; 1.5 equiv.; 229 μL) at 0 °C. The reaction mixture was stirred at r.t. for 12 h and quenched with 2 M HCl aqueous solution. After a reverse extraction, the combined organic layers were dried over $MgSO_4$ and concentrated under reduced pressure to afford **161** (1.55 g; 71 % on 2 steps) as a volatile pale yellow oil.

^{1}H NMR (400 MHz, $CDCl_3$): δ = 2.53 (t, J = 6.1 Hz, 2 H, N–CH_2–CH_2), 2.88 (t, J = 6.2 Hz, 2 H, N–CH_2), 5.83 (d, J = 1.3 Hz, 1 H, = C*H*H), 6.12 (dd, J = 1.3 Hz, 2.6 Hz, 1 H, = CH*H*); ^{13}C NMR (100 MHz, $CDCl_3$): δ = 44.7 (N–CH_2–*C*H_2), 50.2 (N–CH_2), 103.6 (= C), 128.7 (= CH_2); HRMS calcd. for C_4H_9NI ($[M + H]^+$) 197.9774, found 197.9772.

3-Iodo-but-3-enyl-cyanamide (164)

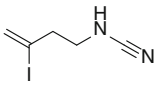

$C_5H_7IN_2$ M = 222.03 g/mol

Following **GP1** with 3-iodo-but-3-enylamine **161** (1 mmol; 197 mg), **164** was purified by flash column chromatography (petroleum ether:EtOAc = 6:4) and isolated as a colorless oil (119 mg; 54 %). This product proved very unstable and was immediately used for the next step.

IR (neat): ν = 3,295, 2,917, 2,222, 1,587, 1,128, 897 cm^{-1}; ^1H NMR (400 MHz, $CDCl_3$): δ = 2.65 (td, J = 6.4, 1.1 Hz, 2 H, N–CH_2–CH_2), 3.23 (t, J = 6.4 Hz, 2 H, N–CH_2), 4.10 (br s, 1 H, NH), 5.87 (d, J = 1.7 Hz, 1 H, = CH*H*), 6.23 (dt, J = 1.5, 1.3 Hz, 1 H, = C*H*H); ^{13}C NMR (100 MHz, $CDCl_3$): δ = 44.9 (N–CH_2–*C*H_2), 45.0 (N–CH_2), 105.7 (C vinyl.), 115.7 (CN), 129.6 (CH_2 vinyl.); HRMS calcd. for $C_5H_7IN_2Na$ ($[M + Na]^+$) 244.9546, found 244.9545.

***N*-acylcyanamide (165)**

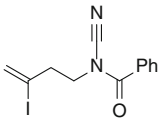

$C_{12}H_{11}IN_2O$ M = 326.13 g/mol

Following **GP2** with cyanamide **164** (2 mmol; 444 mg) and benzoyl chloride (2.4 mmol; 278 μL), *N*-acylcyanamide **165** was purified by flash column chromatography (pentane:Et_2O = 5:1) and isolated as colorless oil (594 mg; 91 %).

IR (neat): ν = 2,958, 2,232, 1,703, 1,447, 1,273, 1,180, 1,143, 1,101, 906, 789, 701 cm^{-1}; ^1H NMR (400 MHz, $CDCl_3$): δ = 2.89 (t, J = 6.7 Hz, 2 H, N–CH_2–CH_2), 3.96 (t, J = 6.7 Hz, 2 H, N–CH_2), 5.92 (d, J = 0.8 Hz, 1 H, = CH*H*), 6.27 (d, J = 0.8 Hz, 1 H, = C*H*H), 7.46–7.50 (m, 2 H, arom.), 7.56–7.63 (m, 1 H, arom.), 7.78–7.80 (m, 2 H, arom.); ^{13}C NMR (100 MHz, $CDCl_3$): δ = 43.2 (N–CH_2–*C*H_2), 46.7 (N–CH_2), 104.3 (C vinyl.), 110.9 (CN), 128.7 (2 CH arom.), 128.8 (CH arom.), 129.7 (CH_2 vinyl.), 130.9 (2 CH arom.), 133.4 (C arom.), 168.3 (CO); HRMS calcd. for $C_{12}H_{11}IN_2ONa$ ($[M + Na]^+$) 348.9808, found 348.9812.

***N*-acylcyanamide (170)**

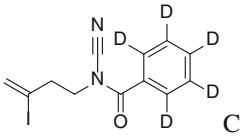

$C_{12}H_6D_5IN_2O$ M = 331.16 g/mol

Following **GP2** with cyanamide **164** (0.55 mmol; 122 mg) and benzoyl-d_5 chloride (0.61 mmol; 71 μL), *N*-acylcyanamide **170** was purified by flash column chromatography (pentane:Et_2O = 5:1) and isolated as a colorless oil (180 mg; 98 %).

IR (neat): ν = 2,952, 2,232, 1,701, 1,381, 1,231 1,179, 906, 720 cm^{-1}; ^1H NMR (400 MHz, $CDCl_3$): δ = 2.88 (t, J = 6.7 Hz, 2 H, N–CH_2–CH_2), 3.95 (t, J = 6.7 Hz, 2 H, N–CH_2), 5.90–5.91 (m, 1 H, = CH*H*), 6.26–6.27 (m, 1 H, = C*H*H); ^{13}C NMR (100 MHz, $CDCl_3$): δ = 43.2 (N–CH_2–*C*H_2), 46.6 (N–CH_2), 104.2 (C vinyl.), 110.8 (CN), 128.2 (t, $^1J_{C-D}$ = 24.0 Hz, 2 CD arom.), 128.3 (t, $^1J_{C-D}$ = 24.8 Hz, 2 CD arom.), 129.6 (CH_2 vinyl.), 130.6 (C arom.), 132.8 (t, $^1J_{C-D}$ = 24.0 Hz, CD arom.), 168.2 (CO); HRMS calcd. for $C_{12}H_6D_5IN_2ONa$ ($[M + Na]^+$) 354.0122, found 354.0120.

***N*-acylcyanamide (172)**

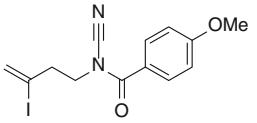

$C_{13}H_{13}IN_2O_2$ M = 356.16 g/mol

Following **GP2** with cyanamide **164** (0.70 mmol; 155 mg) and 4-methoxybenzoyl chloride (0.77 mmol; 104 μL), *N*-acylcyanamide **172** was purified by flash column chromatography (pentane:Et_2O = 10:3) and isolated as a colorless oil (222 mg; 89 %).

IR (neat): ν = 2,934, 2,229, 1,695, 1,603, 1,510, 1,254, 1,173, 1,023, 840, 756 cm^{-1}; ^1H NMR (400 MHz, $CDCl_3$): δ = 2.88 (td, J = 6.7, 0.9 Hz, 2 H, N–CH_2–CH_2), 3.86 (s, 3 H, Me), 3.93 (t, J = 6.7 Hz, 2 H, N–CH_2), 5.90 (d, J = 1.8 Hz, 1 H, = CH*H*), 6.25–6.26 (m, 1 H, = C*H*H), 6.95 (d, J = 9.0 Hz, 2 H, arom.), 7.81 (d, J = 9.0 Hz, 2 H, arom.); ^{13}C NMR (100 MHz, $CDCl_3$): δ = 43.3 (N–CH_2–*C*H_2), 46.8 (N–CH_2), 55.7 (OMe), 104.5 (C vinyl.), 111.4 (CN), 114.0 (2 CH arom.), 122.9 (C arom.), 129.6 (CH_2 vinyl.), 131.2 (2 CH arom.), 163.8 (C arom.), 167.6 (CO); HRMS calcd. for $C_{13}H_{13}IN_2O_2Na$ ($[M + Na]^+$) 378.9914, found 378.9914.

***N*-acylcyanamide (182)**

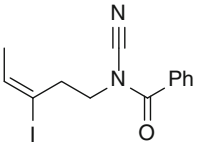

$C_{13}H_{13}IN_2O$ M = 340.16 g/mol

Starting from 3-pentyn-1-ol **184**, similar procedures to those employed for the synthesis of amine **161** led to an unseparable 1/1.4 mixture of (*E*)-3-iodopent-3-en-1-amine **189** and (*E*)-3-iodobut-2-en-1-amine **190**.

Following **GP1** with the mixture of **189** and **190** (3.4 mmol; 725 mg), the corresponding cyanamides were purified by flash column chromatography (petroleum ether:EtOAc = 6:4) and isolated as an unseparable mixture (538 mg; 67 %). The mixture was directly used for the next step owing to the instability of the cyanamide. Following **GP2** with the mixture of cyanamides (1.9 mmol; 454 mg) and benzoyl chloride (2.1 mmol; 245 μL), the two *N*-acylcyanamides **182** and **191** could be separated by flash column chromatography (pentane:Et_2O = 5:1). **182** was isolated as a white solid (178 mg; 67 %).

Mp: 51–52 °C; IR (neat): ν = 2,913, 2,231, 1,702, 1,447, 1,272, 1,176, 699 cm^{-1}; ^1H NMR (400 MHz, $CDCl_3$): δ = 1.79 (d, J = 6.4 Hz, 3 H, Me), 2.97 (t, J = 6.7 Hz, 2 H, N–CH_2–CH_2), 3.96 (t, J = 6.7 Hz, 2 H, N–CH_2), 5.84 (q, J = 6.4 Hz, 1 H, = CH), 7.46–7.50 (m, 2 H, arom.), 7.57–7.63 (m, 1 H, arom.), 7.76 (d, J = 8.3 Hz, 2 H, arom.); ^{13}C NMR (100 MHz, $CDCl_3$): δ = 22.4 (Me), 43.2 (N–CH_2–*C*H_2), 47.1 (N–CH_2), 103.0 (C vinyl.), 111.0 (CN), 128.7

(2 CH arom.), 128.8 (2 CH arom.), 131.0 (C arom.), 133.4 (CH arom.), 134.5 (CH vinyl.), 168.4 (CO); HRMS calcd. for $C_{13}H_{13}IN_2ONa$ ($[M + Na]^+$) 362.9965, found 362.9964.

***N*-acylcyanamide (191)**

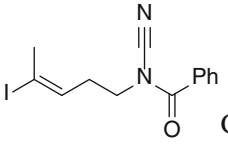

$C_{13}H_{13}IN_2O$ M = 340.16 g/mol

As depicted above, **191** was isolated as a yellow oil (240 mg; 62 %).

IR (neat): ν = 2,231, 1,701, 1,447, 1,272, 1,089, 699 cm^{-1}; ^1H NMR (400 MHz, $CDCl_3$): δ = 2.54–2.55 (m, 3 H, Me), 2.63 (q, J = 6.8 Hz, 2 H, N–CH_2–CH_2), 3.85 (t, J = 6.9 Hz, 2 H, N–CH_2), 5.51–5.56 (m, 1 H, = CH), 7.47–7.52 (m, 2 H, arom.), 7.58–7.63 (m, 1 H, arom.), 7.79–7.85 (m, 2 H, arom.); ^{13}C NMR (100 MHz, $CDCl_3$): δ = 33.9 (Me), 35.4 (N–CH_2–CH_2), 46.7 (N–CH_2), 105.5 (C vinyl.), 111.2 (CN), 128.7 (2 CH arom.), 128.8 (CH arom.), 129.9 (CH vinyl.), 131.1 (C arom.), 133.3 (2 CH arom.), 168.5 (CO); HRMS calcd. for $C_{13}H_{13}IN_2ONa$ ($[M + Na]^+$) 362.9965, found 362.9966.

***N*-acylcyanamide (195)**

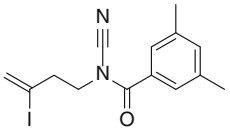

$C_{14}H_{15}IN_2O$ M = 354.19 g/mol

Following **GP2** with cyanamide **164** (1.25 mmol; 277 mg) and 3,5-dimethylbenzoyl chloride (1.38 mmol; 233 mg), *N*-acylcyanamide **195** was purified by flash column chromatography (pentane:Et_2O = 10:1) and isolated as a colorless oil (296 mg; 67 %).

IR (neat): ν = 2,233, 1,704, 1,606, 1,312, 1,219, 907 cm^{-1}; ^1H NMR (400 MHz, $CDCl_3$): δ = 2.37 (s, 6 H, 2 Me), 2.89 (t, J = 6.8 Hz, 2 H, N–CH_2–CH_2), 3.94 (t, J = 6.6 Hz, 2 H, N–CH_2), 5.92 (d, J = 1.5 Hz, 1 H, = C*H*H), 6.26 (d, J = 1.3 Hz, 1 H, = C*H*H), 7.22 (s, 1 H, arom.), 7.37 (s, 2 H, arom.); ^{13}C NMR (100 MHz, $CDCl_3$): δ = 21.4 (2 Me), 43.4 (N–CH_2–CH_2), 46.8 (N–CH_2), 104.3 (C vinyl.), 111.0 (CN), 126.3 (2 CH arom.), 129.7 (CH_2 vinyl.), 130.9 (C arom.), 135.1 (CH arom.), 138.6 (2 C arom.), 168.8 (CO); HRMS calcd. for $C_{14}H_{15}N_2OINa$ ($[M + Na]^+$) 377.0121, found 377.0117.

***N*-acylcyanamide (196)**

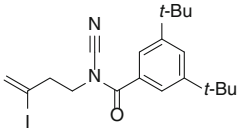

$C_{20}H_{27}IN_2O$ M = 438.35 g/mol

Following **GP2** with cyanamide **164** (1.1 mmol; 244 mg) and 3,5-di-*tert*-butylbenzoyl chloride (1.2 mmol; 252 mg), *N*-acylcyanamide **24** was purified by flash column chromatography (pentane:Et_2O = 20:1) and isolated as a colorless oil (350 mg; 73 %).

IR (neat): ν = 2,963, 2,232, 1,706, 1,598, 1,314, 1,246, 901 cm^{-1}; ^1H NMR (400 MHz, $CDCl_3$): δ = 1.35 (s, 18 H, 6 Me), 2.91 (t, J = 6.8 Hz, 2 H, N–CH_2–CH_2), 3.97 (t, J = 6.6 Hz, 2 H, N–CH_2), 5.93 (d, J = 1.6 Hz, 1 H, = CH*H*), 6.28–6.29 (m, 1 H, = C*H*H), 7.63 (s, 2 H, arom.), 7.64 (s, 1 H, arom.);^{13}C NMR (100 MHz, $CDCl_3$): δ = 31.4 (6 Me), 35.2 (2 CMe_3) 43.4 (N–CH_2–CH_2), 46.7 (N–CH_2), 104.5 (C vinyl.), 111.1 (CN), 123.3 (2 CH arom.), 127.6 (CH_2 vinyl.), 129.6 (CH arom.), 130.2 (C arom.), 151.5 (2 C arom.), 169.2 (CO); HRMS calcd. for $C_{20}H_{27}N_2OINa$ ($[M + Na]^+$) 461.1060, found 461.1055.

***N*-acylcyanamide (199)**

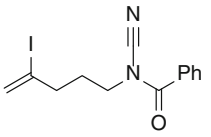

$C_{13}H_{13}IN_2O$ M = 340.16 g/mol

Starting from 5-chloro-1-pentyne **200**, similar procedures to those employed for the synthesis of amine **161** afforded 4-iodopent-4-en-1-amine (47 % in 3 steps) as a volatile yellow oil which was used for the next step without further purification. Following **GP1** with 4-iodopent-4-en-1-amine (3.79 mmol; 800 mg), the corresponding cyanamide was purified by flash column chromatography (petroleum ether:EtOAc = 6:4) and isolated as a pale yellow oil (650 mg; 73 %) which was directly used for the next step owing to its instability. Following **GP2** with the cyanamide (1.9 mmol; 450 mg) and benzoyl chloride (2.09 mmol; 243 μL), *N*-acylcyanamide **199** was purified by flash column chromatography (pentane:Et_2O = 5:1) and isolated as a colorless oil (390 mg; 60 %).

IR (neat): ν = 2,230, 1,701, 1,447, 1,273, 1,105, 898, 699 cm^{-1}; ^1H NMR (400 MHz, $CDCl_3$): δ = 1.99–2.10 (m, 2 H, N–CH_2–CH_2), 2.54 (t, J = 7.1 Hz, 2 H, N–CH_2–CH_2–CH_2), 3.78 (t, J = 7.2 Hz, 2 H, N–CH_2), 5.79 (s, 1 H, = CH*H*), 6.15 (s, 1 H, = C*H*H), 7.49 (t, J = 7.7 Hz, 2 H, arom.), 7.60 (t, J = 7.5 Hz, 1 H, arom.), 7.81 (d, J = 7.7 Hz, 2 H, arom.); ^{13}C NMR (100 MHz, $CDCl_3$): δ = 27.2 (N–CH_2–CH_2), 42.1 (N–CH_2–CH_2–CH_2), 46.5 (N–CH_2), 109.3 (C vinyl.), 111.1 (CN), 127.3 (CH_2 vinyl.), 128.7 (CH arom.), 128.7 (2 CH arom.), 131.0 (C arom.),

133.4 (2 CH arom.), 168.4 (CO); HRMS calcd. for $C_{13}H_{13}IN_2ONa$ ($[M + Na]^+$) 362.9965, found 362.9961.

***N*-acylcyanamide (211)**

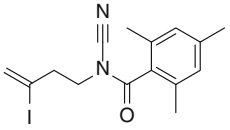

$C_{15}H_{17}IN_2O$ M = 368.21 g/mol

Following **GP2** with cyanamide **164** (0.40 mmol; 89 mg) and 2,4,6-trimethylbenzoyl chloride (0.77 mmol; 73 μL), *N*-acylcyanamide **211** was purified by flash column chromatography (pentane:Et_2O = 10:1) and isolated as a colorless oil (130 mg; 87 %).

IR (neat): ν = 2,952, 2,234, 1,712, 1,612, 1,428, 1,262, 1,185, 849 cm^{-1}; ^1H NMR (400 MHz, $CDCl_3$): δ = 2.28 (s, 6 H, 2 Me), 2.29 (s, 3 H, Me), 2.88 (t, J = 6.6 Hz, 2 H, N–CH_2–CH_2), 3.97 (t, J = 6.6 Hz, 2 H, N–CH_2), 5.92 (d, J = 1.6 Hz, 1 H, = C*H*H), 6.31 (d, J = 1.5 Hz, 1 H, = C*H*H), 6.89 (s, 2 H, arom.);^{13}C NMR (100 MHz, $CDCl_3$): δ = 19.1 (2 Me), 21.4 (Me), 43.2 (N–CH_2–CH_2), 45.2 (N–CH_2), 104.5 (C vinyl.), 109.6 (CN), 128.7 (CH_2 vinyl.), 130.0 (2 CH arom.), 130.1 (2 C arom.), 134.4 (C arom.), 140.8 (C arom.), 170.4 (CO); HRMS calcd. for $C_{15}H_{17}IN_2ONa$ ($[M + Na]^+$) 391.0278, found 391.0280.

***N*-acylcyanamide (212)**

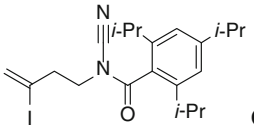

$C_{21}H_{29}IN_2O$ M = 452.37 g/mol

Following **GP2** with cyanamide **164** (0.63 mmol; 140 mg) and 2,4,6-triisopropylbenzoyl chloride (0.69 mmol; 184 mg), *N*-acylcyanamide **212** was purified by flash column chromatography (pentane:Et_2O = 20:1) and isolated as a colorless oil (43 mg; 15 %). This synthesis was not reproducible since this compound was only obtained one time.

IR (neat): ν = 2,962, 2,235, 1,716, 1,461, 1,210, 1,183, 1,151, 878 cm^{-1}; ^1H NMR (400 MHz, $CDCl_3$): δ = 1.22 (d, J = 6.8 Hz, 6 H, 2 Me), 1.25 (d, J = 6.9 Hz, 6 H, 2 Me), 1.32 (d, J = 6.9 Hz, 6 H, 2 Me), 2.74 (dt, J = 6.8, 13.6 Hz, 2 H, N–CH_2–CH_2), 2.85–2.96 (m, 3 H, 3 Me–C*H*–Me), 3.99 (t, J = 6.6 Hz, 2 H, N–CH_2), 5.93 (d, J = 1.6 Hz, 1 H, = C*H*H), 6.29–6.35 (m, 1 H, = C*H*H), 7.04 (s, 2 H, arom.).^{13}C NMR (100 MHz, $CDCl_3$): δ = 23.8 (2 Me), 24.0 (2 Me), 25.1 (2 Me), 31.9 (2 Me–*C*H–Me), 34.5 (Me–*C*H–Me), 43.2 (N–CH_2–CH_2), 45.3 (N–CH_2), 104.8 (C vinyl.), 109.7 (CN), 121.5 (2 CH arom.), 128.6 (C arom.), 129.9 (CH_2 vinyl.), 145.3 (2 C arom.), 151.9 (C arom.), 170.8 (CO); HRMS calcd. for $C_{21}H_{29}IN_2ONa$ ($[M + Na]^+$) 475.12168, found 475.12138.

***N*-acylcyanamide (213)**

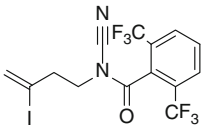

$C_{14}H_9F_6IN_2O$ M = 462.13 g/mol

Following **GP2** with cyanamide **164** (1.27 mmol; 282 mg) and 2,6-ditrifluoromethylbenzoyl chloride (1.40 mmol; 387 mg), *N*-acylcyanamide **213** was purified by flash column chromatography (pentane:Et_2O = 5:1) and isolated as a colorless oil (277 mg; 48 %).

IR (neat): ν = 2,242, 1,728, 1,341, 1,295, 1,211, 1,185, 1,138, 821, 677 cm^{-1}; ^1H NMR (400 MHz, $CDCl_3$): δ = 2.86 (t, J = 6.9 Hz, 2 H, N–CH_2–C*H*$_2$), 3.98 (t, J = 7.0 Hz, 2 H, N–CH_2), 5.92 (d, J = 1.8 Hz, 1 H, = CH*H*), 6.29 (d, J = 1.3 Hz, 1 H, = C*H*H), 7.83 (t, J = 8.4 Hz, 1 H, arom.), 7.99 (d, J = 8.1 Hz, 2 H arom.); ^{13}C NMR (100 MHz, $CDCl_3$): δ = 42.8 (N–CH_2–*C*H_2), 46.6 (N–CH_2), 103.5 (C vinyl.), 108.8 (CN), 122.7 (q, $^1J_{C\text{-}F}$ = 272.5 Hz, 2 CF_3), 129.1 (C arom.), 129.5 (q, $^2J_{C\text{-}F}$ = 32.6 Hz, 2 C arom.), 130.1 (CH_2 vinyl.), 130.6 (q, $^3J_{C\text{-}F}$ = 4.3 Hz, 2 CH arom.), 131.9 (CH arom.), 164.8 (CO); ^{19}F NMR (377 MHz, $CDCl_3$): δ = -59.6; HRMS calcd. for $C_{14}H_9F_6IN_2ONa$ ($[M + Na]^+$) 484.9556, found 484.9550.

***N*-acylcyanamide (214)**

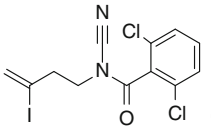

$C_{12}H_9Cl_2IN_2O$ M = 395.02 g/mol

Following **GP2** with cyanamide **164** (1 mmol; 222 mg) and 2,6-dichlorobenzoyl chloride (1.1 mmol; 158 μL), *N*-acylcyanamide **214** was purified by flash column chromatography (pentane:Et_2O = 5:1) and isolated as a colorless oil (336 mg; 85 %).

IR (neat): ν = 2,243, 1,727, 1,294, 823, 677 cm^{-1}; ^1H NMR (400 MHz, $CDCl_3$): δ = 2.91 (t, J = 6.6 Hz, 2 H, N–CH_2–C*H*$_2$), 4.00 (t, J = 6.8 Hz, 2 H, N–CH_2), 5.92 (d, J = 1.3 Hz, 1 H, = CH*H*), 6.31 (d, J = 1.3 Hz, 1 H, = C*H*H), 7.35–7.39 (m, 3 H, arom.); ^{13}C NMR (100 MHz, $CDCl_3$): δ = 43.2 (N–CH_2–*C*H_2), 46.0 (N–CH_2), 103.8 (C vinyl.), 108.8 (CN), 128.2 (C arom.), 128.4 (2 CH arom.), 130.2 (CH arom.), 132.3 (2 C arom.), 132.6 (CH_2 vinyl), 164.8 (CO); HRMS calcd. for $C_{12}H_9Cl_2IN_2O$ Na ($[M + Na]^+$) 416.9029, found 416.9028.

***N*-acylcyanamide (215)**

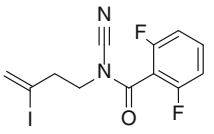

$C_{12}H_9F_2IN_2O$ M = 362.11 g/mol

Following **GP2** with cyanamide **164** (0.5 mmol; 127 mg) and 2,6-difluorobenzoyl chloride (0.55 mmol; 70 μL), *N*-acylcyanamide **215** was purified by flash column chromatography (pentane:Et_2O = 5:1) and isolated as a colorless oil (175 mg; 96 %).

IR (neat): ν = 2,238, 1,717, 1,624, 1,469, 1,284, 1,144, 1,010, 791 cm^{-1}; ^1H NMR (400 MHz, $CDCl_3$): δ = 2.86 (t, J = 6.8 Hz, 2 H, N–CH_2–CH_2), 3.98 (t, J = 6.8 Hz, 2 H, N–CH_2), 5.91 (d, J = 2.0 Hz, 1 H, = CH*H*), 6.27 (s, 1 H, = C*H*H), 7.02 (t, J = 10.8 Hz, 2 H, arom.), 7.48–7.53 (m, 1 H arom.); ^{13}C NMR (100 MHz, $CDCl_3$): δ = 43.4 (N–CH_2–CH_2), 46.1 (N–CH_2), 103.6 (C vinyl.), 109.1 (CN), 110.7 (t, $^2J_{C\text{-}F}$ = 20.2 Hz, C arom.), 112.2 (d, $^2J_{C\text{-}F}$ = 23.7 Hz, 2 CH arom.), 130.2 (CH_2 vinyl.), 134.1 (t, $^3J_{C\text{-}F}$ = 10.0 Hz, CH arom.), 159.4 (dd, $^1J_{C\text{-}F}$ = 252.9 Hz, $^3J_{C\text{-}F}$ = 6.3 Hz, 2 C arom.), 164.8 (CO); HRMS calcd. for $C_{12}H_9F_2IN_2ONa$ ($[M + Na]^+$) 384.9620, found 384.9622.

***N*-acylcyanamide (216)**

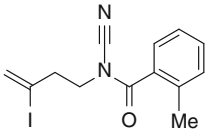

$C_{13}H_{13}IN_2O$ M = 340.16 g/mol

Following **GP2** with cyanamide **164** (1.00 mmol; 222 mg) and *o*-toluyl chloride (1.10 mmol; 144 μL), *N*-acylcyanamide **216** was purified by flash column chromatography (pentane:Et_2O = 5:1) and isolated as a colorless oil (313 mg; 92 %).

IR (neat): ν = 2,921, 2,233, 1,709, 1,263, 1,147, 906, 736 cm^{-1}; ^1H NMR (400 MHz, $CDCl_3$): δ = 2.43 (s, 3 H, Me), 2.91 (td, J = 6.5, 0.9 Hz, 2 H, N–CH_2–CH_2), 3.98 (t, J = 6.6 Hz, 2 H, N–CH_2), 5.96 (d, J = 1.6 Hz, 1 H, = CH*H*), 6.29–6.30 (m, 1 H, = C*H*H), 7.27–7.29 (m, 2 H, arom.), 7.40–7.42 (m, 2 H, arom.); ^{13}C NMR (100 MHz, $CDCl_3$): δ = 19.5 (Me), 43.4 (N–CH_2–CH_2), 45.8 (N–CH_2), 104.4 (C vinyl.), 110.1 (CN), 126.0 (CH arom.), 127.4 (CH arom.), 129.9 (CH_2 vinyl.), 131.3 (CH arom.), 131.6 (C arom.), 131.9 (CH arom.), 136.4 (C arom.), 169.4 (CO); HRMS calcd. for $C_{13}H_{13}IN_2ONa$ ($[M + Na]^+$) 362.9965, found 362. 9960.

3.3.3 Cyclized Products

α-Methyldeoxyvasicinone (129)

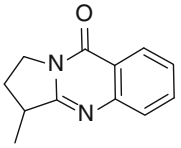

$C_{12}H_{12}N_2O$ M = 200.24 g/mol

Following **GP3** with *N*-acylcyanamide **165** (0.25 mmol; 82 mg) in *t*-BuOH, and with *N*-acylcyanamide **165** (0.29 mmol; 94 mg) in benzene, **129** was purified by flash column chromatography (CH_2Cl_2:EtOAc = 10:1 to 1:1) and isolated as a white solid (38 mg; 77 %) and (38 mg; 66 %), along with quinazolinone **167** (6 mg; 12 %), (11 mg; 20 %) respectively.

See previous part for spectral data.

Quinazolinone (167)

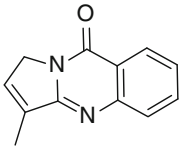

$C_{12}H_{10}N_2O$ M = 198.22 g/mol

White solid. Mp: 147–148 °C; IR (neat): ν = 1,777, 1,681, 1,607, 1,467, 1,312, 775 cm^{-1}; ^1H NMR (400 MHz, $CDCl_3$): δ = 2.24–2.25 (m, 3 H, Me), 4.64 (quint., J = 2.0 Hz, 2 H, N–CH_2), 6.84–6.45 (m, 1 H, = CH), 7.46–7.50 (m, 1 H, arom.), 7.75–7.82 (m, 2 H, arom.), 8.36 (d, J = 7.4 Hz, arom.). ^{13}C NMR (100 MHz, $CDCl_3$): δ = 11.6 (Me), 50.6 (N–CH_2), 120.0 (C arom.), 126.3 (CH arom.), 126.6 (CH arom.), 127.2 (C vinyl.), 127.6 (CH arom.), 134.2 (CH vinyl.), 134.6 (CH arom.), 136.0 (C arom.), 155.1 (N–C–N), 160.4 (CO); HRMS calcd. for $C_{12}H_{11}N_2O$ ($[M + H]^+$) 199.0866, found 199.0869.

Quinazolinone (169)

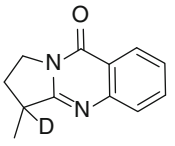

$C_{12}H_{11}DN_2O$ M = 201.24 g/mol

Following **GP3** with *N*-acylcyanamide **165** (0.19 mmol; 62 mg) and Bu_3SnD (0.38 mmol; 103 μL) in benzene, quinazolinone **169** was purified by flash column chromatography (CH_2Cl_2:EtOAc = 10:1 to 1:1) and isolated as a white solid (21 mg; 55 % with 83 % deuterium insertion, as measured by ^1H NMR).

IR (neat): v = 1,674, 1,622, 1,469, 1,384, 1,335, 1,022, 774 cm^{-1}; ^1H NMR (400 MHz, $CDCl_3$): δ = 1.47 (s, 3 H, Me), 1.77–1.85 (m, 1 H, N–CH_2–C*H*H), 2.43–2.53 (m, 1 H, N–CH_2–CH*H*), 3.97–4.05 (m, 1 H, N–C*H*H), 4.23–4.30 (m, 1 H, N–CH*H*), 7.43 (ddd, J = 8.2, 6.6, 1.7 Hz, 1 H, arom.), 7.66–7.75 (m, 2 H, arom.), 8.27–8.29 (m, 1 H, arom.); ^{13}C NMR (100 MHz, $CDCl_3$): δ = 17.3 (Me), 28.6 (N–CH_2–*C*H_2), 38.7 (t, $^1J_{C\text{-}D}$ = 19.7 Hz, CD), 44.7 (N–CH_2), 120.8 (C arom.), 126.3 (CH arom.), 126.5 (CH arom.), 127.2 (CH arom.), 134.2 (CH arom.), 149.5 (C arom.), 161.2 (N–C–N), 162.5 (CO); HRMS calcd. for $C_{12}H_{12}DN_2O$ ($[M + H]^+$) 202.1085, found 202.1081.

Quinazolinone (171)

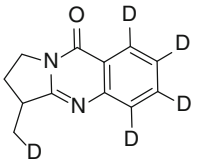

$C_{12}H_7D_5N_2O$ M = 205.27 g/mol

Following **GP3** with *N*-acylcyanamide **170** (0.12 mmol; 40 mg) in *t*-BuOH, following **GP3** with *N*-acylcyanamide **170** (0.43 mmol; 143 mg) in benzene, following **GP4** with *N*-acylcyanamide **172** (0.14 mmol; 50 mg) and *N*-acylcyanamide **170** (0.14 mmol; 46 mg) in *t*-BuOH, quinazolinone **171** was purified by flash column chromatography (CH_2Cl_2:EtOAc = 10:1 to 1:1) and isolated as a white solid (15 mg; 59 %; > 95 % deuterium insertion measured by MS), (43 mg, 48 %), (15 mg; 27 % as a *48*: mixture with **175**) along with quinazolinone **173** (16 mg; 23 % as a *52*: mixture with **174**), respectively.

Mp: 128–129 °C; IR (neat): v = 2,932, 1,661, 1,620, 1,583, 1,538, 1,397, 1,329, 1,267, 786, 698 cm^{-1}; ^1H NMR (400 MHz, $CDCl_3$): δ = 1.45 (dt, J = 5.3, 1.7 Hz, 2 H, CH_2D), 1.87 (dq, J = 12.7 Hz, 8.6 Hz, 1 H, N–CH_2–CH*H*), 2.42–2.56 (m, 1 H, N–CH_2–C*H*H), 3.28–3.35 (m, 1 H, C*H*–CH_2D), 3.96–4.03 (m, 1 H, N–CH*H*), 4.23–4.30 (m, 1 H, N–C*H*H); ^{13}C NMR (100 MHz, $CDCl_3$): δ = 17.1 (t, $^1J_{C\text{-}D}$ = 18.9 Hz, CH_2D), 28.7 (N–CH_2–*C*H_2), 38.7 (*C*H–CH_2D), 44.5 (N–CH_2), 120.8 (C arom.), 125.8 (t, $^1J_{C\text{-}D}$ = 24.0 Hz, CD arom.), 126.1 (m, CD arom.), 126.7 (m, CD arom.), 133.7 (t, $^1J_{C\text{-}D}$ = 24.9 Hz, CD arom.), 149.5 (C arom.), 161.2 (N–C–N), 162.5 (CO); HRMS calcd. for $C_{12}H_8D_5N_2O$ ($[M + H]^+$) 206.1336, found 206.1334.

Quinazolinone (175)

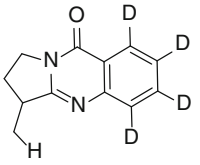

$C_{12}H_8D_4N_2O$ M = 204.26 g/mol

^{1}H NMR (400 MHz, $CDCl_3$): δ = 1.48 (d, J = 7.0 Hz, 3 H, Me), 1.82–1.92 (m, 1 H, N–CH_2–CH*H*), 2.45–2.54 (m, 1 H, N–CH_2–C*H*H), 3.28–3.36 (m, 1 H, C*H*–Me), 3.97–4.03 (m, 1 H, N–CH*H*), 4.25–4.31 (m, 1 H, N–C*H*H); ^{13}C NMR (100 MHz, $CDCl_3$): δ = 17.4 (Me), 28.8 (N–CH_2–*C*H_2), 38.9 (*C*H–Me), 44.7 (N–CH_2), 120.8 (C arom.), 125.8 (t, $^1J_{C\text{-}D}$ = 24.0 Hz, CD arom.), 126.1 (m, CD arom.), 126.7 (m, CD arom.), 133.7 (t, $^1J_{C\text{-}D}$ = 24.9 Hz, CD arom.), 149.5 (C arom.), 161.2 (N–C–N), 162.5 (CO); HRMS calcd. for $C_{12}H_9D_4N_2O$ ([M + H]$^+$) 205.1272, found 205.1273.

Quinazolinone (173)

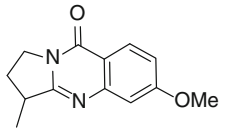

$C_{13}H_{14}N_2O_2$ M = 230.26 g/mol

Following **GP3** with *N*-acylcyanamide **172** (0.12 mmol; 43 mg) in *t*-BuOH, following **GP4** with *N*-acylcyanamide **172** (0.14 mmol; 50 mg) and *N*-acylcyanamide **170** (0.14 mmol; 46 mg) in *t*-BuOH, quinazolinone **173** was purified by flash column chromatography (pentane:Et_2O = 1:9) and isolated as a white solid (20 mg; 72 %), (16 mg; 23 % as a *52*:48 mixture with **174**) along with quinazolinone **171** (15 mg; 27 % as a *48*:52 mixture with **175**), respectively.

Mp: 136–137 °C; IR (neat): ν = 2,933, 1,670, 1,612, 1,487, 1,444, 1,391, 1,312, 1,029, 781, 694 cm^{-1}; ^{1}H NMR (400 MHz, $CDCl_3$): δ = 1.47 (d, J = 7.0 Hz, 3 H, Me), 1.81–1.89 (m, 1 H, N–CH_2–C*H*H), 2.38–2.52 (m, 1 H, N–CH_2–CH*H*), 3.24–3.34 (m, 1 H, Me–C*H*), 3.90 (s, 3 H, OMe), 3.91–4.01 (m, 1 H, N–C*H*H), 4.25 (ddd, J = 12.4, 8.7, 3.9 Hz, 1 H, N–CH*H*), 7.00 (dd, J = 8.8, 2.4 Hz, 1 H, arom.), 7.08 (d, J = 2.4 Hz, 1 H, arom.), 8.17 (d, J = 9.0 Hz, 1 H, arom.); ^{13}C NMR (100 MHz, $CDCl_3$): δ = 17.3 (Me), 28.7 (N–CH_2–*C*H_2), 39.0 (Me–*C*H), 44.6 (N–CH_2), 55.8 (OMe), 107.8 (CH arom.), 114.3 (C arom.), 116.4 (CH arom.), 127.9 (CH arom.), 151.8 (C arom.), 160.8 (C arom.), 163.3 (N–C–N), 164.5 (CO); HRMS calcd. for $C_{13}H_{15}N_2O_2$ ([M + H]$^+$) 231.1128, found 232.1126.

Quinazolinone (174)

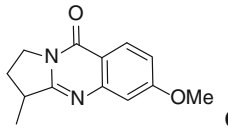

$C_{13}H_{13}DN_2O_2$ M = 231.27 g/mol

^{1}H NMR (400 MHz, $CDCl_3$): δ = 1.45 (dt, J = 7.0, 1.8 Hz, 2 H, CH_2D), 1.81–1.89 (m, 1 H, N–CH_2–C*H*H), 2.38–2.52 (m, 1 H, N–CH_2–CH*H*), 3.24–3.34 (m, 1 H, Me–C*H*), 3.90 (s, 3 H, OMe), 3.91–4.01 (m, 1 H, N–C*H*H), 4.25 (ddd, J = 12.4, 8.7, 3.9 Hz, 1 H, N–CH*H*), 7.00 (dd, J = 8.8, 2.4 Hz, 1 H, arom.), 7.08 (d, J = 2.4 Hz, 1 H, arom.), 8.17 (d, J = 9.0 Hz, 1 H, arom.); ^{13}C NMR (100 MHz, $CDCl_3$): δ = 15.5 (t, $^1J_{C\text{-}D}$ = 19.7 Hz, CH_2D), 28.8 (N–CH_2–*C*H_2),

38.9 (CH_2D–*C*H), 44.6 (N–CH_2), 55.8 (OMe), 107.9 (CH arom.), 114.4 (C arom.), 116.4 (CH arom.), 128.0 (CH arom.), 151.9 (C arom.), 160.8 (C arom.), 163.3 (N–C–N), 164.6 (CO); HRMS calcd. for $C_{13}H_{14}DN_2O_2$ ($[M + H]^+$) 232.1190, found 232.1191.

Quinazolinone (178)

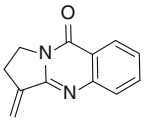

$C_{12}H_{10}N_2O$ M = 198.08 g/mol

Following **GP5** with *N*-acylcyanamide **165** (0.17 mmol; 55 mg) in benzene, quinazolinone **178** (9 mg; 26 %) was purified by flash column chromatography (pentane:CH_2Cl_2 = 3:2) and isolated as a colorless oil, along with reducedd product **177** (21 mg; 79 %) and quinazoline **167** (4 mg; 13 %).

IR (neat): ν = 1,673, 1,612, 1,469, 1,335, 772, 694 cm^{-1}; ^1H NMR (400 MHz, $CDCl_3$): δ = 2.91–3.13 (m, 2 H, N–CH_2–CH_2), 4.18–4.22 (m, 2 H, N–CH_2), 5.57 (t, J = 2.6 Hz, 1 H, = CH*H*), 6.45 (t, J = 2.9 Hz, 1 H, = C*H*H), 7.37–7.55 (m, 1 H, arom.), 7.65–7.78 (m, 2 H, arom.), 8.25–8.38 (m, 1 H, arom.); ^{13}C NMR (100 MHz, $CDCl_3$): δ = 25.7 (N–CH_2–*C*H_2), 43.6 (N–CH_2), 116.3 (CH_2 vinyl.), 121.1 (C arom.), 126.5 (CH arom.), 126.7 (CH arom.), 127.7 (CH arom.), 134.4 (CH arom.), 140.6 (C vinyl.), 149.6 (C arom.), 154.1 (N–C–N), 161.4 (CO); HRMS calcd. for $C_{12}H_{11}N_2O$ ($[M + H]^+$) 199.0866, found 199.0863.

Reduced malonitrile (177)

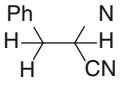

$C_{10}H_8N_2$ M = 156.18 g/mol

Data are in accordance with those described in the literature [9]. ^1H NMR (400 MHz, $CDCl_3$): δ = 2.28 (d, J = 7.0 Hz, 2 H, $PhCH_2$), 3.91 (t, J = 6.8 Hz, 1 H, $(CN)_2CH$), 7.31–7.34 (m, 2 H, arom.), 7.38–7.43 (m, 3 H, arom.); ^{13}C NMR (100 MHz, $CDCl_3$): δ = 25.1 ($(CN)_2$*C*H), 36.9 ($PhCH_2$), 112.3 (2 CN), 128.9 (CH arom.), 129.3 (2 CH arom.), 129.4 (2 CH arom.), 133.1 (C arom.).

Reduced malonitrile (179)

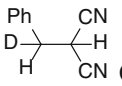

$C_{10}H_7DN_2$ M = 157.07 g/mol

Following **GP5** with *N*-acylcyanamide **170** (0.09 mmol; 30 mg) in benzene, reduced product **179** was purified by flash column chromatography (pentane: CH_2Cl_2 = 3:2) and isolated as a white solid (11 mg; 76 %, 74 % deuterium insertion as measured by ^1H NMR et MS). Data correspond to those described in the literature [9].

IR (neat): ν = 2,916, 2,853, 2,259, 1,495, 1,452, 1,075, 1,032, 745, 701 cm^{-1}; ^1H NMR (400 MHz, $CDCl_3$): δ = 3.28 (dt, J = 6.8, 1.8 Hz, 1 H, PhCHD), 3.90 (d, J = 7.0 Hz, 1 H, $(CN)_2CH$), 7.31–7.34 (m, 2 H, arom.), 7.39–7.43 (m, 3 H, arom.); ^{13}C NMR (100 MHz, $CDCl_3$): δ = 25.1 ($(CN)_2CH$), 36.6 (t, $^1J_{CD}$ = 41 Hz), 112.3 (2 CN), 129.0 (CH arom.), 129.3 (2 CH arom.), 129.5 (2 CH arom.), 133.0 (C arom.); HRMS calcd. for $C_{11}H_{11}DN_2Na$ ($[M + MeOH + H]^+$) 212.0905, found 212.0905.

Quinazolinone (192)

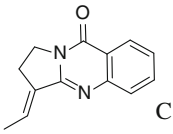

$C_{13}H_{12}N_2O$ M = 212.25 g/mol

Following **GP3** with *N*-acylcyanamide **182** (0.38 mmol; 129 mg) in benzene and following **GP5** with *N*-acylcyanamide **182** (0.12 mmol; 40 mg) in benzene, quinazolinone **192** was purified by flash column chromatography (pentane:EtOAc = 10:1 to 1:1) and isolated as a white solid (39 mg; 49 %; (*E*) isomer) along with an inseparable mixture of (*Z*) isomer and quinazolinone **193** (30 mg; 36 %, **192**(*Z*):**193** = 25:75), (23 mg; 92 %; (*E*)/(*Z*) = 52:48 separable mixture), respectively. The diastereoisomers were identified by NOE experiments.

Mp: 134–135 °C. IR (neat): ν = 1,673, 1,604, 1,469, 1,391, 1,184, 893, 793 cm^{-1}. ***(E) isomer***: ^1H NMR (400 MHz, $CDCl_3$): δ = 1.94 (dt, J = 7.2, 1.9 Hz, 3 H, Me), 2.88–2.98 (m, 2 H, N–CH_2–CH_2), 4.21 (t, J = 7.2 Hz, 2 H, N–CH_2–CH_2), 6.97–7.08 (m, 1 H, vinyl.), 7.42 (ddd, J = 8.1, 6.5, 1.8 Hz, 1 H, arom.), 7.65–7.77 (m, 2 H, arom.), 8.28 (ddd, J = 8.0, 1.4, 0.5 Hz, 1 H, arom.);^{13}C NMR (100 MHz, $CDCl_3$): δ = 15.3 (Me), 23.0 (N–CH_2–CH_2), 43.8 (N–CH_2), 121.0 (C arom.), 126.1 (CH arom.), 126.5 (CH arom.), 127.3 (CH arom.), 129.1 (CH arom.), 133.3 (C vinyl.), 134.3 (CH vinyl.), 149.9 (C arom.), 154.7 (N–C–N), 161.5 (CO). ***(Z) isomer:*** ^1H NMR (400 MHz, $CDCl_3$): δ = 2.36 (dt, J = 5.5 Hz, 3 H, Me), 2.83–2.88 (m, 2 H, N–CH_2–CH_2), 4.06 (td, J = 7.6, 1.8 Hz, 2 H, N–CH_2–CH_2), 6.12–6.19 (m, 1 H, vinyl.), 7.34–7.38 (m, 1 H, arom.), 7.64–7.65 (m, 2 H, arom.), 8.21 (d, J = 7.6 Hz, 1 H, arom.);^{13}C NMR (100 MHz, $CDCl_3$): δ = 13.5 (Me), 26.2 (N–CH_2–CH_2), 42.3 (N–CH_2), 119.5 (C arom.), 125.2 (CH arom.), 125.3 (CH arom.), 126.8 (CH arom.), 129.9 (C vinyl.), 132.4 (CH vinyl.),132.9 (CH arom.), 148.6 (C arom.), 153.7 (N–C–N), 160.5 (CO). HRMS calcd. for $C_{13}H_{12}N_2ONa$ ($[M + Na]^+$) 235.0842, found 235.0841.

Quinazolinone (193)

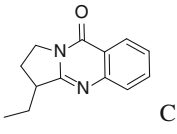

$C_{13}H_{14}N_2O$ M = 214.26 g/mol

^{1}H NMR (400 MHz, $CDCl_3$): $\delta = 0.89$ (t, $J = 7.0$ Hz, 3 H, *Me*–CH_2), 1.60–1.71 (m, 1 H, Me–CH*H*), 1.97–2.01 (m, 1 H, N–CH_2–CH*H*), 2.14–2.28 (m, 1 H, Me–C*H*H), 2.42–2.48 (m, 1 H, N–CH_2–C*H*H), 3.15–3.22 (m, 1 H, N–CH_2–CH_2–C*H*), 4.01–4.08 (dt, $J = 12.3$, 7.8 Hz, 1 H, N–CH*H*), 4.20–4.29 (m, 1 H, N–C*H*H), 7.41–7.46 (m, 1 H, arom.), 7.68–7.74 (m, 2 H, arom.), 8.28–8.30 (m, 1 H, arom.); ^{13}C NMR (100 MHz, $CDCl_3$): $\delta = 11.5$ (Me), 25.4 (N–CH_2–*C*H_2), 25.7 (Me–*C*H_2), 44.9 (N–*C*H_2), 45.4 (N–CH_2–CH_2–*C*H), 120.8 (C arom.), 126.2 (CH arom.), 126.3 (CH arom.), 127.1 (CH arom.), 134.1 (CH arom.), 149.4 (C arom.), 161.1 (N–C–N), 161.7 (CO).

Quinazolinone (194)

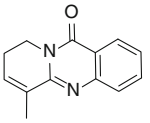

$C_{13}H_{12}N_2O$ M = 212.25 g/mol

Following **GP3** with *N*-acylcyanamide **191** (0.43 mmol; 146 mg) in benzene, quinazolinone **194** was purified by flash column chromatography (pentane: EtOAc = 10:1 to 1:1) and isolated as a white solid (69 mg; 77 %).

Mp: 94–95 °C; IR (neat): ν = 1,673, 1,610, 1,560, 1,473, 1,311, 1,165, 1,052, 773 cm^{-1}; ^{1}H NMR (400 MHz, $CDCl_3$): $\delta = 2.19$–2.20 (m, 3 H, Me), 2.44–2.54 (m, 2 H, N–CH_2–C*H*$_2$), 4.25 (t, $J = 7.0$ Hz, 2 H, N–CH_2), 6.45–6.48 (m, 1 H, = CH), 7.41–7.45 (m, 1 H, arom.), 7.64–7.76 (m, 2 H, arom.), 8.27 (ddd, $J = 8.0$, 1.3, 0.8 Hz, arom.); ^{13}C NMR (100 MHz, $CDCl_3$): $\delta = 18.3$ (Me), 23.0 (N–CH_2–*C*H_2), 39.1 (N–CH_2), 121.3 (C arom.), 126.6 (CH arom.), 126.9 (CH arom.), 127.8 (CH arom.), 131.9 (C vinyl.), 133.5 (CH vinyl.), 134.1 (CH arom.), 147.7 (C arom.), 150.2 (N–C–N), 161.7 (CO); HRMS calcd. for $C_{13}H_{12}N_2ONa$ ($[M + Na]^+$) 235.0842, found 235.0841.

Quinazolinone (197)

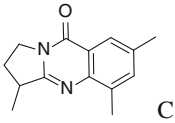

$C_{14}H_{16}N_2O$ M = 228.29 g/mol

Following **GP3** with *N*-acylcyanamide **195** (0.40 mmol; 142 mg) in benzene, quinazolinone **197** was purified by flash column chromatography (pentane: Et_2O = 3:7) and isolated as a white solid (57 mg; 63 %).

Mp: 89–90 °C; IR (neat): ν = 1,668, 1,627, 1,476, 1,345, 872 cm^{-1}; ^{1}H NMR (400 MHz, $CDCl_3$): 1.46 (d, $J = 6.8$ Hz, 3 H, *Me*–CH), 1.79–1.89 (m, 1 H, N–CH_2–CH*H*), 2.43 (s, 3 H, Me–C), 2.43–2.51 (m, 1 H, N–CH_2–C*H*H), 2.58 (s, 3 H, Me–C), 3.25–3.34 (m, 1 H, Me–C*H*), 3.93–4.00 (m, 1 H, N–CH*H*), 4.22–4.29 (m, 1 H, N–C*H*H), 7.39 (s, 1 H, arom.), 7.92 (s, 1 H, arom.); ^{13}C NMR (100 MHz, $CDCl_3$): $\delta = 17.4$ (*Me*–CH), 17.5 (*Me*–C), 21.3 (*Me*–C), 28.9

(N–CH_2–CH_2), 38.8 (*C*H–Me), 44.5 (N–CH_2), 120.5 (C arom.), 123.6 (CH arom.), 135.3 (C arom.), 135.6 (C arom.), 136.3 (CH arom.), 146.2 (C arom.), 160.2 (N–C–N), 161.6 (CO); HRMS calcd. for $C_{14}H_{17}N_2O$ ($[M + H]^+$) 229.1335, found 229.1329.

Quinazolinone (198)

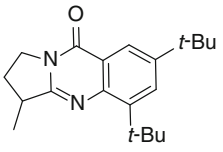

$C_{20}H_{28}N_2O$ M = 312.45 g/mol

Following **GP3** with *N*-acylcyanamide **196** (0.22 mmol; 98 mg) in benzene, quinazolinone **198** was purified by flash column chromatography (pentane:Et_2O = 4:6) and isolated as a white solid (23 mg; 33 %).

Mp: 179–180 °C; IR (neat): ν = 2,959, 1,669, 1,632, 1,477, 1,389, 1,273, 807 cm^{-1}; ^{1}H NMR (400 MHz, $CDCl_3$): 1.38 (s, 9 H, CMe_3), 1.47 (d, J = 7.0 Hz, 3 H, *Me*–CH), 1.59 (s, 9 H, CMe_3), 1.79–1.88 (m, 1 H, N–CH_2–CH*H*), 2.44–2.52 (m, 1 H, N–CH_2–C*H*H), 3.23–3.34 (m, 1 H, Me–C*H*), 3.90–3.98 (m, 1 H, N–CH*H*), 4.25–4.31 (m, 1 H, N–C*H*H), 7.77 (d, J = 2.4 Hz, 1 H, arom.), 8.18 (d, J = 2.4 Hz, 1 H, arom.); ^{13}C NMR (100 MHz, $CDCl_3$): δ = 17.1 (*C*H_3–CH), 29.0 (N–CH_2–*C*H_2), 31.0 (C*Me*$_3$), 31.5 (C*Me*$_3$), 35.2 (*C*Me_3), 36.6 (*C*Me_3), 38.8 (*C*H–CH_3), 44.5 (N–CH_2), 120.4 (CH arom.), 121.2 (C arom.), 128.9 (CH arom.), 145.9 (C arom.), 146.2 (C arom.), 148.5 (C arom.), 158.1 (N–C–N), 162.1 (CO); HRMS calcd. for $C_{20}H_{28}N_2ONa$ ($[M + Na]^+$) 335.2094, found 335.2089.

***N*-acylcyanamide (201)**

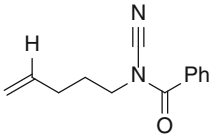

$C_{13}H_{14}N_2O$ M = 214.26 g/mol

Following **GP3** with *N*-acylcyanamide **199** (0.15 mmol; 51 mg), reduced product **201** was purified by flash column chromatography (pentane:Et_2O = 10:1 to 10:2) and isolated as a colorless oil (14 mg; 45 %) along with an inseparable mixture of quinazolinone **203** and **194** (8 mg; 24 %; **203**:**194** = 1:2).

IR (neat): ν = 2,232, 1,703, 1,448, 1,276, 1,102, 701 cm^{-1}; ^{1}H NMR (400 MHz, $CDCl_3$): δ = 1.93 (quint., J = 7.2 Hz, 2 H, N–CH_2–CH_2), 2.22 (q, J = 7.0 Hz, 2 H, N–CH_2–CH_2–CH_2), 3.81 (t, J = 7.0 Hz, 2 H, N–CH_2), 5.09 (d, J = 10.1 Hz, 1 H, HC = C*H*H), 5.14 (d, J = 17.1 Hz, 1 H, *H*C = CHH), 5.81–5.91 (m, 1 H, HC = CH*H*), 7.47–7.51 (m, 2 H, arom.), 7.58–7.62 (m, 1 H, arom.), 7.82 (d, J = 7.2 Hz, 2 H, arom.); ^{13}C NMR (100 MHz, $CDCl_3$): δ = 26.8 (N–CH_2–*C*H_2), 30.5 (N–CH_2–CH_2–*C*H_2), 47.5 (N–CH_2), 111.3 (CN), 116.4 (CH_2 vinyl.), 128.7 (CH arom.), 128.8 (2 CH arom.), 131.3 (C arom.), 133.3 (2 CH

arom.), 136.6 (CH vinyl.), 168.6 (CO); HRMS calcd. for $C_{13}H_{13}N_2ONa$ ($[M + Na]^+$) 237.0998, found 237.0995.

Quinazolinone (203)

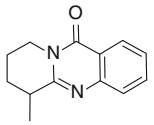

$C_{13}H_{14}N_2O$ M = 214.26 g/mol

^{1}H NMR (400 MHz, $CDCl_3$): $\delta = 1.51$ (d, $J = 7.0$ Hz, 3 H, Me), 1.61–1.71 (m, 1 H, N–CH_2–CH_2–C*H*H), 1.79–1.89 (m, 1 H, N–CH_2–C*H*H), 1.95–2.07 (m, 1 H, N–CH_2–CH_2–CH*H*), 2.08–2.20 (m, 1 H, N–CH_2–CH*H*), 3.00–3.09 (m, 1 H, Me–C*H*), 3.89–4.92 (m, 1 H, N–C*H*H), 4.25–4.30 (m, 1 H, N–CH*H*), 7.40–7.43 (m, 1 H, arom.), 7.65–7.72 (m, 2 H, arom.), 8.25–8.27 (m, 1 H, arom.).

Quinazolinone (217)

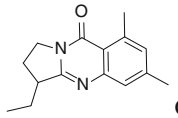

$C_{15}H_{18}N_2O$ M = 242.32 g/mol

Following **GP3** with *N*-acylcyanamide **211** (0.17 mmol; 63 mg) in *t*-BuOH, and with *N*-acylcyanamide **211** (0.34 mmol; 124 mg) in benzene, quinazolinone **217** was purified by flash column chromatography (pentane:EtOAc = 10:4 to 1:2) and isolated as a white solid (19 mg; 47 %), (35 mg; 45 %) respectively.

Mp: 82–83 °C; IR (neat): $\nu = 2{,}963$, 2,360, 1,670, 1,630, 1,613, 1,460, 1,311, 855 cm^{-1}; ^{1}H NMR (400 MHz, DMSO-d_6): $\delta = 0.99$ (t, $J = 7.5$ Hz, 3 H, *Me*–CH_2), 1.50–1.61 (m, 1 H, Me–CH*H*), 1.77–1.87 (m, 1 H, N–CH_2–CH*H*), 1.94–2.01 (m, 1 H, Me–C*H*H), 2.30–2.49 (m, 4 H, N–CH_2–C*H*H + Me), 2.74 (s, 3 H, Me), 3.10–3.16 (m, 1 H, N–CH_2–CH_2–C*H*), 3.83 (dt, $J = 12.3$, 7.8 Hz, 1 H, N–CH*H*), 4.02–4.08 (m, 1 H, N–C*H*H), 7.04 (s, 1 H, arom.), 7.25 (s, 1 H, arom.); ^{13}C NMR (100 MHz, $CDCl_3$): $\delta = 11.2$ (Me), 21.0 (Me), 22.4 (Me), 24.4 (Me–*C*H_2), 25.0 (N–CH_2–*C*H_2), 44.3 (N–*C*H_2), 44.5 (N–CH_2–CH_2–*C*H), 116.4 (C arom.), 124.8 (CH arom.), 129.7 (CH arom.), 139.3 (C arom.), 143.2 (C arom.), 150.9 (C arom.), 160.6 (N–C–N), 161.6 (CO). HRMS calcd. for $C_{15}H_{19}N_2O$ ($[M + H]^+$) 243.1492, found 243.1491.

Quinazolinone (218)

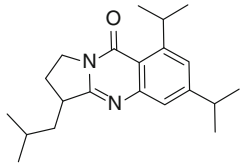

$C_{21}H_{30}N_2O$ M = 326.48 g/mol

Following **GP3** with *N*-acylcyanamide **212** (0.10 mmol; 45 mg) in benzene, quinazolinone **218** was purified by flash column chromatography (pentane:EtOAc = 20:1 to 2:1) and isolated as a colorless oil (17 mg; 52 %).

IR (neat): ν = 2,958, 1,666, 1,609, 1,461, 1,439, 1,367, 1,228, 1,176, 701 cm^{-1}; ^1H NMR (400 MHz, $CDCl_3$): δ = 0.99 (d, J = 6.7 Hz, 3 H, *Me*–CH–Me), 1.03 (d, J = 6.7 Hz, 3 H, Me–CH–*Me*), 1.28–1.33 (m, 12 H, 4 Me), 1.44–1.53 (m, 1 H, Me_2CH–CH*H*), 1.78–1.91 (m, 2 H, Me_2CH + N–CH_2–CH*H*), 2.00–2.06 (m, 1 H, Me_2CH–C*H*H), 2.41–2.49 (m, 1 H, N–CH_2–C*H*H), 2.99 (sept., J = 6.9 Hz, 1 H, Me_2CH), 3.24–3.32 (m, 1 H, N–CH_2–CH_2–C*H*), 3.90–4.02 (m, 1 H, N–CH*H*), 4.17–4.28 (m, 1 H, N–C*H*H), 4.72 (sept., J = 6.8 Hz, 1 H, Me_2CH), 7.26 (s, 1 H, arom.), 7.39 (s, 1 H, arom.); ^{13}C NMR (100 MHz, $CDCl_3$): δ = 21.5 (Me), 23.7 (Me), 23.8 (Me), 23.8 (Me), 24.2 (Me), 24.3 (Me), 26.2 (N–CH_2–CH_2), 26.6 (Me_2CH), 29.3 (Me_2CH), 34.6 (Me_2CH), 41.3 (Me_2CH–CH_2), 42.2 (N–CH_2–CH_2–CH), 45.0 (N–CH_2), 116.0 (C arom.), 122.2 (C arom.), 122.3 (CH arom.), 122.9 (CH arom.), 152.1 (C arom.), 154.9 (C arom.), 161.4 (N–C–N), 161.6 (CO); HRMS calcd. for $C_{21}H_{31}N_2O$ ($[M + H]^+$) 327.24309, found 327.24301.

Quinazolinone (219)

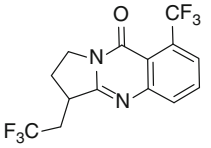

$C_{14}H_{10}F_6N_2O$ M = 336.07 g/mol

Following **GP3** with *N*-acylcyanamide **213** (0.07 mmol; 32 mg) in *t*-BuOH, and with *N*-acylcyanamide **213** (0.07 mmol; 32 mg) in benzene, with a very slow addition of Bu_3SnH (0.06 mmol/h), quinazolinone **219** was purified by flash column chromatography (pentane:Et_2O = 1:2) and isolated as a white solid (12 mg; 55 %), (6 mg; 24 %) respectively.

Mp: 96–97 °C. IR (neat): ν = 1,682, 1,633, 1,447, 1,336, 1,255, 1,135, 1,070, 1,036, 774, 628 cm^{-1}; ^1H NMR (400 MHz, $CDCl_3$): δ = 2.00–2.12 (m, 1 H, N–CH_2–CH*H*), 2.24–2.33 (m, 1 H, CF_3–CH*H*), 2.68–2.78 (m, 1 H, N–CH_2–C*H*H), 3.21–3.39 (m, 1 H, CF_3–C*H*H), 3.53–3.62 (m, 1 H, N–CH_2–CH_2–C*H*), 3.96 (ddd, J = 12.5, 10.9, 7.0 Hz, 1 H, N–CH*H*), 4.40 (ddd, J = 12.5, 9.0, 1.3 Hz, 1 H, N–C*H*H), 7.54–7.56 (m, 1 H, arom.), 8.06 (dd, J = 7.6, 0.8 Hz, 1 H, arom.), 8.49 (dd, J = 7.9, 1.1 Hz, 1 H, arom.).^{13}C NMR (100 MHz, $CDCl_3$): δ = 27.7 (N–CH_2–CH_2), 35.7 (q, $^2J_{C\text{-}F}$ = 29.1 Hz, CF_3–CH_2), 38.8 (N–CH_2–CH_2–CH), 45.1 (N–CH_2), 122.2 (C arom.), 125.9 (q, $^1J_{C\text{-}F}$ = 199.6 Hz, CH_2–CF_3), 126.3 (CH arom.), 126.4 (q, $^2J_{C\text{-}F}$ = 36.8 Hz, C arom.), 126.7 (q, $^1J_{C\text{-}F}$ = 275.0 Hz, C–CF_3), 130.7 (CH arom.), 132.1 (q, $^3J_{C\text{-}F}$ = 5.1 Hz, CH arom.), 146.6 (C arom.), 159.7 (N–C–N), 160.1 (CO); ^{19}F NMR (377 MHz, $CDCl_3$): δ = −65.0 (t, $^3J_{F\text{-}H}$ = 10.3 Hz, CF_3–CH_2), −60.7 (s, Carom.-CF_3); HRMS calcd. for $C_{14}H_{11}F_6N_2O$ ($[M + H]^+$) 337.0770, found 337.0768.

Quinazolinone (222)

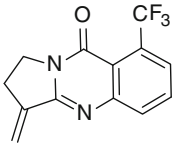

$C_{13}H_9F_3N_2O$ M = 266.22 g/mol

Following **GP3** with *N*-acylcyanamide **213** (0.065 mmol; 30 mg) in THF, with a very slow addition of Bu_3SnH (0.06 mmol/h), quinazolinone **222** was purified by flash column chromatography (pentane:Et_2O = 1:2) and isolated as a colorless oil (13 mg; 75 %).

IR (neat): ν = 1,680, 1,602, 1,445, 1,334, 1,308, 1,134, 1,071, 786 cm^{-1}; ^1H NMR (400 MHz, $CDCl_3$): δ = 3.02–3.06 (m, 2 H, N–CH_2–CH_2), 4.19–4.23 (t, 2 H, J = 7.4 Hz, N–CH_2), 5.64 (td, J = 2.4, 0.7 Hz, 1 H, = CH*H*), 6.56 (td, J = 2.8, 0.7 Hz, 1 H, = C*H*H), 7.49 (t, J = 7.7 Hz, 1 H, arom.), 8.05 (d, J = 7.4 Hz, 1 H, arom.), 8.48 (d, J = 8.1 Hz, 1 H, arom.); ^{13}C NMR (100 MHz, $CDCl_3$): δ = 25.4 (N–CH_2–*C*H_2), 43.8 (N–*C*H_2), 118.1 (CH_2 vinyl.), 122.2 (C arom.), 124.8 (CH arom.), 125.9 (q, $^1J_{C\text{-}F}$ = 294.0 Hz, *C*F_3), 130.6 (CH arom.), 131.1 (C arom.), 131.2 (q, $^2J_{C\text{-}F}$ = 30.2 Hz, C arom.), 132.0 (q, $^3J_{C\text{-}F}$ = 5.5 Hz, CH arom.), 140.0 (C vinyl.), 147.4 (N–C–N), 154.8 (CO); HRMS calcd. for $C_{13}H_9F_3N_2ONa$ ($[M + Na]^+$) 289.0559, found 289.0557.

Quinazolinone (223)

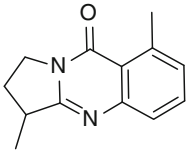

$C_{13}H_{14}N_2O$ M = 214.26 g/mol

Following **GP3** with *N*-acylcyanamide **216** (0.07 mmol; 23 mg) in *t*-BuOH, and with *N*-acylcyanamide **216** (0.12 mmol; 41 mg) in benzene, quinazolinone **223** was purified by flash column chromatography (pentane:Et_2O = 1:4) and isolated as a colorless oil (10 mg; 69 %), (15 mg; 58 %) respectively.

IR (neat): ν = 2,970, 2,361, 1,668, 1,632, 1,600, 1,474, 1,313, 813, 694 cm^{-1}; ^1H NMR (400 MHz, $CDCl_3$): δ = 1.47 (d, J = 7.0 Hz, 3 H, *Me*–CH), 1.81–1.90 (m, 1 H, N–CH_2–CH*H*), 2.40–2.51 (m, 1 H, N–CH_2–C*H*H), 2.89 (s, 3 H, *Me*–C), 3.16–3.39 (m, 1 H, Me–C*H*), 3.93–4.00 (m, 1 H, N–CH*H*), 4.19–4.25 (m, 1 H, N–C*H*H), 7.11–7.21 (m, 1 H, arom.), 7.51–7.57 (m, 2 H, arom.);^{13}C NMR (100 MHz, $CDCl_3$): δ = 17.4 (*Me*–CH), 23.1 (*Me*–C), 28.7 (N–CH_2–*C*H_2), 38.9 (*C*H–CH_3), 44.7 (N–CH_2), 119.4 (C arom.), 125.4 (CH arom.), 129.0 (CH arom.), 133.3 (CH arom.), 141.1 (C arom.), 151.2 (C arom.), 162.0 (N–C–N), 162.1 (CO); HRMS calcd. for $C_{13}H_{15}N_2O$ ($[M + H]^+$) 215.1179, found 215.1175.

Quinazolinone (224)

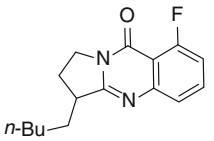

$C_{16}H_{19}FN_2O$ M = 274.33 g/mol

Following **GP3** with *N*-acylcyanamide **215** (0.33 mmol; 120 mg) in benzene, quinazolinone **224** was purified by flash column chromatography (pentane:Et_2O = 4:6) and isolated as a colorless oil (27 mg; 30 %).

IR (neat): ν = 2,924, 1,675, 1,616, 1,474, 1,253, 818 cm^{-1}; ^1H NMR (400 MHz, $CDCl_3$): δ = 0.93 (t, J = 7.0 Hz, 3 H, *Me*–CH_2), 1.32–1.62 (m, 7 H, *Me*–C*H*$_2$–C*H*$_2$–C*H*$_2$–CH*H*), 1.89–1.98 (m, 1 H, N–CH_2–C*H*H), 2.10–2.19 (m, 1 H, Me–CH_2–CH_2–CH_2–C*H*H), 2.40–2.45 (m, 1 H, N–CH_2–CH*H*), 3.18–3.29 (m, 1 H, CH_2–C*H*), 3.95–4.08 (m, 1 H, N–CH*H*), 4.21–4.35 (m, 1 H, N–C*H*H), 7.05–7.11 (m, 1 H, arom.), 7.45–7.47 (m, 1 H, arom.), 7.60–7.66 (m, 1 H, arom.); ^{13}C NMR (100 MHz, $CDCl_3$): δ = 14.2 (*Me*–CH_2), 22.7 (Me–*C*H_2), 26.0 (N–CH_2–*C*H_2), 27.0 (Me–CH_2–CH_2–*C*H_2), 31.8 (Me–CH_2–*C*H_2), 32.2 (Me–CH_2–CH_2–CH_2–*C*H_2), 43.8 (t, $^1J_{C\text{-}D}$ = 19.9 Hz, CH_2–*C*D), 45.0 (N–CH_2), 110.8 (C arom.), 112.7 (d, $^2J_{C\text{-}F}$ = 20.7 Hz, CH arom.), 123.1 (CH arom.), 134.4 (d, $^3J_{C\text{-}F}$ = 10.4 Hz, CH arom.), 151.9 (N–C–N), 158.4 (C arom.), 161.4 (d, $^1J_{C\text{-}F}$ = 263.2 Hz, C arom.), 162.9 (CO); ^{19}F NMR (377 MHz, $CDCl_3$): δ = -111.1 (dd, $^3J_{F\text{-}H}$ = 11.4 Hz, $^4J_{F\text{-}H}$ = 4.6 Hz); HRMS calcd. for $C_{16}H_{20}N_2OF$ ($[M + H]^+$) 275.1554, found 275.1552.

Quinazolinone (226)

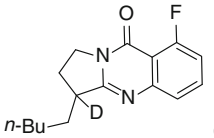

$C_{16}H_{18}DFN_2O$ M = 275.34 g/mol

Following **GP3** with *N*-acylcyanamide **215** (0.6 mmol; 217 mg) and Bu_3SnD (1.2 mmol; 2 equiv.; 325 µL) in benzene, quinazolinone **226** was purified by flash column chromatography (pentane:EtOAc = 5:4) and isolated as a colorless oil (15 mg; 9 %; 95 % deuterium insertion as measured by ^1H NMR et MS).

^1H NMR (400 MHz, $CDCl_3$): δ = 0.90 (t, J = 7.0 Hz, 3 H, *Me*–CH_2), 1.32–1.62 (m, 7 H, *Me*–C*H*$_2$–C*H*$_2$–C*H*$_2$–CH*H*), 1.87–1.98 (m, 1 H, N–CH_2–C*H*H), 2.06–2.19 (m, 1 H, Me–CH_2–CH_2–CH_2–C*H*H), 2.40–2.45 (m, 1 H, N–CH_2–CH*H*), 3.96–4.08 (m, 1 H, N–CH*H*), 4.20–4.35 (m, 1 H, N–C*H*H), 7.05–7.11 (m, 1 H, arom.), 7.45–7.47 (m, 1 H, arom.), 7.60–7.65 (m, 1 H, arom.); ^{13}C NMR (100 MHz, $CDCl_3$): δ = 14.2 (*Me*–CH_2), 22.6 (Me–*C*H_2), 26.1 (N–CH_2–*C*H_2), 27.0 (Me–CH_2–CH_2–*C*H_2), 31.8 (Me–CH_2–*C*H_2), 32.3 (Me–CH_2–CH_2–CH_2–*C*H_2), 44.2 (CH_2–*C*H), 45.0 (N–CH_2), 110.5 (C arom.), 112.6 (d, $^2J_{C\text{-}F}$ = 20.6 Hz, CH arom.), 122.9 (CH arom.), 134.2 (d, $^3J_{C\text{-}F}$ = 10.3 Hz, CH arom.), 151.8

(N–C–N), 158.4 (C arom.), 161.4 (d, $^{1}J_{C\text{-}F} = 263.1$ Hz, C arom.), 162.8 (CO); ^{19}F NMR (377 MHz, $CDCl_3$): $\delta = -111.1$ (dd, $^{3}J_{F\text{-}H} = 10.7$ Hz, $^{4}J_{F\text{-}H} = 5.5$ Hz); HRMS calcd. for $C_{16}H_{19}DN_2OF$ ([M + H]$^+$) 276.16169, found 276.1621.

3.4 Preparation and Cyclization of Azide Precursors

3.4.1 General Procedures

General procedure 1 (GP1): Preparation of *N*-Boc-protected amino alcohols

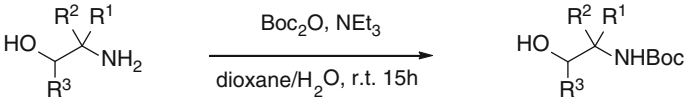

To a solution of amino alcohol in dioxane/H_2O (1:1 mixture, 0.25 M) was added at r.t. di-*t*-butyl dicarbonate (1 equiv.) and NEt_3 (1.1 equiv.). The reaction mixture was stirred at r.t. for 15 h and extracted with CH_2Cl_2. The combined organic layers were washed with water, dried over $MgSO_4$ and concentrated under reduced pressure to afford the pure protected amine as a white solid.

General procedure 2(GP2): Mesylation of *N*-Boc-protected amino alcohols

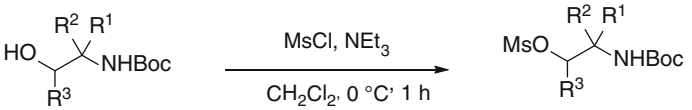

To a solution of *N*-Boc-protected amino alcohol in CH_2Cl_2 (0.15 M) at 0 °C, was added NEt_3 (1.4 equiv.) and dropwise MsCl (1.2 equiv.). The reaction mixture was stirred at 0 °C for 30 min, then at r.t. for an additional hour. The reaction was quenched with H_2O and extracted with CH_2Cl_2. The combined organic layers were washed with water, dried over $MgSO_4$ and concentrated under reduced pressure to afford the pure mesylate as an orange oil.

General procedure 3 (GP3): Preparation of ammonium salts from *N*-Boc-protected aminomesylates [10]

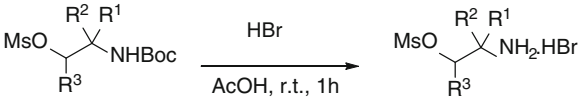

The Boc-protected amine was slowly added to a 2 M solution of HBr in HOAc (1.2 M) at r.t.. After completion of the gas evolution stirring was continued for a further hour followed by the addition of Et_2O (0.3 M). The precipitated product

was filtered off, washed with Et_2O and dried *in vacuo* to afford the ammonium salt as a white solid.

General procedure 4 (GP4): Preparation of azidoamines

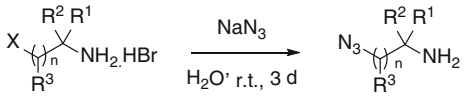

To a solution of alkylamine hydrobromide (1 equiv.) in H_2O (1 M), was added at r.t. sodium azide (3 equiv.). The reaction mixture was stirred at r.t. for 3 d, quenched with a 1 M aqueous NaOH solution and extracted with Et_2O. The combined organic layers were washed with water, dried over $MgSO_4$ and concentrated under reduced pressure to afford the pure azidoamine as an oil.

General procedure 5 (GP5): Preparation of cyanamides

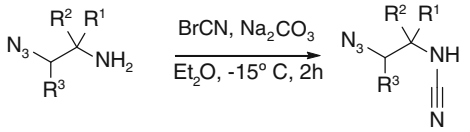

To a solution of cyanogen bromide (1.2 equiv.) in Et_2O (0.5 M) at −15 °C was added Na_2CO_3 (2 equiv.) and the corresponding azidoamine (1 equiv.). The reaction mixture was stirred for 2 h at −15 °C, allowed to reach r.t., and filtered through a short pad of silica. The filtrate was concentrated under reduce pressure and purified by silica gel flash chromatography to afford the cyanamide.

Caution: Cyanogen bromide is a very toxic reagent and must be carefully manipulated under a ventilated hood. All the glassware must be washed with a NaOH solution (0.5 M) and bleach (10 %).

General procedure 6 (GP6): Preparation of *N*-acylcyanamides

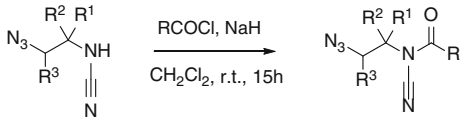

To a solution of cyanamide (1 equiv.) in CH_2Cl_2 (0.05 M) at 0 °C was added the acyl chloride (1.2 equiv.) immediately followed by NaH (1.3 equiv. [60 % in mineral oil]). The reaction mixture was stirred 15 min at 0 °C and an additional hour at r.t., concentrated under reduced pressure and purified by flash column chromatography to give the *N*-acylcyanamide.

General procedure 7 (GP7): Cyclization of aromatic *N*-acylcyanamides

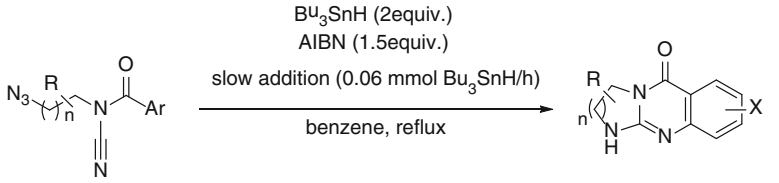

To a degassed solution of *N*-acylcyanamide (1 equiv.) and AIBN (0.3 equiv.) in benzene (0.017 M, 75 % final volume) under reflux was added Bu_3SnH (2 equiv.) and AIBN (1.2 equiv.) in benzene (25 % final volume) over 6.5 h (0.06 mmol Bu_3SnH/h). The reaction mixture was refluxed for an additional hour, cooled to r.t. and concentrated under reduced pressure. Purification of the residue by flash column chromatography afforded the cyclization product.

General procedure 8 (GP8): Cyclization of *N*-enoyl cyanamides

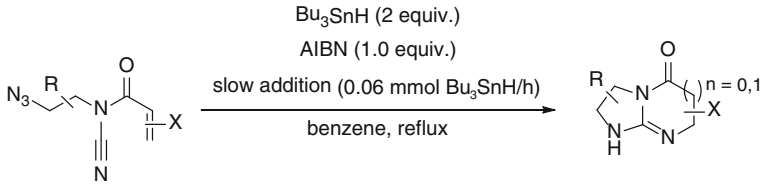

To a degassed solution of *N*-acylcyanamide (1 equiv.) and AIBN (0.2 equiv.) in benzene (0.017 M, 75 % final volume) under reflux was added Bu_3SnH (2 equiv.) and AIBN (0.8 equiv.) in benzene (25 % final volume) over 6.5 h (0.06 mmol Bu_3SnH/h). The reaction mixture was refluxed for an additional hour, cooled to r.t. and concentrated under reduced pressure. Purification of the residue by flash column chromatography afforded the cyclization product.

3.4.2 Azide Precursors

N-(2-azidoethyl)-*N*-cyanobenzamide (169)

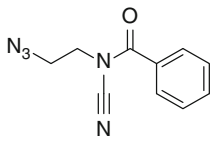

$C_{10}H_9N_5O$ M = 215.21 g/mol

Following **GP4** with 2-bromoethylamine hydrobromide **135** (40 mmol; 8.2 g), 2-azidoethanamine[1] **272** was isolated as a volatile pale yellow oil (2.75 g; 81 %).

Following **GP5** with **272** (1.1 mmol; 95 mg) the corresponding cyanamide was purified by flash column chromatography (petroleum ether:Et_2O = 6:4) and isolated as a pale yellow oil (75 mg; 61 %), which was directly used for the next step owing to its instability. Following **GP6** with the cyanamide (0.68 mmol; 75 mg) and benzoyl chloride (0.74 mmol; 87 μL), *N*-(2-azidoethyl)-*N*-cyanobenzamide **269** was purified by flash column chromatography (pentane:Et_2O = 10:6) and isolated as a yellow oil (134 mg; 92 %).

IR (neat): ν = 2,233, 2,097, 1,703, 1,448, 1,270, 1,058, 700 cm^{-1}; ^1H NMR (400 MHz, $CDCl_3$): δ = 3.72 (t, J = 5.9 Hz, 2 H, N_3–CH_2), 3.96 (t, J = 5.5 Hz, 2 H, N–CH_2), 7.49–7.53 (m, 2 H, arom.), 7.60–7.65 (m, 1 H, arom.), 7.82–7.85 (m, 2 H, arom.); ^{13}C NMR (100 MHz, $CDCl_3$): δ = 47.1 (N–CH_2), 48.6 (N_3–CH_2), 110.7 (CN), 128.8 (2 CH arom.), 128.8 (CH arom.), 130.5 (C arom.), 133.5 (2 CH arom.), 168.3 (C = O); HRMS calcd. for $C_{10}H_9N_5ONa$ ($[M + Na]^+$) 238.0699, found 238.0698.

***N*-(3-azidopropyl)-*N*-cyanobenzamide (270)**

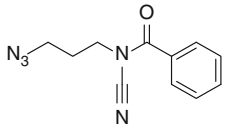

$C_{11}H_{11}N_5O$ M = 229.24 g/mol

Following **GP4** with 3-bromopropylamine hydrobromide **138** (22.8 mmol; 5 g), 3-azidopropan-1-amine [11] **273** was isolated as a volatile pale yellow oil (550 mg; 24 %). Following **GP5** with azidoamine **273** (1.0 mmol; 100 mg) the corresponding cyanamide was purified by flash column chromatography (petroleum ether:Et_2O = 6:4) and isolated as a pale yellow oil (81 mg; 65 %) which was directly used for the next step owing to its instability. Following **GP6** with the cyanamide (0.65 mmol; 81 mg) and benzoyl chloride (0.72 mmol; 83 μL), *N*-acylcyanamide **270** was purified by flash column chromatography (pentane: Et_2O = 10:6) and isolated as a yellow oil (131 mg; 88 %).

IR (neat): ν = 2,231, 2,095, 1,701, 1,448, 1,272, 1,136, 700 cm^{-1}; ^1H NMR (400 MHz, $CDCl_3$): δ = 2.07 (quint., J = 6.9 Hz, 2 H, N_3–CH_2–CH_2), 3.50 (t, J = 6.5 Hz, 2 H, N_3–CH_2), 3.88 (t, J = 6.9 Hz, 2 H, N–CH_2), 7.48–7.52 (m, 2 H, arom.), 7.59–7.63 (m, 1 H, arom.), 7.80–7.83 (m, 2 H, arom.); ^{13}C NMR (100 MHz, $CDCl_3$): δ = 27.3 (N_3–CH_2–CH_2), 45.6 (N–CH_2), 48.6 (N_3–CH_2), 111.0 (CN), 128.7 (CH arom.), 128.8 (CH arom.), 130.9 (C arom.), 133.4 (CH arom.), 168.4 (C = O); HRMS calcd. for $C_{11}H_{11}N_5ONa$ ([M + Na] +) 252.0856, found 252.0862.

4-Azidobutan-1-amine (276)

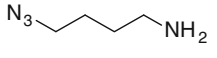

$C_4H_{10}N_4$ M = 114.15 g/mol

To a solution of 1,4-dibromobutane **274** (15 mmol; 1 equiv.; 1.8 mL) in DMF (24 mL), was added sodium azide (90 mmol; 6 equiv.; 5.85 g). The reaction mixture was strirred at 80 °C for 20 h, quenched with H_2O (100 mL) and extracted with Et_2O (3 x 30 mL). The combined organic layers were washed with water (50 mL), dried over $MgSO_4$ and concentrated under reduced pressure to afford the pure 1,4-diazidobutane[11] **275** as a colorless oil (2.16 g; quant.). To a solution of 1,4-diazidobutane **275** (15 mmol; 2.16 g) in Et_2O (10 mL)/EtOAc (10 mL) and 5 % HCl (20 mL), was added triphenylphosphine (0.39 mol) in small portions for 1 h at 0 °C. The mixture was stirred for 24 h at r.t., then, the organic layer was discarded. The aqueous layer was washed twice with CH_2Cl_2 (10 mL), carefully basified with NaOH and then extracted with CH_2Cl_2 (3 × 10 mL). The combined organic layers were washed with water (10 mL), dried over $MgSO_4$ and concentrated under reduced pressure to afford the pure 4-azidobutan-1-amine [11] **276** as a colorless oil (1.20 g; 70 %). Data correspond to those described in the literature [11].

^{1}H NMR (400 MHz, $CDCl_3$): δ = 1.41–1.60 (m, 4 H, N_3–CH_2–CH_2–CH_2), 1.80 (br s, 2 H, NH_2), 2.63 (t, J = 7.04 Hz, 2 H, N_3–CH_2), 3.19 (t, J = 6.8 Hz, 2 H, N–CH_2); ^{13}C NMR (100 MHz, $CDCl_3$): δ = 26.3, 30.8 (N–CH_2–CH_2–CH_2), 41.6 (N–CH_2), 51.3 (N–CH_2).

***N*-(4-azidobutyl)-*N*-cyanobenzamide (271)**

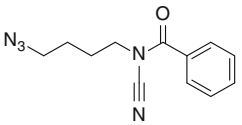

$C_{12}H_{13}N_5O$ M = 243.26 g/mol

Following **GP4** with 4-azidobutan-1-amine **276** (5.0 mmol; 570 mg) the corresponding cyanamide was purified by flash column chromatography (petroleum ether:Et_2O = 6:4) and isolated as a pale yellow oil (418 mg; 60 %) which was directly used for the next step owing to its instability. Following **GP5** with the cyanamide (3.0 mmol; 418 mg) and benzoyl chloride (3.6 mmol; 450 μL), *N*-acylcyanamide **271** was purified by flash column chromatography (pentane:Et_2O = 10:3) and isolated as a colorless oil (520 mg; 71 %).

IR (neat): ν = 2,233, 2,097, 1,703, 1,448, 1,270, 1,058, 700 cm^{-1}; ^{1}H NMR (400 MHz, $CDCl_3$): δ = 1.68–1.75 (m, 2 H, N_3–CH_2–CH_2), 1.87–1.94 (m, 2 H, N–CH_2–CH_2), 3.37 (t, J = 6.6 Hz, 2 H, N_3–CH_2), 3.80 (t, J = 7.1 Hz, 2 H, N–CH_2), 7.47–7.50 (m, 2 H, arom.), 7.58–7.62 (m, 1 H, arom.), 7.79–7.81 (m, 2 H, arom.); ^{13}C NMR (100 MHz, $CDCl_3$): δ = 25.1 N–CH_2–CH_2), 25.9 (N_3–CH_2–CH_2), 47.3 (N–CH_2), 50.8 (N_3–CH_2), 111.0 (CN), 128.7 (CH arom.), 128.7 (CH arom.), 131.0 (C arom.), 133.3 (CH arom.), 168.5 (C = O); HRMS calcd. for $C_{12}H_{13}N_5ONa$ ([M + Na]$^+$) 266.1012, found 266.1012.

Methanesulfonic acid 2-*tert*-butoxycarbonylamino-2-methyl-propyl ester (283)

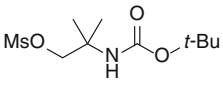

$C_{10}H_{21}NO_5S$ M = 267.34 g/mol

Following **GP1** with 2-amino-2-methylpropanol **280** (50 mmol; 4.50 g), the corresponding *N*-Boc-protected amine [12] was isolated as a pale yellow solid (8.45 g; 90 %). Following **GP2** with the *N*-Boc-protected amine (10.6 mmol; 2.0 g), mesylate **283** was isolated as an orange oil (3.0 g; quant.) [13].

^{1}H NMR (400 MHz, $CDCl_3$): δ = 1.25 (s, 6 H, Me_2C), 1.41 (s, 9 H, Me_3C), 2.98 (s, 3 H, Me–S), 4.28 (s, 2 H, CH_2), 4.56 (br s, 1 H, NH).

***N*-(1-azido-2-methylpropan-2-yl)cyanamide (292)**

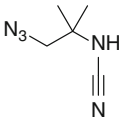

$C_5H_9N_5$ M = 139.16 g/mol

Following **GP3** with mesylate 283 (10.6 mmol; 2.83 g), the corresponding ammonium salt **286** was isolated as a white solid (2.2 g; 83 %). Following **GP4** with ammonium salt **286** (4.8 mmol; 1.20 g), 2-azido-1,1-dimethyl-ethylamine **289** was isolated as a volatile pale yellow oil. Following **GP5** with amine **289** (3.38 mmol; 386 mg), cyanamide **292** was purified by flash column chromatography (petroleum ether:Et_2O = 1:2) and isolated as a colorless oil (210 mg; 34 %) which was quickly used for the next step owing to its instability.

IR (neat): ν = 3,185, 2,211, 2,100, 1,442, 1,300, 1,174 cm^{-1}; ^{1}H NMR (400 MHz, $CDCl_3$): δ = 1.29 (s, 6 H, 2 Me), 3.36 (s, 2 H, N_3–CH_2), 4.17 (br s, 1 H, NH); ^{13}C NMR (100 MHz, $CDCl_3$): δ = 24.8 (Me), 55.8 (Me_2C), 60.3 (N_3–CH_2), 113.8 (CN).

***N*-(1-azido-2-methylpropan-2-yl)-*N*-cyanobenzamide (277)**

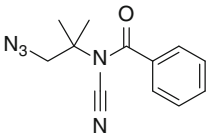

$C_{12}H_{13}N_5O$ M = 243.26 g/mol

Following **GP6** with cyanamide **292** (0.54 mmol; 75 mg) and benzoyl chloride (0.65 mmol; 75 μL), *N*-acylcyanamide **277** was purified by flash column chromatography (pentane:Et_2O = 5:1) and isolated as colorless oil (109 mg; 83 %).

IR (neat): ν = 2,236, 2,097, 1,711, 1,449, 1,274, 1,107, 706 cm^{-1}; ^{1}H NMR (400 MHz, $CDCl_3$): δ = 1.42 (s, 6 H, 2 Me), 3.81 (s, 2 H, N_3–CH_2), 7.47–7.52 (m, 2 H, arom.), 7.59–7.61 (m, 1 H, arom.), 7.82–7.84 (m, 2 H, arom.); ^{13}C NMR

(100 MHz, $CDCl_3$): δ = 24.1 (2 Me), 55.1 (N_3–CH_2), 61.6 (*C*Me_2), 111.6 (CN), 128.8 (2 CH arom.), 128.8 (CH arom.), 130.6 (C arom.), 133.5 (2 CH arom.), 168.6 (C = O); HRMS calcd. for $C_{12}H_{13}N_5ONa$ ($[M + Na]^+$) 306.1325, found 306.1325.

Methanesulfonic acid 2-*tert*-butoxycarbonylamino-2-phenyl–ethyl ester (284)

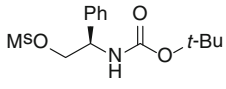

$C_{14}H_{21}NO_5S$ M = 315.39 g/mol

Following **GP1** with (*R*)-2-amino-2-phenylethanol **281** (21.9 mmol; 3.00 g), the corresponding *N*-Boc-protected amine [14] was isolated as a pale yellow solid (4.80 g; 93 %). Following **GP2** with the *N*-Boc-protected amine (16.9 mmol; 4.00 g), mesylate **284** was isolated as an orange oil (5.20 g; 98 %). Data correspond to those described in the litterature [14].

^{1}H NMR (400 MHz, $CDCl_3$): δ = 1.43 (s, 9 H, *Me*$_3$C), 2.87 (s, 3 H, Me–S), 4.37–4.48 (m, 2 H, CH_2), 5.01 (br s, 1 H, N–C*H*), 5.19–5.20 (br s, 1 H, NH), 7.30–7.39 (m, 5 H, arom.); ^{13}C NMR (100 MHz, $CDCl_3$): δ = 28.4 (*Me*$_3$C), 37.6 (Me–S), 53.9 (N–*C*H), 71.4 (CH_2), 80.4 (Me$_3$*C*), 126.8 (2 CH arom.), 128.4 (CH arom.), 129.1 (2 CH arom.), 137.9 (C arom.), 155.2 (C = O).

(*R*)-2-Azido-1-phenylethylamine (290)

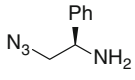

$C_8H_{10}N_4$ M = 162.19 g/mol

Following **GP3** with mesylate **284** (25.7 mmol; 8.10 g), the corresponding ammonium salt **287** was isolated as a white solid (7.50 g; 99 %). Following **GP4** with **287** (25.4 mmol; 7.50 g), azidoamine **290** was isolated as a yellow oil (3.80 g; 92 %). Data correspond to those described in the litterature.[14]

IR (neat): ν = 3,321, 2,093, 1,601, 1,453, 1,242, 844, 699 cm^{-1}; ^{1}H NMR (400 MHz, $CDCl_3$): δ = 1.22 (br s, 2 H, NH_2), 2.94 (d, J = 6.36 Hz, 2 H, CH_2), 4.48 (t, J = 6.32 Hz, 1 H, N–C*H*), 7.29–7.41 (m, 5 H, arom.); ^{13}C NMR (100 MHz, $CDCl_3$): δ = 47.9 (N–*C*H), 69.2 (CH_2), 127.1 (2 CH arom.), 128.5 (CH arom.), 128.9 (2 CH arom.), 137.8 (C arom.); HRMS calcd. for $C_8H_{11}N_4$ ($[M + H]^+$) 163.0978, found 163.0974.

(*R*)-*N*-(2-azido-1-phenylethyl)cyanamide (293)

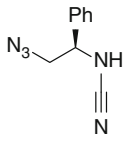

$C_9H_9N_5$ M = 187.20 g/mol

Following **GP5** with amine **290** (3.08 mmol; 500 mg) cyanamide **293** was purified by flash column chromatography (petroleum ether:Et_2O = 1:2) and isolated as a pale orange oil (434 mg; 75 %), which was quickly used for the next step owing to its instability.

IR (neat): ν = 3,185, 2,221, 2,100, 1,603, 1,243, 699 cm^{-1}; ^1H NMR (400 MHz, $CDCl_3$): δ = 3.23–3.27 (m, 2 H, N_3–CH_2), 4.19 (br s, 1 H, NH), 4.73 (dd, J = 7.0, 5.7 Hz, 1 H, PhC*H*), 7.31–7.34 (m, 2 H, arom.), 7.39–7.45 (m, 3 H, arom.); ^{13}C NMR (100 MHz, $CDCl_3$): δ = 51.2 (N_3–CH_2), 65.5 (*C*HPh), 115.5 (CN), 127.1 (2 CH arom.), 129.4 (3 CH arom.), 135.7 (C arom.); HRMS calcd. for $C_9H_{10}N_5$ ($[M + H]^+$) 188.0931, found 188.0929.

(*R*)-*N*-(2-azido-1-phenylethyl)-*N*-cyanobenzamide (278)

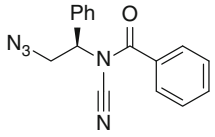

$C_{16}H_{13}N_5O$ M = 291.31 g/mol

Following **GP6** with cyanamide **293** (0.72 mmol; 134 mg) and benzoyl chloride (0.86 mmol; 100 μL), *N*-acylcyanamide **278** was purified by flash column chromatography (pentane:Et_2O = 5:1) and isolated as colorless oil (201 mg; 96 %).

IR (neat): ν = 2,235, 2,104, 1,704, 1,449, 1,269, 1,130, 1,003, 700 cm^{-1}; ^1H NMR (400 MHz, $CDCl_3$): δ = 3.96 (d, J = 7.0 Hz, 2 H, N_3–CH_2), 5.01 (t, J = 7.2 Hz, 1 H, Ph–CH), 7.40–7.52 (m, 7 H, arom.), 7.59–7.63 (m, 1 H, arom.), 7.77–7.79 (m, 2 H, arom.); ^{13}C NMR (100 MHz, $CDCl_3$): δ = 52.1 (N_3–CH_2), 63.4 (*C*HPh), 110.8 (CN), 127.3 (2 CH arom.), 128.7 (3 CH arom.), 128.7 (CH arom.), 129.4 (2 CH arom.), 129.6 (CH arom.), 130.6 (C arom.), 133.5 (CH arom.), 135.3 (C arom.), 168.2 (C = O); HRMS calcd. for $C_{16}H_{13}N_5ONa$ ($[M + Na]^+$) 314.1012, found 314.1006; $[\alpha]_D^{20}$ = + 76.0 (c = 10 g/L, CH_2Cl_2).

Methanesulfonic acid 2-*tert*-butoxycarbonylamino-cyclohexyl ester (285)

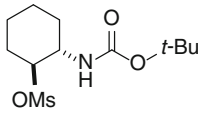

$C_{12}H_{23}NO_5S$ M = 293.38 g/mol

Following **GP1** with *trans*-2-amino-cyclohexanol hydrochloride **282** (25.0 mmol; 3.79 g), the corresponding *N*-Boc-protected amine [15] was isolated as a pale yellow solid (4.77 g; 89 %). Following **GP2** with the *N*-Boc-protected amine (16.9 mmol; 4.77 g), mesylate **284** was isolated as an orange oil (5.20 g; 98 %). Data correspond to those described in the literature [15].

^1H NMR (400 MHz, $CDCl_3$): δ = 1.22–1.30 (m, 3 H, CH_2 cyclohexyl), 1.41 (s, 9 H, Me_3C), 1.58–1.84 (m, 3 H, CH_2 cyclohexyl), 2.05–2.20 (m, 2 H, CH_2 cyclohexyl), 2.84 (s, 3 H, Me–S), 3.57 (br d, 1 H, CH cyclohexyl), 4.30–4.50

(m, 1 H, CH_2 cyclohexyl), 4.70 (br d s, 1 H, NH); ^{13}C NMR (100 MHz, $CDCl_3$): $\delta = 23.8$, 24.0 (2 CH_2 cyclohexyl), 28.5 (Me_3C), 32.0, 32.3 (2 CH_2 cyclohexyl), 38.7 (Me–S), 53.1 (N–CH), 79.3 (Me_3C), 82.6 (O–CH), 155.2 (C = O).

***trans*-2-Azidocyclohexanamine (291)**

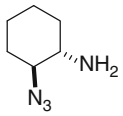

$C_6H_{12}N_4$ M = 140.19 g/mol

Following **GP3** with mesylate **285** (10.2 mmol; 3.00 g), the corresponding ammonium salt **288** was isolated as a whitesolid (2.49 g; 89 %). Following **GP4** with **288** (4.38 mmol; 1.20 g), azidoamine **291** was isolated as a colorless oil (3.80 g; 92 %). Data correspond to those described in the litterature [16].

^1H NMR (400 MHz, $CDCl_3$): $\delta = 1.08$–1.40 (m, 4 H, CH_2 cyclohexyl), 1.46 (br s, 2 H, NH_2), 1.66–2.06 (m, 4 H, CH_2 cyclohexyl), 2.47–2.53 (m, 1 H, N_3–CH), 2.90–2.97 (m, 1 H, NH_2–C*H*); ^{13}C NMR (100 MHz, $CDCl_3$): $\delta = 24.5$, 24.7 (2 CH_2 cyclohexyl), 30.3, 34.2 (2 CH_2 cyclohexyl), 54.7 (N–CH), 68.5 (N–CH).

***N*-(*trans*-2-azidocyclohexyl)cyanamide (294)**

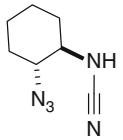

$C_7H_{11}N_5$ M = 165.20 g/mol

Following **GP5** with azidoamine **291** (2.6 mmol; 360 mg), cyanamide **294** was purified by flash column chromatography (petroleum ether:Et_2O = 1:2) and isolated as a colorless oil (140 mg; 33 %) which was quickly used for the next step owing to its instability.

IR (neat): $\nu = 3{,}181$, 2,935, 2,217, 2,092, 1,450, 1,259 cm^{-1}; ^1H NMR (400 MHz, $CDCl_3$): $\delta = 1.24$–1.50 (m, 4 H, cyclohexyl), 1.78–1.85 (m, 2 H, cyclohexyl), 2.10–2.20 (m, 2 H, cyclohexyl), 2.77–2.85 (m, 1 H, N_3–CH), 3.24 (td, $J = 10.3$, 4.2 Hz, 1 H, N–CH), 4.29 (br s, 1 H, NH); ^{13}C NMR (100 MHz, $CDCl_3$): $\delta = 24.0$ (2 CH_2, cyclohex.), 30.1 (CH_2, cyclohex.), 30.2 (CH_2, cyclohex.), 57.9 (N–CH), 64.3 (N_3–CH), 114.2 (CN); HRMS calcd. for $C_7H_{11}N_5Na$ ($[M + Na]^+$) 188.09071, found 188.0906.

***N*-(*trans*-2-azidocyclohexyl)-*N*-cyanobenzamide (279)**

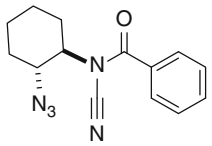

$C_{14}H_{15}N_5O$ M = 269.30 g/mol

Following **GP6** with cyanamide **294** (0.62 mmol; 102 mg) and benzoyl chloride (0.74 mmol; 86 μL), *N*-acylcyanamide **279** was purified by flash column chromatography (pentane:Et_2O = 5:1) and isolated as colorless oil (127 mg; 76 %).

IR (neat): ν = 2,942, 2,865, 2,231, 2,097, 1,707, 1,449, 1,280, 1,105, 711 cm^{-1}; ^1H NMR (400 MHz, $CDCl_3$): δ = 1.34–1.73 (m, 4 H, cyclohex.), 1.87–1.91 (m, 2 H, cyclohex.), 2.05–2.12 (m, 1 H, cyclohex.), 2.26–2.34 (m, 1 H, cyclohex.), 3.59 (td, J = 11.1, 4.4 Hz, 1 H, N–CH), 4.27 (td, J = 11.4, 4.4 Hz, 1 H, N_3–CH), 7.48–7.52 (m, 2 H, arom.), 7.58–7.63 (m, 1 H, arom.), 7.80–7.83 (m, 2 H, arom.); ^{13}C NMR (100 MHz, $CDCl_3$): δ = 24.0 (CH_2 cyclohex.), 24.4 (CH_2 cyclohex.), 29.7 (CH_2 cyclohex.), 31.0 (CH_2 cyclohex.), 58.5 (N_3–CH), 61.1 (N–CH), 109.2 (CN), 128.8 (CH arom.), 128.8 (4 CH arom.), 131.3 (C arom.), 133.3 (CH arom.), 168.5 (C = O); HRMS calcd. for $C_{14}H_{15}N_5ONa$ ($[M + Na]^+$) 292.1169, found 292.1169.

The crystal structure of **279** has been deposited at the Cambridge Crystallographic Data Centre and allocated the deposition number CCDC 766976.

(*R*)-*N*-(2-azido-1-phenylethyl)-*N*-cyano-4-methoxybenzamide (295)

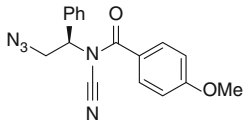

$C_{17}H_{15}N_5O_2$ M = 321.33 g/mol

Following **GP6** with cyanamide **164** (0.43 mmol; 80 mg) and 4-methoxybenzoyl chloride (0.56 mmol; 76 μL), *N*-acylcyanamide **295** was purified by flash column chromatography (pentane:Et_2O = 5:4) and isolated as colorless oil (135 mg; 98 %).

IR (neat): ν = 2,232, 2,104, 1,697, 1,604, 1,511, 1,253, 1,173, 1,025, 841, 756, 701 cm^{-1}; ^1H NMR (400 MHz, $CDCl_3$): δ = 3.86 (s, 3 H, OMe), 3.92–3.96 (m, 2 H, N_3–CH_2), 3.99 (dd, J = 8.1, 6.4 Hz, 1 H, Ph–CH), 6.96 (d, J = 9.0 Hz, 2 H, arom.), 7.39–7.52 (m, 5 H, arom.), 7.80 (d, J = 8.8 Hz, 2 H, arom.); ^{13}C NMR (100 MHz, $CDCl_3$): δ = 52.3 (N_3–CH_2), 59.6 (OMe), 63.5 (*C*HPh), 111.4 (CN), 114.0 (2 CH arom.), 122.5 (C arom.), 127.2 (2 CH arom.), 129.4 (2 CH arom.), 129.5 (CH arom.), 131.2 (2 CH arom.), 135.5 (C arom.), 163.8 (C arom.), 167.4 (C = O); HRMS calcd. for $C_{17}H_{15}N_5O_2Na$ ($[M + Na]^+$) 344.1118, found 344.1119; $[\alpha]_D^{20}$ = + 55.0 (c = 1 g/L, CH_2Cl_2).

(*R*)-*N*-(2-azido-1-phenylethyl)-*N*-cyano-4-(trifluoromethyl)benzamide (296)

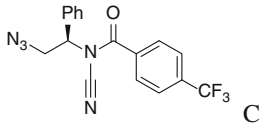

$C_{17}H_{12}F_3N_5O$ M = 359.31 g/mol

Following **GP6** with cyanamide **164** (1.0 mmol; 187 mg) and 4-trifloromethylbenzoyl chloride (1.2 mmol; 179 μL), *N*-acylcyanamide **296** was

purified by flash column chromatography (pentane:Et_2O = 5:1) and isolated as colorless oil (250 mg; 70 %).

IR (neat): ν = 2,238, 2,109, 1,710, 1,325, 1,269, 1,274, 1,173, 1,131, 1,068, 853, 701 cm^{-1}; ^1H NMR (400 MHz, $CDCl_3$): δ = 3.94–4.03 (m, 2 H, N_3–CH_2), 5.01 (dd, J = 8.6, 5.9 Hz, 1 H, Ph–CH), 7.42–7.49 (m, 5 H, arom.), 7.76 (d, J = 8.8 Hz, 2 H, arom.), 7.87 (d, J = 8.8 Hz 2 H, arom.); ^{13}C NMR (100 MHz, $CDCl_3$): δ = 52.1 (N_3–CH_2), 63.3 (*C*HPh), 110.3 (CN), 123.4 (q, CF_3, $^1J_{C\text{-}F}$ = 271.4 Hz), 125.9 (q, 2 CH arom., $^3J_{C\text{-}F}$ = 3.4 Hz), 127.3 (2 CH arom.), 129.2 (2 CH arom.), 129.5 (2 CH arom.), 129.8 (CH arom.), 133.9 (C arom.),135.0 (q, C–CF_3 arom., $^2J_{C\text{-}F}$ = 32.7 Hz), 135.1 (C arom.), 167.2 (C = O); ^{19}F NMR (377 MHz, $CDCl_3$): δ = -63.8; $[\alpha]_D^{20}$ = + 62.0 (c = 2.5 g/L, CH_2Cl_2).

(*R*)-*N*-(2-azido-1-phenylethyl)-*N*-cyano-2,4,6-trimethylbenzamide (297)

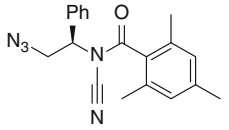

$C_{19}H_{19}N_5O$ M = 333.39 g/mol

Following **GP6** with cyanamide **164** (0.50 mmol; 93 mg) and 2,4,6-trimethylbenzoyl chloride (0.6 mmol; 110 mg), *N*-acylcyanamide **297** was purified by flash column chromatography (pentane:Et_2O = 5:1) and isolated as colorless oil (101 mg; 61 %).

IR (neat): ν = 2,237, 2,104, 1,715, 1,261, 1,197, 701 cm^{-1}; ^1H NMR (400 MHz, $CDCl_3$): δ = 2.19 (s, 3 H, Me), 2.28 (s, 3 H, Me), 2.29 (s, 3 H, Me), 3.92 (A of ABX, $J_{A\text{-}B}$ = 13.9 Hz, $J_{A\text{-}X}$ = 9.5 Hz, 1 H, N_3–CH*H*), 3.99 (B of ABX, $J_{A\text{-}B}$ = 13.8 Hz, $J_{B\text{-}X}$ = 5.5 Hz, 1 H, N_3–C*H*H), 4.97 (X of ABX, 1 H, Ph–C*H*), 6.88 (br s, 2 H, arom.), 7.40–7.49 (m, 5 H, arom.); ^{13}C NMR (100 MHz, $CDCl_3$): δ = 18.8 (Me), 19.0 (Me), 21.4 (Me), 50.4 (N_3–CH_2), 63.5 (*C*HPh), 109.8 (CN), 127.5 (2 CH arom.), 128.8 (CH arom.), 128.8 (CH arom.), 129.5 (CH arom.), 129.8 (2 CH arom.), 129.8 (C arom.), 134.6 (C arom.), 134.6 (C arom.), 135.2 (C arom.), 140.9 (C arom.), 170.5 (C = O); HRMS calcd. for $C_{19}H_{19}N_5ONa$ ($[M + Na]^+$) 356.1482, found 356.1476; $[\alpha]_D^{20}$ = + 80.7 (c = 6 g/L, CH_2Cl_2).

(*R*)-*N*-(2-azido-1-phenylethyl)-*N*-cyano-2-naphthamide (298)

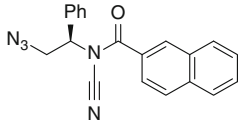

$C_{20}H_{15}N_5O$ M = 341.37 g/mol

Following **GP6** with cyanamide **164** (0.42 mmol; 80 mg) and 2-naphtoyl chloride (0.50 mmol; 48 mg), *N*-acylcyanamide **298** was purified by flash column chromatography (pentane:Et_2O = 5:1) and isolated as colorless oil (130 mg; 91 %).

IR (neat): ν = 2,922, 2,234, 2,106, 1,703, 1,279, 1,231, 1,011, 756, 700 cm^{-1}; ^1H NMR (400 MHz, $CDCl_3$): δ = 4.03 (d, J = 7.2 Hz, 2 H, N_3–CH_2), 5.06 (t, J = 7.2 Hz, 1 H, Ph–CH), 7.44–7.51 (m, 5 H, arom.), 7.57–7.67 (m, 2 H, arom.), 7.76–7.79 (m, 1 H, arom.), 7.89–7.98 (m, 3 H, arom.), 8.34–8.35 (m, 1 H, arom.); ^{13}C NMR (100 MHz, $CDCl_3$): δ = 52.4 (N_3–CH_2), 63.6 (*C*HPh), 111.1 (CN), 124.3 (CH arom.), 127.4 (2 CH arom.), 127.5 (CH arom.), 127.7 (C arom.), 128.0 (CH arom.), 128.9 (CH arom.), 129.1 (CH arom.), 129.5 (CH arom.), 129.5 (CH arom.), 129.7 (2 CH arom.), 130.3 (CH arom.), 132.1 (C arom.), 135.5 (C arom.), 135.6 (C arom.), 168.4 (C = O); HRMS calcd. for $C_{20}H_{15}N_5ONa$ ($[M + Na]^+$) 364.1169, found 364.1169; $[\alpha]_D^{20}$ = + 47.5 (c = 8 g/L, CH_2Cl_2).

(*R*)-*N*-(2-azido-1-phenylethyl)-*N*-cyanothiophene-2-carboxamide (299)

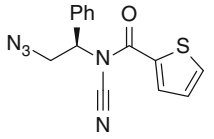

$C_{14}H_{11}N_5OS$ M = 297.34 g/mol

Following **GP6** with cyanamide **164** (0.37 mmol; 69 mg) and 2-thiophencarbonyl chloride (0.44 mmol; 48 μL), *N*-acylcyanamide **299** was purified by flash column chromatography (pentane:Et_2O = 5:1) and isolated as colorless oil (90 mg; 82 %).

IR (neat): ν = 2,235, 2,105, 1,676, 1,412, 1,263, 1,002, 727, 700 cm^{-1}; ^1H NMR (400 MHz, $CDCl_3$): δ = 3.89 (A of ABX, $J_{A\text{-}B}$ = 13.8 Hz, $J_{A\text{-}X}$ = 9.5 Hz, 1 H, N_3–CH*H*), 3.89 (B of ABX, $J_{A\text{-}B}$ = 13.8 Hz, $J_{B\text{-}X}$ = 4.8 Hz, 1 H, N_3–C*H*H), 4.99 (X of ABX, 1 H, Ph–C*H*), 7.16 (dd, J = 4.8, 4.0 Hz, 1 H, arom.), 7.39–7.48 (m, 5 H, arom.), 7.73 (dd, J = 5.0, 0.9 Hz, 1 H, arom.), 8.15 (dd, J = 4.0, 0.9 Hz, 1 H, arom.); ^{13}C NMR (100 MHz, $CDCl_3$): δ = 53.0 (N_3–CH_2), 63.6 (*C*HPh), 111.1 (CN), 127.2 (2 CH arom.), 128.4 (CH arom.), 129.5 (CH arom.), 129.6 (2 CH arom.), 133.5 (C arom.), 134.1 (CH arom.), 134.9 (CH arom.), 135.4 (C arom.), 160.3 (C = O); HRMS calcd. for $C_{14}H_{11}N_5OSNa$ ($[M + Na]^+$) 320.0576, found 320.0573; $[\alpha]_D^{20}$ = + 83.0 (c = 6 g/L, CH_2Cl_2).

(*R*)-*N*-(2-Azido-1-phenylethyl)isonicotinamide (300)

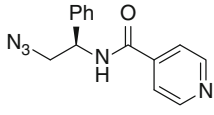

$C_{14}H_{13}N_5O$ M = 267.29 g/mol

To a solution of azidoamine **290** (1.23 mmol; 1 equiv.; 200 mg) in CH_2Cl_2 (40 mL) was added at 0 °C NEt_3 (2.95 mmol; 2.4 equiv.; 415 μL) and after 10 min isonicotinoyl chloride hydrochloride (1.48 mmol; 1.2 equiv.; 264 mg). The reaction was stirred at r.t. for 15 h, hydrolyzed with 50 mL of water, extracted with CH_2Cl_2 (2 x 30 mL) and concentrated under reduced pressure. The residue was

purified by flash column chromatography (petroleum ether:Et_2O = 1:2) to afford the desired amide **300** as a colorless oil (145 mg; 44 %).

IR (neat): ν = 3,270, 2,098, 1,650, 1,536, 1,304, 1,241, 699 $^{-1}$; ^{1}H NMR (400 MHz, $CDCl_3$): δ = 3.45–3.52 (m, 1 H, N_3–CH*H*), 3.86–3.94 (m, 1 H, N_3–C*H*H), 4.84 (dd, J = 9.0, 4.8 Hz, 1 H, PhC*H*), 6.68 (br s, 1 H, NH), 7.38–7.45 (m, 5 H, arom.), 7.57–7.58 (m, 2 H, arom.), 8.73–8.74 (m, 2 H, arom.); ^{13}C NMR (100 MHz, $CDCl_3$): δ = 45.4 (N_3–CH_2), 65.2 (*C*HPh), 121.0 (2 CH arom.), 127.0 (2 CH arom.), 129.2 (2 CH arom.), 129.3 (CH arom.), 136.8 (C arom.), 141.3 (C arom.), 150.8 (2 CH arom.), 165.8 (C = O); HRMS calcd. for $C_{14}H_{13}N_5ONa$ ($[M + Na]^+$) 290.1012, found 290.1013.

(*R*)-*N*-(2-azido-1-phenylethyl)-*N*-cyanoisonicotinamide (301)

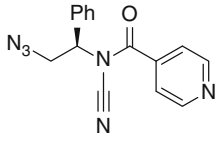

$C_{15}H_{12}N_6O$ M = 292.30 g/mol

To a solution of amide **300** (0.54 mmol; 1 equiv.; 145 mg) in THF (18 mL) at r.t. was added NaH (0.60 mmol; 1.1 equiv.; 24 mg [60 % in mineral oil]). After 45 min, cyanogen bromide (1.62 mmol; 3 equiv.; 540 µL [3.0 M solution in CH_2Cl_2]) was added and the mixture was stirred at r.t. for 15 h. The reaction mixture was filtered through a short pad of silica and concentrated under reduced pressure. The residue was purified by flash column chromatography (petroleum ether:EtOAc = 4:3) to afford the desired *N*-acylcyanamide **301** as a colorless oil (79 mg; 50 %).

IR (neat): ν = 2,238, 2,106, 1,713, 1,409, 1,277, 1,138, 752, 700 cm^{-1}; ^{1}H NMR (400 MHz, $CDCl_3$): δ = 3.91–4.01 (m, 2 H, N_3–CH_2), 4.99 (dd, J = 8.6, 5.7 Hz, 1 H, PhC*H*), 7.40–7.49 (m, 5 H, arom.), 7.55–7.57 (m, 2 H, arom.), 8.81–8.82 (m, 2 H, arom.); ^{13}C NMR (100 MHz, $CDCl_3$): δ = 52.0 (N_3–CH_2), 63.2 (*C*HPh), 109.9 (CN), 121.7 (2 CH arom.), 127.3 (2 CH arom.), 129.5 (2 CH arom.), 129.8 (CH arom.), 134.9 (C arom.), 137.7 (C arom.), 150.8 (2 CH arom.), 166.6 (C = O); HRMS calcd. for $C_{15}H_{13}N_6O$ ($[M + H]^+$) 265.1084, found 265.1083; $[\alpha]_D^{20}$ = + 67.9 (c = 7 g/L, CH_2Cl_2).

(*R*,*E*)-*N*-(2-azido-1-phenylethyl)-*N*-cyanobut-2-enamide (302)

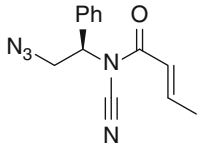

$C_{13}H_{13}N_5O$ M = 255.28 g/mol

Following **GP6** with cyanamide **164** (0.43 mmol; 80 mg) and *trans*-crotonyl chloride (0.47 mmol; 49 mg), *N*-acylcyanamide **302** was purified by flash column chromatography (pentane:Et_2O = 10:3) and isolated as a colorless oil (84 mg; 77 %).

IR (neat): ν = 2,236, 2,110, 1,710, 1,644, 1,224, 702 cm^{-1}; ^1H NMR (400 MHz, $CDCl_3$): δ = 1.99 (dd, J = 7.04, 1.8 Hz, 3 H, Me), 3.75 (A of ABX, $J_{A\text{-}B}$ = 14.0 Hz, $J_{A\text{-}X}$ = 9.4 Hz, 1 H, N_3–CH*H*), 3.81 (B of ABX, $J_{A\text{-}B}$ = 14.0 Hz, $J_{B\text{-}X}$ = 5.2 Hz, 1 H, N_3–C*H*H), 4.86 (X of ABX, 1 H, Ph–C*H*), 6.57 (dq, J = 14.9, 1.7 Hz, 1 H, = C*H*CO), 7.18–7.26 (m, 1 H, = C*H*Me), 7.36–7.49 (m, 5 H, arom.); ^{13}C NMR (100 MHz, $CDCl_3$): δ = 18.6 (Me), 50.9 (N_3–CH_2), 63.6 (*C*HPh), 110.5 (CN), 119.1 (= *C*HCO), 127.2 (2 CH arom.), 129.4 (2 CH arom.), 129.5 (CH arom.), 135.5 (C arom.), 150.2 (= *C*HMe), 164.3 (C = O); HRMS calcd. for $C_{13}H_{13}N_5ONa$ ($[M + Na]^+$) 278.1012, found 278.1013.

(*E*)-*N*-(1-azido-2-methylpropan-2-yl)-*N*-cyano-2-methyl-3-phenylacrylamide (303)

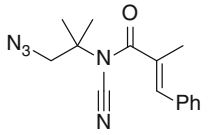

$C_{15}H_{17}N_5O$ M = 283.33 g/mol

Following **GP6** with cyanamide **164** (0.32 mmol; 45 mg) and 2-methyl-3-phenylprop-2-enoyl chloride (0.39 mmol; 70 mg), *N*-acylcyanamide **303** was purified by flash column chromatography (pentane:Et_2O = 5:1) and isolated as a colorless oil (75 mg; 83 %).

IR (neat): ν = 2,234, 2,095, 1,703, 1,445, 1,343, 1,246, 1,212, 1,107, 696 cm^{-1}; ^1H NMR (400 MHz, $CDCl_3$): δ = 1.40 (s, 6 H, 2 Me), 2.21 (d, J = 1.5 Hz, 3 H, = CMe), 3.73 (s, 2 H, N_3–CH_2), 7.28 (q, J = 1.3 Hz, 1 H, = CH), 7.34–7.42 (m, 5 H, arom.); ^{13}C NMR (100 MHz, $CDCl_3$): δ = 15.6 (= C*Me*), 24.2 (2 Me), 54.8 (N_3–CH_2), 61.7 (*C*Me_2), 111.6 (CN), 128.7 (2 CH arom.), 128.8 (C arom.), 129.1 (CH arom.), 129.7 (2 CH arom.), 134.5 (= *C*Me), 138.2 (= CH), 171.0 (C = O).

(*R*)-*N*-(2-azido-1-phenylethyl)-*N*-cyano-3-methylbut-2-enamide (304)

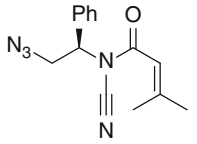

$C_{14}H_{15}N_5O$ M = 269.30 g/mol

Following **GP6** with cyanamide **164** (0.37 mmol; 69 mg) and 3,3′-dimethylacryloyl chloride (0.44 mmol; 50 μL), *N*-acylcyanamide **304** was purified by flash column chromatography (pentane:Et_2O = 10:1) and isolated as colorless oil (75 mg; 75 %).

IR (neat): ν = 2,232, 2,105, 1,703, 1,634, 1,446, 1,232, 1,143, 830, 759, 700 cm^{-1}; ^1H NMR (400 MHz, $CDCl_3$): δ = 2.00 (d, J = 1.3 Hz, 3 H, Me), 2.20 (d, J = 1.3 Hz, 3 H, Me), 3.72 (A of ABX, $J_{A\text{-}B}$ = 14.0 Hz, $J_{A\text{-}X}$ = 9.4 Hz, 1 H, N_3–CH*H*), 3.78 (B of ABX, $J_{A\text{-}B}$ = 14.0 Hz, $J_{B\text{-}X}$ = 5.0 Hz, 1 H, N_3–C*H*H), 4.85

(X of ABX, 1 H, Ph–C*H*), 6.33 (br s, 1 H, = CH), 7.36–7.45 (m, 5 H, arom.); ^{13}C NMR (100 MHz, $CDCl_3$): $\delta = 21.2$ (Me), 28.1 (Me), 50.6 (N_3–CH_2), 63.8 (*C*HPh), 110.9 (CN), 112.8 (= CH), 127.2 (2 CH arom.), 129.4 (2 CH arom.), 129.5 (CH arom.), 135.7 (C arom.), 163.3 (= *C*Me_2), 164.2 (C = O); HRMS calcd. for $C_{14}H_{15}N_5ONa$ ([M + Na]$^+$) 292.1169, found 292.1169; $[\alpha]_D^{20} = +97.4$ (c = 5 g/L, CH_2Cl_2).

2-Phthalimidoaniline (306)

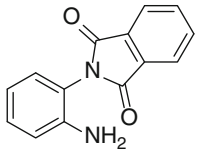

$C_{14}H_{10}N_2O_2$ M = 238.24 g/mol

Phthalic anhydride (100 mmol; 1 equiv.; 13.81 g) and 2-nitroaniline (100 mmol; 1 equiv.; 14.81 g) were melted together in an open flask and heated to 160 °C for 2 h. The reaction mixture was then allowed to cool, and glacial acetic acid (50 mL) was added. The solution was refluxed for 5 min, and slowly cooled. The resulting mixture was filtered and the precipitate was washed with Et_2O until the filtrate was colorless to provide 2-phthalimidonitrobenzene [17] as a yellow crystalline solid (14.50 g; 55 %). To a solution of 2-phthalimidonitrobenzene (13.8 mmol; 3.70 g) in acetone (110 mL), was added glacial acetic acid (11 mL), H_2O (11 mL) and iron powder (166 mmol; 12 equiv.; 9.30 g). The mixture was heated to reflux for 8 h, cooled to r.t. and filtered through a pad of Celite. The filtrate was concentrated *in vacuo*. The resulting residue was dissolved in acetone (50 mL), and a saturated solution of sodium carbonate (70 mL) was then added. Filtration afforded 2-phthalimidoaniline **306** as a yellow solid (2.9 g; 88 %). Spectral data correspond to those described in the literature [17].

^{1}H NMR (400 MHz, $CDCl_3$): $\delta = 3.74$ (br s, 2 H, NH_2), 6.89–6.92 (m, 2 H, arom.), 7.11–7.14 (m, 1 H, arom.), 7.24–7.26 (m, 1 H, arom.), 7.80 (dd, $J = 5.5$, 3.1 Hz, 2 H, arom.), 7.96 (dd, $J = 5.4$, 3.1 Hz, 2 H, arom.).

2-Azidoaniline (307)

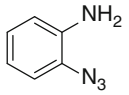

$C_6H_6N_4$ M = 134.14 g/mol

To a solution of 2-phthalimidoaniline **306** (11.75 mmol; 2.80 g) in glacial acetic acid (75 mL) and H_2O (75 mL) at 0 °C was added $NaNO_2$ (16.45 mmol; 1.4 equiv.; 1.14 g). The reaction mixture was stirred at r.t. for 1 h and filtered. To the filtrate, NaN_3 (17.6 mmol; 1.5 equiv.; 1.14 g) was slowly added. During this addition, small portions of ethyl ether were added to prevent excessive foaming. After 0.5 h, the reaction mixture was filtered to give 2-phthalimidophenyl azide [17] as a light yellow solid (2.82 g; 91 %). To a suspension of 2-phthalimidophenyl

azide (1.15 g; 4.35 mmol) in ethanol (45 mL) was added hydrazine hydrate (8.7 mmol; 2 equiv.; 423 μL). The reaction mixture was stirred under reflux for 2 h. Then an aqueous HCl 35 % solution (2 mL) was added and the white precipitate was filtered. The filtrate was neutralized with NaOH 1.0 M aqueous solution, and extracted with Et_2O (2 x 30 mL). The combined organic phases were washed with H_2O, dried over $MgSO_4$ and was concentrated *in vacuo* to afford 2-azidoaniline **307** as a yellow solid (380 mg; 65 %). Spectral data correspônd to those described in the literature [17].

^{1}H NMR (400 MHz, $CDCl_3$): $\delta = 3.81$ (br s, 2 H, NH_2), 6.70 (dd, $J = 7.9$, 1.6 Hz, 1 H, arom.), 6.80 (td, $J = 7.7$, 1.5 Hz, 1 H, arom.), 6.96 (td, $J = 7.7$, 1.4 Hz, 1 H, arom.), 7.04 (td, $J = 7.9$, 1.3 Hz, 1 H, arom.); ^{13}C NMR (100 MHz, $CDCl_3$): $\delta = 116.0$ (CH arom.), 118.5 (CH arom.), 119.2 (CH arom.), 125.3 (C arom.), 125.7 (CH arom.), 138.2 (C arom.).

***N*-(2-azidophenyl)-*N*-cyanobenzamide (308)**

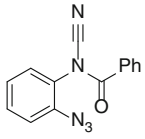

$C_{14}H_9N_5O$ M = 263.25 g/mol

To a solution of 2-azidoaniline **307** (0.37 mmol; 50 mg) in CH_2Cl_2 (8 mL) at 0 °C was added NaH (0.37 mmol; 1 equiv.; 15 mg) and benzoyl chloride (0.74 mmol; 2 equiv.; 86 μL). The reaction mixture was stirred at r.t. during 14 h, then hydrolyzed by a saturated solution of NH_4Cl. The aqueous layer was extracted two times with CH_2Cl_2. The combined organic layers were washed with water, dried over $MgSO_4$ and concentrated *in vacuo*. Purification by flash column chromatography (pentane:CH_2Cl_2:Et_2O = 10:4:1) afforded the corresponding amide as a brown solid. To a solution of the amide (68 mg; 0.28 mmol) in THF (3 mL) at r.t., was added NaH (0.37 mmol; 1.3 equiv.; 15 mg; [60 % in mineral oil]). The reaction mixture was stirred during 45 min, then a 3 M solution of BrCN (0.85 mmol; 3 equiv.; 91 mg) in CH_2Cl_2 was added. The resulting reaction mixture was stirred at r.t. during 24 h and filtered through a short pad of silica. The filtrate was concentrated under reduced pressure and purified by flash column chromatography (pentane:EtOAc = 20:3) to afford *N*-acylcyanamide **308** (58 mg; 77 %) as a pale yellow oil.

IR (neat): ν = 2,239, 2,134, 1,719, 1,494, 1,292, 1,267, 1,244, 705 cm^{-1}; ^{1}H NMR (400 MHz, $CDCl_3$): $\delta = 7.26$–7.30 (m, 2 H, arom.), 7.43–7.52 (m, 4 H, arom.), 7.58–7.62 (m, 1 H, arom.), 7.85–7.91 (m, 2 H, arom.); ^{13}C NMR (100 MHz, $CDCl_3$): $\delta = 109.8$ (CN), 119.8 (CH arom.), 125.9 (CH arom.), 126.1 (C arom.), 1288.8 (2 CH arom.), 129.0 (CH arom.), 129.1 (2 CH arom.), 130.4 (C arom.), 131.4 (CH arom.), 133.6 (CH arom.), 137.3 (C arom.), 167.7 (CO).

3.4.3 Cyclized Guanidines

2,3-dihydroimidazo[2,1-*b*]quinazolin-5(1*H*)-one (309)

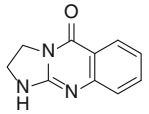

$C_{10}H_9N_3O$ M = 187.20 g/mol

Following **GP7** with *N*-acylcyanamide **269** (0.14 mmol; 30 mg), guanidine **309** was purified by flash column chromatography (EtOAc:EtOH = 4:1) and isolated as a white solid (20 mg; 76 %).

Mp: 258 °C. IR (neat): ν = 2,888, 1,678, 1,651, 1,607, 1,471, 1,286, 1,143, 768 cm^{-1}; ^1H NMR (400 MHz, DMSO-d_6): $\delta = 3.62$ (t, $J = 8.4$ Hz, 2 H, N–CH_2), 4.09–4.13 (m, 2 H, NH–CH_2), 7.08–7.13 (m, 1 H, arom.), 7.21 (d, $J = 7.7$ Hz, 1 H, arom.), 7.55 (ddd, $J = 8.6$, 7.0, 1.5 Hz, 1 H, arom.), 7.76 (br s, 1 H, NH), 7.90 (dd, $J = 7.9$, 1.5 Hz, 1 H, arom.); ^{13}C NMR (100 MHz, DMSO-d_6): $\delta = 39.3$ (NH–CH_2), 42.2 (N–CH_2), 117.2 (C arom.), 121.6 (CH arom.), 124.3 (CH arom.), 125.7 (CH arom.), 133.9 (CH arom.), 151.2 (C arom.), 154.6 (NC = N), 160.2 (C = O); HRMS calcd. for $C_{10}H_{10}N_3O$ ($[M + H]^+$) 188.0818, found 188.0817.

3,4-dihydro-1*H*-pyrimido[2,1-b]quinazolin-6(2*H*)-one (310)

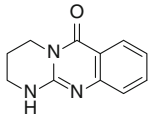

$C_{11}H_{11}N_3O$ M = 201.22 g/mol

Following **GP7** with *N*-acylcyanamide **270** (0.11 mmol; 25 mg), guanidine **310** was purified by flash column chromatography (EtOAc:EtOH = 8:1) and isolated as a colorless oil (13 mg; 59 %).

IR (neat): ν = 2,361, 2,341, 1,676, 1,608, 1,483, 688 cm^{-1}; ^1H NMR (400 MHz, DMSO-d_6): $\delta = 1.92$–1.98 (m, 2 H, NH–CH_2–CH_2), 3.18–3.35 (m, 2 H, N–CH_2), 3.92–3.95 (m, 2 H, NH–CH_2), 7.02 (ddd, $J = 8.0$, 7.0, 1.1 Hz, 1 H, arom.), 7.12 (d, $J = 8.1$ Hz, 1 H, arom.), 7.51 (ddd, $J = 8.4$, 7.0, 1.6 Hz, 1 H, arom.), 7.69 (br s, 1 H, NH), 7.87 (dd, $J = 7.9$, 1.3 Hz, 1 H, arom.); ^{13}C NMR (100 MHz, DMSO-d_6): $\delta = 19.9$ (NH–CH_2–CH_2), 38.4 (NH–CH_2), 39.6 (N–CH_2), 115.9 (C arom.), 120.7 (CH arom.), 123.4 (CH arom.), 126.3 (CH arom.), 134.0 (CH arom.), 149.9 (C arom.), 150.2 (NC = N), 161.5 (C = O); HRMS calcd. for $C_{11}H_{12}N_3O$ ($[M + H]^+$) 202.0975, found 202.0973.

2,3,4,5-tetrahydro-[1, 3]diazepino[2,1-b]quinazolin-7(1*H*)-one (311)

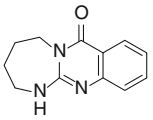

$C_{12}H_{13}N_3O$ M = 215.25 g/mol

Following **GP7** with *N*-acylcyanamide **271** (0.12 mmol; 30 mg), guanidine **311** was purified by flash column chromatography (EtOAc:EtOH = 20:1) and isolated as a colorless oil (6 mg; 24 %).

IR (neat): ν = 3,304, 1,638, 1,600, 1,543, 1,489, 1,309, 696 cm^{-1}; ^1H NMR (400 MHz, $CDCl_3$): δ = 1.74–1.81 (m, 4 H, NH–CH_2–CH_2 + N–CH_2–CH_2), 3.19–3.23 (m, 2 H, N–CH_2), 4.14–4.17 (m, 2 H, NH–CH_2), 6.84 (t, J = 4.3 Hz, 1 H, NH), 7.15–7.19 (m, 1 H, arom.), 7.24 (d, J = 8.2 Hz, 1 H, arom.), 7.60 (ddd, J = 8.6, 7.1, 1.6 Hz, 1 H, arom.), 7.93 (dd, J = 8.1, 1.5 Hz, 1 H, arom.); ^{13}C NMR (101 MHz, DMSO): δ = 25.1 (N–CH_2–*C*H_2), 26.1 (N–*C*H_2–*C*H_2), 42.7 (NH–CH_2), 43.8 (N–CH_2), 117.2 (C arom.), 122.4 (CH arom.), 124.3 (CH arom.), 126.5 (CH arom.), 134.1 (CH arom.), 149.0 (C arom.), 155.9 (NC = N), 162.5 (C = O); HRMS calcd. for $C_{12}H_{14}N_3O$ ($[M + H]^+$) 216.1131, found 216.1125.

3,3-dimethyl-2,3-dihydroimidazo[2,1-b]quinazolin-5(1*H*)-one (312)

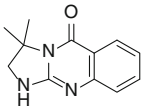

$C_{12}H_{13}N_3O$ M = 215.25 g/mol

Following **GP7** with *N*-acylcyanamide **277** (0.20 mmol; 50 mg), guanidine **312** was purified by flash column chromatography (EtOAc:EtOH = 9:1) and isolated as a white solid (32 mg; 75 %).

Mp: 209 °C. IR (neat): ν = 2,965, 1,644, 1,610, 1,563, 1,474, 1,136, 905, 726 cm^{-1}; ^1H NMR (400 MHz, $CDCl_3$): δ = 1.49 (s, 6 H, 2 Me), 3.99 (s, 2 H, NH–CH_2), 6.71 (br s, 1 H, NH), 7.19 (ddd, J = 8.0, 7.1, 1.1 Hz, 1 H, arom.), 7.30 (dd, J = 8.2, 0.5 Hz, 1 H, arom.), 7.58 (ddd, J = 8.2, 7.2, 1.6 Hz, 1 H, arom.), 8.14 (dd, J = 7.9, 1.8 Hz, 1 H, arom.); ^{13}C NMR (100 MHz, $CDCl_3$): δ = 28.8 (2 Me), 55.3 (NH–CH_2), 55.9 (Me_2*C*) 118.1 (C arom.), 122.9 (CH arom.), 124.1 (CH arom.), 126.9 (CH arom.), 134.5 (CH arom.), 150.6 (C arom.), 153.6 (NC = N), 161.3 (C = O); HRMS calcd. for $C_{12}H_{14}N_3O$ ($[M + H]^+$) 216.1131, found 216.1129.

(*R*)-3-phenyl-2,3-dihydroimidazo[2,1-b]quinazolin-5(1*H*)-one (313)

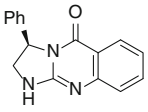

$C_{16}H_{13}N_3O$ M = 263.29 g/mol

Following **GP7** with *N*-acylcyanamide **278** (0.20 mmol; 58 mg), guanidine **313** was purified by flash column chromatography (Pentane:EtOAc:EtOH = 5:5:1) and isolated as a white solid (40 mg; 76 %).

Mp: 239 °C. IR (neat): ν = 1,681, 1,650, 1,608, 1,472, 1,261, 758, 693 cm^{-1}; ^1H NMR (400 MHz, $CDCl_3$): δ = 4.06 (ddd, J = 11.8, 7.2, 2.4 Hz, 1 H, N–CH*H*), 4.66 (dd, J = 11.8, 9.4 Hz, 1 H, N–C*H*H), 5.17 (dd, J = 7.4, 7.2 Hz, 1 H, PhCH), 6.86 (d, J = 8.2 Hz, 1 H, arom.), 7.15 (t, J = 7.5 Hz, 1 H, arom.), 7.34–7.50 (m, 6 H, arom.), 7.57 (br s, 1 H, NH), 8.11 (d, J = 8.0 Hz, 1 H, arom.); ^{13}C NMR (100 MHz, $CDCl_3$): δ = 51.2 (N–CH_2), 56.3 (Ph*C*H), 118.1 (C arom.), 123.1 (CH arom.), 124.2 (CH arom.), 126.5 (2 CH arom.), 126.8 (CH arom.), 129.1 (CH arom.), 129.5 (2 CH arom.), 134.5 (CH arom.), 140.2 (C arom.), 150.3 (C arom.), 154.3 (NC = N), 161.0 (C = O); HRMS calcd. for $C_{16}H_{14}N_3O$ ($[M + H]^+$) 264.1131, found 264.1130; $[\alpha]_D^{20} = -96.0$ (c = 5 g/L, CH_2Cl_2).

Guanidine (314)

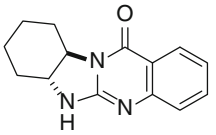

$C_{14}H_{15}N_3O$ M = 241.29 g/mol

Following **GP7** with *N*–acylcyanamide **279** (0.22 mmol; 60 mg), guanidine **314** was purified by flash column chromatography (pentane:EtOAc:EtOH = 10:2:1) and isolated as a white solid (41 mg; 77 %).

Mp: 293 °C. IR (neat): ν = 3,036, 1,681, 1,650, 1,608, 1,472, 1,261, 758, 693 cm^{-1}; ^1H NMR (400 MHz, $CDCl_3$): δ = 1.32–1.82 (m, 4 H, cyclohex.), 1.89–2.00 (m, 2 H, cyclohex.), 2.11–2.26 (m, 1 H, cyclohex.), 3.20–3.24 (m, 1 H, cyclohex.), 3.37 (td, J = 11.5, 3.3 Hz, 1 H, NH–C*H*), 3.71 (td, J = 11.6, 3.2 Hz, 1 H, N–C*H*), 5.83 (br s, 1 H, NH), 7.20–7.23 (m, 1 H, arom.), 7.33 (d, J = 7.9 Hz, 1 H, arom.), 7.57–7.62 (m, 1 H, arom.), 8.13 (dd, J = 7.9, 1.4 Hz, 1 H, arom.); ^{13}C NMR (100 MHz, $CDCl_3$): δ = 23.9 (CH_2 cyclohex.), 24.5 (CH_2 cyclohex.), 29.2 (CH_2 cyclohex.), 29.7 (CH_2 cyclohex.), 61.5 (NH–CH), 64.6 (N–CH), 119.4 (C arom.), 123.5 (CH arom.), 124.6 (CH arom.), 126.8 (CH arom.), 134.4 (CH arom.), 149.9 (C arom.), 155.6 (NC = N), 162.7 (C = O); HRMS calcd. for $C_{14}H_{16}N_3O$ ($[M + H]^+$) 242.1288, found 242.1289.

(*R*)-8-methoxy-3-phenyl-2,3-dihydroimidazo[2,1-*b*]quinazolin-5(1*H*)-one (315)

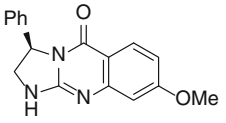

$C_{17}H_{15}N_3O_2$ M = 293.32 g/mol

Following **GP7** with *N*-acylcyanamide **295** (0.27 mmol; 88 mg), guanidine **315** was purified by flash column chromatography (Pentane:EtOAc:EtOH = 8:4:1) and isolated as a white solid (65 mg; 82 %).

Mp: 223 °C. IR (neat): ν = 1,682, 1,641, 1,609, 1,566, 1,455, 1,248, 700 cm^{-1}; ^1H NMR (400 MHz, $CDCl_3$): δ = 3.44 (s, 3 H, OMe), 3.97 (dd, J = 11.7, 7.2 Hz, 1 H, N–CH*H*), 4.64 (dd, J = 11.7, 9.6 Hz, 1 H, N–C*H*H), 5.23 (dd, J = 9.4, 7.3 Hz, 1 H, PhC*H*), 6.28 (br s, 1 H, arom.), 6.70 (dd, J = 8.8, 2.4 Hz, 1 H, arom.), 7.37–7.49 (m, 5 H, arom.), 7.98 (d, J = 8.8 Hz, 1 H, arom.); ^{13}C NMR (100 MHz, $CDCl_3$): δ = 51.2 (N–CH_2), 55.2 (OMe), 56.2 (Ph*C*H), 105.1 (CH arom.), 111.4 (C arom.), 112.9 (CH arom.), 126.2 (2 CH arom.), 128.3 (CH arom.), 128.9 (CH arom.), 129.5 (2 CH arom.), 140.7 (C arom.), 152.4 (C arom.), 155.3 (NC = N), 160.5 (C–OMe), 164.9 (C = O); HRMS calcd. for $C_{17}H_{16}N_3O_2$ ($[M + H]^+$) 294.1237, found 294.1235; $[\alpha]_D^{20}$ = − 28.0 (c = 2 g/L, CH_2Cl_2).

(*R*)-3-phenyl-8-(trifluoromethyl)-2,3-dihydroimidazo[2,1-*b*]quinazolin-5(1*H*)-one (316)

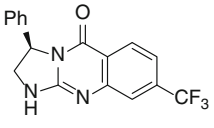

$C_{17}H_{12}N_3F_3O$ M = 331.29 g/mol

Following **GP7** with *N*-acylcyanamide **296** (0.07 mmol; 25 mg), guanidine **316** was purified by flash column chromatography (Pentane:EtOAc:EtOH = 6:3:1) and isolated as a colorless oil (19 mg; 82 %).

IR (neat): ν = 2,958, 1,686, 1,653, 1,501, 1,319, 1,168, 1,128, 1,065, 785 cm^{-1}; ^1H NMR (400 MHz, $CDCl_3$): δ = 4.07 (dd, J = 12.0, 7.1 Hz, 1 H, N–CH*H*), 4.68 (dd, J = 12.0, 9.6 Hz, 1 H, N–C*H*H), 5.22 (dd, J = 9.5, 7.2 Hz, 1 H, PhC*H*), 7.18 (s, 1 H, arom.), 7.35 (d, J = 8.2 Hz, 1 H, arom.), 7.37–7.50 (m, 5 H, arom.), 7.91 (br s, 1 H, NH), 8.20 (d, J = 8.3 Hz, 1 H, arom.); ^{13}C NMR (100 MHz, $CDCl_3$): δ = 51.3 (N–CH_2), 56.3 (Ph*C*H), 119.1 (q, CH arom., $^3J_{C\text{-}F}$ = 3.4 Hz), 120.4 (C arom.), 121.5 (q, CH arom., $^3J_{C\text{-}F}$ = 4.3 Hz), 123.3 (q, CF_3., $^1J_{C\text{-}F}$ = 181.0 Hz), 126.2 (2 CH arom.), 127.9 (CH arom.), 129.4 (2 CH arom.), 129.6 (CH arom.), 136.1 (q, *C*-CF_3, $^2J_{C\text{-}F}$ = 32.7 Hz), 139.7 (C arom.), 150.2 (C arom.), 155.0 (NC = N), 160.1 (C = O); ^{19}F NMR (377 MHz, $CDCl_3$): δ = -63.2; HRMS calcd. for $C_{17}H_{13}N_3F_3O$ ($[M + H]^+$) 332.1005, found 332.1004; $[\alpha]_D^{20}$ = − 18.3 (c = 3 g/L, CH_2Cl_2).

(*R*)-6,8-dimethyl-3-phenyl-2,3-dihydroimidazo[2,1-*b*]quinazolin-5(1*H*)-one (317)

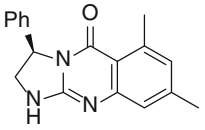

$C_{18}H_{17}N_3O$ M = 291.35 g/mol

Following **GP7** with *N*-acylcyanamide **297** (0.18 mmol; 60 mg), guanidine **317** was purified by flash column chromatography (Pentane:EtOAc:EtOH = 16:3:1) and isolated as a colorless oil (36 mg; 69 %).

IR (neat): ν = 1,675, 1,636, 1,479, 1,364, 1,263, 908, 730, 698 cm^{-1}; ^1H NMR (400 MHz, $CDCl_3$): δ = 2.36 (s, 3 H, Me), 2.40 (s, 3 H, Me), 4.00–4.05 (m, 1 H, N–CH*H*), 4.62 (ddd, J = 14.5, 9.4, 5.2 Hz, 1 H, N–C*H*H), 5.10 (dd, J = 9.2, 7.0 Hz, 1 H, PhC*H*), 7.27 (s, 1 H, arom.), 7.33–7.39 (m, 5 H, arom.), 7.80 (s, 1 H, arom.); ^{13}C NMR (100 MHz, $CDCl_3$): δ = 17.9 (Me), 21.0 (Me), 51.0 (N–CH_2), 56.1 (Ph*C*H), 117.8 (C arom.), 124.0 (2 CH arom.), 126.1 (CH arom.), 128.9 (CH arom.), 129.3 (2 CH arom.), 132.3 (C arom.), 132.6 (C arom.), 136.7 (CH arom.), 140.4 (C arom.), 146.9 (C arom.), 152.9 (NC = N), 161.3 (C = O); HRMS calcd. for $C_{18}H_{17}N_3O$ ($[M + H]^+$) 292.1444, found 292.1441; $[\alpha]_D^{20}$ = − 31.8 (c = 4 g/L, CH_2Cl_2).

(*R*)-3-phenyl-2,3-dihydrobenzo[*g*]imidazo[2,1-b]quinazolin-5(1*H*)-one (318)

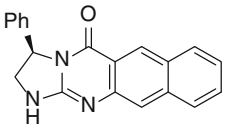

$C_{20}H_{15}N_3O$ M = 313.35 g/mol

Following **GP7** with *N*-acylcyanamide **298** (0.26 mmol; 88 mg), guanidine **318** was purified by flash column chromatography (Pentane:EtOAc:EtOH = 8:1:1) and isolated as a white solid (65 mg; 82 %).

Mp: 237 °C. IR (neat): ν = 3,251, 1,669, 1,618, 1,561, 1,447, 1,268, 800, 763, 734 cm^{-1}; ^1H NMR (400 MHz, $CDCl_3$): δ = 4.15 (dd, J = 11.9, 7.0 Hz, 1 H, N–CH*H*), 4.71 (dd, J = 11.9, 9.6 Hz, 1 H, N–C*H*H), 5.16 (dd, J = 9.5, 7.0 Hz, 1 H, PhC*H*), 6.03 (br s, 1 H, NH), 7.30–7.42 (m, 5 H, arom.), 7.50–7.68 (m, 3 H, arom.), 7.85 (d, J = 8.1 Hz, 1 H, arom.), 8.10 (d, J = 8.8 Hz, 1 H, arom.), 8.78 (d, J = 8.3 Hz, 1 H, arom.); ^{13}C NMR (100 MHz, $CDCl_3$): δ = 51.3 (N–CH_2), 56.3 (Ph*C*H), 113.6 (C arom.), 122.2 (CH arom.), 123.3 (CH arom.), 125.0 (CH arom.), 126.2 (2 CH arom.), 126.3 (CH arom.), 128.0 (CH arom.), 129.0 (2 CH arom.), 129.1 (CH arom.), 129.2 (C arom.), 129.4 (CH arom.), 136.8 (C arom.), 140.1 (C arom.), 149.6 (C arom.), 154.4 (NC = N), 161.1 (C = O);

HRMS calcd. for $C_{20}H_{16}N_3O$ ($[M + H]^+$) 314.1288, found 314.1286; $[\alpha]_D^{20} = + 68.5$ (c = 3 g/L, CH_2Cl_2).

(*R*)-7-phenyl-6,7-dihydroimidazo[1,2-*a*]thieno[3,2-*d*]pyrimidin-9(5*H*)-one (319)

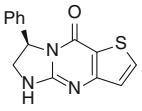

$C_{14}H_{11}N_3OS$ M = 269.32 g/mol

Following **GP7** with *N*-acylcyanamide **299** (0.16 mmol; 49 mg), guanidine **319** was purified by flash column chromatography (EtOAc:EtOH = 20:1) and isolated as a pale yellow solid (21 mg; 49 %).

Mp: 205 °C. IR (neat): ν = 3,132, 1,676, 1,618, 1,517, 1,264, 1,044, 777, 733, 700 cm^{-1}; ^1H NMR (400 MHz, $CDCl_3$): $\delta = 4.06$ (dd, $J = 11.8$, 7.5 Hz, 1 H, N–CH*H*), 4.65 (dd, $J = 11.8$, 9.6 Hz, 1 H, N–C*H*H), 5.19 (dd, $J = 9.5$, 7.5 Hz, 1 H, PhC*H*), 6.51 (d, $J = 5.3$ Hz, 1 H, arom.), 7.39–7.44 (m, 5 H, arom.), 7.51 (br s, 1 H, NH), 7.54 (d, $J = 5.3$ Hz, 1 H, arom.); ^{13}C NMR (100 MHz, $CDCl_3$): $\delta = 51.1$ (N–CH_2), 56.9 (Ph*C*H), 115.1 (C arom.), 123.3 (CH arom.), 126.4 (2 CH arom.), 129.1 (CH arom.), 129.5 (2 CH arom.), 134.0 (CH arom.), 140.1 (C arom.), 156.9 (C arom.), 156.9 (NC = N), 158.7 (C = O); HRMS calcd. for $C_{14}H_{12}N_3OS$ ($[M + H]^+$) 270.0696, found 270.0698; $[\alpha]_D^{20} = - 128.0$ (c = 1 g/L, CH_2Cl_2).

(*R*)-3-phenyl-2,3-dihydroimidazo[1,2-*a*]pyrido[3,4-*d*]pyrimidin-5(1*H*)-one (320)

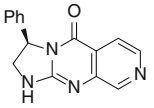

$C_{15}H_{12}N_4O$ M = 264.28 g/mol

Following **GP7** with *N*-acylcyanamide **301** (0.24 mmol; 71 mg), guanidine **320** was purified by flash column chromatography (EtOAc:EtOH = 9:1) and isolated as a pale yellow solid (45 mg; 71 %).

Mp: 203 °C. IR (neat): ν = 3,032, 1,687, 1,636, 1,549, 1,364, 729, 699 cm^{-1}; ^1H NMR (400 MHz, $CDCl_3$): $\delta = 4.10$ (dd, $J = 12.1$, 7.0 Hz, 1 H, N–CH*H*), 4.68 (dd, $J = 12.1$, 9.5 Hz, 1 H, N–C*H*H), 5.23 (dd, $J = 9.5$, 7.3 Hz, 1 H, PhC*H*), 7.44–7.46 (m, 5 H, arom.), 7.88 (d, $J = 8.3$ Hz, 1 H, arom.), 8.37–8.38 (m, 2 H, arom.); ^{13}C NMR (100 MHz, $CDCl_3$): $\delta = 51.2$ (N–CH_2), 56.2 (Ph*C*H), 119.0 (CH arom.), 123.3 (C arom.), 126.3 (2 CH arom.), 129.7 (3 CH arom.), 139.6 (CH arom.), 142.5 (C arom.), 145.3 (C arom.), 147.7 (CH arom.), 155.2 (NC = N), 159.6 (C = O); $[\alpha]_D^{20} = - 95.0$ (c = 1 g/L, CH_2Cl_2).

***cis*-3,3,6-trimethyl-7-phenyl-2,3,6,7-tetrahydroimidazo[1,2-*a*]pyrimidin-5(1*H*)-one (322)**

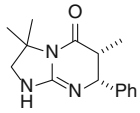

$C_{15}H_{19}N_3O$ M = 257.33 g/mol

Following **GP8** with *N*-acylcyanamide **303** (0.14 mmol; 39 mg), guanidine **322** was purified by flash column chromatography (CH_2Cl_2:MeOH = 9:1) and isolated as a white solid (20 mg; 57 %) along with **321** (9 mg; 26 %).

Mp: 142 °C. IR (neat): ν = 2,925, 1,695, 1,382, 700 cm^{-1}; ^1H NMR (400 MHz, $CDCl_3$): δ = 0.95 (d, J = 7.2 Hz, 3 H, *Me*CH), 1.33 (s, 6 H, 2 Me), 2.75–2.84 (m, 1 H, MeC*H*), 2.82 (br s, 1 H, NH), 3.60 (A of AB, J_{AB} = 10.8 Hz, 1 H, NH–CH*H*), 3.67 (B of AB, J_{AB} = 10.8 Hz, 1 H, NH–C*H*H) 4.77 (d, J = 4.9 Hz, 1 H, PhC*H*), 7.22–7.24 (m, 2 H, arom.), 7.30–7.37 (m, 3 H, arom.); ^{13}C NMR (100 MHz, $CDCl_3$): δ = 11.3 (*Me*CH), 29.0 (Me), 29.3 (Me), 41.3 (Me*C*H), 55.4 (NH–CH_2), 58.7 (Ph*C*H), 59.6 (Me_2C), 126.9 (2 CH arom.), 128.1 (CH arom.), 128.9 (2 CH arom.), 138.6 (C arom.), 151.6 (NC = N), 170.7 (C = O); HRMS calcd. for $C_{15}H_{20}N_3O$ ($[M + H]^+$) 258.1601, found 258.1606.

6-benzyl-3,3,6-trimethyl-2,3-dihydro-1*H*-imidazo[1,2-*a*]imidazol-5(6*H*)-one (321)

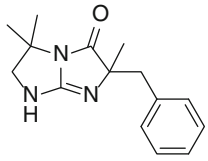

$C_{15}H_{19}N_3O$ M = 257.33 g/mol

IR (neat): ν = 2,966, 1,697, 1,368, 701 cm^{-1}; ^1H NMR (400 MHz, $CDCl_3$): δ = 0.89 (s, 3 H, Me), 1.27 (s, 3 H, Me), 1.49 (s, 3 H, Me), 2.86 (A of AB, J_{AB} = 13.3 Hz, 1 H, Ph–CH*H*), 2.90 (br s, 1 H, NH), 2.97 (A of AB, J_{AB} = 10.3 Hz, 1 H, NH–CH*H*), 3.06 (B of AB, J_{AB} = 13.3 Hz, 1 H, Ph–C*H*H), 3.19 (B of AB, J_{AB} = 10.3 Hz, 1 H, NH–C*H*H), 7.19–7.23 (m, 5 H, arom.); ^{13}C NMR (100 MHz, $CDCl_3$): δ = 24.0 (Me), 29.0 (Me), 29.1 (Me), 45.1 (Ph–CH_2), 51.7 (NH–CH_2), 67.2 (Me_2C), 75.2 (Ph–CH_2–*C*), 126.9 (CH arom.), 128.1 (2 CH arom.), 130.4 (2 CH arom.), 135.9 (C arom.), 157.3 (NC = N), 175.7 (C = O).

(3*R*)-6-isopropyl-3-phenyl-2,3-dihydro-1*H*-imidazo[1,2-*a*]imidazol-5(6*H*)-one (323)

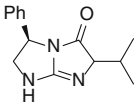

$C_{14}H_{17}N_3O$ M = 243.30 g/mol

Following **GP8** with *N*-acylcyanamide **304** (0.09 mmol; 23 mg), guanidine **323** was purified by flash column chromatography (CH_2Cl_2:MeOH = 10:1) and isolated as a mixture of unseparable diastereoisomers (15 mg; 73 %; dr = 50:50) as a yellow solid.

Mp: 160 °C. IR (neat): ν = 2,962, 1,693, 1,454, 1,365, 1,029, 700 cm^{-1}; ^1H NMR (400 MHz, $CDCl_3$): δ = 0.85–0.89 (m, 12 H, 2 Me, 2 dias), 2.07–2.18 (m, 2 H, Me_2CH, two dias), 3.44 (dd, J = 5.7, 4,6 Hz, 1 H, N–CH*H,* one dia), 3.47 (dd, J = 6.3, 5.3 Hz, 1 H, N–CH*H,* one dia), 4.01–4.09 (m, 2 H, N–C*H*H, two dias), 4.14 (d, J = 3.9 Hz, 1 H, Me_2CH–C*H*, one dia), 4.23 (d, J = 3.7 Hz, 1 H, Me_2CH–C*H*, one dia), 5.33 (dd, J = 9.0, 5.7 Hz, 1 H, PhC*H*, one dia), 5.33 (dd, J = 8.8, 6.6 Hz, 1 H, PhC*H*, one dia), 7.22–7.36 (m, 10 H, arom., two dias); ^{13}C NMR (100 MHz, $CDCl_3$): δ = 16.1 (Me, one dia), 16.3 (Me, one dia), 18.8 (Me, one dia), 19.0 (Me, one dia), 30.6 (Me_2*C*H, one dia), 30.8 (Me_2*C*H, one dia), 47.6 (N–CH_2, one dia), 47.8 (N–CH_2, one dia), 69.9 (Ph*C*H, one dia), 70.4 (Ph*C*H, one dia), 73.2 (Me_2CH–*C*H, one dia), 73.5 (Me_2CH–*C*H, one dia), 126.1 (2 CH arom., one dia), 126.3 (2 CH arom., one dia), 127.9 (CH arom., two dias), 128.8 (2 CH arom., one dia), 128.8 (2 CH arom., one dia), 142.6 (C arom., one dia), 142.7 (C arom., one dia), 161.2 (NC = N, one dia), 161.5 (NC = N, one dia), 170.9 (C = O, one dia), 171.0 (C = O, one dia); HRMS calcd. for $C_{14}H_{18}N_3O$ ($[M + H]^+$) 244.1444, found 244.1447.

Determination of the diastereoisomer **322**:

Optimization of the conformations for each diastereoisomer by MM2 provided us with an estimation of the dihedral angle between C–H_1 and C–H_2.

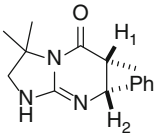

Cis

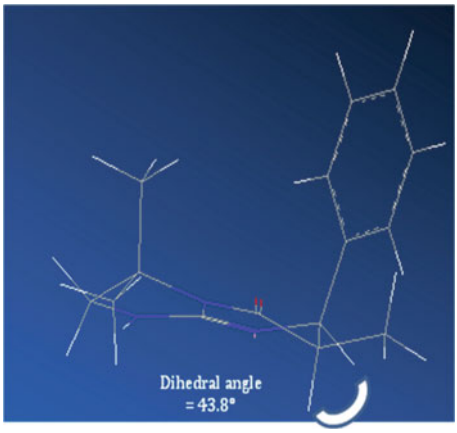

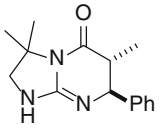

Trans

A dihedral angle of approximately 40° seems to correspond better to the coupling constant observed between H_1 and H_2 ($J = 4.9$ Hz), which involve a *cis* configuration.

References

1. Bowman, W. R., Stephenson, P. T., Terett, N. K., & Young, A. R. (1995). *Tetrahedron, 51*, 7959–7980.
2. Trost, B. M., & Bogdanowicz, M. J. (1973). *Journal of the American Chemical Society, 95*, 5298–5307.
3. Coxon, G. D., Furman, B. L., Harvey, A. L., McTavish, J., Mooney, M. H., Arastoo, M., et al. (2009). *Journal of Medicinal Chemistry, 52*, 3457–3463.
4. Munbunjong, W., Lee, E. H., Chavasiric, W., & Janga, D. O. (2005). *Tetrahedron Letters, 46*, 8769–8771.
5. Toshimitsu, A., Hirosawa, C., Tanimoto, S., & Uemura, S. (1992). *Tetrahedron Letters, 33*, 4017–4020.
6. Liu, J.-F., Ye, P., Sprague, K., Sargent, K., Yohannes, D., Baldino, C. M., et al. (2005). *Organic Letters, 7*, 3363–3366.
7. Elmuradov, B. Z., & Shakhidoyatov, K. M. (2005). *Chemical Natural Compound, 40*, 496–498.
8. Sugiyama, H., Yokokawa, F., & Shiori, T. (2000). *Organic Letters, 14*, 2149–2152.
9. Xue, D., Chen, Y.-C., Cui, X., Wang, Q.-W., Zhu, J., & Deng, J.-G. (2005). *Journal of Organic Chemistry, 70*, 3584–3591.
10. Quirmbach, M., Holz, J., Tararov, V. I., & Börner, A. (2000). *Tetrahedron, 56*, 775–780.
11. Lee, J. W., Jun, S. I., & Kim, K. (2001). *Tetrahedron Letters, 42*, 2709–2711.
12. Chen, C.-T., Kuo, J.-H., Pawar, V. D., Munot, Y. S., Weng, S.-S., Ku, C.-H., et al. (2005). *Journal of Organic Chemistry, 70*, 1188–1197.
13. Shiau, T. P., Houchin, A., Nair, S., Xu, P., Low, E., Najafi, R., et al. (2009). *Bioorganic and Medicinal Chemistry Letters, 19*, 1110–1114.
14. Wannaporn, D., & Tsutomu, I. (2005). *Molecular Diversity, 9*, 321–331.
15. Govindaraju, T., Kumar, V. A., & Ganesh, K. N. (2004). *Journal of Organic Chemistry, 69*, 1858–1865.
16. Swift, G., & Swern, D. (1967). *Journal of Organic Chemistry, 32*, 511–517.
17. Shen, M., & Driver, T. G. (2008). *Organic Letters, 10*, 3367–3370.

Part II
Visible-light Photoreductive Catalysis for an Eco-compatible Generation of Radicals

Chapter 4
Bibliographical Backgrounds: Generation of Radicals by Visible Light Photoredox Catalysis

Visible light has the potential to serve as a sustainable, clean, economical and abundant source of energy. Visible light-induced electron transfer reactions are thus widely used in nature [1]. Photosynthetic organisms absorb visible light by antenna proteins containing chromophores. Subsequent photon-induced electron transfers generate charge-separated states which are used to prepare various high-energy molecules required to fuel organisms. The progressive elucidation of the molecular mechanisms of photosynthesis has raised tremendous hopes that efficient means would be found for artificial conversion of solar energy. Thus, one century ago, Professor Ciamician (University of Bologna), one of the pioneer in photochemistry forecasted: [2]"The photochemical processes, that hitherto have been guarded secret of the plants, will have been mastered by human industry which will know how to make them bear even more abundant fruit than nature, for nature is not in a hurry but mankind is".

Since then, the direct conversion of light into energy by photovoltaic processes has been an area of intense research. In the field of photocatalysis, the main focus of efforts has been the development of artificial photosynthetic systems for the conversion of solar energy into storable chemical fuel (Fig. 4.1). The two main studied reactions have thus been (a) the splitting of water into molecular hydrogen and molecular oxygen[3] and (b) the reduction of carbon dioxide to carbon monoxide with concomitant generation of dioxygen [4].

However, despite the high synthetic potential of visible light as a promoter of electron transfer reactions, its application in organic synthesis has been greatly limited by the inability of most molecules to absorb light in the visible range. The ultraviolet wavelengths required in conventional photochemistry[1] are not abundant in the solar spectrum (Fig. 4.2) and must be generated by specialized photoreactors. The energy costs and scale issues associated with the use of these reactors restrain sharply the potential industrial applications.[2]

[1] Generally for ketones λ_{max} absorption $\sim$280 nm, for non-conjugated alkenes λ_{max} absorption $\sim$180 nm.

[2] Image inspired from http://www.dlt.ncssm.edu/

M.-H. Larraufie, *Development of New Radical Cascades and Multi-Component Reactions*, Springer Theses, DOI: 10.1007/978-3-319-01324-4_4,

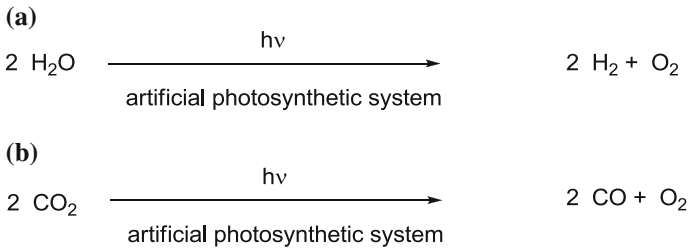

Fig. 4.1 Conversion of solar energy into storable chemical fuel

Fig. 4.2 Solar spectrum

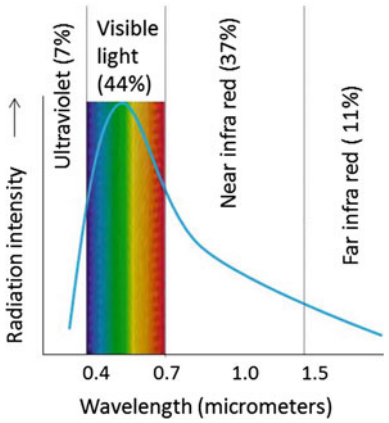

Fig. 4.3 Organic and organometallic dyes for visible light photocatalysis

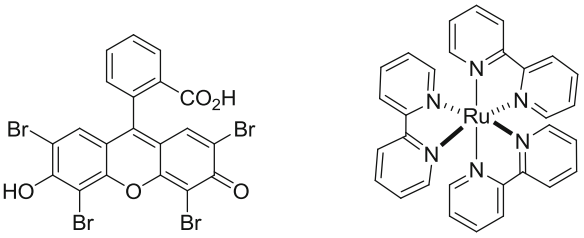

Eosin Y 1 **2**

One major strategy to enable the direct utilization of incident sunlight is the use of homogenous visible light photocatalysts to sensitize organic molecules via electron/energy transfer reactions. Two types of sensitizers have been developed in this objective (Fig. 4.3): organic dyes such as rose Bengal or eosin Y [5, 6] **1** or transition metal polypyridyl complexes such as ruthenium(II) trisbipyridine **2** [7–9].

Despite the heavier cost of organometallic catalysts compared to organic dyes, their good stability and high turnover numbers have made them the tools of choice

to perform visible light photocatalyzed reactions. In a first part, we will present the well characterized photophysical properties of tris(bipyridyl)ruthenium(II) complexes. Subsequently, the applications of organometallic photoredox catalysts in organic synthesis will be described, with a special focus on the scope of substrates amenable to oxidation or reduction using such approach.

4.1 Photophysical Properties of Tris(bipyridyl)ruthenium(II) Complexes

4.1.1 Structure and Excited States

$Ru(bpy)_3^{2+}$ as well as most of the $Ru(LL)_3^{2+}$ complexes (LL = bidentate polypyridine ligand) are octahedral complexes exhibiting a D_3 symmetry. $Ru(bpy)_3^{2+}$ can thus exist as two enantiomers Δ and Λ (Fig. 4.4) which are configurationally stable and have been isolated as early as 1936 via diastereomeric resolution with tartrate salts [10].

Figure 4.5 presents a simplified molecular orbital diagram for Ru(II) polypyridines complexes in an octahedral symmetry. Ru(II) is a d^6 system and the polypyridine ligands possess σ donor orbitals localized on the nitrogen atom, and π and π^* acceptor orbitals delocalized on aromatic rings. In the octahedral strong field, the five degenerate *d*-orbitals of ruthenium are splitted into stabilized t_{2g} and destabilized $e_{.g.}$ orbitals with an energy difference Δ_{oct}. From the ground $(t_{2g})^6$ electronic configuration, four possible types of one electron excitations are possible [11]. Promotions of an electron from t_{2g} to $e_{.g.}$ orbitals represent metal-centered transitions (MCT). Excitations of an electron from t_{2g} to π^* constitute metal–ligand charge transfer transitions (MLCT). Finally, transitions can occur

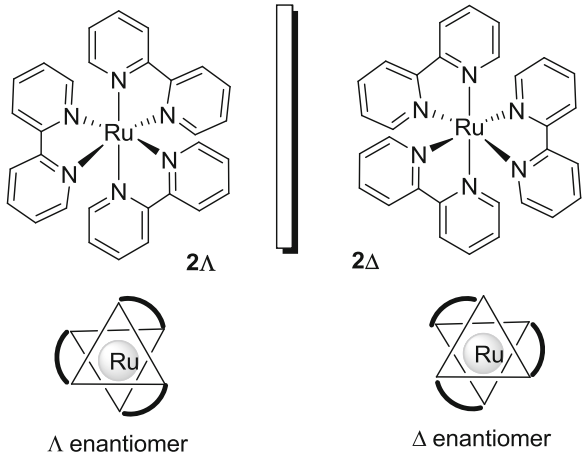

Fig. 4.4 Chirality of C_3-symmetric $Ru(bpy)_3^{2+}$ complex

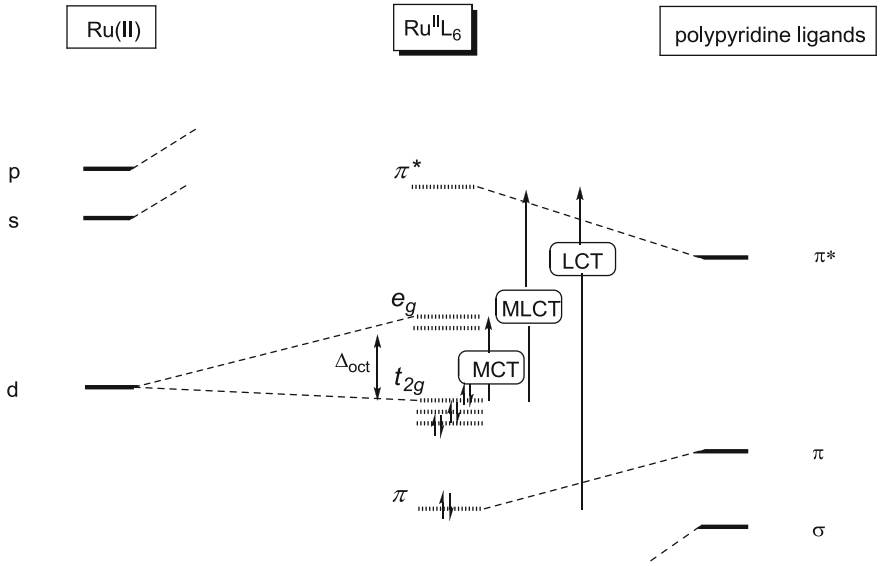

Fig. 4.5 Molecular orbital diagram for $Ru(bpy)_3^{2+}$ complex

within the ligand π-bonding orbital to the π^*-antibonding orbital. Such ligand centered transitions (LCT) usually lie at high energies.

The relative energy positions of the MC, MLCT and LC excited states for Ru(II) polypyridines complexes depend on the ligand field strength and the intrinsic and redox properties of the ligands. For Ru(II) polypyridines ligands, since the Ru(II) metal is easy to oxidize and the ligands are easy to reduce, the lowest triplet and singlet excited states are metal-to-ligand charge-transfers (MLCT).

4.1.2 Absorption Spectrum

The absorption spectrum of $Ru(bpy)_3Cl_2$ has been recorded in aqueous solutions and organic solvents and displayed the general profile shown in Fig. 4.6. Absorption bands at 185 nm (not shown) and 285 nm were assigned to ligand-centered π-π^* transitions (LCT) by comparison with the spectrum of protonated bipyridine ligands [12]. The two remaining intense bands at 240 nm ($\varepsilon \sim 2.5 \times 10^4$ $M^{-1}cm^{-1}$) and 452 nm ($\varepsilon \sim 1.5 \times 10^4$ $M^{-1}cm^{-1}$) have been attributed to spin-allowed *d*- π^* transitions (MLCT) [13]. Finally, the shoulders at 322 and 344 nm might be due to metal-centered *d*–*d* transitions (MCT).

The characteristic absorption band centered at 452 nm is responsible for visible-light excitation.

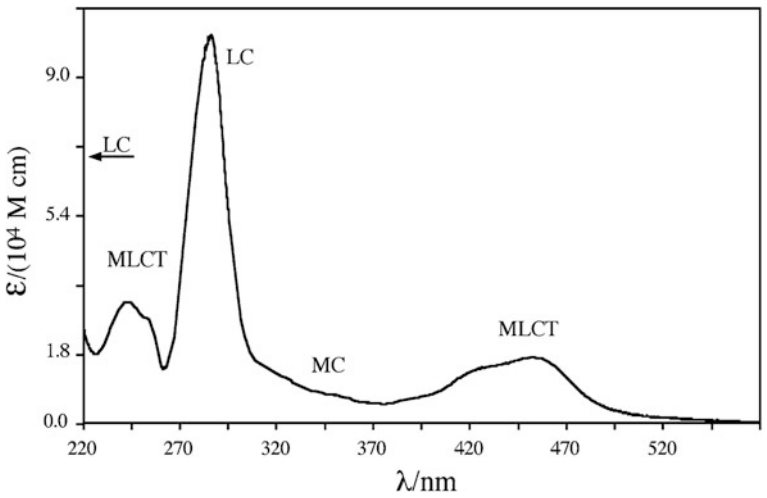

Fig. 4.6 Absorption spectrum of $Ru(bpy)_3Cl_2$ in ethanol/methanol solution at r.t. (from ref [11])

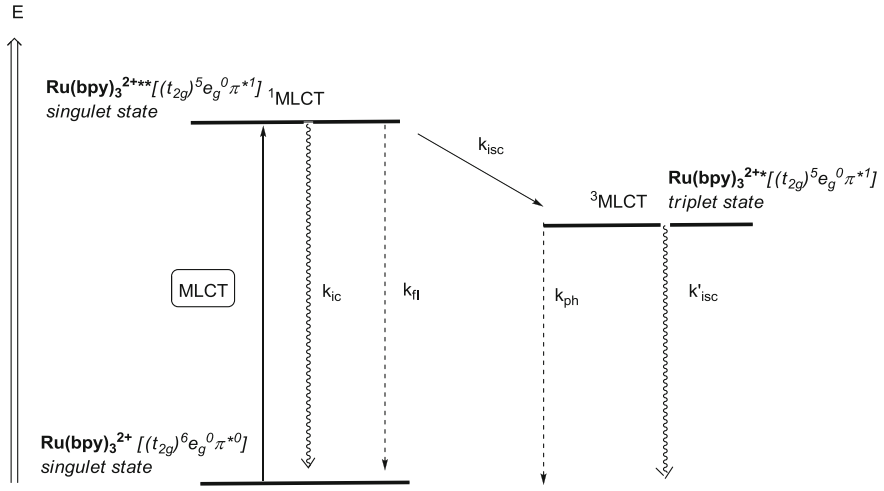

Fig. 4.7 Schematic energy level diagram for photoexcitation of $Ru(bpy)_3^{2+}$

4.1.3 Deactivation and Quenching of Excited State

When Ru(II) polypyridines complexes are excited to spin allowed singulet ^{1}MLCT state, deactivation can occur via three first-order processes (Fig. 4.7):

– Internal conversion: nonradiative decay to the ground state (rate constant k_{ic})
– Fluorescence: radiative decay to the ground state (rate constant k_{fl}).

– Intersystem crossing to the lower triplet state ^{3}MLCT (rate constant k_{isc}). For $Ru(bpy)_3^{2+}$, intersystem crossing occurs in the subpicosecond timescale. The efficiency of formation of ^{3}MLCT ($\Phi(^3MLCT)$) is close to 100 %, meaning that almost all singulet MLCT states created upon absorption of a photon from the ground state become triplet MLCT states through intersystem crossing.

In its turn, ^{3}(MLCT) can undergo deactivation via non radiative ($k'isc$) or radiative (phosphorescence, kph) decay to the ground state (Fig. 4.7). The quantum yield for phosphorescence is low ($\Phi \sim 0.04$) [14], meaning that the majority of molecules relax to the ground state through non-radiative, vibrational relaxation processes if no quenching reaction interplays.

The triplet state is exceptionally long-lived: 890 ns in acetonitrile and 650 ns in water [15]. Thanks to this long lifetime, in addition to the unimolecular processes described above, $Ru(bpy)_3^{2+*}$ can interact through bimolecular reactions with other solute molecules.(see footnote 2) The triplet excited state can play the role of energy donor (energy available = 2.12 eV), electron donor (oxidation potential: $Ru(bpy)_3^{3+}/Ru(bpy)_3^{2+*} = -0.86$ V *vs* SCE in MeCN) and electron acceptor (reduction potential: $Ru(bpy)_3^{2+*}/Ru(bpy)_3^{+} = +0.84$ V *vs* SCE in MeCN).[3]

The excited state $Ru(bpy)_3^{2+*}$ can be quenched by electron donors (blue reductive quenching cycle, Fig. 4.8) or electron acceptors (green oxidative quenching cycle, Fig. 4.8) in one-electron transfer processes. In order to obtain high quenching efficiencies, energy-wasting back reactions between the quench and the ruthenium complex (such as Eq. 4.3) must be prevented. For example, Whitten has demonstrated that trialkylamines such as NEt_3 or i-Pr_2NEt were excellent reductive quenches (Eq. 4.1), since the trialkylamine radical cation formed was rapidly consumed by proton loss (Eq. 4.2) [16]. In other cases, NADPH models such as 1,4-dihydropyridines proved also efficient reductive quenches, due to their adequate oxidation potentials and the good proton-donor abilities of their corresponding radical cations [11].

$$Ru(bpy)_3^{2+*} + NEt_3 \rightarrow Ru(bpy)_3^{+} + NEt_3^{\bullet +} \tag{4.1}$$

(Eq. 4.1, reductive quenching)

$$NEt_3^{\bullet +} \rightarrow H^+ + CH_3 - CH = N(Et)_2^{\bullet} \tag{4.2}$$

(Eq. 4.2, loss of proton)

$$NEt_3^{\bullet +} + Ru(bpy)_3^{+} \rightarrow Ru(bpy)_3^{2+} + NEt_3 \tag{4.3}$$

(Eq. 4.3, competitive back electron transfer)

[3] The free energy changes ΔG involved in such redox reactions can be calculated by: $\Delta G_{ox}(eV) = -F/N_A(0.84 - EQ/Q^{\bullet -})$ or $\Delta G_{red}(eV) = -F/N_A(EQ/Q^{\bullet +} + 0.86)$. With F (Faraday constant) = 96 485 C/mol and N_A (Avogadro constant) = $6{,}022 \times 10^{23}$ mol^{-1}.

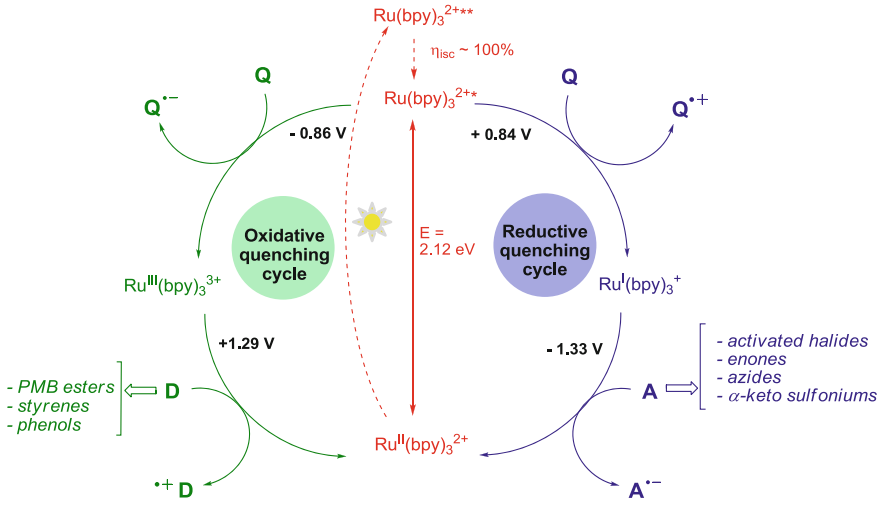

Fig. 4.8 Accessible energy and electron transfer processes using $Ru(bpy)_3^{2+}$ photocatalysis. Q = sacrificial electron donor or acceptor (quench)

Interestingly, if reductive quenching occurs, the strongly reducing species $Ru(bpy)_3^{+}$ is generated ($Ru(bpy)_3^{2+}/Ru(bpy)_3^{+} = -1.33$ V *vs* SCE in MeCN). Electron transfer to a range of substrates **A** can follow, leading to the formation of the corresponding radical anion $\mathbf{A}^{\bullet-}$ and regenerating the $Ru^{II}(bpy)_3^{2+}$ species. On the other hand, if oxidative quenching occurs (green oxidative quenching cycle), strong oxidant $Ru(bpy)_3^{3+}$ is generated ($Ru(bpy)_3^{3+}/Ru(bpy)_3^{2+} = +1.29$ V *vs* SCE in MeCN). Similarly, the oxidation of a range of substrates **D** can take place, forming the corresponding radical cation $D^{\bullet+}$ and closing the catalytic cycle.

Conveniently, the redox properties of ruthenium(II) polypyridines complexes can be fine tuned by appropriate substitution of the ligands. Table 4.1 presents the redox potentials determined by cyclic voltammetric studies of a series of ruthenium complexes [10]. From these data, it can be seen that the redox potential ($Ru(bpy)_3^{2+}/Ru(bpy)_3^{+}$) can be lowered by substituting ligands with electron-donating groups (Table 4.1, entry 2), while the redox potential ($Ru(bpy)_3^{3+}/Ru(bpy)_3^{2+}$) can be increased with ligands bearing electron withdrawing groups as substituents (Table 4.1, entries 3,4,7).

The tunable photoredox properties of ruthenium(II) polypyridines complexes combined to their unique spectral properties and their high chemical stability offer unmatched opportunities to channel visible light into the generation of radicals via electron transfer reactions. The radical generated can then be used in usual radical transformation, allowing the construction of new carbon–carbon bonds and carbon-heteroatom bonds in an eco-compatible fashion.

By optimizing the structure of the photoredox catalyst, the nature of the reductive or oxidative quench and all other reaction parameters, the scope of substrates amenable to visible light photoreductive or photooxidative catalysis has

Table 4.1 Spectral and redox properties of a series of substituted ruthenium(II) polypyridines complexes

Entry	Ligand L	λ absorption (nm)	Oxidative quenching cycle		Reductive quenching cycle	
			$RuL_3^{3+}/RuL_3^{2+}*$	RuL_3^{3+}/RuL_3^{2+} (V)	$RuL_3^{2+}*/RuL_3^{+}$	RuL_3^{2+}/RuL_3^{+} (V)
1	bpy	452	−0.86V	+1.29	+0.84 V	−1.33
2	4,4′-Me_2bpy	460	−0.94 V	+1.10	+0.69 V	−1.44
3	4-NO_2bpy	462	unknown	+1.43	unknown	−1.06
4	4,4′-Cl_2bpy	480	unknown	+1.55	unknown	−0.55
5	phen	447	−0.87 V	+1.26	+0.82 V	−1.36
6	5-Mephen	450	−0.92 V	+1.23	+1.00 V	−1.31
7	5-Clphen	447	−0.77 V	+1.36	unknown	−1.157

all redox potentials were determined *vs*. NHE in aqueous solutions

been progressively expanded, providing new opportunities to conduct radical chemistry under tin-free conditions.

4.2 State of the Art of the Substrates Amenable to Visible Light Photoredox Catalysis

4.2.1 Aromatic Ketones

Early studies by Pac have disclosed that the $Ru(bpy)_3^{2+}$-photosensitized reaction of 1-benzyl-1,4-dihydronicotinamide (BNAH) with electron-poor aromatic ketones such as **3** in methanol, led to their reduction to the corresponding alcohol **4a** [17, 18]. The authors found that the luminescence of $Ru(bpy)_3^{2+}$ was quenched by BNAH but not by the aromatic ketones and proposed the mechanism depicted in Fig. 4.9. Visible-light excitation of the ruthenium complex triggers the formation of $Ru(bpy)_3^{2+}*$ (reduction potential = + 0.86 V *vs* SCE), that would oxidize BNAH to $BNAH^{\bullet+}$ (oxidation potential = + 0.57 V *vs* SCE)[19]. The reductive species $Ru(bpy)_3^{+}$ formed (oxidation potential = −1.33 V *vs* SCE) would transfer an electron to ketone **3** (reduction potential = −1.17 V *vs* SCE) to generate the corresponding radical anion. Facile deprotonation of $BNAH^{\bullet+}$ would deliver radical **5** and $BNA^{\bullet}$, which dimerizes to **4b**. This latter would re-enter the catalytic cycle to undergo second electron and proton transfers.

4.2.2 Activated Halides

Halide substrates are the most commonly used precursors in usual radical chemistry. Using visible light catalysis, the photoreduction of halides can be performed

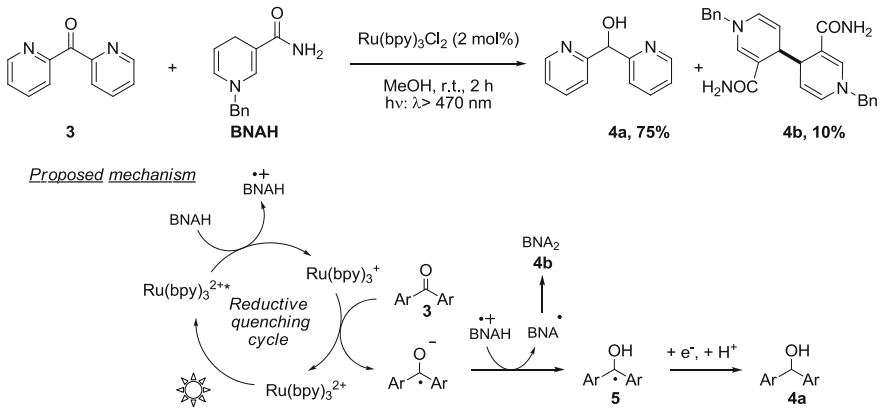

Fig. 4.9 $Ru(bpy)_3^{2+}$-photosensitized reaction of BNAH with electron-poor aromatic ketone

only if the carbon-halide bond is sufficiently activated towards one-electron reduction. Several strategies have been employed to achieve such activation.

Phenacylbromide **6a** (−0.49 V *vs* SCE in MeCN) could be reduced by irradiation with visible light in the presence of *N*-alkyl-2,3-dihydrobenzothiazole[4] **7** and $Ru(bpy)_3Cl_2$, as early as 1985 by the team of Kellogg (Fig. 4.10) [20]. The roles of light and photoredox catalyst were carefully tested. Control reaction in the dark at room temperature did not lead to any conversion. Under visible light irradiation, the reduction could work without any sensitizer but was strongly accelerated in the presence of the ruthenium catalyst. It was also observed that increased electron deficiency at the carbon to be reduced led to higher rates of reduction. Thus diethyl 2-bromomalonate bromide could be reduced in 1 h and 2-bromomalonitrile in 0.7 h under the same conditions. Those results suggested that the reduction proceeded via visible-light induced photoredox catalysis, but no definitive mechanism could be proposed.

A few years later, Fukuzumi reported the visible light photoreduction of phenacyl bromides and chlorides in the presence of dihydroacridine derivative **9** and $Ru(bpy)_3Cl_2$ [21]. Quantum yield determinations and luminescence quenching experiments suggested the mechanism depicted in Fig. 4.11 for the formation of acetophenone **8**. Irradiation of the reaction mixture with visible light would trigger the formation of $Ru(bpy)_3^{2+}*$ in an excited state, that would oxidize acridine to the corresponding radical cation **11**. The reductive species $Ru(bpy)_3^{+}$ formed would transfer an electron to the carbonyl function, leading to a radical anion that after reaction with **11** would afford the reduced product **8**.

In those first examples, the radical formed by visible light photoreduction was directly reduced with hydrogen donors, which provides an interesting proof of concept but limits the usefulness of the methodologies. Starting from 2008, there

[4] Standard redox potential for *N*-alkyl-2,3-dihydrobenzothiazole **6** is −0.33 V.

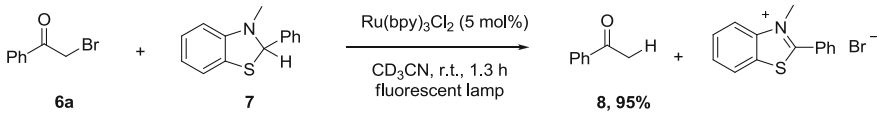

Fig. 4.10 Photoreduction of phenacylbromide using *N*-alkyl-2,3-dihydrobenzothiazole as reductive quench

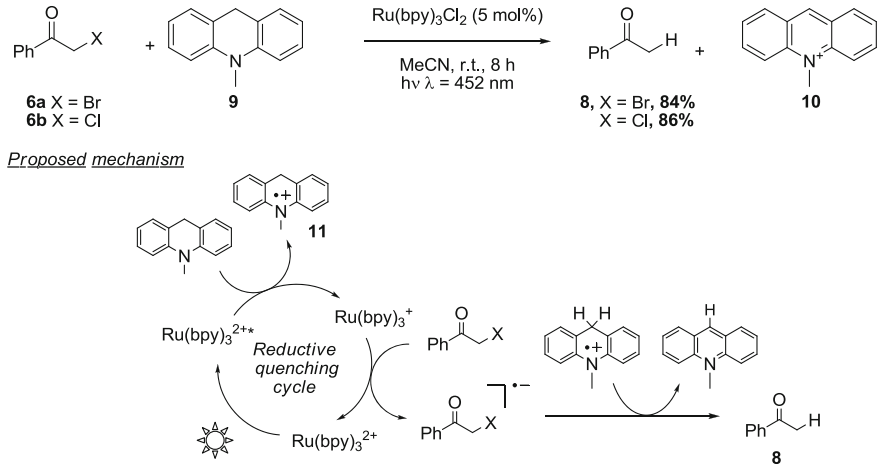

Fig. 4.11 Photoreduction of phenacylbromide using dihydroacridine as reductive quench

was a new surge of interest for the utilization of the radicals formed to build carbon–carbon bonds or carbon-heteroatom bonds.

The visible light photoreduction of bromopyrroindolines such as **12** was investigated by the Stephenson group. In the presence of $Ru(bpy)_3Cl_2$, a tertiary amine as the reductive quench, and Hantzsch ester or formic acid as hydrogen donor, the reduced indoline **13** could be obtained in excellent yield (Fig. 4.12a) [22]. These conditions could be applied to the reductive dehalogenation of α-carbonyl chlorides and bromides and proved particularly mild and selective. When the hydrogen donor was replaced with an excess of indole acceptor **15**, the benzylic radical intermediate could be trapped by radical addition to the indole ring, yielding after rearomatization bisindoles **16** [23]. This strategy was successfully employed to construct the C3-C3′ bisindole core of cytotoxic agent gliocladin C (Fig. 4.12b). During the optimization of this reaction, various trialkylamines were examined and n-Bu_3N resulted in the optimal balance between reactivity and selectivity (C–C bond formation *vs* dehalogenation). Moreover, irradiation by commercially available blue LED light source afforded an appreciable increase in the reaction rate. The reaction mechanism was thought to proceed via reductive quenching of visible-light excited $Ru(bpy)_3^{2+}$* species by tertiary amine. Indeed, luminescence quenching experiments indicated that tertiary

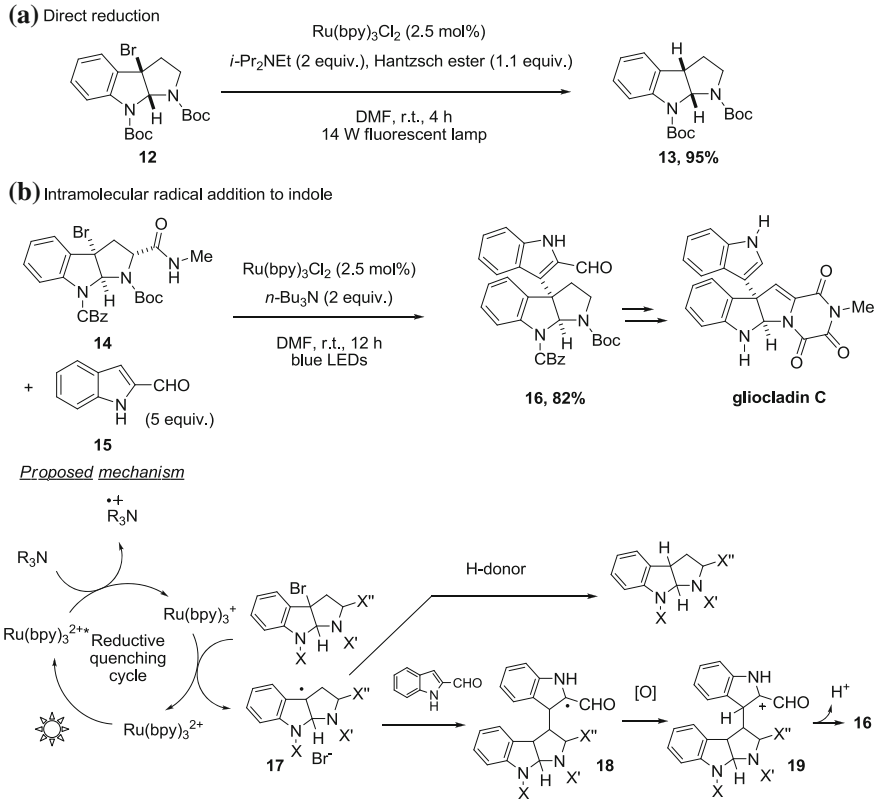

Fig. 4.12 Generation of indolinoyl radical by visible light photoreduction and intermolecular addition to indole

amines were the only reaction components that could quench the excited state. The strongly reducing $Ru(bpy)_3^+$ formed would then perform a single-electron reduction of the activated C–Br bond, delivering tertiary radical **17** and regenerating $Ru(bpy)_3^{2+}$ catalyst. Benzylic radical **17** could either be directly reduced, either add to the indole ring, forming radical **18** which would be subsequently oxidized to cationic intermediate **19**. Several species could play the role of oxidizing agent (i.e. $Ru(bpy)_3^{2+}*$, adventitious oxygen or ammonium radical), which still remains to be formally identified. Loss of a proton would finally afford the bisindole **16**.

Using similar reaction systems, Stephenson could successfully generate malonyl radical by visible light photoreduction of diethyl bromomalonate and have it add intra- and inter-molecularly to heterocyclic aryls such as indoles, pyrroles and furans [24, 25]. The efficiency of the transformation seemed to be related to the electronic properties of the trapping aryl partner. Indeed, the electron-richer pyrroles generally outperformed indoles. Adding a degree of complexity, malonyl type radical **21** was successfully engaged in a photoredox mediated cascade 5-*exo*-*trig*

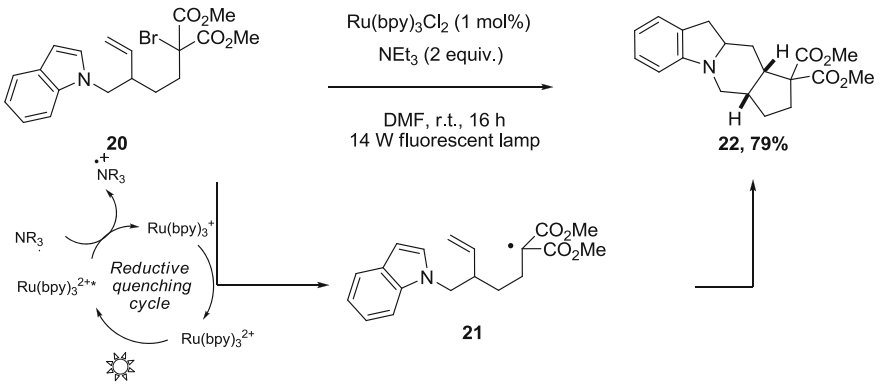

Fig. 4.13 Cascade cyclization of malonyl radical generated by visible light photoreduction

cyclization/radical addition to indole, delivering tetracyclic product **22** in excellent yield as a single diastereoisomer (Fig. 4.13).

Changing from $Ru(bpy)_3Cl_2$ catalyst to $Ir(dtbbpy)(ppy)_2PF_6$ which possesses similar spectral properties and provides a highly reductive Ir(II) species ($Ir^{III}(dtbbpy)(ppy)_2^+/Ir^{II}(dtbbpy)(ppy)_2 = -1.51$ V *vs* SCE in MeCN) [26] allowed to expand the scope of visible light photoreduction. Indeed, α-bromo esters such as **23** and geminally dibrominated cyclopropanes such as **25** which were unreactive under ruthenium-catalyzed conditions, afforded smoothly the corresponding radicals that could be cyclized onto tethered double or triple bonds [27]. Reduction of the resulting vinyl or alkyl radical was thought to occur via abstraction of hydrogen from the triethylammonium radical cation (Fig. 4.14).

α-Glucosyl bromides such as **27** proved sufficiently activated to undergo $Ru(bpy)_3^{2+}$-catalyzed visible light photoreduction (Fig. 4.15) [28]. The generated nucleophilic C1-radical **28** could react intermolecularly with electron-deficient alkenes, providing C-glycosides such as **29** with high α selectivities. The use of Hantzsch ester as efficient hydrogen donor prevented oligomerization side reactions and led to improved yields, while the use of BF_4^- as counter anion of the ruthenium catalyst seemed to improve its solubility in MeCN. This methodology provides a greener alternative to the usual Giese reaction mediated by Bu_3SnH [29].

In 2008, MacMillan group reported a combination of photoredox catalysis and organocatalysis using $Ru(bpy)_3Cl_2$ and a chiral imidazolidinone **30** as catalysts. In the pursuit of enantioselective alkylation of aldehydes, the group observed that electron-deficient radicals generated by photoreduction of activated bromides could add to electron-rich enamines with excellent enantiofacial control. The two cooperative catalytic cycles depicted in Fig. 4.16 were built on this concept [30]. The photoredox catalytic cycle is initiated with the visible light activation of $Ru(bpy)_3^{2+}$ to $Ru(bpy)_3^{2+}*$ which can oxidize a sacrificial quantity of enamine to provide $Ru(bpy)_3^+$. This reductive species can transfer an electron to α-bromocarbonyl **31**, closing the first catalytic cycle. The α-carbonyl radical **32** generated

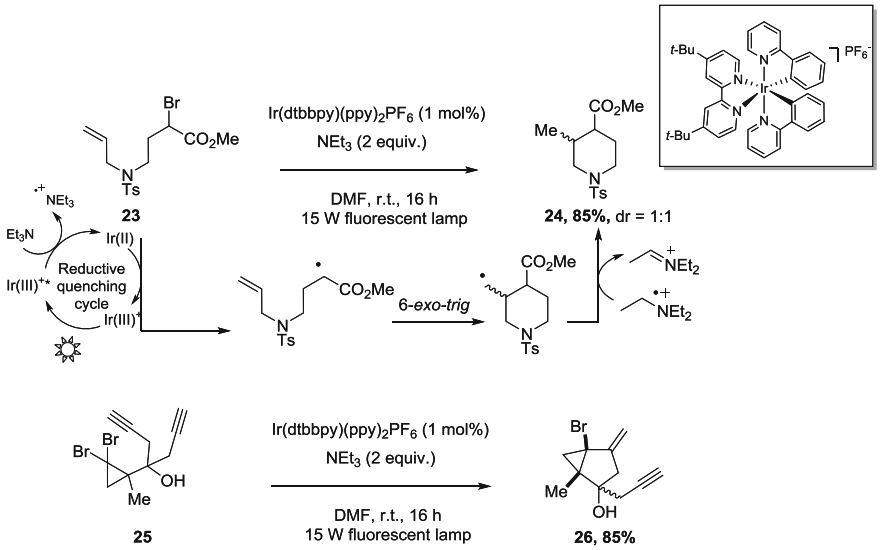

Fig. 4.14 Cyclization of α-keto and cyclopropyl radicals generated by Ir-catalyzed photoreduction

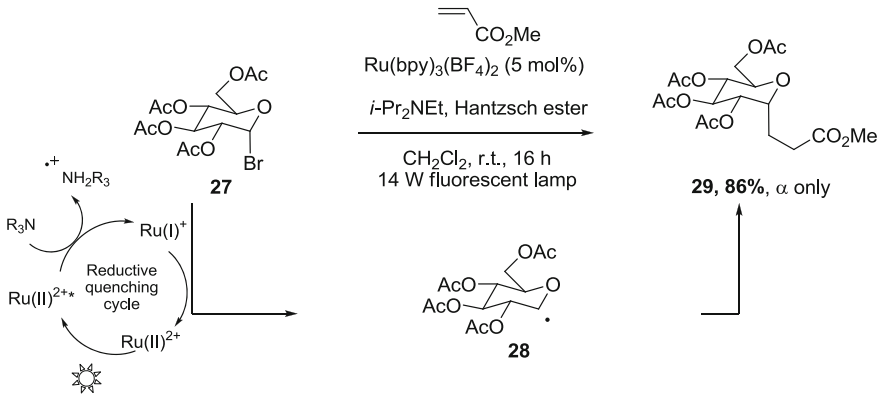

Fig. 4.15 Photoreductive generation of C1 sugar-radical and addition to alkenes

joins the organocatalytic cycle by radical addition to the enamine **33**, formed by condensation of starting aldehyde **36** and proline catalyst. The product of this radical addition is the electron-rich aminyl radical **34** which possesses a low barrier to oxidation (−1.03 V *vs* SCE in MeCN for model (dimethylamino)methyl radical [31]) and can consequently be oxidized by $Ru(bpy)_3^{2+}$* to form the corresponding imminium **35**. Hydrolysis of **35** delivers the enantio-enriched α-alkylated aldehyde **37** while regenerating the organocatalyst. One can notice that

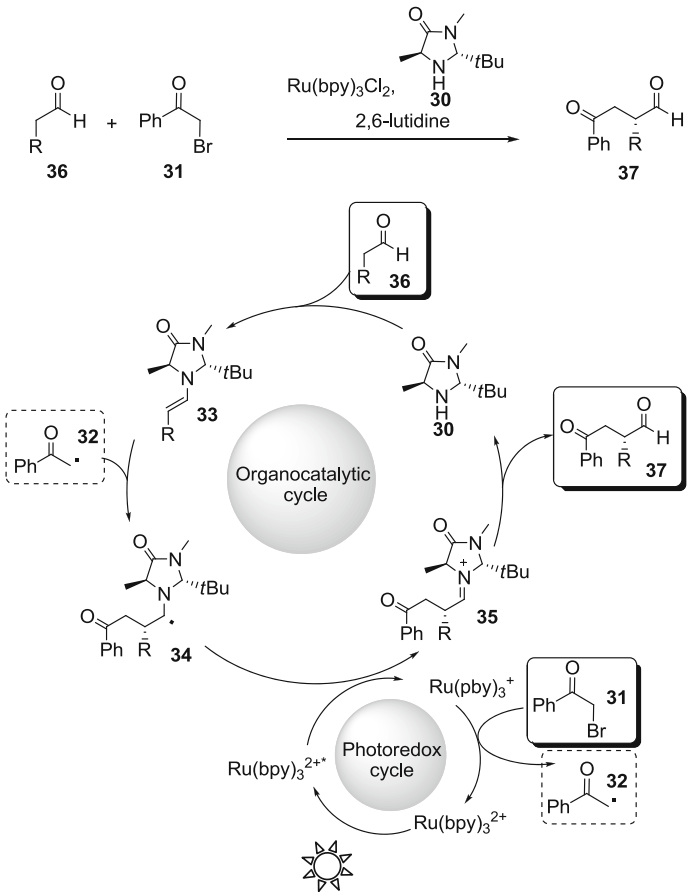

Fig. 4.16 Merger of orgnocatalysis and photoredox catalysis for enantioselective alkylation of aldehydes

in this catalytic system, both oxidation and reduction steps are productive, avoiding the need of an external reductive quench.

Using $Ru(bpy)_3Cl_2$ as the photoredox catalyst, MacMillan was able to use α-bromocarbonyl compounds such as phencyl bromides, malonyl bromides or α-bromoester as radical precursors. Thus irradiation of α-bromoester **38** and aliphatic aldehyde **39** in the presence of ruthenium catalyst, proline derivative **30** and 2,6-lutidine as HBr quench afforded α-alkylated aldehyde **40** in 80 % yield and 92 % ee (Fig. 4.17a) [28]. By changing the catalyst to $Ir(dtbbpy)(ppy)_2PF_6$ the scope of radical precursors could be extended to trifluoromethyl iodide **41**. Under adapted reaction conditions, visible light irradiation of trifluoromethyl iodide and aliphatic aldehydes such as **42** in the presence of the iridium catalyst and proline catalyst **43** allowed the first enantioselective catalytic trifluoromethylation of

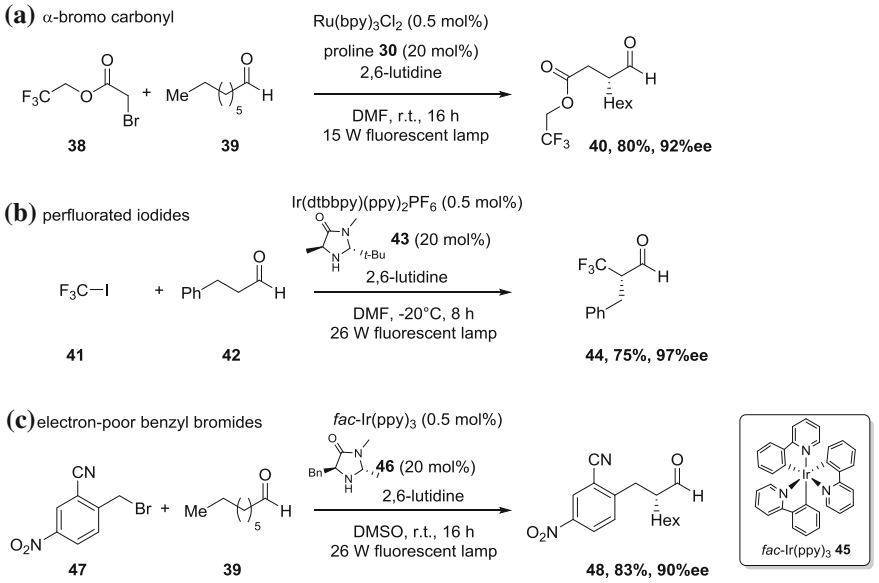

Fig. 4.17 Photoredox Organocatalysis with various halogenated precursors

aldehyde, yielding adduct **44** in 75 % yield and 97 % ee (Fig. 4.17b) [32]. Notably, a wide range of perfluoroalkyl iodides could also participate in the enantioselective alkylation of aldehydes under these reaction conditions. Finally, benzylbromides were tested as radical precursors [33]. Electron-neutral benzylic halides could not be reduced, however the reaction was successful with electron-deficient nitrobenzyl bromides or pyridinyl methylene bromides on the condition to use *fac*-Ir(ppy)$_3$ **45** as the photoredox catalyst (Fig. 4.17c). *fac*-Ir(ppy)$_3$ is a commercially available catalyst widely used as green triplet emitter in OLEDs. Under visible light excitation *fac*-Ir(ppy)$_3$ undergoes excitation to *fac*-$Ir^{III}(ppy)_3$* which is a higly reductive species ($Ir^{IV}(ppy)_3^+/Ir^{III}(ppy)_3$* = −1.73 V *vs* SCE in MeCN) [34]. Oxidative quenching with electron deficient benzyl bromide generates the benzyl radical and affords *fac*-$Ir^{IV}(ppy)_3^+$. Note that in this case the photoredox cycle is an oxidative quenching cycle, so that the reduction and oxidation steps are inverted compared to Fig. 4.16.

The possibility to use highly activated halides as oxidative quench of excited $[Ir^{III}]^+$* species was used to set up a visible light-triggered atom transfer radical addition of halo alkanes to olefins. Thus, irradiation of diethyl 2-bromomalonate **49** and 5-henen-1-ol **50** in the presence of Ir[(dF(CF_3)ppy)$_2$(dtbbpy)]PF_6 ($[Ir^{III}]^+$*/$[Ir^{IV}]$ = −1.21 V; $[Ir^{IV}]/[Ir^{III}]^+$ = +1.69 V) and LiBr afforded bromoalkane **51** in nearly quantitative yield (Figure 4.18).

These atom transfer conditions tolerated as the starting halide perfluorated iodides and bromides, and trichlorobromomethane besides bromomalonate. Electron rich olefins such as allylamines or cyclohexenes could be used as unsaturated

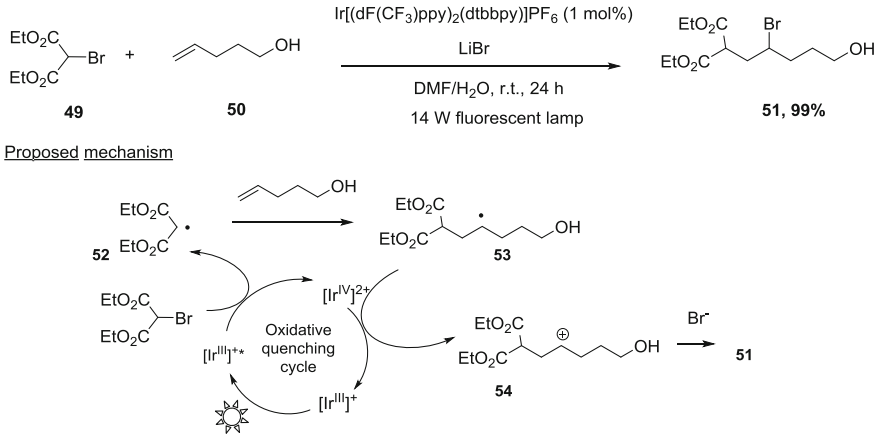

Fig. 4.18 Visible-light triggered intermolecular atom transfer radical addition

partners. The mechanism is thought to proceed via oxidative quenching of the visible-light induced excited state $[Ir^{III}]^{+*}$ with 2-bromomalonate, leading to electrophilic radical **52** and $[Ir^{IV}]^{2+}$. This species would oxidize the alkyl radical **53** formed by addition of malonyl radical **52** to the electron rich olefin. The carbocation **54** generated would recombine with bromide ion from the starting halide or from the LiBr salt to afford the final bromoalkane.[5]

4.2.3 Aryl Enones and Electron-Rich Styrenes

In 2008, in the context of formal [2 + 2] cycloadditions, Yoon reported that aryl enones could be smoothly reduced to the corresponding radical anion under $Ru(bpy)_3Cl_2$-catalyzed photoredox conditions. Since aliphatic enones and enoates had a too low potential to be reduced (−1.64 V *vs* SCE in MeCN for 4-phenylbut-3-en-2-one *vs* −1.41 V for chalcone), they could be employed as Michael acceptor partners, to afford selectively the [2 + 2] adducts via intramolecular [35] or intermolecular [36] reactions (Fig. 4.19). The cyclobutane products were obtained in high diastereoselectivities as *cis* isomers in the case of intramolecular [2 + 2] reactions and as *trans* isomer for intermolecular reactions. The addition of $LiBF_4$ salts to the reaction mixture proved essential to obtain conversion, which has been attributed to both its Lewis acid behavior and its ability to enhance the solubility of $Ru(bpy)_3Cl_2$ in MeCN. The authors proposed as mechanistic pathway the reductive quenching of excited state $Ru(bpy)_3^{2+}$* by *i*-Pr_2NEt forming the corresponding

[5] Evidence for the formation of carbocation intermediate was obtained by isolation of a furan side product when 4-penten-1-ol was used as the olefin. Furthermore, alkyl radicals are known to be easily oxidized (+0.47 V *vs* SCE in MeCN for $Me_2CH^{\bullet}$).

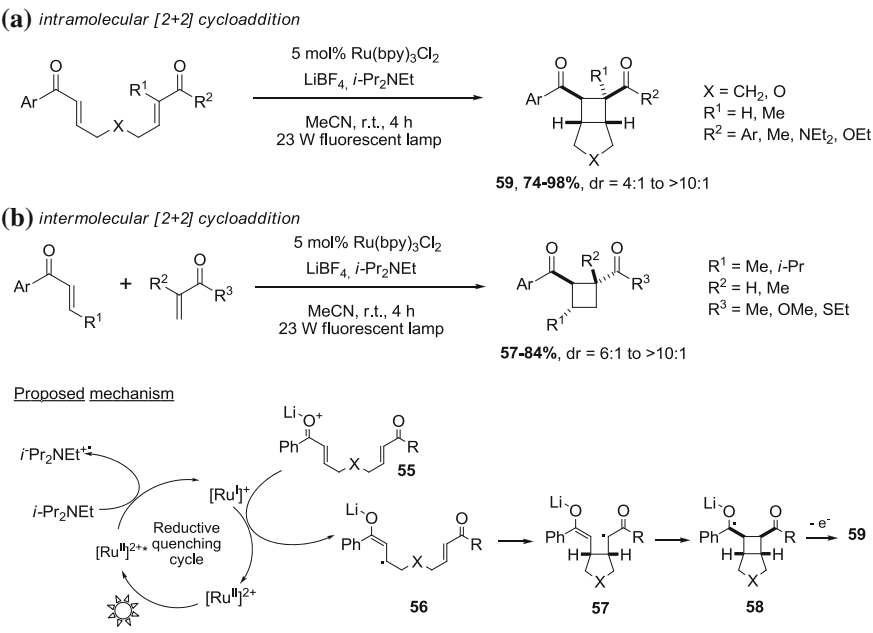

Fig. 4.19 [2 + 2] Cycloadditions of enones via visible light photocatalysis

radical cation and $Ru(bpy)_3^+$. This reductive species can transfer an electron to the activated aryl enone **55**, delivering radical anion **56** which undergoes a formal [2 + 2] cycloaddition with the pendant Michael acceptor. Oxidation of radical anion **58** could be achieved either by $Ru(bpy)_3^{2+}$* or *i*-Pr_2NEt radical cation, but this mechanistic step was not discussed by the authors and the amine was always introduced in stoichiometric quantities. Interestingly, when the length of the tethering group was increased in bisenones precursors, the [2 + 2] adducts were not formed. Instead, a hetero-Diels–Alder cycloadduct was obtained [37].

In 2010, Yoon reported a complementary strategy for the [2 + 2] addition of electron rich diene substrates. Indeed, he found that visible light irradiation of diene **60** possessing a 4-methoxystyrene moiety in the presence of $Ru(bpy)_3Cl_2$ and methyl viologen (oxidation potential = + 0.45 V) as an oxidative quench, triggered a radical cation [2 + 2] cycloaddition pathway leading to cyclobutane adduct **61** (Fig. 4.20) [38].

4.2.4 α-Keto Sulfonium, Ammonium and Phosphonium Salts

Phenacyl sulfonium salts possess adequate potentials for $Ru(bpy)_3Cl_2$-catalyzed visible light photoreduction. Dimethylphenacylsulfonium butyltriphenylborates has thus a reduction potential of −1.01 V *vs* SCE in MeCN [39]. Using Hantzsch

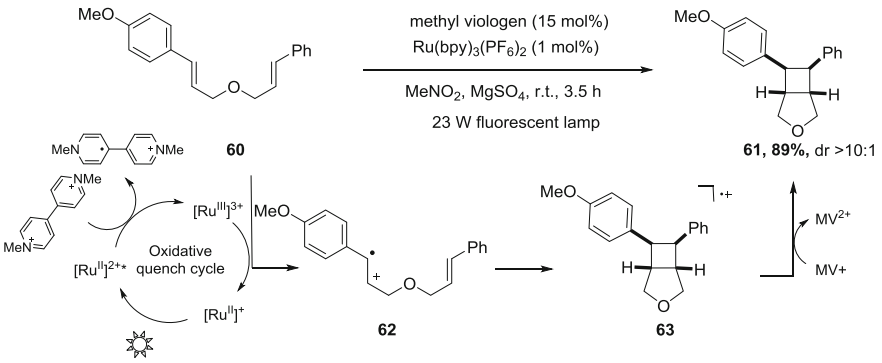

Fig. 4.20 Visible-light induced [2 + 2] cycloaddition of electron rich diene via oxidative quenching of $[Ru(bpy)_3]^{2+*}$

ester derivative **65** as hydrogen donor, Kellog could report in 1978 the reduction of phenacylsulfonium salt **64** in the presence of $Ru(bpy)_3Cl_2$ and under visible light irradiation (Fig. 4.21) [40]. The products isolated were aryl ketone **66**, sulfide **67** and pyridinium **68**. No mechanism could be ascertained for this transformation but the authors described that the reduction was highly accelerated in the presence of ruthenium catalyst. Thus the time needed for full conversion dropped from 48 h without catalyst to 0.3 h in the presence of 1 mol % of catalyst. The rates of reaction were also enhanced using phenacylsulfonium salts bearing electron withdrawing substituents. Using the same reaction conditions, ammonium salt **69a** and phosphonium salt **69b** could also be reduced. Visible light photoreduction of dialkylphenacylsulfonium salts catalyzed by coumarin-type sensitizers has been used to initiate polymerization of acrylates. Nonetheless $Ru(bpy)_3Cl_2$-catalyzed photoreduction of sulfonium salts has never been applied to the construction of C–C bonds.

4.2.5 N-(acyloxy)Phthalimides

Alkyl radical could be generated by the ruthenium-catalyzed decarboxylative photoreduction of *N*-(acyloxy)phthalimides such as **70,** in the presence of BNAH **72** as the reductive quench [41]. The formed radical could be elegantly trapped by Michael acceptors such as methyl vinyl ketone **71** (Fig. 4.22). No reaction took place if $Ru(bpy)_3Cl_2$ or BNAH **72** was omitted. The authors envisioned that the reaction proceeded as depicted in Fig. 4.22. Reductive quenching of $Ru(bpy)_3^{2+*}$ by BNAH would deliver the corresponding ammonium radical and $Ru(bpy)_3^{+}$ that could transfer an electron to phtalamide **70** (reduction potential = −1.37 V *vs* SCE in MeCN) [42]. Decarboxylation would generate alkyl radical **74** that would add to electron deficient olefins forming α-carbonyl radical **75**. This latter abstracts hydrogen from BNAH, as demonstrated by deuterium labeling studies.

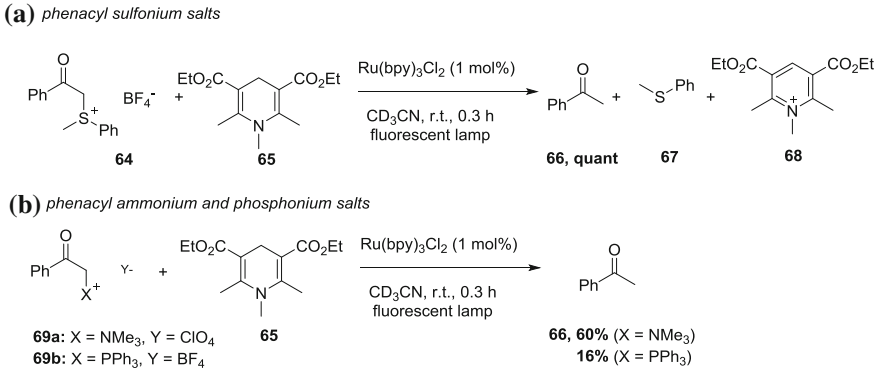

Fig. 4.21 $Ru(bpy)_3Cl_2$-catalyzed visible light photoreduction of α-keto onium salts

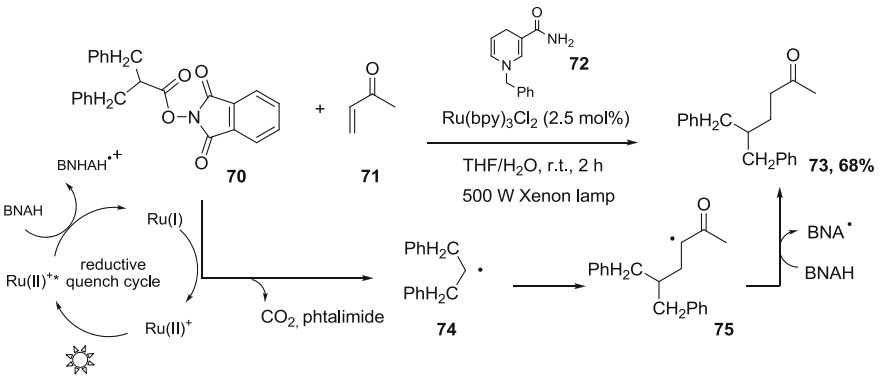

Fig. 4.22 Visible light-triggered decarboxylative Michael addition of *N*-(acyloxy)phthalimides

4.2.6 Diazoniums

Diazoniums salts are readily reduced (reduction potential = −0.1 V *vs* SCE in MeCN) and constitute consequently radical precursors of choice. As early as 1984, Deronzier and Cano-Yelo reported the $Ru(bpy)_3Cl_2$-catalyzed photocatalytic Pschorr reaction for the synthesis of phenanthrenes (Fig. 4.23) [43]. In this reaction, an aryl radical **78** was formed by oxidative quench of $Ru(bpy)_3^{2+}$* with aryldiazonium salt such as **76**. Intramolecular arylation delivers radical **79** which undergoes oxidation by $Ru(bpy)_3^{3+}$ and subsequent loss of proton to afford aromatized product **77**. In that example, no sacrificial oxidative or reductive quench was needed since both steps were productive. In further investigations, Deronzier used aryldiazonium as oxidative quench to perform the $Ru(bpy)_3Cl_2$-catalyzed oxidation of benzylic alcohols to aldehydes [44].

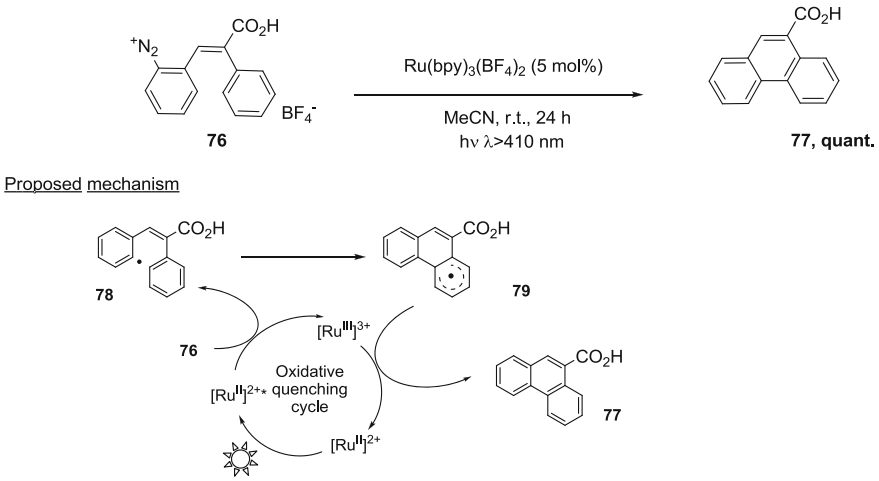

Fig. 4.23 Pschorr reaction via visible-light photoredox catalysis with $Ru(bpy)_3^{2+}$

4.2.7 Azides

In 2011, using a DNA-templated reaction-discovery system, Liu serendipitously discovered that DNA-linked aryl azide **80** irradiated by visible light in the presence of $Ru(bpy)_3Cl_2$ could react with acetonitrile to generate a product identified by LC–MS as imidate adduct **81** (Fig. 4.24a) [45]. When this reaction was studied in a non-DNA linked format, the formation of the new nitrogen-carbon bond could not be reproduced. However, under optimized reaction conditions, various aryl azides such as **82** and one alkyl azide could be reduced to the corresponding amine (Fig. 4.24b). The reaction proceeded optimally in the presence of Hantzsch ester as hydrogen donor, iPr$_2$NEt as reductive quench and acetic acid. The reaction was very selective and was compatible with aryl halides, acids or alcohols functional groups. The proposed general reaction mechanism is depicted in Fig. 4.24. Reductive quenching of $Ru(bpy)_3^{2+}$* by the tertiary amine gives $Ru(bpy)_3^{+}$. This latter would reduce azide through one electron transfer to generate azide radical anion **84**. Extrusion of nitrogen and protonation would afford aminyl radical **85** that would abstract hydrogen from Hantzsch ester or ammonium radical to deliver the amine **86**. This study opens the door to the generation of nitrogen centered radicals by visible light photoredox catalysis and should find a huge number of applications in the future, provided that the radical generated can be channeled for the construction of new N–C bonds.

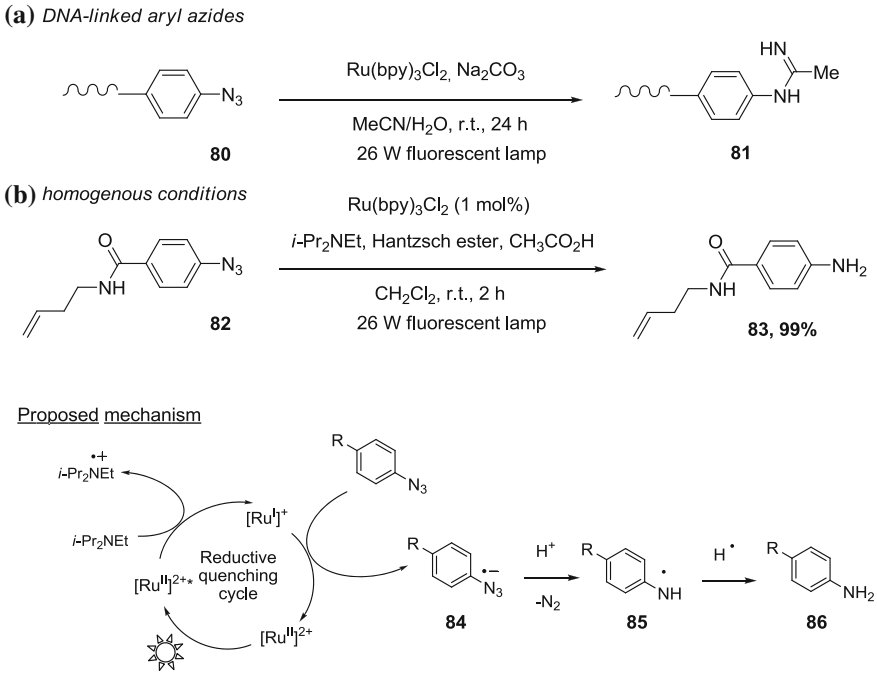

Fig. 4.24 Visible-light induced azide reduction

4.2.8 Iodonium Salts

Very recently, Lalevée and Blanchard exploited iodonium salts ($E_{red}(Ph_2I^+)$ ~ -0.2 V) as oxidative quench of $Ru^{II}(bpy)_3^{2+}$* excited state to generate strong oxidant species $Ru^{III}(bpy)_3^{3+}$ and phenyl radical $Ph^{\bullet}$ (Fig. 4.25) [46]. These intermediates were used to promote the cationic ring-opening polymerization of epoxy monomers such as limonene dioxide LDO **87** upon generation of silylium cation from TTMSS. The mechanism of the initiation is depicted in Fig. 4.25. $Ph^{\bullet}$ radical can abstract hydrogen from TTMSS leading to the corresponding silyl radical that is oxidized by $Ru^{III}(bpy)_3^{3+}$ to the desired silylium cation. Alternatively, silyl radicals can be oxidized by starting iodonium salt. The silylium cations generated are efficient initiators of ring-opening polymerization. Thus, irradiation by a household green bulb of the $Ru(bpy)_3Cl_2$/TTMSS/iodonium salt system provides a rapid free radical promoted photoinitiation of cationic polymerization of epoxides. In a subsequent study, the use of $Ir(ppy)_3$ as photoredox catalyst allowed to further improve the photopolymerization initiating system [47].

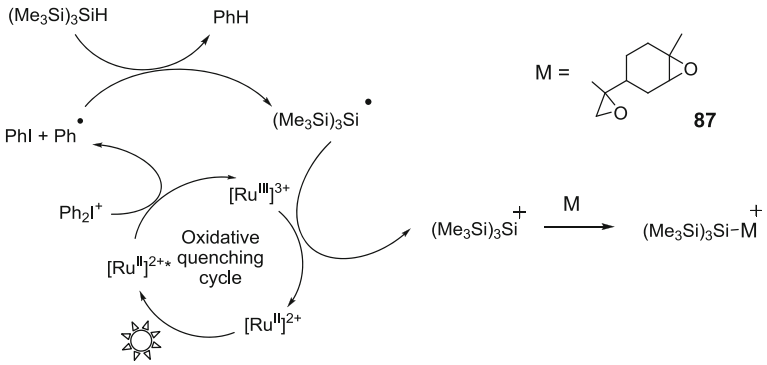

Fig. 4.25 $Ru(bpy)_3Cl_2$/iodonium salt/TTMSS as novel visible light photopolymerization initiating system

4.2.9 Para-Methoxybenzyl Ethers

PMB ether protecting groups are generally removed under oxidative conditions employing stoichiometric quantities of oxidant such as CAN or DDQ. Stephenson reported that using appropriate photoredox catalyst $Ir[dF(CF_3)ppy]_2(dtbbpy)PF_6$ ($[Ir^{III}]^+*/[Ir^{IV}] = -1.21$ V; $[Ir^{IV}]/[Ir^{III}]^+ = +1.69$ V *vs* SCE in MeCN) under oxidative quenching conditions, a visible light photoredox catalyzed deprotection of PMB ethers could be performed (oxidation potential for *p*-methoxybenzyl alcohol = + 1.44 V *vs* SCE in MeCN) [48]. Thus under blue LEDs irradiation, compounds bearing PMB ether functionality such as **88** were converted into the corresponding alcohols in the presence of $Ir[(dF(CF_3)ppy)_2(dtbbpy)]PF_6$, $BrCCl_3$ as the oxidative quench, water and 2,6-lutidine to buffer HBr (Fig. 4.26). These mild conditions allowed selective deprotection of PMB in the presence of THP acetals, benzyl ethers or TBS ethers.

4.2.10 Naphtols

Efficient one-electron oxidation of 2-naphtol (oxidation potential = + 1.34 V *vs* SCE in MeCN) can be performed by ruthenium(II) polypyridines catalysts through visible light-induced oxidative quenching catalytic cycles [49]. Enantioselective oxidative coupling of naphtols was developed by Ohkubo using enantiopure Δ-$[Ru(membpy)_3]^{2+}$ **94** as catalyst (Fig. 4.27) [50]. This latter possesses outstanding photophysical properties: long excited state lifetime (1940 ns in MeCN), extremely low quantum yield of photoracemization ($\Phi_{rac} = 4 \times 10^{-6}$ in MeCN compared to $\Phi_{rac} = 3 \times 10^{-4}$ for Δ-$[Ru(bpy)_3]^{2+}$) and high oxidation potential (+1.55 V *vs* SCE in MeCN). Using $[Co(acac)_3]$ as oxidative quench, visible light irradiation of **92** in the presence of Ru(II) catalyst afforded (*R*)-(+)-1,1′-bi-2-naphtol **93** with 16 % ee.

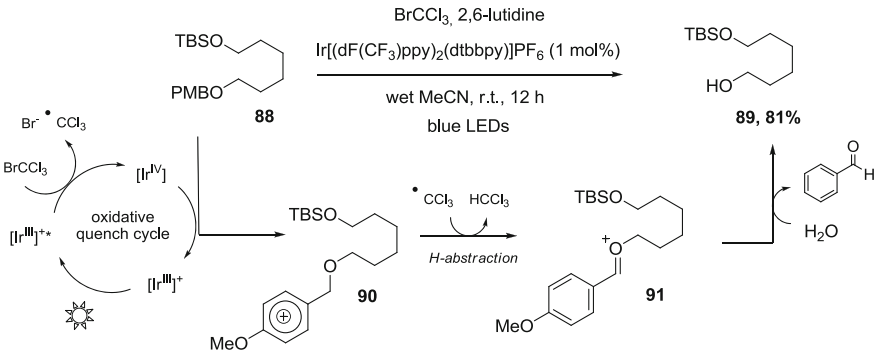

Fig. 4.26 Visible-light mediated photoredox deprotection of PMB ethers

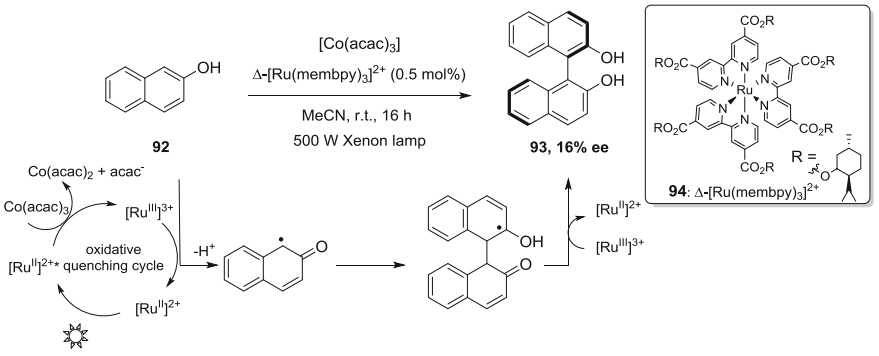

Fig. 4.27 Δ-$[Ru(membpy)_3]^{2+}$-catalyzed enantioselective oxidative homocoupling of 2-naphtol

This enantiomeric excess constitutes a proof of concept that enantioselectivity can be governed by chiral helicity along C_3 axis of the ruthenium complex.

4.2.11 Oxidative Functionalization of Tertiary Amines

As it has been presented throughout this bibliographic account, tertiary amines are very efficient reductive quench of excited states of photoredox catalysts $[Ru^{II}]^{2+*}$ or $[Ir^{III}]^{+*}$. The generated ammonium radicals can serve as hydrogen donors, affording imminium ions which are generally unexploited byproducts. Several groups envisioned that the imminium ion could be intercepted with appropriate nucleophile, thus affording a visible light mediated functionalization of C–H bond adjacent to nitrogen atom. Nitroalkanes were first tested as nucleophiles. Under visible light irradiation, using $Ir(dtbbpy)(ppy)_2PF_6$ as catalyst, tetrahydroquinoline **95** could undergo an aza-Henry reaction with nitromethane leading to compound

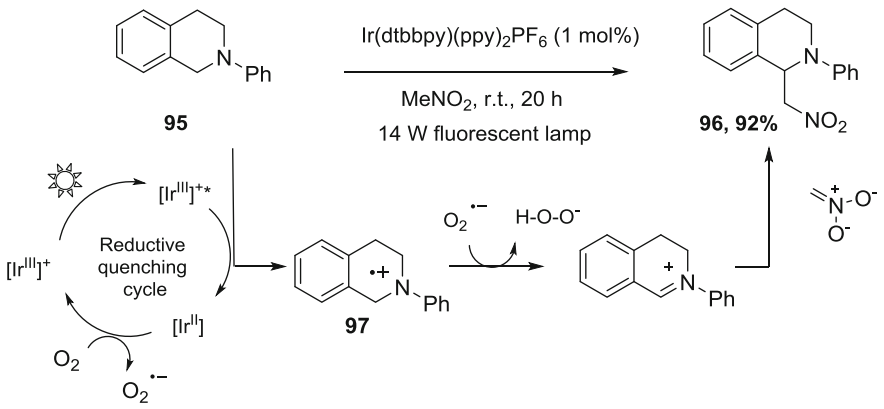

Fig. 4.28 Oxidative aza-Henry reaction via visible light photoredox catalysis

96 (Fig. 4.28) [51]. Interestingly, no external oxidant was needed to perform this reaction, suggesting that adventitious oxygen could play this role, with the corresponding radical anion abstracting hydrogen from ammonium radical.

Subsequently, various nucleophiles were used to intercept imminium ions formed under similar conditions such as ketones [52], phosphite esters [53] or amines [54].

To conclude, Ru and Ir photocatalysts possess dual visible-light induced reactivities, which offer multiple possibilities to access free radical intermediates under tin-free conditions. Radical cyclizations and radical additions to aromatics have been performed with photogenerated radicals, demonstrating that their utilization in carbon–carbon or carbon-heteroatom bond formations was achievable. Thanks to fine tuning of the properties of the photoredox catalysts and the quenches, one can hope that the scope of the substrates amenable to visible-light induced photoredox catalysis will keep growing. The goal is not only to provide an environmental-friendly alternative to tin mediators but furthermore to explore novel reactivities and mechanistic pathways that have never been reported.

References

1. Balzani, V., Credi, A., & Venturi, M. (2008). *ChemSusChem, 1*, 26–58.
2. Ciamician, G. (1912). *Science, 36*, 385–394.
3. Sala, X., Romero, I., Rodriguez, M., Escriche, L., & Llobet, A. (2009). *Angewandte Chemie International Edition, 48*, 2842–2852.
4. Lehn, J.-M., & Ziessel, R. (1982). *Proceedings of the National Academy of Sciences of the United States of America, 79*, 701–704.
5. Hari, D. P., & König, B. (2011). *Organic Letters, 13*, 3852–3855.
6. Neumann, M., Füldner, S., König, B., & Zeitler, K. (2011). *Angewandte Chemie International Edition, 50*, 951–954.

7. Yoon, T. P., Ischay, M. A., & Du, J. (2010). *Nature Chemistry, 2*, 527–532.
8. Narayanam, J. M. R., & Stephenson, C. R. J. (2011). *Chemical Society Reviews, 40*, 102–113.
9. Teply, F. (2011). *Collection of Czechoslovak Chemical Communications, 76*, 859–917.
10. Burstall,F. H. (1936). *Journal of Chemical Society*, 173–175.
11. Kalyanasundaram, K. (1982). *Coordination Chemistry Reviews, 46*, 159–244.
12. Lytle, F. E., & Hercules, D. M. (1969). *Journal of the American Chemical Society, 91*, 253–257.
13. Campagna, S., Puntoriero, F., Nastasi, F., Bergamini, G., & Balzani, V. (2007). *Topics in Current Chemistry, 280*, 117–214.
14. Van Houten, J., & Watts, R. J. (1976). *Journal of the American Chemical Society, 98*, 4853–4858.
15. Montalti, M., Cedi, A., Prodi, L., & Gandolfi, M. T. (2006). *Handbook of photochemistry* (3rd ed.). NY: CRC press and Taylor & Francis Group.
16. Whitten Acc, D. G. (1980). *Chemical Research, 13*, 83–90.
17. Ishitani, O., Pac, C., & Sakurai, H. (1983). *Journal of Organic Chemistry, 48*, 2941–2942.
18. Ishitani, O., Yanagida, S., Takamaku, S., & Pac, C. (1987). *Journal of Organic Chemistry, 52*, 2790–2799.
19. Jin, M., Zhang, D., Yang, L., & Liu, Y. (2000). Z. Liu. *Tetrahedron Letters, 41*, 7357–7360.
20. Mashraqui, S. H., & Kellogg, R. M. (1985). *Tetrahedron Letters, 26*, 1453–1456.
21. Fukuzumi, S., Mochizuki, S., & Tanaka, T. (1990). *Journal of Physical Chemistry, 94*, 722–726.
22. Narayanam, J. M. R., Tucker, J. W., & Stephenson, C. R. J. (2009). *Journal of the American Chemical Society, 131*, 8756–8757.
23. Furst, L., Narayanam, J.M.R. & Stephenson, C.R.J. (2011). *Angewandte Chemie International Edition 50*, early view.
24. Furst, L., Matsuura, B. S., Narayanam, J. M. R., Tucker, J. W., & Stephenson, C. R. J. (2010). *Organic Letters, 12*, 3104–3107.
25. Tucker, J. W., Narayanam, J. M. R., Krabbe, S. W., & Stephenson, C. R. J. (2010). *Organic Letters, 12*, 368–371.
26. Flamigni, L., Barbieri, A., Sabatini, C., Ventura, B., & Barigelleti, F. (2007). *Topics in Current Chemistry, 281*, 143–203.
27. Tucker, J.W., Nguyen, J.D., Narayanam, J.M.R., Krabbe, S.W. & Stephenson, C.R.J. (2010). *Chemical Communications*, 4985–4987.
28. Andrews, R. S., Becker, J. J., & Gagné, M. R. (2010). *Angewandte Chemie International Edition, 49*, 7274–7276.
29. Giese, B., & Dupuis, J. (1983). *Angewandte Chemie International Edition, 22*, 622–623.
30. Nicewicz, D. A., & MacMillan, D. W. C. (2008). *Science, 322*, 77–80.
31. Wayner, D. D. M., Dannenberg, J. J., & Griller, D. (1986). *Chemical Physics Letters, 131*, 189–191.
32. Nagib, D. A., Scott, M. E., & MacMillan, D. W. C. (2009). *Journal of the American Chemical Society, 131*, 10875–10877.
33. Shih, H.-W., Vander Wal, M. N., Grange, R. L., & MacMillan, D. W. C. (2010). *Journal of the American Chemical Society, 132*(13600), 13603.
34. Flamigni, L., Barbieri, A., Sabatini, C., Ventura, B., & Barigelleti, F. (2007). *Topics in Current Chemistry, 281*, 143–203.
35. Ischay, M. A., Anzovino, M. E., Du, J., & Yoon, T. P. (2008). *Journal of the American Chemical Society, 130*, 12886–12887.
36. Du, J., & Yoon, T. P. (2009). *Journal of the American Chemical Society, 131*, 14604–14605.
37. Hurtley, A. E., Cismesia, M. A., Ischay, M. A., & Yoon, T. P. (2011). *Tetrahedron, 67*, 4442–4448.
38. Ischay, M. A., Lu, Z., & Yoon, T. P. (2010). *Journal of the American Chemical Society, 132*, 8572–8574.
39. Toba, Y., & Usui, Y. (1999). *Macromolecules, 32*, 6545–6551.

40. Hedstrand, D. M., Kruizinga, W. H., & Kellog, R. M. (1979). *Journal of Organic Chemistry, 44*, 4953–4962.
41. Okada, K., Okamoto, K., Morita, N., Okubo, K., & Oda, M. (1991). *Journal of the American Chemical Society, 113*, 9401–9402.
42. Okada, K., Okamoto, K., & Oda, M. (1988). *Journal of the American Chemical Society, 110*, 8736–8738.
43. Cano-Yelo, H., & Deronzier, A. (1984). *Journal of Chemical Society Faraday Transactions, 1*(25), 5517–5520.
44. Cano-Yelo, H., & Deronzier, A. (1984). *Tetrahedron Letters, 25*, 5517–5520.
45. Chen, Y., Kamlet, A. S., Steinman, J. B., & Liu, D. R. (2011). *Nature Chemistry, 3*, 146–153.
46. Lalevée, J., Blanchard, N., Tehfe, M.-A., Morlet-Savary, F., & Fouassier, J.-P. (2010). *Macromolecules, 43*(10191), 10195.
47. Lalevée, J., Blanchard, N., Tehfe, M.-A., Peter, M., Morlet-Savary, F., & Fouassier, J.-P. (2011). *Macromolecular Rapid Communications, 32*, 917–920.
48. Tucker, J.W., Narayanam, J.M.R., Shah, P.S. & Stephenson, C.R.J. (2011). *Chemical Communication*, 5040–5042.
49. Irie, R., Masutani, K., & Katsuki, T. (2000). *Synlett, 10*, 1433–1436.
50. Hamada, T., Ishida, H., Usui, S., Watanabe, Y., Tsumura, K. & Ohkubo, KJ. *Chemical Society, Chemical Communication*, 909–911.
51. Condie, G., Gonzalez-Gomez, J. C., & Stephenson, C. R. J. (2010). *Journal of the American Chemical Society, 132*, 1464–1465.
52. Rueping, M., Vila, C., Koenig, R.M., Poscharny, K. & Fabry, D.C. *Chemical Comumunication*, 2360–2362.
53. Rueping, M., Zhu, S. & Koenig, R.M. (2011). *Chemical Communication*, 8679–8681.
54. Xuan, J., Cheng, Y., An, J., Lu, L.-Q., Zhang, X.-X. & Xiao, W.-J. *Chemical Communication*, 8337–8339.

Chapter 5
Results: Visible Light-Induced Photoreductive Generation of Radicals from Epoxides and Aziridines

5.1 Epoxides as New Substrates for Visible-Light Triggered Generation of Radicals

5.1.1 Objectives of the Project

Epoxides are readily available and highly valuable radical precursors, as demonstrated by their omnipresence in radical transformations [1]. Several methodologies have been reported so far for their radical ring-opening. Epoxides are particularly prone to reductive ring-opening via one-electron transfer. Lithium 4,4′-di-tert-butylbiphenylid (LDBB) has thus been widely used to generate lithiated radical anions such as **99**. This latter is immediately reduced to dianion **100** which can add to various electrophiles (Fig. 5.1) [2].

Nugent and Rajanbabu proposed the use of a metal complex that could both act as a Lewis acid for the activation of the oxirane, and reduce the moiety via electron transfer. Titanocene(III) complex Cp_2TiCl proved highly efficient in that role [3]. Further optimization of the conditions by Gansäuer allowed the use of the titanium complex in catalytic amounts [4]. In these conditions, collidine•HCl must be added to the reaction mixture to quench the titanium enolate **106**. Furthermore, manganese has to be introduced in stoichiometric quantities to reduce Ti(IV) species into Ti(III) and hence close the catalytic cycle. The β-titanoxy radicals generated such as **103** can be cyclized efficiently, in diastereoselective manner according to the Beckwith-Houk model (Fig. 5.2a) [5]. These cyclization conditions have been applied in numerous synthetic endeavors [6].

Recently, Hilt reported the ring expansion reaction of styrene oxides with alkenes using preformed [Fe(salen)] complexes, zinc powder and triethylamine (Fig. 5.2b) [7]. The reaction is initiated by single electron transfer from low-valent Fe(I) species to the epoxide, which is coordinated to the iron center. The

M.-H. Larraufie, *Development of New Radical Cascades and Multi-Component Reactions*, Springer Theses, DOI: 10.1007/978-3-319-01324-4_5,

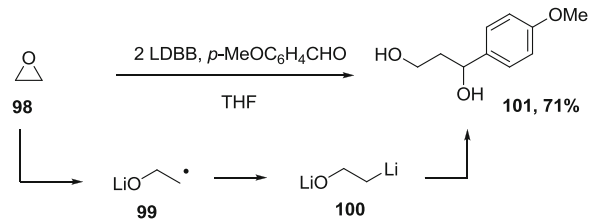

Fig. 5.1 Bu_3SnH- and LDBB-mediated ring-opening of epoxides

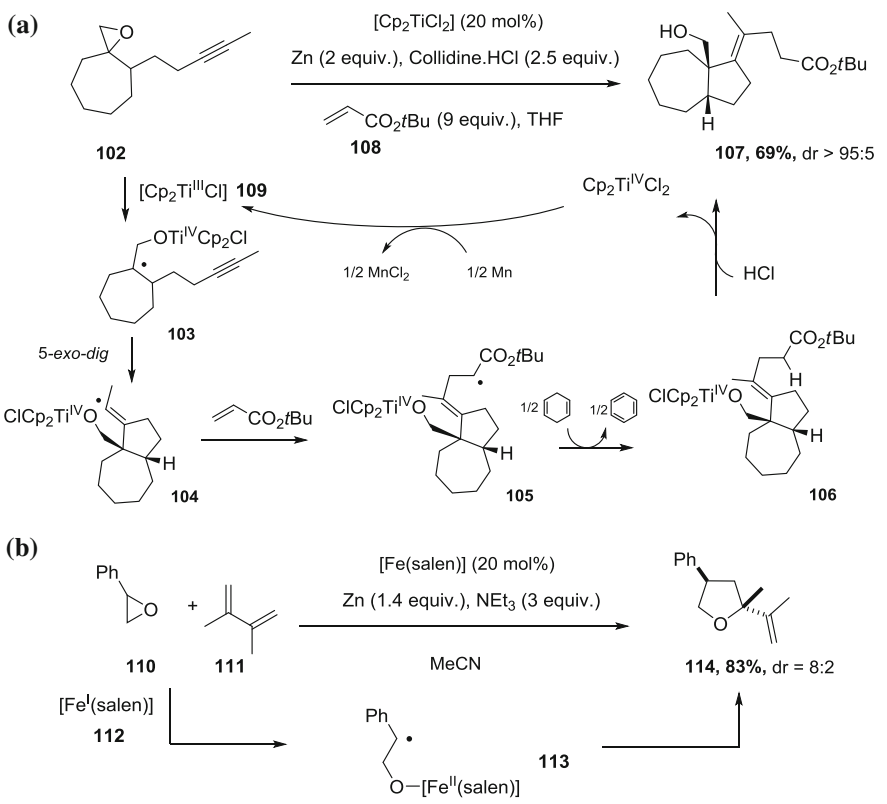

Fig. 5.2 Ti- and Fe-mediated ring-opening of epoxides

methodology was elegant but suffered from narrow scope of application in addition to the use of zinc metal in stoichiometric amounts.

We wondered if it would be possible to expand the scope of visible light sensitization to epoxides, thus accessing a reductive ring-opening reaction under catalytic, mild and eco-compatible conditions. The generated radical anion would be first directly reduced by a H-donor to study the feasibility of the approach in simplified conditions. Subsequently, attempts to use the photogenerated radical in

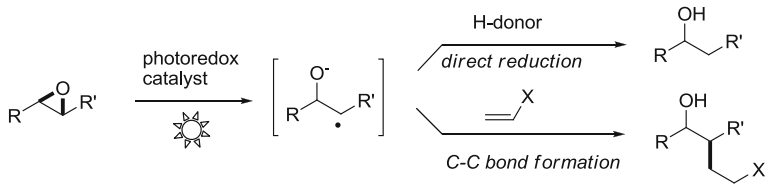

Fig. 5.3 Objectives of the project

carbon–carbon bond formations would be made, in order to demonstrate the synthetic utility of the methodology (Fig. 5.3).

5.1.2 Various Modes of Activation Tested

Epoxides possess a low reduction potential (−1.84 V for stilbene oxide *vs*. SCE in MeCN [8]) compared to $(Rubpy_3)^+$ (−1.33 *vs*. SCE). We consequently anticipated that an appropriate activation of the oxirane ring would be required to favor electron transfers between both species. Several strategies were devised and tested on simple substrates.

5.1.2.1 Strategy 1: Lewis Acid Activation

As expected, visible light irradiation of stilbene oxide **115** in the presence of $Ru(bpy)_3Cl_2$ in the conditions developed by Yoon (for [2+2] cycloaddition), or in the conditions developed by Stephenson (for dehalogenation) did not afford any conversion of the starting epoxide (Fig. 5.4).

Changing the photoredox catalyst for more reductive $Ir(dtbbpy)(ppy)_2PF_6$ ($Ir^{III}(dtbbpy)(ppy)_2^+/Ir^{II}(dtbbpy)(ppy)_2 = -1.51$ V *vs*. SCE in MeCN) and *fac*-$Ir(ppy)_3$ ($Ir^{IV}(ppy)_3^+/Ir^{III}(ppy)_3^* = -1.73$ V *vs*. SCE in MeCN) did not enable any conversion of the starting material. Keeping the more reductive *fac*-$Ir(ppy)_3$ complex, we investigated the influence of Lewis acids on the outcome of the reaction. Several photochemical redox reactions, that would otherwise be unlikely to occur, could proceed efficiently by Lewis acid catalysis on the electron-transfer step. Yoon has thus demonstrated that the Lewis acidity of the lithium cation was

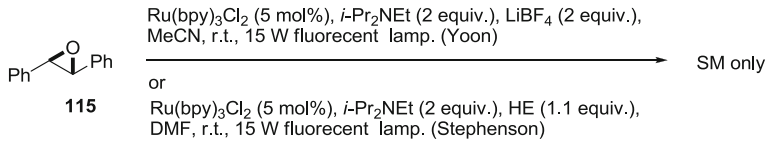

Fig. 5.4 Reactivity of unactivated epoxide in photoreductive conditions

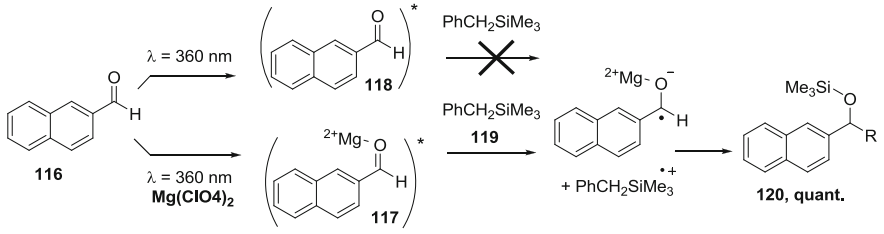

Fig. 5.5 Addition of organosilanes with aromatic carbonyl compounds via photoinduced electron transfer in the presence of magnesium perchlorate

critical to the success of the visible light photoreduction of aryl enones [9]. Fukuzumi has reported that photoinduced electron transfer between benzyltrimethylsilane **119** and 2-naphtaldehyde **116** could occur only in the presence of $Mg(ClO_4)_2$ (Fig. 5.5) [10]. The reason invoked was that the reduction potential of the excited-state of carbonyl-Mg^{2+} complex **117** ($E_{red} = 1.87$ V *vs*. SCE in MeCN) was positively shifted compared to the excited state of uncomplexed carbonyl compound **118** ($E_{red} = 0.90$ V *vs*. SCE in MeCN). This shift would allow electron transfer from benzyltrimethylsilane **119** ($E_{ox} = 1.38$ V *vs*. SCE in MeCN) to the excited state of Mg^{2+}-carbonyl complex to occur efficiently.

We tested various Lewis acids known to readily coordinated epoxides such as BF_3, $MgBr_2$ or lanthanide triflates [11]. *fac*-Ir(ppy)$_3$-induced electron-transfer reactions have been reported in DMSO, so we chose to first test this solvent. We also used acetonitrile and less coordinating solvent dichloromethane. Disappointingly, the desired ring-opening product **121** could not be observed in any cases (Table 5.1), suggesting that Lewis acid activation might not be sufficient to trigger visible light photoreduction of epoxides.

Table 5.1 Activation of stilbene oxide with Lewis acids

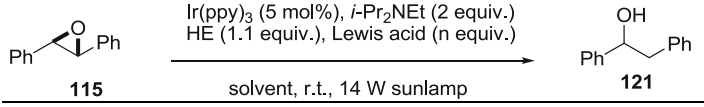

Entry	Solvent	N	Lewis acid	Result
1	DMSO	1	$LiBF_4$, $MgBr_2$, $BF_3.OEt_2$, $Cu(OTf)_2$	SM only
2	DMSO	1	$Yb(OTf)_3$, $La(OTf)_3$, $Y(OTf)_3$, $Sc(OTf)_3$	SM only
3	DMSO	10	$LiBF_4$, $BF_3.OEt_2$, $La(OTf)_3$	SM only
4	MeCN	1	$LiBF_4$, $BF_3.OEt_2$, $La(OTf)_3$	SM only
5	CH_2Cl_2	1, 10	$LiBF_4$, $BF_3.OEt_2$	SM only
6	CH_2Cl_2	1, 10	$La(OTf)_3$, $Y(OTf)_3$, $Sc(OTf)_3$	SM + degradation

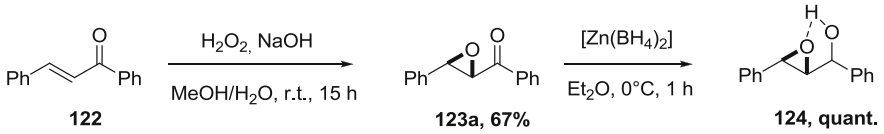

Fig. 5.6 Preparation of α-hydroxy epoxide substrate

5.1.2.2 Strategy 2: Intramolecular Activation via H-bonding

We next sought to activate epoxide towards one-electron transfer via intramolecular hydrogen bonds. In biological redox systems, numerous electron-transfer reactions are achieved with the help of hydrogen bonding formed among vicinally-oriented functional groups of amino acids [12]. We prepared α-hydroxy epoxide **124** by reduction of the corresponding epoxy chalcone **123a**. We hoped that hydrogen bonding between the alcohol and the epoxide functions would be facilitated by the 5-membered ring scaffold involved. Indeed, NMR studies have shown that in weakly hydrogen-bonding solvents, the hydroxyl proton of α-hydroxy epoxides was intramolecularly associated with the oxirane [13] (Fig. 5.6).

We did not find the suitable conditions to initiate the visible-light photoreduction of α-hydroxy epoxide **124**. As shown in the two representative examples of Fig. 5.7, only starting material could be recovered under usual photoreductive conditions. Several parameters still remain to be changed to fully investigate this strategy.

5.1.2.3 Strategy 3: Taking Advantage of the Anomeric Effect

Inspired by the work of Andrews et al. [14] we next sought to take advantage of the anomeric effect to activate epoxyglucals towards visible-light triggered one

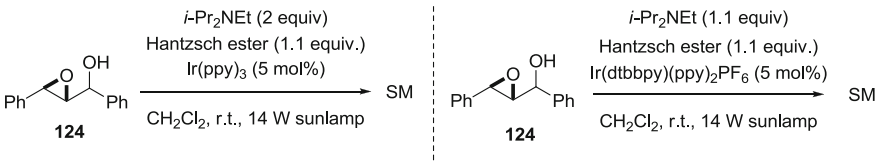

Fig. 5.7 Attempts of visible-light photoreduction of α-hydroxy epoxide

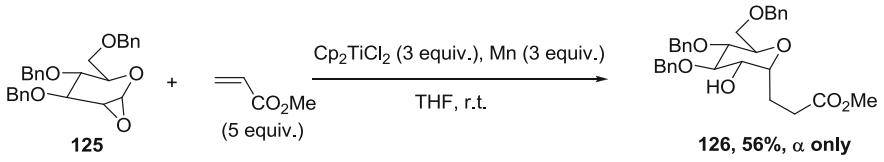

Fig. 5.8 Reported reductive ring opening of 1,2-anhydro sugars with titanocene(III) chloride

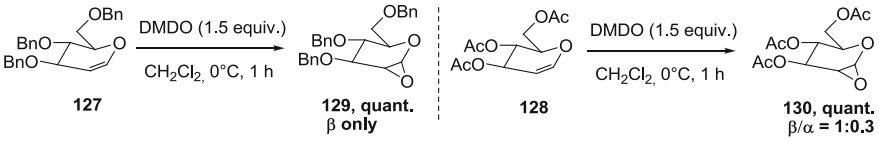

Fig. 5.9 Synthesis of epoxyglucal substrates

electron transfers. Indeed, reductive ring opening of 1,2-anhydro sugars has been reported with titanocene(III) chloride, producing an anomeric radical that can be trapped with a variety of agents (Fig. 5.8) [15]. We wished to investigate whether a visible light photocatalyzed version of such reaction could be developed.

Two differently protected epoxyglucals **129** and **130** were prepared by DMDO-mediated oxidation of tri-*O*-benzyl-D-glucal **127** and tri-*O*-acetate-D-glucal **128** respectively (Fig. 5.9).

Various sets of conditions were tested to trigger ring-opening of the epoxyglucal substrates under visible-light irradiation. Unfortunately, only starting material could be recovered. Addition of Lewis acids to the reaction mixture resulted in degradation of the starting epoxides, possibly due to nucleophilic addition of amines to the activated epoxides (Fig. 5.10).

5.1.2.4 Strategy 4: Use of a α-ketyl Function as a Relay

Since direct electron transfer to the oxirane ring seemed highly disfavored, we had the idea to use an adjacent carbonyl function as a relay for visible light-induced electron transfer. Indeed, we knew that the reduction potential of an aryl ketone function lied around −1.3 V versus SCE [16], appreciably higher than the reduction potential of epoxides. We imagined that electron transfer could first occur from the photoredox catalyst to the carbonyl function, delivering radical

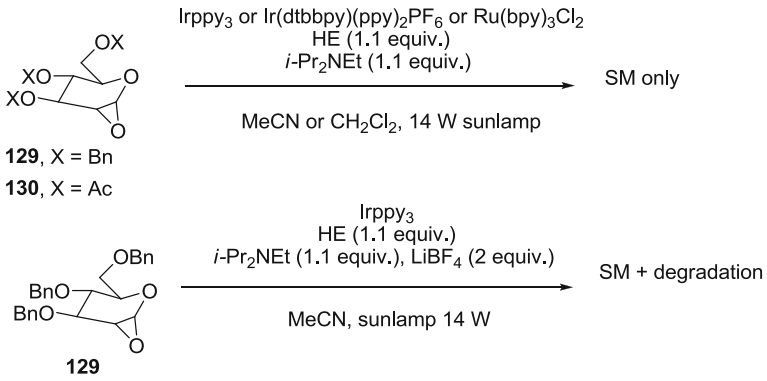

Fig. 5.10 Attempts of visible-light photoreduction of epoxyglucal substrates

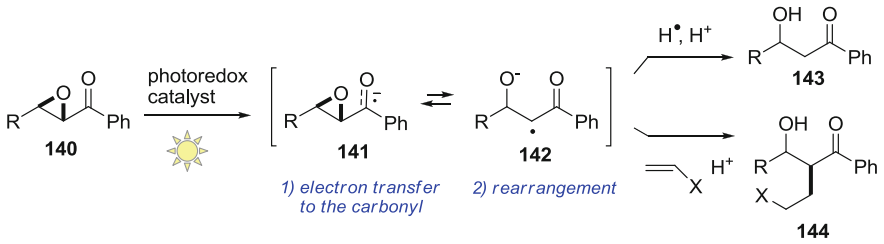

Fig. 5.11 Strategy envisioned for the use of a α-ketyl function as a relay

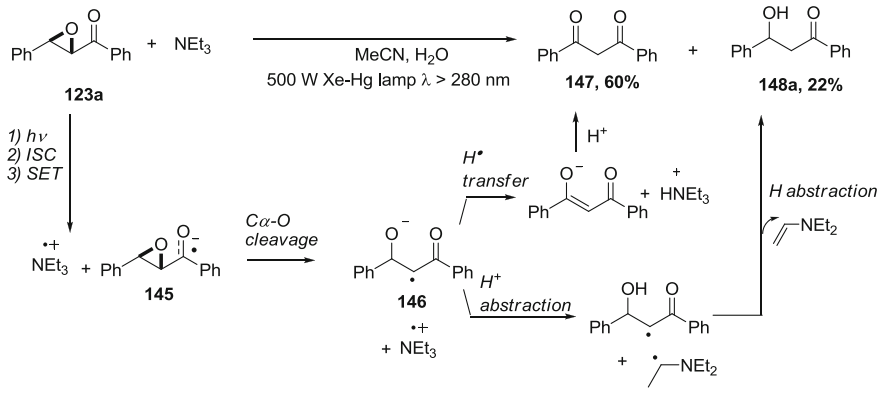

Fig. 5.12 Photoinduced single electron transfer reactions of α,β-epoxy ketones with amines

anion **141**. This latter would rearrange to afford radical anion **142** after desired ring-opening of the epoxide moiety (Fig. 5.11). The carbon-centered radical obtained could be directly reduced or engaged in carbon–carbon bond formation.

UV light-induced ring opening reaction of α,β-epoxy ketones have been studied by several groups [17–21] with particularly important contributions from Hasegawa et al. [22–26], after the pioneering studies of Cossy and Pète. As early as 1991, he reported that the irradiation of epoxychalcone **123a** with triethylamine afforded β-diketone **147** and β-hydroxy ketone **148a** via photoinduced electron-transfer reactions (Fig. 5.12) [23]. The reaction was thought to proceed via photoinduced excitation of **123a** to singulet excited state ^{1}**123a***. Subsequent rapid intersystem crossing (ISC) would lead to triplet excited state ^{3}**123a***. This latter would be quenched by ground-state NEt_3 to afford radical anion **145**. Driven by the release of ring strain, selective Cα-O bond cleavage would occur to afford ring-opened radical anion **146**. At that point, two terminating sequences can take place. Abstraction of β-hydrogen by $NEt_3^{+\bullet}$, followed by protonation would deliver diketone **147** [25]. On the other hand, sequential proton and hydrogen abstractions from $NEt_3^{+\bullet}$ would afford β-hydroxy ketone **148a** along with enamine. The ratio

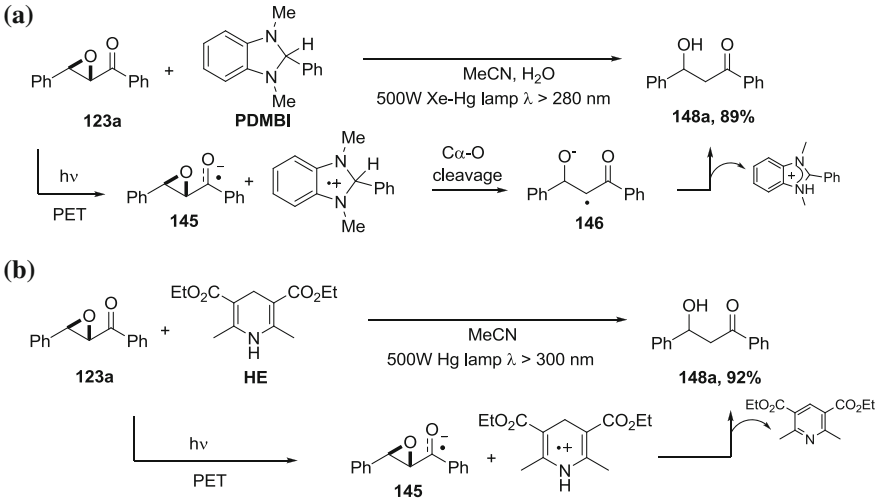

Fig. 5.13 Ring-opening of epoxychalcone by PET. **a** PET with PDMI. **b** PET with HE

between the two products was strongly influenced by the rate of proton transfer to **146**.

By replacing NEt_3 with 2-phenyl,*N*,*N*-dimethylbenzimidazoline (PDMBI) as reductive quench, Hasegawa could obtain *β*-hydroxyketone **148a** selectively (Fig. 5.13a) [24]. Using a similar strategy, Liu described the photoinduced reductive opening of epoxychalcones in the presence of Hantzsch ester (HE), under irradiation with a 500 W high pressure mercury lamp ($\lambda > 300$ nm) (Fig. 5.13b) [27].

A single report described the utilization of the photogenerated radical in carbon–carbon bond formation [23]. UV irradiation of a mixture of epoxychalcone **123a** and allyl tributyltin afforded α-allyl-*β*-hydroxy ketone **149** in 28 % yield, in an undetermined diastereomeric mixture. The mechanism of the reaction was not clearly understood. The authors proposed that the triplet excited state of the ketone ^{3}**123a*** could be quenched by allyl tributyltin (ABT) to afford radical anion **145**

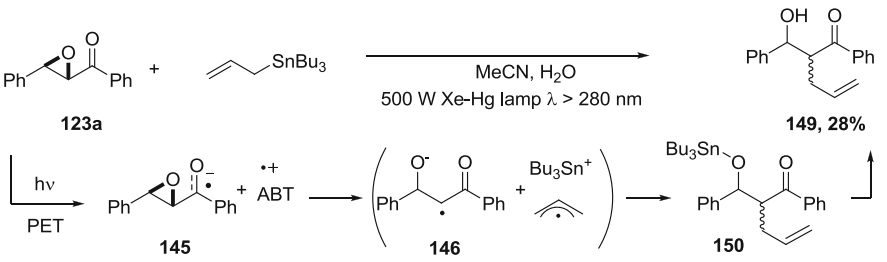

Fig. 5.14 Radical trapping of UV photogenerated α-keto radical derived from α,*β*-epoxy ketone

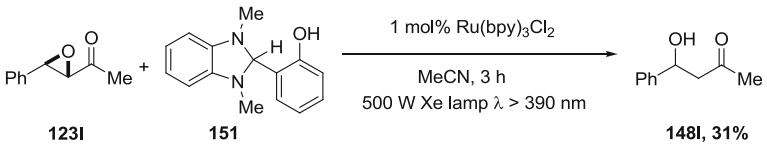

Fig. 5.15 Visible-light photoreductive ring-opening of epoxyketone

and the cation radical of ABT. This latter would undergo C-Sn bond cleavage. The allyl radical and the tin cation formed would couple with the ring-opened radical anion to afford adduct **150** and finally **149** after work-up (Fig. 5.14).

In 2006, Hasegawa reported the photoreductive ring-opening of α,β-epoxy ketone **123 l** under irradiation with a 500 W Xe lamp in the visible range ($\lambda > 390$ nm), in the presence of $Ru(bpy)_3Cl_2$ and HPDMBI **151** (Fig. 5.15) [28]. If no clear mechanism was proposed, $Ru(bpy)_3Cl_2$ was thought to act as a visible-light sensitizer and HPDMBI as an electron and proton donor.

This pioneering methodology suffered from the following drawbacks:

- First only one epoxyketone substrate was successfully reduced, and the desired β-hydroxyketone was obtained in a low yield. The reaction conditions were not mild enough for epoxychalcone **123a.** Indeed, in those reaction conditions, the reduction of **123a** was observed without the need of irradiation.
- The lamp used was highly energetic, which inhibits the advantages of using visible light (see introduction). In addition, the electron and proton donor HPDMI had to be synthesized in a low-yielding 4 steps procedure.
- Finally, the photogenerated radicals were not exploited in carbon–carbon bond formation processes.

Nevertheless, this very interesting report rendered us optimistic about the viability of our approach. In order to develop the mildest and simplest conditions possible, we decided to test the visible light photoreductive ring-opening of epoxychalcone **123a** under irradiation of 14 W fluorescent lamp, at room temperature and in the presence of commercially available reagents. We tested first the Stephenson conditions used for dehalogenation, [29] i. e. $Ru(bpy)_3Cl_2\bullet(H_2O)_6$[1] (5 mol %), *i*-$Pr_2NEt$ (2 equiv.), and Hantzsch ester (1.1 equiv.) in DMF.

To our great delight, after 36 h of irradiation with a 14 W fluorescent lamp,β-hydroxyketone **148a** could be obtained in 74 % yield (with incomplete conversion of **123a**) (Fig. 5.16).

Having devised a successful strategy to trigger the visible-light induced photoreductive ring-opening of epoxides, we sought to optimize the conditions, check the scope of the methodology and apply it to carbon–carbon bond formation processes.

[1] In all the manuscript, the $Ru(bpy)_3Cl_2\bullet(H_2O)_6$ catalyst will be simply designed as $Ru(bpy)_3Cl_2$.

Table 5.2 Optimization of the photoreductive ring-opening of epoxychalcone

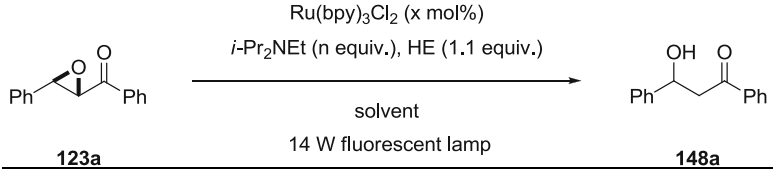

123a **148a**

Entry	Solvent	Catalytic charge (mol %)	*i*-Pr_2NEt (n equiv.)	Time (h)	Conversion (%)[(a)]	Yield 148a (%)
1	DMF	5	2	36	76	74
2	*t*-BuOH	5	2	36	45	41
3	Et_2O	5	2	36	0	0
4	MeCN	5	2	36	30	10
5	MeOH	5	2	3	100	90
6	DMSO	5	2	3	100	86
7	DMSO	2.5	2	12	94	83
8	DMSO	5	1.1	3	100	83
9	DMSO	5	0	3	100	91

[(a)] Conversion determined by ^{1}H NMR analysis

5.1.3 *Optimization of the Photoreductive Ring-Opening of Epoxides and Proposed Mechanism*

In order to optimize the photoreductive ring-opening of epoxychalcone **123a**, we first performed a rapid solvent screening. The desired *β*-hydroxyketone **148a** was formed cleanly in *t*-BuOH (Table 5.2, entry 2), albeit very slowly, probably owing to the lack of solubility of Hantzsch ester and $Ru(bpy)_3Cl_2$. The use of diethyl ether completely shut down the reaction (Table 5.2, entry 3), while the reaction was sluggish in MeCN (Table 5.2, entry 4). Both DMSO and MeOH proved highly beneficial solvents for the reaction, resulting in a sharp decrease of the reaction time (Table 5.2, entries 5–6). We chose to carry on the optimization with less toxic DMSO as solvent. We next sought to reduce the catalytic charge to 2.5 mol %, but it led to prohibitive decrease of the reaction rate (Table 5.2, entry 7). Finally, we tried to reduce the amount of *i*-Pr_2NEt and we disclosed that the tertiary amine was not needed in our reaction conditions (Table 5.2, entries 8–9). This result suggested that the Hantzsch ester could be both the reductive quencher *and* the hydrogen and proton donor. Indeed, in a typical reduction, **123a** led to 91 % of **148a** after 3 h of irradiation in the presence of the Hantzsch ester (1.1 equiv.) and $Ru(bpy)_3Cl_2$ (5 mol %) only in DMSO at room temperature.

With those optimized conditions in hand, we immediately controlled that the formation of **148a** occurred via $Ru(bpy)_3^{2+}$-catalyzed visible-light induced electron transfers (Fig. 5.17). For that purpose, we first ran the reaction without light. We

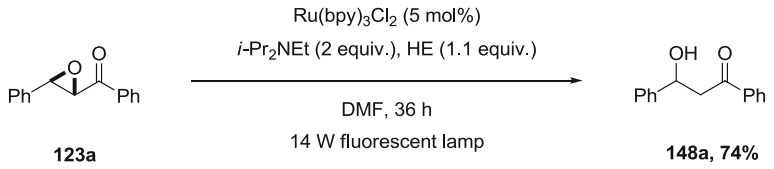

Fig. 5.16 Successful attempts of visible-light photoreduction of α,β-epoxyketone

Fig. 5.17 Control experiments

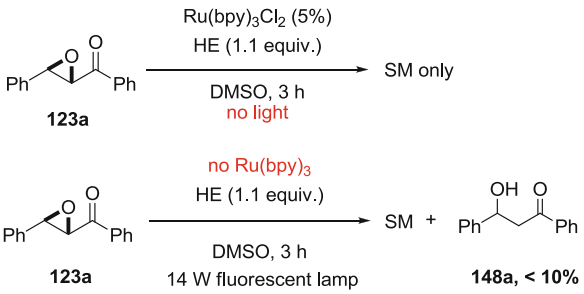

observed no conversion of the starting material, showing that visible-light irradiation was required to trigger the catalytic cycle. Then, we ran the reaction under irradiation but omitting $Ru(bpy)_3Cl_2$ in the reaction mixture. After 3 h, we could only observe a conversion lower than 10 %, demonstrating that the photoreductive ring-opening reaction was catalyzed by $Ru(bpy)_3Cl_2$. The small amount of **148a** formed could arise from photoinduced electron-transfer between excited state of Hantzsch ester and epoxychalcone. Indeed Hantzsch ester exhibits an absorption band in the near UV, with a maximum at 350 nm, but with a weak tail extending in the visible (resulting in a yellow color of this compound).

Based on the literature and those control experiments, we propose the mechanism depicted in Fig. 5.18 for the transformations. The excited state $Ru(bpy)_3^{2+*}$ obtained upon visible-light irradiation of $Ru(bpy)_3^{2+}$ (reduction potential = + 0.84 V *vs*. SCE in MeCN) would be reductively quenched by the Hantzsch ester (oxidation potential = + 0.72 V *vs*. SCE in MeCN [27]) to form the strong reductant $Ru(bpy)_3^{+}$. Single electron transfer to epoxychalcone **123a** would then take place, regenerating the ruthenium(II) complex and providing the radical anion **153a**. This latter would undergo ring-opening to carbon-centered radical **154a** and subsequent proton and electron transfers by Hantzsch ester. It should be noted that the half-wave reduction potential of epoxychalcone **123a** has been reported to stand at −1.70 V versus SCE in MeCN, which makes the electron-transfer from $Ru(bpy)_3^{+}$ theoretically unfavorable. This data demonstrates that the solvent and the Hantzsch ester must play a crucial role via polar effect or H-bonding interactions to lower the activation energy of this electron-transfer step. Furthermore, high rate of proton and hydrogen transfers from Hantzsch ester to

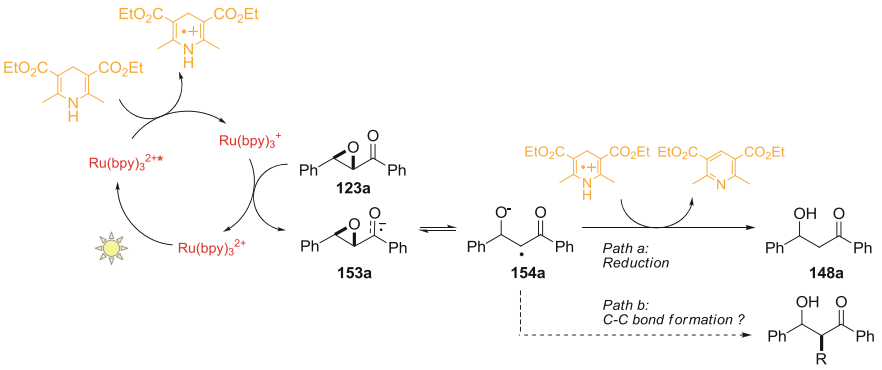

Fig. 5.18 Proposed mechanism for photocatalyzed reduction of 123a

radical anion **153a** might help displace the equilibrium towards the formation of the radical anion.

The formation of radical anion **154a** from **153a** may occur via the two pathways presented in Fig. 5.19. Path a depicts an anionic ring-opening. Otherwise, a radical ring-opening could occur leading to intermediate **153a'**. Kinetic studies have established a full quantitative picture for the ring-opening of epoxycarbinyl radicals and established that it was one of the fastest radical reaction known ($k = 3.2 \times 10^{10}\ s^{-1}$ for epoxy-2-cyclohexyl radical) [30]. Both Cα-O and Cα-Cβ bond cleavage are generally exothermic and the selectivity of the ring-opening depends on the substituents of epoxycarbinyl radical. In our case, the selective Cα-O bond cleavage observed could be rationalized as follow: high electron density at the carbonyl should raise the SOMO of the radical. Since the LUMO and HOMO for the Cα-O bond are lower than those for the Cα-Cβ bond, the favored interaction will be between the nucleophilic SOMO and the LUMO of Cα-O [31]. Radical **153a'** would thus be generated and lead to more stable radical anion **154a** by intramolecular electron transfer [32].

We next wished to explore the scope of precursors that could serve as radical precursors in our optimized conditions.

5.2 Scope and Limitations of the Reductive Ring-Opening Methodology

5.2.1 α,β-epoxyketones

This study was performed in collaboration with a Master 2 student: *Rémy Pellet*.

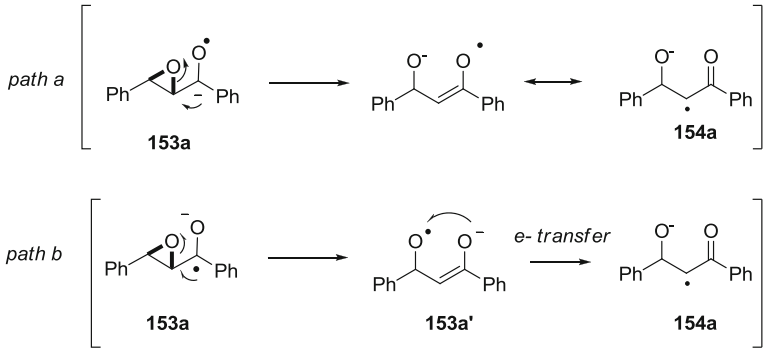

Fig. 5.19 Postulated mechanisms for the formation of 154a

5.2.1.1 Preparation of the α,β-epoxyketone Substrates

We first endeavored to prepare a set of epoxychalcones bearing various kinds of substituents on both aromatic rings via a one-pot two-steps procedure (Fig. 5.20). Treatment of the corresponding aldehydes and ketones with aqueous NaOH afforded in situ the corresponding enones. Base-catalyzed epoxidation was

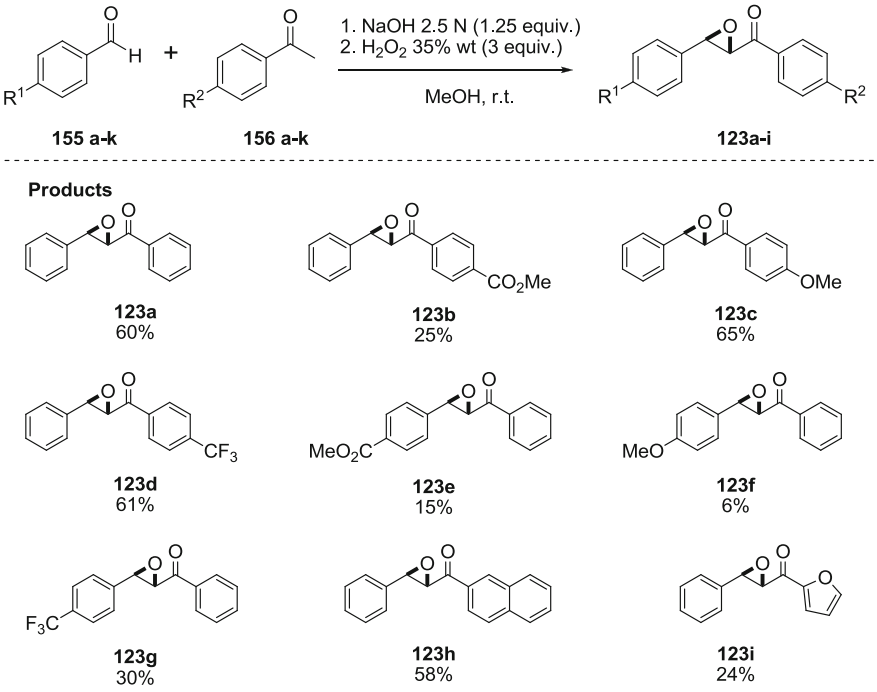

Fig. 5.20 Synthesis of a set of epoxychalcones

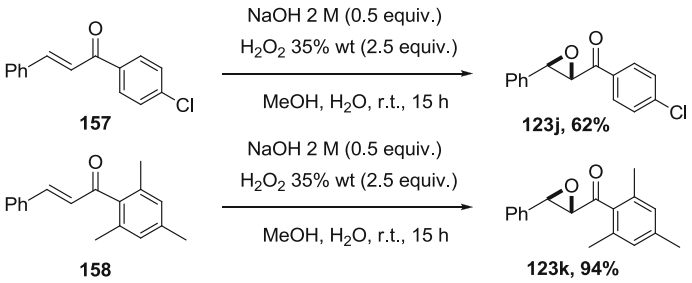

Fig. 5.21 Preparation of epoxychalcone from corresponding enones

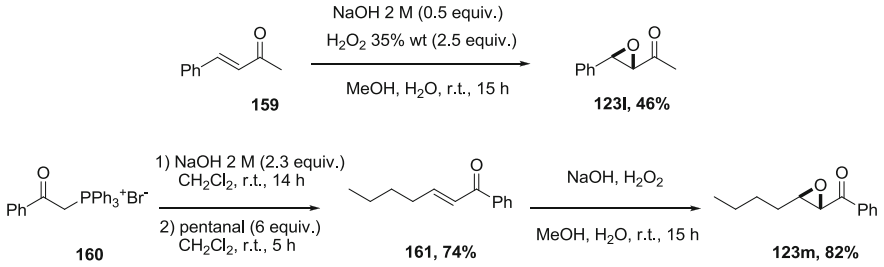

Fig. 5.22 Synthesis of α,β-epoxyketone with alkyl substituents

subsequently performed by adding hydrogen peroxide to the reaction mixture [33]. The desired epoxychalcones were obtained in moderate to good yields.

Other epoxychalcones were synthesized directly from the commercially available enone by base-catalyzed epoxidation with hydrogen peroxide (Fig. 5.21).

Then, we replaced both aryl substituents of epoxychalcone with alkyl chains (Fig. 5.22). The synthesis of methyl ketone **123l** was performed by treatment of 4-phenylbut-3-en-2-one **159** with hydrogen peroxide in basic conditions. Butyl oxirane **123m** was similarly prepared by oxidation of the corresponding enone **161**. This latter had to be previously synthesized by a Wittig reaction between phenacyl triphenylphosphonium bromide **160** and pentanal [34].

Finally, we endeavored to synthesize substrates bearing substituents α to the carbonyl function (Figure 5.23). α-Methyl substituted epoxychalcone **123n** could be prepared by reacting propiophenone **162** and benzaldehyde **163** in carbon tetrachloride in the presence of aqueous NaOH and a phase transfer catalyst [35]. The reaction is thought to proceed via chlorinated intermediate **164** which after deprotonation can act as both a nucleophile and an electrophile towards benzaldehyde. Tetralone derivative **123o** could be prepared by epoxidation of enone **167**, formed by the condensation of tetralone and isobutyraldehyde [36].

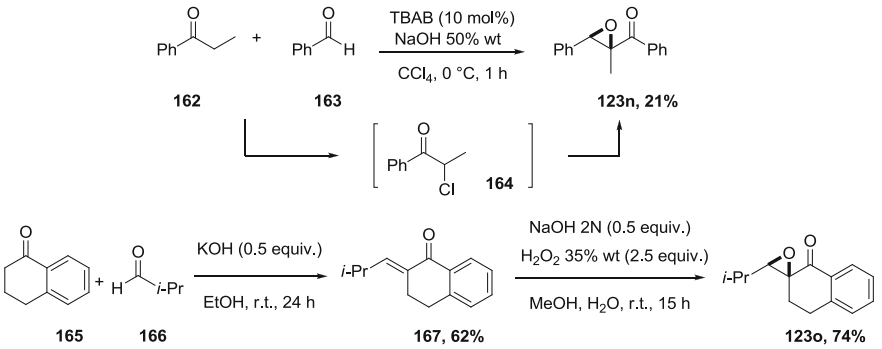

Fig. 5.23 Preparation of α-methyl substituted epoxyketones

Table 5.3 Scope of the photoreductive ring-opening of epoxides

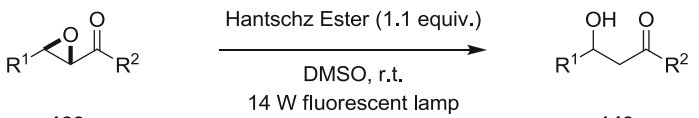

123a-o 148a-o

Entry	Substrate	R^1	R^2	Time (h)	Yield[(b)] (%)
1	123a	C_6H_5	C_6H_5	3	148a, 91
2	123b	C_6H_5	4-CO_2Me-C_6H_4	20	148b, 55
3	123c	C_6H_5	4-MeO-C_6H_4	7	148c, 76
4	123d	C_6H_5	4-CF_3-C_6H_4	5	148d, 76
5	123e	4-CO_2Me-C_6H_4	C_6H_5	4	148e, 60
6	123f	4-MeO-C_6H_4	C_6H_5	6	148f, 54
7	123g	4-CF_3-C_6H_4	C_6H_5	4	148 g, 78
8	123h	C_6H_5	Napht	10	148 h, 42
9	123i	C_6H_5	Furan	60	–
10	123j	4-Cl-C_6H_4	C_6H_5	3	148j, 86
11	123k	C_6H_5	2,4,6-$(Me)_3C_6H_5$	12	–
12	123l	C_6H_5	Me	24	148l, 0 (60[(a)])
13	123m	C_4H_9	C_6H_5	24	148 m, 52

[(a)] HPDMBI used instead of Hantzsch ester

5.2.1.2 Photoreductive Ring-Opening of α,β-epoxyketones

We tested the reactivity of all epoxyketone substrates employing the optimized conditions devised for epoxychalcone **123a** (Table 5.3). The visible-light induced ring-opening worked smoothly with epoxychalcones bearing electron-donating (entries 3, 6), or withdrawing substituents (entries 2, 4, 5, 7, 10) on both aromatic rings. The mild conditions employed were compatible with a range of functionalities

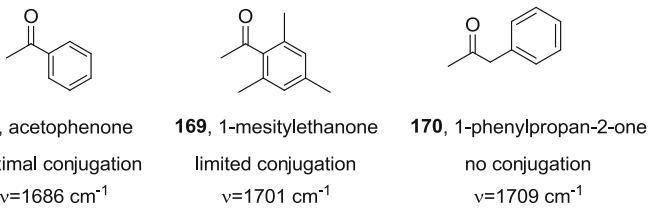

Fig. 5.24 Comparison of IR absorption band for representative ketones

including an ether (entries 3, 6), an ester (entry 2, 5), an aromatic halide (entry 10), or a naphthyl ring (entry 8). For furan derivative **123i** (entry 9), full conversion was reached after 2.5 days, but only degradation product could be detected by NMR.

When the oxirane substituent R^1 was a butyl chain, the desired reduction proceeded as desired (entry 13). However, when the carbonyl substituent R^2 was an alkyl chain, no conversion could be observed (entry 12). This failure might be explained by the much lower redox potential of methyl ketone **123l** (reduction potential = −2.40 V *vs*. SCE in MeCN [27]) compared to epoxychalcone **123a** (−1.70 V *vs*. SCE in MeCN). Using our optimized conditions, but replacing Hantzsch ester with Hasegawa's reductive quench HPDMBI, we could isolate the desired *β*-hydroxyketone **148l** in 60 % yield.[2] We are still trying to rationalize this result. HPDMBI might for instance activate the methyl ketone towards one-electron reduction via H-bonding. Otherwise it could displace the equilibrium of electron transfer thanks to better proton and hydrogen-donating abilities than Hantzsch ester.

Mesityl derivative **123k** was unreactive under our reaction conditions (entry11). We thought that this behavior might be explained by the presence of two *ortho,ortho'*-methyl substituents that could prevent the acyl function from standing in the plan of the aromatic ring because of steric hindrance. **123k** would thus adopt a conformation partially hampering the conjugation between the carbonyl function and the aromatic ring. The occurrence of limited conjugation within mesitylacyl group could be confirmed by the comparison of the relative values of wavenumbers corresponding to C=O absorption bands in the infrared range for the three compounds depicted in Fig. 5.24 [37]. Because of this limited conjugation, it is not surprising that the reactivity of **123k** towards reductive agents stands between the reactivity of aryl ketones and the reactivity of alkyl ketones.

We sought to bypass the low reactivity of **123k** by using more reductive reaction conditions (Table 5.4). First we found out that the reintroduction of *i*-Pr_2NEt as reductive quench was beneficial for the reaction. Then, we anticipated that a stronger reductant would favor the photoreductive process, so we switched

[2] When we performed the reaction in the exact conditions described by Hasegawa, *i.e.* HPDMBI (1.2 equiv.), $Ru(bpy)_3Cl_2$ (1 mol %), 3 h in MeCN but under irradiation by our 14 W fluorescent bulb, we obtained only 9 % of **148l**. This demonstrated that the use of energetic 500 W Xe lamp was required to obtain the results obtained by Hasegawa. Switching to DMSO and increasing the reaction time to 24 h allowed us to obtain **148l** in 60 % yield.

Table 5.4 Influence of the nature of the photocatalyt and the additives on the substrate scope

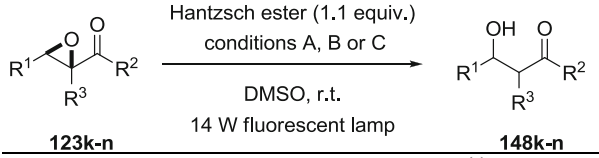

Entry	Substrate	Time (h)	Conditions[(a)]	Yield (%)	Product
1	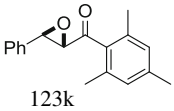 123k	15	A	148k, 0	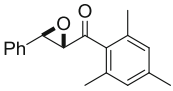
		72	B	148k, 55	
		15	C	148k, 75	
2	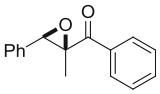 123m	15	A	148m, 0	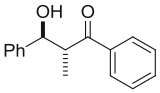
		15	C	148m, 83(dr = 54:46)	
3	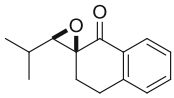 123n	15	A	148n, 0	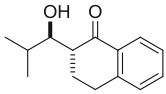
		4	C	148n, 87(dr = 76:24)	

[(a)] *Conditions A* substrate (0.2 mmol, 0.1 M in DMSO), HE (0.22 mmol), $Ru(bpy)_3Cl_2.(H_2O)_6$ (0.01 mmol); *Conditions B* substrate (0.2 mmol, 0.1 mM in DMSO), HE (0.22 mmol), *i*-Pr_2NEt (0.22 mmol), $Ru(bpy)_3Cl_2.(H_2O)_6$ (0.01 mmol); *Conditions C* substrate (0.2 mmol, 0.1 mM in DMSO), HE (0.22 mmol), *i*-Pr_2NEt (0.22 mmol), $Ir(dtbbpy)ppy_2PF_6$ (0.01 mmol)

the catalyst from $Ru(bpy)_3Cl_2.(H_2O)_6$ to $Ir(dtbbpy)(ppy)_2PF_6$ complex [38] ($Ir^{III}(dtbbpy)(ppy)_2^+/Ir^{II}(dtbbpy)(ppy)_2 = -1.51$ V *vs.* SCE in MeCN) (conditions C). To our pleasure, we obtained a full conversion for **123k** after 15 h of irradiation (100 % conversion, 75 % yield, entry 1C). We could subsequently apply those conditions to substrates **123m** and **123n** bearing a substituent α to the ketone, which had proven unreactive under the previous conditions. We were delighted to observe that the photoreduction took place with a total conversion, synthetically useful yields but poor to moderate diastereoselectivities (entries 2 and 3).

5.2.2 α-keto-aziridines

We next sought to investigate whether our methodology was suitable for others strained rings than epoxides. We envisioned that photoreductive ring-opening of aziridines would provide interesting α-amino radicals.

We first wished to test the reactivity of unprotected aziridines **171**. The aziridine was synthesized by *N*-methylmorpholine-promoted aziridination of chalcone **122** using *O*-(diphenylphosphinyl)hydroxylamine ($DppONH_2$) (Fig. 5.25) [39]. Unfortunately, **171** proved unreactive under our optimized conditions. Only starting material could be recovered, even using more reductive conditions (see Table 5.4).

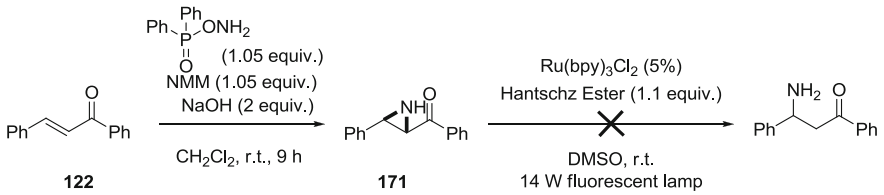

Fig. 5.25 Photoreduction of unprotected aziridines

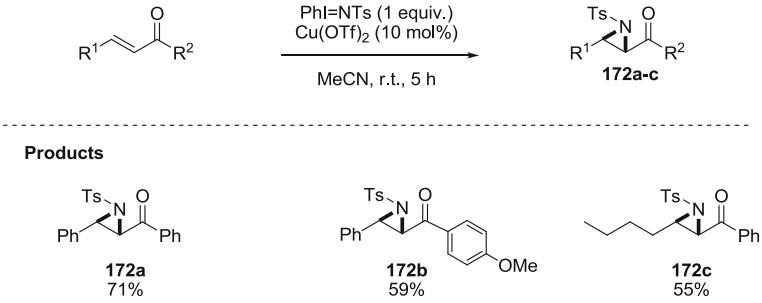

Fig. 5.26 Synthesis of tosylaziridine substrates

Table 5.5 Photoreductive ring-opening of tosylaziridines

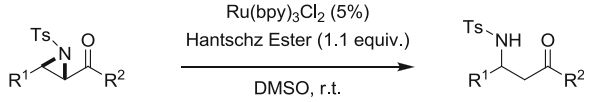

Entry	Substrate	R^1	R^2	Time (h)	Yield (%)
1	172a	C_6H_5	C_6H_5	3	174a, 94
2	172b	C_6H_5	4-MeO-C_6H_4	3	174b, 81
3	172c	C_4H_9	C_6H_5	3	174c, 76

We reasoned that the presence of an electron withdrawing substituent on the nitrogen might activate the aziridines towards one-electron transfer. We chose to synthesize three tosylaziridine substrates **172a–c**. They were prepared by copper-catalyzed aziridination of the corresponding enones, using (*N*-(*p*-toluenesulfonyl)imino)phenyliodinane **173** as nitrene precursor (Fig. 5.26) [40, 41].

We submitted the three aziridines precursors to our optimized conditions. To our great delight, they all underwent $Ru(bpy)_3Cl_2$-catalyzed photoreduction, affording the corresponding *β*-amino ketones **174a–c** in quite high yields (Table 5.5).

Again, we performed control experiment to check that both visible light and ruthenium catalysts were required for the formation of *β*-amino ketones **174a** (Fig. 5.27).

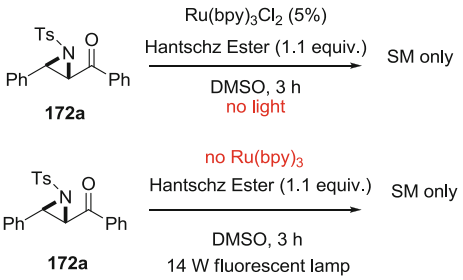

Fig. 5.27 Control experiments

Aziridines are very seldom used in radical chemistry for lack of practical method to make them react. Hence, to our knowledge, aziridines have not been yet reported to be reactive in titanocene chemistry, neither in photocatalyzed one-electron reductions. Our new methodology could be a great way to fill that gap. Many features of our visible-light induced photoreductive ring-opening of aziridines remain to be investigated, such as the influence of other protecting groups on the nitrogen or the functionalities that can replace the ketone function.

5.2.3 α-keto-cyclopropane

Finally, we decided to test the reactivity of α-keto-cyclopropanes in our reaction conditions. We expected that they mode of ring-opening would be different from epoxides and aziridines. Indeed, α-cyclopropyl radicals such as **176** usually adopt a conformation where the SOMO (2p orbital at the carbon of the radical anion) overlaps with the π^* of the C_β-C_γ bond, which will cleave to give the more stabilized radical **177** [42, 43]. For radical anion such as **176**, the rate constant of the ring-opening reaction is significantly lowered by the resonance stabilization afforded by the benzoyl moiety. It has been estimated to lie around 10^5–10^6 s^{-1} depending on the substitution pattern of the cyclopropane (Fig. 5.28) [44].

The UV-light photoinduced reductive fragmentation of cyclopropyl ketones has been thoroughly studied [45–48], however to date no visible-light alternative had been investigated.

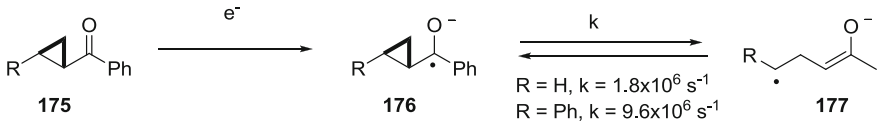

Fig. 5.28 Ring-opening of cyclopropyl ketones

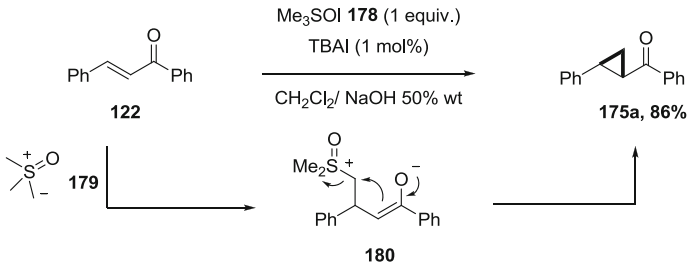

Fig. 5.29 Synthesis of the aryl cyclopropyl ketone 175a

Table 5.6 Optimization of the photoreductive ring-opening of aryl cyclopropyl ketone

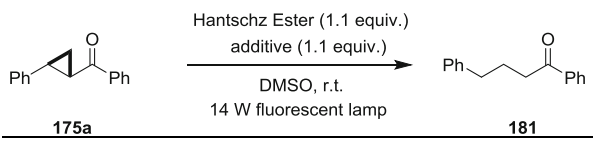

Entry	Catalyst	Additive	Time (h)	Conversion (%)	Yield (%)
1	$Ru(bpy)_3Cl_2$	–	48	–	–
2	$Ir(dtbbpy)(ppy)_2PF_6$	–	15	–	–
3	*fac*-$Ir(ppy)_3$	–	15	25	181, 20
4	*fac*-$Ir(ppy)_3$	*i*-Pr_2NEt	15	100	181, 60

We prepared the desired cyclopropyl ketone **175a** by methylene transfer from dimethylsulfoxonium methylide **179** to chalcone **122** (Fig. 5.29) [49]. The ylide intermediate **179** was generated in situ by deprotonation of trimethyl sulfonium iodide **178** in phase transfer conditions, and reacted selectively at the α,β-carbon–carbon double bond of the enone [50]. This selectivity could be explained by the soft nature of the nucleophilic carbanion in dimethylsulfoxonium methylide.

Under our optimized $Ru(bpy)_3Cl_2$-catalyzed conditions, **175a** proved unreactive (Table 5.6, entry 1). This result might be explained by the lower reduction potential of α-keto cyclopropanes compared to their epoxide counterparts (reduction potential of cyclopropyl(phenyl)methanone = −2.05 V *vs*. SCE[51]). Changing the catalyst for $Ir(dtbbpy)(ppy)_2PF_6$ did not empower any conversion (entry 2). However, when we switched to the more reductive *fac*-$Ir(ppy)_3$ ($Ir^{IV}(ppy)_3^+/Ir^{III}(ppy)_3$* = −1.73 V *vs*. SCE in MeCN), we could observe after 15 h of visible light irradiation the formation of desired ketone **181** with 20 % yield (25 % conversion, entry 3). Reintroducing *i*-Pr_2NEt allowed us to reach full conversion of starting material and isolate the product of ring-opening **181** with 60 % yield (entry 4).

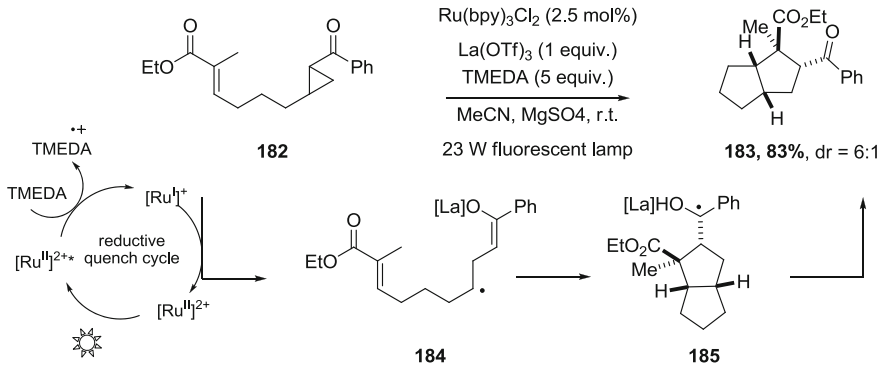

Fig. 5.30 Yoon [3+2] cycloadditions of aryl cyclopropyl ketone by visible light photocatalysis

Encouraged by this successful outcome, we had planned to further investigate the ring-opening of α,β-cyclopropyl ketones. However, just shortly after our first results, Yoon published a methodology describing the $Ru(bpy)_3Cl_2$-catalyzed one-electron reduction of aryl cyclopropyl ketones [52]. The photogenerated radical was beautifully employed in [3+2] cycloadditions with enones (Fig. 5.30). Interestingly, Yoon relied on the addition of strong Lewis acid $La(OTf)_3$ to activate the cyclopropyl ketone towards one-electron reduction by $Ru(bpy)_3^+$, while we had chosen to play with the reductive power of the catalyst.

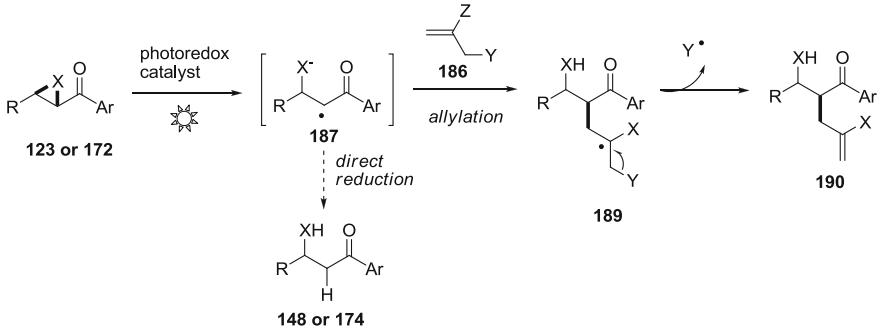

Fig. 5.31 Allylation of photogenerated radical

5.3 Utilization of the Photogenerated Radicals in Carbon–Carbon Bond Formations

The first part of this project had enabled us to disclose that α-keto-epoxides, α-keto-aziridines and α-keto-cyclopropanes were efficient precursors for the visible-light induced photoreductive generation of radicals.

We next attempted to engage the photogenerated radicals in carbon–carbon bond formation. We chose to first test allylation processes which possess several advantages. The polarity of allylating agent **186** can be easily modulated by substituting the double bond with electron withdrawing or electrodonating groups. Besides, after addition of the incoming radical **187** on the double bond, the allyl substituent cleanly *β*-fragments so that no final reduction step is required (Fig. 5.31).

5.3.1 Optimization of the Allylation Conditions

A set of non-commercially available allylating agents was prepared. We synthesized electron-rich allylsulfone **193** by nucleophilic substitution of sodium tosylate **192** at 3-chloro-2-methylpropene **191** [53]. Electron-poor allylsulfone **195** was prepared by addition of in situ-generated tosyl iodide on methyl acrylate **194**, followed by elimination of hydrogen iodide. Final equilibration to the more stable *β*,*γ*-unsaturated isomer delivered the desired allylsulfone **195** [54]. We also wished to prepare allylsulfanes that are known to be efficient allylating agents. Allylsulfane **198** was obtained in excellent yield by treatment of dibromide **196** with two equivalents of *tert*-butylthiol (Fig. 5.32) [55].

Our first thought was that photogenerated radical **187** might be rather electrophilic due to the presence of the α-carbonyl function. We consequently tested first the reactivity of epoxychalcone **123a** with electron rich allylsulfone **193**

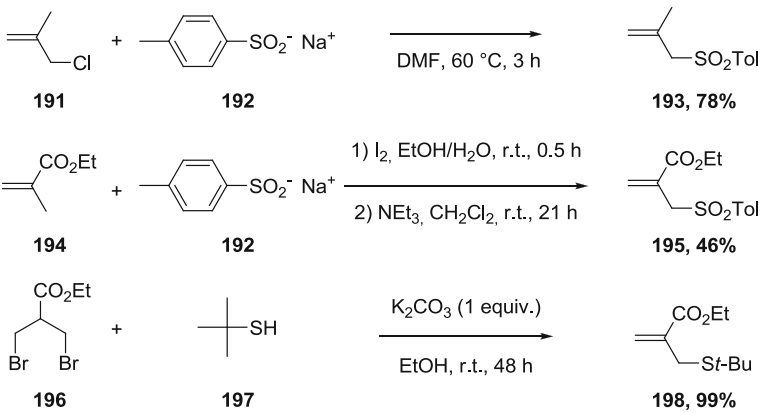

Fig. 5.32 Preparation of allylating agents

Table 5.7 Optimization of the allylation conditions on epoxychalcone 123a

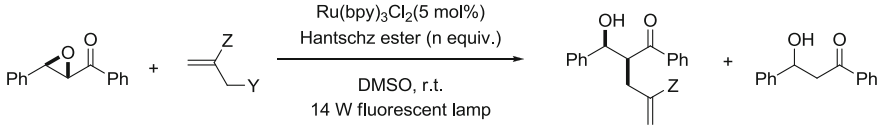

123a 190a/191a 148a

Entry	Allylating agent	n (equiv.)	Time (h)	Conversion (%)	Yield allylation (%)	Yield reduction (%)
1	193 (Z = Me, Y = SO_2Tol)	1.1	5	100	190a, 0	148a, 90
2	195 (Z = CO_2Et, Y = SO_2Tol)	1.1	15	60	191a, 28	148a, 16
3	195 (Z = CO_2Et, Y = SO_2Tol)	2.1	5	100	191a, 41	148a, 30
4	198 (Z = CO_2Et, Y = S*t*-Bu)	2.1	5	100	191a, 54	148a, 32

(Table 5.7). Introduction of 10 equivalents of allylsufone **193** prior to irradiation under optimized conditions A led to only directly reduced β-hydroxy ketone **148a**. We reasoned that, contrary to our first thought, the α-alkoxide function might influence strongly the reactivity of the radical and favor its addition on electron-poor unsaturations. Indeed, to our great pleasure, using electron-poor allylsufone **195** we could observe after 15 h of irradiation the formation of α-allyl ketone **190a** in 28 % yield, albeit together with 16 % of **148a** and incomplete conversion (60 %, entry 1). By doubling the amount of Hantzsch ester, we could obtain a total conversion of the starting material after 5 h. The desired allylation product **190a** was isolated in 41 % yield, together with 30 % of directly reduced **148a** (entry 2). We next tested the reactivity of allylsulfane **198** in those conditions. We were delighted to obtain the desired allylation in 54 % yield along with 32 % of **148a**.

Table 5.8 Optimization of the allylation conditions on epoxychalcone 123a with Hantzsch ester derivatives

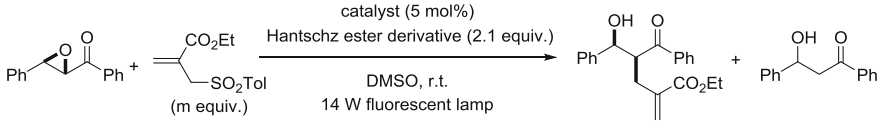

123a 195 191a 148a

Entry	Catalyst	HE derivative	m (equiv.)	Time (h)	Yield allylation (%)	Yield reduction (%)
1	$Ru(bpy)_3Cl_2$	199	10	5	190a, 41	148a, 30
2	$Ru(bpy)_3Cl_2$	200	10	12	191a, 51	*d*-148a,[(a)] 24
3	$Ru(bpy)_3Cl_2$	201	10	24	191a, -	148a, –
4	$Ir(dtbbpy)ppy_2PF_6$	201	10	48	191a, 65	148a, <5
5	$Ir(dtbbpy)ppy_2PF_6$	201	3	100	191a, 67	148a, <5

[(a)] Deuterium incorporation at α-CHD = 54 %

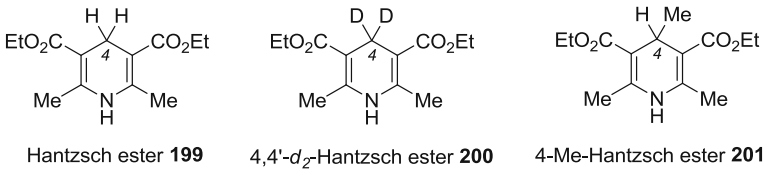

Fig. 5.33 Hantzsh ester derivatives

However, the rest of the optimization was carried out with allylsulfone **195** because the results obtained proved more reproducible than those obtained with allylsulfane **198** (Table 5.7).

We subsequently sought to favor allylation over direct reduction (Table 5.8).We guessed that the best hydrogen donor site of Hantzsch ester **199** was at 4 position (Fig. 5.33). We decided to take advantage of the kinetic isotope effect to favor allylation over reduction [56] and switched to 4,4′d_2-Hantzsch ester **200**. This led to an improved ratio of allyl product (2:1, entry 2). Reasoning that the substitution at the 4 position of Hantzsch esters might be determining for the balance between direct reduction and allylation, we also tested 4-Me-Hantzsch ester **201**. No conversion was observed when employing $Ru(bpy)_3Cl_2$ (entry 3). However, the use of $Ir(dtbbpy)(ppy)_2PF_6$ allowed us to selectively obtain the allylation product **191a** (entry 4). Gratifyingly, lowering the amount of allylating agent to only 3 equivalents of allyl sulfone did not affect this good selectivity (entry 5).

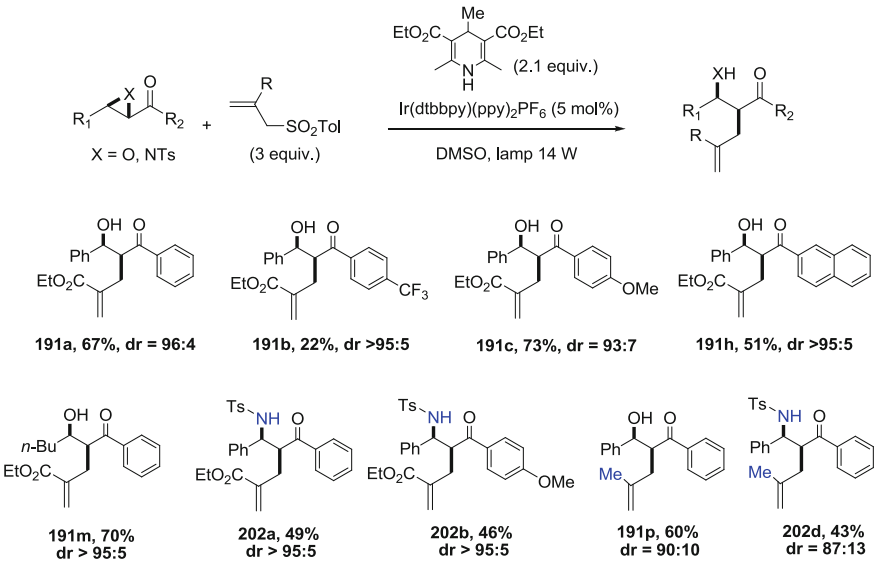

Fig. 5.34 Scope of the visible-light induced allylation process

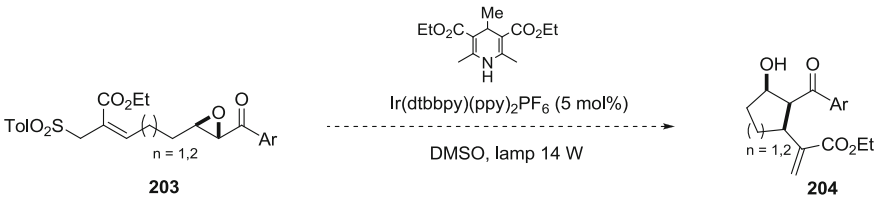

203 **204**

Fig. 5.35 Envisaged intramolecular allylation

5.3.2 Scope of the Allylation Process

The scope of this new radical allylation sequence was examined next (Fig. 5.34). A variety of α-epoxyketones and tosylaziridines could be allylated with fair to good yields, except from α-epoxyketones **123b** with *para*-CF_3substituted aryl ketone. The observed drop in the yield would be coherent with the less nucleophilic nature of the photogenerated radical. In all cases the allylation products were isolated with excellent diastereoselectivities. To our great delight, under our optimized conditions, electron-rich allyl sulfone **193** could also be used efficiently although the diastereoselectivity of the allylation was slightly altered.

Many other allylation reactions have still to be tested, varying the radical precursor and the allylating agent. It might also be interesting to try an intramolecular allylation, leading to five or six-membered cyclized products (Fig. 5.35).

5.3.3 Diastereoselectivity of the Allylations

The diastereomeric ratios were measured on the ^{1}H NMR of the crude and isolated products. To confirm the presence or absence of a minor diastereomer, LCMS experiments were performed on all the isolated products. When possible LCMS experiments were performed as references on diastereomeric mixtures, obtained after overnight stirring of the isolated compound in $CDCl_3$ with silica. As an example the data obtained for product **191p** (dr = 90:10) are presented in Fig. 5.36.

A crystal was obtained for β-amino ketone **202a** whose structure was determined by X-ray diffraction (Fig. 5.37). The major diastereomer was shown to be *syn.*

The *syn* diastereoselectivity would be in accordance with the transition state model developed by Guidon to predict the outcome of the allylation of acyclic β-alkoxy ester under non chelating conditions. This model is based on the assumption of early transition states for radical processes and that the stereoselection occurs in a kinetically controlled process. Guindon considers that the carbon centered radical is not pyramidized but delocalized through the carbonyl group. Because of this delocalization, 1,3-allylic interactions should be taken into account and minimized by locking the smallest substituent (H) in the plane of the

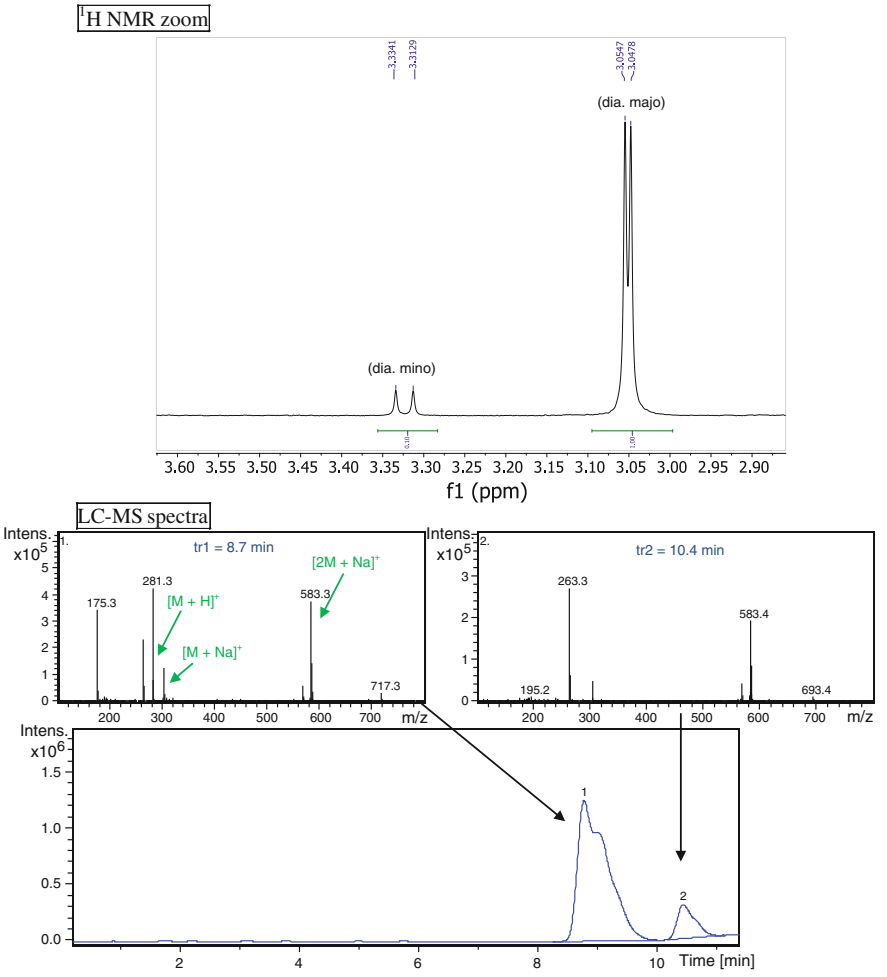

Fig. 5.36 Determination of diastereomeric ratio for 191d (see SI for conditions)

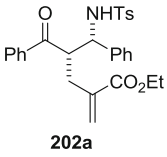

202a

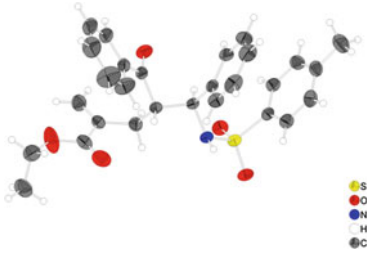

Fig. 5.37 X-Ray structure of 202a

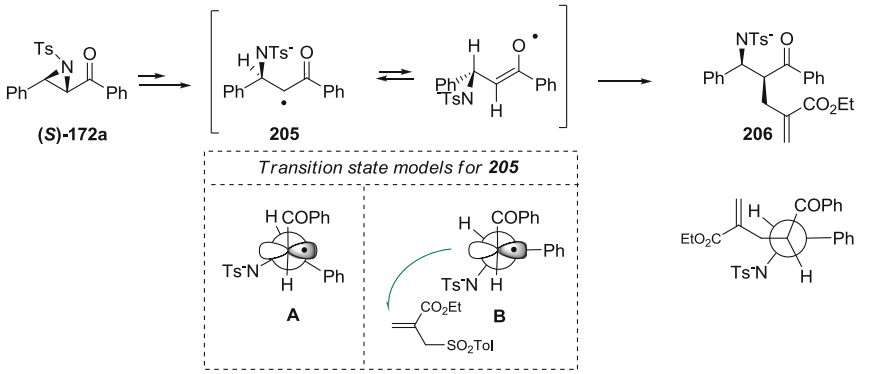

Fig. 5.38 Rationalization of the diastereoselectivity of the allylation

Fig. 5.39 Desymmetrization of *meso*-epoxides

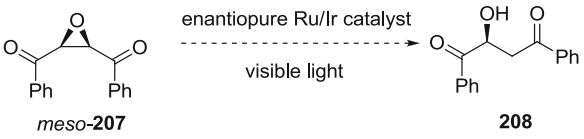

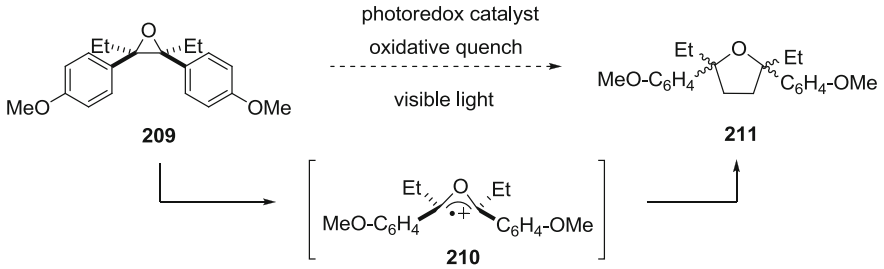

Fig. 5.40 Envisaged photooxidation of epoxides

carbon–carbon double bond. Starting from (*S*) enantiomer of **172a**, minimization of 1,3-allylic strain only would lead to transition state model **A** (Fig. 5.38). In addition, the electrostatic (dipole–dipole) repulsion between the *β*-heteroatom and the carbonyl has to be minimized. Finally, secondary steric interactions can be reduced by orientating the C-Ph bond orthogonal to the radical plane. These two additional considerations favor transition state model **B** that lead to *syn* diastereoisomer. A similar model can be drawn for (*R*) enantiomer and leads to same diastereoselectivity.

To conclude, we extended the scope of visible light photoredox catalysis to the generation of radicals from epoxides and aziridines. To perform this process, we used either $Ir(dtbbpy)ppy_2^+$ or $Ru(bpy)_3^{2+}$ as the photocatalyst in combination with a Hantzsch ester derivative as both quencher and H donor. Then, we took advantage of the reactivity of the photogenerated radical to create new carbon–carbon bonds

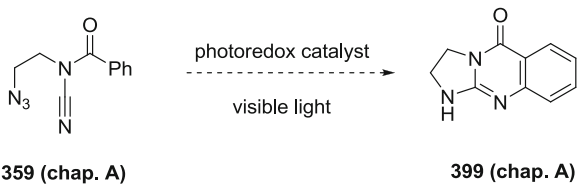

359 (chap. A) 399 (chap. A)

Fig. 5.41 Visible-light induced cascade cyclization of *N*-acylcyanamides

through a highly diastereoselective radical ring-opening/allylation tandem. Many other extensions can be envisaged, such as reductive cyclization or even cascade reactions. It has been demonstrated that the helical chirality of ruthenium photoredox catalysts could be used to perform enantioselective reactions [57]. With this idea in mind, we would like to test the desymmetrization of *meso*-epoxides using an enantiopure photoredox catalyst (Fig. 5.39).

Finally, if direct visible-light induced reduction of epoxides has proven very difficult, it could be the case to investigate their oxidation. Indeed, the oxidation potential of electron-rich epoxystyrene **209** is +1.21 V versus SCE [58], which would be compatible with a one-electron oxidation by $Ru(bpy)_3^{3+}$ species (+1.29 V *vs*. SCE). The radical cation formed could be employed in formal [3+2] cycloadditions with activated double bonds (Fig. 5.40).

The ultimate goal would be to merge the two first parts of my PhD work and design a visible-light induced cascade cyclization of *N*-acylcyanamides (Fig. 5.41). Azidocyanamides precursor such as **359** (chapter A) could be the most promising substrates given the literature backgrounds.

References

1. Gansäuer, A., Lauterbach, T., & Narayan, S. (2003). *Angewandte Chemie International Edition, 42*, 5556–5573.
2. Cohen, T., Jeong, I.-H., Mudryk, B., Bhupathy, M., & Awad, M. M. A. (1990). *Journal of Organic Chemistry, 55*, 1528–1536.
3. Nugent, W. A., & RajanBabu, T. V. (1988). *Journal of the American Chemical Society, 110*, 8561–8562.
4. Gansäuer, A., Bluhm, H., & Pierobon, M. (1998). *Journal of the American Chemical Society, 120*, 12849–12859.
5. Gansäuer, A., Pierobon, M., & Bluhm, H. (2002). *Angewandte Chemie International Edition, 41*, 3206–3208.
6. Gansäuer, A., & Narayan, S. (2002). *Advanced Synthesis & Catalysis, 344*, 465–475.
7. Hilt, G., Bolze, P., & Harms, K. (2007). *Chemistry–A European Journal, 13*, 4312–4325.
8. Boujlel, K., Martigny, P., & Simonet, J. (1983). *Journal of Electroanalytical Chemistry, 144*, 437–442.
9. Ischay, M. A., Anzovino, M. E., Du, J., & Yoon, T. P. (2008). *Journal of the American Chemical Society, 130*, 12886–12887.
10. Fukuzumi, S., & Okamoto, T. (1994). *Journal of the American Chemical Society, 116*, 5503–5504.

11. Lautens, M., Ouellet, S. G., & Raeppel, S. (2000). *Angewandte Chemie International Edition, 39*, 4079–4081.
12. Takahashi, E., & Wraight, C. A. (1992). *Biochemistry, 31*, 855–865.
13. Rastetter, W. H., & Adams, J. (1980). *Journal of Organic Chemistry, 45*, 3534–3535.
14. Andrews, R. S., Becker, J. J., & Gagné, M. R. (2010). *Angewandte Chemie International Edition, 49*, 7274–7276.
15. Parrish, J. D., & Little, R. D. (2002). *Organic Letters, 4*, 1439–1442.
16. Teply, F. (2011). *Collection of Czechoslovak Chemical Communications, 76*, 859–917.
17. Cossy, J., Aclinou, P., Bellosta, V., Furet, N., Baranne-Lafont, J., Sparfel, D., et al. (1991). *Terahedron Letters, 32*, 1315–1316.
18. Hallet, P., Muzart, J., & Pète, J. P. (1981). *Journal of Organic Chemistry, 46*, 4273–4275.
19. Kirschberg, T., & Mattay, J. (1996). *Journal of Organic Chemistry, 61*, 8885–8896.
20. Reynolds, S. C., Wengryniuk, S. E., & Hartel, A. M. (2007). *Tetrahedron Letters, 48*, 6751–6753.
21. Šolomek, T., Štacko, P., Tazhe Veetil, A., Pospíšil, T., & Klán, P. (2010). *Journal of Organic Chemistry, 75*, 7300–7309.
22. Hasegawa, E., Ishiyama, K., Horaguchi, T., & Shimizu, T. (1991). *Journal of Organic Chemistry, 56*, 1631–1635.
23. Hasegawa, E., Ishiyama, K., Horaguchi, T., & Shimizu, T. (1991). *Tetrahedron Letters, 32*, 2029–2032.
24. Hasegawa, E., Kato, T., Kitazume, T., Yanagi, K., Hasegawa, K., & Horaguchi, T. (1996). *Tetrahedron Letters, 37*, 7079–7082.
25. Hasegawa, E., Ishiyama, K., Fujita, T., Kato, T., & Abe, T. (1997). *Journal of Organic Chemistry, 62*, 2396–2400.
26. Hasegawa, E., Yoneoka, A., Suzuki, K., Kato, T., Kitazume, T., & Yanagi, K. (1999). *Tetrahedron, 55*, 12957–12968.
27. Zhang, J., Jin, M.-Z., Zhang, W., Yang, L., & Liu, Z.-L. (2002). *Tetrahedron Letters, 43*, 9687–9689.
28. Hasegawa, E., Takizawa, S., Seida, T., Yamaguchi, A., Yamaguchi, N., Chiba, N., et al. (2006). *Tetrahedron, 62*, 6581–6588.
29. Narayanam, J. M. R., Tucker, J. W., & Stephenson, C. R. J. (2009). *Journal of the American Chemical Society, 131*, 8756–8757.
30. Newcomb, M. (2001). In P. Renaud & M. P. Sibi (Eds.), *Radicals in organic synthesis* (vol. 1, pp. 317–336). Wiley-VCH, Weinheim.
31. Hasegawa, E., Ishiyama, K., Kato, T., Horaguci, T., & Shimizu, T. (1992). *Journal of Organic Chemistry, 57*, 5352–5359.
32. Gloss, G. L., Calcaterra, L. T., Green, N. J., Penfield, K. W., & Miller, J. R. (1986). *Journal of Physical Chemistry, 90*, 3673–3683.
33. Dai, L.-Z., & Shi, M. (2009). *Tetrahedron Letters, 50*, 651–655.
34. Armstrong, A., Baxter, C. A., Lamont, S. G., Pape, A. R., & Wincewicz, R. (2007). *Organic Letters, 9*, 351–353.
35. Makosza, M., Kwast, A., Kwast, E., & Jonczyk, A. (1985). *Journal of Organic Chemistry, 50*, 3722–3727.
36. Liu, S.-M., & Bolm, C. (2008). *Angewandte Chemie International Edition, 47*, 8920–8923.
37. Barbot, F., N'Goma, D., & Miginiac, P. (1991). *Journal of Organometallic Chemistry, 410*, 277–286.
38. Lowry, M. S., Hudson, W.R., Pascal, R.A., & Bernhard, S. (2004). Synthesized in three steps from IrCl3 according to the procedure. *Journal of the American Chemical Society*, *126*, 14129–14135.
39. Armstrong, A., Baxter, C. A., Lamont, S. G., Pape, A. R., & Wincewicz, R. (2007). *Organic Letters, 9*, 351–353.
40. Evans, D. A., Faul, M. M., & Bilodeau, M. T. (1991). *Journal of Organic Chemistry, 56*, 6144–6674.

41. Dauban, P., Sanière, L., Tarrade, A., & Dodd, R. H. (2001). *Journal of the American Chemical Society, 123*, 7707–7708.
42. Nonhebel, D. C. (1993). *Chemical Society Reviews*, 347–349.
43. Kirschberg, T., & Mattay, J. (1996). *Journal of Organic Chemistry, 61*, 8885–8896.
44. Tanko, J. M., Li, X., Chahma, M., Jackson, W. F., & Spencer, J. N. (2007). *Journal of the American Chemical Society, 129*, 4181–4192.
45. Simon, J. D., & Peters, K. S. (1984). *Accounts of Chemical Research, 17*, 277–283.
46. Belotti, D., Cossy, J., Pete, J.-P., & Portella, C. (1986). *Journal of Organic Chemistry, 51*, 4196–4200.
47. Cossy, J., Furet, N., & Bouzbouz, S. (1995). *Tetrahedron, 51*, 11751–11764.
48. Kirshberg, T., & Mattay, J. (1996). *Journal of Organic Chemistry, 61*, 8885–8896.
49. Corey, E. J., & Chaykovsky, M. (1965). *Journal of the American Chemical Society, 87*, 1353–1364.
50. Merz, A., & Markl, G. (1973). *Angewandte Chemie International Edition, 12*, 845–846.
51. Tanko, J. M., Li, X., Chahma, M., Jackson, W. F., & Spencer, J. N. (2007). *Journal of the American Chemical Society, 129*, 4181–4192.
52. Lu, Z., Shen, M., & Yoon, T. P. (2011). *Journal of the American Chemical Society, 133*, 1162–1164.
53. Kocienski, P. (1983). *Journal of the Chemical Society, Perkin Transactions 1*, 945–948.
54. Harvey, l. W., Phillips, E. D., & Whitham, G. H. (1997). *Tetrahedron*, *53*, 6493–6508.
55. Barton, D. H. R., & Crich, D. (1986). *Journal of the Chemical Society, Perkin Transactions 1*, 1613–1619.
56. Giraud, L., Lacote, E., & Renaud, P. (1997). *Helvetica Chimica Acta*, *80*, 2148–2156 (see also references therein).
57. Hamada, T., Ishida, H., Usui, S., Watanabe, Y., Tsumura, K., & Ohkubo, K. (1993). *Journal of the Chemical Society, Chemical. Communications*, 909–911.
58. Futamura, S., Kusunose, S., Ohta, H., & Kamiya, Y. (1984). *Journal of the Chemical Society, Perkin Transactions 1*, 15–19.

Chapter 6
Supporting Information

6.1 General Remarks

Reactions were carried out under argon, with magnetic stirring and redistilled solvents. THF and Et_2O were distilled from sodium/benzophenone. CH_2Cl_2, acetonitrile, DMSO, NEt_3 and *t*-BuOH were distilled from CaH_2. Thin layer chromatography (TLC) was performed on Merck 60 F254 silica gel. Merck Geduran SI 60 Å silica gel (35−70 mm) was used for column chromatography. The melting points reported were measured with a Reichert hot stage apparatus and are uncorrected. IR spectra were recorded with a Bruker Tensor 27 ATR diamant PIKE spectrometer. Optical rotations were measured using a Perkin-Elmer 341 polarimeter. ^1H, ^{13}C and ^{19}F NMR spectra were recorded at 400, 100 and 377 MHz respectively, using a Bruker 400 AVANCE spectrometer fitted with a BBFO probehead. Chemical shifts are given in ppm using the $CDCl_3$ or the d_4-MeOD signal as reference ($^1H = 7.26$ ppm, $^{13}C = 77.16$ ppm and $^1H = 3.31$ ppm, $^{13}C = 49.00$ ppm respectively). Unless noted, NMR spectra were recorded in $CDCl_3$ at 300 K. The terms m, s, d, t, q, quint., and sext. represent multiplet, singlet, doublet, triplet, quadruplet, quintuplet, and sextuplet, respectively, and the term br means a broad signal. Exact masses were recorded at UPMC by the laboratory of Prof. J.-C. Tabet (UMR 7201) (electrospray source). LCMS analysis were conducted using an Agilent series 1100 chromatograph with a Zorbax C18 column (2.1 × 150 mm) coupled with an quadrupole ion trap (Esquire 3000, Brüker) with an ESI source, operated in the positive mode. All the LCMS experiments were conducted with a gradient of acetonitrile/0.5 % formic acid in water/0.5 % formic acid mobile phase (45/55 to 80/20 in 20 min); flow rate: 200 μL/min. Soft desolvation conditions (orifice—skimmer potential difference: 30 V) have been used in order to avoid the degradation of the species. Ir(dtbb-py)$(ppy)_2PF_6$ [1] was synthesized according to literature procedures.

M.-H. Larraufie, *Development of New Radical Cascades and Multi-Component Reactions*, Springer Theses, DOI: 10.1007/978-3-319-01324-4_6,

6.2 General Procedures

General procedure 1 (GP1): Synthesis of the epoxy chalcone-type compounds from the corresponding aldehydes and ketones [2].

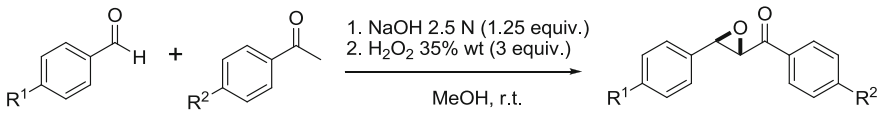

To a mixture of ketone (1.0 equiv.) and aldehyde (1.0 equiv.) in MeOH (0.3 M) was slowly added 2.5 M aqueous NaOH (1.25 equiv.). The resulting mixture was stirred at r.t. until completion of the reaction (monitored by TLC). Then, H_2O_2 35 % wt in water (3.2 equiv.) was added dropwise at 0 °C and the resulting mixture was stirred at r.t. until completion of the reaction. The mixture was filtered and the precipitate was disolved in EtOAc, washed with water, dried over $MgSO_4$, concentrated *in vacuo* and purified by flash column chromatography if necessary to afford the corresponding epoxy chalcone-type compound.

General procedure 2 (GP2): Synthesis of the epoxy chalcone-type compounds from the corresponding enones [3].

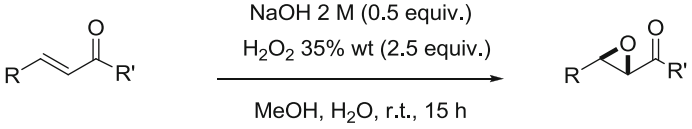

To a solution of enone (1.0 equiv.) in MeOH (0.3 M) at 0 °C was slowly added a mixture of H_2O_2 35 % wt in water (2.5 equiv.) and 2 M aqueous NaOH (0.5 equiv.). The mixture was stirred at r.t; until completion of the reaction. Addition of cold water generally led to the precipitation of a solid which was filtered and washed with water to yield the pure epoxide. With liquid epoxides, the reaction mixture was extracted with EtOAc. The combined organic layers were dried over $MgSO_4$, concentrated *in vacuo* and purified by flash column chromatography if necessary to afford the corresponding epoxide.

General procedure 3 (GP3): Synthesis of chalcone aziridine-type compounds from the corresponding enones [4].

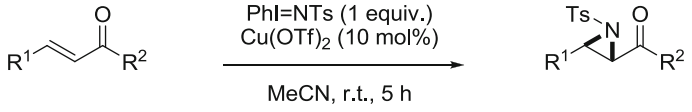

To a solution of $Cu(OTf)_2$ (0.1 equiv.) in distilled MeCN (0.03 M) under argon, was added the chalcone-type derivative (5 equiv.) and (*N*-(*p*-toluenesulfonyl)imino)phenyliodinane (1 equiv.). The resulting green mixture was stirred at r.t. during 5 h, diluted into EtOAc and filtered on a short pad of silica. The filtrate was concentrated *in vacuo* and purified by flash column chromatography to afford the corresponding aziridine.

General procedure 4 (GP4): Photocatalytic reduction of epoxy chalcone-type compounds (Conditions A).

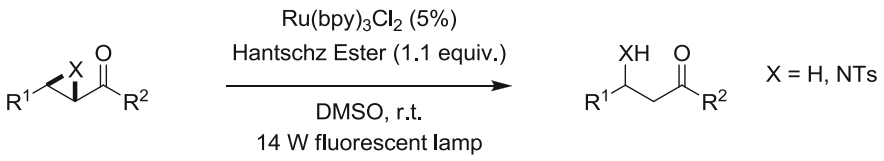

A mixture of epoxychalcone-type derivative (0.2 mmol, 1 equiv.), Hantzsch ester (56 mg, 0.22 mmol, 1.1 equiv.) and $Ru(bpy)_3Cl_2.6H_2O$ (7.5 mg, 0.01 mmol, 5 mol%) in DMSO (2 mL) was deoxygenated by bubbling argon for 20 min., then irradiated with a 14 W light bulb until the reaction was complete (monitored by TLC). The resulting mixture was dissolved in EtOAc (15 mL) and washed with water (2 × 10 mL). The combined aqueous layers were extracted with EtOAc (15 mL). The combined organic layers were dried over $MgSO_4$, concentrated *in vacuo* and purified by flash column chromatography.

General procedure 5 (GP5): Photocatalytic reduction of epoxy chalcone-type compounds (Conditions C).

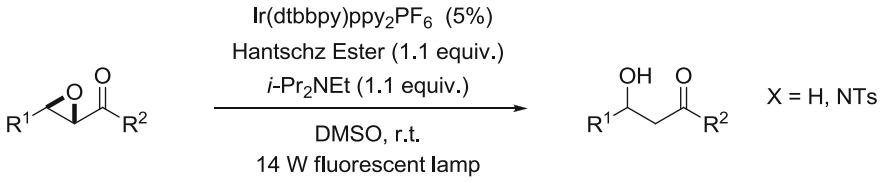

A dried schlenk equipped with a stir bar was loaded with Hantzsch ester (56 mg, 0.22 mmol, 1.1 equiv.), epoxychalcone-type derivative (0.2 mmol, 1 equiv.) and $Ir(dtbbpy)(ppy)_2PF_6$ (9.1 mg, 0.01 mmol, 5 mol%). The schlenk was evacuated and backfilled with argon three times, before degassed DMSO (2 mL) and iPr_2NEt (38 μL, 0.22 mmol, 1.1 equiv.) were added under argon. The yellow reaction mixture was irradiated at r.t. with a 14 W light bulb until the reaction was complete (monitored by RMN). The reaction was quenched with water (15 mL) and extracted with EtOAc (3 × 10 mL). The combined organic layers were dried over $MgSO_4$, concentrated *in vacuo* and purified by flash chromatography over silica gel.

General procedure 6 (GP6): Photoreductive allylation of epoxy chalcone-type compounds.

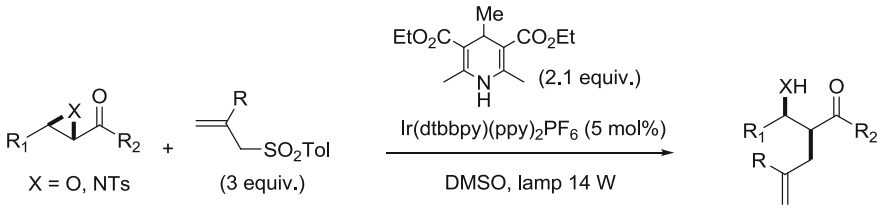

A dried schlenk equipped with a stir bar was loaded with 4-Me Hantzsch ester (112 mg, 0.42 mmol, 2.1 equiv.), allylsulfone (0.6 mmol, 3 equiv.), epoxy chalcone-type derivative or aziridine analog (0.2 mmol, 1 equiv.) and Ir(dtbbpy)$(ppy)_2PF_6$ (9.1 mg, 0.01 mmol, 5 mol%). The schlenk was evacuated and backfilled with argon three times, before degassed DMSO (2 mL) was added under argon. The yellow reaction mixture was irradiated at r.t. with a 14 W light bulb until the reaction was complete (monitored by RMN). The reaction must be stopped as soon as the conversion is complete to avoid degradation. The reaction was quenched with water (15 mL) and extracted with EtOAc (3 × 10 mL). The combined organic layers were dried over $MgSO_4$, concentrated *in vacuo* and purified by flash chromatography over silica gel. The diastereomeric ratio was determined by ^{1}H NMR, and confirmed by LCMS.

6.3 Epoxide, Aziridines and Cyclopropanes Precursors

Phenyl(3-phenyloxiran-2-yl)methanone (123a)

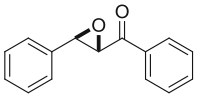

$C_{15}H_{12}O_2$ M = 224.25 g/mol

Following **GP2** with *trans*-chalcone (2.1 g, 10 mmol, 1 equiv.), **1a** was isolated pure after filtration as a white solid (1.4 g, 63 %). Spectral data correspond to those described in the literature [5].

^{1}H NMR (400 MHz, $CDCl_3$): $\delta = 4.08$ (d, $J = 1.8$ Hz, 1 H, PhC*H*O), 4.30 (d, $J = 2$ Hz, 1 H, PhC(O)C*H*O), 7.36–7.43 (m, 5 H, arom.), 7.47–7.51 (m, 2 H, arom.), 7.60–7.64 (m, 1 H, arom.), 8.00–8.03 (m, 2 H, arom.); ^{13}C NMR (100 MHz, $CDCl_3$): $\delta = 59.5$ (Ph*C*HO), 61.2 (PhC(O)*C*HO), 125.9 (2 CH arom.), 128.5 (2 CH arom.), 128.5 (C arom.), 128.9 (2 CH arom.), 129.0 (2 CH arom.), 129.2 (CH arom.), 134.1 (CH arom.), 135.6 (C arom.), 193.2 (C=O).

***anti*-2,3-Epoxy-1,3-diphenylpropan-1-ol (124)**

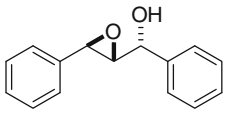

$C_{15}H_{14}O_2$ M = 226.27 g/mol

To an ice-cold solution of epoxychalcone **123a** (1.0 g, 4.46 mmol) in Et_2O (20 mL) was added dropwise a cold solution of $Zn(BH_4)_2$ (0.144 M solution in Et_2O, 9.3 mL, 1.34 mmol). After 30 min, the reaction was quenched with water (5 mL) and stirred vigorously for another 30 min. The aqueous layer was extracted with Et_2O (3 × 15 mL) and the combined organic phases were dried over $MgSO_4$, filtered and evaporated under reduced pressure. Crystallisation of the crude compound from hexane afforded the epoxy alcohol **124** as a white solid (1.0 g, quant.). Data correspond to those described in the literature [6].

^{1}H NMR (400 MHz, $CDCl_3$): δ = 2.41 (br s, 1 H, OH), 3.31 (t, J = 2.1 Hz, 1 H, PhCH(OH)C*H*O), 4.16 (d, J = 1.8 Hz, 1 H, PhC*H*O), 5.06 (s, 1 H, PhC*H*(OH)), 7.26–7.48 (m, 10 H, arom.); ^{13}C NMR (100 MHz, $CDCl_3$): δ = 55.0 (PhCH(OH)*C*HO), 64.9 (PhC*H*O), 71.3 (Ph*C*H(OH)), 125.8 (2 CH arom.), 126.5 (2 CH arom.), 128.5 (2 CH arom.), 128.7 (2 CH arom.), 128.2 (CH arom.), 128.3 (CH arom.), 136.5 (C arom.), 139.2 (C arom.).

Methyl 4-(3-phenyloxirane-2-carbonyl)benzoate (123b)

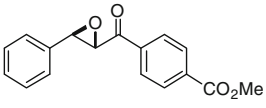

$C_{17}H_{14}O_4$ M = 282.29 g/mol

Following **GP1** with methyl 4-acetylbenzoate (797 mg, 4.47 mmol, 1 equiv.) and benzaldehyde (0.46 mL, 4.46 mmol, 1 equiv.), **123b** was purified by flash column chromatography (pentane: EtOAc = 10 : 2 then 10 : 3) and isolated as a white solid (317 mg, 25 %).

Mp: 112–113 °C; IR (neat): ν = 1723, 1692, 1436, 1415, 1280, 1227, 1108, 1011, 891, 752, 713, 698 cm^{-1}; ^{1}H NMR (400 MHz, $CDCl_3$): δ = 3.96 (s, 3 H, CO_2CH_3), 4.10 (s, 1 H, PhC*H*O), 4.28 (s, 1 H, C(O)C*H*O), 7.37–7.41 (m, 5 H, arom.), 8.07 (d, J = 8.4 Hz, 2 H, arom.), 8.15 (d, J = 8.4 Hz, 2 H, arom.); ^{13}C NMR (100 MHz, $CDCl_3$): δ = 52.7 (CO_2CH_3), 59.7 (Ph*C*HO), 61.3 (C(O)*C*HO), 125.9 (2 CH arom.), 128.4 (2 CH arom.), 129.0 (2 CH arom.), 129.3 (CH arom.), 130.1 (2 CH arom.), 134.8 (C arom.), 135.3 (C arom.), 138.7 (C arom.), 166.1 (CO_2Me), 193.0 (C=O).

(4-Methoxyphenyl)(3-phenyloxiran-2-yl)methanone (123c)

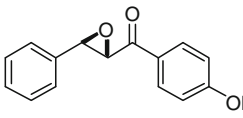

$C_{16}H_{14}O_3$ M = 254.28 g/mol

Following **GP1** with 1-(4-methoxyphenyl)ethanone (1.50 g, 10 mmol, 1 equiv.) and benzaldehyde (1.05 mL, 10 mmol, 1 equiv.), **123c** was isolated pure after filtration as a white solid (1.65 g, 65 %). Spectral data are in accordance with those reported in the literature [7].

^{1}H NMR (400 MHz, $CDCl_3$): δ = 3.88 (s, 3 H, OC*H*$_3$), 4.07 (d, J = 2 Hz, 1 H, PhC*H*O), 4.25 (d, J = 2 Hz, 1 H, C(O)C*H*O), 6.96 (d, J = 9.2 Hz, 2 H, arom.), 7.36–7.39 (m, 5 H, arom.), 8.02 (d, J = 8.8 Hz, 2 H, arom.); ^{13}C NMR (100 MHz, $CDCl_3$): δ = 55.6 (OCH_3), 59.2 (Ph*C*HO), 60.9 (C(O)*C*HO), 114.1 (2 CH arom.), 125.8 (2 CH arom.), 128.6 (C arom.), 128.8 (2 CH arom.), 129.0 (CH arom.), 130.8 (2 CH arom.), 135.7 (C arom.), 164.3 (C arom.), 191.4 (C=O).

(3-Phenyloxiran-2-yl)(4-(trifluoromethyl)phenyl)methanone (123d)

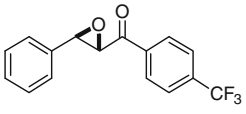

$C_{16}H_{11}F_3O_2$ M = 292.25 g/mol

Following **GP1** with 1-(4-(trifluoromethyl)phenyl)ethanone (1.88 g, 10 mmol, 1 equiv.) and benzaldehyde (1.05 mL, 10 mmol, 1 equiv.), **123d** was isolated pure after filtration as a white solid (1.77 g, 61 %).

Mp: 108–109 °C; IR (neat): ν = 1694, 1666, 1410, 1330, 1171, 1123, 1068, 1015, 897, 755, 728 cm^{-1}; ^{1}H NMR (400 MHz, $CDCl_3$): δ = 4.09 (d, J = 2 Hz, 1 H, PhC*H*O), 4.26 (d, J = 2 Hz, 1 H, C(O)C*H*O), 7.36–7.41 (m, 5 H, arom.), 7.76 (d, J = 8 Hz, 2 H, arom.), 8.13 (d, J = 8.4 Hz, 2 H, arom.); ^{13}C NMR (100 MHz, $CDCl_3$): δ = 59.6 (Ph*C*HO), 61.4 (C(O)*C*HO), 123.5 (q, $^1J_{C\text{-}F}$ = 271.2 Hz, CF_3), 125.9 (2 CH arom.), 126.0 (q, $^3J_{C\text{-}F}$ = 3.7 Hz, 2 CH arom.), 128.9 (2 CH arom.), 129.0 (2 CH arom.), 129.4 (CH arom.), 135.2 (C arom.), 135.3 (q, $^2J_{C\text{-}F}$ = 32.7 Hz, *C*CF_3), 138.1 (C arom.), 192.7 (C=O); ^{19}F NMR (377 MHz, $CDCl_3$): δ = −63.3; HRMS calcd. for $C_{16}H_{11}O_2F_3Na$ ([M + Na]$^+$) 315.06034, found 315.06028.

Methyl 4-(3-benzoyloxiran-2-yl)benzoate (123e)

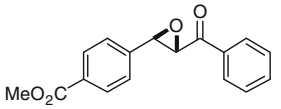

$C_{17}H_{14}O_4$ M = 282.29 g/mol

Following **GP1** with acetophenone (1.17 mL, 10 mmol, 1 equiv.) and methyl 4-formylbenzoate (1.64 g, 10 mmol, 1 equiv.), **123e** was isolated pure after filtration as a white solid (412 mg, 15 %).

IR (neat): v = 1719, 1689, 1450, 1279, 1232, 1110, 1018, 762, 701 cm^{-1}; ^1H NMR (400 MHz, $CDCl_3$): δ = 3.94 (s, 1 H, CO_2CH_3), 4.14 (d, J = 1.6 Hz, 1 H, Ph-C*H*-O), 4.28 (d, J = 2 Hz, 1 H, PHC(O)-C*H*-O), 7.45 (d, J = 8.4 Hz, 2 H, arom.), 7.48–7.52 (m, 2 H, arom.), 7.61-7.66 (m, 1 H, arom.), 8.00–8.02 (m, 2 H, arom.), 8.08 (d, J = 8.4 Hz, 2 H, arom.); ^{13}C NMR (100 MHz, $CDCl_3$): δ = 52.3 (CO_2CH_3), 58.8 (C-*C*H-O), 61.0 (C(O)-*C*H-O), 125.9 (2 CH arom.), 128.5 (2 CH arom.), 129.0 (2 CH arom.), 130.1 (2 CH arom.), 130.9 (*C*-CO_2Me), 134.2 (CH arom.), 135.5 (*C*-C=O), 140.6 (C arom.), 166.6 (*C*O_2Me), 192.7 (C=O).

(3-(4-Methoxyphenyl)oxiran-2-yl)(phenyl)methanone (123f)

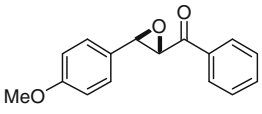

$C_{16}H_{14}O_3$ M = 254.28 g/mol

Following **GP1** with acetophenone (1.17 mL, 10 mmol, 1 equiv.) and paran-isaldehyde (1.22 mL, 10 mmol, 1 equiv.), **123f** was isolated pure after filtration as a light yellow solid (144 mg, 6 %). Data correspond to those described in the literature [7].

^1H NMR (400 MHz, $CDCl_3$): δ = 3.84 (s, 3 H, OCH_3), 4.03 (d, J = 1.6 Hz, 1 H, Ph-C*H*-O), 4.29 (d, J = 2 Hz, 1 H, PhC(O)-C*H*-O), 6.94 (d, J = 8.8 Hz, 2 H, arom.), 7.30 (d, J = 8.8 Hz, 2 H, arom.), 7.47–7.51 (m, 2 H, arom.), 7.60–7.62 (m, 1 H, arom.), 8.00–8.02 (m, 2 H, arom.).

Phenyl(3-(4-(trifluoromethyl)phenyl)oxiran-2-yl)methanone (123g)

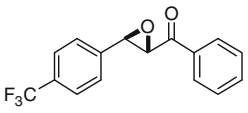

$C_{16}H_{11}F_3O_2$ M = 292.25 g/mol

Following **GP1** with acetophenone (1.17 mL, 10 mmol, 1 equiv.) and 4-(trifluoromethyl)benzaldehyde (1.27 mL, 10 mmol, 1 equiv.), **123g** was isolated after filtration as a white solid (877 mg, 30 %). Spectral data are in accordance with those reported in the literature [8].

^1H NMR (400 MHz, $CDCl_3$): δ = 4.15 (d, J = 1.6 Hz, 1 H, p-CF_3PhC*H*O), 4.26 (d, J = 2 Hz, 1 H, PhC(O)C*H*O), 7.49–7.53 (m, 4 H, arom.), 7.62–7.69 (m, 3 H, arom.), 8.00–8.02 (m, 2 H, arom.); ^{13}C NMR (100 MHz, $CDCl_3$): δ = 58.6 (*p*-CF_3PhC*H*O), 61.0 (C(O)*C*HO), 124.0 (q, $^1J_{C\text{-}F}$ = 270.6 Hz, CF_3), 125.9 (q, $^3J_{C\text{-}F}$ = 3.8 Hz, 2 CH arom.), 126.3 (2 CH arom), 128.5 (2 CH arom.), 129.1 (2 CH arom.), 131.4 (q, $^2J_{C\text{-}F}$ = 32.4 Hz, C arom.), 134.4 (CH arom.), 135.5 (C arom.), 139.7 (C arom.), 192.6 (C=O); ^{19}F NMR (377 MHz, $CDCl_3$): δ = −62.7.

Naphthalen-2-yl(3-phenyloxiran-2-yl)methanone (123 h)

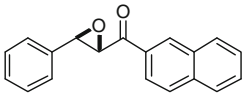

$C_{19}H_{14}O_2$ M = 274.31 g/mol

Following **GP1** with 2-acetylnaphtalene (1.70 mg, 10 mmol, 1 equiv.) and benzaldehyde (1.05 mL, 10 mmol, 1 equiv.), **123 h** was isolated pure after filtration as a light yellow solid (1.59 g, 58 %). Spectral data are in accordance with those reported in the literature [9].

^{1}H NMR (400 MHz, $CDCl_3$): $\delta = 4.16$ (d, $J = 2$ Hz, 1 H, PhC*H*O), 4.44 (d, $J = 1.6$ Hz, 1 H, C(O)C*H*O), 7.40–7.45 (m, 5 H, arom.), 7.55–7.59 (m, 1 H, arom.), 7.62–7.64 (m, 1 H, arom.), 7.88–7.97 (m, 3 H, arom.), 8.05–8.07 (m, 1 H, arom.), 8.58 (s, 1 H, arom.); ^{13}C NMR (100 MHz, $CDCl_3$): $\delta = 59.6$ (C*C*HO), 61.2 (C(O)*C*HO), 123.8 (CH arom.), 126.0 (2 CH arom.), 127.2 (CH arom.), 128.0 (CH arom.), 128.9 (2 CH arom.), 129.0 (CH arom.), 129.1 (CH arom.), 129.2 (CH arom.), 129.8 (CH arom.), 130.5 (CH arom.), 132.5 (C arom.), 133.0 (C arom.), 135.7 (C arom.), 136.0 (C arom.), 193.1 (C=O).

Furan-2-yl(3-phenyloxiran-2-yl)methanone (123i)

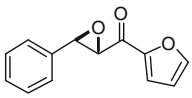

$C_{13}H_{10}O_3$ M = 214.22 g/mol

Following **GP1** with 1-(furan-2-yl)ethanone (1.10 g, 10 mmol, 1 equiv.) and benzaldehyde (1.05 mL, 10 mmol, 1 equiv.), **123i** was purified by flash column chromatography (petroleum ether : $Et_2O = 7 : 3$) and isolated as a light yellow solid (502 mg, 24 %). Data correspond to those described in the literature [10].

^{1}H NMR (400 MHz, $CDCl_3$): $\delta = 4.14$–4.16 (m, 2 H, Ph-C*H*-O + PhC(O)-C*H*-O), 6.60 (dd, $J = 1.2$, 3.6 Hz, 1 H, arom.), 7.33–7.41 (m, 5 H, arom.), 7.46 (d, $J = 3.6$ Hz, 1 H, arom.), 7.67 (d, $J = 1.6$ Hz, 1 H, arom.); ^{13}C NMR (100 MHz, $CDCl_3$): $\delta = 59.7$ (C-*C*H-O), 60.7 (C(O)-*C*H-O), 112.8 (CH arom.), 119.7 (CH arom.), 125.9 (2 CH arom.), 128.8 (2 CH arom.), 129.2 (CH arom.), 135.5 (C arom.), 147.8 (CH arom.), 151.3 (*C*-C=O), 182.2 (C=O).

(3-(4-Chlorophenyl)oxiran-2-yl)(phenyl)methanone (123j)

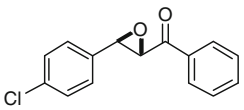

$C_{15}H_{11}ClO_2$ M = 258.70 g/mol

Following **GP2** with 4-chlorochalcone (2.40 g, 10 mmol, 1 equiv.), **123j** was isolated after filtration as a white solid (1.60 g, 62 %). Spectral data are in accordance with those reported in the literature [11].

^{1}H NMR (400 MHz, $CDCl_3$): δ = 4.06 (d, J = 2.0 Hz, 1 H, p-ClPhC*H*O), 4.24 (d, J = 2.0 Hz, 1 H, PhC(O)C*H*O), 7.29–7.39 (m, 4 H, arom.), 7.48–7.52 (m, 2 H, arom.), 7.61–7.65 (m, 1 H, arom.), 7.99–8.01 (m, 2 H, arom.); ^{13}C NMR (100 MHz, $CDCl_3$): δ = 58.8 (*p*-ClPhC*H*O), 61.1 (C(O)*C*HO), 127.3 (2 CH arom.), 128.5 (2 CH arom), 129.1 (2 CH arom.), 129.2 (2 CH arom.), 134.2 (C arom.), 134.2 (CH arom.), 135.1 (C arom.), 135.5 (C arom.), 192.9 (C=O).

Mesityl(3-phenyloxiran-2-yl)methanone (123 k)

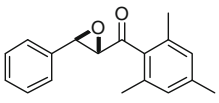

$C_{18}H_{18}O_2$ M = 266.33 g/mol

Following **GP2** with (*E*)-1-mesityl-3-phenylprop-2-en-1-one (600 mg, 2.4 mmol, 1 equiv.), **123 k** was isolated after extraction as a colorless oil (500 mg, 94 %). Spectral data are in accordance with those reported in the literature [12].

^{1}H NMR (400 MHz, $CDCl_3$): δ = 2.29 (s, 9 H, 3 CH_3), 3.77 (d, J = 1.6 Hz, 1 H, PhC*H*O), 3.96 (d, J = 2.0 Hz, 1 H, C(O)C*H*O), 6.87 (s, 2 H, arom.), 7.26–7.29 (m, 2 H, arom.), 7.34–7.36 (m, 3 H, arom.); ^{13}C NMR (100 MHz, $CDCl_3$): δ = 19.6 (2 CH_3), 21.3 (CH_3), 59.8 (Ph*C*HO), 63.9 (C(O)*C*O), 125.8 (2 CH arom.), 128.8 (2 CH arom.), 128.9 (2 CH arom.), 129.2 (CH arom.), 134.7 (2 C arom.), 135.0 (C arom.), 135.4 (C arom.) 139.9 (C arom.), 204.6 (C=O).

1-(3-Phenyloxiran-2-yl)ethanone (123 l)

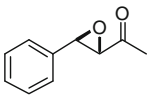

$C_{10}H_{10}O_2$ M = 162.19 g/mol

Following **GP2** with (*E*)-4-phenylbut-3-en-2-one (2.00 g, 13.6 mmol, 1 equiv.), **123 l** was isolated after flash column chromatography (petroleum ether: EtOAc = 5:1) as a white solid (1.02 g, 46 %). Spectral data are in accordance with those reported in the literature [13].

^{1}H NMR (400 MHz, $CDCl_3$): δ = 2.19 (s, 3 H, Me), 3.48 (d, J = 1.8 Hz, 1 H, PhC*H*O), 3.99 (d, J = 1.8 Hz, 1 H, C(O)C*H*O), 7.26–7.28 (m, 2 H, arom.), 7.34–7.37 (m, 3 H, arom.); ^{13}C NMR (100 MHz, $CDCl_3$): δ = 24.9 (Me), 57.9 (Ph*C*HO), 63.6 (C(O)*C*O), 125.8 (2 CH arom.), 128.8 (2 CH arom.), 129.1 (CH arom.), 135.2 (C arom.), 204.2 (C=O).

(*E*)-1-Phenylhept-2-en-1-one (161)

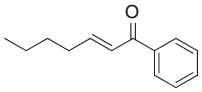

$C_{13}H_{16}O$ M = 188.27 g/mol

To a solution of phenacyl triphenylphosphonium bromide (6.90 g, 15.0 mmol, 1 equiv.) in CH_2Cl_2 (35 mL), was added NaOH as a 2 M aqueous solution (2.5 mL) and the resulting mixture was stirred at r.t. for 14 h. The two phases were separated and the aqueous layer was extracted with CH_2Cl_2 (40 mL). The organic layers were combined, and to this solution was added valeraldehyde (9.8 mL, 90 mmol, 6 equiv.) dropwise over 5 h. The solution was stirred at r.t. for 1 h, then concentrated *in vacuo*. Purification by flash column chromatography (pure pentane to pentane:EtOAc = 9:1), afforded (*E*)-1-phenylhept-2-en-1-one **161** (2.1 g, 74 %) as a clear oil. Data correspond to those described in the literature [14].

^{1}H NMR (400 MHz, $CDCl_3$): δ = 0.94 (t, J = 7.2 Hz, 3 H, CH_3), 1.36–1.54 (m, 4 H, $CH_3CH_2CH_2$), 2.30–2.35 (m, 2 H, CH_2-CH=), 6.87 (dd, J = 15.3, 1.3 Hz, 1 H, CH_2CH=C*H*), 7.07 (dt, J = 15.3, 6.9 Hz, 1 H, CH_2-C*H*=CH), 7.44–7.48 (m, 2 H, arom.), 7.53–7.57 (m, 1 H, arom.), 7.91–7.94 (m, 2 H, arom.).

Phenyl(3-butyloxiran-2-yl)methanone (123 m)

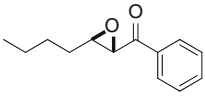

$C_{13}H_{16}O_2$ M = 204.26 g/mol

Following **GP2** with (*E*)-1-phenylhept-2-en-1-one **161** (1.60 g, 7.5 mmol, 1 equiv.), **123 m** was isolated after flash column chromatography (pentane; Et_2O = 10:1 to 10:3) as a colorless oil (1.25 g, 82 %). Spectral data are in accordance with those reported in the literature [15].

^{1}H NMR (400 MHz, $CDCl_3$): δ = 0.93 (t, J = 6.8 Hz, 3 H, CH_3), 1.36–1.77 (m, 6 H, $CH_3CH_2CH_2CH_2$), 3.14–3.16 (m, 1 H, *n*-BuC*H*O), 4.01 (d, J = 2.0 Hz, 1 H, PhC(O)C*H*O), 7.50 (t, J = 7.3 Hz, 2 H, arom.), 7.61 (t, J = 7.3 Hz, 1 H, arom.), 8.01 (d, J = 7.3 Hz, 2 H, arom.); ^{13}C NMR (100 MHz, $CDCl_3$): δ = 14.0 (CH_3), 26.8 (CH_3CH_2), 28.1 ($CH_3CH_2CH_2$), 31.8 ($CH_3CH_2CH_2CH_2$), 57.6 (CH_2CHO), 60.2 (PhC(O)C*H*O), 128.4 (2 CH arom.), 128.9 (2 CH arom.), 133.9 (CH arom.), 135.8 (C arom.), 194.9 (C=O).

(2-Methyl-3-phenyloxiran-2-yl)(phenyl)methanone (123n)

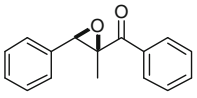

$C_{16}H_{14}O_2$ M = 238.28 g/mol

Propiophenone (4 mL, 30 mmol, 1.0 equiv.), benzaldehyde (3.6 mL, 35 mmol, 1.17 equiv.), tetrabutylammonium bromide (0.101 mg, 0.3 mmol, 0.1 equiv.) and NaOH 50 % wt in water (15 mL) were added to CCl_4 (15 mL) and stirred for 1 h 15 in a cold water bath. The resulting mixture was poured into water (100 mL) and extracted with CH_2Cl_2 (2 × 100 mL). The combined organic layers were washed with water (3 × 200 mL), dried over $MgSO_4$, concentrated *in vacuo* and purified by flash column chromatography (pentane:ether = 98:2) to afford the epoxy chalcone-type compound **123n** as a yellow oil (1.53 g, 21 %). Spectral data are in accordance with those reported in the literature [16].

^{1}H NMR (400 MHz, $CDCl_3$): δ = 1.44 (s, 3 H, CH_3), 4.17 (s, 1 H, PhC*H*O), 7.36–7.44 (m, 5 H, arom.), 7.46–7.52 (m, 2 H, arom.), 7.59–7.62 (m, 1 H, arom.), 8.05–8.07 (m, 2 H, arom.); ^{13}C NMR (100 MHz, $CDCl_3$): δ = 14.5 (CH_3), 61.8 (Ph*C*HO), 66.6 (C(O)*C*O), 126.8 (2 CH arom.), 128.4 (CH arom.), 128.5 (2 CH arom.), 128.7 (2 CH arom.), 129.4 (2 CH arom.), 133.6 (CH arom.), 134.0 (C arom.), 134.5 (C arom.), 198.4 (C=O).

3'-Isopropyl-3,4-dihydro-1*H*-spiro[naphthalene-2,2'-oxiran]-1-one (123o)

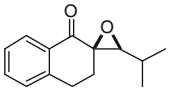

$C_{14}H_{16}O_2$ M = 216.28 g/mol

Following **GP2** with (*E*)-2-(2-methylpropylidene)-3,4-dihydronaphthalen-1(2*H*)-one [17] (1.5 g mg, 7.5 mmol, 1 equiv.), **123o** was isolated after extraction as a colorless oil (1.25 g, 74 %). Spectral data are in accordance with those reported in the literature [18].

^{1}H NMR (400 MHz, $CDCl_3$): δ = 1.00 (d, J = 6.8 Hz, 3 H, CH_3), 1.15 (d, J = 6.8 Hz, 3 H, CH_3), 1.65–1.74 (m, 1 H, Me_2CH), 2.14 (dt, J = 13.8, 4.4 Hz, 1 H, $PhCH_2CHH$), 2.49 (dt, J = 13.6, 8.4 Hz, 1 H, $PhCH_2CHH$), 2.99 (d, J = 9.5 Hz, 1 H, CHO), 3.14 (dd, J = 8.2, 4.4 Hz, 2 H, $PhCH_2$), 7.29 (d, J = 7.7 Hz, 1 H, arom.), 7.36 (t, J = 7.5 Hz, 1 H, arom.), 7.51 (t, J = 7.5 Hz, 1 H, arom.), 8.08 (d, J = 7.8 Hz, 1 H, arom.); ^{13}C NMR (100 MHz, $CDCl_3$): δ = 19.3 (CH_3), 20.2 (CH_3), 26.4 ($PhCH_2CH_2$), 27.6 (Me_2CH), 28.2 ($PhCH_2$), 62.8 (C(O)*C*O), 70.4 (*C*HO), 127.0 (CH arom.), 127.7 (CH arom.), 128.7 (CH arom.), 132.7 (C arom.), 134.1 (CH arom.), 143.4 (C arom.), 194.4 (C=O).

Phenyl(3-phenylaziridin-2-yl)methanone (171)

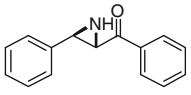

$C_{15}H_{13}NO$ M = 223.27 g/mol

To a solution of $DppONH_2$ (59 mg, 0.25 mmol, 1.05 equiv.) in MeCN (4 mL) at r.t. under argon was added NMM (28 μL, 0.25 mmol, 1.05 equiv.) dropwise.

The reaction mixture was stirred for 30 min at r.t., then NaOH (19 mg, 0.48 mmol, 2.0 equiv.) and *trans*-chalcone (50 mg, 0.24 mmol, 1 equiv.) were added sequentially. The reaction mixture was stirred for 10 h, then quenched by the addition of saturated NH_4Cl solution (2 mL), and extracted with CH_2Cl_2 (3 × 10 mL). The organic layers were combined, dried over $MgSO_4$ and concentrated *in vacuo*. Purification by flash column chromatography (pentane:EtOAc = 20:3) afforded the aziridine (28 mg, 50 %) as a white solid. Data correspond to those described in the literature [19].

^{1}H NMR (400 MHz, $CDCl_3$): δ = 2.67 (br s, 1 H, NH), 3.18 (s, 1 H, C*H*NH), 3.51 (s, 1 H, C*H*NH), 7.30–7.39 (m, 5 H, arom.), 7.47–7.51 (m, 2 H, arom.), 7.59–7.63 (m, 1 H, arom.), 8.00 (d, J = 8.3 Hz, 2 H, arom.).

Phenyl(3-phenyl-1-tosylaziridin-2-yl)methanone (172a)

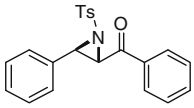

$C_{22}H_{19}NO_3S$ M = 377.46 g/mol

Following **GP3** with *trans*-chalcone (2. 60 g, 12.5 mmol, 5 equiv.), **172a** was isolated after flash column chromatography (pentane:EtOAc = 10:2–10:5) as a white solid (670 mg, 71 %). Spectral data are in accordance with those reported in the literature [20].

^{1}H NMR (400 MHz, $CDCl_3$): δ = 2.40 (s, 3 H, CH_3), 4.29 (d, J = 4.2 Hz, 1 H, PhC*H*N), 4.52 (d, J = 4.2 Hz, 1 H, PhC(O)C*H*N), 7.23 (d, J = 8.1 Hz, 2 H, arom.), 7.26–7.34 (m, 5 H, arom.), 7.46 − 7.51 (m, 2 H, arom.), 7.60–7.64 (m, 1 H, arom.), 7.72 (d, J = 8.2 Hz, 2 H, arom.), 8.04–8.06 (m, 2 H, arom.); ^{13}C NMR (100 MHz, $CDCl_3$): δ = 21.7 (CH_3), 47.6 (Ph*C*HN), 50.3 (PhC(O)*C*HN), 127.7 (2 CH arom.), 127.9 (2 CH arom.), 128.8 (2 CH arom.), 128.9 (2 CH arom.), 129.0 (CH arom.), 129.1 (2 CH arom.), 129.6 (2 CH arom.), 133.0 (C arom.), 134.2 (CH arom.), 136.1 (C arom.), 136.8 (C arom.), 144.5 (C arom.), 190.5 (C=O).

(4-Methoxyphenyl)(3-phenyl-1-tosylaziridin-2-yl)methanone (172b)

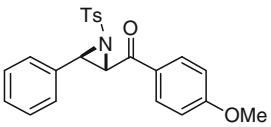

$C_{23}H_{21}NO_4S$ M = 407.48 g/mol

Following **GP3** with 4'-methoxychalcone (1.5 g, 6.2 mmol, 5 equiv.), **172b** was isolated after flash column chromatography (pentane:EtOAc = 10:2–10:5) as a beige oil (301 mg, 59 %). Spectral data are in accordance with those reported in the literature [21].

^{1}H NMR (400 MHz, $CDCl_3$): δ = 2.39 (s, 3 H, C-*C*H_3), 3.87 (s, 3 H, OCH_3), 4.26 (d, J = 4.4 Hz, 1H, PhC*H*N), 4.50 (d, J = 4.4 Hz, 1 H, C(O)C*H*N),

6.93–6.96 (m, 2 H, arom.), 7.21 (d, $J = 8.1$ Hz, 2 H, arom.), 7.31–7.39 (m, 5 H, arom.), 7.71 (d, $J = 8.4$ Hz, 2 H, arom.), 8.02–8.06 (m, 2 H, arom.); ^{13}C NMR (100 MHz, $CDCl_3$): $\delta = 21.7$ (C-*C*H_3), 47.4 (Ph*C*HN), 50.2 (C(O)*C*HN), 55.7 (OCH_3), 114.1(2 CH arom.), 127.6 (2 CH arom.), 127.8 (CH arom.), 128.7 (2 CH arom.), 128.9 (CH arom.), 129.2 (C arom.), 129.6 (2 CH arom.), 131.5 (2 CH arom.), 133.2 (C arom.), 136.8 (C arom.), 144.4 (C arom.), 164.4 (C arom.), 188.5 (C=O).

Phenyl(2-phenylcyclopropyl)methanone (175a)

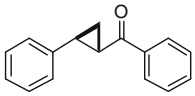

$C_{16}H_{14}O$ M = 222.28 g/mol

To a solution of *trans*-chalcone (5.20 g, 25.0 mmol, 1 equiv.) and TBAI (135 mg, 0.34 mmol, 0.001 equiv.) in CH_2Cl_2 (25 mL) at r.t. were added NaOH as a 50 % wt aqueous solution (25 mL) and trimethylsulfonium iodide (5.50 g, 25 mmol, 1 equiv.). The reaction mixture was stirred at 80 °C for 48 h, quenched with iced-cool water and extracted with CH_2Cl_2 (2 × 25 mL). The combined organic layers were washed with water (50 mL), dried over $MgSO_4$, concentrated *in vacuo* and purified by flash column chromatography (pentane:Et_2O = 20:1) to afford the cyclopropane **175a** as an oily solid (4.70 g, 86 %). Data correspond with those described in the literature [22].

^{1}H NMR (400 MHz, $CDCl_3$): $\delta = 1.54$–1.59 (m, 1 H, C*H*H), 1.94 (ddd, $J = 9.0$, 4.8, 4.4 Hz, 1 H, CH*H*), 2.69–2.74 (m, 1 H, PhC*H*), 2.91 (ddd, $J = 8.6$, 4.4, 4.0 Hz, 1 H, Ph(CO)C*H*), 7.18–7.26 (m, 3 H, arom.), 7.30–7.34 (m, 2 H, arom.), 7.45–7.49 (m, 2 H, arom.), 7.55–7.59 (m, 1 H, arom.), 8.00 (d, $J = 8.0$ Hz, 2 H, arom.); ^{13}C NMR (100 MHz, $CDCl_3$): $\delta = 19.4$ (CH_2), 29.4 (Ph*C*H), 30.1 (Ph(CO)*C*H), 126.4 (2 CH arom.), 126.7 (CH arom.), 128.2 (2 CH arom.), 128.7 (4 CH arom.), 133.0 (CH arom.), 137.9 (C arom.), 140.6 (C arom.), 198.7 (C=O).

6.4 Reductive Ring-Opening Products

3-Hydroxy-1,3-diphenylpropan-1-one (148a)

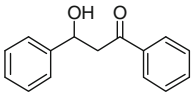

$C_{15}H_{14}O_2$ M = 226.27 g/mol

Following **GP4** with **123a** (44 mg, 0.2 mmol, 1 equiv.), **148a** was purified by flash column chromatography (pentane:EtOAc = 10 :2 then 10 :3) and isolated as

a colorless oil (41 mg, 91 %). Spectral data are in accordance with those reported in the literature [23].

^{1}H NMR (400 MHz, $CDCl_3$): $\delta = 3.38$ (d, $J = 6.4$ Hz, 2 H, CH_2CH), 3.59 (d, $J = 2.6$ Hz, 1 H, O*H*), 5.36 (td, $J = 6.2$, 2.2 Hz, 1 H, CH_2C*H*OH), 7.29–7.31 (m, 1 H, arom.), 7.37–7.41 (m, 2 H, arom.), 7.44–7.47 (m, 4 H, arom.), 7.57–7.61 (m, 1 H, arom.), 7.95–7.97 (m, 2 H, arom.); ^{13}C NMR (100 MHz, $CDCl_3$): $\delta = 47.5$ (CH_2), 70.2 (CHOH), 125.9 (2 CH arom.), 127.8 (CH arom.), 128.3 (2 CH arom.), 128.7 (2 CH arom.), 128.8 (2 CH arom.), 133.8 (CH arom.), 136.4 (C arom.), 143.1 (C arom.), 200.3 (C=O).

Methyl 4-(3-hydroxy-3-phenylpropanoyl)benzoate (148b)

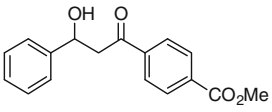

$C_{17}H_{16}O_4$ M = 284.31 g/mol

Following **GP4** with methyl **123b** (57 mg, 0.2 mmol, 1 equiv.), **148b** was purified by flash column chromatography (pentane:EtOAc = 10 :2 then 10 :3) and isolated as a white solid (31 mg, 55 %).

Mp: 96–97 °C; IR (neat): $\nu = 3508$, 2953, 2360, 1723, 1685, 1280, 1109, 755, 700 cm^{-1}; ^{1}H NMR (400 MHz, $CDCl_3$): $\delta = 3.34$ (dd, A of ABX, $J_{AX} = 3.2$ Hz, $J_{AB} = 17.6$ Hz, 1 H, CH*H*CHOH), 3.43 (dd, B of ABX, $J_{BX} = 9.2$ Hz, $J_{AB} = 17.6$ Hz, 1 H, C*H*HCHOH), 3.46 (br s, 1 H, OH), 3.95 (s, 3 H, CO_2CH_3), 5.37 (dd, X of ABX, $J_{AX} = 3.2$, $J_{BX} = 8.8$ Hz, 1 H, CH_2C*H*OH), 7.27–7.44 (m, 5 H, arom.), 8.01 (d, $J = 8.4$ Hz, 2 H, arom.), 8.12 (d, $J = 8.4$ Hz, 2 H, arom.); ^{13}C NMR (100 MHz, $CDCl_3$): $\delta = 48.0$ (CH_2), 52.6 (CO_2CH_3), 70.0 (CH-OH), 125.8 (2 CH arom.), 127.9 (CH arom.), 128.2 (2 CH arom.), 128.7 (2 CH arom.), 130.0 (2 CH arom.), 134.4 (C arom.), 139.9 (C arom.), 142.9 (C arom.), 166.2 (CO_2Me), 199.5 (C=O); HRMS calcd. for $C_{17}H_{16}O_4Na$ ([M + Na]$^+$) 307.09481, found 307.09390.

3-Hydroxy-1-(4-methoxyphenyl)-3-phenylpropan-1-one (148c)

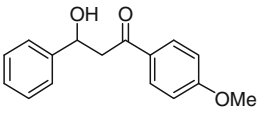

$C_{16}H_{16}O_3$ M = 256.30 g/mol

Following **GP4** with **123c** (50.7 mg, 0.2 mmol, 1 equiv.), **148c** was purified by flash column chromatography (pentane:EtOAc = 10 :3) and isolated as a light yellow solid (39 mg, 76 %). Spectral data are in accordance with those reported in the literature [23].

^{1}H NMR (400 MHz, $CDCl_3$): $\delta = 3.30$–3.32 (m, 2 H, CH_2CHOH), 3.74 (br s, 1 H, O*H*), 3.87 (s, 3 H, OCH_3), 5.33 (dd, $J = 3.6$, 8 Hz, 1 H, CH_2C*H*OH), 6.93 (d,

J = 8.8 Hz, 2 H, arom.), 7.28–7.45 (m, 5 H, arom.), 7.94 (d, J = 8.4 Hz, 2 H, arom.); ^{13}C NMR (100 MHz, $CDCl_3$): δ = 47.0 (CH_2), 55.6 (OCH_3), 70.3 (CHOH), 113.9 (2 CH arom.), 125.9 (2 CH arom.), 127.7 (CH arom.), 128.6 (2 CH arom.), 129.8 (C arom.), 130.6 (2 CH arom.), 143.2 (C arom.), 164.0 (C arom.), 198.8 (C=O); HRMS calcd. for $C_{16}H_{16}O_3Na$ ([M + Na]$^+$) 279.09917, found 279.09920.

3-Hydroxy-3-phenyl-1-(4-(trifluoromethyl)phenyl)propan-1-one (148d)

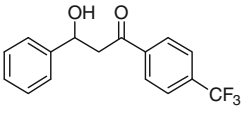

$C_{16}H_{13}F_3O_2$ M = 294.27 g/mol

Following **GP4** with **123d** (59 mg, 0.2 mmol, 1 equiv.), **148d** was purified by flash column chromatography (pentane:EtOAc = 10 :3) and isolated as a white solid (45 mg, 76 %).

Mp: 110–111 °C; IR (neat): ν = 3439, 1686, 1410, 1324, 1169, 1128, 1066, 1015, 701 cm^{-1}; ^{1}H NMR (400 MHz, $CDCl_3$): δ = 3.28 (br s, 1 H, O*H*), 3.33–3.48 (m, 2 H, CH_2CHOH), 5.38 (dd, J = 8.8 Hz, 2.8 Hz, 1 H, CH_2C*H*OH), 7.30–7.45 (m, 5 H, arom.), 7.74 (d, J = 8.4 Hz, 2 H, arom.), 8.06 (d, J = 8.0 Hz, 2 H, arom.); ^{13}C NMR (100 MHz, $CDCl_3$): δ = 48.0 (CH_2), 70.1 (CHOH), 123.7 (q, $^1J_{C\text{-}F}$ = 271.1 Hz, *C*F_3), 125.8 (2 CH arom.), 125.9 (q, $^3J_{C\text{-}F}$ = 3.7 Hz, 2 CH arom.), 128.0 (CH arom.), 128.7 (2 CH arom.), 128.8 (2 CH arom.), 135.0 (q, $^2J_{C\text{-}F}$ = 32.7 Hz, C arom.), 139.4 (C arom.), 142.9 (C arom.), 199.1 (C=O); ^{19}F NMR (377 MHz, $CDCl_3$): δ = −63.1; HRMS calcd. for $C_{16}H_{13}F_3O_2Na$ ([M + Na]$^+$) 317.0760, found 317.0756.

Methyl 4-(1-hydroxy-3-oxo-3-phenylpropyl)benzoate (148e)

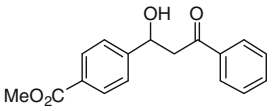

$C_{17}H_{16}O_4$ M = 284.31 g/mol

Following **GP4** with **123e** (56.6 mg, 0.2 mmol, 1 equiv.), **148e** was purified by flash column chromatography (pentane:AcOEt = 10:3) and isolated as a white solid (34 mg, 60 %).

IR (neat): ν = 3486, 2952, 1718, 1681, 1411, 1279, 1112, 1018, 754, 690 cm^{-1}; ^{1}H NMR (400 MHz, $CDCl_3$): δ = 3.28 (br s, 1 H, OH), 3.36–3.38 (m, 2 H, CH_2), 3.92 (s, 3 H, CO_2CH_3), 5.41 (dd, J = 3.6, 8 Hz, 1 H, CH_2-C*H*-OH), 7.46–7.53 (m, 4 H, arom.), 7.58–7.62 (m, 1 H, arom.), 7.95 (d, J = 7.6 Hz, 2 H, arom.), 8.05 (d, J = 8 Hz, 2 H, arom.); ^{13}C NMR (100 MHz, $CDCl_3$): δ = 47.2 (CH_2), 52.2 (CO_2CH_3), 69.7 (CH-OH), 125.8 (2 CH arom.), 128.2 (2 CH arom.), 128.8 (2 CH

arom.), 130.0 (2 CH arom.), 133.9 (CH arom.), 136.4 (C arom.), 139.4 (C arom.), 148.2 (C arom.), 167.0 (CO_2CH_3), 199.9 (C=O).

3-Hydroxy-3-(4-methoxyphenyl)-1-phenylpropan-1-one (148f)

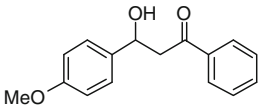

$C_{16}H_{16}O_3$ M = 256.30 g/mol

Following **GP4** with **123f** (50.6 mg, 0.2 mmol, 1 equiv.), **148f** was purified by flash column chromatography (pentane:Et_2O = 6:4) and isolated as a colorless oil (28 mg, 54 %). Data correspond to those described in the literature [23].

^{1}H NMR (400 MHz, $CDCl_3$): δ = 3.36–3.38 (m, 2 H, CH_2-CHOH), 3.82 (s, 3 H, OCH_3), 5.30 (dd, J = 4.8, 7.6 Hz, 1H, CH_2-CH-OH), 6.92 (d, J = 8.8 Hz, 2 H, arom.), 7.36 (d, J = 8.8 Hz, 2 H, arom.), 7.45-7.49 (m, 2 H, arom.), 7.57–7.61 (m, 1H, arom.), 7.95–7.97 (m, 2 H, arom.).

3-Hydroxy-1-phenyl-3-(4-(trifluoromethyl)phenyl)propan-1-one (148g)

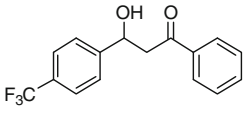

$C_{16}H_{13}F_3O_2$ M = 294.27 g/mol

Following **GP4** with **123g** (59 mg, 0.2 mmol, 1 equiv.), **148g** was purified by flash column chromatography (pentane:EtOAc = 10:3) and isolated as a white solid (46 mg, 78 %).

Mp: 101–102 °C; IR (neat): ν = 3453, 2923, 1680, 1450, 1325, 1164, 1122, 1067, 1017, 841, 758, 689 cm^{-1}; ^{1}H NMR (400 MHz, $CDCl_3$): δ = 3.31–3.43 (m, 2 H, CH_2CHOH), 3.72 (d, J = 3.2 Hz, 1 H, OH), 5.41–5.43 (m, 1 H, CH_2CHOH), 7.46–7.50 (m, 2 H, arom.), 7.56–7.63 (m, 5 H, arom.), 7.94–7.97 (m, 2 H, arom.); ^{13}C NMR (100 MHz, $CDCl_3$): δ = 47.3 (CH_2), 69.6 (CHOH), 121.5 (q, $^1J_{C\text{-}F}$ = 275.1 Hz, CF_3), 125.7 (q, $^3J_{C\text{-}F}$ = 3.8 Hz, 2 CH arom.), 126.2 (2 CH arom.), 128.3 (2 CH arom.), 129.0 (2 CH arom.), 130.4 (q, $^2J_{C\text{-}F}$ = 32.1 Hz, C arom.) 134.0 (CH arom.), 136.5 (C arom.), 147.0 (C arom.), 200.0 (C=O); ^{19}F NMR (377 MHz, $CDCl_3$): δ = −62.5; HRMS calcd. for $C_{16}H_{13}O_2F_3Na$ ([M + Na]$^+$) 317.0760, found 317.0756.

3-Hydroxy-1-(naphthalen-2-yl)-3-phenylpropan-1-one (148 h)

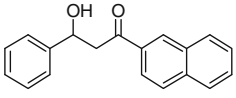

$C_{19}H_{16}O_2$ M = 276.33 g/mol

Following **GP4** with **123 h** (55 mg, 0.2 mmol, 1 equiv.), **148 h** was purified by flash column chromatography (pentane:EtOAc = 10:3) and isolated as white solid (23 mg, 42 %). Spectral data are in accordance with those reported in the literature [24].

^{1}H NMR (400 MHz, $CDCl_3$): δ = 3.52 (d, J = 6.0 Hz, 2 H, CH_2CHOH), 3.73 (br s, 1 H, O*H*), 5.42 (t, J = 6.0 Hz, 1 H, CH_2C*H*OH), 7.31–7.35 (m, 1 H, arom.), 7.39–7.43 (m, 2 H, arom.), 7.48–7.50 (m, 2 H, arom.), 7.54–7.64 (m, 2 H, arom.), 7.87–7.94 (m, 3 H, arom.), 8.02–8.05 (m, 1 H, arom.), 8.45 (s, 1 H, arom.); ^{13}C NMR (100 MHz, $CDCl_3$): δ = 47.6 (CH_2), 70.3 (CH-OH), 123.7 (CH arom.), 125.9 (2 CH arom.), 127.1 (CH arom.), 127.8 (CH arom.), 127.9 (CH arom.), 128.7 (3 CH arom.), 128.9 (CH arom.), 129.8 (CH arom.), 130.3 (CH arom.), 132.6 (C arom.), 134.0 (C arom.), 136.0 (C arom.), 143.2 (C arom.), 200.2 (C=O).

3-(4-Chlorophenyl)-3-hydroxy-1-phenylpropan-1-one (148j)

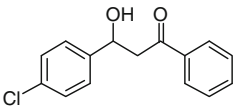

$C_{15}H_{13}ClO_2$ M = 260.72 g/mol

Following **GP4** with **123j** (52 mg, 0.2 mmol, 1 equiv.), **148j** was purified by flash column chromatography (pentane:EtOAc = 10:2) and isolated as a colorless oil (45 mg, 86 %). Spectral data are in accordance with those reported in the literature [24].

^{1}H NMR (400 MHz, $CDCl_3$): δ = 3.33–3.35 (m, 2 H, CH_2CHOH), 3.66 (d, J = 3.0 Hz, 1 H, O*H*), 5.30–5.34 (m, 1 H, C*H*OH), 7.33–7.37 (m, 4 H, arom.), 7.45–7.49 (m, 2 H, arom.), 7.58–7.62 (m, 1 H, arom.), 7.95 (d, J = 7.1 Hz, 2 H, arom.); ^{13}C NMR (100 MHz, $CDCl_3$): δ = 47.4 (CH_2), 69.6 (CH-OH), 127.3 (2 CH arom.), 128.3 (2 CH arom.), 128.8 (2 CH arom.), 128.9 (2 CH arom.), 133.5 (C arom.), 133.9 (CH arom.), 136.6 (C arom.), 141.6 (C arom.), 200.1 (C=O).

4-Hydroxy-4-phenylbutan-2-one (148 l)

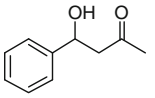

$C_{10}H_{12}O_2$ M = 164.20 g/mol

Following **GP4** (with HPDMBI [25] (1.1 equiv.) instead of Hantzsch ester) with **123 l** (47 mg, 0.3 mmol, 1 equiv.), after 24 h of irradiation, **148 l** was purified by flash column chromatography (pentane:EtOAc = 10 :2 then 10 :3) and isolated as a colorless oil (30 mg, 60 %). Spectral data are in accordance with those reported in the literature [26].

^{1}H NMR (400 MHz, $CDCl_3$): δ = 2.20 (s, 3 H, Me), 2.78–2.94 (m, 2 H, CH_2), 3.23 (br s, 1 H, OH), 5.14–5.17 (m, 1 H, CH_2C*H*OH), 7.26–7.36 (m, 5 H, arom.);

^{13}C NMR (100 MHz, $CDCl_3$): δ = 30.9 (Me), 52.1 (CH_2), 70.0 (CHOH), 125.8 (2 CH arom.), 127.8 (CH arom.), 128.7 (2 CH arom.), 143.1 (C arom.), 209.0 (C=O).

3-Hydroxy-1-phenylheptan-1-one (148 m)

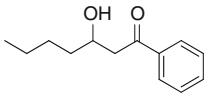

$C_{13}H_{18}O_2$ M = 206.28 g/mol

Following **GP4** with **123 m** (102 mg, 0.5 mmol, 1 equiv.), **148 m** was purified by flash column chromatography (pentane:EtOAc = 10:3) and isolated as a colorless oil (54 mg, 52 %). Spectral data are in accordance with those reported in the literature [27].

^{1}H NMR (400 MHz, $CDCl_3$): δ = 0.92 (t, J = 6.8 Hz, 3 H, CH_3), 1.33–1.64 (m, 6H, $CH_3CH_2CH_2CH_2$), 3.03 (dd, A of ABX, J_{AX} = 8.9 Hz, J_{AB} = 17.6 Hz, 1 H, C(O)CH*H*), 3.17 (dd, B of ABX, J_{BX} = 2.8 Hz, J_{AB} = 17.6 Hz, 1 H, C(O)C*H*H), 3.24 (br s, 1 H, O*H*), 4.19–4.23 (m, 1 H, CH_2CHOH), 7.45–7.49 (m, 2 H, arom.), 7.56–7.60 (m, 1 H, arom.), 7.94–7.97 (m, 2 H, arom.); ^{13}C NMR (100 MHz, $CDCl_3$): δ = 14.2 (CH_3), 22.8 (CH_3CH_2), 27.9 ($CH_3CH_2CH_2$), 36.4 ($CH_3CH_2CH_2CH_2$), 45.2 (C(O)CH_2), 67.9 (CHOH), 128.2 (2 CH arom.), 128.8 (2 CH arom.), 133.6 (CH arom.), 137.0 (C arom.), 201.2 (C=O).

3-Hydroxy-1-mesityl-3-phenylpropan-1-one (123 k)

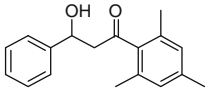

$C_{18}H_{20}O_2$ M = 268.35 g/mol

Following **GP5** with **123 k** (53 mg, 0.2 mmol, 1 equiv.), **148 k** was purified by flash column chromatography (pentane:EtOAc = 20:3) and isolated as a colorless oil (38 mg, 70 %). Spectral data correspond to those described in the literature [28].

^{1}H NMR (400 MHz, $CDCl_3$): δ = 2.20 (s, 6 H, 2 CH_3), 2.27 (s, 3 H, CH_3), 3.08 (dd, A of ABX, J_{AX} = 3.6 Hz, J_{AB} = 18.2 Hz, 1 H, CH*H*CHOH), 3.15 (dd, B of ABX, J_{BX} = 8.6 Hz, J_{AB} = 18.2 Hz, 1 H, C*H*HCHOH), 3.44 (d, J = 3.1 Hz, 1 H, OH), 5.33–5.37 (m, 1 H, CH_2CHOH), 6.83 (s, 2 H, arom.), 7.28–7.42 (m, 5 H, arom.); ^{13}C NMR (100 MHz, $CDCl_3$): δ = 19.2 (2 CH_3), 21.2 (CH_3), 53.4 (CH_2), 70.0 (CHOH), 125.9 (2 CH arom.), 127.9 (CH arom.), 128.7 (2 CH arom.), 128.8 (2 CH arom.), 132.8 (3 C arom.), 139.0 (C arom.), 142.9 (C arom.), 211.1 (C=O).

3-Hydroxy-2-methyl-1,3-diphenylpropan-1-one (148 m)

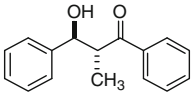

$C_{16}H_{16}O_2$ M = 240.30 g/mol

Following **GP5** with **123 m** (53 mg, 0.2 mmol, 1 equiv.), **148 m** was purified by flash column chromatography (pentane:EtOAc = 10:2) and isolated as a colorless oil [40 mg, 83 %, inseparable mixture of diastereomers (*syn/anti* = 46:54)]. Data correspond to those described in the litterature [29].

^{1}H NMR (400 MHz, $CDCl_3$): δ = 1.07 (d, J = 7.2 Hz, 3 H, CH_3, dia. anti), 1.20 (d, J = 7.6 Hz, 3 H, CH_3, dia. syn), 2.97 (br s, 1 H, OH, dia. anti), 3.63 (br s, 1 H, OH, dia. syn), 3.71 (qd, J = 7.2, 3.2 Hz, 1 H, CH_3CH, dia. syn), 3.84 (quint, J = 7.8 Hz, 1 H, CH_3CH, dia. anti), 5.00 (d, J = 7.8 Hz, 1 H, C*H*OH, dia. anti), 5.25 (d, J = 2.8 Hz, 1 H, C*H*OH, dia. syn), 7.28–7.47 (m, 14 H, arom., 2 dia.), 7.55–7.59 (m, 2 H, arom., 2 dia.), 7.93–7.94 (m, 2 H, arom., dia. syn), 7.96–7.98 (m, 2 H, arom., dia. anti); ^{13}C NMR (100 MHz, $CDCl_3$): δ = 11.3 (CH_3, dia. syn), 15.9 (CH_3, dia. anti), 47.2 (CH_3CH, dia. syn), 48.1 (CH_3CH, dia. anti), 73.2 (CHOH, dia. syn), 77.0 (CHOH, dia. anti), 126.2 (2 CH arom., dia. syn), 126.9 (2 CH arom., dia. anti), 127.5 (CH arom., dia. syn), 128.1 (CH arom., dia. anti), 128.4 (2 CH arom., dia. syn), 128.6 (2 CH arom., dia. anti), 128.7 (4 CH arom., 2 dia.), 128.8 (2 CH arom, dia. anti), 128.9 (2 CH arom, dia. syn), 133.4 (CH arom., dia. anti), 133.7 (CH arom., dia. syn), 135.8 (C arom., dia. syn), 136.9 (C arom., dia. anti), 142.0 (C arom., dia. syn), 142.3 (C arom., dia. anti), 205.1 (C=O, dia. anti), 205.9 (C=O, dia. syn).

2-(1-Hydroxy-2-methylpropyl)-3,4-dihydronaphthalen-1(2*H*)-one (148n)

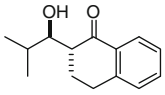

$C_{14}H_{18}O_2$ M = 218.29 g/mol

Following **GP5** with **123n** (43 mg, 0.2 mmol, 1 equiv.), **148n** was purified by flash column chromatography (pentane:EtOAc = 10:1) and isolated as a yellow solid (38 mg, 87 %, separable mixture of diastereomers (syn/anti = 24:76)). Spectral data are in accordance with those reported in the literature [30].

anti isomer (majo): ^{1}H NMR (400 MHz, $CDCl_3$): δ = 0.90 (d, J = 6.4 Hz, 3 H, CH_3), 1.09 (d, J = 6.8 Hz, 3 H, CH_3), 1.76–1.82 (m, 1 H, $(CH_3)_2CH$), 2.13–2.16 (m, 2 H, Ph-CH_2-CH_2), 2.28–2.30 (m, 1 H, OH), 2.66–2.69 (m, 1 H, C(O)-CH), 3.03–3.06 (m, 2 H, Ph-CH_2), 4.05–4.09 (m, 1 H, OH-C*H*), 7.25 (d, J = 7.6 Hz, 1 H, arom.), 7.30 (t, J = 7.6 Hz, 1 H, arom.), 7.47 (t, J = 7.6 Hz, 1 H, arom.), 8.02 (d, J = 7.6 Hz, 1 H, arom.); ^{13}C NMR (100 MHz, $CDCl_3$): δ = 19.1 (CH_3), 19.8 (CH_3), 22.2 (Ph-CH_2-*C*H_2), 29.2 (Ph-*C*H_2), 30.1 (Me_2CH), 50.9 (C(O)-*C*H), 75.1 (CH-OH), 126.7 (CH arom.), 127.4 (CH arom.), 128.9 (CH arom.), 133.2 (C arom.), 133.7 (CH arom.), 144.3 (C arom.), 201.1 (C=O).

syn isomer (mino): ^{1}H NMR (400 MHz, $CDCl_3$): δ = 0.96 (d, J = 6.8 Hz, 3 H, CH_3), 1.06 (d, J = 7.2 Hz, 3 H, CH_3), 1.82–1.99 (m, 2 H, $(CH_3)_2CH$ + Ph-CH_2CH*H*), 2.15–2.18 (m, 1 H, Ph-CH_2-C*H*H), 2.55–2.59 (m, 1 H, C(O)-CH), 2.95–3.16 (m, 2 H, Ph-CH_2), 3.76 (dd, J = 6.8, 3.2 Hz, 1 H, OH-C*H*), 4.08 (br s, 1 H, OH), 7.24 (d, J = 8.0 Hz, 1 H, arom.), 7.31 (t, J = 8.0 Hz, 1 H, arom.),

7.47–7.51 (m, 1 H, arom.), 8.02 (d, $J = 8.0$ Hz, 1 H, arom.); ^{13}C NMR (100 MHz, $CDCl_3$): $\delta = 15.0$ (CH_3), 20.2 (CH_3), 25.9 (Ph-CH_2-CH_2), 29.0 (Ph-CH_2), 29.7 (Me_2CH), 50.9 (C(O)-CH), 76.1 (CH-OH), 126.9 (CH arom.), 127.6 (CH arom.), 128.8 (CH arom.), 132.7 (C arom.), 133.9 (CH arom.), 144.3 (C arom.), 203.2 (C=O).

4-Methyl-N-(3-oxo-1,3-diphenylpropyl)benzenesulfonamide (174a)

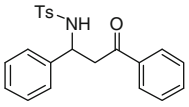

$C_{22}H_{21}NO_3S$ M = 379.47 g/mol

Following **GP4** with **172a** (38 mg, 0.1 mmol, 1 equiv.), **174a** was purified by flash column chromatography (pentane:EtOAc = 10:3) and isolated as a white solid (36 mg, 94 %). Spectral data are in accordance with those reported in the literature [31].

^{1}H NMR (400 MHz, $CDCl_3$): $\delta = 2.36$ (s, 3 H, CH_3), 3.46 (dd, A of ABX, $J_{AB} = 17.2$ Hz, $J_{AX} = 6.2$ Hz, 1 H, C(O)-CHH), 3.58 (dd, B of ABX, $J_{AB} = 17.3$ Hz, $J_{BX} = 5.5$ Hz, 1 H, C(O)-CHH), 4.84–4.89 (m, 1 H, CH-NH), 5.71 (d, $J = 6.8$ Hz, 1 H, NH), 7.15 −7.18 (m, 7H, arom.), 7.41 (t, $J = 7.9$ Hz, 2 H, arom.), 7.54 (t, $J = 7.2$ Hz, 1 H, arom.), 7.62 (d, $J = 8.4$ Hz, 2 H, arom.), 7.80 (d, $J = 7.2$ Hz, 2 H, arom.); ^{13}C NMR (100 MHz, $CDCl_3$): $\delta = 21.6$ (CH_3), 44.9 (CH_2), 54.6 (CH-NH), 126.8 (2 CH arom.), 127.3 (2 CH arom.), 127.8 (CH arom.), 128.2 (2 CH arom.), 128.7 (2 CH arom.), 128.8 (2 CH arom.), 129.6 (2 CH arom.), 133.7 (CH arom.), 136.5 (C arom.), 137.4 (C arom.), 140.0 (C arom.), 143.4 (C arom.), 197.9 (C=O).

N-(3-(4-Methoxyphenyl)-3-oxo-1-phenylpropyl)-4-methylbenzenesulfonamide (174b)

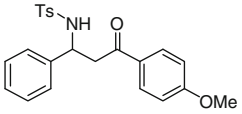

$C_{23}H_{23}NO_4S$ M = 409.50 g/mol

Following **GP4** with **172b** (67 mg, 0.17 mmol, 1 equiv.), **174b** was purified by flash column chromatography (pentane:EtOAc = 10:4) and isolated as a oily solid (55 mg, 81 %).

IR (neat): $\nu = 3300$, 1672, 1599, 1259, 1156 cm^{-1}; ^{1}H NMR (400 MHz, $CDCl_3$): $\delta = 2.34$ (s, 3 H, C-CH_3), 3.36 (dd, A of ABX, $J_{AB} = 17.2$ Hz, $J_{AX} = 6.4$ Hz, 1 H, C(O)-CHH), 3.49 (dd, B of ABX, $J_{AB} = 17.2$ Hz, $J_{BX} = 6.0$ Hz, 1 H, C(O)-CHH), 3.84 (s, 3 H, O-CH_3), 4.82–4.87 (m, 1 H, CH-NH), 5.94 (d, $J = 6.8$ Hz, 1 H, NH), 6.84 −6.87 (m, 2 H, arom.), 7.12–7.16 (m, 7H, arom.), 7.60 (d, $J = 8.4$ Hz, 2 H, arom.), 7.75–7.79 (m, 2 H, arom.); ^{13}C NMR

(100 MHz, $CDCl_3$): δ = 21.6 (C-CH_3), 44.4 (CH_2), 54.7 (CH-NH), 55.6 (O-CH_3), 113.9 (2 CH arom.), 126.8 (2 CH arom.), 127.3 (2 CH arom.), 127.6 (CH arom.), 128.6 (2 CH arom.), 129.5 (2 CH arom.), 129.6 (C arom.), 130.5 (2 CH arom.), 137.4 (C arom.), 140.0 (C arom.), 143.2 (C arom.), 164.0 (C arom.), 196.4 (C=O); HRMS calcd. for $C_{23}H_{23}O_4NSNa$ ([M + Na]$^+$) 432.1240, found 432.1240.

4-Methyl-N-(1-oxo-1-phenylheptan-3-yl)benzenesulfonamide (174c)

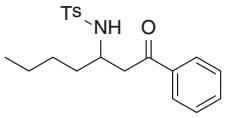

$C_{20}H_{25}NO_3S$ M = 359.48 g/mol

Following **GP4** with **172c**[1] (36 mg, 0.1 mmol, 1 equiv.), **174c** was purified by flash column chromatography (pentane:EtOAc = 10:2) and isolated as a white solid (28 mg, 78 %).

Mp: 95–96 °C; IR (neat): ν = 3284, 2956, 1681, 1597, 1326, 1157, 665 cm^{-1}; ^{1}H NMR (400 MHz, $CDCl_3$): δ = 0.77 (t, J = 7.2 Hz, 3 H, CH_2-CH_3), 1.03–1.25 (m, 4 H, CH_3-CH_2-CH_2), 1.50–1.54 (m, 2 H, CH_3-CH_2-CH_2-CH_2), 2.32 (s, 3 H, C-CH_3), 3.02 (dd, A of ABX, J_{AX} = 6.3 Hz, J_{AB} = 17.3 Hz, 1 H, C(O)-CH*H*), 3.18 (dd, B of ABX, J_{BX} = 3.9 Hz, J_{AB} = 17.3 Hz, 1 H, C(O)-C*H*H), 3.63–3.68 (m, 1 H, C*H*-NH), 5.26 (d, J = 8.4 Hz, 1 H, NH), 7.21 (d, J = 8.0 Hz, 2 H, arom.), 7.41–7.45 (m, 2 H, arom.), 7.53–7.57 (m, 1 H, arom.), 7.73 (d, J = 8.3 Hz, 2 H, arom.), 7.79–7.82 (m, 2 H, arom.); ^{13}C NMR (100 MHz, $CDCl_3$): δ = 13.8 (CH_2-*C*H_3), 21.6 (C-*C*H_3), 22.3 (CH_3-*C*H_2), 28.2 (CH_3-CH_2-*C*H_2), 34.6 (CH_3-CH_2-CH_2-*C*H_2), 42.6 (C(O)-*C*H_2), 51.1 (CH-NH), 127.2 (2 CH arom.), 128.1 (2 CH arom.), 128.7 (2 CH arom.), 129.7 (2 CH arom.), 133.6 (CH arom.), 136.8 (C arom.), 137.8 (C arom.), 143.3 (C arom.), 198.8 (C=O); HRMS calcd. for $C_{20}H_{25}O_3NSNa$ ([M + Na]$^+$) 382.1447, found 382.1446.

1,4-Diphenylbutan-1-one (181)

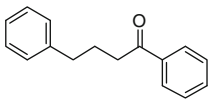

$C_{16}H_{16}O$ M = 224.30 g/mol

A dried schlenk equipped with a stir bar was loaded with Hantzsch ester (28 mg, 0.11 mmol, 1.1 equiv.), cyclopropanes derivative **175a** (22 mg; 0.1 mmol, 1 equiv.) and $Irppy_3$ (3.3 mg, 0.005 mmol, 5 mol%). The schlenk was evacuated and back-filled with argon three times, before degassed DMSO (1 mL) and *i*Pr_2NEt (19 µL,

[1] (3-butyl-1-tosylaziridin-2-yl)(phenyl)methanone was synthesized in one step from (*E*)-1-phenylhept-2-en-1-one. Spectral data are in accordance with those described in the literature: [32].

0.11 mmol, 1.1 equiv.) were added under argon. The yellow reaction mixture was irradiated at r.t. with a 14 W light bulb for 15 h. The reaction was quenched with water (15 mL) and extracted with EtOAc (3 × 10 mL). The combined organic layers were dried over $MgSO_4$, concentrated *in vacuo* and purified by flash column chromatography (pentane:EtOAc = 10:1) to afford 181 (13 mg, 60 %) as a colorless oil. Spectral data correspond to those described in the literature [33].

^{1}H NMR (400 MHz, $CDCl_3$): δ = 2.05–2.13 (m, 2 H, $PhCH_2$-CH_2), 2.71 (t, J = 6.0 Hz, 2 H, PhCH_2), 2.98 (t, J = 7.2 Hz, 2 H, PhC(O)CH_2), 7.18–7.31 (m, 5 H, arom.), 7.42–7.46 (m, 2 H, arom.), 7.53–7.56 (m, 1 H, arom.), 7.91 (d, J = 7.5 Hz, 2 H, arom.); ^{13}C NMR (100 MHz, $CDCl_3$): δ = 25.8 ($PhCH_2$-CH_2), 35.4 (PhCH_2), 37.8 (PhC(O)CH_2), 126.1 (CH arom.), 128.2 (2 CH arom.), 128.5 (2 CH arom), 128.7 (4 CH arom.), 133.1 (CH arom.), 141.8 (C arom.), 142.4 (C arom.), 200.3 (C=O).

6.5 Allylation Products

6.5.1 Allylating Agents

1-Methyl-4-(2-methylallylsulfonyl)benzene (193)

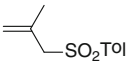

$C_{11}H_{14}O_2S$ M = 210.3 g/mol

A mixture of 3-chloro-2-methyl propene **191** (2.7 mL, 27.6 mmol, 1 equiv.) and sodium *p*-toluene sulfinate **192** (10.0 g, 56.1 mmol, 2 equiv.) in DMF (40 mL) was stirred at 60 °C for 3 h. The reaction mixture was quenched with water (200 mL) and extracted with EtOAc (3 × 70 mL). The combined organic layers were dried over $MgSO_4$, concentrated *in vacuo* and recristallized from pentane to afford the pure allylsulfone **193** as a white solid (4.5 g, 78 %). Spectral data are in accordance with those reported in the literature [34].

^{1}H NMR (400 MHz, $CDCl_3$): δ = 1.85 (s, 3 H, CH_3C), 2.44 (s, 3 H, CH_3C), 3.74 (s, 2 H, CH_2), 4.68 (br s, 1 H, =CHH), 5.01–5.03 (m, 1 H, =CHH), 7.33 (d, J = 7.9 Hz, 2 H, arom.), 7.74 (d, J = 7.9 Hz, 2 H, arom.); ^{13}C NMR (100 MHz, $CDCl_3$): δ = 21.7 (CH_3C), 22.8 (CH_3C), 64.6 (CH_2S), 120.7 (=CH_2), 128.5 (2 CH arom.), 129.7 (2 CH arom.), 133.6 (C arom.), 135.6 (C arom.), 144.7 (=C).

Ethyl 2-(tosylmethyl)acrylate (195)

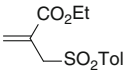

$C_{13}H_{16}O_4S$ M = 268.34 g/mol

A saturated solution of iodine (15.0 g, 59 mmol, 1 equiv.) in ethanol (100 mL) was added dropwise, in the dark, to a stirred solution of sodium p-toluenesulfinate hydrate (12.5 g, 70 mmol, 1.19 equiv.) in water (700 mL). The yellow precipitate was collected, washed with water, dissolved in CH_2Cl_2 (200 mL) and dried over $MgSO_4$. A solution of ethyl methacrylate (8.55 g, 74.9 mmol, 1.26 equiv., prealably purified of inhibitor by washing with 2 M aqueous NaOH) in CH_2Cl_2 (50 mL) was added to the previous yellow solution. The reaction mixture was stirred at r.t. in the light for 15 h. The solvent was evaporated and the residue was redissolved in CH_2Cl_2 (200 mL). NEt_3 (283 mmol, 4.8 equiv., 40 mL) was added, and the resulting mixture was heated under reflux for 6 h. After cooling the solution was washedwith 1 M aqueous HCl and water, dried over $MgSO_4$ and concentrated under reduced pressure. Flash column chromatography (petroleum ether:-EtOAc = 10:1 to 10:3) afforded the allyl sulfone **195** as a white solid (8.10 g, 43 %). Spectral data are in accordance with those reported in the literature [35].

^{1}H NMR (400 MHz, $CDCl_3$): δ = 1.14 (t, J = 7.3 Hz, 3 H, CH_3-CH_2), 2.41 (s, 3 H, CH_3-C), 4.00 (q, J = 7.3 Hz, 2 H, CH_3-CH_2), 4.11 (s, 2 H,CH_2-S), 5.86 (br s, 1 H, =C*H*H), 6.46–6.47 (m, 1 H, =CH*H*), 7.30 (d, J = 7.9 Hz, 2 H, arom.), 7.70 (d, J = 7.9 Hz, 2 H, arom.); ^{13}C NMR (100 MHz, $CDCl_3$): δ = 14.0 (*C*H_3-CH_2), 21.7 (*C*H_3-C), 57.6 (CH_2-S), 61.5 (CH_2-O), 128.9 (2 CH arom.), 129.3 (C arom.), 129.7 (2 CH arom.), 133.2 (=CH_2), 135.6 (C arom.), 144.9 (=C), 164.9 (C=O).

Ethyl 2-(*tert*-butylthiomethyl)acrylate (198)

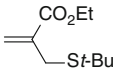

$C_{10}H_{18}O_2S$ M = 202.31 g/mol

To a solution of 1,3-dibromopropane-2-carboxylate **196** (1.00 g, 3.74 mmol, 1.05 equiv.) in ethanol (5 mL), were added K_2CO_3 (500 mg, 3.55 mmol, 1.02 equiv.), and 1,1-dimethylethanethiol **197** (400 µL, 3.55 mmol, 1 equiv.). The reaction mixture was stirred at r.t. for 48 h, quenched with water and extracted with Et_2O (2 x 10 mL). The combined organic layers were dried over $MgSO_4$ and concentrated under reduced pressure. Flash column chromatography (pentane:EtOAc = 20:1) afforded **198** as a colorless oil (750 mg, 99 %). When prepared on higher scale, 198 could also be isolated by distillation (b.p. = 54 °C/0.3 mmHg). Spectral data are in accordance with those reported in the literature [36].

^{1}H NMR (400 MHz, $CDCl_3$): δ = 1.30–1.35 (m, 12 H, CH_3-CH_2 + Me_3C), 3.46 (s, 2 H, CH_2-S), 4.21 (q, J = 7.0 Hz, 2 H, CH_3-CH_2), 5.81 (br s, 1 H, =C*H*H), 6.23 (br s, 1 H, =CH*H*).

4,4-Dideuterio-1,2,6-trimethyl-3,5-dicarboethoxy-l,4-dihydropyridine (200)

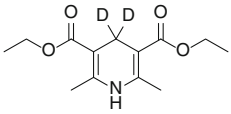

$C_{13}H_{17}D_2NO_4$ M = 255.29 g/mol

A mixture of ethyl acetoacetate (6.0 mL, 47 mmol, 2 equiv.), d_2-paraformaldehyde (750 mg, 23.4 mmol, 1 equiv.) and ammonium acetate (2.7 g, 35 mmol, 1.5 equiv.) was heated at 70 °C in a water bath for 10 min and then allowed to cool down to r.t.. Cold water (40 mL) was added and the resulting mixture was stirred for 10 min and filtered. The precipitate was recristallized from EtOH (25 mL) to afford the pure deuterated Hantzsch ester **200** as a pale yellow solid (2.1 g, 35 %). Spectral data are in accordance with those reported in the literature [37].

^{1}H NMR (400 MHz, $CDCl_3$): δ = 1.27 (t, J = 9.2 Hz, 6 H, 2 CH_3CH$_2$), 2.18 (s, 6 H, 2 CH$_3$), 4.16 (q, J = 9.2 Hz, 4 H, 2 CH$_3$CH_2).

Diethyl 2,4,6-trimethyl-1,4-dihydropyridine-3,5-dicarboxylate (201)

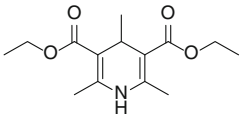

$C_{14}H_{21}NO_4$ M = 267.32 g/mol

A mixture of ethyl acetoacetate (3.8 mL, 30 mmol, 2 equiv.), acetaldehyde (0.85 mL, 15 mmol, 1 equiv.) and ammonium acetate (1.7 g, 22.5 mmol, 1.5 equiv.) was stirred at r.t. for 2 h. Cold water (20 mL) was added and the resulting mixture was stirred for 10 min and filtered. The precipitate was recristallized from EtOH (10 mL) to afford the pure methylated Hantzsch ester **201** as a pale yellow solid (3.2 g, 40 %). Spectral data are in accordance with those reported in the literature [38].

^{1}H NMR (400 MHz, $CDCl_3$): δ = 0.96 (d, J = 8.8 Hz, 3 H, CH_3CH), 1.29 (t, J = 9.6 Hz, 6 H, 2 CH_3CH$_2$), 2.26 (s, 6 H, 2 CCH$_3$), 3.83 (q, J = 8.8 Hz, 1 H, CH$_3$CH), 4.10–4.24 (m, 4 H, 2 CH$_3$-CH_2), 5.48 (br s, 1 H, NH).

6.5.2 Allylated Products

Ethyl 4-benzoyl-5-hydroxy-2-methylene-5-phenylpentanoate (191a)

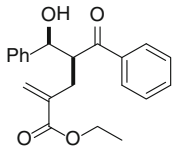

$C_{21}H_{22}O_4$ M = 338.40 g/mol

Following **GP6** with **123a** (44 mg, 0.2 mmol, 1 equiv.) and allylsulfone **195** (161 mg, 0.6 mmol, 3 equiv.); after 48 h of irradiation, **191a** was purified by flash column chromatography (pentane/CH_2Cl_2/Et_2O = 5:5:1) and isolated as a colorless oil (45 mg, 67 %, dr = 96/4).

IR (neat): ν = 3494, 3100, 2923, 1712, 1676, 1448, 1302, 1194, 1143, 1027, 700 cm^{-1}. *Dia. majo*: ^{1}H NMR (400 MHz, $CDCl_3$): δ = 1.16 (t, J = 7.3 Hz, 3 H, C*H*$_3$CH$_2$), 2.76 (dd, A of ABX, J_{AB} = 13.8 Hz, J_{AX} = 4.4 Hz, 1 H, =CC*H*H), 2.87 (dd, B of ABX, J_{AB} = 13.8 Hz, J_{BX} = 9.4 Hz, 1 H, =CCH*H*), 3.39 (br s, 1 H, O*H*), 4.01–4.10 (m, 2 H, CH$_3$C*H*$_2$), 4.23–4.26 (m, 1 H, C*H*C(O)), 5.08 (d, J = 4.6 Hz, 1 H, C*H*OH), 5.42 (d, J = 0.9 Hz, 1 H, =CH*H*), 5.96 (d, J = 1.3 Hz, 1 H, =C*H*H), 7.19–7.21 (m, 1 H, arom.), 7.28–7.31 (m, 2 H, arom.), 7.39–7.42 (m, 4 H, arom.), 7.51–7.54 (m, 1 H, arom.), 7.82–7.84 (m, 2 H, arom.); ^{13}C NMR (100 MHz, $CDCl_3$) : δ = 14.2 (CH_3), 30.6 (=C*C*H$_2$), 51.7 (*C*HC(O)), 60.8 (CH$_3$*C*H$_2$O), 73.7 (CHOH), 126.3 (2 CH arom.), 127.6 (CH arom.), 128.0 (=CH_2), 128.4 (2 CH arom.), 128.5 (2 CH arom.), 128.8 (2 CH arom.), 133.6 (CH arom.), 137.3 (=C), 137.7 (C arom.), 141.6 (C arom.), 167.0 (C=O ester), 204.3 (C=O ketone). *Dia. mino*: ^{1}H NMR (400 MHz, $CDCl_3$): (characteristic signals) δ = 3.55 (d, J = 7.2 Hz, 1 H, OH), 4.94–5.00 (m, 1 H, C*H*OH), 5.63 (d, J = 1.1 Hz, 1 H, =CH*H*), 6.11 (d, J = 1.3 Hz, 1 H, =C*H*H); HRMS calcd. for $C_{21}H_{22}O_4Na$ ([M + Na]$^+$) 361.1410, found 361.1411; LCMS analysis: dia. majo: tr = 8.9 min, dia. mino: tr = 10.0 min.

Ethyl 5-hydroxy-4-(4-methoxybenzoyl)-2-methylene-5-phenylpentanoate (191c)

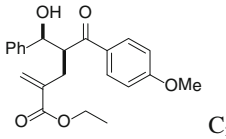

$C_{22}H_{24}O_5$ M = 368.42 g/mol

Following **GP6** with **123c** (51 mg, 0.2 mmol, 1 equiv.) and allylsulfone **195** (161 mg, 0.6 mmol, 3 equiv.); after 17 h of irradiation, **191c** was purified by flash column chromatography (pentane/CH_2Cl_2/Et_2O = 5:5:1) and isolated as a colorless oil (54 mg, 73 %, dr = 93/7).

IR (neat): ν = 3472, 2979, 1709, 1664, 1598, 1245, 1170, 1027, 701 cm^{-1}; *Dia. majo:* ^{1}H NMR (400 MHz, $CDCl_3$): δ = 1.16 (t, J = 7.1 Hz, 3 H, C*H*$_3$CH$_2$), 2.70–2.87 (m, 2 H, =CC*H*$_2$), 3.61 (br s, 1 H, O*H*), 3.85 (s, 3 H, OCH$_3$), 4.01–4.10 (m, 2 H, CH$_3$C*H*$_2$), 4.16–4.21 (m, 1 H, C*H*C(O)), 5.07 (d, J = 4.0 Hz, 1 H, C*H*OH), 5.40 (d, J = 1.1 Hz, 1 H, =CH*H*), 5.94 (d, J = 1.4 Hz, 1 H, =C*H*H), 6.86–6.89 (m, 2 H, arom.), 7.19–7.22 (m, 1 H, arom.), 7.28–7.31 (m, 2 H, arom.), 7.39–7.42 (m, 2 H, arom.), 7.84–7.88 (m, 2 H, arom.); ^{13}C NMR (100 MHz, $CDCl_3$): δ = 14.2 (CH$_2$*C*H$_3$), 30.4 (=C*C*H$_2$), 50.9 (*C*HC(O)), 55.6 (OCH$_3$), 60.8 (CH$_3$*C*H$_2$O), 73.6 (CHOH), 114.0 (2 CH arom.), 126.3 (2 CH arom.), 127.5 (CH arom.), 127.9 (=CH_2), 128.4 (2 CH arom.), 130.2 (C arom.), 131.0 (2 CH arom.), 137.7 (=C), 141.6 (C arom.), 164.1 (C arom.), 167.0 (C=O ester), 203.0 (C=O

ketone); *Dia. mino*: ^{1}H NMR (400 MHz, $CDCl_3$): (characteristic signals) $\delta = 4.92$–4.95 (m, 1 H, C*H*OH), 5.65 (d, $J = 0.8$ Hz, 1 H, =CH*H*), 6.13 (d, $J = 1.4$ Hz, 1 H, =C*H*H); HRMS calcd. for $C_{22}H_{24}O_5Na$ ([M + Na]$^+$) 391.1516, found 391.1520; LCMS analysis: dia. majo: tr = 8.1 min, dia. mino: tr = 9.2 min.

Ethyl 5-hydroxy-2-methylene-5-phenyl-4-(4-(trifluoromethyl)benzoyl)pentanoate (191d)

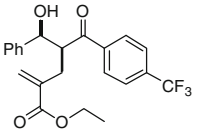

$C_{22}H_{21}F_3O_4$ M = 406.39 g/mol

Following **GP6** with **123d** (58 mg, 0.2 mmol, 1 equiv.) and allylsulfone **195** (161 mg, 0.6 mmol, 3 equiv.), after 48 h of irradiation, **191c** was purified by flash column chromatography (pentane/CH_2Cl_2/Et_2O = 5:5:1) and isolated as a colorless oil (18 mg, 22 %, dr > 95/5).

IR (neat): $\nu = 3495, 3099, 1712, 1677, 1450, 1300, 700$ cm^{-1}; ^{1}H NMR (400 MHz, $CDCl_3$): $\delta = 1.18$ (t, $J = 7.2$ Hz, 3 H, C*H*$_3$-CH$_2$), 2.87 (d, $J = 6.8$ Hz, 2 H, CH$_2$-CHC(O)), 3.05 (br s, 1 H, O*H*), 4.07 (dq, $J = 2.4$, 7.2 Hz, 2 H, CH$_3$-CH$_2$), 4.25 (q, $J = 6.8$ Hz, 1 H, CH$_2$-C*H*-C(O)), 5.05 (d, $J = 5.6$ Hz, 1 H, C*H*-OH), 5.46 (d, $J = 1.2$ Hz, 1 H, =CH*H*), 5.99 (d, $J = 1.6$ Hz, 1 H, =C*H*H), 7.17–7.19 (m, 1 H, arom.), 7.21–7.29 (m, 2 H, arom.), 7.34–7.37 (m, 2 H, arom.), 7.63 (d, $J = 8.0$ Hz, 2 H, arom.), 7.87 (d, $J = 8.0$ Hz, 2 H, arom.); ^{13}C NMR (100 MHz, $CDCl_3$): $\delta = 14.2$ (CH$_2$*C*H$_3$), 31.4 (=C*C*H$_2$), 52.7 (*C*HC(O)), 60.9 (CH$_3$*C*H$_2$O), 74.1 (CHOH), 124.1 (q, $^1J_{C\text{-}F} = 271.0$ Hz, *C*F$_3$), 125.7 (q, $^3J_{C\text{-}F} = 3.5$ Hz, 2 CH arom.), 126.4 (2 CH arom.), 127.9 (CH arom.), 128.1 (q, $^2J_{C\text{-}F} = 32.7$ Hz, C arom.), 128.3 (=CH$_2$), 128.5 (2 CH arom.), 128.7 (2 CH arom.), 137.5 (=C), 140.2 (C arom.), 141.5 (C arom.), 167.0 (C=O ester), 201.0 (C=O ketone).

Ethyl 4-(2-naphthoyl)-5-hydroxy-2-methylene-5-phenylpentanoate (191 h)

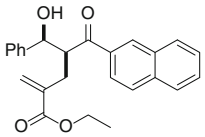

$C_{25}H_{24}O_4$ M = 388.46 g/mol

Following **GP6** with **123 h** (27 mg, 0.1 mmol, 1 equiv.) and allylsulfone **195** (80 mg, 0.3 mmol, 3 equiv.); after 8 h of irradiation, **191 h** was purified by flash column chromatography (pentane/CH_2Cl_2/Et_2O = 5:5:1) and isolated as a colorless oil (20 mg, 51 %, dr > 95/5).

IR (neat): ν = 3472, 2925, 1711, 1668, 1627, 1466, 1369, 1186, 1026, 777, 702 cm^{-1}; ^1H NMR (400 MHz, $CDCl_3$): δ = 1.10 (t, J = 6.8 Hz, 3 H, CH_3CH$_2$), 2.83 (dd, A of ABX, J_{AB} = 14.0 Hz, J_{AX} = 4.4 Hz, 1 H, =CC*H*H), 2.93 (dd, B of ABX, J_{AB} = 14.0 Hz, J_{BX} = 9.6 Hz, 1 H, =CCH*H*), 3.49 (br s, 1 H, O*H*), 3.96–4.05 (m, 2 H, CH$_3$CH_2), 4.40–4.44 (m, 1 H, C*H*C(O)), 5.14–5.16 (m, 1 H, C*H*-OH), 5.44 (d, J = 0.8 Hz, 1 H, =CH*H*), 5.96 (d, J = 1.2 Hz, 1 H, =C*H*H), 7.18–7.21 (m, 1 H, arom.), 7.28–7.31 (m, 2 H, arom.), 7.44–7.49 (m, 2 H arom.), 7.52–7.59 (m, 2 H, arom.), 7.82–7.85 (m, 2 H, arom.), 7.92–7.94 (m, 2 H, arom.), 8.35 (s, 1 H, arom.); ^{13}C NMR (100 MHz, $CDCl_3$): δ = 14.1 (CH_3), 30.8 (=C-*C*H$_2$), 51.6 (*C*H-C(O)), 60.8 (CH$_3$-*C*H$_2$-O), 73.8 (CH-OH), 124.0 (CH arom.), 126.4 (2 CH arom.), 127.0 (CH arom.), 127.7 (CH arom.), 127.9 (CH arom.), 128.0 (=CH$_2$), 128.4 (2 CH arom.), 128.7 (CH arom.), 128.9 (CH arom.), 129.9 (CH arom.), 130.6 (CH arom.), 132.5 (C arom.), 134.8 (C arom.), 135.2 (C arom.), 137.7 (=C), 141.6 (C arom.), 167.0 (C=O ester), 204.3 (C=O ketone); HRMS calcd. for $C_{25}H_{24}O_4Na$ ([M + Na]$^+$) 411.1567, found 411.1572. LCMS analysis: dia. majo: tr = 12.8 min (dia. mino obtained by isomerisation on silica: tr = 13.8 min).

Ethyl 4-(hydroxy(phenyl)methyl)-2-methylene-5-oxononanoate (191 m)

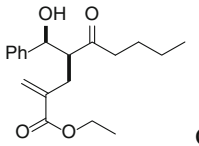

$C_{19}H_{26}O_4$ M = 318.41 g/mol

Following **GP6** with **128 m** (41 mg, 0.2 mmol, 1 equiv.) and allylsulfone **195** (161 mg, 0.6 mmol, 3 equiv.); after 7 h of irradiation, **191 m** was purified by flash column chromatography (pentane/CH_2Cl_2/Et_2O = 5:5:1) and isolated as a colorless oil (45 mg, 70 %, dr > 95/5).

IR (neat): ν = 3493, 2956, 2931, 2861, 1711, 1674, 1447, 1368, 1300, 1194, 1146, 1026, 949, 689 cm^{-1}. ^1H NMR (400 MHz, $CDCl_3$): δ = 0.88 (t, J = 6.8 Hz, 3 H, CH_3CH$_2$CH$_2$), 1.23–1.60 (m, 9H, CH_3CH$_2$O + CH$_3$CH_2CH_2CH_2), 2.72–2.86 (m, 3 H, =CCH_2 + OH), 3.87–3.93 (m, 2 H, C*H*C(O) + C*H*OH), 4.12–4.16 (m, 2 H, CH$_3$CH_2), 5.49 (s, 1 H, =CH*H*), 6.04 (d, J = 1.2 Hz, 1 H, =C*H*H), 7.43–7.47 (m, 2 H, arom.), 7.55–7.58 (m, 1 H, arom.), 7.88–7.90 (m, 2 H, arom.); ^{13}C NMR (100 MHz, $CDCl_3$): δ = 14.1 (CH$_2$CH$_2$*C*H$_3$), 14.3 (OCH$_2$*C*H$_3$), 22.7 (CH$_3$*C*H$_2$), 28.4 (CH$_3$CH$_2$*C*H$_2$), 30.3 (=C*C*H$_2$), 34.6 (CH$_3$CH$_2$CH$_2$*C*H$_2$), 49.7 (*C*H-C(O)), 60.9 (CH$_3$*C*H$_2$O), 71.9 (CHOH), 128.0 (=CH$_2$), 128.6 (2 CH arom.), 128.9 (2 CH arom.), 133.6 (CH arom.), 137.4 (C arom.), 138.0 (=C), 167.2 (C=O ester), 204.5 (C=O ketone); HRMS calcd. for $C_{19}H_{26}O_4Na$ ([M + Na]$^+$) 341.1723, found 341.1721. LCMS analysis: dia. majo: tr = 10.2 min.

Ethyl 4-benzoyl-2-methylene-5-(4-methylphenylsulfonamido)-5-phenylpentanoate (202a)

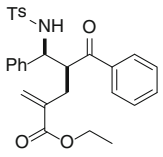

$C_{28}H_{29}NO_5S$ M = 491.60 g/mol

Following **GP6** with **172a** (75 mg, 0.2 mmol, 1 equiv.) and allylsulfone **195** (161 mg, 0.6 mmol, 3 equiv.); after 11 h of irradiation, **202a** was purified by flash column chromatography (pentane/CH_2Cl_2/Et_2O = 5:5:1) and isolated as a colorless solid (48 mg, 49 %, dr > 95/5).

IR (neat): ν = 3274, 2924, 1711, 1677, 1447, 1329, 1158, 700 cm^{-1}. ^1H NMR (400 MHz, $CDCl_3$): δ = 1.18 (t, J = 7.2 Hz, 3 H, C*H*$_3$CH$_2$), 2.28 (s, 3 H, C-CH$_3$), 2.67 (dd, A of ABX, J_{AB} = 13.6 Hz, J_{AX} = 10.3 Hz, 1 H, =CC*H*H), 2.92 (dd, B of ABX, J_{AB} = 13.6 Hz, J_{BX} = 2.4 Hz, 1 H, =CCH*H*), 4.04–4.15 (m, 2 H, CH$_3$C*H*$_2$), 4.18–4.24 (m, 1 H, C*H*C(O)), 4.57 (t, J = 7.5 Hz, 1 H, C*H*NH), 5.43 (s, 1 H, =CH*H*), 5.54 (d, J = 7.2 Hz, 1 H, NH), 5.96 (d, J = 1.3 Hz, 1 H, =C*H*H), 7.01–7.05 (m, 7H, arom.), 7.23–7.27 (m, 2 H, arom.), 7.40–7.43 (m, 1 H, arom.), 7.47–7.50 (m, 4 H, arom.); ^{13}C NMR (100 MHz, $CDCl_3$): δ = 14.2 (CH$_2$*C*H$_3$), 21.5 (C*C*H$_3$), 32.7 (=C*C*H$_2$), 50.9 (*C*HC(O)), 59.7 (CHNH), 61.0 (CH$_3$*C*H$_2$O), 127.2 (2 CH arom.), 127.3 (2 CH arom.), 127.6 (CH arom.), 128.1 (2 CH arom.), 128.4 (2 CH arom.), 128.4 (2 CH arom.), 128.5 (=CH$_2$), 129.4 (2 CH arom.), 133.2 (CH arom.), 136.9 (=C), 137.0 (C arom.), 137.4 (C arom.), 138.9 (C arom.), 143.1 (C arom.), 166.9 (C=O ester), 201.7 (C=O ketone); HRMS calcd. for $C_{28}H_{29}O_5SNa$ ([M + Na]$^+$) 514.1659, found 514.1650; LCMS analysis: dia. majo: tr = 14.7 min.

CCDC 802059 contains the supplementary crystallographic data for this paper. These data can be obtained free of charge from The Cambridge Crystallographic Data Centre *via* www.ccdc.cam.ac.uk/data_request/cif.

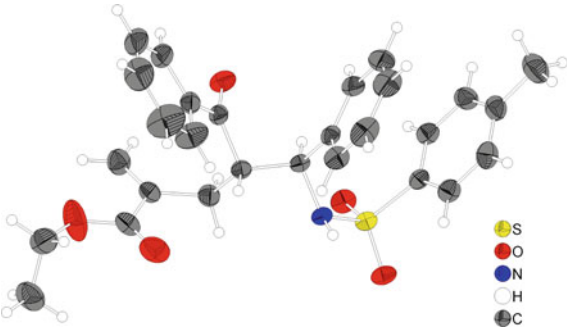

Ethyl 4-(4-methoxybenzoyl)-2-methylene-5-(4-methylphenylsulfonamido)-5-phenylpentanoate (202b)

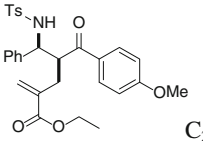

$C_{29}H_{31}NO_6S$ M = 521.62 g/mol

Following **GP6** with **172b** (41 mg, 0.1 mmol, 1 equiv.) and allylsulfone **195** (81 mg, 0.3 mmol, 3 equiv.); after 11 h of irradiation **202b** was purified by flash column chromatography (pentane:Et_2O = 5:5) and isolated as a viscous solid (22 mg, 45 %, dr > 95/5).

IR (neat): ν = 3286, 2937, 1711, 1599, 1247, 1160, 942, 667 cm^{-1}; ^1H NMR (400 MHz, $CDCl_3$): δ = 1.19 (t, J = 7.2 Hz, 3 H, C*H*$_3$-CH_2), 2.28 (s, 3 H, C-CH_3), 2.64 (dd, A of ABX, J_{AB} = 13.6 Hz, J_{AX} = 10.4 Hz, 1 H, =C-C*H*H), 2.86 (dd, B of ABX, J_{AB} = 13.6 Hz, J_{BX} = 2.4 Hz, 1 H, =C-CH*H*), 3.80 (s, 3 H, OCH_3), 4.05–4.19 (m, 3 H, C*H*-C(O) + CH_3-C*H*$_2$), 4.56 (t, J = 7.2 Hz, 1 H, C*H*-NH), 5.41 (s, 1 H, =CH*H*), 5.48 (d, J = 7.0 Hz, 1 H, NH), 5.96 (d, J = 1.2 Hz, 1 H, =C*H*H), 6.73 (d, J = 8.8 Hz, 2 H, arom.), 7.01–7.07 (m, 7H, arom.), 7.48 (d, J = 8.0 Hz, 2 H, arom.), 7.53 (d, J = 8.8 Hz, 2 H, arom.); ^{13}C NMR (100 MHz, $CDCl_3$): δ = 14.3 (CH_2-*C*H_3), 21.5 (C-*C*H_3), 32.5 (=C-*C*H_2), 50.4 (*C*H-C(O)), 55.6 (OCH_3), 59.8 (CH-NH), 60.9 (CH_3-*C*H_2-O), 113.7 (2 CH arom.), 127.2 (2 CH arom.), 127.4 (2 CH arom.), 127.6 (CH arom.), 128.3 (=CH_2), 129.3 (2 CH arom.), 130.4 (CH arom.), 130.6 (2 CH arom.), 137.0 (=C), 137.2 (C arom.), 143.1 (C arom.), 163.8 (C arom.), 166.9 (C=O ester), 199.7 (C=O ketone); HRMS calcd. for $C_{29}H_{31}O_6SNa$ ($[M + Na]^+$) 544.1764, found 544.1751; LCMS analysis: dia. majo: tr = 14.7 min.

2-(Hydroxy(phenyl)methyl)-4-methyl-1-phenylpent-4-en-1-one (191p)

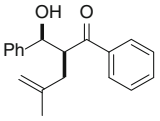

$C_{19}H_{20}O_2$ M = 280.36 g/mol

Following **GP6** with **123a** (44 mg, 0.2 mmol, 1 equiv.) and allylsulfone **193** (126 mg, 0.6 mmol, 3 equiv.); after 28 h of irradiation, **191p** was purified by flash column chromatography (pentane:Et_2O = 10:3) and isolated as a colorless oil (34 mg, 60 %, inseparable 90:10 mixture of two diast.).

IR (neat): ν = 3458, 3064, 2966, 1673, 1596,, 1448, 1232, 1054, 1027, 894, 760, 699 cm^{-1}.^1H NMR (400 MHz, $CDCl_3$): δ = 1.16 (s, 3 H, C*H*$_3$C, dia. majo), 1.16 (s, 3 H, C*H*$_3$C, dia. mino), 2.26 (dd, A of ABX, J_{AB} = 14.4 Hz, J_{AX} = 5.6 Hz, 1 H, =CC*H*H, dia. mino), 2.42 (dd, A of ABX, J_{AB} = 18.3 Hz,

J_{AX} = 4.8 Hz, 1 H, =CC*H*H, dia. majo), 2.50 (dd, B of ABX, J_{AB} = 14.4 Hz, J_{BX} = 9.4 Hz, 1 H, =CCH*H,* dia. mino), 2.68 (dd, B of ABX, J_{AB} = 18.6 Hz, J_{BX} = 10.0 Hz, 1 H, =CCH*H,* dia. majo), 3.06 (d, J = 2.4 Hz, 1 H, O*H,* dia. majo), 3.33 (d, J = 6.4 Hz, 1 H, O*H,* dia. mino), 3.98–4.05 (m, 4 H, C*H*C(O), 2 dia.), 4.56 (br s, 1 H, =CH*H,* dia. majo), 4.59 (br s, 1 H, =C*H*H, dia. majo), 4.69 (br s, 2 H, $=CH_2$, dia. mino), 4.96 (t, J = 6.0 Hz, 1 H, C*H*OH, dia. mino), 5.05–5.07 (m, 1 H, C*H*OH, dia. majo), 7.19–7.22 (m, 4 H, arom., 2 dia.), 7.28–7.32 (m, 4 H, arom., 2 dia.), 7.36–7.44 (m, 8H, arom., 2 dia.), 7.52–7.56 (m, 2 H, arom., 2 dia.), 7.75–7.76 (m, 2 H, arom., dia. mino), 7.83–7.86 (m, 2 H, arom., dia. majo); ^{13}C NMR (100 MHz, $CDCl_3$): δ = 22.7 (CH_3, dia. mino), 22.9 (CH_3, dia. majo), 35.4 (=C*C*H_2, dia. majo), 38.8 (=C*C*H_2, dia. mino), 51.0 (*C*HC(O), dia. mino), 51.8 (*C*HC(O), dia. majo), 74.3 (CHOH, dia. majo), 76.2 (CHOH, dia. mino), 112.6 ($=CH_2$, dia. majo), 113.3 ($=CH_2$, dia. mino), 126.2 (4 CH arom., 2 dia.), 127.6 (CH arom., dia. majo), 127.8 (CH arom., dia. mino), 128.2 (2 CH arom., dia. mino), 128.2 (2 CH arom., dia. majo), 128.3 (2 CH arom., dia. majo), 128.5 (4 CH arom., dia. mino), 128.6 (2 CH arom., dia. majo), 133.1 (CH arom., dia. mino), 133.3 (CH arom., dia. majo), 138.4 (C arom., dia. majo), 139.0 (C arom., dia. mino), 141.5 (C arom., dia. majo), 141.7 (C arom., dia. mino), 142.6 (=C, dia. mino), 143.1 (=C, dia. majo), 204.4 (2 C=O ketone, 2 dia.); HRMS calcd. for $C_{19}H_{20}O_2Na$ ([M + Na]$^+$) 303.1356, found 303.1359; LCMS analysis: dia. majo: tr = 8.7 min, dia. mino: tr = 10.4 min.

***N*-(2-benzoyl-4-methyl-1-phenylpent-4-enyl)-4-methylbenzenesulfonamide (202d)**

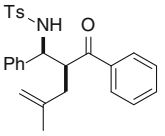

$C_{26}H_{27}NO_3S$ M = 433.56 g/mol

Following **GP6** with **172a** (75 mg, 0.2 mmol, 1 equiv.) and allylsulfone **193** (126 mg, 0.6 mmol, 3 equiv.); after 13 h of irradiation, **202d** was purified by flash column chromatography (Silica gel, pentane/CH_2Cl_2/Et_2O 6: 4:1) and isolated as a white solid (40 mg, 43 %, inseparable 87:13 mixture of two diast.).

IR (neat): ν = 3276, 3065, 2923, 1677, 1597, 1447, 1158, 941, 701, 670 cm^{-1}; ^{1}H NMR (400 MHz, $CDCl_3$): δ = 1.56 (s, 6H, C*H*$_3$C=, 2 dia.), 2.28 (s, 3 H, C-CH_3, dia. majo), 2.29 (s, 3 H, C-CH_3, dia. mino), 2.29–2.58 (m, 4 H, =CCH_2, 2 dia.), 3.96–4.00 (m, 2 H, C*H*C(O), 2 dia.), 4.54–4.64 (m, 3 H, C*H*NH+ =CH*H*+ =C*H*H, dia majo), 4.64 (s, 1 H, =CH*H*, dia. mino), 4.95–4.99 (m, 1 H, =C*H*H, dia. mino), 5.06–5.11 (m, 1 H, C*H*NH, dia. mino), 5.33–5.39 (m, 2 H, NH, 2 dia.), 7.01–7.49 (m, 4 H, arom., 2 dia.), 7.62 (d, J = 8.0 Hz, 2 H, arom., dia. majo), 7.77 (d, J = 7.2 Hz, 2 H, arom., dia. mino); ^{13}C NMR (100 MHz, $CDCl_3$): δ = 21.2 (C*C*H_3, dia. mino), 21.5 (C*C*H_3, dia; majo), 22.7 (=C*C*H_3, dia. mino), 23.0 (=C*C*H_3, dia. majo), 36.0 (2 =C*C*H_2, 2 dia.), 50.6 (2 *C*HC(O), 2 dia.), 59.3

(CHNH, dia. mino), 59.4 (CHNH, dia. majo), 112.6 (=CH_2, dia. majo), 119.7 (=CH_2, dia. mino), 127.1 (4 CH arom., 2 dia.), 127.4 (4 CH arom., 2 dia.), 127.7 (2 CH arom., 2 dia.), 128.2 (2 CH arom., dia. majo), 128.5 (2 CH arom., dia. majo), 128.6 (2 CH arom., dia. majo), 128.6 (2 CH arom., dia. mino), 128.7 (2 CH arom., dia. mino), 128.8 (2 CH arom., dia. mino), 129.4 (2 CH arom., dia. majo), 130.3 (2 CH arom., dia; mino), 133.3 (2 CH arom., 2 dia.), 136.6 (2 C arom., 2 dia.), 136.9 (2 C arom., 2 dia.), 139.1 (2 C arom., 2 dia.), 140.2 (=C, dia. mino), 142.5 (=C, dia. majo), 143.2 (2 C arom., 2 dia.), 197.2 (C=O ketone, dia. mino), 201.3 (C=O ketone, dia majo); HRMS calcd. for $C_{26}H_{27}NO_3SNa$ ($[M + Na]^+$) 456.1604, found 456.1600; LCMS analysis: dia. mino: tr = 9.0 min, dia. majo: tr = 9.5 min.

References

1. Lowry, M. S., Hudson, W. R., Pascal, R. A., & Bernhard, S. (2004). *Journal of the American Chemical Society, 126*, 14129–14135.
2. Dai, L.-Z., & Shi, M. (2009). *Tetrahedron Letters, 50*, 651–655.
3. Hasegawa, E., Ishiyama, K., Horaguchi, T., & Shimizu, T. (1991). *Journal of Organic Chemistry, 56*, 1631–1635.
4. Evans, D. A., Faul, M. M., & Bilodeau, M. T. (1991). *Journal of Organic Chemistry, 56*, 6744–6746.
5. Geng, X., Wang, Z., Li, X., & Zhang, C. (2005). *Journal of Organic Chemistry, 70*, 9610–9613.
6. Carde, L., Davies, D. H., & Roberts, S. M. (2000). *Journal of Chemistry Society of Perkin Transactions, 1*, 2455–2463.
7. Adam, W., Hadjiarapoglou, L., & Smerz, A. (1991). *Chemische Berichte, 124*, 227–232.
8. Bickley, J. F., Gillmore, A. T., Roberts, S. M., Skidmore, J., & Steiner, A. (2001) *Journal of Chemistry Social Perkin Transactions*, *1*, 1109–1115.
9. Hallet, P., Muzart, J., & Pete, J.-P. (1981). *Journal of Organic Chemistry, 46*, 4275–4279.
10. Liu, W., Shi, H.-M., Jin, H., Zhao, H.-Y., Zhou, G.-P., Wen, F., et al. (2009). *Chemical Biology and Drug Design, 73*, 661–667.
11. Li, J.-T., Liu, X.-F., Yin, Y., & Du, C. (2009). *Organic Letters*, *2*:1, 1–6.
12. Barnes, R. P. (1935). *Journal of the American Chemical Society, 57*, 935–940.
13. Hasegawa, E., Takizawa, S., Seida, T., Yamaguchi, A., Yamaguchi, N., Chiba, N., et al. (2006). *Tetrahedron, 62*, 6581–6588.
14. Armstrong, A., Baxter, C. A., Lamont, S. G., Pape, A. R., & Wincewicz, R. (2007). *Organic Letters, 9*, 351–353.
15. Chang, C.-L., & Kumar, M. P. (2004). R.-S Liu. *Journal of Organic Chemistry, 69*, 2793–2796.
16. Makosza, M., Kwast, A., Kwast, E., & Jonczyk, A., (1985). *Journal of Organic Chemistry, 50*, 3722–3727.
17. Lu, S., & Bolm, C. (2008). *Angewandte Chemie International Edition, 47*, 8920–8923.
18. Arai, S., Shirai, Y., Ishida, T., & Shioiri, T. (1999). *Tetrahedron, 55*, 6375–6386.
19. Armstrong, A., Baxter, C. A., Lamont, S. G., Pape, A. R., & Wincewicz, R. (2007). *Organic Letters, 9*, 351–353.
20. Xu, J., Ma, L., & Jiao, P. (2004). *Chemical Communications, 14*, 1616–1617.
21. Chen, D., Timmons, C., Guo, L., Xu, X., & Li, G. (2004). *Synthesis, 15*, 2479–2484.
22. Concellón, J. M., Rodríguez-Solla, H., Mejica, C., & Blanco, E. G. (2007). *Organic Letters*, *9*, 2981–2984.
23. Xu, H.-J., Liu, Y.-C., Fu, Y., & Wu, Y.-D. (2006). *Organic Letters, 8*, 3449–3451.

24. Xu, J., Ma, L., & Jiao, P. (2004). *Chemical Communications*, *14*, 1616–1617.
25. Hasegawa, E., Takizawa, S., Seida, T., Yamaguchi, A., Yamaguchi, N., Chiba, N., Takahashi, T., Ikedab, H., Akiyama, K. (2006). *Tetrahedron, 62*, 6581–6588.
26. Shintani, R., Okamoto, K., & Hayashi, T. (2005). *Organic Letters, 7*, 4757–4759.
27. Curran, D. P. (1983). *Journal of the American Chemical Society, 105*, 5826–5833.
28. House, H. O., Crumrine, D. S., Teranishi, A. Y., & Olmstead, H. D. (1973). *Journal of the American Chemical Society*, *95*, 3310–3324.
29. Denmark, S. E., Wong, K.-T., & Stavenger, R. A. (1997). The relative configuration has been established in the literature. *Journal of the American Chemical Society*, *119*, 2333.
30. Hojo, M., Horada, H., Ito, H., & Hosomi, A. (1997). *Journal of the American Chemical Society*, *119*, 5459–5460.
31. Das, B., Balasubramanyam, P., Veeranjaneyulu, B., Chinna Reddy, G. (2009). *Journal of Organic Chemistry*, *74*, 9505–9508.
32. Yadav, L. D. S. (2009). *Synlett, 19*, 3123–3126.
33. Murphy, J. A. (2005). *Organic Letters*, *7*, 1427–1429.
34. Kocienski, P. (1983). *Journal of Chemistry Society of Perkin Transactions*, *1*, 945–948.
35. Harvey, I. W., Phillips, E. D., & Whitham, G. H. (1997). *Tetrahedron, 53*, 6493–6508.
36. Barton, D. H., & Crich, D. (1986). *Journal of Chemistry Society of Perkin Transactions, 1*, 1613–1619.
37. Norcrossp, B. E., Klinedinstjr, E., & Westheim, F. H. (1962). *Journal of the American Chemical Society, 84*, 797–802.
38. Zolfigol, M. A., & Safaiee, M. (2004). *Synlett*, 827–828.

Part III
New developments in Aryl–Aryl Couplings via Palladium/Norbornene Dual Catalysis: Synthesis of Phenanthridines and Phenanthrenes

Chapter 7
Bibliographical Background: The Ortho Effect in The Catellani Reaction

7.1 The Catellani Reaction

Pallado-catalyzed sequential reactions involving direct C–H bond activations have emerged as powerful tools for rapid access to complex polycyclic scaffolds, starting from simple precursors [1–3]. In this context, Professor Marta Catellani has pioneered in the mid 1980s the utilization of norbornene in cooperation with palladium to achieve sequential C-halide and C–H activations via the formation of a five-membered alkylaromatic palladacycle. In 1985, she published the synthesis of dihydrophenanthrene **1** by coupling of two molecules of bromobenzene and one of norbornene, through the proposed formation of palladacycle **2** (Fig. 7.1) [4].

Since then, numerous applications of palladium/norbornene-mediated domino processes have been reported, allowing the synthesis of various polycyclic frameworks and the construction of up to three carbon–carbon bonds in a single reaction [5–7]. The catalytic cycle of the Catellani reaction, involving multiple oxidation state of palladium (0, II and potentially IV), will be presented first. Several examples of the synthetic scope of this methodology will follow, with a special focus on the sequences involving aryl-aryl coupling.

7.1.1 Palladacycle Formation

The Catellani reaction is based on the formation of palladium(II) metallacycles **7** and their ability to react with electrophiles such as aryl and alkyl halides. The palladacycle is generated from palladium(0) complex **3**, aryl halide **4** and norbornene. Generally, Pd(0) catalysts are not air stable, so the in situ generation of Pd(0) species by reaction of palladium(II) salts with phosphines [8, 9] or coordinating solvent such as DMF [10] is often used. $PdCl_2$ and $Pd(OAc)_2$ are the most commonly employed catalysts. Phosphine-free conditions have also been developed [11] but they generally show lower functional group tolerance than conditions involving the use of triphenylphosphine or trifuryl phosphine. Once a suitable

M.-H. Larraufie, *Development of New Radical Cascades and Multi-Component Reactions*, Springer Theses, DOI: 10.1007/978-3-319-01324-4_7,

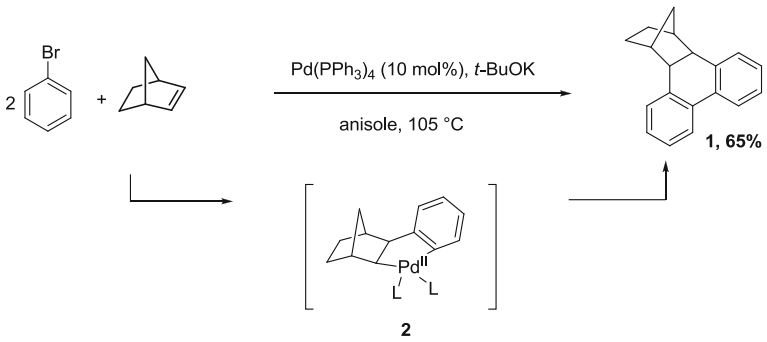

Fig. 7.1 Initial report of the Catellani reaction

$PdL_2^{(0)}$ species has been generated, it can enter the mechanistic pathway depicted in Fig. 7.2.

7.1.1.1 Oxidative Addition and Carbopalladation

Palladium(0) complexes undergo readily oxidative addition with aryl or heteroaryl halides to form the corresponding arylpalladium(II) complexes **5**. The use of aryl triflates has been reported recently, allowing an interesting extension of the substrate scope [12].

As demonstrated by Heck, Pd(II) complexes can coordinate olefins and perform carbopalladation of double bonds [13]. When norbornene is used as the olefin, this process is favored by the release of the steric strain involved (norbornene strain energy = 21.6 kcal/mol [14]). The *cis,exo*-arylnorbornyl palladium(II) complex **6** formed is stable towards β-H elimination because of the bicycle's inability to provide a hydrogen atom in a *syn* relationship to the Pd center. In 1991, Cheng managed to isolate and characterize a series of norbornenylpalladium complexes such as **8** after treatment of $ArPdI(PPh_3)_2$ with excess norbornadiene (Fig. 7.3) [15]. X-Ray crystallography revealed that the aryl group and the palladium metal were *cis* and *exo* to the norbornyl ring, as expected from preferential carbopalladation via the less hindered face of norbornadiene. In addition, the aryl ring is weakly bound to the palladium in a η^2 fashion. Phosphine, iodide and norbornenyl

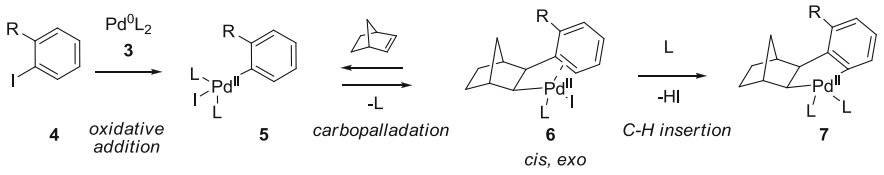

Fig. 7.2 Palladacycle formation

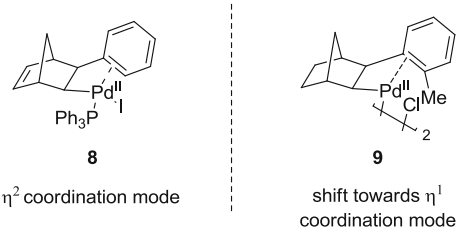

Fig. 7.3 Different coordination modes in arylnorbornyl palladium(II) complexes depending on the aryl substituents

complete the coordination sphere of the palladium atom which has a square-planar geometry. As shown by NMR, in solution the rotation of the C–C bond connecting the aryl and the norbornenyl groups is facile at room temperature, making the two *ortho* and the two *meta* carbons equivalent. A few years later, Catellani examined dimeric arylnorbornylpalladium complexes such as **9** bearing *ortho* substituents [16]. She disclosed that in that case the coordination of the aromatic ring by palladium was dissymmetric and shifted towards a η^1 coordination with the *ipso* carbon of the aromatic ring. Furthermore, the rotation around the C(aryl)-C(norbornyl) bond was hindered at room temperature and only the conformation with the methyl group pseudo *anti* to the bridge carbon atom was observed.

7.1.1.2 C–H Insertion

In the presence of a mild base, ring closure of palladium complex **6** occurs, probably favored by the coordination of the aromatic ring to the metal, which provides the right steric arrangement. This step allowing the formation of palladacycle **7** implies the activation of a usually inert aromatic C–H bond. The mechanism of this process has been investigated thanks to kinetic studies. Catellani has found that the rate of formation of *para*-substituted palladacycle **10** increased with electron-donating substituents and decreased with electron withdrawing substituents ($X = MeO > H > NO_2$) (Fig. 7.4) [17]. Echavarren confirmed that intramolecular C–H activations by alkylpalladium(II) complexes followed this trend and occurred with a lack of isotopic effect, demonstrating that the deprotonation was not the rate limiting step [18]. These data might suggest that the formation of palladacycle **10** proceeds through an electrophilic aromatic substitution pathway via the formation of Wheeland-type intermediate **11** and subsequent loss of proton (Fig. 7.4a).

This mechanism would be in sharp contrast with the one proposed for C–H activations by arylpalladium(II) complexes. The pallado-catalyzed arylations of arenes have indeed demonstrated kinetic effects and regioselectivities which better fit with a σ-bond metathesis-type mechanism. In that pathway, the rate-determining step would be the formation of the Pd–carbon bond, concerted with the breaking of the C–H bond (Fig. 7.4b) [19, 20].

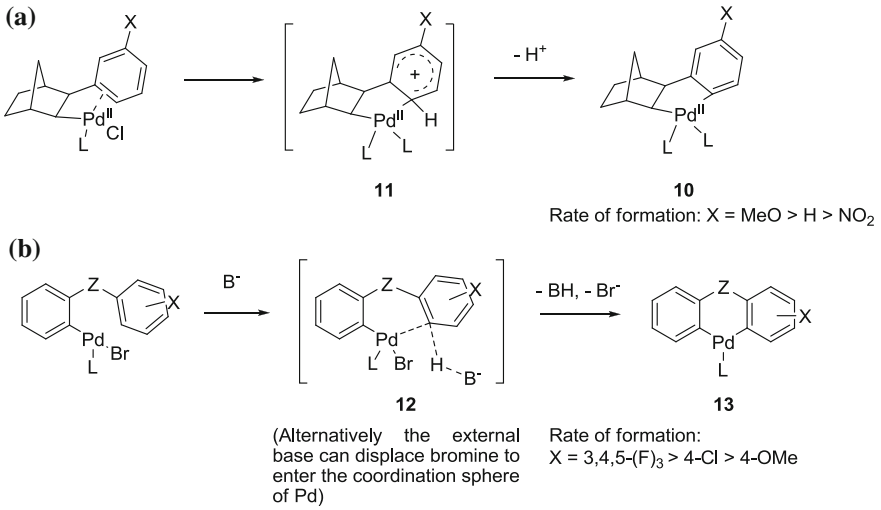

Fig. 7.4 Proposed S_EAr mechanism for the formation of arylnorbornyl palladacycle and comparison with proposed C–H activation mechanism by arylPd(II) complexes. **a** Proposed SEAr-type mechanism for intramolecular C-H activation by alkylpalladium(II) complexes, **b** σ-bond metathesis-type mechanism for intramolecular C-H activation by arylpalladium(II) complexes

Palladacycles such as **7** could be isolated [21, 22]. The structures displayed a square planar environment around the palladium with two ancillary ligands in addition to the aryl and the norbornyl moieties.

7.1.2 Palladacycle Reaction with Alkyl Halides

In the presence of alkyl halides, palladacycle **7** can perform a second oxidative addition into a C–X bond, leading to palladium(IV) complex **14** (Fig. 7.5).

In 1986, Canty was first to isolate such a complex prepared by oxidative addition of iodomethane to dimethyl(2,2'-bipyridyl)palladium(II) [23]. The *fac*-trimethyl(2,2'-bipyridyl)iodopalladium(IV) complex generated was structurally characterized by NMR and X-Ray diffractions. It reductively eliminated ethane in solution. Using 1,10-phenanthroline as the ligand, Catellani could prepare and isolate several palladium(IV) metallacycles resulting from the reaction of palladacycle **15** with methyl iodide, benzyl or allyl bromide and chloride (Fig. 7.6)

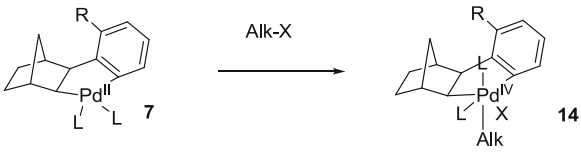

Fig. 7.5 Reaction of palladacycle with alkyl halides

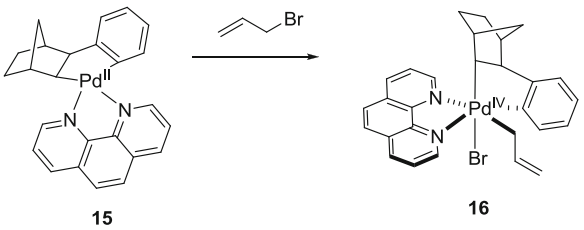

Fig. 7.6 Isolation of palladium(IV) metallacycle with 1,10-phenanthroline ligand

[24]. Octahedral palladium(IV) complexes such as **16** were formed selectively as a single isomer resulting from a *cis* oxidative addition of the alkyl halide to the palladacycle via the less hindered side.

The oxidative addition of alkyl halides to these Pd(II) palladacycles is thought to occur via a SN_2 mechanism, generally accepted for the oxidative additions to Pd(0). Experimental evidence includes the observation of second order kinetics for the formation of Pd(IV) complexes and the disclosure of an inversion of stereochemistry at the alkyl halide occurring during that step [25].

After the formation of complex **14**, reductive elimination occurs, selectively forming a C(sp^2)–C(sp^3) bond between the alkyl and the aryl groups (Fig. 7.7). This is consistent with the fact that usual rates for C–C bond forming reductive elimination from late transition metals follow the order: sp^2-sp^2 > sp^2-sp^3 > sp^3-sp^3.[1] When R ≠ H, owing to the steric strain induced by the presence of the two *ortho*-substituents, norbornene extrusion occurs via *β*-carbon elimination (decarbopalladation) [29]. This deinsertion steps allows the regeneration of norbornene, which can consequently be used in catalytic amount, and the formation of *ortho*, *orho'*-disubstituted arylpalladium(II) species **19a**. In the case where the aryl ring does not bear any *ortho* substituent (R = H), the new norbornylpalladium(II) **17** can undergo a second sequential C–H activation/oxidative addition with alkyl halide. Reductive elimination leads to palladium(II) complex **18** with a bifunctionnalized aryl ring, before norbornene deinsertion.

Various termination steps can be employed to complete the catalytic cycle and generate a Pd(0) complex, allowing access to a wide variety of scaffolds (Fig. 7.8) [30]. These palladium(II)-catalyzed reactions can be simple hydrogen transfers [31], Heck [32], Suzuki [33] or Sonogashira cross-couplings [34] affording the corresponding arenes **20**, vinylarenes **21**, biaryl derivatives **22** or phenylacetylenic compounds **23**.

A beautiful example of tandem *ortho*-alkylations/Heck coupling was reported by Lautens in 2010. Tricyclic heterocycles such as annulated silaoxacycle **25** were synthesized by treatment of precursor **24**, where the alkyl halide is tethered to the aryl iodide, with palladium and norbornene in the presence of *tert*-butyl acrylate (Fig. 7.9) [35]. The reaction tolerates alkyl halide tethers of various lengths and containing besides silicon and oxygen, sulfur or nitrogen moieties.

[1] For theoretical explanations on competitive C–C reductive eliminations see: [26–28].

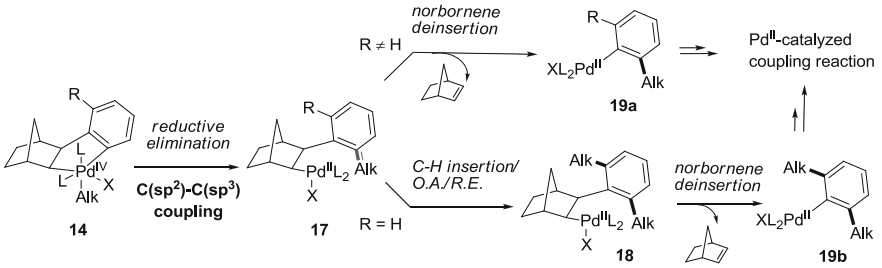

Fig. 7.7 Mono- or dialkylation of aryl ring

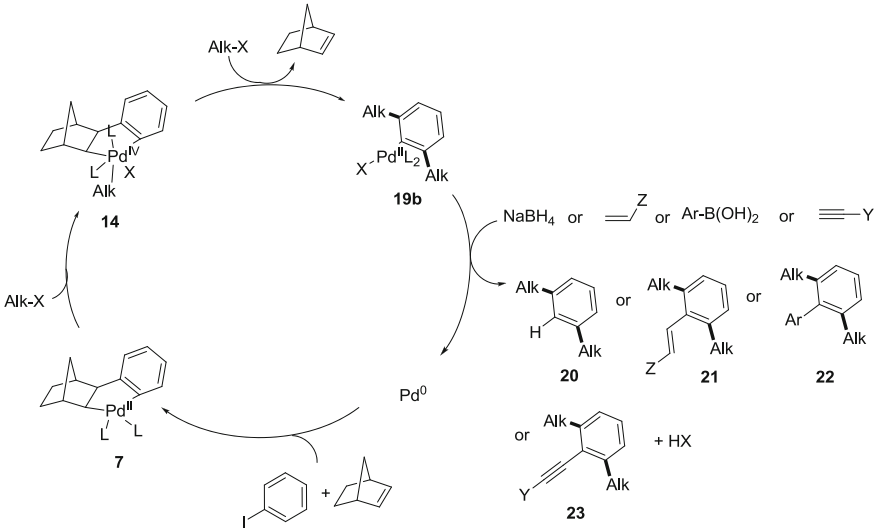

Fig. 7.8 General catalytic cycle for the coupling of aryl halide and alkyl halide using palladium/norbornene cocatalysis

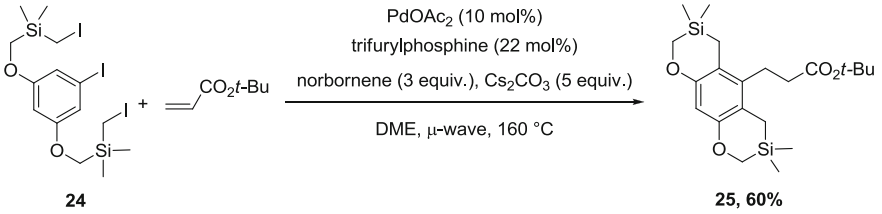

Fig. 7.9 Synthesis of tricyclic heterocycles via a tandem aryl alkylation/Heck coupling sequence

7.1.3 Palladacycle Reaction with Aryl Halides

The reaction of palladacycle **7** with aryl halides is more complex than with alkyl halides. First, there is no experimental evidence for the intermediate palladium species involved in this type of reaction. Indeed, the formation of palladium(IV) complex by oxidative addition of aryl halide to palladium(II) has never been observed, possibly owing to a fast reductive elimination process. In a different context, stable Pd(IV) complexes could be obtained by reacting aryliodonium salts and Pd(II) complexes. However, this oxidation occurring by a formal transfer of Ph^+ might follow a significantly different pathway [37, 38].[2]

Second, the outcome of the reaction depends on the substitution pattern of the palladacycle aryl ring (Fig. 7.10). When this aryl ring does not bear any *ortho* substituent (R = H), the reaction is often unselective. The incoming aryl group is mainly transferred to the palladium-bound norbornyl carbon (sp^2–sp^3 coupling) leading to arylpalladium(II) complex **26a,** but arylpalladium(II) complex **26b** can also be formed. This minor pathway involves the transfer of the incoming aryl on the aryl site of the palladacycle (sp^2–sp^2 coupling). Intramolecular pallado-catalyzed ring-closure termination delivers regioisomeric dihydrophenanthrenes **27a** and **27b** (indistinct when the aryl rings are unsubstituted) incorporating the norbornyl moiety [40].

When the palladacycle aryl ring possesses an *ortho* substituent (R ≠ H), the incoming aryl group is exclusively transferred to the aromatic site of the palladacycle (sp^2–sp^2 coupling) leading to norbornylpalladium(II) complex **28**. In a similar fashion to what was described for reactions with alkyl halides, as a consequence of the steric hindrance introduced by the presence of two *ortho* substituents, norbornene extrusion occurs to give arylpalladium(II) complex **29** [41]. The latter can react in various Pd(II)-catalyzed coupling reactions allowing the regeneration of the Pd(0) species.

To date, only a few examples of arylations using the palladium/norbornene system with non *ortho*-substituted aryl halides have been reported. Apart from Catellani's pioneering work, de Meijere described the domino coupling of heteroaryl iodides such as 3-iodopyridine **31** with norbornene to form adduct **32a** in 45 % yield along with traces of regioisomer **32b** [39] (Fig. 7.11).

Annelation reactions similar to the one at norbornene can occur at other strained olefins such as norbornadiene, bicyclo[2.2.2]octane or acenaphtol[1,2-a]acenaphtylene [42]. Vinyl sulfones could also be employed successfully. Thus dihydrophenanthrene **34** could be synthesized from iodobenzene and vinyl sulfone **33** in the presence of $Pd(OAc)_2$ and Ag_2CO_3 (Fig. 7.12) [43]. Vinyl sulfones and α,β-unsaturated phosphine oxides are the only non-strained olefins to allow this kind of reaction. This peculiar reactivity might be due to their ability to readily form, via C–H activation palladacycle intermediate **35**, where one sulfonylic oxygen atom coordinates the palladium [44].

[2] Alternatively, radical intermediates have been proposed for this type of processes: [36].

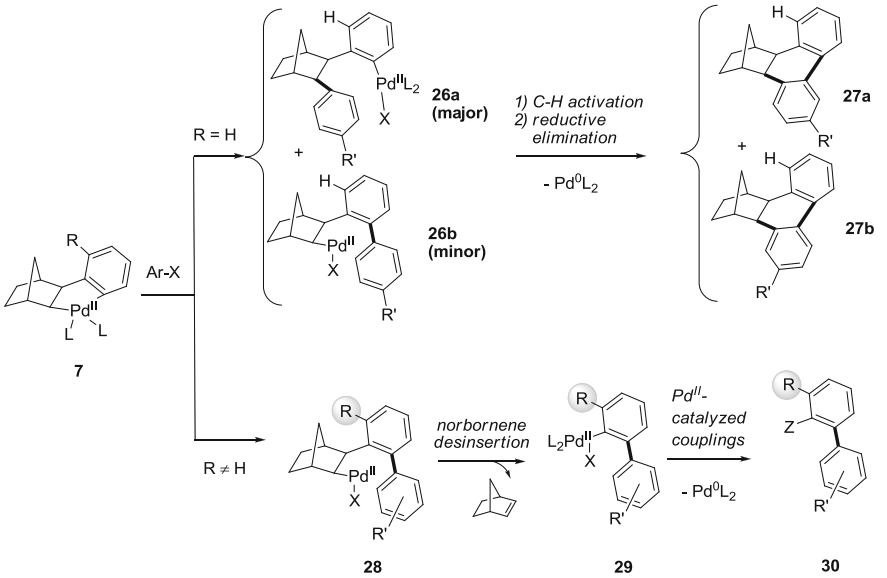

Fig. 7.10 Reactivities of palladacycle with aryl halides depending on the presence of an *ortho*-substituent

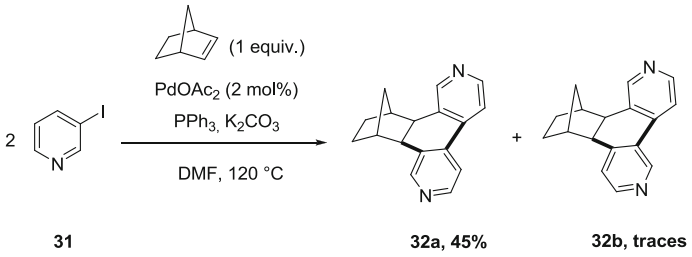

Fig. 7.11 Coupling of iodopyridine with norbornene

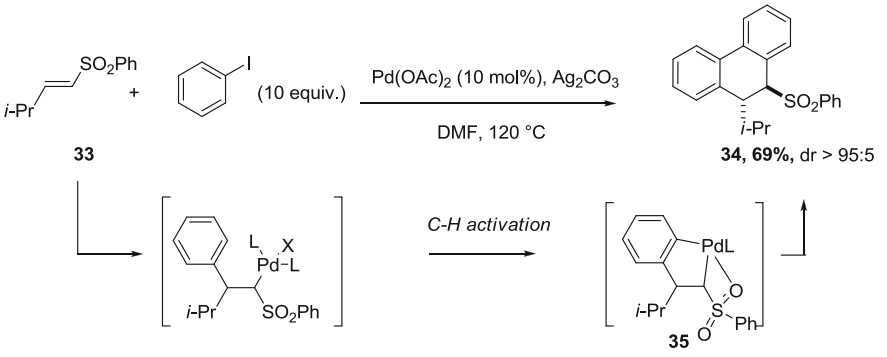

Fig. 7.12 Coupling of iodobenzene using vinyl sulfone instead of norbornene

The presence of an *ortho* substituent on the palladacycle aryl ring allows the selective aryl–aryl (sp^2–sp^2) coupling, higher degree of complexity in the functionalization and the catalytic use of norbornene. This key finding has been called "the *ortho* effect" and numerous applications have been reported since its discovery.

7.2 Synthetic Applications of the *Ortho* Effect

As we have seen, the *ortho* effect gives rise to the formation of biarylpalladium(II) complex **29** which can further react with different trapping agents, according to the known reactivity of arylpalladium(II) species (Fig. 7.13). These multi-component sequences offer a straightforward access to a wide variety of polycyclic scaffolds from simple precursors. The choice of a trapping agent is not trivial since it must selectively react with *ortho, ortho'*-disubstituted arylpalladium(II) **29** but not with all the other different palladium species formed during the complex reaction sequence. We will present here the successful strategies reported for the trapping of biarylpalladium(II) complex **29**.

7.2.1 Aromatic Arylations Coupled with Heck Reaction

Heck coupling was historically the first coupling reaction tested as terminating event of a Catellani catalytic cycle. The major challenge was that the tandem

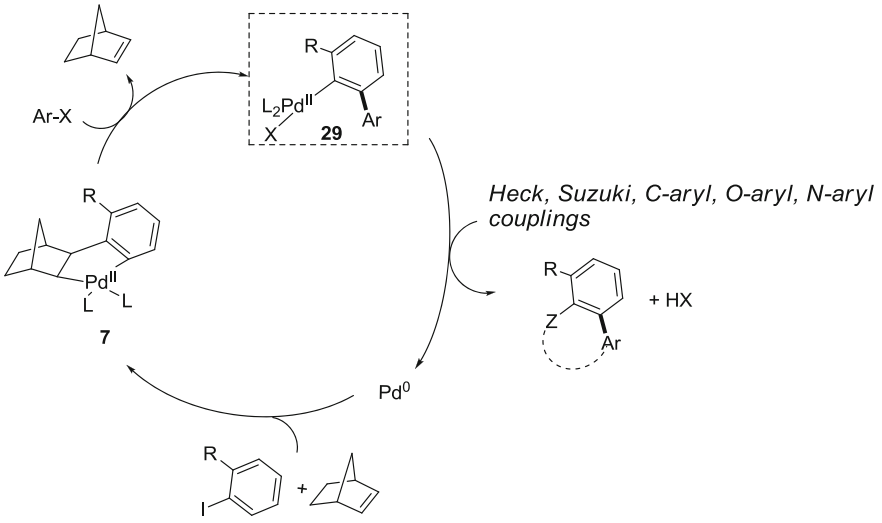

Fig. 7.13 Domino C–H arylation/Pd^{II} catalyzed coupling via palladium and norbornene cocatalysis

reaction would occur in the presence of two olefins. However, excellent selectivity was observed owing to steric effect contol: because of the steric strain release, only norbornene inserted into the unsubstituted aryl-palladium(II) bond, while only the terminal olefin could undergo Heck reaction with the doubly *ortho*-arylated arylpalladium(II) intermediate. Thus, treatment of *ortho*-substituted aryl iodides **36** with methyl acrylate in the presence of $Pd(OAc)_2$, norbornene and K_2CO_3 efficiently afforded vinylbiphenyl **37** (Fig. 7.14a) [45]. When allylic alcohols were employed as terminal alkenes, homobiaryl alkylketones such as **38** could be formed (Fig. 7.14b) [46].

Furthermore, coupling of two differently substituted aryl groups could be achieved. Aryl iodides react generally faster than aryl bromides with Pd(0) and Pd(II) complexes. Nethertheless, selectivity can be reached using *o*-alkyl substituted iodides that react readily with Pd(0) but slowly with the Pd(II) metallacycle for steric and electronic reasons. Smaller bromides, substituted with electron withdrawing groups or bearing chelating groups can on the contrary react preferentially with the palladacycle, giving access to an efficient multi-component process. For example, sequential aryl coupling/Heck reaction of iodotoluene with electron-poor aryl bromide **39** and methyl acrylate was achieved in the presence of norbornene, $Pd(OAc)_2$ and K_2CO_3, affording unsymmetrical vinylbiphenyl **40** (Fig. 7.15) [47].

Functional groups such as MeO, Me_2N or CF_3 are well tolerated as *ortho* substituents on the aryl iodide. However free hydroxyl and amino groups inhibit the reaction, probably because they can complex the Pd atom. Satisfactory results were also obtained with a wide range of substituents on the aryl bromide. Both electron-poor (such as acrylates or enones) and electron rich (such as stilbenes) terminal olefins could be used with high efficiency. However, in the case of electron rich alkenes, arylation at both the terminal and internal vinylic carbons led to a mixture of linear and branched products. Finally, although norbornene is

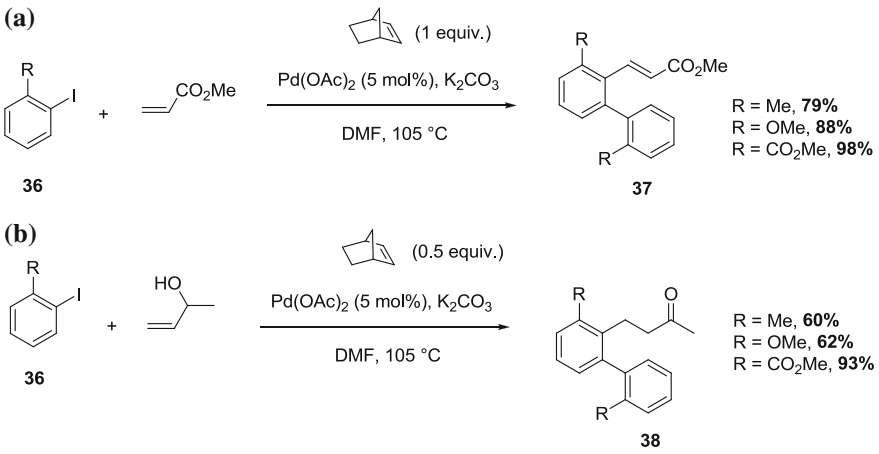

Fig. 7.14 Synthesis of vinylbiphenyls via sequential arylation/Heck reaction

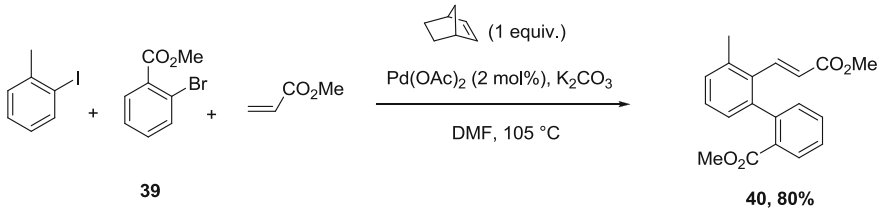

Fig. 7.15 Unsymmetrical aryl–aryl coupling/olefination sequence

regenerated during the catalytic cycle, it has generally to be used in stoichiometric quantities to allow an efficient insertion step.

7.2.2 Aromatic Arylation Coupled with Suzuki Reaction

Arylboronic acids could be used to terminate the sequence, with a very selective Suzuki cross-coupling occurring exclusively at the doubly *ortho*-substituted arylpalladium(II) **29**. *o*-Terphenyl derivatives such as **43** were obtained in good yields and with high catalytic efficiencies (Fig. 7.16) [48]. The reaction was compatible with a variety of substituents for the aryl boronic acid, even at the *ortho* position. However, complete shutdown of the reaction was observed with *ortho, ortho'*-disubstituted boronic acids, certainly because of the steric hindrance.

1-Iodonaphtalene and 4-bromopyridine have been recently coupled with phenyl boronic acid providing the first example of sequential cross *ortho*-arylation/Suzuki coupling [49].

7.2.3 Aromatic Arylations Coupled with Cyanation

Using potassium hexacyanoferrate **44** as a cyanide source, a cross-arylation/cyanation sequence could be performed under the cooperation of palladium and

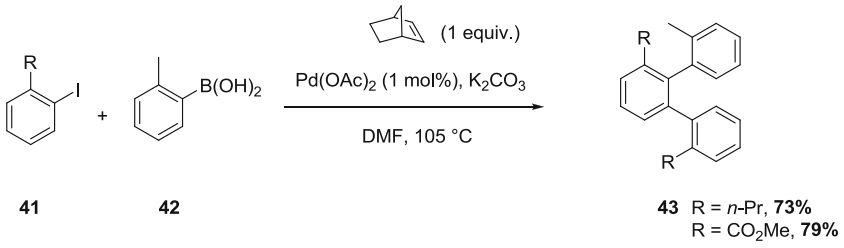

Fig. 7.16 *Ortho* arylation/Suzuki coupling sequence

norbornene. Starting from electron-poor aryl bromides such as **45** and *ortho*-substituted aryl iodide **46**, a wide variety of substituted benzonitriles such as **47** could be prepared from readily available starting materials (Fig. 7.17) [50]. Since the nitrile is amenable to numerous transformations, the prepared products can serve as valuable biaryl building blocks. The mechanism of the cyanation probably involves transmetalation between the metal cyanide and arylpalladium(II), followed by reductive elimination. Selective cyanation at the end of the Catellani sequence was difficult to achieve since several intermediates were found to readily undergo cyanation. The use of potassium hexacyanoferrate **44** bearing a strong iron-cyanide bond slows down the transmetalation rate and thus allows obtaining the desired selectivity.

7.2.4 Aromatic Arylations Coupled with Addition to C=O or C=N Bonds

Recently, Lautens reported that arylpalladium(II) **50**, generated by the coupling of *ortho*-substituted aryl iodide **48** with acetophenone **49**, could add intramolecularly to the pendant ketone. This sequence afforded fluorenol **51** (Fig. 7.18) [51]. This nucleophilic behavior of Pd(II) species [52] was triggered by the specific reaction conditions and particularly by the presence of water. Indeed, in the absence of water, the arylpalladium(II) complex returned to its usual electrophilic behavior and the reaction proceeded by sequential *ortho*-arylation/α-arylation of the ketone to provide phenanthrene derivatives (vide infra). Under optimized conditions, additions to other carbonyl functionalities such as esters or aldehydes were possible, along with additions on *N*-sulfinyl imine **52**. In this latter case, a poor diastereoselectivity was observed (dr = 2:1).

7.2.5 Aromatic Arylations Coupled with C–H Activations

The coupling of the Catellani reaction with the functionalization of aryl C–H bond as the terminating event has been reported for the synthesis of phenanthrene **56**, starting from *ortho*-substituted aryliodide **54** and diphenylacetylene **55** (Fig. 7.19)

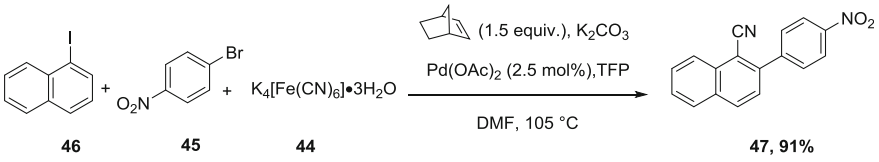

Fig. 7.17 Sequential arylation/cyanation

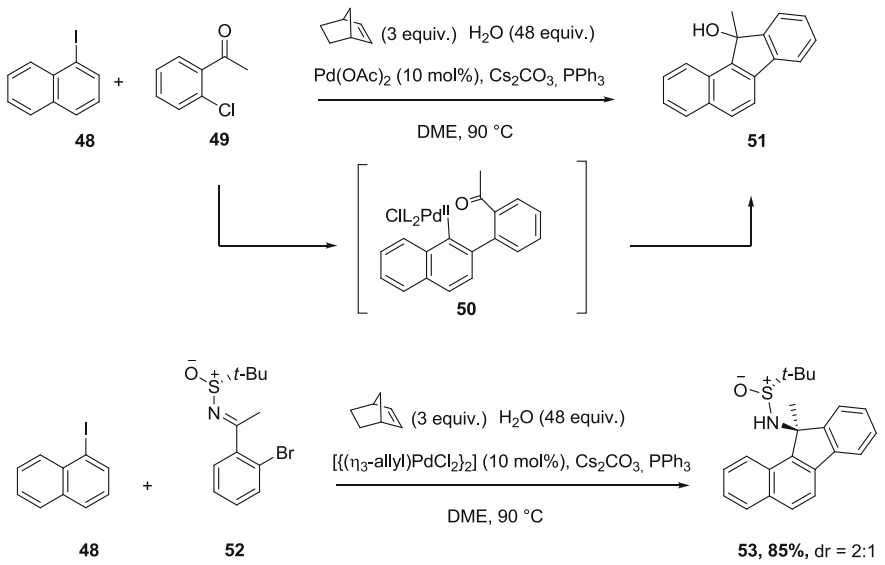

Fig. 7.18 Sequential *ortho*-arylation/C=O or C=N bond addition

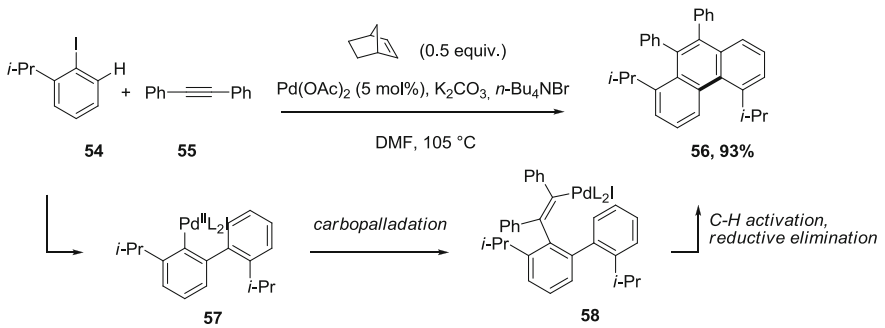

Fig. 7.19 Sequential *ortho*-arylation/carbopalladation/C–H vinylation

[53]. The reaction proceeds via the formation of biarylpalladium(II) complex **57** which undergoes carbopalladation of the alkyne, leading to vinylpalladium(II) **58**. Ring-closure by C–H activation followed by reductive elimination delivered phenanthrene **56**. The use of diarylalkynes is essential for the desired outcome of the reaction, since dialkylalkynes generate allene products via elimination.

More recently norbornene/Pd-catalyzed sequences involving the *ortho*-arylation/C–H arylation of heteroarenes have been introduced [54]. Heteroaryl substrates such as furan, thiophene, and pyrroles could be employed successfully, allowing an expeditious synthesis of heteroatom-containing *o*-teraryl derivatives such as **59** (Fig. 7.20).

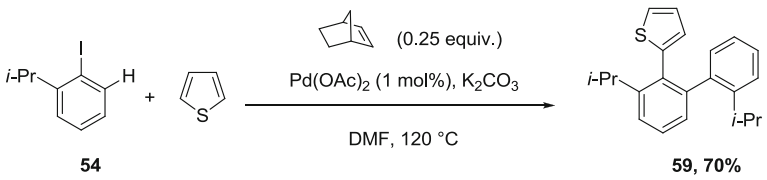

Fig. 7.20 Sequential *ortho*-arylation/C–H arylation

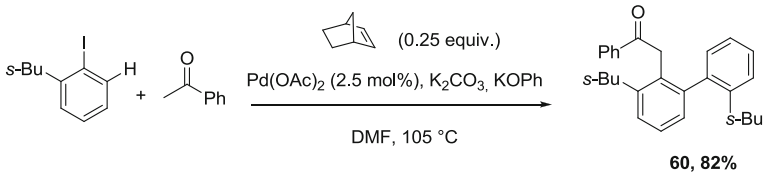

Fig. 7.21 Sequential *ortho*-arylation/C–H activation of ketone

Using the α-arylation of ketones as the terminating step of a Catellani sequence, substituted biaryls containing a ketone function could be obtained in mild conditions. Products such as **60** could be synthesized in efficient yields by reaction between *ortho*-substituted aryl iodides and ketones in the presence of norbornene, palladium and bases (Fig. 7.21) [55]. Acetone, acetophenone and cyclopentanone could be successfully employed for the intermolecular C–H functionalization step.

7.2.6 Aromatic Arylations Coupled with O-aryl Couplings

C–O Couplings have been reported as terminating events of Catellani sequences, using *o*-bromophenols as coupling partners. Thus reaction of *o*-trifluoromethyliodobenzene **61** with *o*-bromophenol **62**, in the presence of $Pd(OAc)_2$ and norbornene led to the synthesis of benzofuran derivative **63** (Fig. 7.22) [49].

When *ortho*-substituted aryliodides and *o*-bromophenol were reacted in the presence of an electron-poor olefin, an elegant sequential *ortho*-arylation/Heck reaction/Michael-type addition sequence took place, leading to 6*H*-dibenzopyrans

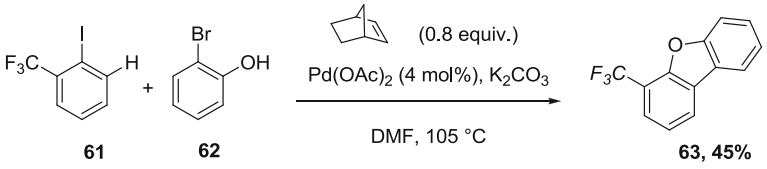

Fig. 7.22 Sequential *ortho*-arylation/O-aryl coupling

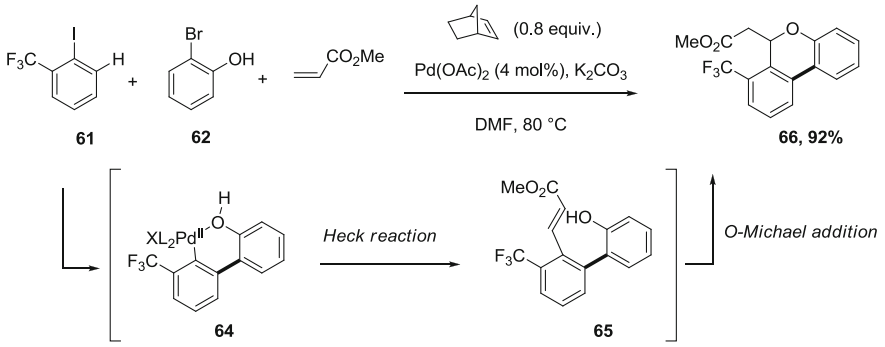

Fig. 7.23 Sequential *ortho*-arylation/Heck reaction/Michael addition

in good yields (Fig. 7.23) [56]. Interestingly, the replacement of *o*-bromophenol with *p*-bromophenol led to the homocoupling of the aryliodide, showing that the selective reaction of *o*-bromophenol with the palladacycle was driven by its chelating ability.

7.2.7 Aromatic Arylations Coupled with N-aryl Couplings

Extension of the termination to palladium-catalyzed C–N coupling (Buchwald-Hartwig) opens access to polycyclic nitrogen-containing compounds. Starting from *ortho*-substituted aryl iodides and *o*–bromobenzamide, 6-phenanthridinones could be synthesized via sequential *ortho*-arylation/amide-aryl coupling (Fig. 7.24a) [57]. The addition of a tertiary phosphine was essential for the successful outcome of the reaction, possibly to counteract the coordination of the amide. Interestingly, the reaction could be extended to several heterocyclic *o*-bromocarboxamides (Fig. 7.24b).

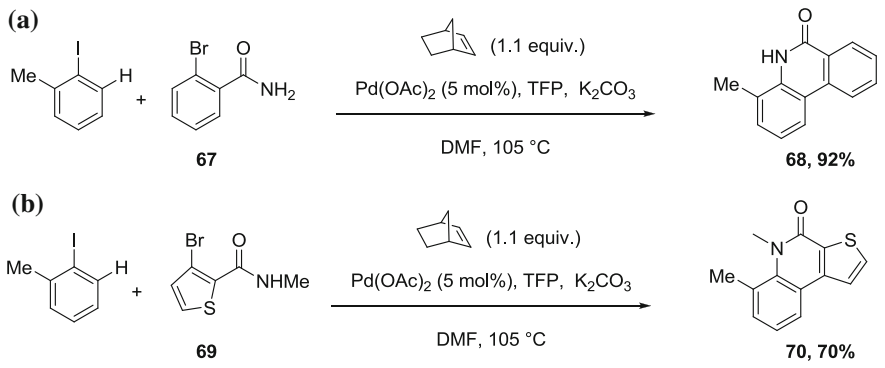

Fig. 7.24 Sequential *ortho*-arylation/amide-aryl coupling

o-Bromoarenesulfanilides such as **71** could also react with *o*-alkylaryl iodides, yielding carbazoles through aryl amination (Fig. 7.25) [58]. It should be noted that bromoanilines had to be *N*-tosyl or *N*-acetyl protected to be tolerated. This catalytic procedure was applied to the synthesis of interesting pharmaceutical compounds such as antibiotic carbazomycin A **74**.

Finally, silylimines could be coupled to *ortho*-substituted aryl iodides via domino arylation/C–N(sp^2) coupling to yield phenanthridines such as **76**. The reaction was thought to proceed trough cleavage of the N–Si bond resulting in the formation of the palladium-imido intermediate **78** [59, 60], followed by reductive elimination (Fig. 7.26) [61]. Along with *N*-silylaldimines, unsubstituted ketimines could be conveniently used in this procedure. Remarkably, silylimine **79** could react smoothly with aryl triflate **80** to deliver benzo[*c*]phenanthridine **81**, a key precursor of natural phenanthridinium alkaloid nitidine [12].

As a conclusion, the *ortho* effect has wide synthetic potential, allowing the straightforward synthesis of complex scaffolds in a single step from simple precursors. However, until recently, no rational explanation had been proposed to account for this selectivity. Pleasingly, theoretical investigations by Echavarren and our group (in collaboration with Catellani's group) shed light on the different mechanistic pathways at stake in the absence and in the presence of an *ortho* substituent on the key—palladacycle intermediate.

7.3 Mechanistic Explanations for the *Ortho* Effect

As we saw in the Sect. 7.1., there is no experimental evidence for the intermediate palladium species involved in the reaction of palladacycles **7** with C(sp^2)-X electrophiles (Fig. 7.27). In analogy to the known reactivity of alkyl halides, the

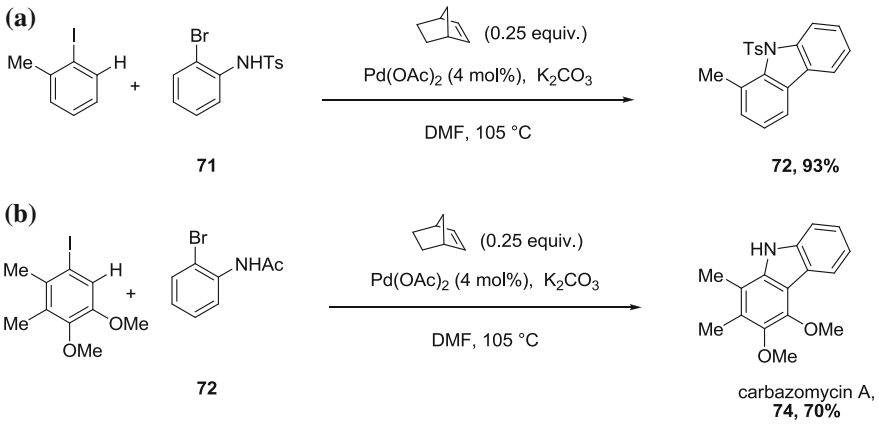

Fig. 7.25 Sequential *ortho*-arylation/amine arylation

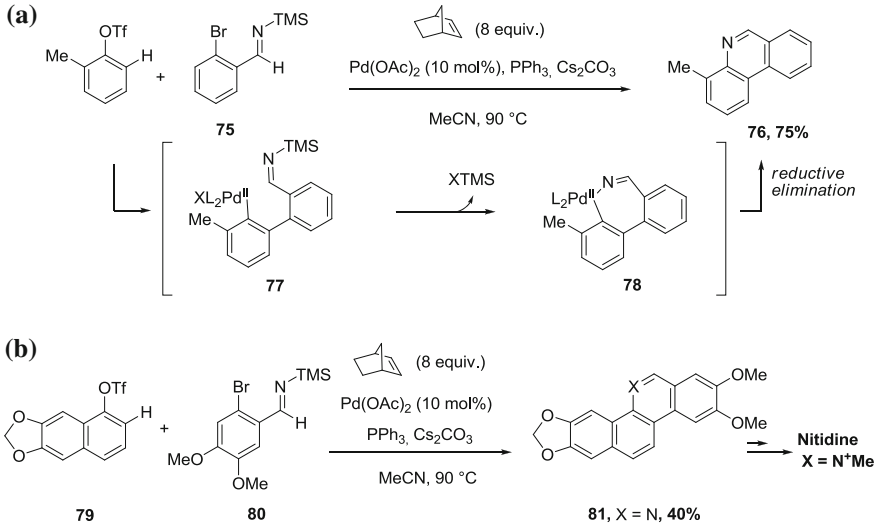

Fig. 7.26 Sequential *ortho* arylation/*N*-arylation of imines

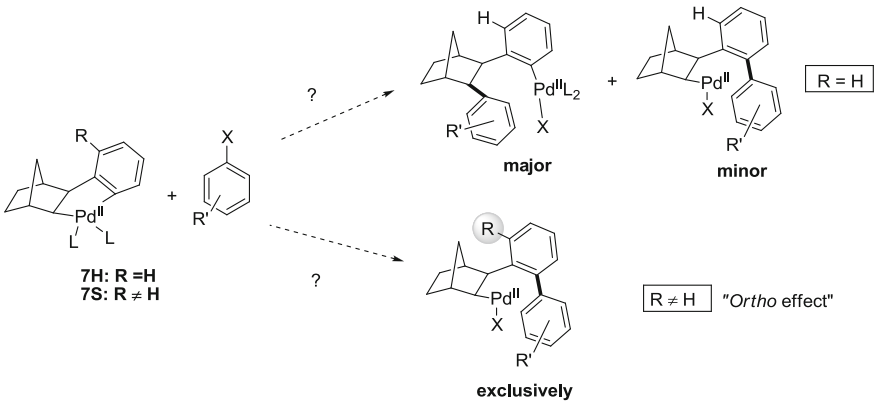

Fig. 7.27 Unknown intermediates in the reactions of *ortho*-substituted and unsubstituted palladacycles with aryl halides

formation of a palladium(IV) complex has been postulated for a long time. However, recent DFT investigations seem to demonstrate that two alternative mechanistic routes can be involved, depending on the presence or absence of an *ortho* substituent. Please note that we will continue with the usual numbering of molecules to designate calculated models.

7.3.1 *Mechanistic Pathway Followed by Palladacycle 7H Bearing No Ortho-substituent*

A transmetalation-type exchange of aryl ligands [62, 63] has been proposed (path b) as an alternative mechanism to the oxidative addition of aryl halides to palladium(II) metallacycle **7H** (path a). In that scenario, the aryl halide would react preferentially with another Pd(0) species present in the reaction mixture, forming an arylpalladium(II) complex **82.** The latter would undergo a transmetalation-type reaction with palladacycle **7H**, leading to binuclear complex **83**. Reductive elimination would create the new $C(sp^2)$–$C(sp^3)$ bond in **84** (Fig. 7.28).

Experimental evidence for the transmetalation of aryl group between two Pd^{II} centers has been reported by Osakada. Formation of macrocyclic biaryl product **86** was indeed observed starting from the binuclear aryl Pd^{II} complex **85** (Fig. 7.29) [64].

Echavarren was the first to undertake computational studies to discriminate between the two pathways: Pd(IV) intermediate or transmetalation-type reaction [65]. Palladacycle **87** bearing one Pd-$C(sp^2)$ bond and one Pd-$C(sp^3)$ bond in a *cis* arrangement was used as a model for **7H** and iodoethylene **88** was used as a model for the aryl halide. Two types of ancillary ligands were tested. H_2O could mimic the behavior of oxygenated coordinating solvent such as DMA or DMF; and PH_3 represented a simplified model for tertiary phosphine ligands. The phenyl ligand exchange was studied with a more complete model using formamide as ligand and demonstrated a moderate activation energy. Comparison of the free energy profiles (not shown) of the two alternatives by DFT calculation supported the reaction pathway described in Fig. 7.30 (way b), that do not involve Pd(IV) species. The oxidative addition of $C(sp^2)$-X electrophile to Pd(0) followed by transmetalation was facilitated by the easy formation of the bridged binuclear complex **94**. This alternative proved highly favorable over endothermic ligand substitution at

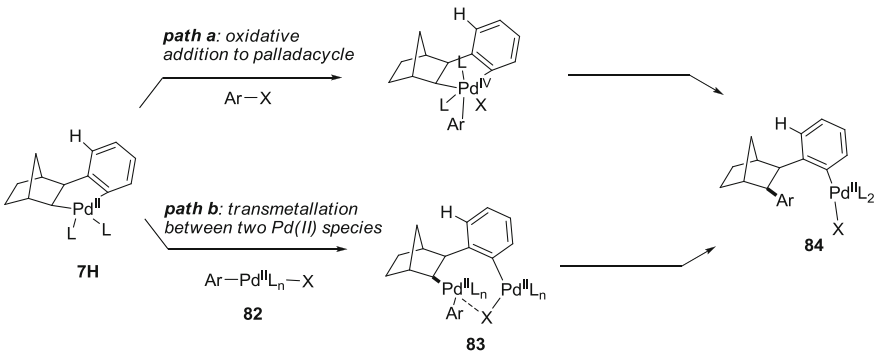

Fig. 7.28 Two mechanistic pathways proposed for reaction of palladacycle 7H with $C(sp^2)$-X electrophiles

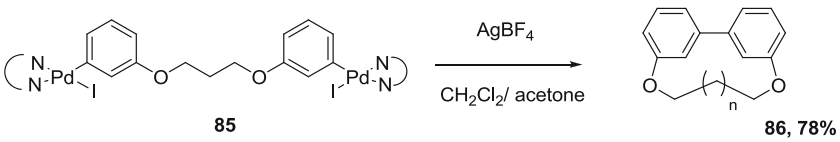

Fig. 7.29 Experimental evidence for transmetalation-type reaction between Pd^{II} complexes

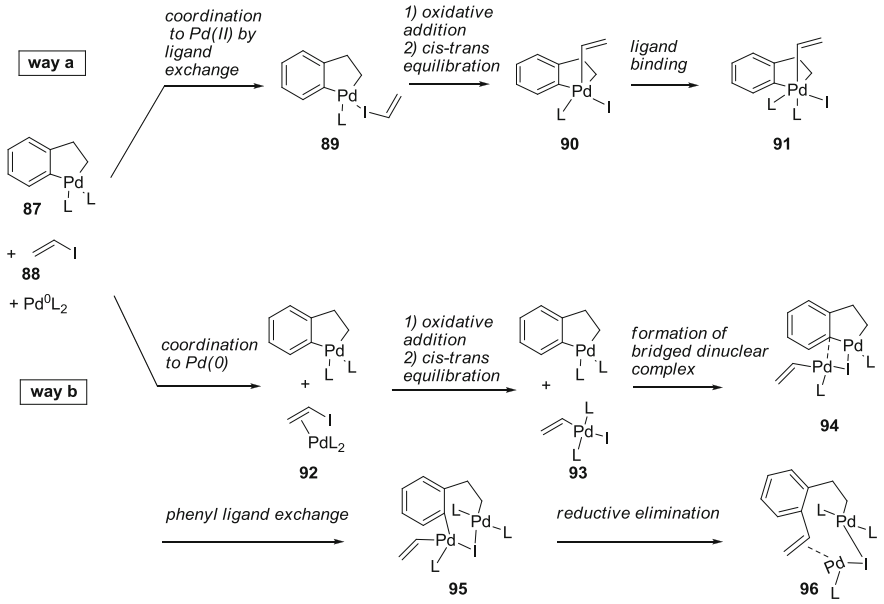

Fig. 7.30 Pd(IV) and transmetalation-type reaction pathways calculated by Echavarren

palladium(II) metallacycle followed by oxidative addition to form Pd(IV) derivative **91** (Fig. 7.30 way a).

The pioneering findings disclosed by Echavarren study were completed by our group in collaboration with Catellani. We compared both pathways on palladacycle **97** model, which is closer to the putative intermediate [66]. Two types of ancillary ligands were tested (DMF and PMe_3). On the most representative steps, the steric contribution of the phosphine was fully assessed by employing PPh_3 as the ligand. To obtain a picture as general as possible, three incoming aryl halides were examined: iodobenzene, 4-iodotoluene and 4-bromobenzaldehyde. Calculations were performed by DFT to evaluate the energy profiles of the Pd(IV) and the transmetalation-type pathways. As a representative example, the calculated free energy profiles for these two pathways with PMe_3 as ligand and iodobenzene as the aryl halide are depicted in Fig. 7.31.

The first step of *way a* is the coordination of iodobenzene to palladacycle **97**. It proceeds via displacement of one phosphorus ligand to form **98**. This process is

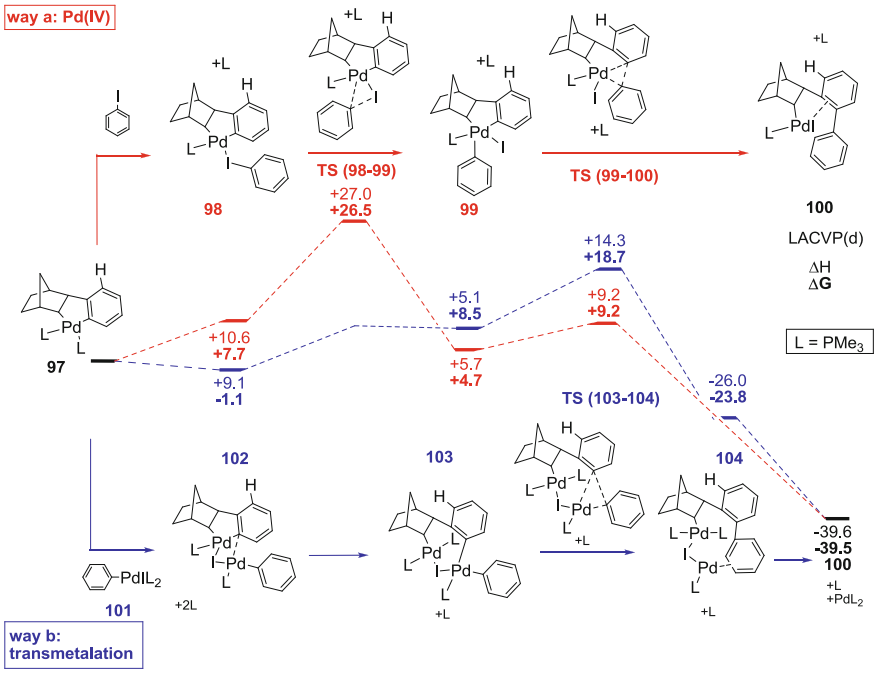

Fig. 7.31 Calculated energy profiles for Pd(IV) and transmetalation pathways for unsubstituted palladacycle with PMe_3 as the ligand. Optimization: M06/LACVP(d), values in kcal/mol at 298 K

endothermic but accompanied by a positive entropic (ΔS) variation (ΔH = +10.6 kcal/mol; ΔG = +7.7 kcal/mol at 298 K). Then, oxidative addition leads to pentacoordinated Pd(IV) complex **99,** which features a Y-distorted trigonal bipyramidal geometry, with a high transition state (ΔG = + 26.5 kcal/mol with respect to the entry channel **97**). Finally, reductive elimination involving the axial C(sp^2) from metallacycle and the equatorial C(sp^2) from the incoming aryl halide occurs with an easily accessible transition state (ΔG = +4.5 kcal/mol relative to **99**). The formation of alkylpalladium(II) complex **100** is highly exothermic. Octahedral transition states (involving two ligands L) for this pathway could also be found but were of higher energy.

On the other hand, the first step of *way b* is the complexation of arylpalladium(II) **101**, formed by oxidative addition of iodobenzene to a Pd(0) species, with palladacycle **97**. The formation of bimetallic complex **102**, presenting a clamshell conformation, occurs with displacement of two phosphorus ligands and a negative free energy (ΔG = −1.1 kcal/mol). In binuclear complex **102**, both bridged Pd nuclei possess a slightly distorted square planar geometry. Transfer of the aryl ring from the palladacycle to the incoming palladium center occurs with concomitant coordination of one phosphorus ligand, which leads to binuclear complex **103**. No transition state could be found for this step. This could be explained by a very flat

potential energy surface around **103** ($\Delta G = +9.6$ kcal/mol relative to **102**). Finally, a reductive elimination from **103** leads to alkylpalladium(II) complex **100** via transition state **TS(103-100)** situated at $\Delta G = +10.2$ kcal/mol relative to **103**.

Comparison of the two energy profiles demonstrated that the transmetalation pathway is always favored over the Pd(IV) pathway by at least 5 kcal/mol at the temperature range in which these reactions usually take place (80–130 °C). This trend was confirmed using the other aryl halides and DMF as the ancillary ligand. This study proved that the coupling of *ortho unsubstituted* aryl halides in the presence of norbornene and palladium had a high probability to occur via a transmetalation-type mechanism rather than via a palladium(IV) intermediate.

It has been observed experimentally that the final reductive elimination was unselective, leading to both $C(sp^2)$–$C(sp^2)$ and $C(sp^2)$–$C(sp^3)$ couplings. To understand this poor selectivity, our group compared the energy profiles for the transfer of the aryl ring from the palladacycle to the incoming palladium center from **102** (Fig. 7.32, way b, $C(sp^2)$–$C(sp^2)$ coupling, previously shown in Fig. 7.31) and for the transfer of the norbornyl moiety from the palladacycle to the incoming palladium (Fig. 7.32, way b', $C(sp^2)$–$C(sp^3)$ coupling, experimentally observed). A very narrow energy gap was calculated between both pathways, which could explain the lack of selectivity experimentally observed for these reactions.

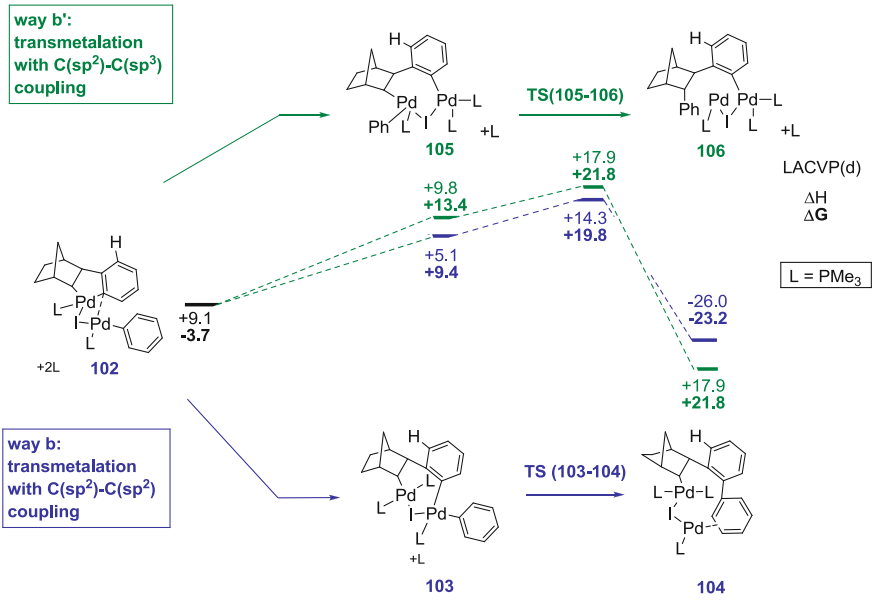

Fig. 7.32 Reaction pathways and energies for the formation of $C(sp^2)$–$C(sp^2)$ bond and $C(sp^2)$–$C(sp^3)$ bond from 102. Optimization: M06/LACVP(d), values in Kcal/mol at 373 K

7.3.2 *Mechanistic Pathway Followed by Palladacycle 7S with an Ortho-substituent*

Our group similarly compared the energy profiles of the Pd(IV) and transmetalation pathways, but starting from the palladacycle bearing an *ortho*-methyl substituent **107** [66]. The calculated free energy profiles for these two pathways, with PMe_3 as ligand and iodobenzene as the aryl halide are depicted in Fig. 7.33.

The newly calculated Pd(IV) pathway (*way a*) is very similar to the unsubstituted palladacycle one. The intermediate Pd(IV) complex **109** has the same Y-distorted trigonal bipyramidal geometry as **99** and leads to C(sp^2)–C(sp^2) coupling via reductive elimination. The similarity in the energy values for the oxidative addition of iodobenzene on unsubstituted palladacycle **97** and on *ortho*-methyl substituted palladacycle **107** can be explained by analyzing the geometries of these palladacycles and the geometries of the transition states **TS(98–99)** and **TS(108–109)**. In the modeled structure of **107**, two carbons sp^3 of the norbornyl moiety, the aryl ring and the palladium center are coplanar. The methyl substituent points toward a free space, far away from the bulky norbornene bridge. The geometry of **TS(108–109)** (Fig. 7.34) is similar to that of **107**. Consequently, the orientation of the methyl substituent implies that oxidative addition on

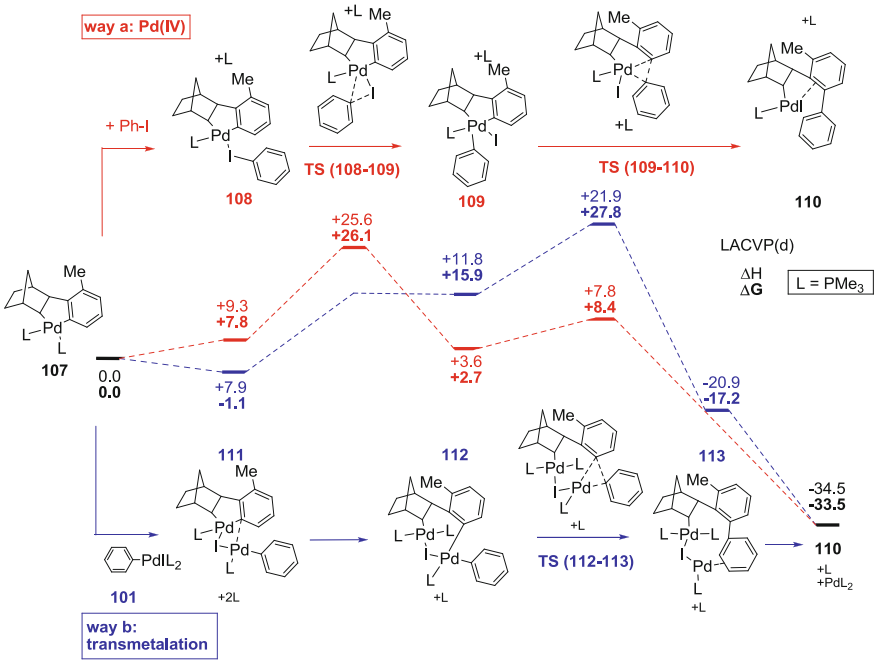

Fig. 7.33 Calculated energy profiles for Pd(IV) and transmetalation pathways for *ortho*-methyl substituted palladacycle with PMe_3 as the ligand. M06/LACVP(d), values in kcal/mol at 298 K

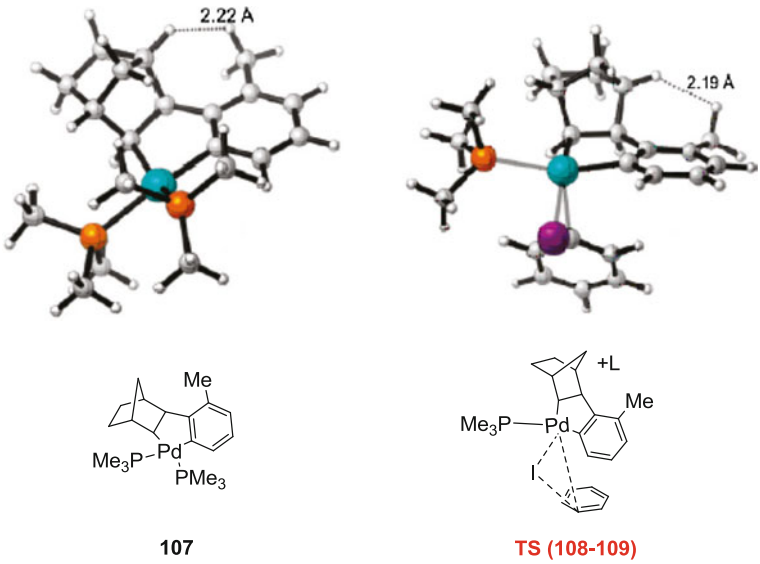

Fig. 7.34 Modeled structures of palladacycle 107 and transition state of the oxidative addition leading to Pd(IV) intermediate

palladacycle **107** would not suffer from an additional steric clash due to the *ortho*-substituent, compared to oxidative addition on **97**.

In the transmetalation pathway (Fig. 7.33, *way b*), the calculated energy profiles are very different in the absence and in the presence of an *ortho*-methyl substituent. The formation of the association complex **111** remains unchanged, but the transfer of the palladacycle aryl ring between the two palladium nuclei, leading to **112** is much more costly ($\Delta G = +17$ kcal/mol from **111**, compared to 9,6 kcal/mol between **102** and **103**). Reductive elimination from binuclear complex **112** occurs via a transition state **TS(112-113)** ($\Delta G = +27.8$ kcal/mol in respect to the entry channel **107**) which is 1.7 kcal/mol higher than the highest transition state in the Pd(IV) pathway (**TS(108-109)**, $\Delta G = +26.1$ kcal/mol in respect to the entry channel). Besides, the energy gap ($\Delta G = \Delta H - T\Delta S$) between the two pathways increases with temperature since the entropy variation (ΔS) is negative for the transmetalation pathway while almost constant for the Pd(IV) pathway.

The sharp increase in the energy values for the transfer of the palladacycle aryl ring in the presence of an *ortho* substituent can be explained by the geometries of the relevant transition state **TS(112-113)** (Fig. 7.35). Compared to the geometry of the starting palladacycle **107**, **TS(112–113)** presents a rotated C(aryl)-C(norbornyl) bond relative to the plan of the palladacycle. As a consequence, the *ortho*-substituent now points *towards* the bridging CH_2 of the norbornyl, creating an important steric clash.

Thus, in the presence of an *ortho*-methyl substituent, the Pd(IV) pathway becomes favored over the transmetalation pathway especially at high temperatures.

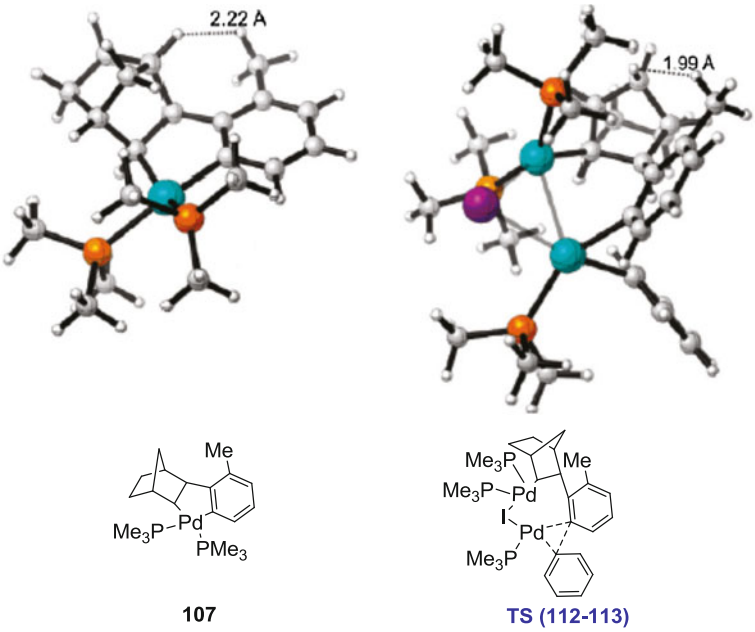

Fig. 7.35 Calculated structures of palladacycle 107 and transition state of the transmetalation-type process

This trend was confirmed using the other aryl halides and DMF as the ancillary ligand. In every cases, the steric effects are the main factors that disfavor the transmetalation pathway.

Experimentally, selective $C(sp^2)$–$C(sp^2)$ coupling is obtained starting from an *ortho*-substituted palladacycle. In accordance with this experimental observation, calculations show that the barrier of the reductive elimination from Pd(IV) complex **109** is much higher for norbornyl-aryl coupling (Fig. 7.36, $C(sp^2)$–$C(sp^3)$ coupling, *way a'*) than for aryl–aryl coupling (Fig. 7.36, $C(sp^2)$–$C(sp^2)$ coupling, *way b*). Calculated Mulliken formal charges for the atoms of complex **109** offer a rationalization for this selectivity. Indeed, the electrophilic $C(sp^2)$ from the incoming aryl halide (Mulliken atomic charge = 0.071492) reacts preferentially with the more nucleophilic carbon [$C(sp^2)$ from metallacycle aryl ring (Mulliken atomic charge = −0.011069), to be compared to the $C(sp^3)$ from norbornyl moiety (Mulliken atomic charge = 0.017381)].

To conclude, recent calculations have elucidated the probable pathways both in the absence and in the presence of an *ortho* substituent in the starting palladacycle. Without an *ortho* substituent, the reaction likely proceeds via a transmetalation-type mechanism between two palladium(II) centers. On the other hand, in the presence of an *ortho* substituent it likely proceeds through a trigonal bipyramidal Pd(IV) intermediate which allows selective $C(sp^2)$–$C(sp^2)$ coupling by reductive elimination. Therefore, the *ortho* effect has its roots in a fundamental switch in the

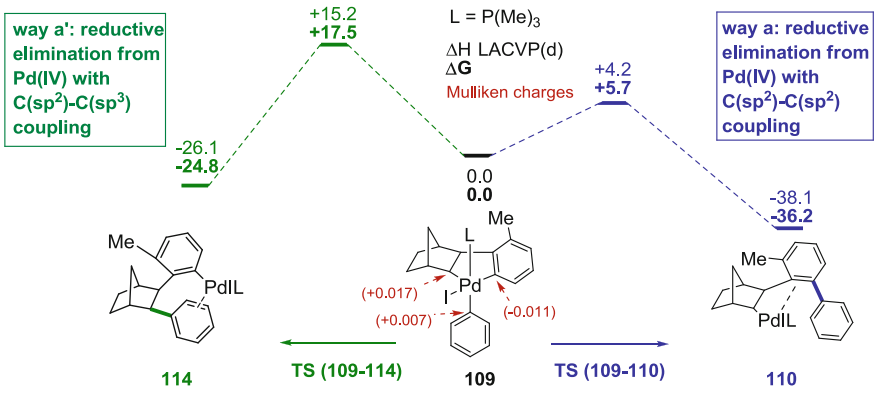

Fig. 7.36 Reaction pathways and energies for the formation of $C(sp^2)$–$C(sp^2)$ bond and $C(sp^2)$–$C(sp^3)$ bond from 109. Optimization: M06/LACVP(d), values in kcal/mol at 298 K

reaction mechanism introduced by steric effects. This finer understanding of the intermediates involved in the mechanism of the *ortho* effect should help chemists to extend the scope of this reactivity and get better insights into the role of chelating functions present on the aryl halides.

References

1. Yu, J. Q., Shi, Z. (Eds.). (2010). C-H activation. Topics in current chemistry, *292*, 1–379.
2. Wencel-delord, J., Dröge, T., Liu, F., & Glorius, F. (2011). *Chemical Society Reviews, 40*, 4740–4761.
3. Chiusoli, G. P., Catellani, M., Costa, M., Motti, E., Della Ca, N., & Maestri, G. (2010). *Coordination Chemistry Reviews, 254*, 456–469.
4. Catellani, M., & Chiusoli, G. P. (1985). *Journal of Organometallic Chemistry, 286*, C13–C16.
5. Catellani, M. (2003). *Synlett,* 298–313.
6. Catellani, M., Motti, E., & Della Ca, N. (2008). *Accounts of Chemical Research, 41*, 1512–1522.
7. Martins, A., Mariampillai, B., & Lautens, M. (2010). *Topics in Current Chemistry, 292*, 1–33.
8. Amatore, C., & Jutand, A. (2000). *Accounts of Chemical Research, 33*, 314–321.
9. Amatore, C., Jutand, A., Khalil, F. (2006). *ARKIVOC*, *iv*, 38–48.
10. Zawisza, A. M., & Muzart, J. (2007). *Tetrahedron Letters, 48*, 6738–6742.
11. Jeffery, T. (1999). *Tetrahedron Letters, 40*, 1673–1676.
12. Blanchot, M., Candido, D. A., Larnaud, F., & Lautens, M. (2011). *Organic Letters, 13*, 1486–1489.
13. Dieck, H. A., & Heck, R. F. (1974). *Journal of the American Chemical Society, 96*, 1133–1135.
14. Khoury, P. R., Goddard, J. D., & Tam, W. (2004). *Tetrahedron, 60*, 8103–8112.
15. Li, C.-S., Cheng, C.-H., Liao, F.-L., Wang, S. L. (1991). *Journal of the Chemical Society, Chemical Communications*, 710–712.

16. Catellani, M., Mealli, C., Motti, E., Paoli, P., Perez-Carreno, E., & Pregosin, P. S. (2002). *Journal of the American Chemical Society, 124*, 4336–4346.
17. Catellani, M., & Chiusoli, G. P. (1992). *Journal of Organometallic Chemistry, 425*, 151–154.
18. Martin-Matute, B., Mateo, C., Cardenas, D. J., & Echavarren, A. M. (2001). *Chemistry–A European Journal, 7*, 2341–2348.
19. Garcia-Cuadrado, D., Braga, A. A. C., Maseras, F., & Echavarren, A. M. (2006). *Journal of the American Chemical Society, 128*, 1066–1067.
20. Garcia-Cuadrado, D., Mendoza, P., Braga, A. A. C., Maseras, F., & Echavarren, A. M. (2007). *Journal of the American Chemical Society, 129*, 6880–6886.
21. Chiusoli, G. P., & Catellani, M. (1992). *Journal of Organometallic Chemistry, 437*, 369–373.
22. Liu, C.-H., Li, C.-S., & Cheng, C.-H. (1994). *Organomettallics, 13*, 18–20.
23. Byers, P. K., Canty, A. J., Skelton, B. W., White, A. H. (1986). *Journal of the Chemical Society, Chemical Communications*, 1722–1724.
24. Bocelli, G., Catellani, M., & Ghelli, S. (1993). *Journal of Organometallic Chemistry, 458*, C12–C15.
25. Rudolph, A., Rackelmann, N., & Lautens, M. (2007). *Angewandte Chemie International Edition, 46*, 1485–1488.
26. Ananikov, V. P., Musaev, D. G., & Morokuma, K. (2005). *Organometallics, 24*, 715–723.
27. Ananikov, V. P., Musaev, D. G., & Morokuma, K. (2007). *European Journal of Inorganic Chemistry, 34*, 5390–5399.
28. Ananikov, V. P., Musaev, D. G., Morokuma, K. (2002). *Journal of the American Chemical Society*, *124*, 2839–2852 and references cited therein.
29. Terpko, M. O., & Heck, R. F. (1979). *Journal of the American Chemical Society, 101*, 5281–5283.
30. Catellani, M. (2003). *Synlett,* 298–313.
31. Wilhem, T., & Lautens, M. (2005). *Organic Letters, 7*, 4053–4056.
32. Catellani, M., Frignani, F., & Rangoni, M. (1997). *Angewandte Chemie International Edition, 36*, 119–122.
33. Catellani, M., Motti, E., Minari, M. (2000). *Journal of the Chemical Society, Chemical Communications,* 157–158.
34. Motti, E., Rosseti, M., Bocelli, G., & Catellani, M. (2004). *Journal of Organometallic Chemistry, 689*, 3741–3749.
35. Alberico, D., Rudolph, A., & Lautens, M. (2007). *Journal of Organic Chemistry, 72*, 775–781.
36. Lyons, T. W., & Sanford, M. S. (2010). *Chemical Reviews, 110*, 1147–1169.
37. Canty, A. J., Patel, J., Rodeman, T., Ryan, J. H., Skelton, B. W., & White, A. H. (2004). *Organometallics, 23*, 3466–3473.
38. Dick, A., Kampf, J. W., & Sanford, M. S. (2005). *Journal of the American Chemical Society, 127*, 12790–12791.
39. Albrecht, K., Reiser, O., Weber, M., Knieriem, B., & de Meijere, A. (1994). *Tetrahedron, 50*, 383–401.
40. Catellani, M., Motti, E. (1998). *New Journal of Chemistry,* 759–761.
41. Catellani, M., Motti, E., & Baratta, S. (2001). *Organic Letters, 3*, 3611–3614.
42. Dyker, G., Korning, P. J., Jones, P. G., & Bubenitschek, P. (1993). *Angewandte Chemie International Edition, 32*, 1733–1735.
43. Mauleón, P., Núñez, A. A., Alonso, I., & Carretero, J. C. (2003). *Chemistry–A European Journal, 9*, 1511–1520.
44. Alonso, I., Alcami, M., Mauleon, P., & Carretero, J. C. (2006). *Chemistry–A European Journal, 12*, 4576–4583.
45. Motti, E., Ippomei, G., Deledda, S., Catellani, M. (2003). *Synthesis*, 2671–2678.
46. Catellani, M., Deledda, S., Ganchegi, B., Henin, F., Motti, E., & Muzart, J. (2003). *Journal of Organometallic Chemistry, 687*, 473–482.
47. Faccini, F., Motti, E., & Catellani, M. (2004). *Journal of the American Chemical Society, 126*, 78–79.

48. Motti, E., Catellani, M. (2003). *Journal of Molecular Catalysis A: Chemical*, *204–205*, 115–124.
49. Catellani, M., Motti, E., & Della Ca, N. (2008). *Accounts of Chemical Research, 41*, 1512–1522.
50. Mariampillai, B., Alliot, J., Li, M., & Lautens, M. (2007). *Journal of the American Chemical Society, 129*, 15372–15379.
51. Zhao, Y.-B., Mariampillai, B., Candito, D. A., Laleu, B., Li, M., & Lautens, M. (2009). *Angewandte Chemie International Edition, 48*, 1849–1852.
52. Quan, L. G., Gevorgyan, V., & Yamamoto, Y. (1999). *Journal of the American Chemical Society, 121*, 3545–3546.
53. Catellani, M., Motti, E., & Baratta, S. (2001). *Organic Letters, 3*, 3611–3614.
54. Della Ca, N., Maestri, G., & Catellani, M. (2009). *Chemistry–A European Journal, 15*, 7850–7853.
55. Maestri, G., Della Ca, N., Catellani, M. (2009). *Chem. Commun,* 4892–4894.
56. Motti, E., Faccini, F., Ferrari, I., Catellani, M., & Ferracioli, R. (2006). *Organic Letters, 8*, 3967–3970.
57. Ferraccioli, R., Carenzi, D., Rombola, O., & Catellani, M. (2004). *Organic Letters, 6*, 4759–4762.
58. Catellani, M., Motti, E., & Della Ca, N. (2010). *Topics in Catalysis, 53*, 991–996.
59. Mann, G., Hartwig, J. F., Driver, M. S., & Fernandez-Rivas, C. (1998). *Journal of the American Chemical Society, 120*, 827–828.
60. Barluenga, J., Aznar, F., & Valdes, C. (2004). *Angewandte Chemie International Edition, 43*, 343–345.
61. Candito, D. A., & Lautens, M. (2009). *Angewandte Chemie International Edition, 48*, 6713–6716.
62. Dyker, G. (1994). *Chemische Berichte, 127*, 739–742.
63. Ozawa, F., Fujimori, M., Yamamoto, T., & Yamamoto, A. (1986). *Organometallics, 5*, 2144–2149.
64. Suzaki, Y., & Osakada, K. (2003). *Organometallics, 22*, 2193–2197.
65. Cardenas, D. J., Martin-Matute, B., & Echavarren, A. (2006). *Journal of the American Chemical Society, 128*, 5033–5040.
66. Maestri, G., Motti, E., Della Ca, N., Malacria, M., Derat, E., & Catellani, M. (2011). *Journal of the American Chemical Society, 133*, 8574–8585.

Chapter 8
Results: New Partners for Ortho-Substituted Aryl Iodides in Palladium/Norbornene Cocatalysis

8.1 Coupling of *Ortho*-Substituted Aryl Iodides and Bromobenzyl Amines: First Reported Catellani Sequence Terminated by *N*-aryl Coupling with Unprotected Amines

8.1.1 Objectives of the Project

As we have seen in Sect. 7.2, the incorporation of a *N*-aryl coupling reaction with unprotected amines in a Catellani sequence has never been reported. Only amides, imines and tosylated and acetylated anilines have been used successfully as coupling partners. The use of free amines would be atom and time economic since no prefunctionalization of starting material would be required. Furthermore the scope of accessible nitrogen heterocycles would be nicely extended. In collaboration with Giovanni Maestri, a third year Ph.D. student from the Catellani group (Parma University) who had joined our laboratory, we wished to develop such a C-amination coupling variant with unprotected amines. We decided to use bromobenzylamine **115** as a test substrate. We reasoned that successful coupling of **115** and *ortho* substituted aryl iodides in the presence of norbornene and palladium would lead to dihydrophenanthridine **117** via sequential cross-*ortho*-arylation and C-amination. We anticipated that dihydrophenanthridine **117** could be further easily oxidized to afford phenanthridines such as **118** which are interesting bioactive compounds (Fig. 8.1).

Phenanthridines are indeed a well known class of natural alkaloids. Quaternary benzo[*c*]phenanthridines are commonly isolated from *Papaveraceae* and *Rutaceae* plants. Nitidine **119**, isolated from *Toddalia asiatica* extracts, exhibits anti-HIV [1], antimalaria [2–4] as well as strong antitumor activities [5]. Chelerythrine **120** isolated from *Greater celandine* is a potent protein kinase C inhibitor [6]. In addition, many synthetic phenanthridine analogues display wide activity spectra [7], and methodologies enabling their synthesis from simple precursors might speed up the discovery of new hit compounds for pharmaceutical applications (Fig. 8.2).

M.-H. Larraufie, *Development of New Radical Cascades and Multi-Component Reactions*, Springer Theses, DOI: 10.1007/978-3-319-01324-4_8,

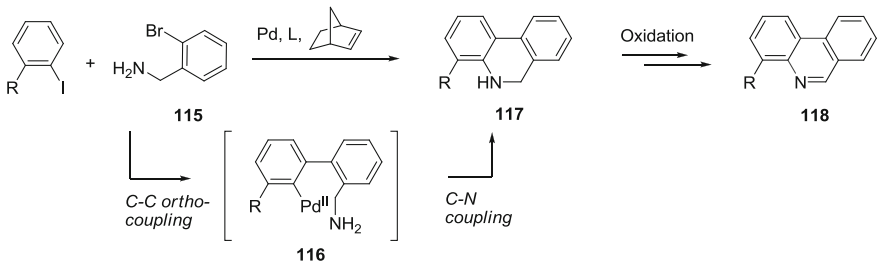

Fig. 8.1 Objectives of the project

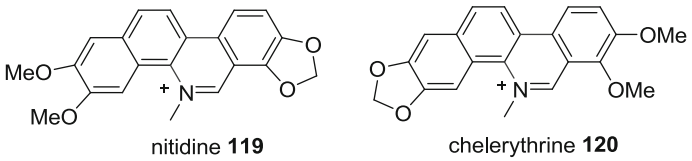

Fig. 8.2 Natural phenanthridines with interesting biological activities

8.1.2 Optimization of the Catalytic Synthesis of Phenanthridines and Proposed Mechanism

8.1.2.1 Optimization of the Conversion

We tested the feasibility of the planned reaction by submitting 2-iodotoluene and 2-bromobenzylamine **115** to the usual Catellani reaction conditions i.e.: $Pd(OAc)_2$ (5 mol %), norbornene (1 equiv.), triphenylphosphine (10 mol %) and Cs_2CO_3 as a base (Table 8.1, entry 1). To our delight, we could isolate the desired 5,6-dihydrophenanthridine **121a** but, surprisingly, as an approximately 4:1 mixture with oxidized phenanthridine **122a** (66 % overall yield). First, we endeavored to optimize the conversions of the starting aryl halides and the overall yield by varying several parameters of the reaction conditions.

We first tested the required conditions for obtaining the desired reactivity. We found that the presence of norbornene was necessary for the reaction to occur (Table 8.1, entry 2). This result suggests that the reaction proceeded through a C-Arylation followed by intramolecular C-Amination and not in the opposite order. The phosphine ligand was important to obtain a satisfying conversion (Table 8.1, entry 3). This is probably due to the presence of the free amino group on aryl bromide that might interact with palladium.

The optimal amount of norbornene was subsequently checked. Reducing the amount of norbornene to 0.5 equiv. limited the formation of the usual byproducts arising from its reactivity with the aryl iodide only [8]. The consumption of the aryl iodide by side-reactions being limited, the conversion of the aryl bromide **115** could be improved to an overall yield of 85 % (Table 8.1, entry 4). Further

Table 8.1 Optimization of the overall yield

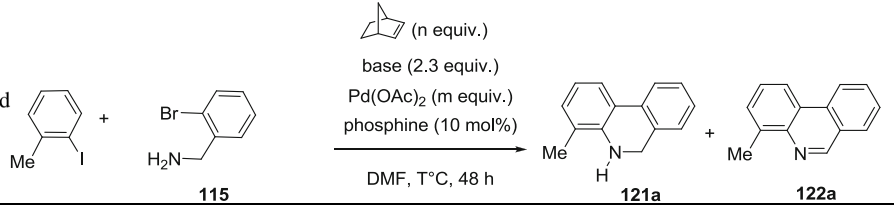

Entry	Norbornene equiv.	Phosphine	T (°C)	Base	Catalytic charge Pd (%)	Conversion Ar–I (%)	Conversion Ar-Br (%)	Yield **1a** + **2a** (%)
1	1	PPh_3	130	Cs_2CO_3	5 mol	100	75	66 (4:1)
2	–	PPh_3	130	Cs_2CO_3	5 mol	10	5	–
3	1	–	130	Cs_2CO_3	5 mol	35	25	20
4	0.5	PPh_3	130	Cs_2CO_3	5 mol	98	95	85
5	0.25	PPh_3	130	Cs_2CO_3	5 mol	75	60	55
6	0.5	PPh_3	105	Cs_2CO_3	5 mol	60	45	40
7	0.5	TFP	105	Cs_2CO_3	5 mol	90	85	70
8	0.5	PPh_3	130	K_2CO_3	5 mol	100	90	75
9	0.5	PPh_3	130	Cs_2CO_3	2.5 mol	98	95	75

reduction of norbornene amount proved detrimental for the conversion (Table 8.1, entry 5), which is quite unusual for this kind of intramolecularly terminated catalytic sequences (vide infra).

Finally, the influence of various parameters on the reaction outcome was checked. Reducing the temperature of the reaction lowered the conversion with PPh_3 as the phosphine (Table 8.1, entry 6). Replacing PPh_3 with tri-2-furyl phosphine allowed a return to good conversion but with a medium overall yield of 70 % (Table 8.1, entry 7). Switching the base for K_2CO_3 (entry 8) or lowering the catalytic charge (entry 9) proved again detrimental to the overall yield.

8.1.2.2 Optimization of the Phenanthridine Formation

Having optimized the conditions for the overall yield, we sought to favor the formation of phenanthridine **122a** which was the most interesting compound given its significant bioactivities (Table 8.2). Checking the influence of the reaction conditions on the **121a:122a** ratio moreover allowed us to get a better insight into the surprising one-pot dehydrogenation of dihydrophenanthridine **121a** into **122a**.

We reasoned that dehydrogenation of **121a** required a sacrificial hydrogen acceptor and that this role could be played by norbornene, yielding norbornane. Addition of norbornene after full conversion did not affect the ratio between the two products (Table 8.2, entry 2). However, addition of 3 equivalents of norbornene at 90 % conversion seemed to favor the dehydrogenation (Table 8.2, entry 3), resulting in an increased amount of phenanthridine product (65 % yield). Employing stilbene as the sacrificial olefin, it was also possible to favor the formation of **122a** (Table 8.2, entry 4) and furthermore to identify diphenylethane as the expected coproduct of the dehydrogenation. We finally found that simple introduction of dioxygen via a balloon even after full conversion (evidenced by precipitation of palladium(0) black) allowed us to get exclusively phenanthridine **122a**, isolated in 85 % yield (Table 8.2, entry 5).

These features suggest a palladium(II) species as catalyst of the dehydrogenation process. When no more aryl halide is present in solution to regenerate palladium(II) species from Pd(0), the addition of a sacrificial olefin has no effect. Dioxygen could both regenerate Pd(II) from Pd(0) and act as the hydrogen scavenger in the dehydrogenation step. Both Pd(II) catalyzed disproportionation between two olefins and dehydrogenations of olefins with dioxygen catalyzed by palladium are reported in the literature. Thus, treatment of cyclic olefin **123** with 5 mol % of palladium trifluoroacetate led to a 40:60 mixture of *tert*-butylphenyl derivative **124** and cyclohexyl derivative **125** (Fig. 8.3) by disproportionation [9].

Using the same palladium catalyst, oxidative aromatization of cyclohexene **126** with dioxygen was depicted (Fig. 8.4) [10]. The reaction was thought to proceed via insertion of the electrophilic palladium into the allylic C–H bond of cyclohexane, followed by elimination of trifluoroacetic acid to give intermediate **129**. β-hydride elimination would deliver cyclohexadiene and palladium hydride species **130**. In the absence of dioxygen, this complex would decompose to give Pd(0). On

Table 8.2 Optimization of the yield of phenanthridine 122a

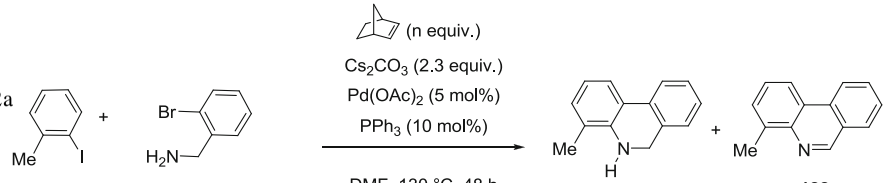

115 121a 122a

Entry	Norbornene equiv. (n)	Additive (equiv.)	Yield **121a** (%)	Yield **122a** (%)
1	0.5	–	58	27
2	0.5 + 3 after full conv.	–	47	31
3	0.5 + 3 before full conv.	–	17	65
4	0.5	Stilbene (3) before full conv.	12	58
5	0.5	O_2 after full conv.	–	85

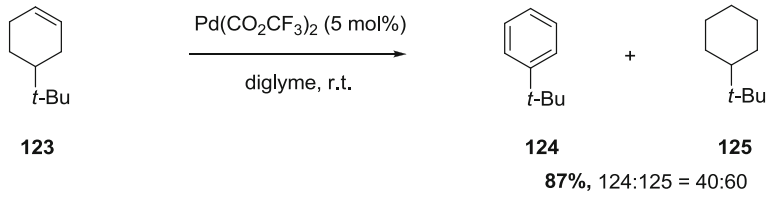

Fig. 8.3 Pd(II) catalyzed disproportionation of endocyclic olefin

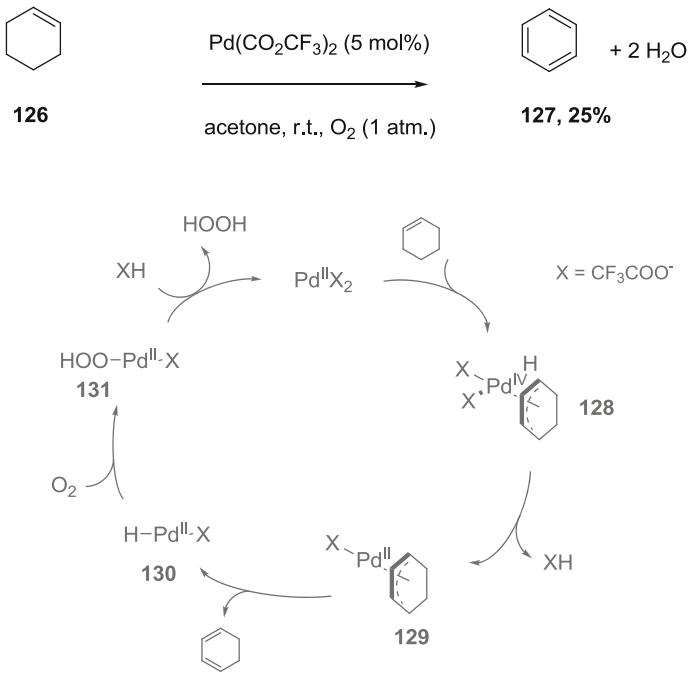

Fig. 8.4 Pd(II) catalyzed oxidative aromatization of endocyclic olefin with dioxygen

the other hand, quick insertion of O_2 into the Pd-H bond is thought to produce peroxy intermediate **131** that reacts with trifluoroacetic acid to regenerate the catalyst. The absence of detectable hydrogen peroxide might indicate that the catalytic system efficiently decomposes it into dioxygen and water [11].

Several catalytic sequences report the regeneration of palladium(II) catalysts from Pd(0) species in the presence of dioxygen [12]. The mechanistic pathway is not perfectly understood and might depend on the reaction conditions. For instance, Stahl has demonstrated that the reaction of Pd(0) complex **132** bearing bidentate nitrogen ligands with dioxygen led to peroxopalladium(II) complex **134** (Fig. 8.5) [13]. This oxidation was proposed to occur via the [(η^1-O_2)Pd^I] diradical **133** [14].

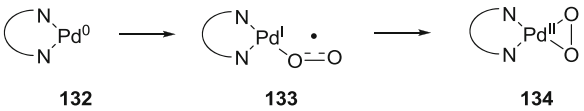

Fig. 8.5 Oxidation of Pd(0) complex to Pd(II) and theoretical intermediate

This literature background as well as the mechanistic studies on the Catellani reaction (see Chap. 7) drove us to propose dual palladium catalysis for our synthesis of phenanthridine **122a** (Fig. 8.6). The first catalytic cycle would correspond to the expected Catellani sequence ending with an aryl-NH_2 coupling. Thus, iodotoluene would oxidatively add to Pd(0) to give arylpalladium(II) complex **135** that would insert norbornene into the aryl palladium bond. Arene C–H activation would deliver palladacycle **137** that would react with bromobenzylamine to afford Pd(IV) complex **138** in which the amine moiety likely completes the Pd(IV) coordination sphere. This chelation and the small size of the bromide substituent may explain the good selectivity obtained for the reaction of palladacycle **137** with aryl bromide rather than aryl iodide. Reductive elimination would selectively afford $C(sp^2)$-$C(sp^2)$ coupling, generating biarylpalladium(II) complex **139**. Extrusion of norbornene would then be triggered by the steric hindrance. A final intramolecular amination step [15] would deliver 5,6-dihydrophenanthridine **121a** and regenerate the Pd(0) species. Dioxygen allows to switch from this first catalytic cycle to a dehydrogenation cycle by oxidizing Pd(0) to Pd(II) species. Coordination of the dihydrophenanthridine by Pd(II) would lead to formation of palladium amide complex **142**. β-hydride elimination would then deliver

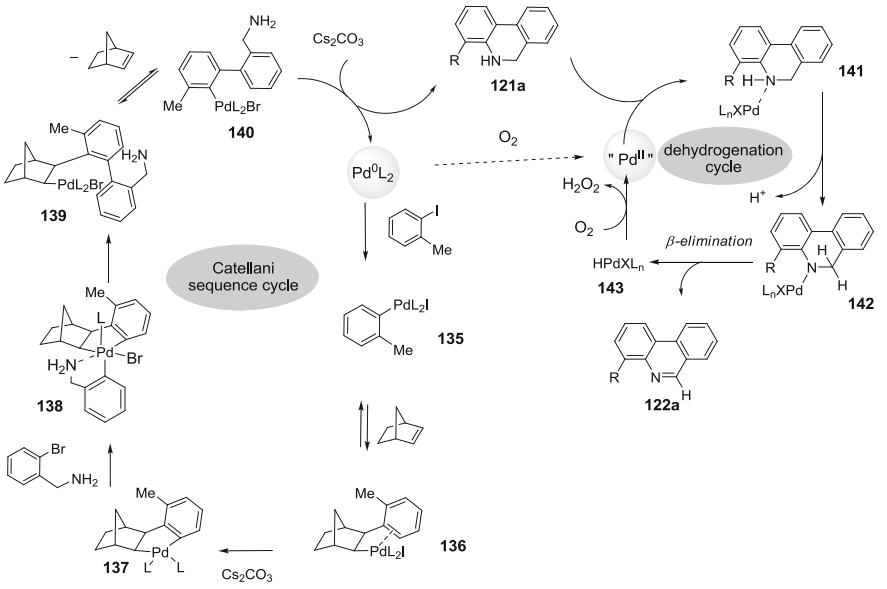

Fig. 8.6 Proposed reaction mechanism

phenanthridine **122a** and palladium hydride species **143** that could react with O_2 to regenerate the initial Pd(II) catalyst.

To confirm the role of palladium in the oxidation step, we heated isolated 5,6-dihydrophenanthridine **121a** at 130 °C in DMF in the presence of Cs_2CO_3 and O_2 but without metal catalyst. The oxidation occurred but was much slower than in the presence of palladium, confirming the role of the latter in the dehydrogenation step.

8.1.3 Scope of the Synthesis of Phenanthridines

8.1.3.1 Preparation of the Aryl Bromide and Aryl Iodides Precursors

Most of the aryl bromides and iodides that we used to check the scope of our methodology were commercially available. A few others were easily accessible via short synthetic sequences.

Bromobenzylamines **146** and **147** were prepared in two steps from the corresponding aldehydes **144** and **145** [16]. Treatment of the latter with hydroxylamine hydrochloride afforded the corresponding oximes which were conveniently reduced to primary amines using zinc powder and aqueous HCl (Fig. 8.7).

α-Substituted benzylamines could also be synthesized starting from the corresponding ketones. Oxime formation using *O*-benzylhydroxylamine was reported in the literature to afford the optimal oxime precursors for secondary amines. [17] We consequently treated ketones **148** and **149** with *O*-benzylhydroxylamine, but only oxime **150**, bearing an α-methyl substituent, could be successfully obtained, as a *cis*/*trans* mixture (Fig. 8.8a). The two isomers were subsequently reduced under mild conditions using borane-THF, affording 1-(2-bromophenyl)acetamine **152**. Pleasingly, under the reaction conditions previously used for the aldehyde precursors, α-phenyl substituted ketone **149** could be converted to the desired secondary amine **154** (Fig. 8.8b).

With the idea of developing an expeditious synthesis of natural quaternary phenanthridine nitidine **119** in mind, we wished to prepare aryl iodide **155** which was not commercially available (Fig. 8.9).

Only one literature report described the synthesis of aryl iodide **155**. Starting from 1,2–bis(ethynyl)benzene derivative **156**, the latter proceeded via $PtCl_2$

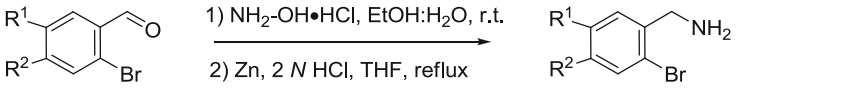

144, $R^1 + R^2$ = O-CH_2-O
145, R^1 = F; R^2 = H, **61%** (2 steps)

146, $R^1 + R^2$ = O-CH_2-O, **71%** (2 steps)
147, R^1 = F; R^2 = H, **61%** (2 steps)

Fig. 8.7 Synthesis of bromobenzylamines from corresponding aldehydes

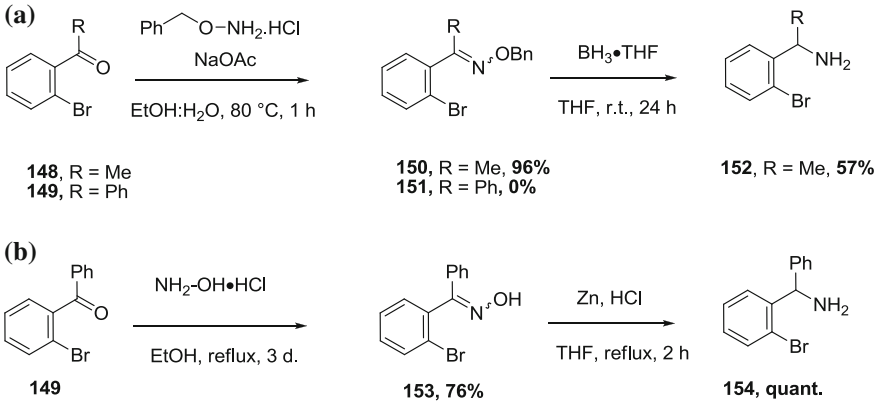

Fig. 8.8 Synthesis of α-substituted bromobenzylamines from corresponding ketones

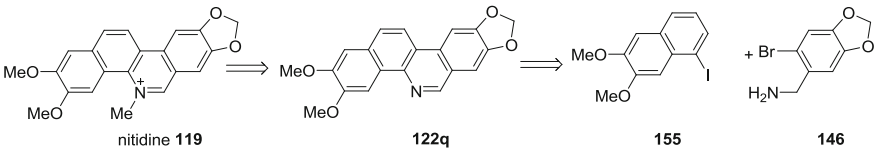

Fig. 8.9 Planned retrosynthesis of nitidine

catalyzed sequential hydroiodination/6-π electrocyclization/dehalogenation [18]. Bis(ethynyl)benzene **156** was readily prepared from 1,2-dibromo-4,5-dimethoxybenzene **157** by Sonogashira coupling with (trimethylsilyl)acetylene and subsequent desylilation of the alkyne functions (Fig. 8.10). Unfortunately, treatment of substrate **156** under the described conditions [18] did not afford the desired naphthalene iodide **155** in our hands, but mostly degradation. Analysis of the

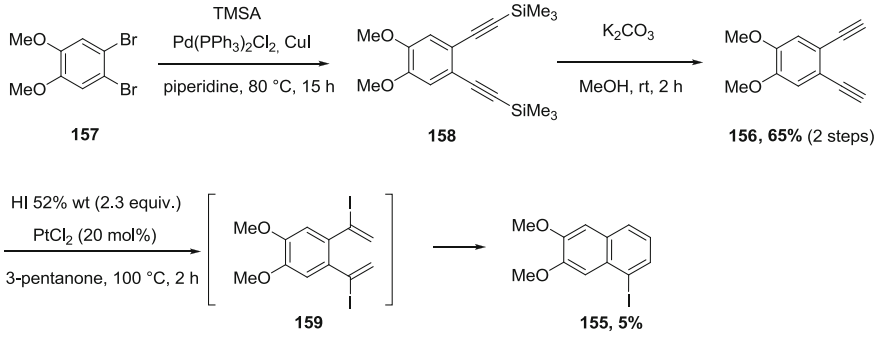

Fig. 8.10 Attempt to synthesize naphtyl iodide 155

reaction course showed that intermediate **159** was well formed (full conversion after one hour at 100 °C), but then reacted sluggishly. Very recently, Lautens mentioned that the synthesis of this kind of naphtyl iodides were inefficient and smartly developed the use of naphtyl triflates as coupling partners instead [19]. This certainly represents a nice alternative that would be tested in the future.

8.1.3.2 Scope: Variation of the Aryl Iodides

With our various aryl halide precursors in hand, we examined the scope of our methodology using the optimized conditions, namely: 1 equiv. of aryl bromide and 1.1 equiv. of aryl iodide stirred in the presence of 5 mol % of $Pd(OAc)_2$, 10 mol % of triphenylphosphine, 2.3 equiv. of Cs_2CO_3 and 50 mol % of norbornene at 130 °C under argon for 36 h, then under dioxygen for 15 h. We firstly investigated the influence of the aryl iodide substitution on the outcome of the reaction by reacting bromobenzylamine **115** with diversely substituted aryl iodides (Table 8.3).

Good results were obtained with electrodonating substituents, whether alkyl (Table 8.3, entries 1−3; yields = 80−91 %) or alkoxy groups (Table 8.3, entries 4−5; yields = 65−95 %). Since natural phenanthridines usually bear alkyl or alkoxy substituents, we were delighted by such an outcome. Benzo[*c*]phenanthridines could also be formed smoothly starting from substituted iodonaphthalenes (Table 8.3, entries 7−6). On the other hands, iodides bearing electron withdrawing groups, such as chloride or trifluoromethyl, at the *ortho* position led to moderate to poor yields (Table 8.3, entries 8 and 9). This is in agreement with previous reports on these sequences employing electron-rich aryl bromides [20–23].

We next investigated the substitution of the bromide partner, and tested various combinations of substituted bromobenzylamine and aryl iodides. The results are depicted in Table 8.4.

Diversely 6-substituted phenanthridines were obtained in excellent yields both from secondary α-methylbenzylamine (Table 8.4, entries 1−3) and dibenzylamine derivatives (Table 8.4, entries 8−9). Aromatic substituents of different electronic and steric properties did not disrupt the reaction, which proved much more tolerant of substitution of the benzylamine part (Table 8.4, entries 4−7), than it was at substitution of the iodide partner. Thus, fluorinated phenanthridines as well as chlorinated phenanthridines could be synthesized with good yields. Again this was in agreement both with previous findings and the proposed reaction mechanism.

To conclude, we developed a novel strategy for the synthesis of phenanthridines by successfully coupling a palladium and norbornene catalyzed domino sequence with an intramolecular amination followed by an oxidative dehydrogenation [24]. Products could be obtained in good to excellent yields, without the requirement of either any protecting group on the primary or secondary amine or any sacrificial reagent for dehydrogenation. This opens a new route towards the synthesis of biologically relevant compounds with minimized production of chemical wastes.

Table 8.3 Scope of the phenanthridine synthesis, effect of substituents on the aryl iodide

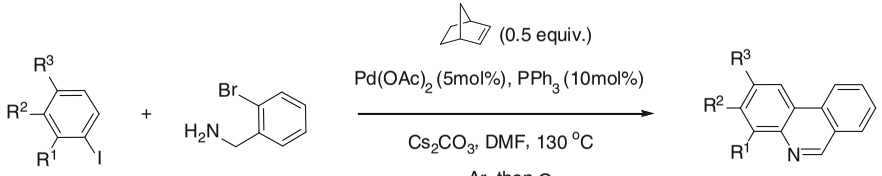

Entry	Aryl Iodide R^1, R^2, R^3	Product	Yield (%)
1	R^1 = Et	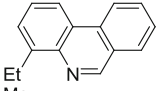	122b, 82
2	R^1, R^3 = Me	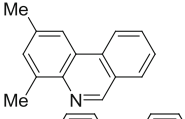	122c, 81
3	R^1, R^2 = Me	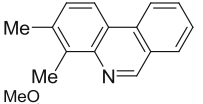	122d, 91
4	R^1 = Me R^3 = OMe	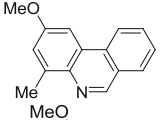	122e, 65
5	R^1 = Me R^2, R^3 = OMe	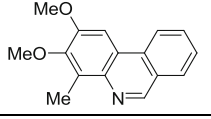	122f, 95

(continued)

Table 8.3 (continued)

Entry	Aryl Iodide R^1, R^2, R^3	Product	Yield (%)
6	$R^1 = R^2 = (CH)_4$	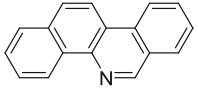	122 g, 80
7	$R^1 = R^2 = (CH)_4$ $R^3 = OMe$	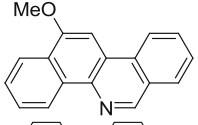	122 h, 77
8	$R^1 = Cl$	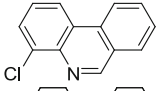	122i, 31
9	$R^2 = CF_3$	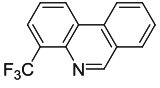	122j, 22

Table 8.4 Scope of the phenanthridine synthesis: effect of the substituents on the aryl bromide

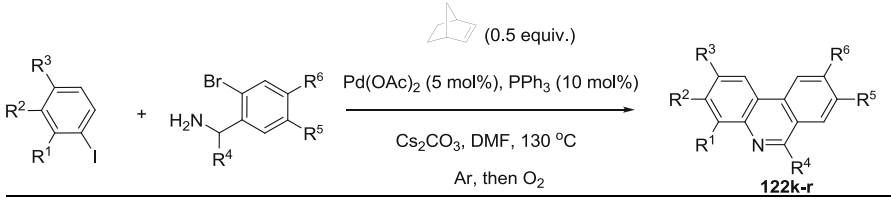

Entry	Aryl Bromide R^4, R^5, R^6	Product	Yield
1	R^4 = Me	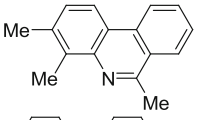	122 k, 90
2	R^4 = Me	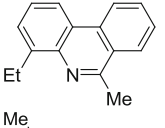	122 l, 88
3	R^4 = Me	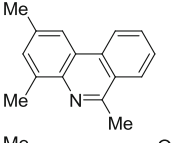	122 m, 90
4	$R^5 = R^6$ = -OCH_2O-	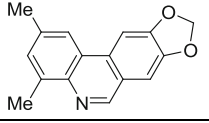	122n, 82

(continued)

Table 8.4 (continued)

Entry	Aryl Bromide R^4, R^5, R^6	Product	Yield
6	$R^5 = F$	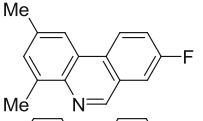	122o, 86
7	$R^5 = F$	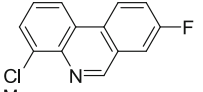	122p, 46
8	$R^4 = Ph$	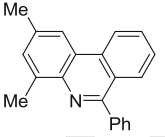	122q, 97
9	$R^4 = Ph$	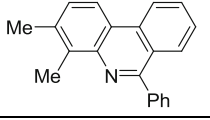	122r, 92

Developing a similar methodology using *ortho*-substituted aryl triflates as partners should allow us to further expand the scope of our methodology and access natural phenanthridines.

8.2 Coupling of *Ortho*-Substituted Aryl Iodides and 2-Bromophenyl Acetamides: An Exception to the *Ortho* Effect

8.2.1 Previous Work and Objectives of the Project

Previously in our laboratory, the synthesis of seven-membered lactam **161** was proposed featuring a key Catellani sequence ending with an intramolecular amide-aryl coupling. Starting materials would be iodotoluene and 2-bromophenylacetamide **160** (Fig. 8.11). The development of an efficient synthesis of this type of lactam ring was interesting because it was envisioned to apply it to the synthesis of paullone derivatives **162**, which are well known inhibitors of cyclin-dependent kinases.

However, when iodotoluene and 2-bromophenylacetamide **160** were reacted in the presence of norbornene and palladium, the formation of lactam **161** was not observed but dihydrophenanthrene **163a** was isolated instead as the major product (Table 8.5, entry 1). A short optimization was performed varying the reaction parameters. In all cases **163a** was obtained as the major product. Increasing the reaction temperature and the catalytic charge improved the isolated yield (Table 8.5, entries 2−3). On the contrary, changing the phosphine or the solvent, or doubling the amount of norbornene proved detrimental (Table 8.5, entries 4−7). Finally, an improved purification procedure led to **163a** in 75 % isolated yield by treatment of iodotoluene and 2-bromophenyl acetamide with $Pd(OAc)_2$ (10 mol %), tri-2-furylphosphine (20 mol %), norbornene (1.1 equiv.) and Cs_2CO_3 (2 equiv.) in DMF at 130 °C during 48 h (Table 8.5, entry 3) [25].

The observation of dihydrophenanthrene 163a under similar conditions to those used for our synthesis of phenanthridines was very surprising. Indeed, this type of structure incorporating the norbornyl ring has only been obtained with aryl iodides

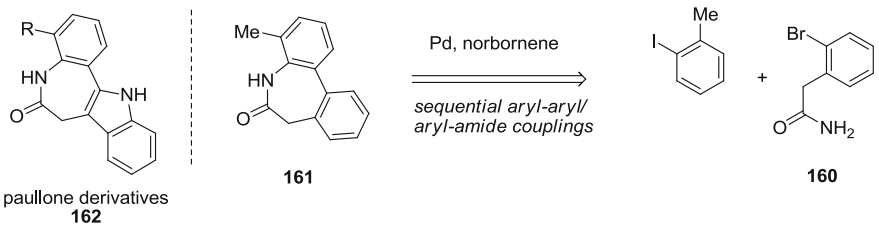

Fig. 8.11 Planned retrosynthesis of paullone core

Table 8.5 Optimization of the synthesis of dihydrophenanthrene 163a

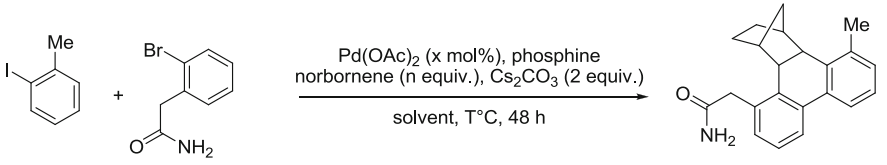

160a **163a**

Entry	$Pd(OAc)_2$ (mol %)	Phosphine (mol %)	Norbornene (equiv.)	Solvent	T (°C)	Yield **163** (%)
1	5	TFP (10)	1	DMF	105	26
2	5	TFP (10)	1	DMF	130	39
3	10	TFP (20)	1	DMF	130	56 (75[a])
4	10	PPh_3 (20)	1	DMF	130	36
5	10	TFP (20)	2	DMF	130	43
6	10	TFP (20)	1	MeCN	85	–
7	10	TFP (20)	1	Toluene	110	21

[a] Without acidic work up before purification on flash column chromatography

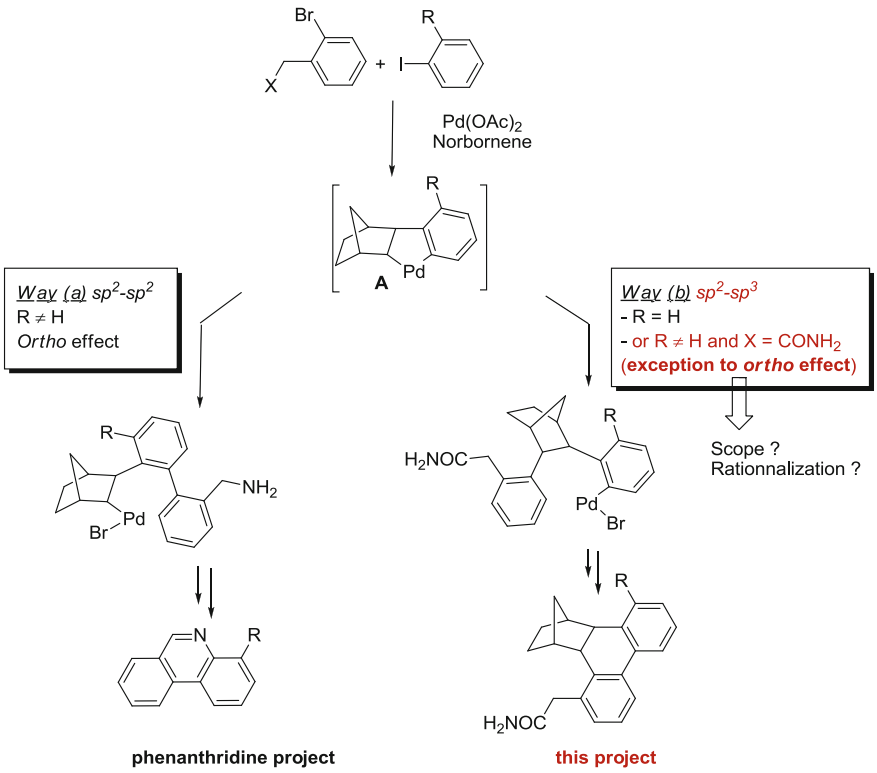

Fig. 8.12 Comparison of the reactivity of bromobenzylamine and bromophenylacetamide

that do not bear *ortho*-substituents, which is not the case of iodotoluene. We suspected that replacing the bromobenzyl amine arm with an acetamide one had resulted in a completely different reactivity, which would correspond to the first reported exception to the *ortho* effect (Fig. 8.12).

As presented in the bibliographical part, the *ortho* effect has been widely exploited for aryl–aryl couplings by palladium/norbornene cocatalysis and to date, not a single exception to this effect had been reported. Our objectives were consequently to check the scope of this peculiar reactivity and to try to rationalize it thanks to DFT calculations.

8.2.2 Scope of the Synthesis of Dihydrophenanthrenes

We first reacted 2-bromophenylacetamide **160a** with differently substituted aryl iodides, varying both their steric and electronic properties (Table 8.6). We were delighted to observe the same deviation to the *ortho* effect with all the examined

Table 8.6 Scope of the multi-components synthesis of phenanthrenes

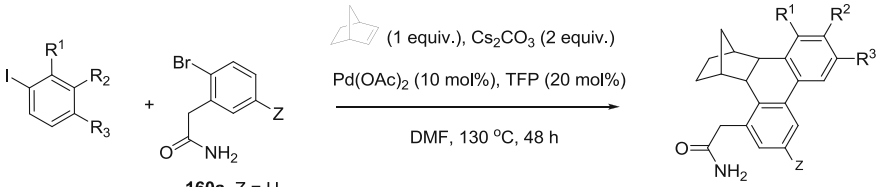

160a, Z = H
160b, Z = CF_3

163b-m

Entry	Aryl iodide	Z	Yield (%)
1	R^1 = Et; R^2 = R^3 = H	H	163b, 57
2	R^1 = CH_2-CO_2Me; R^2 = R^3 = H	H	163c, 55
3	R^1 = Me; R^2 = Me; R^3 = H	H	163d, 60
4	R^1 = Me; R^2 = H; R^3 = Me	H	163e, 82
5	R^1 = Me; R^2 = H; R^3 = OMe	H	163f, 65
6	R^1 = Me; R^2 = R^3 = OMe	H	163 g, 60
7	1-iodonaphtalene	H	163 h, 61
8	9-iodophenanthrene	H	163i, 81
9	R^1 = Cl; R^2 = R^3 = H	H	163j, 47
10	R^1 = CF_3; R^2 = R^3 = H	H	163 k, 71
11	R^1 = Me; R^2 = R^3 = H	CF_3	163 l, 45
12	R^1 = Me; R^2 = H; R^3 = Me	CF_3	163 m, 52

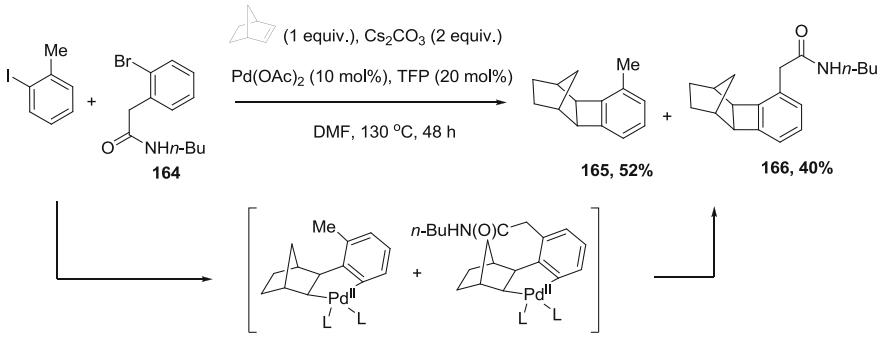

Fig. 8.13 Reactivity of secondary amide 164

substrates. Good results could be obtained employing alkyl or alkoxy substituents (Table 8.6, entries 2−6). Polyaryl iodides (Table 8.6, entries 7−8) or aryl iodides bearing chloride or trifluoromethyl substituents (Table 8.6, entries 9−10) could also be employed successfully.

We then tried to vary the substituents on the aryl bromide. Satisfactorily, 2-bromophenylacetamide **160b** substituted with a trifluoromethyl group could follow the same sequence in synthetically useful yields (Table 8.6, entries 11−12).

On the other hand, the reaction of secondary amide **164** with iodotoluene under the optimized conditions did not result in the same outcome (Fig. 8.13). Products **165** and **166** were obtained, resulting from direct reductive elimination of the corresponding palladacycle before reaction with another aryl halide molecule [25].

The phenanthrene core is present in numerous natural alkaloids exhibiting interesting activities, e.g. antitumor properties [26]. We thus sought to demonstrate a possible synthetic application of our methodology by accessing phenanthrene derivatives via tandem palladium/norbornene catalyzed step/retro Diels–Alder sequence. Pleasingly, employing our previously optimized conditions with norbornadiene instead of norbornene afforded the desired 1-acetamido-8-methylphenanthrene **168** in 61 % yield (Fig. 8.14).

8.2.3 The Powerful Effect of Water

Upon determining the scope of the synthesis of dihydrophenanthrenes, we observed that when the substrates were not carefully dried, an appreciable amount of an original tricyclic compound was isolated as a byproduct together with phenanthrene **163a**. Careful analysis of NMR spectra and X-ray diffraction (vide infra) allowed us to determine that the structure of this mysterious byproduct corresponded to *spiro* derivative **169a** obtained as a single diastereoisomer. We wondered whether adding water in a controlled manner to our reaction mixture

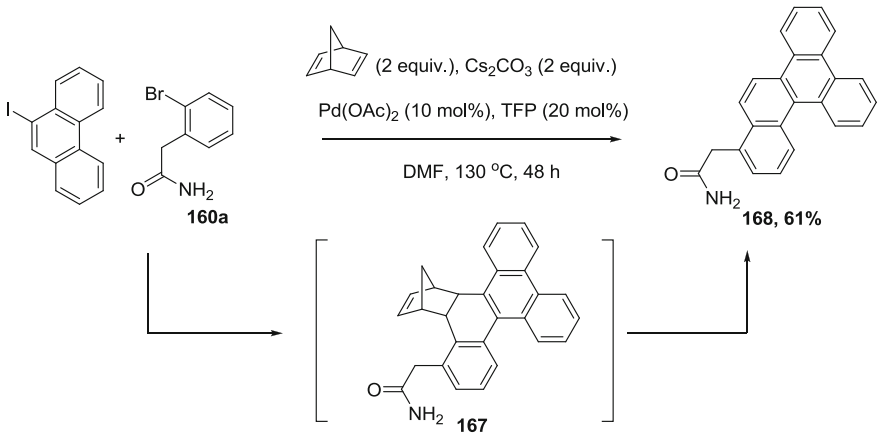

Fig. 8.14 Tandem Catellani sequence/retro Diels–Alder

would completely switch the selectivity of the reaction. To check this hypothesis, we used perfectly dried reagents and gradually increased the quantity of water in the reaction mixture (Table 8.7). We observed the ratio (**169a/163a**) progressively rise. Finally, when 110 equivalents of water regarding to palladium were added, **169a** was obtained selectively (entry 3). Further increase of the amount of water led to degradation.

Our best conditions were thus the same as before plus 11 equivalents of water. With those in hands, we investigated the behavior of various aryl iodides in the presence of water (Table 8.7). We were pleased to find out that, although with limited yields, it was possible in all cases to completely inhibit the formation of the phenanthrene products, totally switching the selectivity of the reaction towards the formation of *spiro* derivatives.

A crystal structure was obtained for 169b. Its structure confirmed the *spiro* junction and allowed us to identify the diastereoisomer obtained (Fig. 8.15).

Interestingly, contrary to what was the case for the formation of dihydrophenanthrenes, *spiro* derivatives could be obtained also starting from secondary amides. For example, treatment of amide **164** with iodotoluene in the presence of norbornene, $Pd(OAc)_2$ and water afforded *spiro* derivative **169 l**, albeit in a modest 35 % yield (Fig. 8.16).

Prior to our work, only a few examples of palladium-catalyzed dearomatization have been reported both in intermolecular [27, 28] and intramolecular processes. In 1999, Catellani described the formation of spirocyclohexadienone **170** starting from *p*-iodophenol and norbornene [29]. The complex mechanistic sequence leading to **170** ended with an intramolecular dearomatization of the phenol ring of norbornylpalladium(II) complex **171**. The mechanism was thought to involve a nucleophilic attack of C-4 from the phenol at the palladium, generating arenium complex **172** (Fig. 8.17).

Table 8.7 Effect of water on the selectivity of the reaction

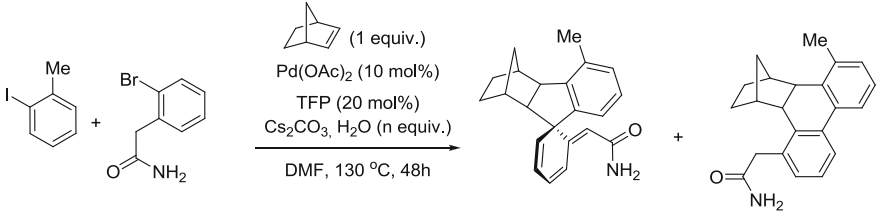

160a **169a** **163a**

Entry	Equiv. of water	Ratio 169a:163a[a]
1	0	163a only
2	2.5	1:1
3	6	6:1
4	11	169a only
5	14	Degradation

[a] Estimated on ^{1}H NMR of the crude reaction mixture

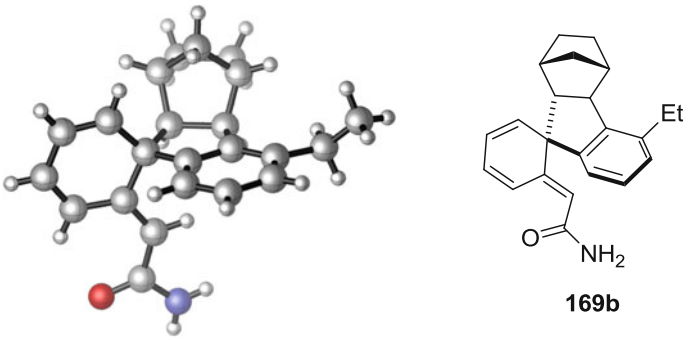

Fig. 8.15 X-ray structure of *spiro* derivative 169b

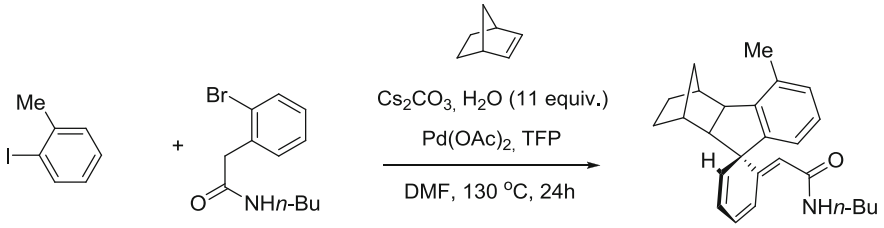

Fig. 8.16 Reaction of secondary amide 164 in the presence of water

Ten years later, Buchwald described a palladium-catalyzed asymmetric dearomatization of naphtolenes using chiral phosphine ligands [30]. Shortly after, Bedford reported the synthesis of dihydroindolo[2,3-*b*]indole **174** by treatment of precursor **173** with $Pd(OAc)_2$, *N*-heterocyclic carbene ligand SIPr and NaO^tBu (Fig. 8.18) [31]. Two pathways were considered for the dearomatization of the Pd(II) intermediate **175** formed by oxidative addition of **173**: an electrophilic pathway (path a) or a Heck pathway (path b). The reaction proved highly base-dependent, which made the authors postulate that the electrophilic pathway was more likely in their reaction conditions.

Based on these literature precedent, we postulated that *spiro* derivative **169a** could be obtained by palladium-catalyzed dearomatization of norbornylpalladium(II) complex **177,** instead of the usual norbornene deinsertion (Fig. 8.19). This could occur either via a tandem deprotonation/nucleophilic attack (path a) or via a 5-*exo* migratory insertion and subsequent *β*-hydrogen elimination (path b). Complex **177** would be obtained by sp^2-sp^2 coupling from palladacycle **176** and aryl bromide, which corresponds to the usual *ortho* effect. The formation of *spiro* derivative **169a** would thus derive from a switch of the reaction back towards the *ortho* rule, under the influence of water.

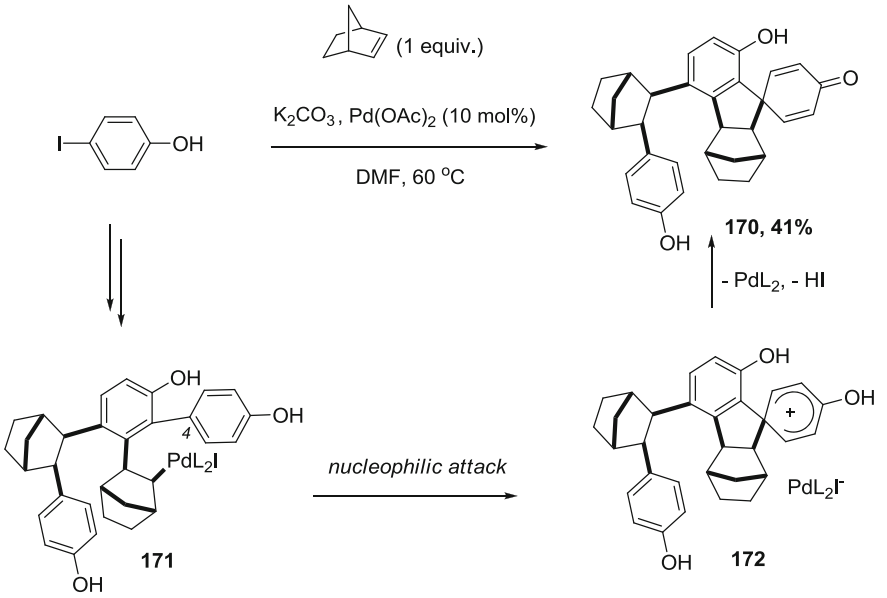

Fig. 8.17 Reported palladium-catalyzed dearomatization of phenol in a Catellani sequence

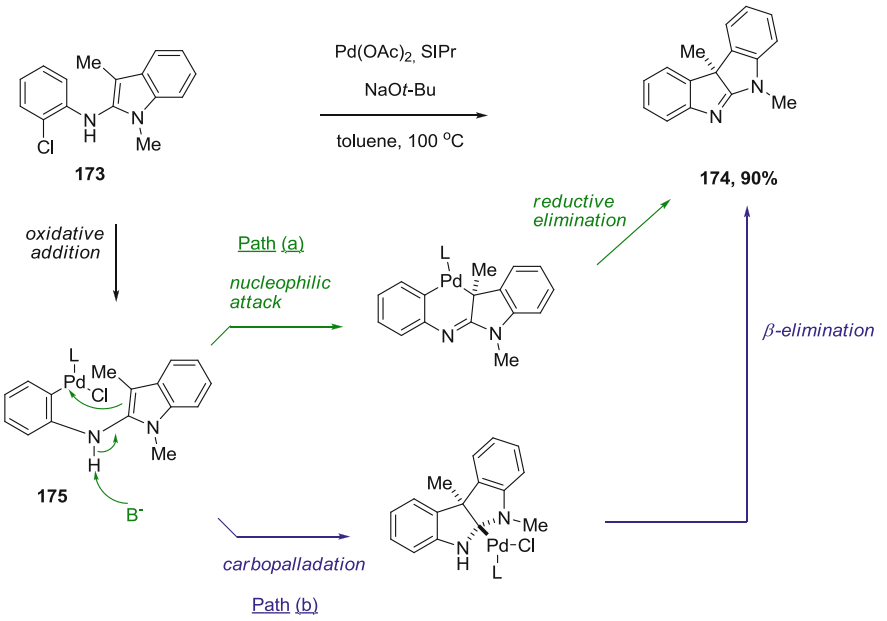

Fig. 8.18 Proposed mechanism for the synthesis of dihydroindoloindole via palladium-catalyzed dearomatization

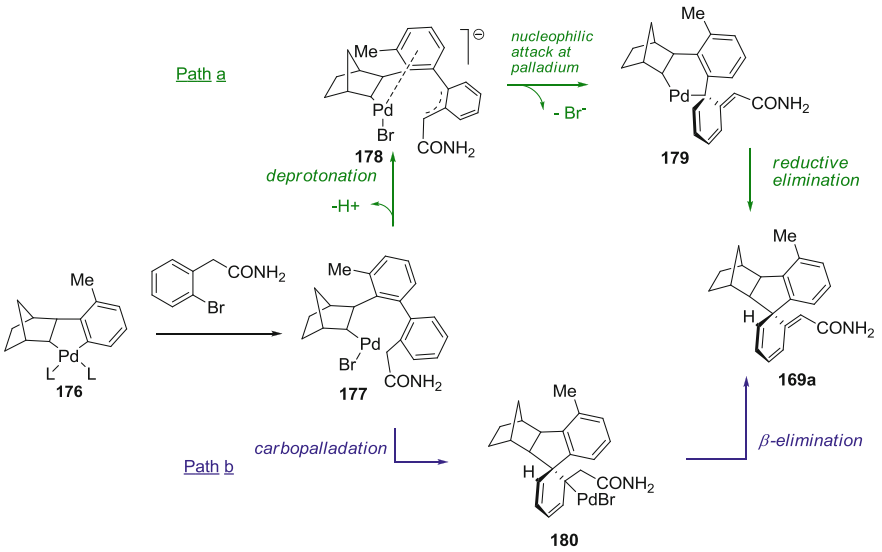

Fig. 8.19 Postulated reaction pathways for the formation of *spiro* derivative

Thus, many mechanistic questions were raised by these experimental results:

- What is the origin of the deviation from the *ortho* rule observed with bromophenylacetamide as the substrate? Is there a chelation of the palladium center with the amide moiety and does this chelation play a role?
- What is the exact role of water in the reaction?

To answer these questions and get precious insights into the reaction mechanism, we turned to DFT modeling. All the DFT calculations were performed by Giovanni Maestri and Dr. Etienne Derat.

8.2.4 Mechanistic Investigations by DFT Calculations

8.2.4.1 Reactions in the Absence of Water

In the absence of water, we observed the formation of dihydrophenanthrene **163a** by multi-component reaction of iodoluene, 2-bromophenylacetamide and norbornene. Postulating the formation of palladacycle **176** as a starting point, we wished to compare the energy profiles of two mechanistic pathways for two steps of the mechanism of formation of **163a**.

Firstly, we wanted to check whether the reaction of palladacycle **176** with 2-bromophenylacetamide occurred via a transmetalation-type mechanism or via the formation of a Pd(IV) intermediate. As presented in the bibliographical part, in

collaboration with Catellani, our group has demonstrated that for *ortho* substituted palladacycle such as **176**, oxidative addition of the aryl halide followed by selective sp^2-sp^2 coupling upon reductive elimination from Pd(IV) complex, was favored over a transmetalation-type pathway [32]. It was proven that the nature of the reacting aryl halide had a limited impact on Pd(IV) formation. However, the situation of an aryl bromide possessing a potentially chelating substituent had not been considered and was consequently missing.

Secondly, according to the favored pathway involved, we wished to compare, the energy profiles for the sp^2-sp^3 coupling and the sp^2-sp^2 coupling, after the reaction of palladacycle **176** with the aryl bromide. Indeed, we thought that the possible chelation of the amide might change the relative energies of the transition states involved (Fig. 8.20).

– *Discrimination between the Pd(IV) and the bimetallic pathways.*

First, the oxidative addition of 2-bromoarylacetamide on palladacycle **176**, leading to the formation of Pd(IV) complexes of type **183** was considered. We modeled the coordination step and the oxidative addition step of the aryl bromide onto the starting Pd(II) metallacycle with and without amide chelation and in the two possible attacking geometries in both cases. We obtained the four energy profiles depicted in Fig. 8.21.

Among the various pathways considered, we always found that chelation by the oxygen atom of the amide group is present at the Pd(IV) stage. Indeed, optimized geometries always converged to minima in which Pd–O distances are lower than 2.3 Å. Calculated barriers delivering complexes **183a–d** are in the range of those reported for aryl bromides without chelating group. Among the pathways presented above, the most stable Pd(IV) complex is octahedral complex **183a**, which

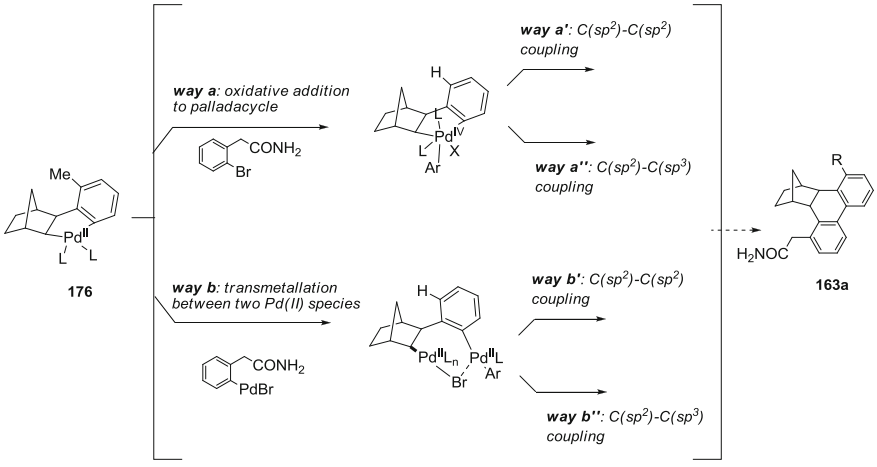

Fig. 8.20 Energy profiles to be examined by DFT calculations

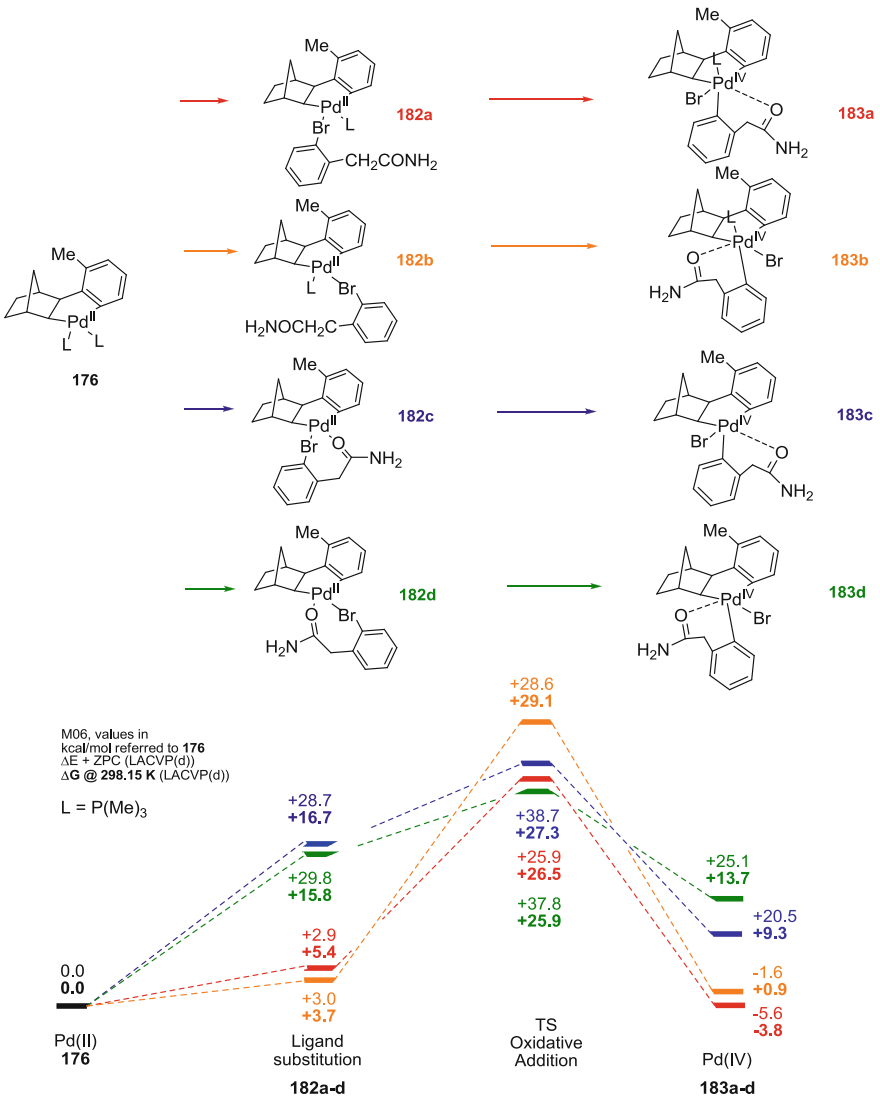

Fig. 8.21 Comparison of different oxidative additions on 181 yielding Pd(IV) complexes

features the halide *cis* to the norbornene unit. This is in contrast with previous calculations on octahedral Pd(IV) complexes with apical aliphatic or benzyl group. A slightly lower barrier for oxidative addition was found for **183d** (green pathway, $\Delta\Delta G = -0.9$ kcal/mol), mainly due to a positive entropic contribution resulting from displacement of the two ligands from palladacycle **176**. However, the resulting Pd(IV) species is much less stable than **183a** (ΔG (**183d**–**183a**) = +17.5 kcal/mol). Thus, if **183d** forms in solution it probably incorporates

a ligand molecule to deliver **183b**, and then **183a** upon isomerization. These processes occur under thermodynamic control and likely present negligible (*if any*) barriers.

Then, we considered the bimetallic pathway to compare it with the Pd(IV) pathway in the present catalytic sequence. In that alternative mechanistic pathway, palladacycle **176** would undergo association with a Pd(II) complex arisen from oxidative addition of the aryl bromide on Pd(0)L_2. Subsequent transmetalation would lead to bimetallic complex of type **184**. Both these processes should have limited impact on the energetic convenience of this mechanism, which is rather decided by the C–C reductive elimination leading to complexes of type **185**. The energy profiles involving two types of bimetallic complexes **184a** and **184b**, differing from the coordination site of the acetamide, were calculated and are depicted in Fig. 8.22.

Intermediates **184a–b** converged to structures in which once again the oxygen atom is coordinated to one metal center. Higher energies were found for analogous complexes with one more phosphine ligand bound to the metal. Both complexes **184a** and **184b** which were tested are already higher in energy with respect to all transition states presented in Fig. 8.21 for the Pd(IV) alternative. The more stable complex **184b**, featuring oxygen chelation on the metal center involved in the reductive elimination lays +34.3 kcal/mol above the entry channel (Fig. 8.22, purple path). The subsequent C–C bond formation has a barrier of +49.1 kcal/mol in ΔG with respect to the reagents, thus more than 20 kcal/mol higher than those

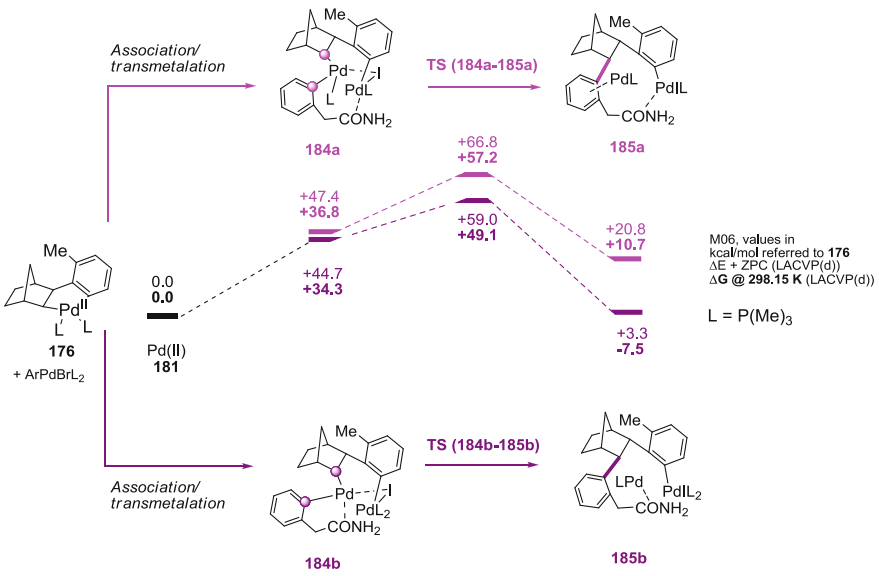

Fig. 8.22 Comparison of relevant transition states for the bimetallic alternative

presented in Fig. 8.21. This large energy gap strengthens the high probability for Pd(IV) involvement in the present catalytic sequence.

– *Discrimination between C(sp^2)-C(sp^2) and C(sp^2)-C(sp^3) couplings.*

Starting from octahedral complex **183a** possessing the halide *cis* to the norbornene unit, which was previously shown to be the favored intermediate, we calculated the energies of the transition states leading to the C(sp^2)-C(sp^2) and C(sp^2)-C(sp^3) couplings via reductive elimination (Fig. 8.23).

We found that the activation barrier for the sp^2-sp^3 C–C bond formation (Fig. 8.23, *path a*, ΔG + 17.7 kcal/mol with respect to **183a**) was lower than the barrier leading to the usual sp^2-sp^2 C–C bond formation (Fig. 8.23, *path b*, ΔG + 21.9 kcal/mol with respect to **183a**).

An explanation for this peculiar reactivity stems from analysis of the two competitive transition states involved. It revealed the reason why the usually disfavored pathway could become favored in our reaction conditions (Fig. 8.24).

Considering the geometry of **TS(183a'–186a')** (same as 183a and 186a but with TFP as ligand), which leads to sp^2-sp^3 coupling, we observed that amide chelation on palladium was released. Instead, a hydrogen bond between the $-NH_2$ group and the halide occurred. Thus, in this transition state, the metal centre was pentacoordinated. On contrary, in **TS(183a'–186b')** the chelation between the amide and Pd was still present and the palladium atom was hexacoordinated. From our previous study, [32] we knew that barriers for reductive elimination from octahedral Pd(IV) complexes were slightly higher compared to their pentacoordinated counterparts, which gives a first rationale for the observed favorability of sp^2-sp^3 coupling.

In addition, a steric strain emerges in the transition state **TS(183a–186b)**, as a result of its overall lower flexibility. This is evidenced by the lowest H–H distances which shrinks from 2.21 Å in **TS(183a–186a)** to 2.01 Å in **TS(183a–186b)**.

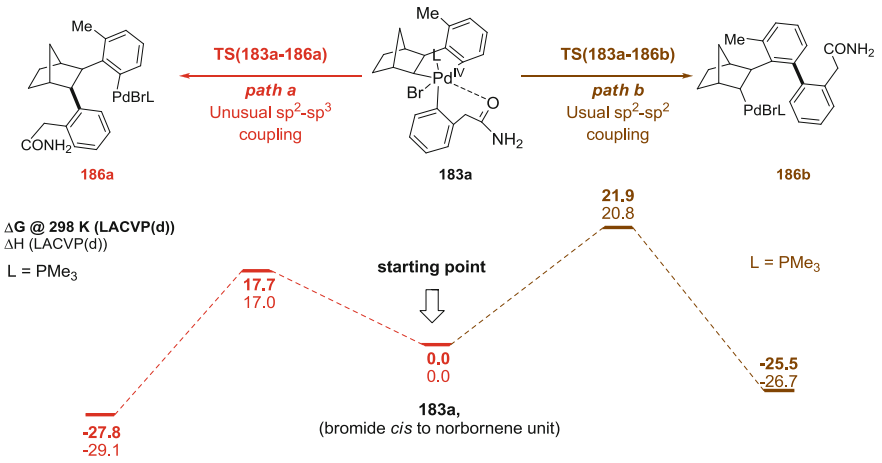

Fig. 8.23 Comparison of possible reductive elimination pathways from Pd(IV) complex 183a

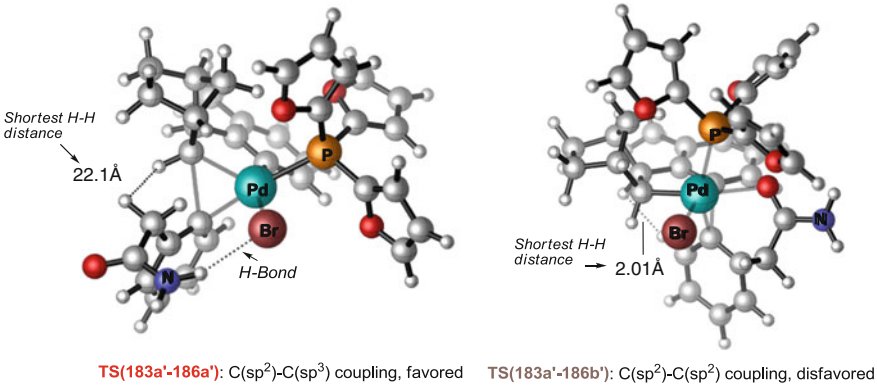

Fig. 8.24 Structure of the modeled transition states for reductive eliminations from 183

The synergic contribution of these two effects increases the barrier for sp^2-sp^2 coupling, allowing the usually disfavored sp^2-sp^3 one to prevail (by 3.3 kcal/mol in ΔG).

To conclude, according to the DFT calculations, the amide moiety is therefore crucial for the exception to the *ortho* rule. Chelation forces the Pd(IV) complex in a *cis*-Br/norbornene geometry, and it also likely hampers the transition state leading to sp^2-sp^2 coupling.

8.2.4.2 Reactions in the Presence of Water

In the presence of water, we observed the formation of the *spiro* derivative **169a** by multi-components reaction of iodoluene, 2-bromophenylacetamide and norbornene.

– *Rationalization for the favored C(sp^2)-C(sp^2) coupling.*

Our initial assumption was that, through hydrogen bonding with the amide group, the water was reducing the chelation on the metal center, thus allowing the system to evolve according to the usual reactivity. We have then investigated the reductive eliminations from systems **187a–b** (Fig. 8.25, same as systems **183a–b** respectively but with an additional water molecule forming an hydrogen bonds with the amide group). However, calculated barriers for reductive elimination from complex **187a** and **187b** could not account for the selective sp^2-sp^2 bond formation experimentally observed, being in both cases more energy demanding than sp^2-sp^3 coupling (Fig. 8.25, green pathway for **187a** and pink pathway for **187b**). We have then tested the reactivity of a pentacoordinated species **187c** and **187d** resulting from displacement of the apical ligand. In this case we did not observe the above mentioned Y-distorted trigonal bipyramidal geometry but instead, a distorted square-based pyramid as a result of the chelating amide (clearly visible in the

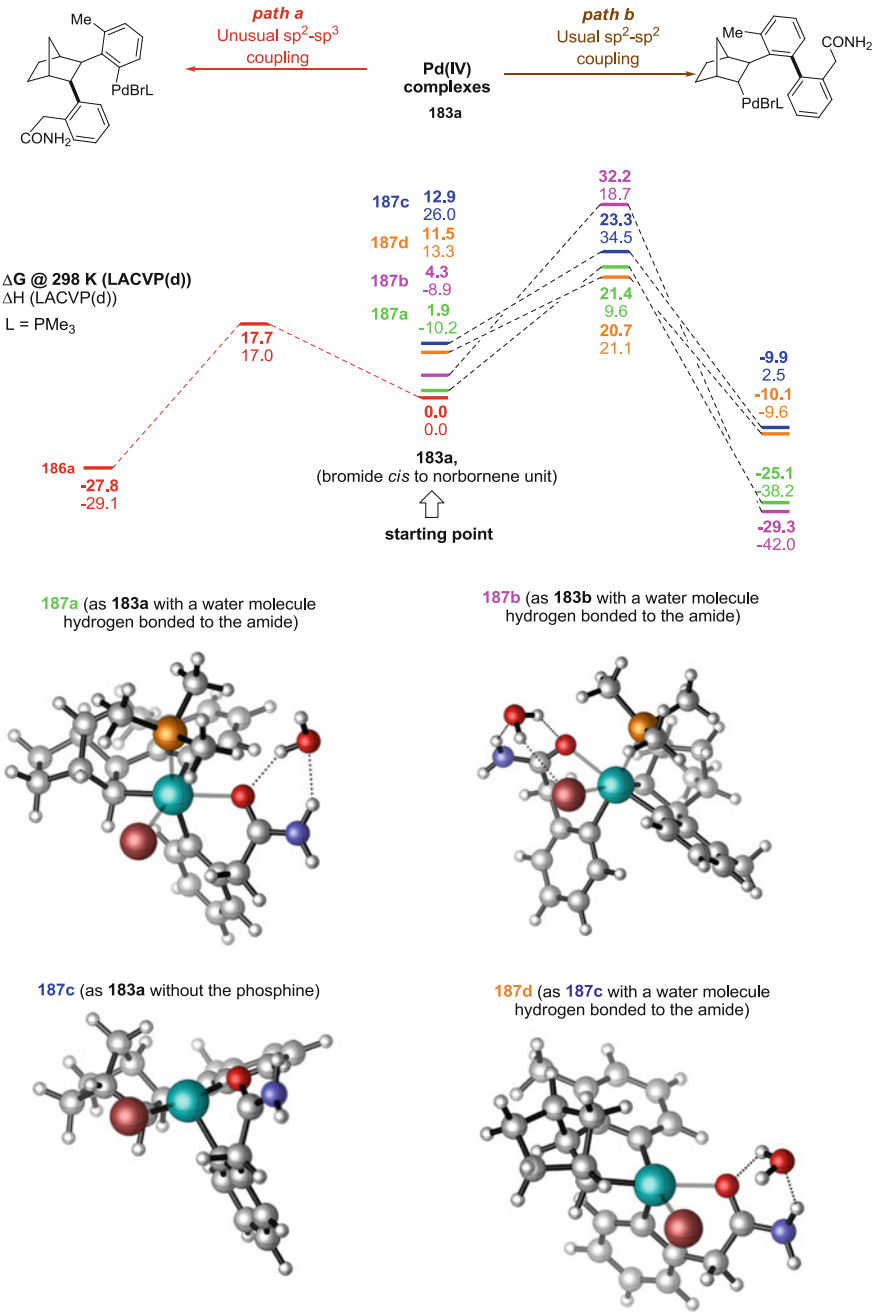

Fig. 8.25 Different modeled pathways considered but unable to explain the formation of *spiro* derivative (Calculated values for sp^2-sp^3 couplings from 187a–d are not presented for clarity but have been characterized.). All values are in kcal/mol and plotted referring to complex 183a to help comparison

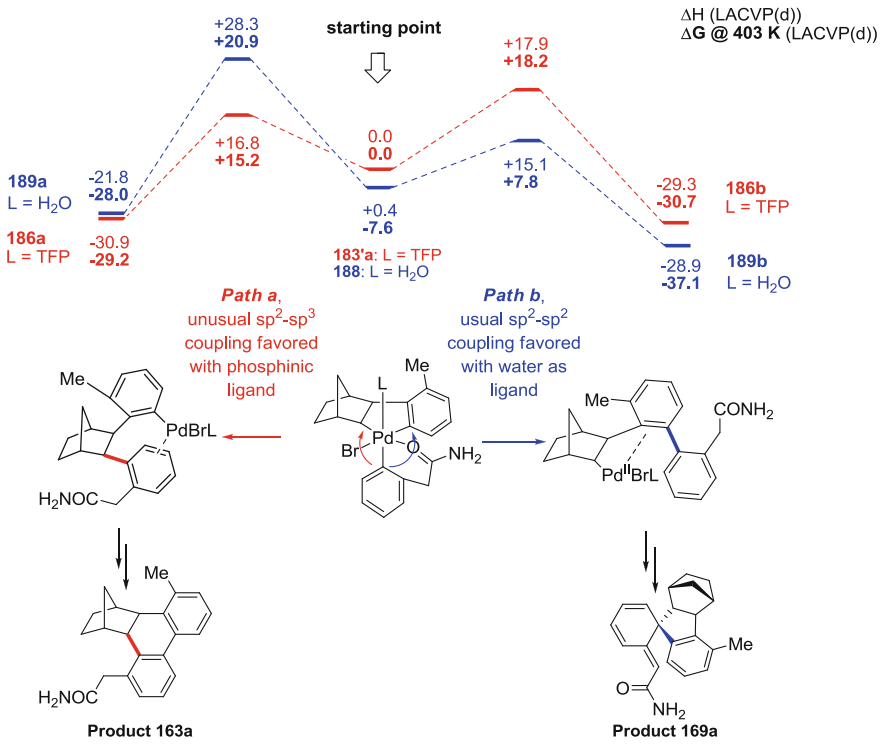

Fig. 8.26 Inversion in the favored reductive elimination pathway by replacing phosphine ligand with water

image of complex **187c**). As in the previous case, calculated sp^2-sp^2 coupling barriers were higher than sp^2-sp^3 ones (Fig. 8.25, blue pathway for **187c**), even by adding a water molecule hydrogen bonded to the chelating amide (Fig. 8.25, orange pathway for **187d**). These models could consequently not explain the experimental observations.

We have eventually imagined that due to its limited steric hindrance, water could play the role of apical ligand of the Pd(IV) complex instead of phosphine.[1] Gratifyingly, calculated barriers from complex **188** (corresponding to **183a** with L = H_2O) matched the experimentally observed role of water. **TS(188–189b)**, leading to sp^2-sp^2 coupling, was not just lower than **TS(188–189a)** but also than **TS(183a–186a)** (by 12.1 and 7.4 kcal/mol in ΔG respectively, Fig. 8.26), which was responsible for the formation of dihydrophenanthrene **163a**. Figure 8.26 shows the inversion in the energetic convenience for C–C bond forming reductive eliminations from Pd(IV) complexes **183′a** and **188**. ΔG were calculated at 403 K, the temperature adopted in these catalytic sequences. To move even closer to the

[1] For other examples of intermediate stabilization by water, see: [33], and ref. therein.

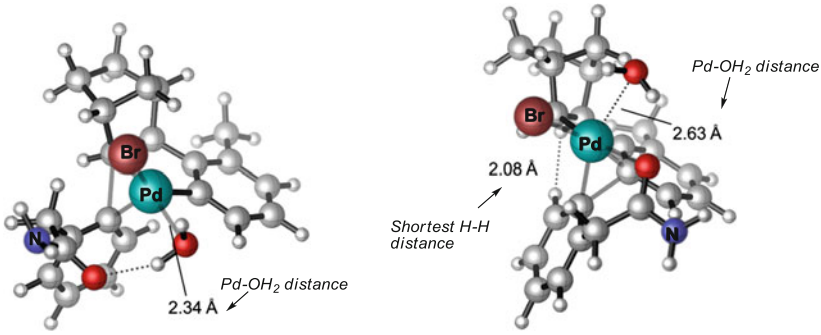

Fig. 8.27 Structure of the transition state for sp^2-sp^3 coupling and sp^2-sp^2 coupling from 188

real systems, we modeled **183′a** with trifuryl phosphine, the real ligand adopted in catalysis. We neglected solvation effects since we have shown previously that they have very limited impact in the description of these complexes.

The geometry of **TS(188–189b)** indicated why the expected reactivity was restored in the presence of water (Fig. 8.27). The steric strain observed in the phosphine case was indeed partially released, as showed by the shorted H–H distance of 2.01 Å in **TS(183a–186b)** (Fig. 8.24) which goes up to 2.08 Å in **TS(188-189b)**. In addition, the coordination of the metal resembled more that of a more reactive pentacoordinated species. This is evidenced by the distance between Pd and the oxygen atom of the water molecule which goes up to 2.63 Å in **TS(188–189b)** from 2.34 Å found in **TS(188–189a)**. The combination of these two features restores the usual and expected energetic convenience for the system to undergo sp^2-sp^2 rather than sp^2-sp^3 coupling, in perfect agreement with the experimentally observed output of reactions performed in the presence of water.

Thus, the water would reduce the steric strain and increase the flexibility of the intermediate Pd(IV) complex by replacing the phosphine as the apical ligand. This is also in agreement with the results of Table 8.8. Since **183a** is a closed-shell, 18-electron complex, replacement of the phosphine with water likely occurs through a dissociative mechanism [34, 35], and the two complexes are in thermodynamic equilibrium. We postulate that an approximately 1:1 mixture is formed when the two ligands are present in nearly equimolar amounts (Table 8.8, entry 2). Formation of **183a** is excluded only when the excess of water is large enough to overcome the contribution of the free enthalpy of the Pd–P bond.

– *Mechanism of the dearomatization step.*

Finally, we analyzed the mechanism of dearomatization leading to *spiro* derivative **169a** from **189a'** (same as **189a** but with the palladium atom coordinated to the other aryl ring). Two mechanisms have been considered (Fig. 8.28). In the first path (*anionic pathway*), deprotonation at the benzylic position of the

Table 8.8 Exemplification of the formation of *spiro* derivatives in the presence of water

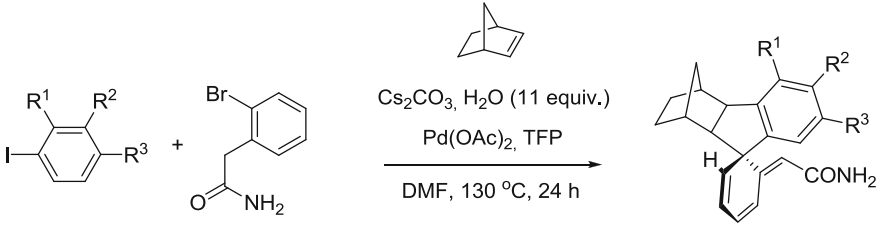

160a **169a-k**

Entry	Aryl iodide	Yield (%)
1	$R^1 = Me$; $R^2 = R^3 = H$	169a, 65
2	$R^1 = Et$; $R^2 = R^3 = H$	169b, 40
3	$R^1 = Me$; $R^2 = Me$; $R^3 = H$	169d, 45
4	$R^1 = Me$; $R^2 = H$; $R^3 = Me$	169e, 39
5	$R^1 = Me$; $R^2 = R^3 = OMe$	169g, 60
6	1-iodonaphtalene	169h, 47
7	$R^1 = Cl$; $R^2 = R^3 = H$	169j, 28
8	$R^1 = CF_3$; $R^2 = R^3 = H$	169k, 60

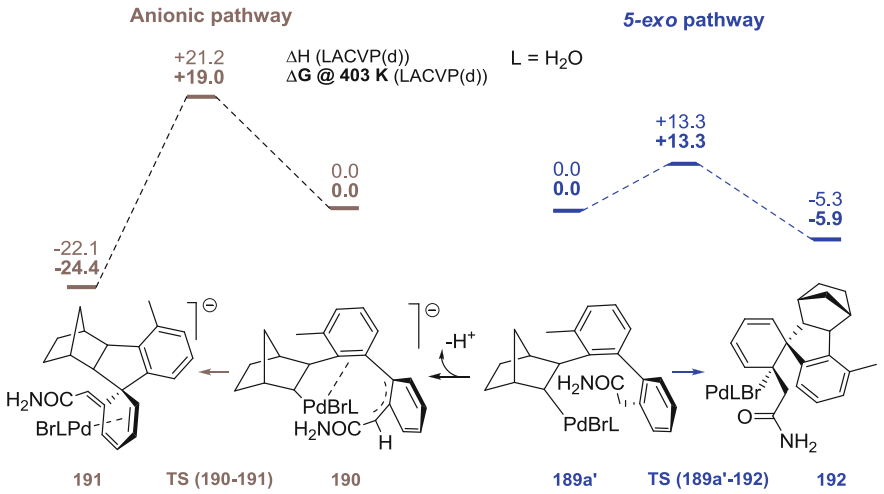

Fig. 8.28 Comparison of ionic and neutral pathway in the dearomatization step

acetamide group could deliver the anionic complex **190** in which the partially delocalized negative charge might allow a nucleophilic attack onto the Pd–C bond through **TS(190–191)**. Alternatively (*5-exo pathway*), complex **189a'** might undergo a *5-exo* migratory insertion via **TS(189a'–192)**, followed by *β*-hydrogen elimination to deliver the experimentally observed diastereoisomer of product **169a**. Figure 8.28 compares the barriers of these mechanisms. Our calculations indicated that in our case, a *5-exo* insertion was favored by 7.7 kcal/mol in ΔG with respect to the anionic pathway. We did not directly compare complex **189a'** with its anionic counterpart **190** because from a computational point of view, the proper evaluation of the energetic contribution of this deprotonation is difficult. However, the pKa of the benzylic proton of phenylacetamide in DMSO is similar to that of acetone (26.6 and 26.5 respectively). The latter has proven experimentally to be efficiently deprotonated in very similar reaction conditions [36], so we believe that this step could be energetically accessible also in our case.

As *spiro* derivative **169a** was obtained as a single diastereoisomer, we tried to model the reaction pathway leading to the unobserved diastereoisomer (Fig. 8.29). We were pleased to find that the transition state leading to the unobserved diastereoisomer of **169a**, **TS(189a'–192b)**, was disfavored over **TS(189a'-192)** by 6.3 kcal/mol in ΔG, as shown in Fig. 8.29. The relatively big gap between these two transition states can perfectly account for the experimental evidence that **169a** is obtained as a single diastereoisomer.

Norbornene extrusion could be a competitive pathway to the dearomatization process, starting from norbornylpalladium(II) complex **189a'**. This process is usually observed in these sequences to deliver the biaryl unit (Fig. 8.30). In our reaction, norbornene extrusion would lead to lactam **194**. This product **194** has only been observed as traces in the presence of water. This experimental result was

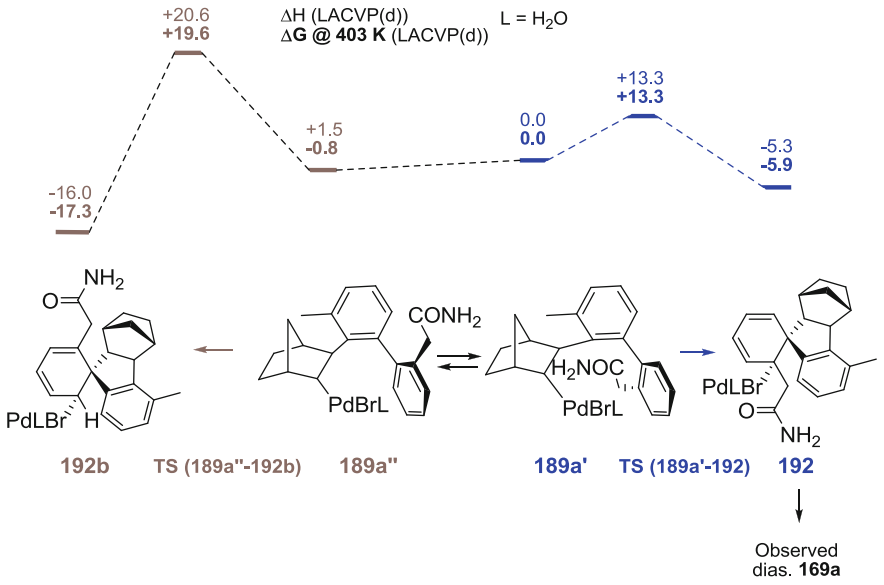

Fig. 8.29 DFT results correlating with the observed diastereoselectivity in the dearomatization step

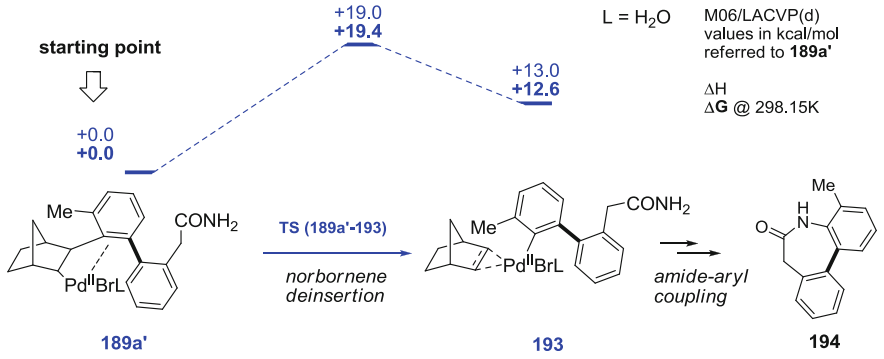

Fig. 8.30 Calculated barrier for norbornene deinsertion

confirmed by calculations (Fig. 8.30). Indeed, the calculated barrier for norbornene extrusion (+19.4 kcal/mol in ΔG with respect to **189a**', Fig. 8.30) was +5.9 kcal/mol higher than the barrier for the 5-*exo* migratory insertion (**TS**(**189a**'–**192**), Fig. 8.28). These results correlate with literature reports on Pd/norbornene sequences which usually state that olefin extrusion at this stage is favored by steric hindrance. In the present case, the small water molecule should decrease the feasibility of this step, allowing the unusual dearomatization reaction to take place.

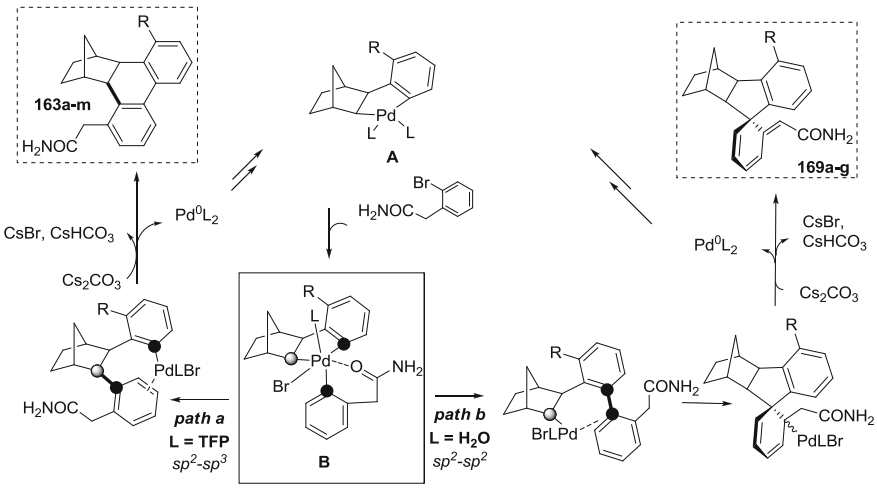

Fig. 8.31 Summary of the proposed mechanistic pathways

To summarize, we can resume the results of the theoretical analysis undertaken in Fig. 8.31. Reaction of 2-bromoarylacetamide likely involves a chelated Pd(IV) complex of type **B**. In the presence of a phosphine ligand, as a result of the particular chelation by the acetamide group, this complex can undergo sp^2-sp^3 reductive elimination which is usually not observed in similar sequences. When this ligand is replaced by a water molecule, the geometry of the transition state is modified, which restores the preference for the usual sp^2-sp^2 coupling. At this point, however, the minimal size of the apical ligand disfavors the expected norbornene extrusion and instead triggers dearomatization.

To conclude, we have evidenced the first deviation from the *ortho* effect in palladium/norbornene catalysis [37]. DFT calculations demonstrated the powerful influence of specific chelation on the mechanistic pathway. Experimental and theoretical studies pointed out that water could play an important role in the coordination of palladium and strongly influence the outcome of the reaction. Chelation is a tool that is new in Pd/norbornene catalysis. We believe its systematic study will open new avenues for further research.

References

1. Rashid, M. A., Gustafson, K. R., Kashman, Y., Cardellina, J. H, I. I., McMahon, J. B., & Boyd, M. R. (1995). *Natural Products Letters, 6*, 153–156.
2. Phillips, S. D., & Castle, R. N. (1981). *Journal Heterocyclic Chemistry, 18*, 223–232.
3. Gakunju, D. M. N., Mberu, E. K., Dossaji, S. F., Gray, A. I., Waigh, R. D., Waterman, P. G., et al. (1995). *Antimicrobial Agents and Chemotherapy, 39*, 2606–2609.
4. Nakanishi, T., Suzuki, M., Saimoto, A., & Kabasawa, T. (1999). *Journal of Natural Products, 62*, 864–867.

5. Makhey, D., Gatto, B., Yu, C., Liu, A., Liu, L. F., & LaVoie Bioorg, E. J. (1996). *Medicinal Chemistry, 4*, 781–791.
6. Herbert, J. M., Augereau, J. M., Gleye, J., & Maffrand, J. P. (1990). *Biochemical and Biophysical Research Communications, 172*, 993–999.
7. Ishikawa, T. (2001). *Medicinal Research Reviews, 21*, 61–72.
8. Catellani, M., & Ferioli, L. (1996). *Synthesis*, 769–772.
9. Trost, B. M., & Metzner, P. J. (1980). *Journal of the American Chemical Society, 102*, 3572–3577.
10. Bercaw, J. E., Hazari, N., & Labinger, J. A. (2008). *Journal of Organic Chemistry, 73*, 8654–8657.
11. Steinhoff, B. A., & Stahl, S. S. (2006). *Journal of the American Chemical Society, 128*, 4348–4355.
12. Muzart, J. (2006). *Chemistry: An Asian Journal, 1*, 508–515.
13. Stahl, S. S., Thorman, J. L., Nelson, R. C., & Kozee, M. A. (2001). *Journal of the American Chemical Society, 123*, 7188–7189.
14. Landis, C. R., Morales, C. M., & Stahl, S. S. (2004). *Journal of the American Chemical Society, 126*, 16302–16303.
15. Driver, M. S., & Hartwig, J. F. (1997). *Journal of the American Chemical Society, 119*, 8232–8245.
16. Chapsal, B., & Ojima, I. (2006). *Organic Letters, 8*, 1395–1398.
17. Klingensmith, L. M., Nadeau, K. A., & Moniz, G. A. (2007). *Tetrahedron Letters, 48*, 4589–4593.
18. Lo, C. Y., Kumar, M. P., Chang, H. K., Lush, S. F., & Liu, R. S. (2005). *Journal of Organic Chemistry, 70*, 10482–10487.
19. Blanchot, M., Candido, D. A., Larnaud, F., & Lautens, M. (2011). *Organic Letters, 13*, 1486–1489.
20. Catellani, M. (2003). *Synlett, 3*, 298–313.
21. Catellani, M., Motti, E., & Della Ca, N. (2008). *Acc. Chem. Res*, *41*, 1512–1522.
22. Martins, A, Mariampillai, B., & Lautens, M. (2010). *Top. Curr. Chem, 292*, 1–33.
23. Cardenas, D. J., Martin-Matute, B., & Echavarren, A. (2006). *Journal American Chemistry Society*, *128*, 5033–5040.
24. Maestri, G., Larraufie, M. H., Derat, E., Ollivier, C., Fensterbank, L., Malacria, M., et al. (2010). *Organic Letters, 12*, 5692–5695.
25. Beaume, A., Courillon, C., & Malacria, M. (2008). UPMC-Paris VI, *Thesis*.
26. Li, S. T., Han, L., Sun, L., Zheng, D., Liu, J., Fu, Y. B., et al. (2009). *Molecules, 14*, 5042–5053.
27. Bao, M., Nakamura, H., & Yamamoto, Y. (2001). *Journal of the American Chemical Society, 123*, 759–760.
28. Peng, B., Feng, X., Zhang, X., Zhang, S., & Bao, M. (2010). *Journal of Organic Chemistry, 75*, 2619–2627.
29. Catellani, M., Cugini, F., & Bocelli, G. (1999). *Journal of Organometallic Chemistry, 584*, 63–67.
30. Garcia-Fortanet, J., Kessler, F., & Buchwald, S. L. (2009). *Journal of the American Chemical Society, 131*, 6676–6677.
31. Bedford, R. B., Fey, N., Haddow, M. F., & Sankey, R. F. (2011). *Chemistry Communications, 47*, 3649–3651.
32. Maestri, G., Motti, E., Della Ca, N., Malacria, M., Derat, E., & Catellani, M. (2011). *Journal American Chemistry Society*, *133*, 8574–8585.
33. Baumgarten, S., Lesage, D., Gandon, V., Goddard, J. P., Malacria, M., Tabet, J. C., et al. (2009). *ChemCatChem, 1*, 138–143.
34. Tolman, C. A. (1972). *Chemical Society Reviews, 1*, 337–353.
35. Howell, J. A. S., & Burkinshaw, P. M. (1983). *Chemical Reviews, 83*, 557–599.
36. Maestri, G., Della Ca, N., & Catellani, M. (2009). *Chemistry Communication,* 4892–4894.
37. Larraufie, M. H., Maestri, G., Beaume, A., Derat, E., Ollivier, C., Fensterbank, L., et al. (2011). *Angewandte Chemie International Edition, 50*, 12253–12258.

Chapter 9
Supporting Information

9.1 General Remarks

Reagents were obtained from commercial sources and used as received. 4-Methoxy-2-methyliodobenzene, 3,4-dimethoxy-2-methyliodobenzene [1], 4-methoxyiodonaphthalene [2], were prepared according to reported procedures. Reactions were carried out with redistilled solvents. THF and Et_2O were distilled from sodium/benzophenone. CH_2Cl_2, acetonitrile, NEt_3 were distilled from CaH_2. DMF was dried and degassed using an MBraun Solvent Purification System, from which it was collected in a Schlenk-type flask immediately prior to use. Reactions were carried out under argon using standard Schlenk technique. Gas chromatography analyses were performed with a Carlo Erba HRGC 8000Top instrument using a 12 m HSP-5 capillary column. Flash column chromatography was performed on Merck Geduran SI 60 A silica gel (35–70 mm) and thin-layer chromatography on Merck $60F_{254}$ plates. Melting points were determined with a Reichert hot stage apparatus and are uncorrected. IR spectra were recorded with a Bruker Tensor 27 ATR diamant PIKE spectrometer. ^{1}H NMR, ^{13}C NMR and ^{19}F NMR spectra were recorded in $CDCl_3$ and CD_2Cl_2 at 300 K on Bruker 400 AVANCE spectrometer fitted with a BBFO probehead at 400.1, 100.5 and 377 MHz respectively, using the solvent as internal standard (7.26 and 5.23 ppm for ^{1}H NMR and 77.00 and 55.24 ppm for ^{13}C NMR) and $CFCl_3$ (0.00 ppm) for ^{19}F. The reported assignments are based on decoupling, COSY, NOESY, HMBC, HMQC correlation experiments. The terms m, s, d, t, q represent multiplet, singlet, doublet, triplet, quadruplet respectively, and the term br means a broad signal. Exact masses were recorded at UPMC by the laboratory of Prof. J.-C. Tabet (UMR 7201) (electrospray source).

Calculations were performed with Gaussian 09 at DFT level [3]. The geometries of all complexes here reported were optimized without any constraints at the generalized gradient approximation using the M06 hybrid functional of Zhao and Truhlar.[1] Optimizations were carried out using LACVP(d) basis set [5, 6]. It consists of the standard 6-31G(d) basis set for lighter atoms (H, C, N, O and P) and

[1] Gaussian 09, Revision **A1** [4].

M.-H. Larraufie, *Development of New Radical Cascades and Multi-Component Reactions*, Springer Theses, DOI: 10.1007/978-3-319-01324-4_9,

the LANL2DZ basis set for Pd, Br and I. For more accurate energy values, single-point calculations were performed on the optimized geometries using a larger basis set, Def2-TZVP defined by Weigand and Ahlrichs, essentially a valence triple-ζ one [7–9]. Harmonic frequencies were calculated at the same level of theory with LACVP(d) basis set to characterize stationary points and to determine zero-point energies corrections (ZPC). Energies calculated with both basis sets were corrected with these ZPCs without scaling. The starting approximate geometries for transition states (TS) were obtained through scans of the relative reaction coordinate starting from the corresponding reagents. Calculations data can be found in the SI of our publication [10].

9.2 Coupling of *Ortho*-Substituted Aryl Iodides and Bromobenzyl Amines

9.2.1 General Procedures

General procedure 1 (**GP1**): Synthesis of bromobenzyloximes from corresponding aldehyde or ketone [11].

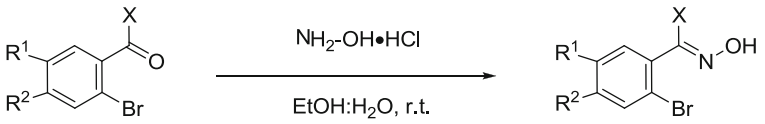

To a solution of $NaHCO_3$ (1 equiv.) in H_2O (0.44 M) were added hydroxylamine hydrochloride (1.02 equiv.) and a solution of the carbonyl compound (1 equiv.) in ethanol (0.44 M). The reaction mixture was stirred at r.t. for 5 h, and left at −20 °C for 1 h. The suspension was filtered, washed with a few mL of cold ethanol and dried under vacuum to afford the pure oxime as a white solid.

General procedure 2 (**GP2**): Synthesis of bromobenzylamines from corresponding oximes [5, 6].

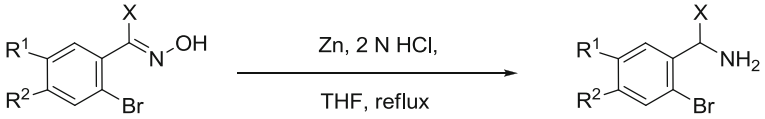

To a solution of oxime (1 equiv.) in THF (0.08 M) were a 2 M HCl solution (10 equiv.) and zinc powder (10 equiv.). The reaction mixture was stirred under reflux until the reaction was complete, cooled to r.t., filtered on a Celite pad, and concentrated under reduced pressure to one third of its volume. The aqueous layer was extracted with EtOAcand its pH was adjusted to >10 by addition of saturated ammonia solution. It was then extracted with EtOAc. The combined organic layers

were washed with water, dried over $MgSO_4$ and concentrated under reduced pressure to afford the pure amine as an oil.

General procedure 3 (**GP3**): Reaction of *ortho*-substituted aryl iodide and a bromobenzylamine.

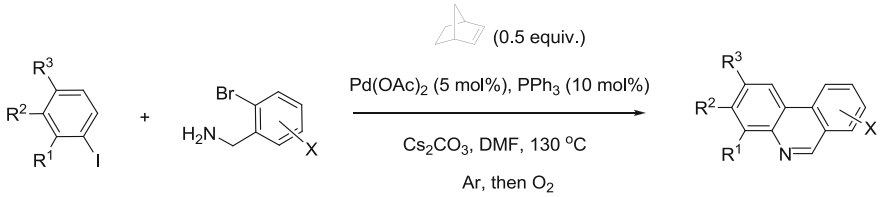

To a Schlenk-type flask were added under argon Cs_2CO_3 (185 mg; 0.6 mmol; 2.1 equiv), triphenylphosphine (7 mg; 0.026 mmol; 0.10 equiv), a solution of DMF (3 mL) containing the aryl iodide (0.29 mmol; 1.1 equiv), the (substituted) 2-bromobenzylamine (0.26 mmol; 1 equiv) and norbornene (12 mg, 0.13 mmol; 0.5 equiv), and a solution of $Pd(OAc)_2$ (3 mg, 0.013 mmol; 0.05 equiv) in 3 mL of DMF. The same procedure could be adopted when using 2-bromobenzylamines hydrochloric salts by adding 1 more equiv of base in the reaction vessel. The resulting suspension was stirred with a magnetic bar at 130 °C until visible formation of palladium black (24–48 h). Oxygen was then added to the reaction mixture via balloon, and the suspension was kept at 130 °C under stirring until complete oxidation (12 h to overnight), as evidenced by ^{1}H NMR. The mixture was then allowed to cool to room temperature, diluted with EtOAc (30 mL), washed three times with a saturated K_2CO_3 solution (3 × 30 mL) and dried over $MgSO_4$. The solvent was removed under reduced pressure and the crude mixture was analyzed by GC and ^{1}H NMR spectroscopy. The products were isolated by flash column chromatography on silica gel.

9.2.2 Preparation of Starting Bromides

1-Bromo-6-aminomethyl-3,4-(methylenedioxy)benzene (146)

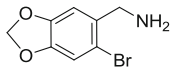

$C_8H_8BrNO_2$ M = 230.06 g/mol

Following **GP1** with 6-bromopiperonal (5.0 g, 21.8 mmol, 1 equiv.), the corresponding oxime was isolated as a white solid (4.60 g, 87 %). Following **GP2** with the oxime (4.00 g, 16.3 mmol, 1 equiv.), amine **146** was isolated as a pale yellow oil (2.8 g, 75 %). Spectral data are in accordance with those reported in the literature [5, 6].

^{1}H NMR (400 MHz, $CDCl_3$): $\delta = 6.99$ (s, 1 H, arom.), 6.88 (s, 1 H, arom.), 5.96 (s, 2 H, CH_2-O), 3.81 (s, 2 H, CH_2-N), 1.59 (br s, 2H, NH_2); ^{13}C NMR (100 MHz, $CDCl_3$): $\delta = 147.5$ (C arom.), 147.2 (C arom.), 135.5 (C arom.), 113.5 (C arom.), 112.8 (CH arom.), 109.1 (CH arom.), 101.6 (CH_2-O), 46.8 (CH_2-N).

2-Bromo-5-fluorobenzylamine (**147**)

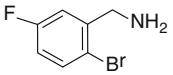

C_7H_7BrFN M = 204.04 g/mol

Following **GP1** with 2-bromo-5-fluorobenzaldehyde (1.0 g, 4.92 mmol, 1 equiv.), the corresponding oxime was isolated as a white solid (900 mg, 84 %). Following **GP2** with the oxime (700 mg, 3.2 mmol, 1 equiv.), amine **147** was isolated as a pale yellow oil (400 mg, 61 %). Spectral data are in accordance with those reported in the literature [12].

^{1}H NMR (400 MHz, $CDCl_3$): $\delta = 7.50$ (dd, $J = 8.6$, 5.3 Hz, 1 H, arom.), 7.19 (dd, $J = 9.4$, 3.0 Hz, 1 H, arom.), 6.86 (ddd, $J = 8.2$, 8.2, 3.0 Hz, 1 H, arom.), 3.90 (s, 2 H, CH_2-N), 1.55 (s, 2 H, NH_2); ^{13}C NMR (100 MHz, $CDCl_3$): $\delta = 162.3$ (d, $^{1}J_{C-F} = 245.1$ Hz, C–F), 144.4 (d, $^{3}J_{C-F} = 6.9$ Hz, C arom.), 133.9 (d, $^{3}J_{C-F} = 7.7$ Hz, CH arom.), 117.2 (d, $^{4}J_{C-F} = 3.4$ Hz, C arom.), 116.0 (d, $^{2}J_{C-F} = 23.1$ Hz, CH arom.), 115.4 (d, $^{2}J_{C-F} = 22.3$ Hz, CH arom.), 46.6 (CH_2-N).

1-Aminoethylbromobenzene (**152**)

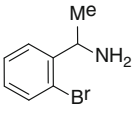

$C_8H_{10}BrN$ M = 200.08 g/mol

To a solution of 2-bromoacetophenone (2.50 g, 12.5 mmol, 1 equiv.) in ethanol (10 mL) was added *O*-benzylhydroxyamine hydrochloride (2.2 g, 13.8 mmol, 1.1 equiv.) and H_2O (6.2 mL). The reaction mixture was stirred at 80 °C for 1 h, then cooled to r.t. and quenched with HCl 2 M aqueous solution (25 mL). The aqueous layer was extracted with EtOAc (2 × 30 mL). The combined organic layers were washed with water, dried over $MgSO_4$, and concentrated under reduced pressure to afford the pure amine as a colorless oil (3.65 g, 96 %). To a solution of the oxime (3.60 g, 11.9 mmol) in THF (18 mL) was added dropwise BH_3.THF (24 mmol, 2 equiv.). The reaction mixture was stirred at r.t. for 24 h, then quenched with HCl 4 M aqueous solution (20 mL) and extracted with EtOAc (3 × 15 mL). The combined organic layers were washed with water, dried over $MgSO_4$, and concentrated under reduced pressure to afford the pure amine **152** as a colorless oil (3.65 g, 96 %). Data correspond to those described in the literature [13].

^{1}H NMR (400 MHz, $CDCl_3$): $\delta = 7.53$ (d, $J = 8.0$ Hz, 2 H, arom.), 7.32 (t, $J = 7.2$ Hz, 1 H, arom.), 7.11 − 7.06 (m, 1 H, arom.), 4.50 (q, $J = 6.4$ Hz, 1 H, MeC*H*), 1.54 (br s, 2 H, NH_2), 1.38 (d, $J = 6.4$ Hz, 3 H, Me); ^{13}C NMR

(100 MHz, $CDCl_3$): δ = 146.4 (C arom.), 133.1 (CH arom.), 128.4 (CH arom.), 128.1 (CH arom.), 126.7 (CH arom.), 123.3 (C arom.), 50.2 (MeCH), 24.0 (Me).

9.2.3 Phenanthridine-Type Products

4-Methylphenanthridine (122a)

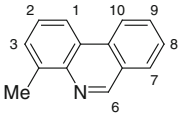

$C_{14}H_{11}N$ M = 193.24 g/mol

Isolated as a white solid. Yield: 85 %. Mp: 73–75 °C. Eluent: pentane/EtOAc = 95:5. Data correspond to those described in the literature [14].

^{1}H NMR (400 MHz, $CDCl_3$): δ = 9.34 (1 H, s, H6), 8.62 (1 H, d, J = 8.4 Hz, H10), 8.46 (1 H, dd, J = 8.0, 1.2 Hz, H1), 8.06 (1 H, d, J = 8.0 Hz, H7), 7.86 (1 H, ddd, J = 8.0, 6.8, 1.2 Hz, H9), 7.73 − 7.67 (1 H, m, H8), 7.64 − 7.55 (2 H, m, H2, H3), 2.92 (3 H, s, Me); ^{13}C NMR (100 MHz, $CDCl_3$): δ = 152.5 (C6), 143.5 (C4a), 138.0 (C4), 133.2 (C10a), 131.1 (C9), 129.8 (C3), 129.0 (C7), 127.6 (C8), 127.0 (C2), 126.4 (C6a), 124.2 (C10b), 122.4 (C10), 120.4 (C1), 19.0 (Me).

5,6-Dihydro-4-methylphenanthridine (121a)

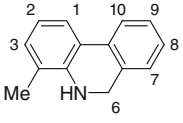

$C_{14}H_{13}N$ M = 195.26 g/mol

^{1}H NMR (400 MHz, $CDCl_3$): δ = 7.69 (1 H, d, J = 8.0 Hz, H10), 7.60 (1 H, d, J = 8.0 Hz, H1), 7.31 (1 H, td, J = 8.0, 1.6 Hz, H9), 7.22 (1 H, td, J = 7.6, 1.2 Hz, H8), 7.13 (1 H, dd, J = 7.6, 0.8 Hz, H7), 7.03 (1 H, dd, J = 7.6, 0.8 Hz, H3), 6.78 (1 H, t, J = 7.6 Hz, H2), 4.43 (2 H, s, CH_2), 4.05 (1 H, br s, NH), 2.19 (3 H, s, Me); ^{13}C NMR (100 MHz, $CDCl_3$): δ = 144.1 (C4a), 132.8 (C6a), 132.7 (C10a), 130.4 (C3), 127.9 (C9), 127.2 (C8), 126.0 (C7), 122.9 (C10), 122.4 (C10b), 121.9 (C1), 121.7 (C4), 118.7 (C2), 46.6 (C6), 17.3 (Me).

4-Ethylphenanthridine (122b)

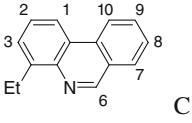

$C_{15}H_{13}N$ M = 207.27 g/mol

Isolated as a colorless oil. Yield: 82 %. Eluent: pentane/EtOAc = 95:5.

IR (neat): ν = 2,961, 1,616, 1,589, 1,525, 1,462, 1,444, 750 cm^{-1}; ^1H NMR (400 MHz, $CDCl_3$): δ = 9.34 (1 H, s, H6), 8.62 (1 H, d, J = 8.4 Hz, H10), 8.47 (1 H, dd, J = 8.0, 2.4 Hz, H1), 8.05 (1 H, d, J = 7.6 Hz, H7), 7.85 (1 H, t, J = 8.0 Hz, H9), 7.74 − 7.67 (1 H, m, H8), 7.65 − 7.58 (2 H, m, H2, H3), 3.42 (2 H, q, J = 7.6 Hz, CH_2), 1.46 (3 H, t, J = 7.6 Hz, Me); ^{13}C NMR (100 MHz, $CDCl_3$): δ = 152.1 (C6), 143.6 (C4), 142.6 (C4a), 132.9 (C10a), 130.7 (C9), 128.6 (C7), 128.0 (C3), 127.2 (C8), 126.9 (C2), 126.1 (C6a), 124.0 (C10b), 122.0 (C10), 120.0 (C1), 25.1 (CH_2), 15.5 (Me); HRMS calcd. for $C_{15}H_{14}N$ ($[M + H]^+$) 208.1121, found 208.1120.

2,4-Dimethylphenanthridine (122c)

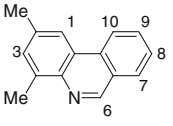

$C_{15}H_{13}N$ M = 207.27 g/mol

Isolated as a white solid. Yield: 81 %. Mp: 117–118 °C. Eluent: pentane/EtOAc = 95:5.

IR (neat): ν = 2,922, 1,616, 1,588, 1,454, 754 cm^{-1}; ^1H NMR (400 MHz, $CDCl_3$): δ = 9.27 (1 H, s, H6), 8.58 (1 H, d, J = 8.4 Hz, H10), 8.22 (1 H, s, H1), 8.03 (1 H, d, J = 8.0 Hz, H7), 7.82 (1 H, td, J = 8.0, 1.2 Hz, H9), 7.67 (1 H, td, J = 8.0, 1.2 Hz, H8), 7.46 (1 H, s, H3), 2.91 (3 H, s, Me(C2)), 2.64 (3 H, s, Me(C4)); ^{13}C NMR (100 MHz, $CDCl_3$): δ = 151.2 (C6), 141.0 (C4a), 137.0 (C4), 136.5 (C2), 132.6 (C10a), 131.4 (C3), 130.7 (C9), 128.7 (C7), 127.1 (C8), 126.0 (C6a), 123.8 (C10b), 122.0 (C10), 119.6 (C1), 21.8 (Me(C4)), 18.5 (Me(C2)); HRMS calcd. for $C_{15}H_{14}N$ ($[M + H]^+$) 208.1121, found 208.1118.

3,4-Dimethylphenanthridine (122d)

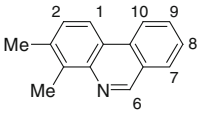

$C_{15}H_{13}N$ M = 207.27 g/mol

Isolated as a white solid. Yield: 91 %. Mp: 90–91 °C. Eluent: pentane/EtOAc = 95:5.

IR (neat): ν = 2,918, 1,616, 1,589, 1,469, 1,444, 748 cm^{-1}; ^1H NMR (400 MHz, $CDCl_3$): δ = 9.31 (1 H, s, H6), 8.59 (1 H, d, J = 8.4 Hz, H10), 8.35 (1 H, d, J = 8.4 Hz, H1), 8.04 (1 H, d, J = 7.6 Hz, H7), 7.81 (1 H, td, J = 8.0, 1.2 Hz, H9), 7.73 − 7.67 (1 H, m, H8), 7.51 (1 H, d, J = 8.4 Hz, H2), 2.85 (3 H, s, Me(C4)), 2.56 (3 H, s, Me(C3)); ^{13}C NMR (100 MHz, $CDCl_3$): δ = 152.0 (C6), 143.1 (C4a), 136.9 (C3), 135.5 (C4), 133.0 (C10a), 130.7 (C9), 129.2 (C7), 128.6 (C2), 126.8 (C8), 125.7 (C6a), 121.9 (C10b), 121.8 (C10), 119.0 (C1), 20.7 (Me(C4)), 20.6 (Me(C3)); HRMS calcd. for $C_{15}H_{14}N$ ($[M + H]^+$) 208.1121, found 208.1118.

CCDC 787343 contains the supplementary crystallographic data for 3,4-dimethylphenanthridine (**122d**). These data can be obtained free of charge from The Cambridge Crystallographic Data Centre via www.ccdc.cam.ac.uk/data_request/cif.

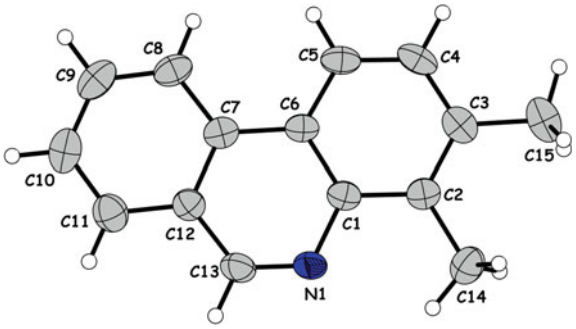

2-Methoxy-4-methylphenanthridine (**122e**)

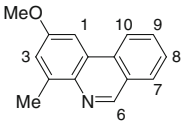

$C_{15}H_{13}NO$ M = 223.27 g/mol

Isolated as a white solid. Yield: 65 %. Mp: 76–77 °C. Eluent: pentane/EtOAc = 85:15.

IR (neat): ν = 2,955, 1,611, 1,523, 1,494, 1,456, 1,401, 1,354, 1,206, 1,052, 753 cm^{-1}; ^1H NMR (400 MHz, $CDCl_3$): δ = 9.17 (1 H, s, H6), 8.51 (1 H, d, J = 8.0 Hz, H10), 8.01 (1 H, dd, J = 8.0, 0.8 Hz, H7), 7.80 (1 H, td, J = 8.0, 1.2 Hz, H9), 7.75 (1 H, d, J = 2.4 Hz, H1), 7.67 (1 H, td, J = 8.0, 1.2 Hz, H8), 7.24 (1 H, d, J = 2.4 Hz, H3), 3.99 (3 H, s, OMe), 2.85 (3 H, s, Me); ^{13}C NMR (100 MHz, $CDCl_3$): δ = 157.9 (C2), 149.6 (C6), 139.5 (C4), 138.7 (C4a), 132.3 (C10a), 130.2 (C9), 128.6 (C7), 127.2 (C8), 126.4 (C6a), 125.1 (C10b), 122.0 (C10), 119.3 (C3), 100.6 (C1), 55.4 (OMe), 18.7 (Me); HRMS calcd. for $C_{15}H_{14}NO$ ($[M + H]^+$) 224.1070, found 224.1066.

2,3-Dimethoxy-4-methylphenanthridine (**122f**)

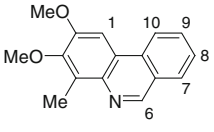

$C_{16}H_{15}NO_2$ M = 253.30 g/mol

Isolated as a white solid. Yield: 95 %. Mp: 86–87 °C. Eluent: pentane/EtOAc = 75:25.

IR (neat): v = 2,928, 1,606, 1,475, 1,403, 1,272, 1,239, 1,077, 751 cm^{-1}; ^1H NMR (400 MHz, $CDCl_3$): δ = 9.17 (1 H, s, H6), 8.45 (1 H, d, J = 8.4 Hz, H10), 7.99 (1 H, dd, J = 8.0, 0.8 Hz, H7), 7.78 (1 H, td, J = 8.4, 1.2 Hz, H9), 7.74 (1 H, s, H1), 7.63 (1 H, td, J = 8.0, 0.8 Hz, H8), 4.07 (3 H, s, OMe), 3.93 (3 H, s, OMe), 2.80 (3 H, s, Me(C4)); ^{13}C NMR (100 MHz, $CDCl_3$): δ = 152.5 (C3 or C2), 150.0 (C6), 148.7 (C2 or C3), 139.2 (C4a), 132.1 (C4), 130.4 (C10a), 130.2 (C9), 128.6 (C7), 126.7 (C8), 125.9 (C6a), 121.7 (C10), 121.0 (C10b), 99.9 (C1), 60.6 (OMe), 55.7 (OMe), 10.9 (Me); HRMS calcd. for $C_{16}H_{16}NO_2$ ($[M + H]^+$) 254.1176, found 254.1175.

Benzo[*c*]phenanthridine (122g)

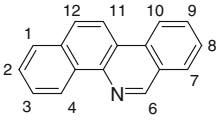

$C_{17}H_{11}N$ M = 229.28 g/mol

Isolated as a white solid. Yield: 80 %. Mp: 126–129 °C. Eluent: pentane/EtOAc = 95:5. Data correspond to those described in the literature [14].

^1H NMR (400 MHz, $CDCl_3$): δ = 9.48 (1 H, s, H6), 9.42 (1 H, d, J = 8.4 Hz, H4), 8.65 (1 H, d, J = 8.4 Hz, H10), 8.53 (1 H, d, J = 8.8 Hz, H1), 8.13 (1 H, d, J = 8.0 Hz, H12), 8.02 (1 H, d, J = 8.8 Hz, H2), 7.98 (1 H, d, J = 8.0 Hz, H11), 7.88 (1 H, t, J = 7.2 Hz, H9), 7.79 (1 H, t, J = 7.2 Hz, H8), 7.73 − 7.67 (2 H, m, H7 + H3); ^{13}C NMR (100 MHz, $CDCl_3$): δ = 151.9, 141.5, 133.2, 132.8, 132.1, 130.8, 128.6, 127.8, 127.6, 127.3, 127.1, 127.0, 126.9, 124.7, 122.2, 121.0, 119.9.

12-Methoxybenzo[*c*]phenanthridine (122h)

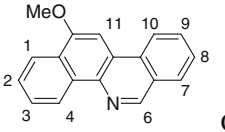

$C_{18}H_{13}NO$ M = 259.30 g/mol

Isolated as a white solid. Yield: 77 %. Mp: 114–115 °C. Eluent: pentane/EtOAc = 85:15.

IR (neat): v = 2,957, 1,620, 1,598, 1,518, 1,452, 1,408, 1,254, 1,232, 1,215, 1,094, 761 cm^{-1}; ^1H NMR (400 MHz, $CDCl_3$): δ = 9.36 (1 H, d, J = 8.3 Hz, H10), 9.31 (1 H, s, H6), 8.51 (1 H, d, J = 8.7 Hz, H4), 8.38 (1 H, d, J = 8.3 Hz, H1), 8.07 (1 H, d, J = 8.0 Hz, H7), 7.85 − 7.76 (2 H, m, H3, H9), 7.72 − 7.65 (2 H, m, H2, H8), 7.64 (1 H, s, H11), 4.16 (3 H, s, OMe); ^{13}C NMR (100 MHz, $CDCl_3$): δ = 154.6 (C12), 149.3 (C6), 137.2 (C4b), 132.8 (C4a), 132.2 (C10a), 130.1 (C3), 128.6 (C7), 127.5 (C9), 127.0 (C6a), 127.0 (C2), 126.9 (C8), 126.8 (C10b), 124.5 (C10), 122.0 (C4), 121.84 (C12a), 121.81 (C1), 95.7 (C11), 55.5 (OMe); HRMS calcd. for $C_{18}H_{14}NO$ ($[M + H]^+$) 260.1070, found 260.1071.

4-Chlorophenanthridine (122i)

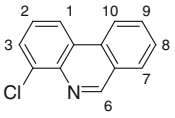

$C_{13}H_8NCl$ M = 213.66 g/mol

Isolated as a yellow solid. Yield: 31 %. Mp: 98–100 °C. Eluent: pentane/EtOAc = 95:5. Data correspond to those described in the literature [14].

^{1}H NMR (400 MHz, $CDCl_3$): δ = 9.40 (1 H, s, H6), 8.67 (1 H, d, J = 8.0 Hz, H10), 8.58 (1 H, dd, J = 8.0, 0.8 Hz, H1), 8.14 (1 H, d, J = 8.0, 0.8 Hz, H7), 7.94 (1 H, ddd, J = 8.0, 7.4, 1.2 Hz, H9), 7.88 (1 H, dd, J = 7.6, 1.2 Hz, H3), 7.80 (1 H, ddd, J = 8.0, 7.4, 1.2 Hz, H8), 7.68 − 7.60 (1 H, m, H2); ^{13}C NMR (100 MHz, $CDCl_3$): δ = 154.9 (C6), 141.6 (C4a), 134.6 (C4), 133.0 (C10a), 132.0 (C3), 129.9 (C9), 129.7 (C7), 129.0 (C8), 127.8 (C2), 127.3 (C6a), 126.7 (C10b), 123.0 (C10), 122.2 (C1).

4-Trifluoromethylphenanthridine (122j)

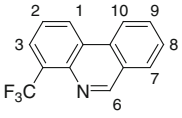

$C_{14}H_8F_3N$ M = 247.22 g/mol

Isolated as a pale yellow solid. Yield: 22 %. Mp: 132–134 °C. Eluent: pentane/EtOAc = 95:5. Data correspond to those described in the literature [14].

^{1}H NMR (400 MHz, $CDCl_3$): δ = 9.46 (1 H, s, H6), 8.81 (1 H, d, J = 8.4 Hz, H1), 8.65 (1 H, d, J = 8.4 Hz, H10), 8.13 (1 H, d, J = 8.0 Hz, H3), 8.11 (1 H, d, J = 7.6 Hz, H7), 7.94 (1 H, J = 8.0 Hz, H8), 7.80 (1 H, t, J = 8.0 Hz, H2), 7.75 (1 H, t, J = 8.0 Hz, H9); ^{13}C NMR (100 MHz, $CDCl_3$): δ = 154.4 (C6), 141.4 (C4a), 132.0 (C10a), 131.6 (C9), 129.0 (C7), 128.6 (q, $^2J_{C-F}$ = 18.2 Hz, C4), 128.3 (C8), 126.8 (q, $^3J_{C-F}$ = 5.5 Hz, C3), 126.5 (C2), 126.2 (C6a), 125.9 (C10), 124.9 (C10b), 124.3 (q, $^1J_{C-F}$ = 273.2 Hz, CF_3), 121.9 (C1); ^{19}F NMR: δ = −60.9.

3,4,6-Trimethylphenanthridine (122k)

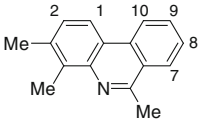

$C_{16}H_{15}N$ M = 221.30 g/mol

Isolated as a white solid. Yield: 90 %. Mp: 120–121 °C. Eluent: pentane/EtOAc = 95:5.

IR (neat): ν = 2,920, 1,612, 1,588, 1,482, 1,447, 1,375, 757 cm^{-1}; ^{1}H NMR (400 MHz, $CDCl_3$): δ = 8.57 (1 H, d, J = 8.4 Hz, H10), 8.28 (1 H, d, J = 8.4 Hz,

H1), 8.16 (1 H, d, $J = 8.4$ Hz, H7), 7.77 (1 H, td, $J = 8.4$, 1.2 Hz, H9), 7.63 (1 H, td, $J = 8.0$, 1.2 Hz, H8), 7.42 (1 H, d, $J = 8.4$ Hz, H2), 3.05 (3 H, s, Me(C6)), 2.85 (3 H, s, Me(C4)), 2.53 (3 H, s, Me(C2)); ^{13}C NMR (100 MHz, $CDCl_3$): $\delta = 157.1$ (C6), 142.2 (C4a), 136.7 (C4), 134.8 (C3), 133.0 (C10a), 129.9 (C9), 128.2 (C2), 126.5 (C8), 126.2 (C7), 125.1 (C6a), 122.2 (C10), 121.5 (C10b), 118.7 (C1), 23.7 (Me(C6)), 20.7 (Me(C3)), 13.5 (Me(C4)); HRMS calcd. for $C_{16}H_{16}N$ ($[M + H]^+$) 222.1277, found 222.1274.

4-Ethyl-6-methylphenanthridine (122l)

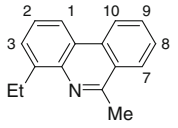

$C_{16}H_{15}N$ M = 221.30 g/mol

Isolated as a white solid. Yield: 88 %. Mp: 75–76 °C. Eluent: pentane/EtOAc = 95:5.

IR (neat): $\nu = 2{,}962$, 1,585, 1,527, 1,446, 1,375, 1,319, 752 cm^{-1}; ^{1}H NMR (400 MHz, $CDCl_3$): $\delta = 8.61$ (1 H, d, $J = 8.3$ Hz, H10), 8.40 (1 H, dd, $J = 8.0$, 1.6 Hz, H1), 8.19 (1 H, dd, $J = 8.3$, 0.8 Hz, H7), 7.79 (1 H, t, $J = 8.3$ Hz, H9), 7.66 (1 H, t, $J = 8.3$ Hz, H8), 7.62 − 7.52 (2 H, m, H2, H3), 3.40 (2 H, q, $J = 7.6$ Hz, CH_2(C4)), 3.05 (3 H, s, Me(C6)), 1.44 (3 H, t, $J = 7.6$ Hz, Me); ^{13}C NMR (100 MHz, $CDCl_3$): $\delta = 157.1$ (C6), 143.1 (C4), 141.8 (C4a), 132.9 (C10a), 129.9 (C9), 127.6 (C2), 126.9 (C8), 126.3 (C7), 125.9 (C3), 125.6 (C6a), 123.5 (C10b), 122.5 (C10), 119.6 (C1), 24.7 CH_2(C4), 23.6 Me(C6), 15.4 (Me); HRMS calcd. for $C_{16}H_{16}N$ ($[M + H]^+$) 222.1277, found 222.1278.

2,4,6-Trimethylphenanthridine (122m)

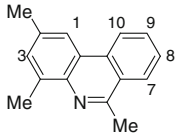

$C_{16}H_{15}N$ M = 221.30 g/mol

Isolated as a white solid. Yield: 90 %. Mp: 87–88 °C. Eluent: pentane/EtOAc = 95:5.

IR (neat): $\nu = 2{,}920$, 1,612, 1,585, 1,451, 1,374, 755 cm^{-1}; ^{1}H NMR (400 MHz, $CDCl_3$): $\delta = 8.57$ (1 H, d, $J = 8.0$ Hz, H10), 8.16 (1 H, d, $J = 8.0$ Hz, H7), 8.15 (1 H, s, H1), 7.77 (1 H, t, $J = 8.0$ Hz, H9), 7.63 (1 H, t, $J = 7.6$ Hz, H8), 7.40 (1 H, s, H3), 3.03 (3 H, s, Me(C6)), 2.85 (3 H, s, Me(C4)), 2.56 (3 H, s, Me(C2)); ^{13}C NMR (100 MHz, $CDCl_3$): $\delta = 156.2$ (C6), 140.7 (C4a), 136.7 (C4), 135.2 (C2), 132.5 (C10a), 131.0 (C3), 129.8 (C9), 126.7 (C8), 126.2 (C7), 125.6 (C6a), 123.3 (C10b), 122.4 (C10), 119.3 (C1), 23.5 (Me(C6)), 21.8 (Me(C2)), 18.1 (Me(C4)); HRMS calcd. for $C_{16}H_{16}N$ ($[M + H]^+$) 222.1277, found 222.1277.

2,4-Dimethyl-8,9-methylenedioxyphenanthridine (122n)

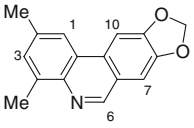

$C_{16}H_{13}NO_2$ M = 251.28 g/mol

Isolated as a white solid. Yield: 82 %. Mp: 98–99 °C. Eluent: pentane/EtOAc = 80:20.

IR (neat): ν = 2,912, 1,619, 1,488, 1,461, 1,252, 1,217, 1,239, 1,037, 940, 835 cm^{-1}; ^1H NMR (400 MHz, $CDCl_3$): δ = 9.04 (1 H, s, H6), 7.99 (1 H, s, H1), 7.87 (1 H, s, H10), 7.38 (1 H, s, H3), 7.30 (1 H, s, H7), 6.14 (2 H, s, CH_2), 2.82 (3 H, s, Me(C4)), 2.56 (3 H, s, Me(C2)); ^{13}C NMR (100 MHz, $CDCl_3$): δ = 151.1 (C8), 149.6 (C6), 147.9 (C9), 141.3 (C4a), 137.2 (C4), 135.9 (C2), 130.6 (C3), 130.1 (C10a), 124.0 (C6a), 122.9 (C10b), 119.4 (C1), 105.2 (C7), 101.7 (CH_2), 100.0 (C10), 21.8 (Me(C2)), 18.6 (Me(C4)); HRMS calcd. for $C_{16}H_{14}NO_2$ ($[M + H]^+$) 252.1019, found 252.1016.

2,4-Dimethyl-8-fluorophenanthridine (122o)

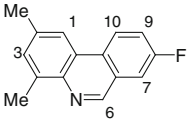

$C_{15}H_{12}NF$ M = 225.26 g/mol

Isolated as a white solid. Yield: 86 %. Mp: 112–113 °C. Eluent: pentane/EtOAc = 95:5.

IR (neat): ν = 2,920, 1,620, 1,525, 1,264, 1,198, 1,153, 958, 825 cm^{-1}; ^1H NMR (400 MHz, $CDCl_3$): δ = 9.17 (1 H, s, H6), 8.55 (1 H, dd, J = 9.0, 5.1 Hz, H10), 8.13 (1 H, s, H1), 7.63 (1 H, dd, J = 8.4, 2.6 Hz, H7), 7.57 − 7.52 (1 H, m, H9), 7.43 (1 H, s, H3), 2.83 (3 H, s, Me(C4)), 2.57 (3 H, s, Me(C2)); ^{13}C NMR (100 MHz, $CDCl_3$): δ = 161.2 (d, $^1J_{C-F}$ = 248.2 Hz, C8), 150.1 (C6), 141.2 (C4a), 137.5 (C4), 136.9 (C2), 131.1 (C3), 129.2 (d, $^4J_{C-F}$ = 1.9 Hz, C10a), 127.3 (d, $^3J_{C-F}$ = 7.8 Hz, C6a), 124.7 (d, $^3J_{C-F}$ = 8.2 Hz, C10), 123.5 (C10b), 119.8 (d, $^2J_{C-F}$ = 23.9 Hz, C9), 119.4 (C1), 112.4 (d, $^2J_{C-F}$ = 20.5 Hz, C7), 21.9 (Me(C2)), 18.5 (Me(C4)); ^{19}F NMR: δ = −113.71. HRMS calcd. for $C_{15}H_{13}NF$ ($[M + H]^+$) 226.1026, found 226.1025.

4-Chloro-8-fluorophenanthridine (122p)

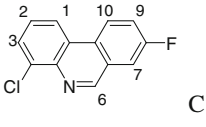

$C_{13}H_7NClF$ M = 231.65 g/mol

Isolated as a white solid. Yield: 46 %. Mp: 73–74 °C. Eluent: pentane/EtOAc = 95:5.

IR (neat): ν = 2,922, 2,852, 1,597, 1,495, 1,455, 1,366, 806 cm^{-1}; ^1H NMR (400 MHz, CD_2Cl_2): δ = 9.36 (1 H, s, H6), 8.67 (1 H, dd, J = 9.2, 5.2 Hz, H10), 8.52 (1 H, dd, J = 8.4, 0.9 Hz, H1), 7.88 (1 H, dd, J = 7.6, 1.2 Hz, H3), 7.75 (1 H, dd, J = 8.4, 2.4 Hz, H7), 7.68 − 7.60 (2 H, m, H9, H2); ^{13}C NMR (100 MHz, CD_2Cl_2): δ = 162.7 (d, $^1J_{C-F}$ = 248.2 Hz, C8), 153.8 (d, $^4J_{C-F}$ = 3.8 Hz, C6), 141.3 (C4a), 135.4 (C4), 129.84 (d, $^4J_{C-F}$ = 1.1 Hz, C10a), 129.80 (C3), 128.6 (d, $^3J_{C-F}$ = 8.2 Hz, C6a), 128.3 (C2), 126.4 (C10b), 125.9 (d, $^3J_{C-F}$ = 8.5 Hz, C10), 121.9 (C1), 121.5 (d, $^2J_{C-F}$ = 24.4 Hz, C7), 113.6 (d, $^2J_{C-F}$ = 20.8 Hz, C9); ^{19}F NMR: δ = −111.63; HRMS calcd. for $C_{13}H_8NClF$ ($[M + H]^+$) 232.0324, found 232.0322.

2,4-Dimethyl-6-phenylphenanthridine (122q)

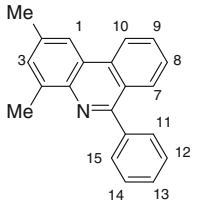

$C_{21\,H17}N$ M = 283.37 g/mol

Isolated as a pale yellow solid. Yield: 97 %. Mp: 132–133 °C. Eluent: pentane/EtOAc = 95:5.

IR (neat): ν = 2,920, 2,849, 1,599, 1,488, 1,445, 1,362, 816 cm^{-1}; ^1H NMR (400 MHz, $CDCl_3$): δ = 8.68 (1 H, d, J = 8.4 Hz, H10), 8.26 (1 H, s, H1), 8.19 (1 H, dd, J = 8.4, 0.8 Hz, H7), 7.87 − 7.83 (2 H, m, H11, H15), 7.80 (1 H, td, J = 8.0, 1.2 Hz, H9), 7.61 − 7.50 (4 H, m, H8, H12, H13, H14), 7.48 (1 H, s, H3), 2.89 (3 H, s, Me(C4), 2.62 (3 H, s, Me(C2)); ^{13}C NMR (100 MHz, $CDCl_3$): δ = 158.2 (C6), 140.9 (C4a), 140.4 (C11a), 137.8 (C4), 136.1 (C2), 133.5 (C10a), 131.2 (C13), 130.2 (C11, C15), 129.8 (C3), 128.5 (C8), 128.4 (C7), 128.1 (C12, C14), 126.6 (C9), 124.7 (C6a), 123.3 (C10b), 122.4 (C10), 119.2 (C1), 21.9 (Me(C2)), 18.2 (Me(C4)); HRMS calcd. for $C_{21\,H18}N$ ($[M + H]^+$) 284.1434, found 284.1437.

6-Phenylbenzo[*c*]phenanthridine (122r)

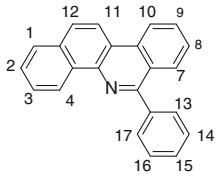

$C_{23}H_{15}N$ M = 305.37 g/mol

Isolated as a pale yellow solid. Yield: 92 %. Mp: 189–190 °C. Eluent: pentane/EtOAc = 95:5.

IR (neat): v = 2,921, 2,853, 1,564, 1,493, 1,445, 1,372, 799 cm^{-1}; ^1H NMR (400 MHz, $CDCl_3$): $\delta = 9.50$ (1 H, dd, $J = 8.4$, 0.8 Hz, H4), 8.76 (1 H, d, $J = 8.4$ Hz, H10), 8.59 (1 H, d, $J = 9.0$ Hz, H11), 8.31 (1 H, d, $J = 8.0$ Hz, H1), 8.04 (1 H, d, $J = 9.0$ Hz, H12), 7.99 (1 H, d, $J = 8.0$ Hz, arom.), 7.96 − 7.92 (2 H, m, H13, H17), 7.88 (1 H, ddd, $J = 8.4$, 8.0, 1.2 Hz, arom.), 7.77 − 7.56 (6H, m, arom.); ^{13}C NMR (100 MHz, $CDCl_3$): δ = 159.4 (C6), 140.7 (C4b), 140.3 (C13a), 133.8 (C10a), 133.4 (C12a), 132.2 (C4a), 130.4 (C13, C17), 130.2 (C9), 128.6 (C14, C16), 128.3 (C7, C15), 127.6 (C1), 127.5 (C2), 127.3 (C8), 126.8 (C3), 126.7 (C12), 125.3 (C6a), 125.2 (C4), 122.6 (C10), 120.4 (C10b), 119.7 (C11); HRMS calcd. for $C_{23}H_{16}N$ ($[M + H]^+$) 306.1277, found 306.1278.

9.3 Coupling of *Ortho*-Substituted Aryl Iodides and 2-Bromophenyl Acetamides

9.3.1 General Procedures

General procedure 1 (**GP1**): Reaction of an *ortho*-substituted aryl iodide and 2-(2-bromophenyl) acetamide without water.

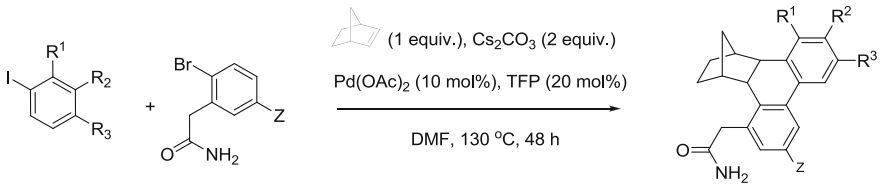

To a Schlenk-type flask containing a magnetic stir bar were added under argon Cs_2CO_3 (270 mg; 0.83 mmol; 2.3 equiv.), trifurylphosphine (17 mg; 0.07 mmol; 0.2 equiv.), the aryl iodide (0.36 mmol; 1 equiv.), 2-(2-bromophenyl)-acetamide (80 mg; 0.36 mmol; 1 equiv.), norbornene (46 mg; 0.48 mmol: 1.33 equiv.) and $Pd(OAc)_2$ (8 mg, 0.036 mmol; 0.1 equiv.). DMF (8 mL) was added to give a final palladium concentration of 0.004 M, and the resulting suspension was stirred at 130 °C for 48 h. At the end of the reaction the mixture was allowed to cool to room temperature, diluted with EtOAc (30 mL) and passed through a subtle pad of Celite. The solvent was removed under reduced pressure and the crude mixture was subjected to flash column chromatography on silica gel using a mixture of pentane/EtOAc as eluent.

General procedure 2 (**GP2**): Reaction of an *ortho*-substituted aryl iodide and 2-(2-bromophenyl) acetamide in the presence of water.

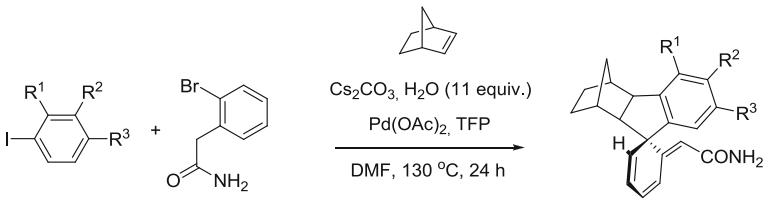

Following the above mentioned procedure, water (80 μL, 4.4 mmol; 11 equiv. in respect to palladium) was eventually added through a syringe inside the Schlenk-type flask to the resulting suspension before heating the reaction mixture at 130 °C for 24 h. Owing to the high temperature adopted, the partition of water between the solution and the head space of the vessel is influenced by the total volume of the latter. Formation of dihydrophenanthrene product is completely inhibited with the above reported amount of water when reactions are performed in a 20 mL Schlenk, while the use of larger reactors demands for a proportional increase in its amount (for example, 120 μL for 30 mL vessels).

Spiro compounds are stable at the solid state, while they decompose in few hours in solution, especially in an acidic environment (as in chloroform).

9.3.2 Preparation of Bromide Precursors

2-(2-Bromophenyl)-acetamide (160a)

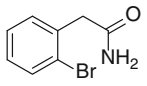

C_8H_8BrNO M = 214.06 g/mol

To a solution of 2-bromophenyl acetonitrile (4.40 g, 22.4 mmol, 1 equiv.) in *t*-BuOH (22 mL), was added potassium hydroxide (5.00 g, 89.8 mmol, 4 equiv.). The resulting mixture was refluxed for 2 h, turning red. It was then allowed to cool to room temperature, quenched with water (50 mL) and extracted with $CHCl_3$ (2 × 70 mL). The organic layers were combined and dried over $MgSO_4$. The solvent was removed under reduced pressure, yielding 2-(2-bromophenyl)-acetamide **160a** (3.5 g, 73 %) as a white solid.

Mp: 186–188 °C; IR (neat): ν = 3,387, 3,190, 1,661, 1,403, 1,026, 750 cm^{-1}; ^1H NMR (400 MHz, $CDCl_3$): $\delta = 7.63 - 7.57$ (m, 1 H, H3), 7.34 (dtd, J = 8.6, 7.6, 1.4 Hz, 2 H, H3, H5), 7.18 (td, J = 7.8, 1.8 Hz, 1 H, H4), 5.44 (br s, 2 H, NH_2), 3.74 (s, 2 H, CH_2); ^{13}C NMR (100 MHz, $CDCl_3$): δ = 171.8 (CO), 134.8 (C2), 133.2 (C3), 131.6 (C6), 129.2 (C5), 128.1 (C4), 124.9 (C1), 43.5 (CH_2); HRMS calcd. for $C_8H_8NOBrNa$ ($[M + Na]^+$, ^{79}Br) 235.9681, found 235.9682.

2-(2-Bromo-5-trifluoromethyl-phenyl)-acetamide (160b)

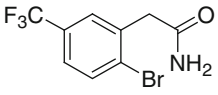

$C_9H_7BrF_3NO$ M = 282.06 g/mol

To a solution of 2-bromo, 4-trifluoromethyl acetonitrile (649 μL, 4.0 mmol, 1 equiv.) in a acetone/H_2O 1:1 mixture (6 mL), was added K_2CO_3 (80 mg, 0.58 mmol, 0.15 equiv.) and hydrogen peroxide-urea adduct (2.25 g, 24 mmol, 6 equiv.). The resulting mixture was stirred at r.t. for 24 h. Acetone was removed under reduced pressure and the resulting suspension filtered, yielding 2-(2-Bromo-5-trifluoromethylphenyl)-acetamide **160b** (800 mg; 71 %) as a white solid.

Mp: 162–164 °C; IR (neat): ν = 3,412, 3,209, 1,658, 1,399, 1,324, 1,079 cm^{-1}; ^1H NMR (400 MHz, DMSO-d_6): δ = 7.83 (d, J = 7.8 Hz, 1 H, H3), 7.75 (d, J = 1.2 Hz, 1 H, H6), 7.59 (br s, 1 H, N*H*H′), 7.52 (dd, J = 7.8, 1.2 Hz, H4), 7.05 (br s, 1 H, NH*H*′), 3.70 (s, 2 H, CH_2); ^{13}C NMR (DMSO-d_6): δ = 171.0 (CO), 137.9 (C2), 133.7 (C3), 129.5 (q, $^4J_{C-F}$ = 2 Hz, C1), 128.9 (q, $^3J_{C-F}$ = 4 Hz, C6), 128.5 (q, $^2J_{C-F}$ = 32 Hz, C5), 125.5 (q, $^3J_{C-F}$ = 4 Hz, C4), 124.7 (q, $^2J_{C-F}$ = 271 Hz, CF_3), 42.1 (CH_2); HRMS calcd. for $C_9H_7NOBrF_3Na$ ($[M + Na]^+$, ^{79}Br) 303.9555, found 303.9556.

9.3.3 Dihydrophenanthrene and Spiro Products

1,2,3,4,4a,12b-Hexahydro-1,4-methano-5-(carbamoylmethyl)-12-methyltriphenylene 163a

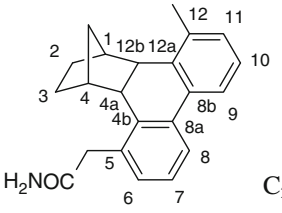

$C_{22}H_{23}NO$ M = 317.42 g/mol

Prepared using **GP1** and isolated as an oil. Yield: 75 %. Eluent: pentane/EtOAc = 6:4.

IR (neat): ν = 3,469, 3,326, 3,186, 2,952, 1,670 cm^{-1}; ^1H NMR (400 MHz, $CDCl_3$): δ = 7.86 (d, J = 7.8 Hz, 1 H, H8), 7.74 (d, J = 7.8 Hz, 1 H, H9), 7.23 − 7.09 (m, 4H, H7 + H10 + H6 + H11), 5.88 (br s, 1 H, N*H*H′), 5.39 (br s, 1 H, NH*H*′), 3.79 (A of AB, J_{AB} = 16.9 Hz, 1 H, C*H*H′(C5)), 3.57 (B of AB, J_{AB} = 16.9 Hz, 1 H, CH*H*′(C5)), 3.25 (s, 2 H, H4a + H12b), 2.34 (s, 3 H, CH_3(C12)), 2.19 (br s, 1 H, H4), 2.12 (br s, 1 H, H1), 1.74 – 1.69 (m, 4H, 2 H3 + 2 H2), 1.42 (A′ of A′B′, $J_{A'B'}$ = 10.4 Hz, 1 H, C*H*H′(C1)), 1.03 (B′ of

A′B′, $J_{A'B'}$ = 10.4 Hz, 1 H, CH*H*′(C1)); ^{13}C NMR ($CDCl_3$): δ = 173.7 (CO), 136.5 (C12), 136.4 (C4b), 135.9 (C12a), 133.5 (C5), 133.2 (C8a), 131.4 (C8b), 130.4, 130.3 (C6, C11), 126.7 (C7), 126.1 (C10), 122.5 (C8), 120.7 (C9), 48.2 (C1), 47.1 (C1), 44.2, 43.9 (C4a, C12b), 41.1 (CH_2(C5)), 33.0 (CH_2(C1)), 30.3, 30.1 (C2, C3), 19.8 (CH_3(C12)); HRMS calcd. for $C_{22}H_{23}NONa$ ([M + Na]$^+$) 340.1672, found 340.1672.

1,2,3,4,4a,12b-Hexahydro-1,4-methano-5-(carbamoylmethyl)-12-ethyltriphenylene (163b)

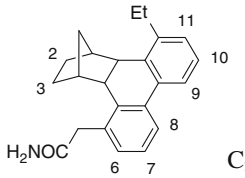

$C_{23}H_{25}NO$ M = 331.45 g/mol

Prepared using **GP1** and isolated as an oil. Yield: 57 %. Eluent: pentane/EtOAc = 6:4.

IR (neat): ν = 3,334, 3,189, 29,557, 2,871, 1,669, 1,452, 767 cm^{-1}; ^{1}H NMR (400 MHz, $CDCl_3$): δ = 7.86 (d, J = 7.6 Hz, 1 H, H8), 7.74 (d, J = 7.2 Hz, 1 H, H9), 7.29 − 7.10 (m, 4H, H7 + H10 + H11 + H6), 5.64 (br s, 1 H, N*H*H′), 5.35 (br s, 1 H, NH*H*′), 3.81 (A of AB, J_{AB} = 17.2 Hz, 1 H, C*H*H′(C5)), 3.58 (B of AB, J_{AB} = 16.8 Hz, 1 H, CH*H*′(C5)), 3.33 (d, J = 10.0 Hz, 1 H, H12b), 3.25 (d, J = 10.0 Hz, 1 H, H4a), 2.76 (dq, J = 14.9, 7.5 Hz, 1 H, C*H*H′(C12)), 2.64 (dq, J = 14.9, 7.5 Hz, CH*H*′(C12)), 2.15 (br s, 1 H, H4), 2.12 (br s, 1 H, H1), 1.77 − 1.62 (m, 4H, 2 H3 + 2 H2), 1.43 (A′ of A′B′, $J_{A'B'}$ = 10.4 Hz, 1 H, C*H*H′(C1)), 1.26 (t, J = 7.6 Hz, 3 H, C*H*$_3$–CH_2), 1.01 (B′ of A′B′, $J_{A'B'}$ = 10.4 Hz, 1 H, CH*H*′(C1)); ^{13}C NMR ($CDCl_3$): δ = 173.6 (CO), 142.6 (C12), 136.4 (C4b), 135.2 (C12a), 133.5 (C5), 133.4 (C8a), 131.4 (C8b), 130.4 (C6), 128.4 (C11), 126.8 (C7), 126.4 (C10), 122.6 (C8), 120.5 (C9), 48.5 (C1), 48.4 (C4), 43.9 (C12b), 43.6 (C4a), 41.1 (CH_2(C5)), 32.9 (CH_2(C1)), 30.3, 30.2 (C2, C3), 25.2 (CH_2(C12)), 15.0 (CH_3–CH_2); HRMS calcd. for $C_{23}H_{25}NONa$ ([M + Na]$^+$) 354.1828, found 354.1829.

1,2,3,4,4a,12b-Hexahydro-1,4-methano-5-(carbamoylmethyl)-12-methoxymethyltriphenylene (163c)

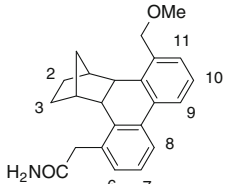

$C_{23}H_{25}NO_2$ M = 347.45 g/mol

Prepared using **GP1** and isolated as an oil. Yield: 60 %. Eluent: pentane/EtOAc = 3:7.

IR (neat): $v = 3{,}188$, 2,952, 2,924, 2,869, 1,669, 731 cm^{-1}; ^1H NMR (400 MHz, $CDCl_3$): $\delta = 7.84$ (d, $J = 7.1$ Hz, 1 H, H8), 7.82 (d, $J = 7.3$ Hz, 1 H, H9), 7.33 (d, $J = 7.3$ Hz, 1 H, H6), 7.24 − 7.20 (m, 2 H, H7, H10), 7.11 (d, $J = 6.7$ Hz, 1 H, H11), 5.75 (br s, 1 H, N*H*H′), 5.37 (br s, 1 H, NH*H*′), 4.61 (A of AB, $J_{AB} = 11.8$ Hz, 1 H, C*H*H′(C12)), 4.44 (B of AB, $J_{AB} = 11.8$ Hz, 1 H, CH*H*′(C12)), 3.78 (A′ of A′B′, $J_{A'B'} = 16.8$ Hz, 1 H, C*H*H′(C5)), 3.56 (B′ of A′B′, $J_{A'B'} = 16.8$ Hz, 1 H, CH*H*′(C5)), 3.44 (s, 3 H, OCH_3), 3.40 (d, $J = 9.7$ Hz, 1 H, H12b), 3.26 (d, $J = 9.7$ Hz, 1 H, H4a), 2.16 (br s, 1 H, H4), 2.12 (br s, 1 H, H1), 1.81 − 1.60 (m, 4H, 2 H3 + 2 H2), 1.43 (A″ of A″B″, $J_{A''B''} = 10.3$ Hz, 1 H, C*H*H′(C1)), 1.02 (A″ of A″B″, $J_{A''B''} = 10.3$ Hz, 1 H, CH*H*′(C1)); ^{13}C NMR ($CDCl_3$): $\delta = 173.5$ (CO), 136.4 (C5), 136.3 (C12a), 135.7 (C4b), 133.6 (C12), 133.1 (C8a), 131.7 (C8b), 130.5, 129.0 (C6, C11), 126.8 (C7), 126.4 (C10), 122.5 (C8), 122.4 (C9), 72.2 (CH_2(C12)), 58.6 (OCH_3), 48.4, 48.2 (C1, C4), 43.8 (C12b), 43.2 (C4a), 41.1 (CH_2(C5)), 33.0 (CH_2(C1)), 30.3, 30.2 (C2, C3); HRMS calcd. for $C_{23}H_{25}NO_2Na$ ([M + Na]$^+$) 370.1778, found 370.1773.

1,2,3,4,4a,12b-Hexahydro-1,4-methano-5-(carbamoylmethyl)-11,12-dimethyltriphenylene (163d)

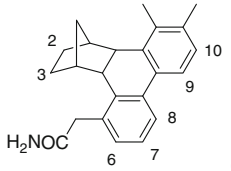

$C_{23}H_{25}NO$ M = 331.45 g/mol

Prepared using **GP1** and isolated as an oil. Yield: 60 %. Eluent: pentane/EtOAc = 6:4.

IR (neat): $v = 3{,}184$, 2,948, 1,665, 1,456, 1,385, 908, 731 cm^{-1}; ^1H NMR (400 MHz, $CDCl_3$): $\delta = 7.84$ (d, $J = 7.5$ Hz, 1 H, H8), 7.66 (d, $J = 8.1$ Hz, 1 H, H9), 7.21 (t, $J = 7.5$ Hz, 1 H, H7), 7.09 (d, $J = 7.2$ Hz, 1 H, H6), 7.05 (d, $J = 8.2$ Hz, 1 H, H10), 5.53 (br s, 1 H, N*H*H′), 5.34 (br s, 1 H, NH*H*′), 3.81 (A of AB, $J_{AB} = 17.0$ Hz, 1 H, C*H*H′(C5)), 3.58 (B of AB, $J_{AB} = 17.0$ Hz, 1 H, CH*H*′(C5)), 3.35 (d, $J = 9.7$ Hz, 1 H, H4a), 3.22 (d, $J = 9.7$ Hz, 1 H, H12b), 2.29 (s, 3 H, CH_3(C12)), 2.23 (s, 3 H, CH_3(C11)), 2.16 (br s, 1 H, H4), 2.13 (br s, 1 H, H1), 1.74–1.69 (m, 4H, 2 H3 + 2 H2), 1.40 (A′ of A′B′, $J_{A'B'} = 10.1$ Hz, 1 H, C*H*H′(C1)), 1.03 (B′ of A′B′, $J_{A'B'} = 10.1$ Hz, 1 H, CH*H*′(C1)); ^{13}C NMR ($CDCl_3$): $\delta = 173.7$ (CO), 137.3 (C11), 136.0 (C12a), 135.7 (C4b), 135.0 (C12), 133.5 (C5), 133.4 (C8a), 130.0 (C6), 129.3 (C8b), 128.0, 126.8 (C7, C10), 122.3 (C8), 120.1 (C9), 48.5 (C1), 47.3 (C4), 44.7, 44.0 (C4a, C12b), 41.1 (CH_2(C5)), 33.0 (CH_2(C1)), 30.5, 30.0 (C2, C3), 20.7 (CH_3(C11)), 15.9 (CH_3(C12)); HRMS calcd. for $C_{23}H_{25}NONa$ ([M + Na]$^+$) 354.1828, found 354.1826.

1,2,3,4,4a,12b-Hexahydro-1,4-methano-5-(carbamoylmethyl)-10,12-dimethyltriphenylene (163e)

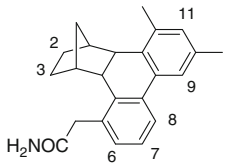

$C_{23}H_{25}NO$ M = 331.45 g/mol

Prepared using **GP1** and isolated as an oil. Yield: 82 %. Eluent: pentane/EtOAc = 6:4.

IR (neat): ν = 3,187, 2,950, 2,867, 1,666, 1,450, 1,386, 731 cm^{-1}; ^1H NMR (400 MHz, $CDCl_3$): δ = 7.87 (d, J = 7.6 Hz, 1 H, H8), 7.56 (s, 1 H, H9), 7.20 (t, J = 7.6 Hz, 1 H, H7), 7.10 (d, J = 7.6 Hz, 1 H, H6), 6.95 (s, 1 H, H11), 5.76 (br s, 1 H, N*H*H′), 5.37 (br s, 1 H, NH*H*′), 3.80 (A of AB, J_{AB} = 17.0 Hz, 1 H, C*H*H′(C5)), 3.56 (B of AB, J_{AB} = 17.0 Hz, 1 H, CH*H*′(C5)), 3.23 (s, 2 H, H4a + H12b), 2.33 (s, 3 H, CH_3(C12)), 2.31 (s, 3 H, CH_3(C10)), 2.17 (br s, 1 H, H4), 2.11 (br s, 1 H, H1), 1.75 − 1.62 (m, 4H, 2 H3 + 2 H2), 1.42 (A′ of A′B′, $J_{A'B'}$ = 10.6 Hz, 1 H, C*H*H′(C1)), 1.02 (B′ of A′B′, $J_{A'B'}$ = 10.6 Hz, 1 H, CH*H*′(C1)); ^{13}C NMR ($CDCl_3$): δ = 173.7 (CO), 136.6 (C4b), 136.4 (C12), 135.3 (C10), 133.5 (C5), 133.4 (C8a), 133.0 (C12a), 131.4 (C11), 131.3 (C8b), 130.3 (C6), 126.7 (C7), 122.4 (C8), 121.3 (C9), 48.3 (C1), 47.1 (C4), 44.0, 43.9 (C4a, C12b), 41.1 (CH_2(C5)), 33.0 (CH_2(C1)), 30.3, 30.1 (C2, C3), 21.2 (CH_3(C12)), 19.7 (CH_3(C10)); HRMS calcd. for $C_{23}H_{25}NONa$ ($[M + Na]^+$) 354.1828, found 354.1826.

1,2,3,4,4a,12b-Hexahydro-1,4-methano-5-(carbamoylmethyl)-10-methoxy-12-methyltriphenylene (163f)

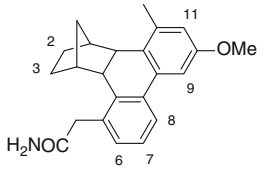

$C_{23}H_{25}NO_2$ M = 347.45 g/mol

Prepared using **GP1** and isolated as an oil. Yield: 65 %. Eluent: pentane/EtOAc = 5:5.

IR (neat): ν = 3,343, 2,950, 1,669, 1,601, 1,456, 1,320, 1,062 cm^{-1}; ^1H NMR (400 MHz, $CDCl_3$): δ = 7.80 (d, J = 8.0 Hz, 1 H, H8), 7.27 (s, 1 H, H9), 7.21 (t, J = 7.7 Hz, 1 H, H7), 7.15 − 7.06 (m, 1 H, H6), 6.71 (s, 1 H, H11), 5.77 (br s, 1 H, N*H*H′), 5.38 (br s, 1 H, NH*H*′), 3.83 (s, 3 H, OCH_3), 3.80 (A of AB, J_{AB} = 17.4 Hz, 1 H, C*H*H′(C5)), 3.57 (B of AB, J_{AB} = 16.9 Hz, 1 H, CH*H*′(C5)), 3.23 − 3.17 (m, 2 H, H4a, H12b), 2.32 (s, 3 H, CH_3(C12)), 2.16 (br s, 1 H, H4),

2.07 (br s, 1 H, H1), 1.79 − 1.55 (m, 4H, 2 H3 + 2 H2), 1.39 (A′ of A′B′, $J_{A'B'}$ = 10.2 Hz, 1 H, C*H*H′(C1)), 1.01 (B′ of A′B′, $J_{A'B'}$ = 10.1 Hz, 1 H, CH*H*′(C1)); ^{13}C NMR ($CDCl_3$): δ = 173.7 (CO), 157.8 (C10), 138.0 (C12), 136.9 (C4b), 133.5 (C5), 133.1 (C8a), 132.5 (C8b), 130.5 (C6), 128.4 (C12a), 126.7 (C7), 122.5 (C8), 116.2 (C11), 106.0 (C9), 55.2 (OCH_3), 48.2 (C1), 47.0 (C4), 43.8, 43.7 (C4a, C12b), 41.1 (CH_2(C5)), 32.9 (CH_2(C1)), 30.4, 30.0 (C2, C3), 20.1 (CH_3(C12)); HRMS calcd. for $C_{23}H_{25}NO_2Na$ ([M + Na]$^+$) 370.1777, found 370.1778.

1,2,3,4,4a,12b-Hexahydro-1,4-methano-5-(carbamoylmethyl)-10,11-dimethoxy-12-methyltriphenylene (163g)

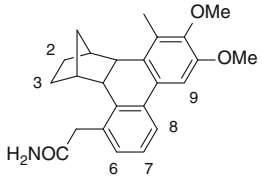

$C_{24}H_{27}NO_3$ M = 377.48 g/mol

Prepared using **GP1** and isolated as an white solid. Yield: 60 %. Eluent: pentane/EtOAc = 5:5. Colorless crystals were obtained by slow evaporation of EtOH.

Mp: 228–229 °C; IR (neat): ν = 3,343, 2,948, 1,670, 1,460, 1,088 cm^{-1}; ^{1}H NMR (400 MHz, $CDCl_3$): δ = 7.75 (d, J = 7.6 Hz, 1 H, H8), 7.27 (s, 1 H, H9), 7.20 (t, J = 7.6 Hz, 1 H, H7), 7.08 (d, J = 7.6 Hz, 1 H, H6), 5.49 (br s, 1 H, N*H*H′), 5.33 (br s, 1 H, NH*H*′), 3.92 (s, 3 H, OCH_3(C10)), 3.80 (s, 3 H, OCH_3(C11)), 3.77 (A of AB, J_{AB} = 17.2 Hz, 1 H, C*H*H′(C5)), 3.55 (B of AB, J_{AB} = 17.2 Hz, 1 H, CH*H*′(C5)), 3.22 (s, 2 H, H4a + H12b), 2.24 (s, 3 H, CH_3(C12)), 2.14 (br s, 1 H, H4), 2.11 (br s, 1 H, H1), 1.75-1.58 (m, 4H, 2 H3 + 2 H2), 1.40 (A′ of A′B′, $J_{A'B'}$ = 10.0 Hz, 1 H, C*H*H(C1)), 1.01 (B′ of A′B′, $J_{A'B'}$ = 10.0 Hz, 1 H, C*H*H(C1)); ^{13}C NMR ($CDCl_3$): δ = 173.5 (CO), 151.0 (C10), 148.1 (C11), 136.4 (C4b), 133.6 (C5), 133.3 (C8a), 130.4 (C12), 133.1 (C6), 129.6 (C12b), 127.2 (C8b), 126.7 (C7), 122.1 (C8), 104.7 (C9), 60.2 (OCH_3(C11)), 55.7 (OCH_3(C10)), 48.4 (C1), 47.1 (C4), 44.3, 43.9 (C4a, C12b), 41.1 (CH_2(C5)), 33.0 (CH_2(C1)), 30.4, 30.0 (C2, C3), 12.4 (CH_3(C12)); HRMS calcd. for $C_{24}H_{27}NO_3Na$ ([M + Na]$^+$) 400.1883, found 400.1886.

CCDC 827669 contains the supplementary crystallographic data for dihydrophenanthrene **163g**. These data can be obtained free of charge from The Cambridge Crystallographic Data Centre via www.ccdc.cam.ac.uk/data_request/cif.

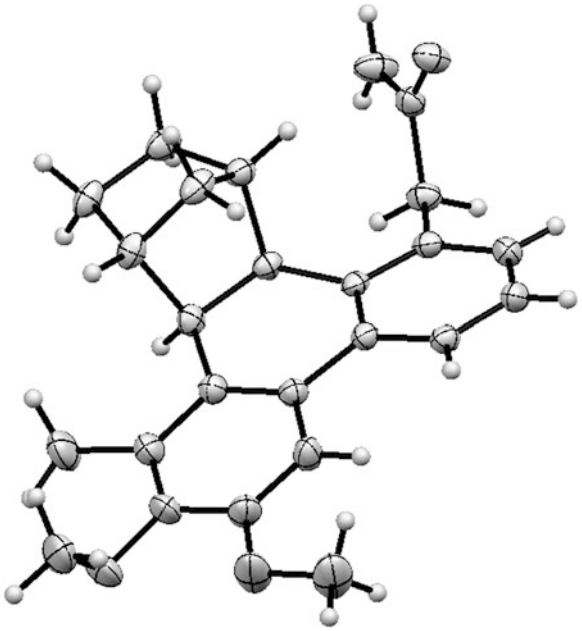

1,2,3,4,4a,14c-Hexahydro-1,4-methano-5-(carbamoylmethyl)-benzo[g]chrysene (163h)

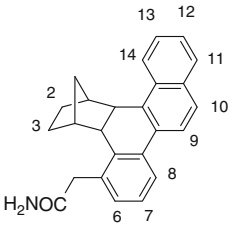

$C_{25}H_{23}NO$ M = 353.46 g/mol

Prepared using **GP1** and isolated as an oil. Yield: 61 %. Eluent: pentane/EtOAc = 5:5.

IR (neat): ν = 3,325, 2,927, 2,865, 1,639, 1,452, 1,394, 1,118, 773 cm^{-1}; ^1H NMR (400 MHz, DMSO-d_6): δ = 8.13 (d, J = 9.0 Hz, 1 H, H9), 8.01 (d, J = 9.0 Hz, 1 H, H14), 7.95 (dd, J = 7.0, 1.2 Hz, 1 H, H8), 7.85 (d, J = 8.0 Hz, 1 H, H11), 7.77 (d, J = 8.2 Hz, 1 H, H10), 7.57 (t, J = 7.0 Hz, 1 H, H13), 7.51 (br s, 1 H, N*H*H′), 7.47 (t, J = 8.0 Hz, 1 H, H12), 7.23 − 7.17 (m, 2 H, H7, H6), 6.98 (br s, 1 H, NH*H*′), 3.87 (d, J = 10.1 Hz, 1 H, H4a), 3.59 (A of AB, J_{AB} = 16.0 Hz, 1 H, CH*H*′(C5)), 3.50 (B of AB, J_{AB} = 16.0 Hz, 1 H, CH*H*′(C5)), 3.49 (d, J = 10.1 Hz, 1 H, H12b), 2.27 (br s, 1 H, H4), 2.18 (br s, 1 H, H1), 1.92 − 1.62 (m, 4H, 2 H3 + 2 H2), 1.27 (A′ of A′B′, $J_{A'B'}$ = 10.0 Hz, 1 H, C*H*H(C1)), 0.96 (B′ of A′B′, $J_{A'B'}$ = 10.0 Hz, 1 H, C*H*H(C1)); ^{13}C NMR (DMSO-d_6): δ = 172.3 (CO), 135.7 (C4b), 135.2 (C8a), 133.0 (C10a), 131.59

(C5), 131.58 (C14a), 131.4 (C7), 130.6 (C6), 128.9 (C8b), 128.3 (C11), 126.9 (C10), 126.3 (C13), 126.1 (C8), 125.4 (C12), 124.4 (C14), 121.7 (C8), 121.2 (C9), 48.4 (C1), 47.3 (C4), 42.9 (C4a, C12b), 39.2 (CH_2(C5)), 33.0 (CH_2(C1)), 29.8, 29.4 (C2, C3); HRMS calcd. for $C_{25}H_{23}NO$ ($[M + H]^+$) 354.1852, found 354.1830.

12b,13,14,15,16,16a-Hexahydro-13,16-methano-12-(carbamoylmethyl)-dibenzo[g,p]chrysene (163i)

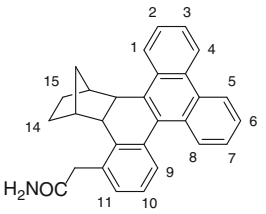

$C_{29}H_{25}NO$ M = 403.51 g/mol

Prepared using **GP1** and isolated as a white solid. Yield: 81 %. Eluent: Pentane/DCM/EtOAc = 2:3:5.

Mp: 238–239 °C; IR (neat): ν = 2,922, 2,855, 1,667, 1,456, 1,261, 732 cm^{-1}; ^{1}H NMR (400 MHz, $CDCl_3$): δ = 8.67 − 8.59 (m, 2 H, H5, H3), 8.52 (dd, J = 8.0, 1.2 Hz, 1 H, H8), 8.10 − 8.04 (m, 1 H, H2), 7.83 (dd, J = 8.0, 1.2 Hz, 1 H, H9), 7.64 − 7.57 (m, 3 H, H1, H4, H6), 7.54 (ddd, J = 8.0, 7.8, 1.2 Hz, 1 H, H7), 7.20 (t, J = 7.8 Hz, 1 H, H10), 7.17 (dd, J = 7.8, 1.2 Hz, 1 H, H11), 5.80 (br s, 1 H, N*H*H′), 5.46 (br s, 1 H, NH*H*′), 4.00 (d, J = 10.0 Hz, 1 H, H12b), 3.82 (A of AB, J_{AB} = 16.8 Hz, 1 H, C*H*H′(C5)), 3.65 (B of AB, J_{AB} = 16.8 Hz, 1 H, CH*H*′(C5)), 3.28 (d, J = 10.0 Hz, 1 H, H16a), 2.49 (br s, 1 H, H16), 2.26 (br s, 1 H, H13), 1.85 − 1.69 (m, 4H, 2 H14 + 2 H15), 1.49 (A′ of A′B′, $J_{A'B'}$ = 10.4 Hz, 1 H, C*H*H′(C13)), 1.03 (B′ of A′B′, $J_{A'B'}$ = 10.4 Hz, 1 H, CH*H*′(C13)); ^{13}C NMR ($CDCl_3$): δ = 173.6 (CO), 137.1 (C12a), 133.9 (C8c), 133.8 (C12), 133.1 (C16b), 130.9 (C4b), 130.7 (C8b), 130.6 (C16c), 129.7 (C11), 129.6 (C4a), 129.2 (C9), 128.8 (C8a), 127.0 (C8), 126.8, 126.3 (C1, C4), 126.2 (C10), 125.7 (C7), 125.6 (C6), 124.4 (C2), 123.3 (C5), 122.8 (C3), 47.9 (C16), 46.1 (C13), 45.4 (C12b), 44.4 (C16a), 41.0 (CH_2(C12)), 34.7 (CH_2(C13)), 31.8, 29.0 (C15, C14); HRMS calcd. for $C_{29}H_{25}NONa$ ($[M + Na]^+$) 426.1828, found 426.1828.

1,2,3,4,4a,12b-Hexahydro-1,4-methano-5-(carbamoylmethyl)-12-chlorotriphenylene (163j)

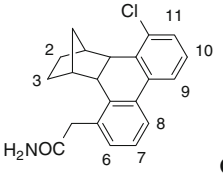

$C_{21\ H20}ClNO$ M = 337.84 g/mol

Prepared using **GP1** and isolated as an oil. Yield: 47 %. Eluent: pentane/EtOAc = 6:4.

IR (neat): ν = 3,331, 2,952, 2,871, 1,668, 1,448, 1,412, 768 cm^{-1}; ^1H NMR (400 MHz, $CDCl_3$): δ = 7.81 (d, J = 8.0 Hz, 1 H, H8), 7.77 (d, J = 7.8 Hz, 1 H, H9), 7.29 − 7.13 (m, 4H, H11 + H7 + H6 + H10), 5.98 (br s, 1 H, N*H*H′), 5.41 (br s, 1 H, NH*H*′), 3.78 (A of AB, J_{AB} = 16.8 Hz, 1 H, C*H*H′(C5)), 3.57 (B of AB, J_{AB} = 16.8 Hz, 1 H, CH*H*′(C5)), 3.41 (d, J = 10.0 Hz, 1 H, H12b), 3.24 (d, J = 10.0 Hz, 1 H, H4a), 2.45 (br s, 1 H, H4), 2.12 (br s, 1 H, H1), 1.77 − 1.62 (m, 4H, 2 H3 + 2 H2), 1.34 (A′ of A′B′, $J_{A'B'}$ = 10.4 Hz, 1 H, C*H*H′(C1)), 1.04 (B′ of A′B′, $J_{A'B'}$ = 10.4 Hz, 1 H, CH*H*′(C1)); ^{13}C NMR ($CDCl_3$): δ = 173.5 (CO), 136.6 (C4b), 135.14 (12a), 135.11 (12), 133.9 (8b), 133.8 (C8a), 132.0 (C5), 131.1 (C6), 129.2 (C9), 127.1 (C7), 126.9 (C10), 122.5 (C8), 121.3 (C11), 48.5 (C1), 46.9 (C4), 44.5 (C12b), 43.5 (C4a), 40.9 (CH_2(C5)), 33.0 (CH_2(C1)), 30.3, 29.9 (C2, C3); HRMS calcd. for C_{21} H_{20}ClNONa ([M + Na]$^+$) 360.1126, found 360.1127.

1,2,3,4,4a,12b-Hexahydro-1,4-methano-5-(carbamoylmethyl)-12-trifluoromethyltriphenylene (163k)

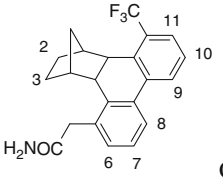

$C_{22}H_{20}F_3NO$ M = 371.40 g/mol

Prepared using **GP1** and isolated as an oil. Yield: 71 %. Eluent: pentane/EtOAc = 6:4.

IR (neat): ν = 3,190, 2,956, 2,873, 1,667, 1,388, 1,314, 1,114, 775 cm^{-1}; ^1H NMR (400 MHz, $CDCl_3$): δ = 8.05 (d, J = 8.0 Hz, 1 H, H11), 7.82 (d, J = 8.4 Hz, 1 H, H8), 7.57 (d, J = 7.8 Hz, 1 H, H9), 7.31 (t, J = 8.0 Hz, 1 H, H10), 7.24 (t, J = 8.0 Hz, 1 H, H7), 7.17 (d, J = 8.0 Hz, 1 H, H6), 5.91 (br s, 1 H, N*H*H′), 5.42 (br s, 1 H, NH*H*′), 3.80 (A of AB, J_{AB} = 16.4 Hz, 1 H, C*H*H′(C5)), 3.59 (B of AB, J_{AB} = 16.4 Hz, 1 H, CH*H*′(C5)), 3.58 (d, J = 9.6 Hz, 1 H, H12b), 3.32 (d, J = 9.6 Hz, 1 H, H4a), 2.21 (br s, 1 H, H1), 2.11 (br s, 1 H, H4), 1.75 − 1.62 (m, 4H, 2 H3 + 2 H2), 1.41 (A′ of A′B′, $J_{A'B'}$ = 10.4 Hz, 1 H, C*H*H′(C1)), 0.99 (B′ of A′B′, $J_{A'B'}$ = 10.4 Hz, 1 H, CH*H*′(C1)); ^{13}C NMR ($CDCl_3$): δ = 173.3 (CO), 136.6 (q, $^3J_{C-F}$= 1.3 Hz, C12a), 136.4 (C8a), 133.6 (C8b), 133.4 (C4b), 132.4 (C5), 131.2 (C6), 128.9 (q, $^2J_{C-F}$ = 29 Hz, C12), 126.9 (C9), 126.6 (q, $^3J_{C-F}$ = 6 Hz, C11), 126.4 (C7), 126.2 (C10), 124.7 (q, $^1J_{C-F}$ = 273 Hz, CF_3), 122.6 (C8), 50.6 (q, $^5J_{C-F}$ = 2.2 Hz, C1), 47.9 (C4), 44.2 (C4a), 43.0 (q, $^4J_{C-F}$ = 1.6 Hz, C12b), 40.7 (CH_2(C5)), 32.4 (CH_2(C1)), 30.5, 29.7 (C2, C3); ^{19}F NMR ($CDCl_3$): δ = −58.40. HRMS calcd. for $C_{22}H_{20}NF_3ONa$ ([M + Na]$^+$) 394.1389, found 394.1394.

1,2,3,4,4a,12b-Hexahydro-1,4-methano-5-(carbamoylmethyl)-7-trifluoromethyl-12-methyltriphenylene (163l)

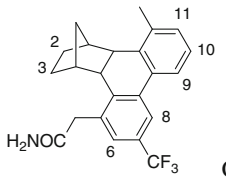

$C_{23}H_{22}F_3NO$ M = 385.16 g/mol

Prepared using **GP1** and isolated as an oil. Yield: 45 %. Eluent: pentane/EtOAc = 5:5.

IR (neat): ν = 3,187, 2,951, 1,667, 1,347, 1,272, 119, 905, 730 cm^{-1}; ^1H NMR (400 MHz, $CDCl_3$): δ = 8.08 (s, 1 H, H8), 7.74 (dd, J = 7.4, 1.8 Hz, 1 H, H9), 7.35 (s, 1 H, H6), 7.22 − 7.09 (m, 2 H, H10 + H11), 5.59 (br s, 1 H, N*H*H′), 5.33 (br s, 1 H, NH*H*′), 3.85 (A of AB, J_{AB} = 16.7 Hz, 1 H, C*H*H′(C5)), 3.63 (B of AB, J_{AB} = 16.7 Hz, 1 H, CH*H*′(C5)), 3.30 (s, 2 H, H4a + H12b), 2.34 (s, 3 H, CH_3(C12)), 2.21 (br s, 1 H, H4), 2.13 (br s, 1 H, H1), 1.76–1.59 (m, 4H, 2 H3 + 2 H2), 1.43 − 1.36 (m, 1 H, C*H*H′(C1)), 1.11 − 1.02 (m, 1 H, CH*H*′(C1)); ^{13}C NMR ($CDCl_3$): δ = 172.4 (CO), 140.4 (C5), 136.8 (C4a), 136.0 (C12), 134.5 (C8a), 134.3 (C12a), 131.3 (C11), 130.3 (C8b), 129.0 (q, $^2J_{C-F}$ = 34 Hz, C7), 126.4 (C 10), 126.4 (q, $^3J_{C-F}$ = 4 Hz, C6), 124.6 (q, $^1J_{C-F}$ = 272 Hz, CF_3), 120.9 (C9), 119.3 (q, $^3J_{C-F}$ = 4 Hz, C8), 48.4 (C1), 47.0 (C4), 44.3, 44.0 (C4a, C12b), 40.9 (CH_2(C5)), 33.1 (CH_2(C1)), 30.5, 30.1 (C2, C3), 19.8 (CH_3(C12)); ^{19}F NMR ($CDCl_3$): δ = −62.56. HRMS calcd. for $C_{23}H_{22}F_3NONa$ ($[M + H]^+$) 408.1546, found 408.1546.

1,2,3,4,4a,12b-Hexahydro-1,4-methano-5-(carbamoylmethyl)-7-trifluoromethyl-10,12-dimethyltriphenylene (163m)

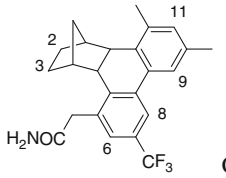

$C_{24}H_{24}F_3NO$ M = 399.49 g/mol

Prepared using **GP1** and isolated as an oil. Yield: 52 %. Eluent: pentane/DCM/EtOAc = 2:3:5.

IR (neat): ν = 3,337, 2,952, 1,668, 1,349, 1,288, 1,157, 1,120 cm^{-1}; ^1H NMR (400 MHz, $CDCl_3$): δ = 8.07 (s, 1 H, H8), 7.53 (s, 1 H, H9), 7.34 (s, 1 H, H6), 6.99 (s, 1 H, H11), 5.78 (br s, 1 H, N*H*H′), 5.36 (br s, 1 H, NH*H*′), 3.84 (A of AB, J_{AB} = 16.8 Hz, 1 H, C*H*H′(C5)), 3.62 (B of AB, J_{AB} = 16.8 Hz, 1 H, CH*H*′(C5)), 3.26 (s, 2 H, H4a + H12b), 2.35 (s, 3 H, CH_3(C12)), 2.31 (s, 3 H, CH_3(C10)), 2.19 (br s, 1 H, H4), 2.11 (br s, 1 H, H1), 1.76 − 1.56 (m, 4H, 2 H3 + 2 H2), 1.37 (A′ of A′B′, $J_{A'B'}$ = 10.4 Hz, 1 H, C*H*H′(C1)), 1.04 (B′ of A′B′, $J_{A'B'}$ = 10.4 Hz, 1 H,

CH*H′*(C1)); ^{13}C NMR ($CDCl_3$): δ = 172.6 (CO), 140.6 (C5), 136.6 (C4a), 135.7 (C12), 134.41 (C8a), 134.31 (C12a), 133.0 (C10), 132.3 (C11), 130.1 (C8b), 128.9 (q, $^2J_{C-F}$ = 32 Hz, C7), 126.2 (q, $^3J_{C-F}$ = 4 Hz, C6), 124.2 (q, $^1J_{C-F}$ = 271 Hz, CF_3), 121.4 (C9), 119.2 (q, $^3J_{C-F}$ = 4 Hz, C8), 48.3 (C1), 46.9 (C4), 44.0, 43.9 (C4a, C12b), 40.9 (CH_2(C5)), 33.0 (CH_2(C1)), 30.4, 30.0 (C2, C3), 21.1 (CH_3(C12)), 19.7 (CH_3(C10)); ^{19}F NMR ($CDCl_3$): δ = −62.63. HRMS calcd. for $C_{24}H_{24}F_3NONa$ ([M + Na]$^+$) 422.1702, found 422.1701.

2-(Benzo[g]chrysen-11-yl)acetamide (168)

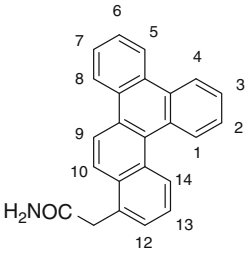

$C_{24}H_{17}NO$ MW = 335.39 g/mol

Prepared using **GP1** using 2 equiv. of norbornadiene instead of norbornene and isolated as a white solid.Yield: 55 %. Eluent: CH_2Cl_2/EtOAc = 1:1.

Mp: 202–204 °C; IR (neat): ν = 3,390, 1,655, 1,387, 998 cm^{-1}; ^{1}H NMR (400 MHz, DMSO-d_6): δ = 9.08 − 8.75 (m, 6H, H4, H5, H8, H10, H1, H14), 8.32 (d, 1 H, J = 8.8 Hz, 1 H, H9), 7.81 − 7.69 (m, 4H, H6, H3, H7, H2), 7.67 (br s, 1 H, N*H*H′), 7.61 − 7.55 (m, 2 H, H13, H12), 7.12 (br s, 1 H, NH*H′*), 4.04 (s, 2 H, CH_2); ^{13}C NMR (DMSO-d_6): δ = 172.2 (CO), 133.3 (C10a), 132.1 (C14a), 130.4 (C4b), 129.7 (C11), 129.3 (C8b), 129.1 (C8a), 129.0 (C14c), 128.6 (C1), 128.2 (C12), 127.8 (C6), 127.6 (C14), 127.2 (C3), 127.0 (C14b), 126.9 (C4a), 126.6 (C7), 126.5 (C2), 125.7 (C13), 124.2 (C9), 124.0 (C4), 123.8 (C8), 123.3 (C5), 120.9 (C10), 54.9 (CH_2); HRMS calcd. for $C_{24}H_{17}NONa$ ([M + Na]$^+$) 358.1202, found 358.1191.

6-(Carbamoyl)methylene-5′-methyl-1′,2′,3′,4′,4a′,9a′-hexahydro-1′, 4′-methanospirocyclohexa[2, 4]diene-1,9′-fluorene (169a)

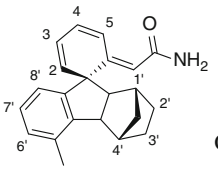

$C_{22}H_{23}NO$ M = 317.42 g/mol

Prepared using **GP2** and isolated as an oil. Yield: 65 %. Eluent: pentane/ EtOAc = 6:4.

IR (neat): ν = 2,910, 2,850, 1,653, 1,460, 745 cm^{-1}; ^{1}H NMR (400 MHz, CD_2Cl_2): δ = 7.64 (d, J = 10.8 Hz, 1 H, H2), 7.15 − 7.05 (m, 2 H, H6′ + H7′),

6.71 (d, $J = 7.6$ Hz, 1 H, H8′), 6.32 − 6.18 (m, 2 H, H3 + H4), 6.14 (d, $J = 9.6$ Hz, 1 H, H5), 5.27 (br s, 2 H, NH_2), 4.91 (s, 1 H, C*H*(C6)), 3.43 (d, $J = 7.5$ Hz, 1 H, H9a′), 2.57 (d, $J = 3.4$ Hz, 1 H, H4′), 2.44 (br s, 4H, CH_3 + H1′), 2.40 (d, $J = 7.4$ Hz, 1 H, H4a′), 1.70 − 1.50 (m, 2 H, H2′ + H3′), 1.48 − 1.38 (m, 1 H, H2′), 1.29 − 1.18 (m, 1 H, H3′), 1.05 (br s, 2 H, CH_2(C1′)); ^{13}C NMR (CD_2Cl_2): $\delta = 168.5$ (CO), 162.4 (C6), 150.8 (C4b′), 144.2 (C8a′), 136.9 (C5), 134.4 (C5′), 129.4, 128.1, 128.0 (C3 + C6′ + C7′), 122.8 (C8′), 121.6 (C4), 121.4 (C2), 118.0 (CH(C6)), 64.5 (C4a′), 59.0 (C1), 55.1 (C9a′), 40.1 (C4′), 38.9 (C1′), 34.3 (CH_2(C1′)), 29.8, 29.0 (C2′ + C3′), 19.4 (CH_3(C5′)); HRMS calcd. for $C_{22\ H24}NO$ ([M + H]$^+$) 318.1852, found 318.1854.

6-(Carbamoyl)methylene-5′-ethyl-1′,2′,3′,4′,4a′,9a′-hexahydro-1′, 4′-methanospirocyclohexa[2,4]diene-1,9′-fluorene (169b)

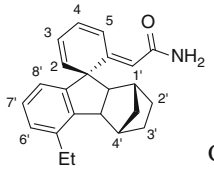

$C_{23}H_{25}NO$ M = 331.45 g/mol

Prepared using **GP2** and isolated as a pale yellow solid. Pale yellow crystals were obtained by slow evaporation of EtOH. Yield: 40 %. Eluent: pentane/ EtOAc = 65:35.

Mp: 220–222 °C; IR (neat): $\nu = 3{,}172$, 2,955, 2,871, 1,654, 1,570, 1,448, 1,400, 1,351, 733 cm^{-1}; ^{1}H NMR (400 MHz, CD_2Cl_2): $\delta = 7.59$ (dd, $J = 9.7$, 1.0 Hz, 1 H, H2), 7.16 − 7.08 (m, 2 H, H6′ + H7′), 6.68 (dd, $J = 6.5$, 2.1 Hz, 1 H, H8′), 6.29 − 6.14 (m, 2 H, H3 + H4), 6.11 (d, $J = 9.6$ Hz, 1 H, H5), 5.14 (br s, 2 H, NH_2), 4.85 (s, 1 H, C*H*(C6)), 3.42 (d, $J = 7.5$ Hz, 1 H, H9a′), 2.75 (q, $J = 7.5$ Hz, 2 H, CH_2(C5′)), 2.49 (br s, 1 H, H4′), 2.39 (br s, 1 H, H1′), 2.35 (d, $J = 7.5$ Hz, 1 H, H4a′), 1.57 − 1.45 (m, 2 H, H2′ + H3′), 1.41 − 1.23 (m, 4H, H2′ + CH_3), 1.19 − 1.11 (m, 1 H, H3′), 1.00 (br s, 2 H, CH_2(C1′)); ^{13}C NMR (CD_2Cl_2): $\delta = 168.4$ (CO), 162.5 (C6), 150.8 (C4b′), 143.6 (C8a′), 140.6 (C5′), 137.0 (C5), 128.2, 128.1, 127.4 (C4 + C6′ + C7′), 122.8 (C8′), 121.6, 121.5 (C2, C3), 118.0 (CH(C6)), 64.4 (C4a′), 59.0 (C1), 54.9 (C9a′), 40.0 (C4′), 39.0 (C1′), 34.3 (CH_2(C1′)), 29.8, 29.1 (C2′ + C3′), 25.8 (CH_2(C5′)), 15.2 (CH_3(CH_2)); HRMS calcd. for $C_{23}H_{26}NO$ ([M + H]$^+$) 332.2009, found 332.2010.

CCDC 826530 contains the supplementary crystallographic data for *spiro* product **169b.** These data can be obtained free of charge from The Cambridge Crystallographic Data Centre via www.ccdc.cam.ac.uk/data_request/cif.

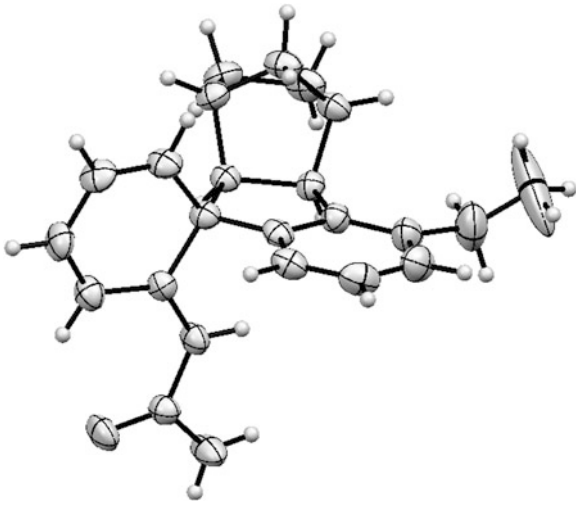

6-(Carbamoyl)methylene-5′,6′-dimethyl-1′,2′,3′,4′,4a′,9a′-hexahydro-1′, 4′-methanospirocyclohexa[2,4]diene-1,9′-fluorene (169d)

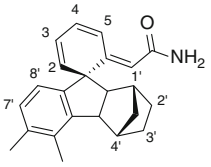

$C_{23}H_{25}NO$ M = 331.45 g/mol

Prepared using **GP2** and isolated as a pale yellow solid. Yield: 45 %. Eluent: pentane/EtOAc = 65:35.

Mp: 182–184 °C; IR (neat): ν = 3,332, 3,176, 2,952, 2,870, 1,660, 1,451, 1,398, 1,350, 735 cm^{-1}; ^1H NMR (400 MHz, CD_2Cl_2): δ = 7.60 (d, J = 10.0 Hz, 1 H, H2), 6.97 (d, J = 7.6 Hz, 1 H, H7′), 6.57 (d, J = 7.6 Hz, 1 H, H8′), 6.29 − 6.16 (m, 2 H, H3 + H4), 6.11 (d, J = 9.7 Hz, 1 H, H5), 5.23 (br s, 2 H, NH_2), 4.91 (s, 1 H, C*H*(C6)), 3.40 (d, J = 7.8 Hz, 1 H, H9a′), 2.49 (d, J = 3.6 Hz, 1 H, H1′), 2.39 (d, J = 3.6 Hz, 1 H, H4′), 2.36 (d, J = 7.8 Hz, 1 H, H4a′), 2.29 (s, 3 H, CH_3(C5′)), 2.26 (s, 3 H, CH_3(C6′)), 1.65 − 1.47 (m, 2 H, H2′ + H3′), 1.42 − 1.32 (m, 1 H, H2′), 1.19 − 1.11 (m, 1 H, H3′), 0.99 (s, 2 H, CH_2(C1′)); ^{13}C NMR (CD_2Cl_2): δ = 168.5 (CO), 162.7 (C6), 148.4 (C8a′), 144.4 (C4b′), 137.2 (C5), 136.5 (C6′), 132.7 (C5′), 129.7 (C7′), 128.1 (C3), 122.2 (C8′), 121.5 (C4), 121.3 (C2), 117.8 (CH(C6)), 64.7 (C4a′), 58.8 (C1), 55.2 (C9a′), 40.7 (C1′), 39.0 (C4′), 34.2 (CH_2(C1′)), 29.8, 29.0 (C2′ + C3′), 19.8 (CH_3(C5′)), 16.6 (CH_3(C6′)); HRMS calcd. for $C_{23}H_{26}NO$ ($[M + H]^+$) 332.2009, found 332.0010.

6-(Carbamoyl)methylene-5′,7′-dimethyl-1′,2′,3′,4′,4a′,9a′-hexahydro-1′, 4′-methanospirocyclohexa[2,4]diene-1,9′-fluorene (169e)

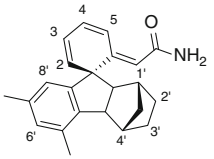

$C_{23}H_{25}NO$ M = 331.45 g/mol

Prepared using **GP2** and isolated as a yellow solid. Yield: 39 %. Eluent: Pentane/EtOAc = 65:35.

Mp: 206–208 °C; IR (neat): ν = 3,327, 3,181, 3,041, 2,957, 2,869, 1,653, 1,609, 1,574 cm^{-1}; ^1H NMR (400 MHz, CD_2Cl_2): δ = 7.64 (dd, J = 10.0, 0.8 Hz, 1 H, H2), 6.87 (s, 1 H, H6′), 6.48 (s, 1 H, H8′), 6.28 − 6.08 (m, 3 H, H3 + H4 + H5), 5.22 (br s, 2 H, NH_2), 4.90 (s, 1 H, C*H*(C6)), 3.34 (d, J = 7.4 Hz, 1 H, H9a′ or H4a′), 2.53, 2.42 (2 br s, 2 H, H4′ + H1′), 2.38 (s, 3 H, CH_3(C5′)), 2.37 (d, J = 7.4 Hz, 1 H, H4a′ or H9′a), 2.26 (s, 3 H, CH_3(C7′)), 1.58 − 1.49 (m, 2 H, H2′ + H3′), 1.39 − 1.29 (m, 1 H, H2′), 1.22 − 1.11 (m, 1 H, H3′), 1.03 (br s, 2 H, CH_2(C1′)); ^{13}C NMR (CD_2Cl_2): δ = 168.7 (CO), 162.8 (C6), 151.2 (C8a′), 141.4 (C4b′), 137.7 (C7′), 137.9 (C5), 134.2 (C5′), 130.6 (C6′), 128.3 (C3), 123.4 (C8′), 121.8 (C2), 121.4 (C4), 118.1 (CH(C6)), 65.2 (C4a′ or C9a′), 59.0 (C1), 54.6 (C9a′ or C4a′), 40.2 (C4′), 39.0 (C1′), 34.5 (CH_2(C1′)), 30.0, 29.1 (C2′ + C3′), 21.4 (CH_3(C7′)), 19.6 (CH_3(C5′)); HRMS calcd. for $C_{23}H_{26}NO$ ($[M + H]^+$) 332.2009, found 332.2010.

6-(Carbamoyl)methylene-5′-methyl-6′,7′-dimethoxy-1′,2′,3′,4′,4a′,9a′-hexahydro-1′,4′-methanospirocyclohexa[2,4]diene-1,9′-fluorene (169g)

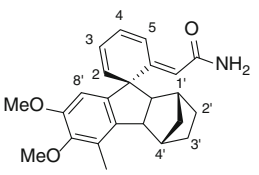

$C_{24}H_{27}NO_3$ M = 377.48 g/mol

Prepared using **GP2** and isolated as a pale yellow solid. Yield: 60 %. Eluent: pentane/EtOAc = 65:35.

Mp: 214–216 °C; IR (neat): ν = 3,338, 3,182, 2,953, 2,871, 1,658, 1,576, 1,473, 1,324, 1,230, 1,088, 735 cm^{-1}; ^1H NMR (400 MHz, CD_2Cl_2): δ = 7.61 (dd, J = 10.0, 1.2 Hz, 1 H, H2), 6.31 − 6.17 (m, 3 H, H3 + H8′ + H4), 6.09 (d, J = 9.5 Hz, 1 H, H5), 5.26 (br s, 2 H, NH_2), 4.92 (s, 1 H, C*H*(C6)), 3.74 (s, 3 H, OCH_3(C7′)), 3.72 (s, 3 H, OCH_3(C6′)), 3.29 (d, J = 7.6 Hz, 1 H, H9a′), 2.45 (d, J = 0.4 Hz, 1 H, H4′), 2.40–2.31 (m, 2 H, H1′, H4a′), 2.28 (s, 3 H, CH_3(C5′)), 1.64 − 1.48 (m, 2 H, H2′, H3′), 1.39 − 1.32 (m, 1 H, H2′), 1.19 − 1.11 (m, 1 H, H3′), 1.08 − 0.95 (m, 2 H, CH_2(C1′)); ^{13}C NMR (CD_2Cl_2): δ = 168.6 (CO), 162.2 (C6), 153.0 (C6′), 147.6 (C7′), 145.2 (C4b′), 137.2 (C8a′), 137.0 (C5), 128.0

(C3), 127.4 (C5′), 121.7 (C4), 121.6 (C2), 118.1 (CH(C6)), 106.1 (C8′), 64.9 (C4a′), 60.2 (OCH_3(C7′)), 59.2 (C1), 55.9 (OCH_3(C6′)), 54.8 (C9a′), 40.3 (C4′), 38.9 (C1′), 34.2 (CH_2(C1′)), 29.8 (C2′), 28.9 (C3′), 13.2 (CH_3(C5′); HRMS calcd. for $C_{24}H_{27}NO_3Na$([M + Na]$^+$) 400.1883, found 400.1890.

6-(Carbamoyl)methylene-7a',8′,9′,10′,11′,11a'-hexahydro-8′, 11′-methanospirocyclohexa[2,4]diene-1,7′-benzo[c]fluorene (169h)

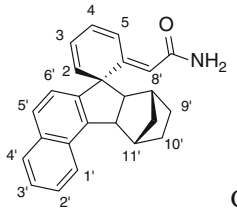

$C_{25}H_{23}NO$ M = 353.46 g/mol

Prepared using **GP2** and isolated as a pale yellow solid. Yield: 47 %. Eluent: pentane/EtOAc = 65:35.

Mp: 210–212 °C; IR (neat): ν = 3,173, 3,045, 2,954, 2,869, 1,654, 1,573, 1,348, 953, 817, 710; ^{1}H NMR (400 MHz, CD_2Cl_2): δ = 8.07 (d, J = 8.0 Hz, 1 H, H1′), 7.86 (d, J = 8.0 Hz, 1 H, H4′), 7.73 − 7.65 (m, 2 H, H5′, H2), 7.55 (td, J = 8.0 Hz, 1.2 Hz, 1 H, H2′), 7.48 (td, J = 8.0 Hz, 1.2 Hz, 1 H, H3′), 7.01 (d, J = 8.4 Hz, 1 H, H6′), 6.33 − 6.24 (m, 2 H, H3, H4), 6.21 − 6.16 (m, 1 H, H5), 5.13 (br s, 2 H, NH_2), 4.90 (s, 1 H, CH(C6)), 3.81 (d, J = 7.2 Hz, 1 H, H11a′), 2.77 (d, J = 4.0 Hz, 1 H, H11′), 2.54 (d, J = 7.2 Hz, 1 H, H7a′), 2.47 (d, J = 3.6 Hz, 1 H, H8′), 1.73 − 1.63 (m, 1 H, H10′), 1.62 − 1.48 (m, 2 H, H10′ + H9′), 1.28 − 1.20 (m, 1 H, H9′), 1.04 (s, 2 H, CH_2(C8′)); ^{13}C NMR (CD_2Cl_2): δ = 168.4 (CO), 161.7 (C6), 147.1 (C6a′), 140.8 (C11b′), 136.1 (C5), 134.2 (C4a′), 130.3 (C11c′), 129.0 (C4′), 128.9 (C5′), 128.1 (C3), 126.4 (C2′), 125.8 (C3′), 125.3 (C1′), 123.6 (C6′), 122.3 (C4), 122.0 (C2), 118.5 (CH(C6)), 64.9 (C7a′), 59.6 (C1), 54.9 (C11a′), 41.0 (C11′), 39.0 (C8′), 34.7 (CH_2(C8′)), 29.8 (C10′), 29.1 (C9′); HRMS calcd. for $C_{25}H_{23}NONa$ ([M + Na]$^+$) 376.1672, found 376.1676.

6-(Carbamoyl)methylene-5′-chloro-1′,2′,3′,4′,4a′,9a′-hexahydro-1′, 4′-methanospirocyclohexa[2,4]diene-1,9′-fluorene (169j)

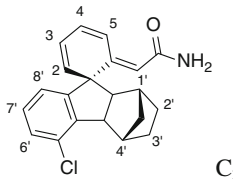

$C_{21}H_{20}NOCl$ M = 337.84 g/mol

Prepared using **GP2** and isolated as a white solid. Yield: 28 %. Eluent: pentane/EtOAc = 6:4.

Mp: 117–119 °C; IR (neat): ν = 3,325, 3,178, 2,952, 2,870, 1,655, 1,573, 1,446, 1,348, 733 cm^{-1}; ^1H NMR (400 MHz, CD_2Cl_2): δ = 7.63 (dd, J = 9.7, 1.0 Hz, 1 H, H2), 7.23 (dd, J = 7.9, 1.0 Hz, 1 H, H6′), 7.14 (td, J = 7.8, 0.7 Hz, 1 H, H7′), 6.80 (dd, J = 7.6, 0.7 Hz, 1 H, H8′), 6.31 – 6.16 (m, 2 H, H3, H4), 6.07 (d, J = 9.4 Hz, 1 H, H5), 5.19 (br s, 2 H, NH_2), 4.89 (s, 1 H, C*H*(C6)), 3.46 (d, J = 7.5 Hz, 1 H, H9a′), 2.84 (d, J = 4.1 Hz, 1 H, H4′), 2.49 – 2.34 (m, 2 H, H1′ + H4a′), 1.59 – 1.12 (m, 6H, H2′ + H3′ + CH_2(C1′)); ^{13}C NMR (CD_2Cl_2): δ = 168.1 (CO), 161.5 (C6), 153.0 (C5′), 143.3 (C4b′), 135.8 (C5), 130.9 (C8a′), 129.6 (C7′), 128.7 (C6′), 128.0 (C3), 124.0 (C8′), 122.0 (C4), 121.8 (C2), 118.4 (CH(C6)), 64.1 (C4a′), 59.4 (C1), 54.4 (C9a′), 39.8, 39.1 (C1′, C4′), 34.4 (CH_2(C1′)), 29.7, 28.8 (C2′ + C3′); HRMS calcd. for $C_{21}H_{20}NOClNa$ ([M + Na]$^+$) 360.1126, found 360.1125.

6-(Carbamoyl)methylene-5′-trifluoromethyl-1′,2′,3′,4′,4a′,9a′-hexahydro-1′,4′-methanospirocyclohexa[2,4]diene-1,9′-fluorene (169k)

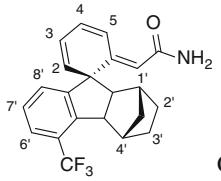

$C_{22}H_{20}F_3NO$ M = 371.40 g/mol

Prepared using **GP2** and isolated as an oil. Yield: 60 %. Eluent: pentane/EtOAc = 6:4.

IR (neat): ν = 3,180, 2,953, 1,655, 1,575, 1,318, 1,162, 1,118, 735 cm^{-1}; ^1H NMR (400 MHz, CD_2Cl_2): δ = 7.69 − 7.60 (m, 1 H, H2), 7.55 (d, J = 7.7 Hz, 1 H, H6′), 7.32 (t, J = 7.3 Hz, 1 H, H7′), 7.10 (d, J = 7.7 Hz, 1 H, H8′), 6.34 − 6.21 (m, 2 H, H3 + H4), 6.19 − 6.03 (m, 1 H, H5), 5.32 (br s, 2 H, NH_2), 4.83 (s, 1 H, C*H*(C6)), 3.67 (d, J = 7.4 Hz, 1 H, H9a′), 2.60 (s, 1 H, H4′), 2.46 − 2.42 (m, 2 H, H4a′ + H1′), 1.8 − 0.85 (m, 6H, H2′ + H3′ + CH_2(C1′)); ^{13}C NMR (CD_2Cl_2): δ = 168.7 (CO), 162.0 (C6), 153.4 (C8a′), 143.7 (q, $^3J_{C-F}$ = 2 Hz, C4b′), 136.2 (C5), 129.9 (C8′), 128.9 (C7′), 128.4 (C3 or C4), 127.1 (q, $^2J_{C-F}$ = 31 Hz, C5′) 126.6 (q, $^3J_{C-F}$ = 5 Hz, C6′), 125.7 (q, CF_3, $^1J_{C-F}$ = 272 Hz), 122.8 (C3 or C4), 122.2 (C2), 119.0 (CH(C6)), 64.8 (C4a′), 58.8 (C1), 55.6 (C9a′), 42.4 (q, $^5J_{C-F}$ = 2.4 Hz, C4′), 39.6 (C1′), 34.6 (CH_2(C1′)), 30.1, 29.5 (C2′ + C3′); ^{19}F NMR ($CDCl_3$): δ = −58.96; HRMS calcd. for $C_{22}H_{20}F_3NONa$ ([M + Na]$^+$) 394.1389, found 394.1390.

***Spiro* derivative (169l)**

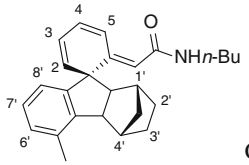

$C_{26}H_{31}NO$ M = 373.53 g/mol

Prepared using **GP2** and isolated as an oil. Yield: 35 %. Eluent: pentane/EtOAc = 2:1.

IR (neat): ν = 3,281, 2,956, 2,870, 2,358, 1,630, 1,578, 1,137 cm^{-1}; ^1H NMR (400 MHz, CD_2Cl_2): δ = 7.64 (d, J = 10.8 Hz, 1 H, arom.), 7.09 − 7.03 (m, 2 H, arom.), 6.71 (d, J = 7.6 Hz, 1 H, arom.), 6.19 − 6.06 (m, 3 H, arom.), 5.33 (br s, 1 H, NH), 4.80 (s, 1 H, = C*H*), 3.39 (d, J = 7.5 Hz, 1 H, H9a′), 3.16 − 3.14 (m, 2 H, NH-CH_2), 2.54 (br s, 1 H, H4′), 2.38 (br s, 5 H, C-CH_3 + H1′ + H4a′), 1.70 − 0.86 (m, 13 H, CH_2 norbornene + butyl); ^{13}C NMR (CD_2Cl_2): 166.7, 160.6, 151.2, 144.4, 136.6, 134.5, 129.5, 128.2, 127.5, 123.0, 122.1, 121.7, 119.9, 64.7, 59.0, 55.2, 40.3, 39.5, 39.1, 34.5, 32.3, 30.0, 29.2, 20.7, 19.6, 14.1.

References

1. Della Ca, N., Motti, E., Mega, A., Catellani, M. (2010). *Advanced Synthesis and Catalysis*, *352*, 1451–1454.
2. Castanet,A.-S., Colobert, F., Broutin, P.-E.(2002). *Tetrahedron Letters*, *43*, 5047–5048.
3. Zhao,Y., Truhlar, D. G. (2008). *Theoretical Chemistry Accounts*, *120*, 215–241.
4. Frisch, M. J., Trucks, G. W., Schlegel, H. B., Scuseria, G. E., Robb, M. A., Cheeseman, J. R. (2009). *Gaussian, Inc*., *Wallingford CT*.
5. Hay, J. P., Wadt, W. R. (1985). *The Journal of Chemical Physics*, *82*, 299–308.
6. Friesner, R. A., Murphy, R. B., Beachy, M. D., Ringlanda, M. N., Pollard, W. T., Dunietz, B. D. et al. (1999). *Journal of Physical Chemistry A*, *103*, 1913–1928.
7. Weigen, F., Ahlrichs, R. (2005). *Physical Chemistry Chemical Physics*, *7*, 3297.
8. Andrae, D., Haeussermann, U., Dolg, M., Stoll, H., Preuss, H., (1990). *Theoretica Chimica Acta*, *77*, 123–141.
9. Peterson, K. A., Figgen, D., Goll, E., Stoll, H., Dolg, M. (2003). *The Journal of Chemical Physics*, *119*, 11113–11123.
10. Larraufie, M.-H., Maestri, G., Beaume, A., Derat, E., Ollivier, C., Fensterbank, L. (2011). *Angewandte Chemie International Edition*, *50*, 12253–12258.
11. Chapsal, B. D., Ojima, I. (2006). *Organic Letters*, *8*, 1395–1398.
12. Coulomb, J., Certal, V., Larraufie, M.-H., Ollivier, C., Corbet, J.-P., Mignani, G. (2009). *Chemistry–A European Journal*, *15*, 10225–10232.
13. Klingensmith, L. M., Nadeau, K. A., Moniz, G. A. (2007). *Tetrahedron Letters*, *48*, 4589–4593.
14. Candito, D. A., Lautens, M. (2009). *Angewandte Chemie International Edition*, *48*, 6713–6716.

General Conclusion

During this Ph.D. work we have developed new radical and pallado-catalyzed methodologies, and we have endeavored to apply them to the synthesis of biologically-relevant polycyclic compounds. We first explored the scope of radical cascades using *N*-acylcyanamides as original partners. The generation of an alkyl radical at the γ or δ position of the cyanamide led in one step, after two consecutive cyclizations to the formation of quinazolinones. Among the small library of compounds synthesized in this fashion, two were natural products: deoxyvasicinone and mackinazolinone.

Switching the starting radical to a vinyl one led to a more complex cascade. Indeed, the aryl ring *ortho*-substituent extruded during the re-aromatization step was trapped by the initially formed exo methylene, in a formal bond-forming migration. In depth mechanistic studies allowed us to control this new domino process. In particular, this unprecedented radical migration was possible with a trifluoromethyl group.

The next challenge was the addition of aminyl radicals to the cyanamide moiety, which would lead to the first radical synthesis of guanidines. This was achieved employing azide precursors, and led to synthesis of a dozen of tricyclic guanidines. We are currently seeking to evaluate the biological activity of our compounds which could potentially act as DNA intercalating agents. It would also be interesting to examine their use as chiral bases for enantioselective applications.

In order to allow the translation of these pioneering results to industrial applications, we have next endeavored to find eco-compatible alternatives for the generation of radicals using visible light, the most abundant source of energy. Under 14 W light bulb irradiation, electrons could be transferred to α-keto epoxides *via* a Ruthenium or Iridium catalyst in the presence of Hantzsch ester. The resulting α-hydroxy radicals were allylated with high diastereoselectivity. Significantly, α-amino radicals were obtained and reacted under the same conditions by visible-light photoreduction of α-keto aziridines.

The main challenge to undertake in the future, will be to merge the first two axis of my Ph.D., i.e. to devise complex cascades triggered by visible-light photoredox catalysis.

M.-H. Larraufie, *Development of New Radical Cascades and Multi-Component Reactions*, Springer Theses, DOI: 10.1007/978-3-319-01324-4,

In a complementary approach, we used the palladium/norbornene cocatalysis for the synthesis of nitrogen-containing heterocyclic compounds. In collaboration with the group of Pr. Catellani, we developed a new methodology for the direct synthesis of phenanthridines. Commercially available aryl iodides and benzyl bromides could be coupled in the presence of a palladium catalyst and norbornene, to form a library of biologically relevant phenanthridines in one step and excellent yields. Aside to this synthetic study, we brought new insights into the mechanism of the Catellani reaction. Indeed, we evidenced the first deviation from the *ortho* effect in this chemistry using bromobenzylacetamides as substrates. DFT calculations indicated that this likely originated in a distortion in the reductive elimination pathway from the Pd(IV) intermediate initially formed, caused by specific chelation. Addition of water restored the normal selectivity, however it led to de-aromatization. Thorough modelisation studies allowed us to understand the role of water. We showed that it could take the place of an apical ligand of the Pd(IV) intermediate, thus reducing the steric strain, and increasing the flexibility of the complex. Further work should seek to expand the synthetic applications of the chelate approach in Pd(IV) chemistry. Finally, the best opportunity to combine the two facets of my Ph.D. work would be to explore the possibility to control the various oxidation states of palladium thanks to visible-light induced electron transfers.